



# UNIVERSIDAD DE GRANADA

FACULTAD DE CIENCIAS

Departamento de Química Analítica

Grupo de investigación FQM-297 "Control Analítico, Ambiental, Bioquímico y Alimentario"

## Programa de Doctorado en Química

### METABOLOMICS APPLIED TO THE STUDY OF DIFFERENT PLANT MATRICES IN AREAS OF INTEREST TO THE AGRI-FOOD SECTOR

CONTRIBUCIÓN DE LA METABOLÓMICA APLICADA AL ESTUDIO DE  
DIVERSAS MATRICES VEGETALES EN ÁREAS DE INTERÉS PARA EL  
SECTOR AGROALIMENTARIO

Memoria presentada por **Dña. Irene Serrano García** para optar al título  
de Doctora Internacional por la Universidad de Granada

*Tesis dirigida por*

Dra. Dña. Alegría Carrasco Pancorbo

Dra. Dña. Lucía Olmo García

**Granada, 2024**

Editor: Universidad de Granada. Tesis Doctorales  
Autor: Irene Serrano García  
ISBN: 978-84-1195-648-2  
URI: <https://hdl.handle.net/10481/101991>





UNIVERSIDAD  
DE GRANADA



Dpto. de Química Analítica  
Prof. Fermín Capitán García

La doctoranda / *The doctoral candidate* Dña. IRENE SERRANO GARCÍA y los directores de la Tesis / *and the thesis supervisors* Dra. Dña. ALEGRÍA CARRASCO PANCORBO y Dra. Dña. LUCÍA OLMO GARCÍA

Garantizamos, al firmar esta Tesis Doctoral, que el trabajo ha sido realizado por la doctoranda bajo la dirección de los directores de la Tesis y, hasta donde nuestro conocimiento alcanza, en la realización del trabajo, se han respetado los derechos de otros autores a ser citados cuando se han utilizado sus resultados o publicaciones.

/

*Guarantee, by signing this Doctoral Thesis, that the work has been done by the doctoral candidate under the direction of the thesis supervisors and, as far as our knowledge reaches, in the performance of the work, the rights of other authors to be cited (when their results or publications have been used) have been respected.*

Granada, 25 de septiembre de 2024

Directoras de la Tesis / *Thesis supervisors*:

**Dra. Dña. Alegría Carrasco Pancorbo**

**Dra. Dña. Lucía Olmo García**

Doctoranda / *Doctoral candidate*:

**Dña. Irene Serrano García**





UNIVERSIDAD  
DE GRANADA



Dpto. de Química Analítica  
Prof. Fermín Capitán García

Dra. Dña. ALEGRÍA CARRASCO PANCORBO, Catedrática del Departamento de Química Analítica de la Facultad de Ciencias de la Universidad de Granada,

CERTIFICA QUE:

El trabajo presentado en esta Tesis Doctoral, titulado "CONTRIBUCIÓN DE LA METABOLÓMICA APLICADA AL ESTUDIO DE DIVERSAS MATRICES VEGETALES EN ÁREAS DE INTERÉS PARA EL SECTOR AGROALIMENTARIO", realizado bajo mi dirección, cumple con todos los requisitos legales, académicos y científicos necesarios para que la doctoranda Dña. Irene Serrano García pueda optar al título de Doctora Internacional en Química.

Esta Tesis ha sido realizada en los laboratorios del grupo FQM-297 en el Departamento de Química Analítica de la Universidad de Granada y, parcialmente, en el Centro de Instrumentación Científica de la Universidad de Granada, y en las instalaciones del grupo TrAMS (Trace Analysis and Mass Spectrometry Group) de la Universidad Nacional y Kapodistriaca de Atenas (Grecia).

Y para que así conste, expido y firmo el presente certificado en Granada, a 25 de septiembre de 2024:





UNIVERSIDAD  
DE GRANADA



Dpto. de Química Analítica  
Prof. Fermín Capitán García

Dra. Dña. LUCÍA OLMO GARCÍA, Profesora Titular del Departamento de Química Analítica de la Facultad de Ciencias de la Universidad de Granada,

CERTIFICA QUE:

El trabajo presentado en esta Tesis Doctoral, titulado "CONTRIBUCIÓN DE LA METABOLÓMICA APLICADA AL ESTUDIO DE DIVERSAS MATRICES VEGETALES EN ÁREAS DE INTERÉS PARA EL SECTOR AGROALIMENTARIO", realizado bajo mi dirección, cumple con todos los requisitos legales, académicos y científicos necesarios para que la doctoranda Dña. Irene Serrano García pueda optar al título de Doctora Internacional en Química.

Esta Tesis ha sido realizada en los laboratorios del grupo FQM-297 en el Departamento de Química Analítica de la Universidad de Granada y, parcialmente, en el Centro de Instrumentación Científica de la Universidad de Granada, y en las instalaciones del grupo TrAMS (Trace Analysis and Mass Spectrometry Group) de la Universidad Nacional y Kapodistriaca de Atenas (Grecia).

Y para que así conste, expido y firmo el presente certificado en Granada, a 25 de septiembre de 2024:



## FINANCIACIÓN PERSONAL RECIBIDA DURANTE LA TESIS DOCTORAL

La presente Tesis Doctoral ha sido financiada por el Ministerio de Ciencia, Innovación y Universidades del Gobierno de España mediante la "Ayuda para la Formación de Profesorado Universitario (FPU)" otorgada a la doctoranda, con inicio el 31 de octubre de 2019 (**ref. FPU19/00700**).

La Estancia Internacional se financió a través del Programa 10: Ayudas para Realizar Estancias Breves en Centros de Investigación Nacionales y Extranjeros, otorgado en diciembre de 2022 por el Vicerrectorado de Investigación y Tránsito de la Universidad de Granada.



MINISTERIO  
DE CIENCIA, INNOVACIÓN  
Y UNIVERSIDADES



UNIVERSIDAD  
DE GRANADA



# AGRADECIMIENTOS

Quiero expresar mi más sincero agradecimiento a todas las personas e instituciones que han hecho posible la realización de esta Tesis Doctoral.

En primer lugar, quiero agradecer a mis directoras de tesis, la Dra. Alegría Carrasco Pancorbo y la Dra. Lucía Olmo García, por su guía, apoyo y confianza durante todos estos años de doctorado. Su conocimiento, paciencia y dedicación han sido fundamentales para el desarrollo de este trabajo. Agradezco también al Departamento de Química Analítica de la Universidad de Granada, por proporcionar los recursos y el ambiente académico necesario para llevar a cabo esta investigación. A todos los integrantes que forman o formaron parte del grupo de investigación FQM-297, por su amistad, colaboración y apoyo constante. En especial a Carmencita, ¡gracias por esos desayunos y esas escapadas tan necesarias e invaluable! También quiero agradecer a los compañeros del grupo FQM-302 por haber compartido grandes momentos tanto dentro como fuera de la becaria, y a todos los amigos de otros departamentos de la Facultad de Ciencias (incluyendo Química Orgánica, Química Inorgánica, Ingeniería Química, etc.) por los buenos momentos compartidos.

En especial me gustaría darle las gracias a Pedro porque siempre tiene una sonrisa para todos y una actitud ante la vida que es de admirar. Gracias por haberme aguantado en tu casa como si fuera una más, y estar siempre atento a lo que pudiéramos necesitar. También darle las gracias a Marcos por los desayunos, los partidos de pádel compartidos y por todas las charlas exprés en el pasillo de Química General. A las chicas del fútbol, que, aunque empecé tarde en la peña, se convirtió en una vía de escape maravillosa todos los martes.

En segundo lugar, me gustaría dar las gracias a toda mi familia, y en especial a mi madre, padre, tía y hermanos, por su amor incondicional y su complicidad, por su paciencia y su comprensión constantes durante este largo camino. Vuestro apoyo y buenas palabras han sido mi refugio en los momentos difíciles y mi motivación en los días de mayores dudas. Gracias por creer en mí y celebrar cada uno de mis pequeños avances como si fueran propios y por todos vuestros viajes a Granada, incluyendo a Ekko, ¡aun y con el calorazo que hacía en alguna época!

Tota aquesta etapa tampoc hauria estat possible sense el gran recolzament rebut per part de tots els amics de Barcelona: Cami, Quar, Anna, Óscar, Marc, Dani, Laia, Tetxos, Laia Indukern, etc. Tornar a marxar lluny de casa va ser un repte molt difícil, i més encara després de l'època viscuda durant la Covid-19. Per tot això, us vull agrair la vostra presència, preocupació, missatges, trucades, i tot allò que heu fet per ajudar a desfogar-me en moments difícils, entendre les meves absències i celebrar sempre les bones notícies. La vostra amistat sempre ha estat un pilar sòlid en aquest procés. També agrair-vos totes les visites rebudes en aquests cinc anys, tant a Granada com a Atenes, els dinars de Nadal, Setmana Santa, vacances d'estiu, etc., i les celebracions d'aniversari

per tot lo alt. També vull agrair als companys de la Universitat de Barcelona (Ainoha, Paula, Sandra, Pau..) per estar sempre atents als meus progressos, les múltiples visites i tot el temps compartit durant el anys d'universitat.

A més, diuen que coneixes a les millors persones quan menys ho esperes, i quanta raó tenen. Moltes gràcies, Sandra, pel suport tan gran que vas ser durant la meva estada a Grècia. Totes les escapades, els dinars, els cafès i les llargues xerrades a la universitat són records d'Atenes que perduraran molt de temps i que agrairé tota la vida. Arribaràs molt lluny amb tot el que et proposis, no en tinc dubtes! I also want to thank Ilinca and Chris for being the best flatmates in Athens and, of course, the best restaurant tasters. You are wonderful people and I wish you all the best. I would also like to thank TrAMS group for receiving me.

Por último, quiero dedicar unas palabras especiales de agradecimiento a Aritz. Gracias por ser mi apoyo incondicional, en casa, en la universidad, en el pádel y donde haga falta. Gracias por estar a mi lado cuando las fuerzas escaseaban, y por celebrar cada éxito como si fuera tuyo. Por recorrer juntos Andalucía (Granada, Sevilla, Ronda, Málaga, Jaén, etc.), Cataluña, País Vasco, y otros rincones maravillosos de España y Europa. Admiro tu capacidad para empatizar y tus infinitas muestras de afecto que dan motivación para seguir adelante. Eres un refugio de serenidad y este logro no habría sido posible sin ti. Vivir la etapa del doctorado juntos, ha sido una experiencia gratificante. También quiero dar las gracias a toda tu familia por el apoyo y las muestras de cariño recibido a lo largo de todos estos años.

*¡Infinitas gracias a todos los que habéis formado parte de esta etapa!*

# INDEX

---

OBJECTIVES / OBJETIVOS .....	15
SUMMARY / RESUMEN .....	23
INTRODUCTION .....	33
<b>1. <i>Persea americana</i> Mill.</b> .....	35
<b>1.1.</b> Avocado origin and botany .....	35
<b>1.2.</b> Avocado production .....	38
<b>1.3.</b> Dynamics of world avocado trade and importance of consumption .....	40
<b>1.4.</b> Development of avocado fruit: Special features of <i>Persea americana</i> Mill. ....	41
<b>1.5.</b> Composition and health benefits of avocado fruit .....	43
<b>2. <i>Olea europaea</i> L.</b> .....	46
<b>2.1.</b> Origin, botanical classification, and cultivation of the olive tree .....	46
<b>2.2.</b> Olive tree morphology, composition, and key metabolites .....	48
<b>2.2.1.</b> Olive fruit .....	49
<b>2.2.2.</b> Other olive tree matrices (leaves, stems, roots...) .....	50
<b>2.2.3.</b> <i>Olea europaea</i> L. secondary metabolites .....	50
<b>2.3.</b> Olive tree pathologies: Verticillium wilt .....	54
<b>2.3.1.</b> Pathogen life cycle and infection symptomatology .....	54
<b>2.3.2.</b> Management of Verticillium wilt of olive disease .....	55
<b>2.4.</b> Genetic resources and olive breeding programs .....	56
<b>2.4.1.</b> Breeding objectives and selection criteria in olive cultivation .....	56
<b>3. Metabolomics applied to food analysis</b> .....	59
<b>3.1.</b> Terminology and metabolomics strategies .....	59
<b>3.2.</b> Metabolomics workflow .....	61
<b>3.3.</b> Main applications fields of metabolomics .....	64
<b>3.4.</b> Metabolomics-based research on the matrices under investigation .....	66
<b>3.4.1.</b> Metabolomics applied to the study of avocado fruit .....	67
<b>3.4.2.</b> Metabolomics applied to the study of olive-related matrices .....	68
<b>4. References</b> .....	70
EXPERIMENTAL PART, RESULTS AND DISCUSSION .....	83
Section I: "Metabolomic approaches applied to the study of avocado fruit" .....	87
Chapter 1. Prolonged on-tree maturation vs. cold storage of <i>Hass</i> avocado fruit: Changes in metabolites of bioactive interest at edible ripeness .....	89

<b>Chapter 2.</b> Uncovering phytochemicals quantitative evolution in avocado fruit mesocarp during ripening: A targeted LC-MS metabolic exploration of <i>Hass</i> , <i>Fuerte</i> and <i>Bacon</i> varieties .....	115
<b>Chapter 3.</b> Assessing the RP-LC-MS-based metabolic profile of <i>Hass</i> avocados marketed in Europe from different geographical origins (Peru, Chile, and Spain) over the whole season .....	145
<b>Chapter 4.</b> Comprehensive LC-IMS-MS characterisation of avocado fruits from different Iberian regions: Integrating ion mobility as a valuable descriptor in non-targeted metabolomics .....	171
<b>Section II: “Metabolomic approaches applied to the study of olive-related matrices” .....</b>	<b>209</b>
<b>Chapter 5.</b> Fruit phenolic and triterpenic composition of progenies of <i>Olea europaea</i> subsp. <i>cuspidata</i> , an interesting phytochemical source to be included in olive breeding programs .....	211
<b>Chapter 6.</b> Characterization of the metabolic profile of olive tissues (roots, stems and leaves): Relationship with cultivars’ resistance/susceptibility to the soil fungus <i>Verticillium dahliae</i> .....	239
<b>Chapter 7.</b> Application of LC-ion mobility spectrometry-MS-based metabolomics to investigate the basal chemical profile of olive cultivars differing in <i>Verticillium dahliae</i> resistance .....	275
<b>CONCLUSIONS / CONCLUSIONES .....</b>	<b>309</b>

**OBJECTIVES**

**OBJETIVOS**





The avocado is the most widespread tropical crop in Spain, with a predominant presence in the southern part of the country, although production has also expanded to other regions of the Iberian Peninsula. However, Spanish production is not sufficient to meet the demands of the European market, leading to the need for imports from other countries such as Chile and Peru. The proximity of Spanish avocado plantations to European Union markets offers a major competitive advantage over those imported from more distant countries. On the one hand, it is crucial to evaluate how this factor influences the compositional profile of avocado, and consequently, its nutritional quality. On the other hand, appropriate analytical tools are essential for certifying the origin of avocados available on the market, ensuring accurate labelling.

While the lipid fraction of the avocado is the most well-recognized and extensively studied, the fruit also contains a wide range of phytochemicals belonging to different chemical families, such as phenolic compounds, amino acids, nucleosides, vitamins, phytohormones, etc., which are partially responsible for many of its organoleptic and nutritional properties. Fruit composition is directly modulated by various pre- and postharvest factors, including growing area, maturity stage, and storage conditions. Therefore, characterizing the profile of minor compounds can be highly useful in studies on nutritional quality or geographical authentication, among others.

Additionally, Spain is by far the world's leading producer of both olive oil and table olives. However, the olive sector faces diseases and pests that could jeopardize plantation viability and cause significant economic losses. In fact, there are breeding programs that not only aim to identify varieties suitable for high-quality oil production but also focus on finding cultivars that exhibit high resistance to certain pathogens. To support the progress of these programs, it is essential to thoroughly characterize unexplored subspecies that may serve as genetic resources before considering their inclusion. It is also important to investigate at the molecular level the natural defense mechanisms present in certain varieties that show greater resistance to pests to inform potential crossbreeding efforts aimed at developing improved cultivars.

Metabolomics provides valuable tools to address some of the challenges faced by both the avocado and olive sectors. The use of omics strategies, particularly those approaches based on the use of liquid chromatography coupled to mass spectrometry (LC-MS), allows for the comprehensive characterization of metabolite profiles in plant tissues (different plant organs or various parts of the fruit). Advances in analytical platforms and data processing tools enable increasingly complete and precise information about the metabolome of the samples under study, facilitating their grouping and/or discrimination, the description of distinctive compositional patterns, or the discovery of specific markers. Furthermore, qualitative and quantitative information on certain metabolites allows for deeper understanding of plant physiology, covering

aspects such as tissue distribution, ripening, genetic influence, and natural defense mechanisms against pathogens.

Based on the above, the **main objective** of this Doctoral Thesis has been to develop and apply powerful metabolomic tools that can contribute to the improvement, evolution, and profitability of the avocado and olive sectors in Spain. To achieve this overall goal, several **specific objectives** were pursued, as outlined below. Some of the partial objectives have a more analytical focus, while others are more oriented towards the practical application of the developed methodologies. The analytically focused objectives include:

- ✚ To design an appropriate sampling plan to obtain representative samples that can lead to relevant and well-founded conclusions useful to the avocado and olive sectors.
- ✚ To optimize pre-treatment and sample processing systems, as well as the most relevant variables for the separation and detection of compounds of interest, using advanced analytical platforms.
- ✚ To apply optimized and validated analytical methods to the analysis of samples of interest to the agri-food sector (olive and avocado matrices), ensuring accuracy and reliability of the results.
- ✚ To assess the potential of coupling ion mobility to LC-MS for metabolomic studies of highly complex matrices, such as those studied in this thesis.
- ✚ To properly process the data and employ chemometric tools to extract useful information in an efficient and reliable manner.
- ✚ To interpret the results obtained to provide well-supported responses to the issues addressed in each study.

The specific objectives related to the application of the methodologies proposed in this thesis can be formulated as follows:

- ✚ To evaluate the impact of prolonged on-tree maturation on the metabolic profile of avocados compared with cold storage.
- ✚ To study the effect of ripening on the avocado compositional profile, and to assess the possible dependence of this physiological process on the variety.
- ✚ To identify possible biomarkers that can be used to define the typical compositional profiles of avocados from different regions or olive genotypes with varying levels of tolerance to the soil fungus *Verticillium dahliae*.
- ✚ To evaluate the potential of *Olea europaea* subsp. *cuspidata* for inclusion in olive breeding programs, considering the richness and diversity of its metabolic profile.

El aguacate es el cultivo tropical más extendido en España, con una presencia predominante en la zona sur del país, aunque su producción se ha expandido a otras regiones de la Península Ibérica. Sin embargo, la producción española no es suficiente para cubrir toda la demanda del mercado europeo, lo que obliga a importar frutos provenientes de otros países como Chile y Perú, mayoritariamente. La proximidad de nuestras plantaciones a los mercados de la Unión Europea constituye la principal ventaja competitiva de los productos nacionales frente a los importados de países lejanos. Por un lado, es fundamental evaluar cómo este factor influye en el perfil composicional del aguacate y, por ende, en su calidad nutricional. Por otro lado, es indispensable disponer de las herramientas analíticas adecuadas para poder certificar el origen de los aguacates que se encuentran en el mercado, garantizando su correcto etiquetado.

Si bien la fracción lipídica es la más reconocida y estudiada del aguacate, el fruto también contiene una amplia gama de fitoquímicos pertenecientes a diferentes familias químicas, como compuestos fenólicos, aminoácidos, nucleósidos, vitaminas, fitohormonas, etc., que son responsables parcialmente de muchas de sus propiedades organolépticas y nutricionales. La composición de los frutos está directamente modulada por la influencia de diversos factores pre- y postcosecha, entre los que se incluyen la zona de cultivo, el estado de madurez o las condiciones de almacenamiento. Por tanto, la caracterización del perfil de compuestos minoritarios puede ser de gran ayuda a la hora de abordar estudios sobre calidad nutricional o de autenticación geográfica, entre otros.

Asimismo, nuestro país es, con diferencia, el principal productor mundial tanto de aceite de oliva como de aceitunas de mesa. Sin embargo, cada año, el sector oleícola se enfrenta a enfermedades y plagas, que podrían poner en riesgo la viabilidad de las plantaciones y producir graves pérdidas económicas. De hecho, existen programas de mejora que, además de identificar variedades adecuadas para la producción de aceite de alta calidad, se enfocan en la búsqueda de variedades con elevada resistencia a determinados patógenos. Para contribuir al avance de estos programas, es indispensable caracterizar de forma exhaustiva subespecies inexploradas que puedan emplearse como recursos genéticos antes de considerar su introducción en los mismos. Asimismo, es importante investigar a nivel molecular los mecanismos de defensa natural que poseen ciertas variedades que presentan una mayor resistencia a las plagas, para ayudar a definir posibles cruzamientos que den lugar a cultivares mejorados.

La metabolómica ofrece herramientas que podrían ser de gran ayuda a la hora de abordar algunos de los desafíos a los que se enfrentan tanto el sector del aguacate como el oleícola. El uso de estrategias ómicas, en particular el de aquellas aproximaciones basadas en el empleo de la cromatografía líquida acoplada a espectrometría de masas (LC-MS), permite caracterizar de

forma exhaustiva el perfil de metabolitos de interés de tejidos vegetales (distintos órganos de la planta o diversas partes del fruto). La evolución de las plataformas analíticas, así como de las herramientas de tratamiento de datos, favorece la obtención de información cada vez más completa y precisa acerca del metaboloma de las muestras estudiadas, posibilitando su agrupamiento y/o discriminación, la descripción de patrones composicionales distintivos o la identificación de ciertos marcadores. Además, la obtención de información cualitativa y cuantitativa de determinados metabolitos permite profundizar en el conocimiento de la fisiología de la planta, abarcando aspectos como la distribución entre tejidos, la evolución durante la maduración, la influencia genética, los mecanismos de autodefensa frente a patógenos, etc.

En base a todo lo expuesto, el **objetivo principal** de esta Tesis Doctoral ha sido desarrollar y aplicar potentes herramientas metabolómicas que puedan contribuir a la mejora, evolución y aumento de la rentabilidad del sector del aguacate y del olivar en nuestro país. Para alcanzar este objetivo general, ha sido necesario conseguir una serie de **objetivos parciales** que se detallan a continuación. Como podrá observarse, algunos de los objetivos parciales tienen un enfoque más analítico, mientras que otros están más orientados a las aplicaciones específicas de las metodologías desarrolladas; en cuanto a los primeros:

- ✚ Diseñar un plan de muestreo adecuado que facilite la obtención de muestras representativas que permitan alcanzar conclusiones relevantes y con fundamento suficiente para poder ser aprovechadas por los responsables del sector oleícola y del aguacate.
- ✚ Optimizar el pretratamiento y los sistemas de tratamiento de muestra, así como las variables más relevantes para llevar a cabo la separación y detección de los compuestos de interés empleando potentes plataformas analíticas.
- ✚ Aplicar los métodos analíticos optimizados y validados para el análisis de muestras de interés para el sector agroalimentario (matrices oleícolas y aguacate), asegurando la exactitud y fiabilidad de los resultados.
- ✚ Evaluar el potencial que tiene el acoplamiento de la dimensión de movilidad iónica a LC-MS para llevar a cabo estudios metabolómicos de matrices altamente complejas como las que se han estudiado en la presente tesis.
- ✚ Procesar correctamente los datos y emplear herramientas quimiométricas que permitan extraer información útil del modo más efectivo y fiable posible.
- ✚ Interpretar los resultados obtenidos con el fin de dar una respuesta fundamentada a la problemática tratada en cada estudio.

Los objetivos parciales directamente relacionados con la aplicación de las metodologías puestas a punto en el transcurso de la presente tesis podrían formularse tal y como sigue:

- ✦ Evaluar el impacto de una maduración prolongada en árbol sobre el perfil metabólico del aguacate, en comparación con el almacenamiento en frío.
- ✦ Estudiar la influencia que ejerce el proceso de maduración del aguacate sobre su perfil composicional, y evaluar la posible dependencia de este proceso fisiológico en función de la variedad.
- ✦ Identificar posibles biomarcadores que puedan ser empleados para definir el perfil composicional típico de aguacates provenientes de distintas regiones o de genotipos de olivo con diferentes niveles de tolerancia al hongo de suelo *Verticillium dahliae* Kleb.
- ✦ Evaluar el potencial de *Olea europaea* subsp. *cuspidata* para su inclusión en programas de mejora genética del olivo, teniendo en cuenta la riqueza y diversidad de su perfil metabólico.



**SUMMARY**

**RESUMEN**





## SUMMARY

---

This dissertation presents the results achieved within the frame of the Doctoral Thesis entitled **“METABOLOMICS APPLIED TO THE STUDY OF DIFFERENT PLANT MATRICES IN AREAS OF INTEREST TO THE AGRI-FOOD SECTOR”**. The report has been structured into two main sections. The first section, the **Introduction**, provides a general overview of the covered topics and contextualizes the work. The second section, which encompasses the **Experimental Part, Results, and Discussion**, details the experimental work and presents the findings of each investigation along with the corresponding discussion, key conclusions, and the main future perspectives.

Since this Doctoral Thesis explored two different species (*Persea americana* Mill. and *Olea europaea* L.), the **Introduction** focuses on describing the most relevant aspects of both. It covers their botanical and taxonomic descriptions, as well as their significance in terms of global production, cultivation, and trade. For each species, the necessary information has been organized into specific sections to ensure a comprehensive understanding of all the topics addressed in the experimental part of this work. To conclude the introductory section, the final part introduces metabolomics, describing the strategies that can be followed, and the typical workflow used in metabolomic studies. The most relevant applications of metabolomics are also highlighted, with a particular emphasis on those related to the scope of this thesis.

The second major section refers to the **Experimental Part, Results, and Discussion**, and is divided into two distinct parts, according to the matrix under study in each chapter. The first part is entitled **“Section I: Metabolomic approaches applied to the study of avocado fruit”** and includes four chapters. The second part, entitled **“Section II: Metabolomic approaches applied to the study of olive-related matrices”** encompasses three studies focused on the olive sector. Each chapter includes a brief introduction to the topic, followed by detailed descriptions of the materials and reagents used, the procedures for sample collection and treatment, the instrumental conditions for analysis, and the tools employed for data processing. In the *Results and Discussion*, the findings are presented using tables, graphs, and figures to facilitate the extraction of relevant information, often through the application of statistical analysis. The results are compared with previous studies to contextualize the findings within the existing literature. Additionally, the possible theoretical and practical implications of the results are discussed, recognizing possible limitations of the study and its potential impact, and suggesting future research directions based on the study’s findings.

In **Section I**, devoted to the study of avocados, two main topics are addressed: the first two studies investigate the phenomena of fruit maturation and ripening at the metabolic level, while the following two chapters focus on the differentiation of avocados based on their geographical origin. The key aspects of each work are presented below:

- ✚ **Chapter 1:** The objective of this study was to compare the effect of prolonged on-tree maturation with the impact of cold storage (common in intercontinental exports) on the final composition of avocados. The evolution of 9 bioactive compounds (7 phenolic compounds, as well as pantothenic and abscisic acids) was investigated over a 40-day period (in 10-day intervals), using LC-MS for the determination of the target analytes. The results were discussed considering both the individual evolution of each compound and broader trends through statistical analysis.
- ✚ **Chapter 2:** In this work, the quantitative evolution of 30 metabolites (including phenolic compounds, amino acids, nucleosides, vitamins, phytohormones, etc.) was studied using LC-MS throughout the different stages of avocado ripening after harvesting (green, intermediate, ripe, and overripe), examining whether the observed trends were shared across different varieties (*Hass*, *Fuerte*, and *Bacon*). Significant metabolic differences were found according to genetic origin, and potential varietal markers were identified. Quantitative variations over time were also observed for most of the metabolites examined, with a noticeable increase in the concentration of phenolic compounds during the ripening process.
- ✚ **Chapter 3:** This study focused on a comprehensive characterization of the metabolic profile of *Hass* avocados marketed in Europe and sourced from Spain, Chile and Peru by means of high and low resolution LC-MS. Twenty-two metabolites from different chemical families were identified and quantified, their concentrations were compared between samples, and the proportion of each class of compounds (amino acids and nucleotides, phenolic acids and derivatives, etc.) was estimated with respect to the sum concentration of all of them. Statistical analyses (PCA and PLS-DA) revealed metabolic patterns specific to each producing country.
- ✚ **Chapter 4:** Avocado production has expanded across different regions of the Iberian Peninsula. To explore how the geographical origin (location, soil, climate) influences the metabolic profile of the fruit, this study employed an advanced LC-MS platform coupled to ion mobility spectrometry (IMS) to analyze *Hass* avocados from eight different plantations across several Iberian regions. The analytical platform employed enabled the annotation of over 100 primary and secondary metabolites, providing CCS (Collision Cross Section) values as an additional descriptor that significantly improves identification accuracy. In addition, by employing a non-targeted approach and appropriate statistical tools, distinctive compositional patterns for each region were described, revealing the most notable differences between avocados grown in the north and south of the peninsula.

On the other hand, the studies presented in [Section II](#), dedicated to the examination of olive-related matrices are framed within the olive breeding programs. The first chapter focuses on the exploration of a previously under-studied subspecies (subsp. *cuspidata*), while the remaining two chapters are centered on one of the most devastating diseases affecting olive groves (verticillium

wilt), seeking cultivars with the highest possible resistance to this pathogen. The key aspects of each study are summarized below:

- ✚ **Chapter 5:** The subspecies *cuspidata* has been relatively unexplored so far due to its low commercial value, but it may hold significant potential as a genetic resource for olive breeding programs. In this study, the drupe metabolic composition of a progeny of 27 *cuspidata* genotypes coming from free pollination and their female parent was characterized, identifying 62 compounds through LC-MS and quantifying the 27 most relevant. Simultaneously, four traditional cultivars (*Arbequina*, *Frantoio*, *Koroneiki*, and *Picual*) were analyzed for comparison and used as controls. The metabolic profiles of *cuspidata* showed significant differences compared to common olive cultivars, standing out for their higher content of certain bioactive compounds such as rutin, hydroxytyrosol glucoside, and some secoiridoids.
- ✚ **Chapter 6:** Understanding the resistance mechanism of olive to the pathogen causing verticillium wilt is crucial to control this devastating disease. In this targeted study, the basal metabolic profiles of leaves, stems, and roots from 10 olive cultivars with varying levels of resistance/susceptibility were analyzed using LC-MS. A total of 56 metabolites were identified, and their distribution across different plant organs was described in qualitative and quantitative terms. Multivariate analysis was applied to evaluate the relationship between the compositional profile and the resistance exhibited by the different cultivars, successfully distinguishing resistant from susceptible cultivars. Additionally, compositional patterns were described, and potential metabolic markers of resistance and/or susceptibility were identified.
- ✚ **Chapter 7:** Building on the work from the previous chapter, this study examined the basal metabolome of tissues from 43 cultivars with varying levels of resistance to verticillium wilt, aiming to provide new insights for olive breeding programs. A non-targeted metabolomics strategy was applied using an innovative UHPLC-ESI-TimsTOF MS/MS analytical platform, which allowed the creation of a preliminary database that includes experimental <sup>TIMS</sup>CCS<sub>N<sub>2</sub></sub> values. More than 70 metabolites were identified in roots, stems, and leaves, and chemometric analysis of the data revealed significant metabolic variability between resistant and susceptible cultivars, establishing disease susceptibility markers and typical compositional patterns.



Esta memoria presenta los resultados obtenidos durante la realización de la Tesis Doctoral titulada “**CONTRIBUCIÓN DE LA METABOLÓMICA APLICADA AL ESTUDIO DE DIVERSAS MATRICES VEGETALES EN ÁREAS DE INTERÉS PARA EL SECTOR AGROALIMENTARIO**”. Se ha estructurado en dos secciones principales. La primera, la **Introducción**, ofrece una visión general de los temas tratados y contextualiza el trabajo realizado. La segunda sección, que incluye la **Parte Experimental, Resultados y Discusión**, detalla el trabajo experimental llevado a cabo y recoge los resultados de cada investigación junto con su correspondiente discusión, las conclusiones más relevantes, así como las principales perspectivas futuras.

Dado que en esta Tesis Doctoral se ha abordado el estudio de dos especies distintas (*Persea americana* Mill. y *Olea europaea* L.), la **Introducción** se ha centrado en describir los aspectos más relevantes de ambas. Esto incluye su descripción botánica y taxonómica, así como su relevancia en términos de producción, cultivo y comercio a nivel mundial. Para cada una de las especies, se ha procurado incluir la información necesaria, estructurada en secciones específicas, que permita comprender plenamente todas las temáticas tratadas en la parte experimental de este trabajo. Para concluir el bloque introductorio, el último apartado se ha ocupado de introducir la metabolómica, describiendo las estrategias que pueden seguirse y las distintas etapas de los estudios metabolómicos. Además, se han destacado sus aplicaciones más relevantes, haciendo especial hincapié en aquellas relacionadas con el ámbito de esta tesis.

El segundo gran bloque hace referencia a la **Parte Experimental, Resultados y Discusión** y se ha dividido en dos secciones distintas, según la matriz objeto de estudio en cada capítulo. La primera de las secciones se ha denominado “**Sección I. Aproximaciones metabolómicas aplicadas al estudio del fruto del aguacate**”, e incluye cuatro capítulos. La segunda sección, denominada “**Sección II. Aproximaciones metabolómicas aplicadas al estudio de matrices relacionadas con el olivar**”, abarca tres trabajos enfocados al sector oleícola. Cada capítulo incluye una breve introducción a la temática tratada y detalla los materiales y reactivos empleados, los procedimientos aplicados para la toma y tratamiento de muestras, las condiciones instrumentales utilizadas para realizar los análisis, así como las herramientas empleadas para el tratamiento de los datos. En *Resultados y Discusión*, se presentan los resultados obtenidos haciendo uso de tablas, gráficas y figuras, que facilitan la extracción de información relevante, en muchos casos, mediante la aplicación de análisis estadísticos. Asimismo, se comparan los resultados con los de estudios anteriores para situar los hallazgos en el contexto de la literatura existente. Del mismo modo, se discuten las posibles implicaciones teóricas y prácticas de los resultados, se reconocen las posibles limitaciones del estudio y su impacto potencial, y se sugieren futuras líneas de investigación basadas en los hallazgos del estudio.

En la **sección I**, dedicada al estudio del aguacate, se abordan dos temáticas principales: los primeros dos trabajos investigan el fenómeno de maduración del fruto a nivel metabólico, mientras que los dos capítulos siguientes se centran en la diferenciación de aguacates atendiendo a su origen geográfico. A continuación, se presentan los aspectos más destacados de cada trabajo:

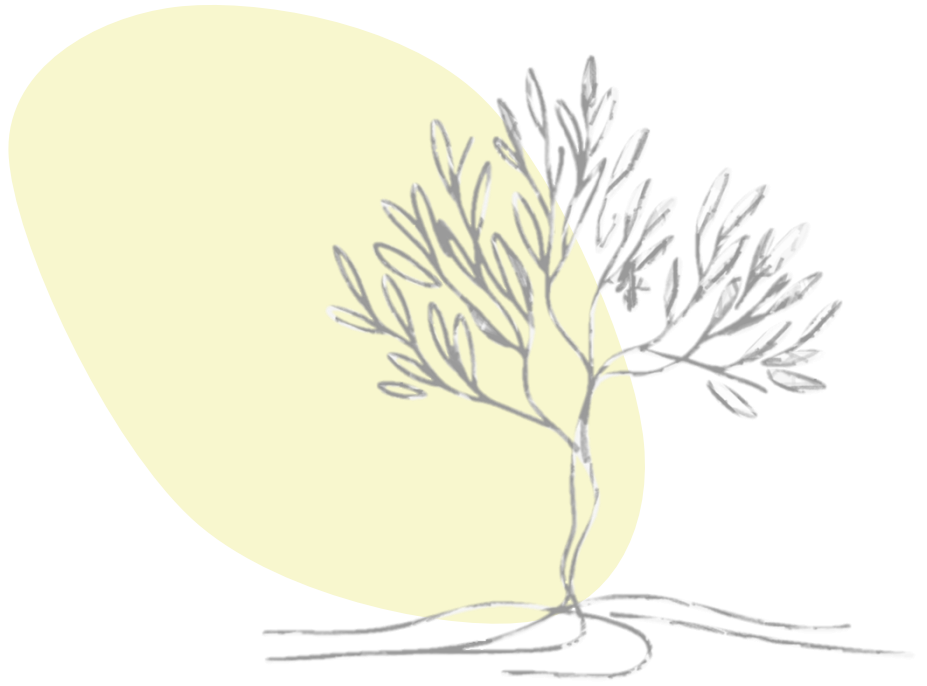
- ✚ **Capítulo 1:** El objetivo de este estudio fue comparar el efecto de la maduración prolongada en el árbol con el impacto de un almacenamiento en frío (común en exportaciones intercontinentales) sobre la composición final del aguacate. Para ello, se investigó la evolución de 9 compuestos bioactivos (7 compuestos fenólicos, y los ácidos pantoténico y abscísico) a lo largo de un periodo de 40 días (en intervalos de 10 días), empleando LC-MS para la determinación de los analitos de interés. Los resultados se discutieron considerando tanto la evolución individual de cada compuesto como en términos más globales mediante el empleo de análisis estadísticos.
- ✚ **Capítulo 2:** En este trabajo se estudió, mediante LC-MS, la evolución cuantitativa de 30 metabolitos (compuestos fenólicos, aminoácidos, nucleósidos, vitaminas, fitohormonas, etc.) a lo largo de las distintas etapas de maduración del aguacate tras su recolección (verde, madurez intermedia, maduro y sobremaduro), examinando si las tendencias observadas eran compartidas entre distintas variedades (*Hass*, *Fuerte* y *Bacon*). Se encontraron diferencias metabólicas significativas atendiendo al origen genético y se identificaron potenciales marcadores varietales. También se observaron variaciones cuantitativas a lo largo del tiempo para la mayoría de los metabolitos examinados, resultando evidente el aumento de la concentración de compuestos fenólicos durante el proceso de maduración.
- ✚ **Capítulo 3:** En este capítulo se realizó la caracterización exhaustiva del perfil metabólico de aguacates *Hass* comercializados en Europa y procedentes de España, Chile y Perú utilizando LC-MS de alta y baja resolución. Se identificaron y cuantificaron 22 metabolitos de diversas familias químicas, se compararon sus concentraciones entre muestras y se estimó la proporción que representaba cada clase de compuestos (aminoácidos y nucleótidos, ácidos fenólicos y derivados, etc.) respecto de la concentración sumatoria de todos ellos. Los análisis estadísticos realizados (PCA y PLS-DA) revelaron patrones metabólicos específicos de cada país productor.
- ✚ **Capítulo 4:** La producción de aguacate se ha expandido por distintas regiones de la Península Ibérica. Para investigar cómo el origen geográfico (localización, suelo, clima...) puede condicionar el perfil metabólico de los frutos, en este estudio se utilizó una plataforma avanzada LC-MS acoplada a movilidad iónica (IMS) para analizar aguacates de la variedad *Hass* procedentes de ocho plantaciones distintas de varias regiones de la península. La plataforma analítica empleada permitió la anotación de más de 100 metabolitos primarios y secundarios, aportando el valor de CCS (*Collision Cross Section*) como un descriptor adicional que mejora significativamente la precisión en la identificación. Además, aplicando un enfoque no dirigido y haciendo uso de las pertinentes herramientas estadísticas, se pudieron describir patrones composicionales

distintivos de cada región, hallando las diferencias más notables entre aguacates cultivados en el norte y el sur de la península.

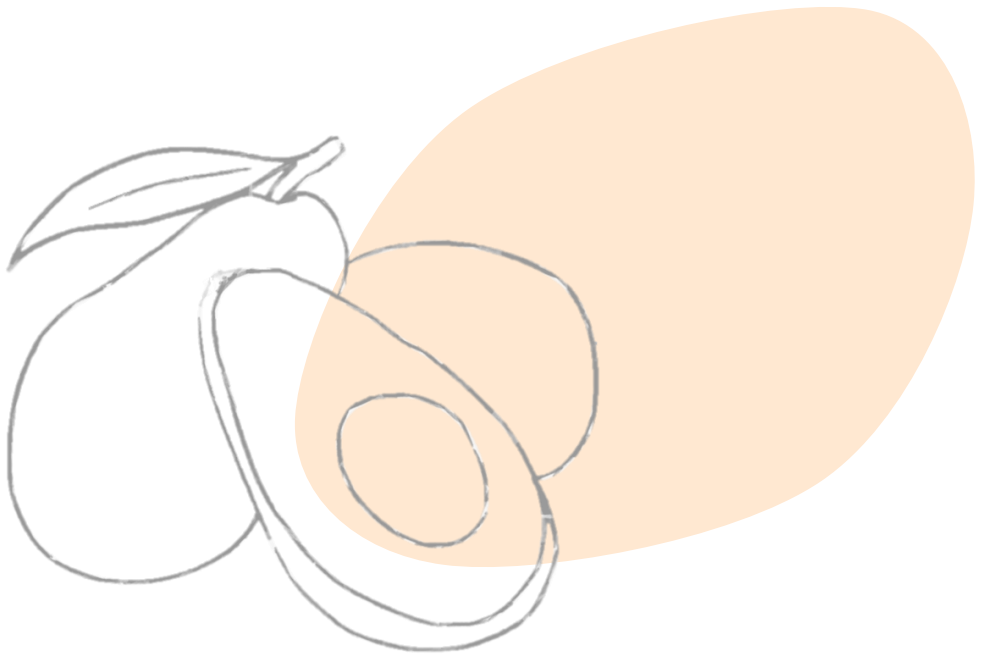
Por otro lado, los trabajos presentados en la **sección II** dedicada al estudio de matrices oleícolas, se enmarcan dentro de los programas de mejora para el cultivo del olivo. El primer capítulo se centra en la exploración de una subespecie poco considerada hasta ahora (la subsp. *cuspidata*), mientras que los dos capítulos restantes se focalizan en una de las enfermedades más devastadoras que afectan al olivar, la verticilosis, buscando cultivares lo más resistentes posible al ataque de este patógeno. A continuación, se resumen los aspectos más relevantes de cada estudio:

- ✚ **Capítulo 5:** La subespecie *cuspidata* ha sido poco explorada hasta el momento debido a su bajo valor comercial, pero podría esconder un gran potencial como recurso genético en programas de mejora del olivo. Por ello, en este trabajo se caracterizó la composición metabólica de las drupas de 27 genotipos de *cuspidata* y su progenitora, identificando 62 compuestos mediante LC-MS y cuantificando los 27 más relevantes. Simultáneamente, se analizaron cuatro cultivares tradicionales (*Arbequina*, *Frantoio*, *Koroneiki* y *Picual*) que se usaron como controles con el propósito de comparar sus composiciones. Los perfiles metabólicos de *cuspidata* mostraron diferencias significativas respecto a los cultivares comunes de olivo, destacando por su mayor contenido en ciertos compuestos bioactivos, como la rutina, el hidroxitirosol glicosilado y algunos secoiridoides.
- ✚ **Capítulo 6:** Conocer el mecanismo de resistencia del olivo al patógeno causante de la verticilosis es clave para controlar esta demoledora enfermedad. En este estudio dirigido, se analizaron los perfiles metabólicos basales de hojas, tallos y raíces de 10 cultivares de olivo con diferentes niveles de resistencia/susceptibilidad mediante LC-MS. Se identificaron 56 metabolitos y se describió su distribución en términos cualitativos y cuantitativos en las distintas partes de la planta. Mediante la aplicación de análisis multivariante se evaluó la relación del perfil composicional con la resistencia mostrada por los distintos cultivares, logrando diferenciar los resistentes de los susceptibles. Asimismo, se describieron patrones composicionales y se identificaron posibles marcadores metabólicos de resistencia y/o susceptibilidad.
- ✚ **Capítulo 7:** Siguiendo con la línea abierta en el capítulo anterior, en este trabajo se estudió el metaboloma basal de tejidos de 43 cultivares con distintos niveles de resistencia a la verticilosis, con la intención de brindar nuevas perspectivas para los programas de mejora genética del olivo. Para ello, se aplicó una estrategia metabolómica no dirigida basada en el empleo de una innovadora plataforma UHPLC-ESI-TimsTOF MS/MS, que permitió la creación de una base de datos preliminar que incluye valores de <sup>TIMS</sup>CCS<sub>N2</sub> experimentales. Se identificaron más de 70 metabolitos en raíces, tallos y hojas, y el tratamiento quimiométrico de los datos reveló una significativa variabilidad metabólica entre los cultivares resistentes y los susceptibles, estableciendo marcadores de susceptibilidad a la enfermedad y patrones composicionales típicos.





## **INTRODUCTION**





## 1. *PERSEA AMERICANA* MILL.

### 1.1. Avocado origin and botany

The avocado is a tropical fruit originated in a wide geographical area of Mesoamerica, extending from the eastern and central highlands of Mexico through Guatemala to the Pacific coast of Central America [1]. Archaeological seed evidence from the Tehuacan Valley in Puebla, Mexico, suggest that avocados were consumed by humans as early as 8000–7000 B.C., with domestication by Mesoamerican groups probably dating back to at least 5000 B.C. [2]. After America's conquest, Spaniards introduced the avocado to Europe [3]. The avocado tree belongs to the Lauraceae family and the *Persea* genus, which is divided in three different subgenera – *Machilus*, *Eriodaphne* and *Persea* – that enclose more than 150 species. Although the *Persea* subgenus only comprises three recognized species (*P. schiedeana* Nees, *P. parvifolia* Williams, and *P. americana* Mill.), it is the most economically significant as it includes the cultivated avocado [4].

The avocado tree (*P. americana* Mill.) is a woody evergreen tree, but often loses its leaves for a short period of time before and during flowering (no longer than 12 months). The tree canopy varies in form, ranging from low and dense with a uniform shape to tall and irregularly structured, and the tree itself can reach heights of up to 30 meters. The root system is remarkably shallow as it grows in a horizontal pattern, concentrated in the first 50 cm of the soil, resulting in limited water uptake and hydraulic conductance. Leaves ranges in length from 7 to 41 cm with variable shapes (elliptical, oval, lanceolate, etc.), colors (reddish, dark green, etc.), and textures (hairy, smooth, leathery, etc.) [4,5]. The flowers are bisexual with both functional male and female organs and exhibit a singular synchronous protogynous dichogamy breeding system. Each tree produces an abundance of flowers blooming for weeks and even months, which facilitates both cross- and self-pollination. However, despite this prolific flowering, only 0.01% to 1% of the flowers successfully develop into fruit [6,7]. **Figure 1** shows an illustration of an avocado tree (a), flowers (b), and fruits (c).

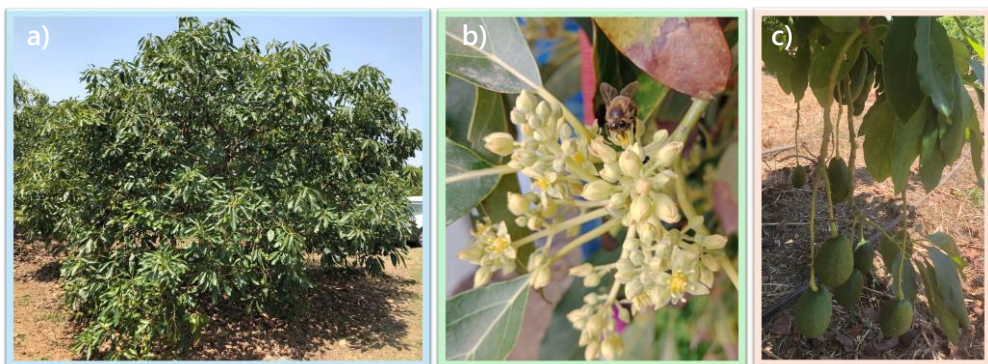


**Figure 1.** *Persea americana* Mill. (a) tree, (b) flowers, and (c) fruits

Botanically, avocado fruit is considered a one-seeded berry with an exceedingly variable in size (50 g to nearly 2 Kg), shape (round, oval, pyriform, ellipsoid, etc.), peel (color, thickness, roughness, etc.), and seed characteristics (size, surface, etc.) [4]. The structure of the avocado fruit is made up of the seed (10-25% of the total weight of the fruit), and the pericarp, which in turn is composed of the epicarp, also called exocarp or peel (7-15% of total weight), the mesocarp (65-80% of fruit weight) and a thin layer around the seed called the endocarp [8,9] (Figure 2).

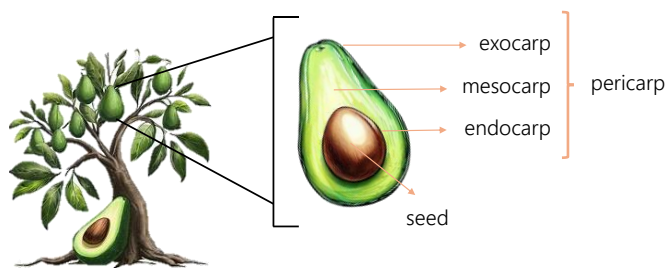


Figure 2. Scheme of the distinct structural components of the avocado fruit

Several botanical varieties or subspecies of *P. americana* Mill., also referred as horticultural races, are commercially recognized by horticulturists, including the Guatemalan (*P. americana* var. *guatemalensis*), Mexican (*P. americana* var. *drymifolia*), and West Indian (*P. americana* var. *americana*) races. Each of these races has distinct morphological, physiological, and ecological characteristics, which are summarized in Table 1 [4,10].

Table 1. Major characteristics of the three commercial horticultural races of avocado

Characteristics	Guatemalan race	Mexican race	West Indian race
Origin	Tropical highlands	Tropical highlands	Tropical lowlands
<b>TREE</b>			
Climatic adaptation	Subtropical	Semi-tropical	Tropical
Cold tolerance	Intermediate	High	Sensible
Salinity tolerance	Medium tolerant	Sensitive	Most tolerant
Leaf length	8-20 cm	5-20 cm	10-30 cm
Leaf anise	Absent	Present	Absent
Young leaf colour	Green with red tinge	Green	Pale yellow
Mature leaf colour	Dark green	Dark green	Pale green
<b>FRUIT</b>			
Flowering-mature interval	10-16 months	6-9 months	5-9 months
Fruit color	Green	Often dark	Green or reddish
Fruit shape	Rounded	Elongated	Elongated
Fruit size	Variable intermediate	Variable to small	Variable to large
Pulp flavour	Rich	Anise-like, rich	Sweeter, milder
Presence of fibres	Rare	Common	Rare
Oil content	Medium-High	High	Low
Fruit ripening	On-tree storage	On-tree storage	No on-tree storage
Skin thickness	Thick	Very thin	Medium
Skin surface	Rough	Waxy bloom	Shiny
Seed size	Small	Large	Variable
Seed cavity	Tight	Loose	Variable
Seed surface	Smooth	Smooth	Rough

There are no reported sterility barriers in avocado fruit, which has facilitated racial hybridization. Hybrids are usually developed from random seedlings, although breeding efforts have also been made to obtain varieties with selected agronomic traits (resistance to pests, salinity or cold tolerance, enhanced yields, extended harvesting seasons, etc.) or traits related to fruit quality (flavor, size, oil content, etc.). There are two flower-type cultivars, referred to as “A” and “B” according to the timing of the male and female phases [5]. Most commercial avocado cultivars in subtropical climates are Guatemalan × Mexican hybrids with different degrees of hybridization. The *Hass* variety (A flower-type) originated by chance in California almost 100 years ago and is now the most widely planted and commercialized variety in the world. Indeed, such hybrid replaced the *Fuerte* variety as the international avocado market standard in the 1970s. In addition to these two valued hybrids, other popular varieties include *Bacon*, *Carmen*, *Maluma*, *Lamb Hass*, *Pinkerton*, *Reed*, *Edranol*, and *Zutano*. Some of these varieties, such as *Bacon* and *Fuerte* (B-types), are used as *Hass* pollinators in many countries. Although *Hass* avocado flowers are capable of self-pollination, cross-pollination usually gives better results [9].

Most traits in hybrids are derived from their parental races, although they are often enhanced or diversified as a result of the hybridization process. With around 10-15% of Mexican genes and 85-90 % of the Guatemalan race, the *Hass* variety stands out mostly for its high quality, enhanced productivity, storage, and transport capacity and later maturity (long on-tree storage). Other varieties, such as *Fuerte* and *Bacon* (both M × G) also have a significant commercial presence in Spain due to their quality and the need to ensure year-round coverage. Figure 3 compiles some of the most relevant fruit characteristics of these three varieties, which were the subject of the present Thesis [11–13].

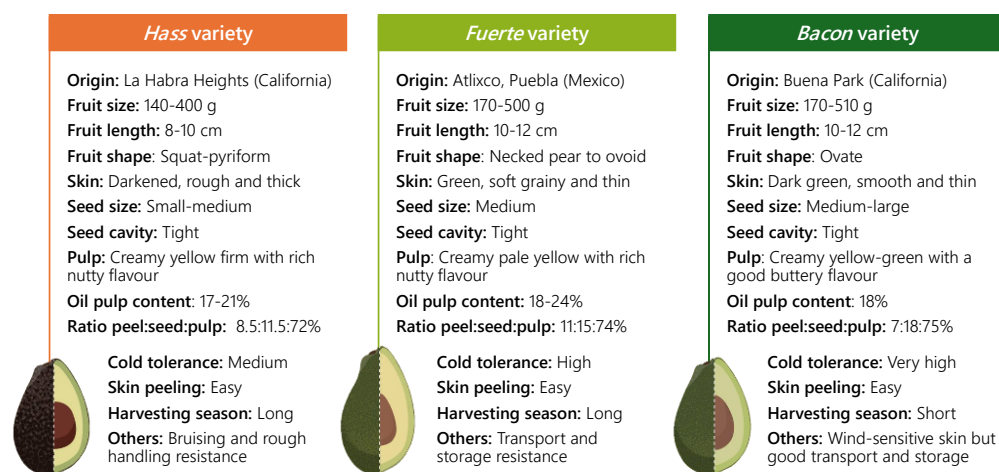


Figure 3. Some recognised traits of *Hass*, *Fuerte*, and *Bacon* avocado varieties

## 1.2. Avocado production

Since the 1960s, both the area under cultivation and the production of avocados have gradually increased worldwide (see Figure 4). Over a four-decade period (1960-2000), production increased from 716,353 tons (t) to around 2.7 million tons. Similarly, the area under cultivation expanded from 78,690 hectares (ha) to 329,288 hectares [14]. It is noteworthy that although the area harvested increased at a higher rate than production in the intervening years (1976-1995), this did not result in higher yields. This phenomenon may be attributed to poor crop management, but it is more likely due to the fact that avocado production stabilizes after 8 years of planting, often at 12–14 years [12].

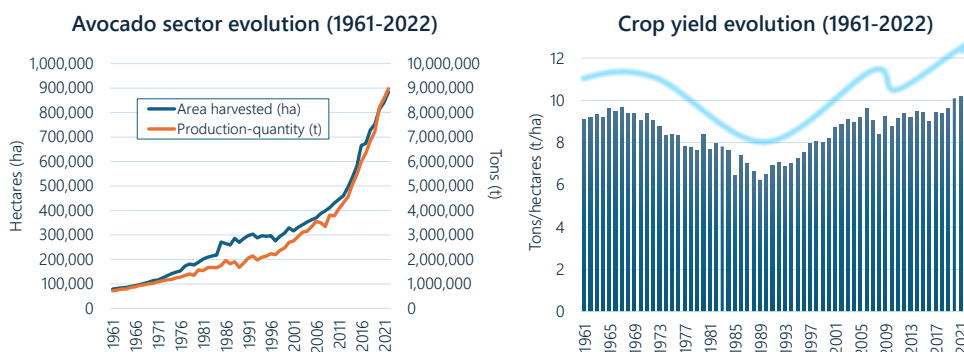
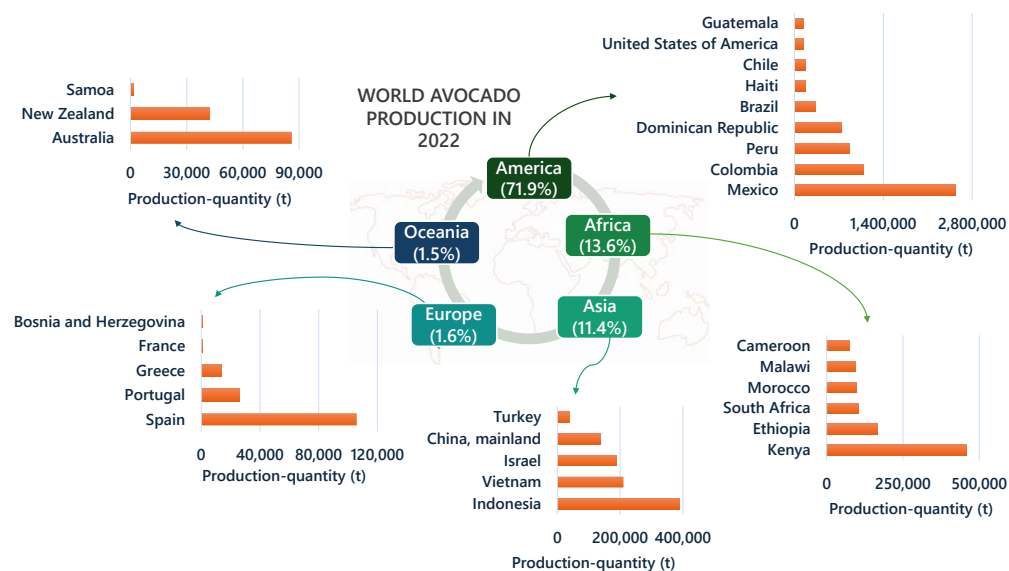


Figure 4. Global avocado harvested area, production, and yield data from 1961 to 2022

Among major tropical fruits, the avocado has the lowest production levels, but has experienced the most rapid expansion in recent years. The exponential growth of the sector began in the second decade of the 2000s, driven by the increasing consumer appreciation for avocado’s attractive attributes and the favourable price levels that benefit both farmers and marketing companies [15]. In just 12 years (2010-2022), avocado production has increased 2.4-fold to nearly 9 million tonnes (Mt) at present, while the harvested area has doubled to over 884,000 hectares. Moreover, avocado crop yield has increased from 8.8 t/ha in 2010 to 10.2 t/ha [14]. Based on the agriculture prospects 2021-2030 published by FAO and the Organisation for Economic Co-operation and Development (OECD), avocado production is expected to reach 12 million tonnes by 2030, three times the level reached in 2010 [16].

More than 60 countries contribute to world avocado production, thanks to the crop’s adaptability to different climatic regions. Several of them are included in Figure 5, which presents fruit production statistics by continent (data from 2022). The American continent accounts for 71.9% of global production, with Mexico as the world’s leading producer (2.5 Mt), followed by Colombia (1 Mt), Peru (≈0.9 Mt), and the Dominican Republic (≈0.7 Mt). The African continent follows with 13.6% of fruit production, with Kenya as the main producing country (0.45 Mt). Asia contributes 11.4%, led by Indonesia (≈0.4 Mt). The European continent accounts for only a modest 1.6% of world production, with Spain leading the way (0.1 Mt). Portugal, among other emerging

producers, shows good potential though it does not match the scale of Spain. Lastly, Oceania ranks the lowest, accounting for 1.5% of the total, with Australia as the principal producing region [14].



**Figure 5.** Major avocado producing countries and associated production by continent (2022)

When comparing producing avocado regions, it is also important to consider crop yield in addition to production. In general, the world's largest producers do not have the highest yields. For instance, Mexico had a yield of 10.7 t/ha, while the Dominican Republic, Brazil, Kenya, and Israel had yields of 18.7 t/ha, 17.4 t/ha, 16.5 t/ha and 14.9 t/ha, respectively. Indonesia reached 13.3 t/ha and Peru 12.3 t/ha. Chile, with 5.2 t/ha, is far behind. The leading countries in production yield are El Salvador (47.7 t/ha), Samoa (30.4 t/ha) and Panama (29.0 t/ha) [14]. Climatic conditions, crop management, genetic factors, and biological barriers could be some of the factors that modify yield rates.

Although Spanish production remains limited, with around 105,930 tons and 19,520 hectares of harvested area in 2022, it represents a significant 72% of total European production. The first national avocado plantation dates back to the 16th century, but it was not until the mid-20th century when avocados were planted for commercial purposes [17]. Cultivation is steadily increasing, although production has decreased by about 9% compared to 2021, probably due to increased temperatures and insufficient water supply. The current yield is about 5.4 t/ha, which is lower than the world average and lower than in previous years [14].

The main cultivars thrive in Andalusia (southern of Spain) due to favourable climatic conditions (temperatures above 20–23°C, adequate relative humidity, minimal wind, free-frost occurrences, etc.). Andalusia dominates the national production, with approximately 83% of the plantations spread over 13,700 hectares of cultivation. Within this region, the coastal areas of the provinces of

Malaga and Granada lead in production ( $\approx 62\%$  and  $30\%$ , respectively), followed by other regions such as Huelva, Cadiz, Almería or Seville, which have recently adopted avocado cultivation. This tropical fruit is also well-established in the Canary Islands, with a consistent  $10\%$  of national production, although the product is primarily reserved for local markets. Interestingly, the Valencian Community has become the third largest producing region in Spain, covering the  $7.7\%$  of total production [18]. Climate change has favoured this latter area, as frosts are now less frequent, and temperatures are rising. Other trials of avocado plantations have been conducted in provinces such as Murcia, Pontevedra, Asturias, and Vizcaya. The feasibility of these plantations depends largely on the climatic conditions, especially the occurrence of frosts, as the fruit cannot tolerate temperatures below  $0^{\circ}\text{C}$  [17].

### 1.3. Dynamics of world avocado trade and importance of consumption

Demand for avocado fruit is booming around the globe. Nearly 3.1 million tonnes were exported in 2022, valued at USD 7,613 million. In fact, avocados are expected to become the most traded tropical fruit by 2030, with exports of 3.9 million tonnes, surpassing pineapple and mango in terms of quantity [16]. Mexico is the leading exporter, with a  $34\%$  share of the market. The second largest exporter is Peru ( $19\%$ ), followed by the Netherlands ( $13.6\%$ ), Spain ( $4.9\%$ ), and Chile ( $3.6\%$ ). Figure 6 lists the major world exporters and importers of avocados in the world and the percentage that the country represents in each category (data from 2022) [14].



Figure 6. Major exporting and importing countries for avocados worldwide (data from 2022)

More than 3.1 million tons of fruits were imported all over the world in 2022 with value of USD 8,275 million. The United States of America (USA) and the European Union (EU) stand as the primary destinations for globally traded avocados. The USA accounts for  $36.5\%$  of the total import volume, whereas the Netherlands is the second most relevant country in this regard [14]. It is noteworthy that the Netherlands handles similar quantities of imported and exported fruits, with product coming mainly from South America, Spain and Israel. Thus, although the Netherlands is a non-producing country, it is the main trading hub for avocados in Europe, with large volumes re-exported to Germany, France, the United Kingdom, and the Scandinavian countries [19,20].

Avocados from Mexico are mainly exported to the United States, Canada, and Japan, with a relatively smaller share reaching European markets compared to the Spanish, Chilean or Peruvian fruits. However, Spanish production accounts for less than 10% to European consumption. Spanish imports are mainly used to supplement domestic production seasons and to fulfil international supply contracts coming from Peru, Chile, Mexico, Morocco, Colombia, or Kenya. With a similar import rate, France stands out as the largest destination market for avocados in Europe. Most of these imports (around 27.6%) are fruits cultivated in Spain, but some are re-exports from Spain or direct imports from Peru. France also imports from Mexico, Chile, and Kenya [19,20].

The Spanish avocado is held in high esteem by major European consumers. A key advantage is the significantly reduced delivery time to European markets, achieved within days, in contrast to the several weeks required for avocados produced in South America. This approach has encouraged the current trend in the markets to supply ready-to-eat avocados, as the fruit can ripen progressively during transport. Additionally, while concerns remain about the sustainability and environmental impact of avocado production, the carbon footprint is significantly reduced in short distances compared to the trans-oceanic exports [21].

Building on the high standard of the fruit, many national producers have long sought to establish prestigious product labels such as the Protected Designation of Origin (PDO) or Protected Geographical Indication (PGI). Nevertheless, these designations have yet to materialize. To date, the avocado sector has been an important national socio-economic support, particularly in the Andalusian region. Its expansion throughout the territory not only increases the national product available, but also generates employment opportunities in field work, industry, and transport. These efforts are aimed at meeting both national and international demand, highlighting the sector's vital contribution to the economy and community development.

Despite a global increase in avocado consumption, the European eating habits remain underdeveloped. On average, Europeans consume 1.16 kg per capita, which is notably low compared to 3.5 kg in the United States and 2.5 kg in Canada. Mexico, the world's largest avocado producer, boasts a per capita consumption ranging from 6.5 to 7 kg. Within the EU, France has the highest consumption with 2.3 kg per person in 2022/2023, followed by the Scandinavian countries (2.2 kg), the United Kingdom (1.6 kg), Germany (1.3 kg), Spain (1.1 kg) and Italy (0.8 kg) [20,22].

#### **1.4. Development of avocado fruit: Special features of *Persea americana* Mill.**

The growth pattern of the avocado follows a single sigmoid curve. Rapid cell division and enlargement are characteristic of the initial growth stage but persist until the fruit is harvested. Throughout fruit development (growth and maturation), numerous physicochemical changes occur to reach the physiological fruit maturity. Fruit is considered mature when it possesses the ability to ripen to a desirable level of edibility [23]. Determining the optimal harvest time can be a complex task that often lacking clear external indicators (color or textural changes). In this sense,

the measurement of parameters such as oil and dry matter content at harvest is an essential aid for growers, as they have been shown to correlate very well with the post-harvest ripening ability of avocado [24]. The codex standard from FAO sets a minimum dry content of 21% for *Hass* and 20% for other commercial varieties, such as *Fuerte*, *Pinkerton*, and *Reed* [25]. Despite these guidelines, each country sets its own minimum avocado harvest requirements.

This tropical fruit does not ripen while on the tree; instead, the ripening process begins after harvest and cannot be reversed. As a climacteric fruit, avocado ripening is associated with a marked increase in respiration rate, which is referred to as the climacteric rise. There are three distinct stages in this process: the pre-climacteric stage, characterized by minimum fruit respiration; the climacteric maximum, marked by peak fruit respiration; and the post-climacteric stage, during which respiration declines and fruit senescence occurs [23,26]. Ripening is also associated with the autocatalytic production of ethylene (a volatile phytohormone) which is the primary stimulator of the climacteric phase. The ethylene production pattern is parallel to respiration and its peak usually precedes the respiratory climacteric stage [23]. The delineated physiological developmental stages of avocado, alongside their corresponding gas respiration and ethylene production rates are illustrated in Figure 7. Compared to other tropical and subtropical fruits, avocado displays a high respiration rate (150-300 mg/CO<sub>2</sub>/kg/hr) and ethylene production rate (10-100 µg/kg/hr) at 20°C. These ratios indicate that avocado fruit is a highly perishable commodity, since the higher the respiration rate, the shorter the shelf life of fresh products [24].

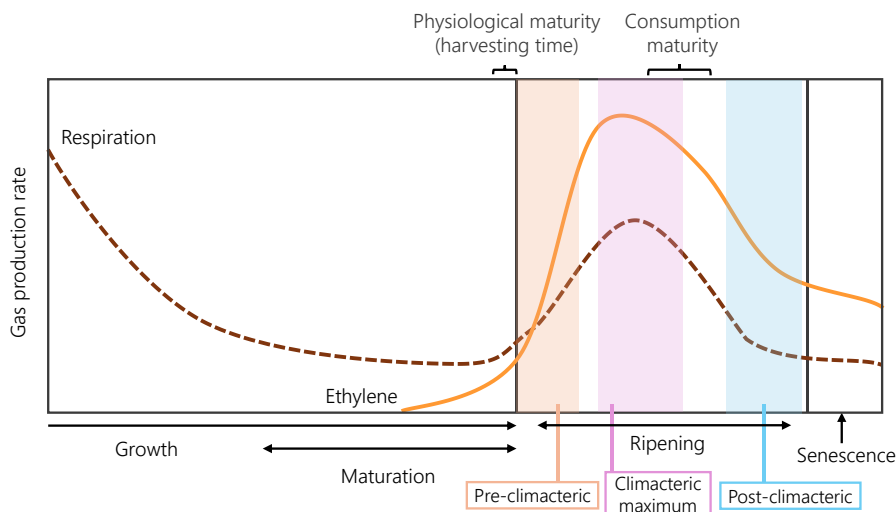


**Figure 7.** Physiological development stages of avocado fruit with associated gas respiration and ethylene production rates (adapted from [27])

Many complex, energy-intensive catabolic and anabolic biochemical processes occur during ripening. The most substantial changes take place during the pre-climacteric and climacteric stages, with a rapid effects on fruit acceptability attributes such as texture, firmness, color and

flavor [28]. Fruit softening that occurs during ripening is mainly associated with cell wall disassembly as the result of alterations in the structure and composition of primary cell wall polysaccharides and their interactions [29]. Softening improves fruit texture but also increases susceptibility to pathogen attack, which could lead to a decline in fruit quality at post-climacteric stages. Other fruit alterations, such as peel darkening due to elevated anthocyanin levels and reduced chlorophyll content, are unique to the *Hass* variety at edible ripeness and constitute an exceptionally valuable feature for consumers to recognize the ready-to-eat stage [30]. The nutritional composition also changes during ripening being closely linked to the overall fruit quality.

Given the unique characteristics of the avocado fruit, ensuring optimum quality at destination is a major concern in the export process. Postharvest handling conditions adopted to enhance the quality of avocados and prolong their shelf life aim at reducing respiration and ethylene production, thereby slowing metabolic rates. This can be accomplished through the use of lower temperatures (cold storage), increasing carbon dioxide levels, and reducing oxygen concentrations within acceptable limits (controlled or modified atmosphere storage). Fruits must be maintained at the pre-climacteric stage, but prolonged storage at low temperatures may induce chilling injury symptoms. Effective cold chain management is paramount for maintaining the quality of avocados from harvest to their ultimate market destination with temperature oscillations not exceeding  $\pm 1^{\circ}\text{C}$  [5]. The duration of ripening in avocado can vary significantly from less than 7 days at room temperature to up to one month when stored at  $5^{\circ}\text{C}$ . The recommended storage temperature and relative humidity range from  $4$  to  $13^{\circ}\text{C}$  and  $85$ - $90\%$  of relative humidity to prevent water loss. For controlled or modified atmosphere storage, it is recommended to maintain around  $2$ - $5$   $\text{O}_2$  kPa and  $3$ - $10$   $\text{CO}_2$  kPa [24,26,31]. Ripening and fruit softening can also be inhibited by the application of 1-methylcyclopropene (1-MCP) which is an ethylene antagonist. Air circulation through boxes, containers or chambers should be guaranteed during avocados storage to control the temperature and minimize ethylene accumulation [32].

### **1.5. Composition and health benefits of avocado fruit**

According to the United States Department of Agriculture (USDA) FoodData Central, the nutritional composition of the pulp of raw avocados, specifically comprising 86% California and 14% Florida varieties, is summarized in Table 2. However, it is important to note that the macro- and micronutrient composition depends on the variety, ripening degree, climate of the growing area, cultivation conditions, soil composition, and even the fertilizers used.

The avocado is an energetic fruit used as a versatile culinary ingredient. It is the main ingredient of the popular guacamole, but it is also consumed in salads and used in sauces. In general, the edible part of the avocado contains 67 to 78% moisture (water), 13.5 to 24% lipids, 0.8 to 4.8% carbohydrates, 1 to 3% proteins, and 1.4 to 3% fiber [33,34].

**Table 2.** Avocado composition information (100 g edible portion) [35]

Component	Value	Unit	Component	Value	Unit
<b>Proximate</b>			<b>Fats</b>		
total lipid (fat)	14.7	g	monounsaturated fatty acids	9.8	g
protein, total	2	g	18:1	9.07	g
water	73.2	g	16:1	0.70	g
energy	670 (160)	kJ (kcal)	polyunsaturated fatty acids	1.82	g
ash, g	1.58	g	18:2	1.67	g
carbohydrate, by difference	8.64	g	18:3	0.125	g
fiber, total dietary	6.7	g	saturated fatty acids	2.13	g
total sugars	0.66	g	16:0	2.08	g
starch	0.11	g	18:0	0.05	g
<b>Vitamins and phytochemicals</b>			cholesterol	0	mg
vitamin A, RAE	7	µg	stigmasterol	2	mg
β-carotene	62	µg	campesterol	5	mg
α-carotene	24	µg	β-sitosterol	76	mg
β-cryptoxanthin	28	µg	<b>Minerals</b>		
Lutein + zeaxanthin	271	µg	calcium, Ca	12	mg
vitamin E (α-tocopherol)	2.07	mg	iron, Fe	0.55	mg
β-tocopherol	0.05	mg	potassium, K	485	mg
γ-tocopherol	0.33	mg	magnesium, Mg	29	mg
δ-tocopherol	0.02	mg	sodium, Na	7	mg
vitamin K (phylloquinone)	21	µg	phosphorus, P	52	mg
folate, total	81	µg	copper, Cu	0.19	mg
betaine	0.7	mg	zinc, Zn	0.64	mg
choline, total	14.2	mg	manganese, Mn	0.14	mg
niacin	1.74	mg	fluoride, F	7	µg
riboflavin	0.13	mg	selenium, Se	0.4	µg
thiamin	0.07	mg	<b>Carbohydrates</b>		
pantothenic acid (vit. B5)	1.39	mg	sucrose	0.06	g
vitamin B6	0.26	mg	glucose	0.37	g
vitamin C, ascorbic acid	10	mg	fructose	0.12	g

The avocado is commonly known as the "butter fruit" because of the high fat content of its mesocarp. The accumulation of oil in the pulp initiates a few weeks after fruit setting and persists throughout its growth and development until maturation (instead of carbohydrates and organic acids as in other fruits). The oil in avocado fruit is primarily stored as triacylglycerols, which are predominantly composed of monounsaturated fatty acids (MUFA) (oleic acid, 18:1n-9) with a low content of polyunsaturated fatty acids (PUFA) (linolenic acid, 18:2n-6) and saturated fatty acids (palmitic acid, 16:0). It also contains other fatty acids, such as stearic, myristic, and arachidonic acids at low levels. The ratio of unsaturated to saturated fatty acids is roughly 6:1 in avocados, although it can vary depending on several pre- and postharvest conditions, such as production location, cultivar, and environmental conditions [36–38].

Avocado pulp is also a rich source of potassium, vitamin B, vitamins C and E (antioxidants), and β-carotene. Luteolin, zeaxanthin, and phytosterols, mainly β-sitosterol followed by campesterol and stigmasterol, are also relevant. Avocado pulp contains high levels of both insoluble and soluble fiber (70% and 30%, respectively), along with a high protein content. In contrast, the sugar

content is low, mainly *D*-mannoheptulose and its reduced form, perseitol. These  $C_7$  sugars inhibit the ripening process, serve as transportable and storage sugars, and act as antioxidants in avocado flesh. Organic acids and amino acids are also part of the fruit matrix, although their metabolisms have been less studied. In addition to these substances, significant levels of other non-nutritive compounds such as pigments (anthocyanins, chlorophyll, etc.), alkanols, and phenolic substances are found in the avocado fruit, which contribute to fruit organoleptic properties and may also have potential benefits for human health [9,37,38]. The key health-promoting benefits attributed to this nutrient-dense fruit have been summarized in Figure 8.

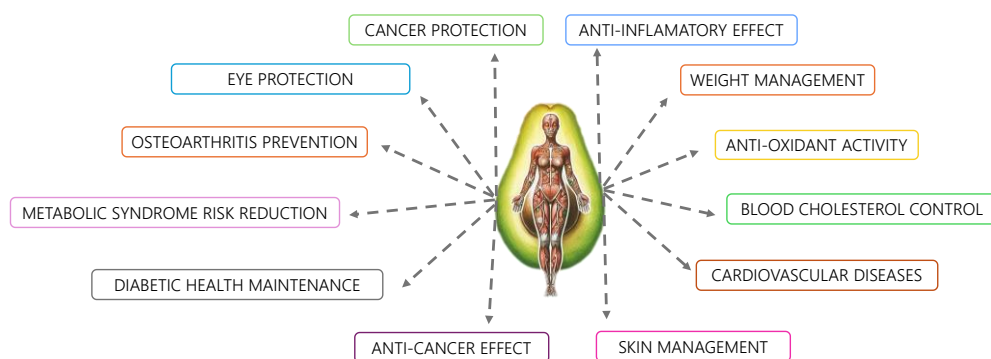


**Figure 8.** Health-promoting effects of avocado pulp consumption

Research on the health benefits of avocado consumption has grown alongside its increasing popularity. The first clinical study was conducted by Grant in 1960, who observed a reduction in total serum cholesterol [39]. Since then, several studies have proven that avocado consumption contributes to improved cholesterol levels, diabetes management, weight control, and prevention/treatment of several interrelated chronic conditions, including cardiovascular diseases [40–46]. The closest link between fat and these effects is the reason why they have been extensively explored, but avocado intake also has benefits for osteoarthritis management [47–49], metabolic syndrome risk control [50,51], eye health [52,53], anticancer/anti-inflammatory/anti-oxidant properties [54–58], or skin health [59–61]. The described health-related effects are not only associated with the fatty acids content (mainly MUFA), but also with fiber, vitamins B, C, E, and K, potassium, magnesium, carotenoids, phytosterols, and phenolic compounds, among others. In addition, oleic acid and water emulsions have been shown to increase carotenoid absorption from low-fat fruits and vegetables (e.g. salad) when consumed with avocados, thereby supporting secondary health and wellness [62]. Given the numerous health benefits, promoting a diet rich in avocados is advisable for maintaining overall well-being.

## 2. OLEA EUROPAEA L.

### 2.1. Origin, botanical classification, and cultivation of the olive tree

Since ancient times, the olive tree has played both a practical and symbolic role in the economy, health, religion, worship, and cuisine of Mediterranean inhabitants. Believed to be one of the earliest fruit trees cultivated by humans, it has been regarded as a divine gift since prehistoric times. Many civilizations have considered the olive tree as a symbol of peace, dignity, hope, prosperity, health, abundance, fertility, and wisdom. Beyond its nutritional value, the oil extracted from olive drupes and various by-products (wood, leaves, seeds, etc.) have also been used for heating, construction, lighting, medicinal applications, and cosmetics. Today, table olives and olive oil remain vital sectors in Mediterranean regions and are indispensable elements of the so-called Mediterranean diet, while some of the traditional uses are still maintained [63,64].

The geographical origin and domestication of the olive tree remain unclear. It is believed that its cultivation started around the fourth millennium B.C., with a primary domestication occurring in the Middle East (modern Turkey, Syria, Jordan, Lebanon, Palestine and Israel) around 6000 years ago. From this region, olive groves gradually spread throughout the Mediterranean basin, facilitated by the Phoenicians, Etruscans, Romans and Greeks. After the discovery of America in the 15<sup>th</sup> century, olive cultivation spread beyond the Mediterranean confines to the regions now occupied by countries such as Mexico, Argentina, California, and Chile. More recently, the olive tree has expanded far beyond its origins to southern Africa, Australia, Japan, and China [65,66].

The olive belongs to the family Oleaceae and the genus *Olea*, which is divided into three different subgenera: *Olea*, *Tetrapilus*, and *Paniculatae*. The subgenera *Olea* has been separated into two sections –*Olea* and *Ligustroides*– the first of which includes the complex of *Olea europaea* L. (popularly known as “The Olive Complex”), which comprises six subspecies. The subsp. *europaea* (diploid, 2x), found throughout the entire Mediterranean basin, is represented by two botanical varieties, including the cultivated olive (var. *europaea*) and the wild olive (var. *sylvestris*), commonly known as oleaster. Five additional non-cultivated subsp. have been described, although with some taxonomic discrepancies: subsp. *laperrini* (diploid, 2x) in the Saharan massifs, subsp. *cuspidata* (diploid, 2x) from southern Africa to southern Egypt and from Arabia to China, subsp. *guanchica* (diploid, 2x) in the Canary Islands, subsp. *maroccana* (polyploid, 6x) in southern Morocco, and subsp. *cerasiformis* (polyploid, 4x) in Madeira. All diploid forms are probably cross-compatible, whereas inter-subspecies hybrids involving polyploids have never been reported. The habitat of wild olives is limited compared to the extensive regions where cultivated olives are currently grown [63,67–69].

The most valued olives are the cultivated varieties, but their identification and classification is a highly complex task. There are about 2500 known olive varieties in the Mediterranean region, of which about 250 are recognized as commercial cultivars by the International Olive Council (IOC). These commercial cultivars are used to produce either olive oil, table olives, or both, depending

on pit size and fruit morphology. Detailed information on the main cultivated olive varieties is collected in the “*World catalogue of olive varieties*”, which includes comprehensive data on their morphological characteristics, synonyms, origin, distribution, agronomic performance, and commercial significance [70,71]. A brief summary of some relevant cultivars from the world’s major olive producers is presented in [Table 3](#).

**Table 3.** Some relevant olive cultivars and total numbers described from the world’s top producing countries (adapted from [71,72])

Country	No.	Cultivar name
Spain	262	<i>Picual, Cornicabra, Hojiblanca, Manzanilla de Sevilla, Arbequina, Morisca de Badajoz, Empeltre, Manzanilla Cacerena, Lechin de Sevilla, Picudo, Lechin de Granada, Verdial de Badajoz, Morrut, Sevillena, Villalonga, Castellana, Farga, Verdial de Huevar, Blanqueta, Gordal Sevillana, Verdial de Velez-Malaga, Aloreña, Changlot Real, Alfafara, etc.</i>
Greece	52	<i>Koroneiki, Kalamata, Mastoidis, Adramitini, Amigdalolia, Chalkidiki, Kalamon, Koservolia, Megaritiki, Valanolia, etc.</i>
Italy	538	<i>Coratina, Ogliarola Salentina, Cellina di Nardò, Carolea, Frantoio, Leccino, Ogliarola Barese, Moraiolo, Bosana, Cima di Mola, Dolce di Rossano, Ogliarola Messinese, Ottobratica, Sinopolese, Nocellara del Belice, Canino, Carboncella, Itrana, Moresca, Rotondella, Taggiasca, Tondina, Grossa di Gerace, Nocellara Etnea, etc.</i>
Turkey	80	<i>Ayvalik, Memecik, Gemlik, Uslu, Memeli, Gemlik, etc.</i>
Morocco	6	<i>Picholine Marocaine, Meslala, Menara, Houzia, etc.</i>
Portugal	24	<i>Galega Vulgar, Cobrançosa, Cordovil de Serpa, Carrasquenha, Cordovil de Castelo Branco, Redondal, etc.</i>

Olive cultivation is typically concentrated between latitudes 30° and 45° in both the northern and southern hemispheres, with Mediterranean-type climates characterized by mild and wet winters and hot and dry summers ([Figure 9](#)). There are currently about 11.0 Mha of olive groves that annually produce almost 21 Mt of olive fruit. Spain is the leading producer with about 8.3 Mt of fruit and 2.6 Mha of olive groves, followed by Greece (≈3.0 Mt), Italy (≈2.3 Mt), Turkey (≈1.7 Mt), Morocco (≈1.6 Mt) and Portugal (≈1.4 Mt). It is estimated that 90% of olive production is earmarked for oil extraction, while the remaining 10% is used for table olives. Accordingly, Spain leads the world olive oil production, contributing nearly 1.4 Mt annually out of a global production of 3.3 Mt. Indeed, Europe concentrates approximately 70% of the world’s olive oil production, with Italy (≈0.34 Mt), Greece (≈0.29 Mt) and Portugal (≈0.23 Mt) as the next leading producers [14,73].

Olive groves in Spain are cultivated in 15 of the 17 autonomous communities, predominantly in the central, southern and eastern regions of the peninsula. Andalusia, located in the south, is the heart of this economic activity, concentrating around 80% of the national production (≈6.6 Mt) and 61% of the olive growing area (≈1.6 Mha). The main production area is Jaen, but contributions also come from Cordoba, Seville, Almeria, Granada, Malaga, Cadiz, and Huelva. Other regions with significant but smaller production capacities include Castilla-La Mancha (≈8%), Extremadura (≈5%) and Cataluña (≈2%). The country is also the world’s largest exporter of olive oil (≈1.1Mt) with more than 150 destination countries and a favorable trade balance of 2,932.8 million euros [18,73,74].

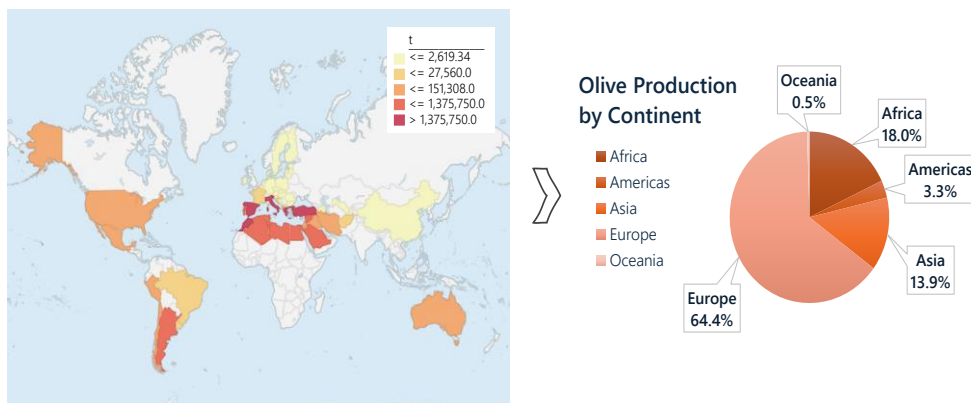


**Figure 9.** Map of olive production by country and percentage by continent (data from 2021 [14])

The significance of the olive sector in Spain is undeniable, not only because of its considerable economic importance, but also because of its social, environmental, and territorial impact. It generates employment and income in rural areas and contributes to the establishment of regions with high environmental and landscape value. More than 350,000 farmers are involved to olive growing in Spain, and the sector supports 15,000 jobs in the industry and generates more than 32 million daily wages per season [18,74].

## 2.2. Olive tree morphology, composition, and key metabolites

The cultivated olive (*Olea europaea* subsp. *europaea* var. *europaea*) is a broad evergreen tree of slow growth and remarkable longevity. It typically grows as a tree with a large, gnarled central trunk or as a multi-trunk, bush-like structure, with a height varying from 5-10 meters, up to 20 meters. Its small, thick, oppositely arranged leaves vary in shape from elliptic to lanceolate and obovate with 4-10 cm long and 1-3 cm wide. They are pale green on top and silver-white underneath. Flower buds are borne in the axil of each leaf and are yellowish-white in color. There are hundreds of flowers per twig (most bisexual), and each inflorescence contains 15-30 flowers of which only one or few will bear fruit. The root system is generally shallow, reaching 0.9-1.2 m even in deep soils. The olive fruit is a single-seeded drupe which range from green to blackish violet when ripe, and is 1-4 cm long and 0.5-2 cm in diameter. Fruit shapes vary from spherical to ellipsoidal or elongated with several degrees of asymmetry and rounded or pointed apex [75,76]. Wild olive subspecies tend to have smaller fruits (diameter generally <8 mm), with small fleshy mesocarp, and low oil content, resulting in lower commercial value compared to cultivated varieties [77]. **Figure 10** illustrates an example of an olive tree (a), flowers (b), and fruits (c).

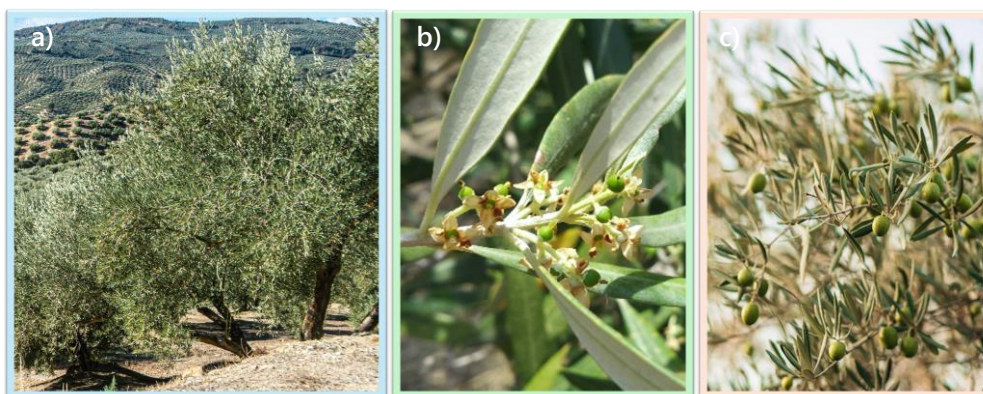


**Figure 10.** *Olea europaea*, L. (a) tree, (b) flowers, and (c) fruits

### 2.2.1. Olive fruit

The drupe consists of a pericarp and an endocarp and typically weights 2-12 g, with some varieties reaching up to 20 g (Figure 11). The pericarp is composed of the mesocarp or pulp (70-80% of the total weight), and the epicarp or skin (1-3% of the total drupe weight). The endocarp or stone accounts for 12-22% of drupe weight and contains the seed [70,78].

The chemical composition of olive fruit is primarily determined by genetic factors but also by climatic conditions, stage of maturity, cultivation practices, and geographical origin. The average chemical composition of the fruit includes water, which accounts for about 50-60% (w/w), followed by oil, which represents around 15-30%. Varieties with a lower oil content ( $\leq 12\%$ ) are used as table olives, while those with higher oil content are preferred for oil production. Sugars, mainly glucose and fructose, account for 3.5-6% and proteins represent a relatively low percentage (1.5-3.0%). Other relevant compounds present in olive fruit are cellulose (4-6%), inorganic substances (1-2%), phenolic compounds (1-3%), organic acids (1.2-2.1%), and pigments. The texture of olive pulp is determined by the composition of polysaccharides and pectic substances [70,78].

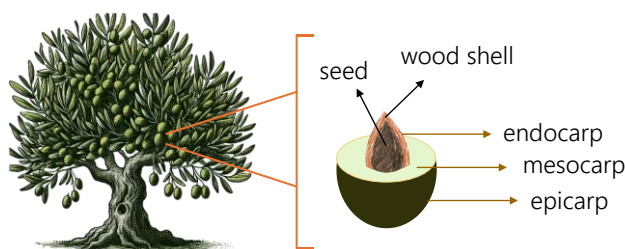


**Figure 11.** Scheme of the structural components of the olive fruit

### 2.2.2. Other olive tree matrices (leaves, stems, roots...)

Olive leaves are an important by-product of olive growing. Approximately, 25 kg (per tree) of twigs and leaves are collected each year from pruning olive trees, and a significant amount (about 5-10% of the fruit weight) is separated from the olives during oil extraction. Leaves are the primary site of plant metabolism at the level of both primary and secondary plant products [79]. The chemical composition of the leaf varies depending on the cultivar, agronomic conditions, tree age, and pruning period. The organic matter content is variable (89.1-94.9% of total dry weight), with a relatively low crude protein content (6.1-13.1%). Other components include crude fat (2.5%-9.6%) and neutral detergent fiber (32.5-55.7%), with lignin content standing out (15-17% of total dry weight) [80]. Much recognition has been given to phenolic compounds, which represent 1.5-6.4% of leaf dry matter and pentacyclic triterpenes (3.5-4.7%) [80,81]. Olive leaves are currently used in traditional herbal medicine and dietary products, in addition to animal feed [79].

Other tissues of *O. europaea* trees (e.g. stems or roots) comprise multiple specialized cell types (epidermis, guard cells, hairs, etc.), each of which has a specific metabolism to effectively perform its function. The primary function of stems is to support the plant and provide transport between its various organs, but they can also accumulate and assimilate different substances and have photosynthetic functions. Roots, on the other hand, anchor the plant to the ground, absorb water and mineral salts, and store substances. Both organs have been described as natural sources of phenolic compounds and pentacyclic triterpenes with interesting bioactivity in specific biological processes [82,83].

### 2.2.3. *Olea europaea* L. secondary metabolites

Secondary metabolites are biologically active compounds that are not directly involved in the basic functions of growth, development, and reproduction of the organism, but are considered essential for many adaptive roles, such as defense mechanisms or signaling molecules in ecological interactions, symbiosis, metal transport and competition, and other functions. These compounds are categorized into three main groups –phenolic compounds, terpenoids, and alkaloids– based on their biosynthetic pathways [84]. The first two groups have been investigated in this Thesis and will be further developed.

#### Phenolic compounds

Phenolic compounds are one of the largest and most prevalent groups of phytochemicals in the plant kingdom. They are synthesized from pentose phosphate, shikimate, and phenylpropanoid pathways in plants and play protective role against UV light and pathogens. These compounds are also important for the sensory properties of olives and have significant nutritional, physiological, and pharmaceutical effects on human health [78,85]. The main beneficial effects of the phenolic compounds of *Olea europaea* L. are illustrated in [Figure 12](#).

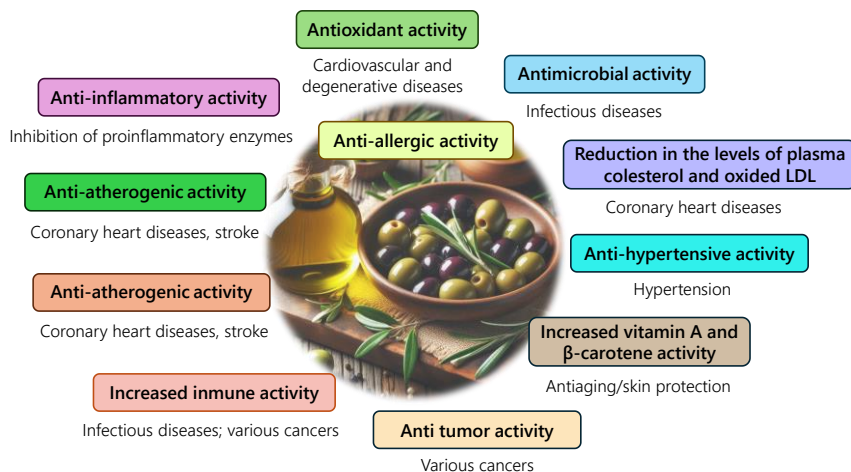


**Figure 12.** Biological activities and potential health-related benefits associated with olive phenolic compounds [70].

A wide variety of structures and functional groups are found within this chemical family, ranging from simple molecules to highly polymerized compounds. Natural phenols are commonly characterized by an aromatic ring with one or more hydroxyl substituents (including esters and glycosidic derivatives). Most of them are conjugated to sugar molecules (primarily glucose, but also rhamnose or others), although they can also be associated with other compounds, such as carboxylic acids, organic acids, amines, lipids, and other phenols [86].

Phenolic compounds can be classified based on their basic carbon skeleton and the type and number of substituents. Tables 4 and 5 outline the main subgroups described in olive matrices, which includes simple phenols, phenolic acids, flavonoids, coumarins, lignans, and secoiridoids [70,85,87]. Most of these compounds are found as glycosylated and aglycone forms.

**Table 4.** Phenolic classes found in *Olea europaea* L. with some examples

Compound name	Substituents	MW	Molecular structure
<b>Simple phenols</b>			
tyrosol	R <sub>1</sub> -H, R <sub>2</sub> -H	138	
hydroxytyrosol	R <sub>1</sub> -OH, R <sub>2</sub> -H	154	
hydroxytyrosol glucoside	R <sub>1</sub> -glucosyl, R <sub>2</sub> -H	316	
<b>Phenolic acids</b>			
<i>Benzoic acids and derivatives</i>			
4-hydroxybenzoic acid	4-OH	138	
vanillic acid	3-OCH <sub>3</sub> , 4-OH	168	
gallic acid	3,4,5-OH	170	
syringic acid	3,5-OCH <sub>3</sub> , 4-OH	198	
<i>Cinnamic acids and derivatives</i>			
<i>p</i> -coumaric	4-OH	164	
caffeic acid	3,4-OH	180	
ferulic acid	3-OCH <sub>3</sub> , 4-OH	194	
sinapic acid	3,5-OCH <sub>3</sub> , 4-OH	224	

Compound name	Substituents	MW	Molecular structure
<b>Flavonoids</b>			
apigenin	R <sub>1</sub> -H, R <sub>2</sub> -OH, R <sub>3</sub> -H	270	
luteolin	R <sub>1</sub> -H, R <sub>2</sub> -OH, R <sub>3</sub> -OH	286	
quercetin	R <sub>1</sub> -OH, R <sub>2</sub> -OH, R <sub>3</sub> -OH	302	
luteolin 7-glucoside	R <sub>1</sub> -H, R <sub>2</sub> -glucosyl, R <sub>3</sub> -OH	448	
apigenin 7-rutinoside	R <sub>1</sub> -H, R <sub>2</sub> -rutinosyl, R <sub>3</sub> -H	578	
rutin	R <sub>1</sub> -rutinosyl, R <sub>2</sub> -OH, R <sub>3</sub> -OH	610	
<b>Coumarins</b>			
aesculetin	R-H	178	
aesculin	R-glucosyl	340	
<b>Lignans</b>			
(+)-pinoresinol	R <sub>1</sub> -H, R <sub>2</sub> -H	358	
(+)-1-hydroxypinoresinol	R <sub>1</sub> -OH, R <sub>2</sub> -H	374	
(+)-1-acetoxypinoresinol	R <sub>1</sub> -OCOCH <sub>3</sub> , R <sub>2</sub> -H	416	
syringaresinol	R <sub>1</sub> -H, R <sub>2</sub> -OCH <sub>3</sub>	418	

Simple phenols consist of a single benzene ring (C<sub>6</sub>) with one or more hydroxyl groups. Phenolic acids, which have the same structure as simple phenols, have a carboxylic group among the substituents on the benzene ring. They are generally divided into benzoic acid derivatives (C<sub>6</sub>-C<sub>1</sub>) and hydroxycinnamic acid derivatives (C<sub>6</sub>-C<sub>3</sub>). Flavonoids are composed by two aromatic rings linked through a three-carbon chain, usually forming an oxygenated heterocycle. Coumarins consist of a benzene ring linked to a pyrone, whereas lignans are derived from two β-β'-linked phenylpropanoid subunits (C<sub>6</sub>-C<sub>3</sub>) [88].

**Table 5.** Characteristic structures of secoiridoids found in *Olea europaea* L.

Compound name	Substituents	MW	Molecular structure
<b>Secoiridoids</b>			
oleoside	R-H —	390	
secologanoside	R-H —	390	
comselogoside	R- <i>p</i> -coumaroyl —	536	
<i>Elenolic acid linked to phenyl ethyl alcohols</i>			
ligstroside	R <sub>1</sub> -glucosyl, R <sub>2</sub> -H	524	
ligstroside aglycone	R <sub>1</sub> -H, R <sub>2</sub> -H	362	
oleuropein	R <sub>1</sub> -glucosyl, R <sub>2</sub> -OH	540	
oleuropein aglycone	R <sub>1</sub> -H, R <sub>2</sub> -OH	378	
<i>Dialdehydic forms of secoiridoids</i>			
decarboxymethyl ligstroside aglycone or oleocanthal	R <sub>2</sub> -H	302	
decarboxymethyl oleuropein aglycone or oleacein	R <sub>2</sub> -OH	304	

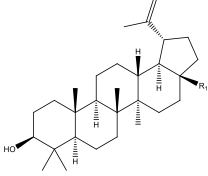
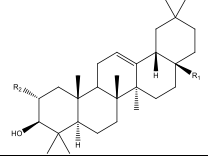
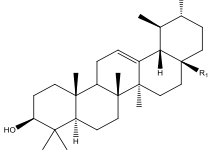
The most complex phenols are the secoiridoids, which are exclusively synthesized in plants of the *Oleaceae* family. They originate from the secondary metabolism of terpenes and are characterized by the presence of elenolic acid in its glycosidic or aglyconic form. The main glycoside in the olive fruit is oleuropein, which is converted to its aglycone by the  $\beta$ -glucosidase enzyme activity during fruit ripening and technological processing [83,87]. Table 5 lists some examples of secoiridoids reported in different olive matrices.

### ✚ Triterpenoids

Triterpenoids are structurally diverse group of natural products that are biosynthesized via the cytosolic acetate/mevalonate pathway. They are derived from squalene or related acyclic 30-carbon precursors and are composed of six  $C_5$  isoprene units. Most of triterpene skeletons are 6-6-6-5 tetracycles, 6-6-6-6-5 pentacycles, or 6-6-6-6-6 pentacycles types [89]. *Olea europaea* L. is a rich source of both bioactive pentacyclic triterpenoids and sterols. The latter, also known as phytosterols, are among the major components of the unsaponifiable fraction of olive oil [70].

Pentacyclic triterpenes are the predominant secondary metabolites in cuticle wax (leaves and fruits) and stem bark. They share a common skeleton of five 5- or 6- membered cycles substituted by different functional groups. Table 6 describes the three main groups, including acids, alcohols and dialcohol types.

**Table 6.** Triterpene characterizations and molecule structures [90]

Triterpene family	Triterpene	R <sub>1</sub>	R <sub>2</sub>	MW	Molecular structures
lupane	lupeol	CH <sub>3</sub>		426	
	betulin	CH <sub>2</sub> OH		442	
	betulinic acid	COOH		456	
oleanane	$\beta$ -amyrin	CH <sub>3</sub>	H	426	
	erythrodiol	CH <sub>2</sub> OH	H	442	
	oleanolic acid	COOH	H	456	
	maslinic acid	COOH	OH	472	
ursane	$\alpha$ -amyrin	CH <sub>3</sub>		426	
	uvaol	CH <sub>2</sub> OH		442	
	ursolic acid	COOH		456	

Pentacyclic triterpenes function as part of the plant's defense system, protecting against environmental stresses, assisting in wound and injury repair mechanisms, and enhancing resistance to plant pathogens (fungi, viruses, and bacteria) [82]. They also exhibit pharmacological properties such as antioxidant, hepatoprotective, gastroprotective, antiallergic, hypolipidemic, anticancer, antiatherosclerotic, anti-inflammatory, and antidiabetic effects [81,90].

The profile and concentration of pentacyclic triterpenes are influenced by the tissue type, olive variety, fruit development stage, and environmental conditions, etc. The total triterpenoid content in olive leaves (~25 mg/g dry weight) is higher than that in fruits or stems (~10 mg/g dry weight), with oleanane-type triterpenoids being predominant. Roots are the tissue with the lowest content (1-2 mg/g dry weight) [81,91].

### **2.3. Olive tree pathologies: Verticillium wilt**

The olive tree is affected by several diseases, of which Verticillium wilt of olive (VWO) is considered to be one of the most devastating biotic threats worldwide. Since it was first reported in Sicily (Italy) in 1946, it has spread to other European (e.g. Spain, France, Greece) and Asian countries, as well as to Australia, California, Syria, Morocco, and Argentina. Indeed, it has been detected in most regions where olives are grown. This disease results in substantial tree mortality and significant decreases in crop yields, presenting considerable challenges for agricultural producers, tree nurseries, and the olive oil industry. Currently, it stands as one of the primary limiting factors in olive oil production. Furthermore, the commercial value of virgin olive oil is adversely affected by VWO, as the infection disrupts the biosynthesis of critical volatile and phenolic compounds, thereby negatively impacting flavor and sensory quality [92–94].

#### **2.3.1. Pathogen life cycle and infection symptomatology**

VWO is caused by the soil-borne hemi-biotrophic fungus *Verticillium dahliae* Kleb., which can infect over 400 plant species. Its life cycle consists of two separated phases: (1) the parasitic phase, during which the fungus infects and lives in its host, and (2) the non-parasitic phase, during which it remains dormant (Figure 13). In the non-parasitic phase, the fungus survives in the soil as microsclerotia, which are resistant structures (even chemical tolerant) that allow it to persist for long periods without a host and under adverse conditions. These microsclerotia facilitate easy dispersal of the pathogen by wind, rain, irrigation water, human and animal activities, or various agricultural practices [95,96].

The parasitic phase begins when the resistant structures are stimulated to germinate by root exudates. The hyphae of germinating microsclerotia penetrate the host roots and colonize the root cortex. The hyphae then reach the xylem vessels, where conidia are formed. Vascular colonization occurs when conidia are transported upwards by the xylem fluid, leading to the deposition of aggregates resulting from fungal enzymatic activity and host defense reaction products, which partially block the xylem vessels. As a result, the vascular system becomes plugged, preventing water and nutrients from reaching the upper parts of the plant and causing symptoms. The main symptoms of VWO include wilting, foliar desiccation, early senescence, chlorosis, necrosis, stunting, xylem discoloration, vessel plugging (vascular congestion), and, eventually, the death of the infected tree. In a later stage of the parasitic phase, the pathogen forms microsclerotia in dead or dying tissues (mainly leaves, branches and herbaceous stems), which persist in the soil for a long time in the non-parasitic stage [97,98].

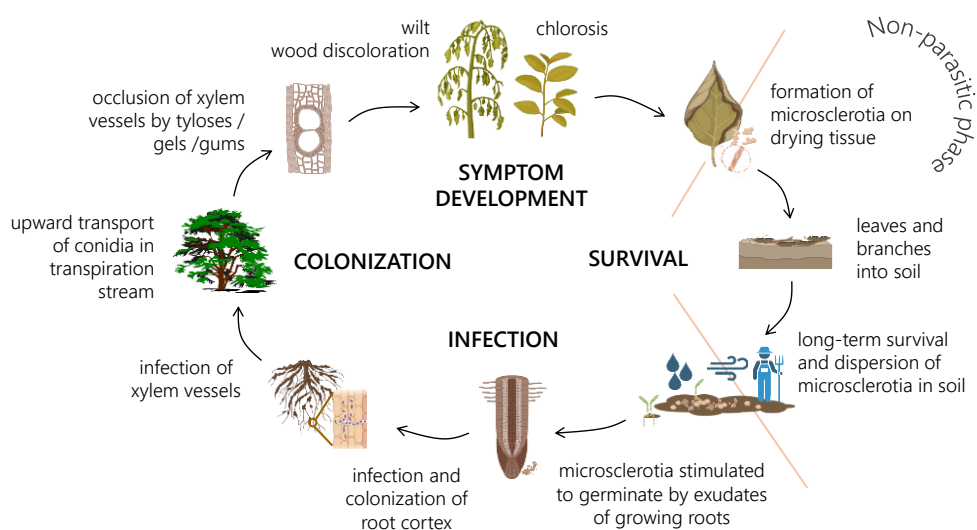


**Figure 13.** Schematic representation of the disease cycle of *Verticillium* wilt in trees (adapted from [97])

The severity of the attack depends on the virulence of the *V. dahliae* pathotypes infecting olive orchards, which are classified based on their virulence and symptoms as defoliating (D) (highly virulent) and not defoliating (ND) (less virulent) pathotypes. Additionally, two different syndromes ‘apoplexy’ and ‘slow decline’ could be observed depending on the season. The latter typically affects trees older than 20-25 years. The severity of symptoms is also influenced by soil inoculum density, environmental conditions, and host genotype. Remission of symptoms has been observed in cultivars infected with ND isolates. However, this disease requires close attention since the D pathotype gradually exceeds and spreads in most olive-growing regions in southern Spain [93,99,100].

### 2.3.2. Management of *Verticillium* wilt of olive disease

Effective control of VWO requires the implementation of an integrated management strategy, which includes the application of control measures both before and after planting. These actions are summarized in the following points [93,101]:

- ✓ **Preventive measures:** Use of tolerant/resistant olive varieties, use of non-infected soils and rootstocks, and the early and reliable detection of infection both *in planta* and soil.
- ✓ **Sustainable measures:** Effective management of irrigation systems, implementation of cultivation practices to prevent root damage, utilization of sanitized equipment, thermal treatments, application of endo-therapy (direct administration of active compounds into plant’s vascular system), and harnessing the potential of beneficial bacterial endophytes.

Since chemicals have no effect on the pathogen, the most recommended preventive measure is the use of VWO-resistant cultivars due to their long-term effectiveness, superior cost-efficiency, and environmental safety. In this context, the classification of olive cultivars based on their VWO susceptibility, from highly resistant to extremely susceptible genotypes, has been achieved. Despite these efforts, most of the resistant cultivars evaluated have negative agronomic traits that limit their commercial viability (e.g. *Frantoio*, *Empeltre* or *Changlot Real*). So far, no olive cultivar resistant to both isolates and with high agronomic profitability is known. The main Spanish cultivars *Picual*, *Cornicabra*, and *Hojiblanca* are susceptible or extremely susceptible to both pathogenic variants of *V. dahliae* [102,103].

#### **2.4. Genetic resources and olive breeding programs**

The diversity of cultivars in olive-growing countries represents significant genetic variability that is crucial for the breeding and future growth of olives. Consequently, the exploration, conservation, evaluation, and sustainable use of genetic resources have become a priority in many countries. As a first effort to categorize olive genetic resources, the Olive World Germplasm Bank (OWGB) of Spain was established in 1970 at the Alameda del Obispo farm of the National Institute for Agrarian Research in collaboration with the University of Cordoba. Over the years, this genetic repository continued to expand its accessions and was integrated into the Andalusian Institute of Agricultural and Fisheries Research (IFAPA), which took over its management in 2013. Two years later, the OWGB of Cordoba was recognized by the IOC as an International Bank of Reference of its Network of Germplasm Banks. To date, only three such international OWGBs, located in Córdoba (Spain), Marrakech (Morocco), and Izmir (Turkey) have been recognized by the IOC [104,105].

Olive breeding initiatives began later than those for other fruit species, with the first olive crossbreeding programs starting between 1960 and 1971 in Israel and Italy, respectively. Since the mid-1980s, additional olive breeding projects have been established in other countries around the world. In Spain, these initiatives began in 1991 [104,106]. Traditional breeding strategies include planned crosses between cultivars of known merit, progeny evaluation and selection, and cloning processes. The multi-stage strategy is time-consuming, but a thorough evaluation of the produced genotypes is essential to promptly discard undesirable crosses. In this regard, the breeding scheme and genotype selection criteria must be adapted to the financial and human resources of each program [107]. Until now, only a limited number of new olive cultivars have been registered. *Sikitita* was the first in Spain and is well adapted to high-density hedgerow planting. Other genotypes from Israel and Italy that have been commercially successful are *Barea* and *Fs-17* [108,109].

##### **2.4.1. Breeding objectives and selection criteria in olive cultivation**

Olive breeding programs target multiple objectives focused on the enhancement of both plant and agronomic traits. A primary focus is the reduction of the juvenile period, which represents a significant constraint in cross-breeding efforts, alongside decreasing pollinator dependency,

promoting precocious flowering, improving adaptation to mechanical harvesting, and increasing overall productivity [106,110,111]. Further objectives emphasize improvements in fruit characteristics, including size, flesh-to-pit ratio, and composition, as well as optimizing oil quality, particularly in terms of its stability and composition [112,113]. Considerable attention is also devoted to enhancing tolerance to abiotic stresses, such as environmental factors, and biotic stresses, including pathogens like bacteria and fungi [104,114,115]. Therefore, new sustainable progenies need to be evaluated from multiple perspectives to ensure that they can thrive in different climatic conditions and meet agricultural demands. The prioritization of olive breeding objectives in Spain has recently been evaluated (Table 7).

**Table 7.** Average score for olive breeding objectives in Spain by researchers and growers/managers (common scale from 0 to 10) [116]

Olive breeding objectives	Average	Olive breeding objectives	Average
<b>Plant traits</b>		<b>Pests' resistance</b>	
Easiness of pruning	3.3	Fruit fly	5.2
Early bearing	4.3	Prays	3.7
High productivity	9.9	<b>Resistance to diseases</b>	
Low biennial bearing	5.8	Peacock eye	4.2
Efficient harvesting	5.5	Verticillium wilt	7.4
<b>Flowering / fructification</b>		Anthracnose	3.4
High fruit set	3.6	Tuberculosis	3.6
High fruit size	2.3	Xylella fastidiosa	6.5
High oil content	7.2	<b>Tolerance to abiotic stresses</b>	
Early / late harvesting	4.3 / 0.0	Frost	3.8
<b>Oil</b>		Water stress	6.7
High stability	5.1	Water lodging	2.5
Improved oil composition	4.0	High temperatures	4.3
Organoleptic profile	5.4	Calcareous soils	2.9

While high and early yields are crucial traits, resistance to *V. dahliae* has emerged as a key criterion in modern olive breeding programs. Traditionally, breeders have focused on cultivated olives, overlooking the extensive genetic diversity provided by wild olives. Interestingly, wild olive germplasm is now being recognized for its resistance to fungal infection, suggesting a great potential as a rootstock or breeding parent [117,118].

Bioassay infection models and the monitoring of wilt symptoms over time are commonly employed for the selection of resistant olive cultivars. This approach is essential for olive growers and breeders, but it often falls short of elucidating which defense-related systemic responses are mainly involved in pathogen resistance. Plant defenses against pathogens encompass constitutive (or basal) and inducible protective mechanisms acting at the genomic, transcriptomic, and metabolomic levels. In this regard, constitutive defenses present prior to *V. dahliae* infection are associated with differences in physical traits (in particular root system architecture), genetic expression, and biochemical composition (basal lignin and phenolic contents in roots). Upon pathogen attack, the host plant activates a set of defense mechanisms to combat the infection. These include the activation of signaling pathway molecules such as reactive oxygen species,

induction of the antioxidant system, reinforcement by lignin and suberin deposition in roots, and induction of pathogenesis-related genes [101,119–121].

From a quality standpoint, selection criteria for olive oil cultivars mainly include oil content, fatty acid composition –especially oleic acid content– and phenolic profile. Equally important are sensory attributes of the oil, along with squalene, sterols, and tocopherols content. Notably, wild olives have been identified as valuable genetic resources for enhancing tocopherol content, despite their smaller size [122]. Fruit morphology and phenolic composition are essential quality traits for processed table olives. In addition, triterpenic acids and sugar content should also be evaluated in the raw fruit of progenies [109,123,124].

### 3. METABOLOMICS APPLIED TO FOOD ANALYSIS

The concurrent development of the Human Genome Project in the late 20<sup>th</sup> century catalyzed substantial transformations in fields such as Molecular Biology and Biochemistry, leading to the emergence of various techniques and methodologies collectively referred to as omics sciences. The term “omics” is derived from the Greek root “ome”, referring to completeness or totality. In this context, the hallmark of omics technologies lies in their holistic capability to comprehensively analyze cells, fluids, tissues, or entire organisms [125,126].

Although numerous disciplines have emerged from the suffix -omics (foodomics, lipidomics, interactomics, ecotoxicogenomics, epigenomics, etc.), four interrelated omics areas of study are primary considered (Figure 14). The era of omics began with genomics, which involves the complete study of the DNA, followed by transcriptomics, which analyzes gene expression (total RNA). Proteomics focuses on the characterization, quantification, and evaluation of protein interactions, while metabolomics takes a large-scale approach to assess the compounds involved in cellular processes, providing metabolic profiles in a single assay. With the advent of metabolomics, the physiological flow of biological information –from gene expression to protein synthesis and metabolites changes– was successfully completed [126,127].

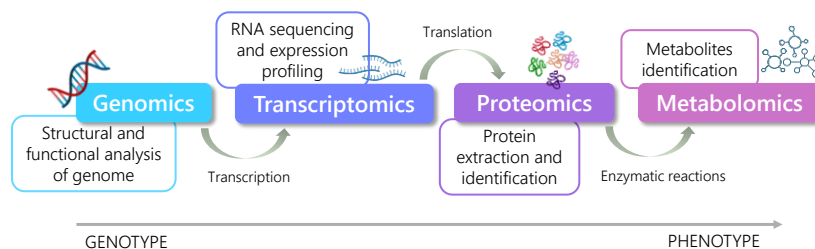


**Figure 14.** Interrelationship among the omics used in systems biology studies

To this extent, the integrative approach of metabolomics with genomics, transcriptomics, and proteomics sciences significantly enhances our understanding of complex molecular interactions within biological systems. Metabolomics is particularly linked to phenotypic expression. This interdisciplinary science not only leverages cutting-edge analytical chemistry techniques but also requires expertise in organic chemistry, chemometrics, advanced computational methods, and other related disciplines. Unlike the other omics sciences, which often rely on a single instrument for measurement, metabolomics demands a diverse array of instrumentation. While this presents technical challenges, it also offers unique insights into metabolic pathways and dynamic biological processes, making metabolomics an invaluable component of systems biology [128,129].

#### 3.1. Terminology and metabolomics strategies

Over the years, several definitions of metabolomics have emerged in the literature. One of the earliest definitions was proposed by Oliver Fiehn in 2001, describing metabolomics as “a

comprehensive and quantitative analysis of all the metabolites of a biological system under study” [130]. Prior to this definition, Nicholson et al. (1999), introduced the term “metabonomics” to refer to the “quantitative measurement of the dynamic multiparametric metabolic response of living systems to pathophysiological stimuli or genetic modifications” [131]. While the two terms have slight differences in focus, they are now used interchangeably and are largely viewed as a historical distinction rather than separate or different disciplines.

Some authors consider it more appropriate to define metabolomics as “the characterization of metabolic phenotypes (the metabolome) under specific conditions (i.e. developmental stages, environmental conditions, genetic modifications) and the association of these phenotypes with their corresponding genotypes” [132]. The term metabolome was introduced by Stephen G. Oliver and co-workers in 1998 and represents the set of low-molecular weight molecules (typically <1,500 Da) present in biological cells, tissues, fluids, organs, or organisms, resulting from a dynamic and interconnected network of biochemical pathways and metabolic reactions occurring within a biological system. The wide range of molecules detectable in the metabolome includes amino acids, peptides, lipids, nucleic acids, carbohydrates, organic acids, vitamins, alkaloids, and phenolic compounds. A single biological specimen contains extensive physicochemical diversity (polarity acidity, volatility, etc.) and these metabolites are found in a wide dynamic range of concentrations, making it challenging to simultaneously analyze such a broad spectrum of compounds [127,133].

More specific terminologies have emerged to define and classify the various types of metabolomics studies. The following four terms represent the most commonly used approaches, categorized by the depth of metabolome exploration (Figure 15) [134,135].

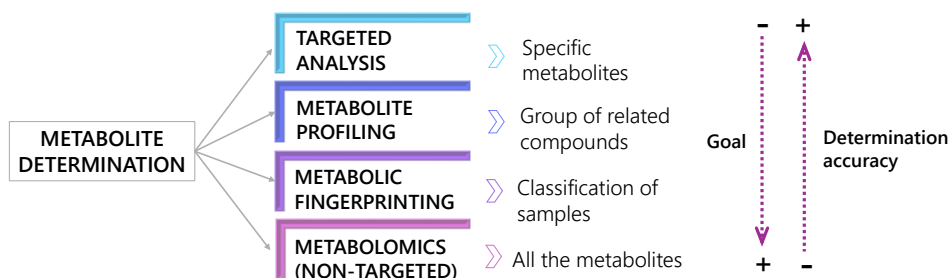


Figure 15. Most common approaches used in metabolomics studies

- i. **Metabolite targeted analysis:** It is restricted to the detection and quantification of a single and small group of metabolites.
- ii. **Metabolic profiling:** It focuses on the qualitative and quantitative analysis of a related group of metabolites (e.g. lipids, polar compounds, etc.) or those associated with a specific pathway.

- iii. **Metabolic fingerprinting:** It involves the rapid screening of the entire metabolic composition but does not provide detailed information about specific metabolites; instead, it classifies samples based on biological relevance, origin, or class.
- iv. **Metabolomics (non-targeted):** It is a comprehensive analysis of the entire metabolome (all measurable metabolites) under a given set of conditions.

A simpler categorization is based primarily on the study objective (discovery vs. hypothesis testing) and method validation requirements. A non-targeted metabolomics approach is hypothesis-generating and allows a full scanning of the metabolome (includes metabolic fingerprinting and metabolomics). In contrast, a targeted metabolomics approach is hypothesis-testing and focuses on pre-known metabolites. This approach is typically performed for the validation of non-targeted analyses and includes targeted analysis and metabolic profiling strategies [136]. Additionally, an intermediate-term “semi-quantitative” metabolomics has also been employed in the literature when the hypothesis is often undefined, but the list of metabolites is predefined and tentatively identified.

### 3.2. Metabolomics workflow

There is no one-size-fits-all workflow for metabolomics strategies, as each approach is distinct. Generally, the process involves several sequential steps, starting with the formulation of the biological question. This is followed by experimental design, sample collection and preparation, data acquisition and processing, and ultimately, the interpretation of results. The general workflow is graphically represented in Figure 16. While not every step is required in every study, detection and data analysis are essential in all metabolomics studies.

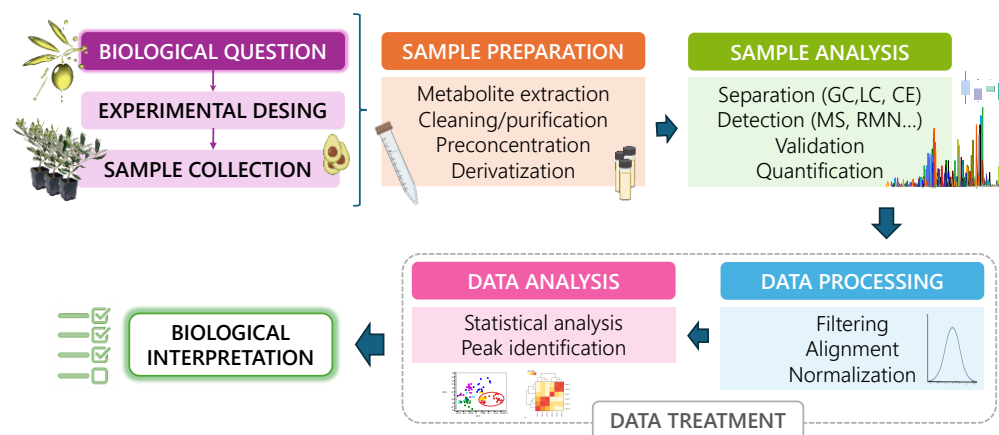


Figure 16. General analytical workflow of metabolomics studies

- ✓ **Identification of the problem to be addressed, experimental design, and sampling**

The first step in metabolomics research involves a clear and straightforward identification of the biological or agri-food or any other problem to be addressed. Depending on the question,

the experimental design is tailored to select the most suitable metabolomics approach and analytical platform, as well as to determine the appropriate sample type and size (ensuring representativeness), experimental conditions, sample collection frequency, and storage conditions. This phase is crucial for ensuring the robustness and reproducibility of the results by incorporating appropriate controls and replicates. Once the experimental design has been clearly established, sample collection and management must be conducted under controlled conditions to minimize variability among the samples. Metabolic quenching to interrupt enzymatic activity (e.g. snap-freezing in liquid nitrogen, immediate freezing with dry-ice or the use of organic solvents) are essential to halt enzymatic activity and preserve heat-labile components. Sample preservation methods, including freeze-drying, oven-drying, or air-drying, are equally important. For long-term storage, biological samples are typically recommended to be stored at  $-80^{\circ}\text{C}$ , particularly for biofluids. Additionally, grinding, particle size reduction, and homogenization of solid matrices are necessary to enhance the release of metabolites during sample extraction [137,138].

#### ✓ **Sample preparation and analysis**

The next step is sample preparation, which aims at generating suitable extracts that are suitable for instrumental analysis. This is a critical stage in metabolomics studies, as the validity of conclusions relies heavily on effective sample preparation. While not every step is always necessary, sample preparation may include metabolite extraction, cleaning, purification, derivatization, and pre-concentration processes. The extraction procedure depends on the study's objective (targeted or untargeted) and sample characteristics. Typically, this involves optimizing type of extraction to be applied, extractant solvent ratios (pure solvents or mixtures), time, and temperature, followed by centrifugation and filtration. In targeted metabolomics, a cleanup step is often added to remove sample matrix interferences, and pre-concentration strategies can be applied if required. In contrast, non-targeted approaches generally utilize a more unselective, simpler, and faster extraction method. Gas chromatography analysis frequently requires a derivatization step aimed at enhancing metabolite volatility [137,139].

The most commonly used analytical techniques in plant and food metabolomics are nuclear magnetic resonance (NMR) and mass spectrometry (MS) in combination with liquid chromatography and gas chromatography (LC-MS and GC-MS). Notably, hyphenated techniques offer improved resolution and metabolite identification capabilities [140]. The choice of the analytical platform largely depends on the specific chemical classes of metabolites of interest and the study's objectives. Each platform has its own limitations that must be carefully considered during the experimental design and sample preparation phases. Key factors to balance include the sensitivity and selectivity of the analytical platform, as well as the required analysis time. [Figure 17](#) presents the main advantages and disadvantages of the analytical technique used in this thesis (LC-MS).

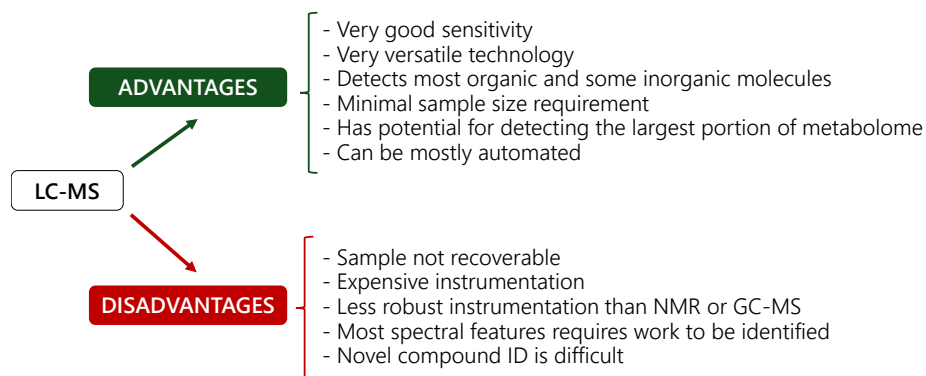


**Figure 17.** Main advantages and disadvantages of LC-MS [129,141]

Ion mobility spectrometry (IMS) coupled to MS is increasingly being used in metabolomics. IMS is a gas-electrophoretic technique capable of separating ions in the gas phase under electric fields influence, differentiating them based on their structural features—mass, size and shape— and charge. This technology allows for the separation of isomers, isobars and conformers. IMS-MS improves resolution and specificity in the analysis of complex food matrices by adding an extra data dimension. The collision cross-section (CCS) value, derived from ion mobility measurements, serves as an additional molecular descriptor to characterize compounds within the metabolome. However, a challenge associated with IMS technology is the need for improved CCS databases and more accessible *in-silico* CCS prediction tools. Despite this, IMS-MS holds significant promise for advancing our understanding of the molecular composition of foods [142,143].

At this stage, validating the method is crucial to ensure that the analytical procedure used is appropriate for its intended purpose. This process typically involves assessing several key parameters: accuracy (which encompasses trueness and precision -both repeatability and reproducibility-), specificity (considering impurities and matrix effects), limits of detection (LOD) and quantification (LOQ), as well as linearity and the linear dynamic range. Accurate metabolite quantification is achieved using either external or internal standards. In non-targeted approaches, quality control samples (composed of a pool of test samples) are commonly used to validate the analytical methodology. The quality of instrumental analysis is often confirmed through statistical tools [144].

#### ✓ **Data treatment and results interpretation**

Data treatment includes both data pre-processing and analysis. Pre-processing is required to convert raw data into an analyzable and comparable format. In hyphenated MS techniques, this includes peak picking, detection and deconvolution, alignment, background spectra filtering (e.g. noise reduction), peak normalization, and chromatogram alignment. The subsequent steps depend on the specific scientific question. Data normalization methods are required to remove unwanted variations between samples and facilitate quantitative comparisons. Moreover,

centering, scaling, and data transformation methods are used as data pretreatment prior to statistical analysis. A range of commercially available and open-source bioinformatics tools can automate data processing, evaluation, and even relative quantification [136,145].

Despite the complexity of most metabolomics datasets, chemometric tools offer effective solutions for data analysis. Multivariate statistical analysis, which examines many variables simultaneously, is frequently employed for sample overview and classification. These strategies may be unsupervised (e.g. principal component analysis (PCA) or hierarchical cluster analysis (HCA)) or supervised (e.g. partial least squares discriminant analysis (PLS-DA), orthogonal PLS-DA (OPLS-DA), etc.). Supervised methods are widely used in non-targeted metabolomics for (bio)marker discovery, typically followed by a labor-intensive metabolite identification process. All those statistical models must be carefully validated to ensure the accuracy of the results. Conversely, univariate analysis (e.g. t-test, analysis of variance (ANOVA)) generally does not require data normalization or pretreatment, as each metabolic feature is evaluated separately. Univariate statistical methods assess variations in individual variables and evaluate their statistical significance across samples or groups [145,146].

At the final step, biological interpretation requires translating the processed data into meaningful insights that address the research objectives. After identifying significant metabolites –at least tentatively– the next step is to explore their associated biological pathways, which aids in addressing the original research question [137].

### **3.3. Main application fields of metabolomics**

The remarkable versatility of metabolomics has enabled its application across a wide range of fields. Until recently, most metabolomics research has focused on pharmaceutical and clinical applications (e.g. drug discovery, drug assessment, clinical toxicology and clinical chemistry). However, in recent years, metabolomics has expanded into numerous other areas, such as plant biotechnology (e.g. plant cell physiology, plant-pathogen interactions), environmental toxicology (e.g. exposure to chemical pollutants), microbiology (e.g. microbial interactions and cellular functions), veterinary and animal health (e.g. monitoring drug residues in food-producing animals), food chemistry (e.g. fermentation monitoring, ripening, and postharvest storage), and nutrition research (e.g. studying food composition and the effects of consumption) [129,141,147]. More detailed applications are summarized in [Figure 18](#).

Plant metabolomics has been applied not only to study the metabolic profiles of different crops or medicinal plants but also to delve into plant physiology and biology-related aspects. This research encompasses the study of complex biological pathways and regulatory networks involved in plant growth and development, as well as the metabolic responses of plants to biotic (heat, cold, drought, salinity, etc.) and abiotic (fungi, bacteria, viruses, pests, etc.) stresses. Additional applications include examining plant-insect interactions, mycorrhizal relationships, and identifying metabolic differences between wild, domesticated and transgenic plants. Metabolomics plays a

crucial role in discovering valuable plant-derived natural metabolites for the development of novel drugs and food supplements in the pharmaceutical industry or biocides (e.g. fungicides and insecticides) in agriculture. Beyond enhancing crop quality and commercial value (physical properties, shelf life, etc.), the characterization of metabolic profiles in plant tissues (including seeds, fruits, peels, leaves, etc.) also provides essential insights for the industrial use of plant by-products (fibers, polymers, biomass, fuels, cosmetics, etc.) [138,148,149].

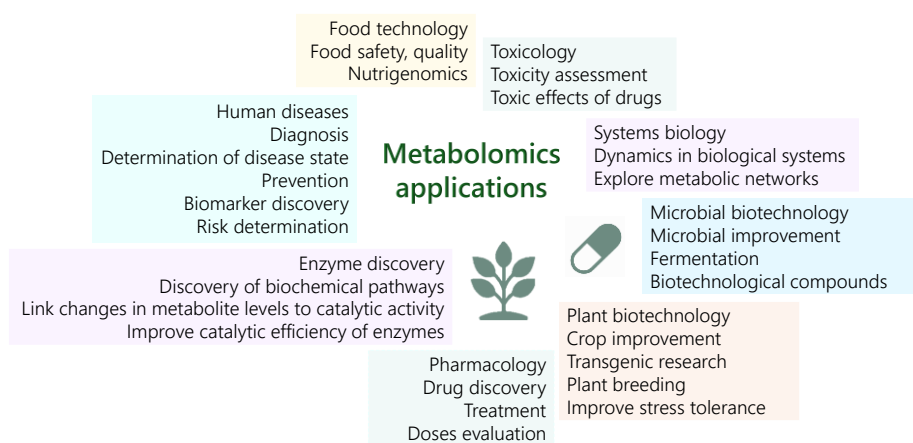


**Figure 18.** Main application fields of metabolomics (adapted from [150])

There is a direct connection between plant and food metabolomics, given that fruits, vegetables and plant-based products constitute a significant proportion of the human diet. These foods are estimated to contain over 15,000 compounds from more than 100 chemical classes at varying concentrations. Through the study of food constituents, specialists in food and nutrition explore the interactions between food and the human body to correlate them with consumer benefits. This focus has led to the emergence of the term “foodomics”, defined as “the comprehensive, high-throughput approach for the exploitation of food science to improve human health and well-being” [151,152].

Overall, food and nutrition metabolomics encompasses many aspects of molecular nutrition, including: (i) food component analysis, (ii) food quality, safety and authenticity detection, (iii) food consumption monitoring, and (iv) health-diet intervention studies [141]. The latter two areas are particularly interrelated and can be grouped under nutrition and dietary health research.

### **i. Food component analysis**

Traditional approaches to food composition have primarily focused on the analysis of macro- (proteins, carbohydrates and fats) and micronutrients (vitamins and minerals). However, the advent of modern metabolomics technologies has transformed this process, allowing for comprehensive analysis that rapidly detects a wide array of both nutritive and non-nutritive metabolites in a single run. These metabolites are not only related to nutritional value but also to valuable organoleptic

properties, such as texture, aroma, flavor, taste, and physical appearance. Beyond understanding the final composition of food, it is crucial to assess compositional changes that occur during processing and storage within the industry. Metabolomics techniques enable the monitoring of these alterations during fermentation and help food scientists identify optimal preservation methods (such as heat treatment, drying, freezing, smoking processes, etc.) as well as preparation techniques (e.g. frying, boiling, baking, etc.), all of which aim to minimize impacts on food composition. Moreover, effectively managing the ripening physiology and optimizing food storage conditions are critical for maintaining food quality [141,153,154].

#### **i. Food quality and authenticity detection**

Ensuring food quality involves adhering to industry-specific standards and meeting consumer expectations. Most quality parameters are often related to sensory attributes, nutritional value, and product shelf life, all of which can be evaluated through metabolomics, including analyses of, for instance, phenolic compounds, organic acids, volatile substances, and macro- and micronutrients. Food safety is central to quality assurance, and metabolomics analysis facilitates the detection of chemical compounds and microbial contamination in both fresh and processed food. This includes identifying toxins, hormones, residues of pesticides and surfactants, spoilage reactions, drug residues, and bacterial presence. Other safety concerns encompass allergens and synthetic food additives. Metabolomics has also been applied to identify food adulteration, classify food products, verify food origins, and enhance food traceability. By leveraging characteristic metabolic profiles and concentration levels of specific compounds (such as fatty acids, organic acids, etc.), researchers can compare suspect products with target foods to detect fraud within the food industry [139,154,155].

#### **i. Nutrition and dietary health studies**

The advancement of nutrition and dietary health studies is significantly enhanced by metabolomics-based food consumption monitoring. By comprehensively analyzing the vast array of metabolites present in human biofluids or tissues, researchers can effectively characterize body deficiencies or excesses of nutrients and identify biomarkers indicative of dietary intake and the metabolic pathways involved in nutrient metabolism. This approach facilitates the identification of dietary patterns associated with several health outcomes (e.g. obesity, diabetes, chronic inflammation, cardiovascular diseases, etc.). Furthermore, monitoring biochemical responses to long-term or short-term dietary or lifestyle interventions enables the development of personalized nutritional strategies tailored to individual needs. These beneficial aspects are often supported by bioactivity assays, and both *in-vitro* and *in-vivo* analyses [141,152].

### **3.4. Metabolomics-based research on the matrices under investigation**

This subsection aims to identify key research areas in which plant and food metabolomics have significantly contributed to the study of the matrices investigated in this Thesis. Rather than providing an exhaustive review of the existing literature, it focuses on the main lines of

investigation pursued in recent years, accompanied by a selection of relevant applications in these areas.

### 3.4.1. Metabolomics applied to the study of avocado fruit

Both targeted and non-targeted metabolomics, along with fingerprinting methods, have been applied to evaluate several aspects related to the phytochemical profile of the avocado. The main applications of metabolomics can be categorized into three major areas, as shown in Figure 19: (i) characterization and authentication purposes, (ii) agro-technological and industrial studies, and (iii) investigation of nutritional and health benefits.



**Figure 19.** Relevant areas in which food metabolomics contributes to the avocado sector

The comprehensive analysis of avocados initially focused on the edible pulp using LC-MS metabolic profiling, identifying several metabolites such as sugars, phenolic compounds, amino acids, vitamins, etc. [156]. Subsequent research has expanded to thoroughly characterize the main avocado by-products (seeds and peels), which are produced in significant industrial quantities [157–159]. The in-depth examination of avocado's unique composition has enabled its use in authentication applications. Metabolic profiling approaches have allowed the differentiation of avocado varieties [160,161] and assessed the influence of geographical origin on the fruit's final composition [162,163].

Beyond detailing avocado's phytochemical composition, metabolomics has been used for several agro-technological and industrial applications. Many studies have evaluated pre- and postharvest physiological processes, particularly metabolic changes during fruit maturation and ripening [36,164–166], and the correlation of physiological disorders with specific bioactive compounds [167,168]. Metabolomics has also facilitated the valorization of avocado by-products; peels and seeds are repurposed for functional food products, pharmaceuticals or cosmetics because of their valuable bioactive composition [8]. They can also be used to produce activated carbons for contaminant removal [169] or to extract natural pigments from seeds [170]. Avocado leaf waste may also be used in herbal tea production [171].

Metabolomics also strongly supports the search for specific metabolites for disease prevention and treatment. A recent review has summarized the biological activities of some specific bioactive metabolites (fatty alcohols, phenolic compounds, carotenoids, carbohydrates, furans, etc.) isolated from various parts of *P. americana* [172]. Targeted metabolomic studies have analyzed individual phenolic compounds (e.g. catechin, epicatechin or (neo)chlorogenic acid) and linked them to

antioxidant, neuroprotective or antimicrobial activities [173,174]. Dietary interventions have also been supported by metabolomics. For instance, studies have investigated the metabolic biomarkers of avocado consumption in relation to glycaemia [175] and intestinal microbiota [176]. Other studies applying metabolomics-based approaches have focused on exploring the bioavailability of avocado metabolites through *in-vitro* and *in-vivo* assays [177,178].

### 3.4.2. Metabolomics applied to the study of olive-related matrices

The body of metabolomics studies focused on olive tree-related matrices and their health impacts is extensive and diverse. Generally, the main application areas closely align with those described in avocado research, although there are some differences, as shown in Figure 20.

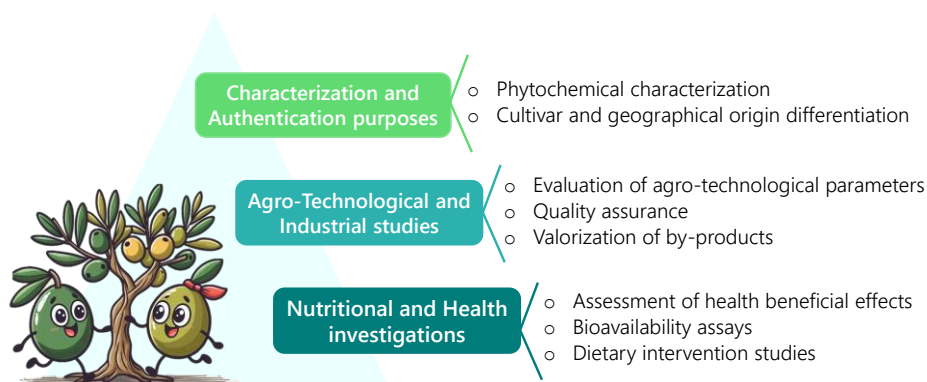


**Figure 20.** Key areas in which food metabolomics contributes to the olive sector

Over the last decades, metabolic characterization studies have extensively explored olive tree derived products, mainly olive oil and table olives [179–181]. This research has expanded to investigate phytochemicals in various parts of olive trees (e.g. leaves, bark, stems, roots, etc.) [182–184], and numerous olive by-products (e.g. seeds, olive seed oil, olive pomace, olive mill water, etc.) [180,185]. Additionally, several researchers have also addressed authenticity concerns in olive oil, particularly regarding varietal and geographical origin discrimination. For instance, phenolic profiling has been effective in distinguishing virgin olive oils from Northern Morocco [186] and in classifying olives according to variety [187]. Furthermore, different non-targeted approaches have been used to differentiate extra virgin olive oils from six protected geographical indications [188] and to discriminate oils based on cultivar and geographical origin [189].

Concerning agro-technological and industrial studies, metabolomics has become a pivotal tool for assessing the impact of different agricultural practices [190–192] and processing methods [193–195] on the final product. It has also been used to detect markers associated with several olive diseases [196,197]. These parameters directly influence olive yield, quality, and crop sustainability, requiring careful evaluation. Besides, non-targeted metabolomics approaches have been employed to detect olive oil adulteration [198]. Metabolomic tools are increasingly being

harnessed to drive innovation in the olive sector, particularly in the valorization of by-products because of their value-added components [199–201].

Increasing attention has been directed toward the health benefits associated with olive bioactive compounds, particularly phenolic compounds, as noted earlier. These beneficial effects are typically validated through bioavailability assays that investigate their absorption, metabolism and excretion in the organism via both *in-vitro* (gastrointestinal digestion, cell culture, etc.) [202–204] and *in-vivo* (human or animals) studies [205,206]. With advancements in metabolomics, research on dietary interventions has gained popularity. For instance, metabolomics has been used to study the impact of long-term olive oil consumption and the effect of consuming olive pomace-enriched biscuits on the gut microbiota [207,208].

#### 4. REFERENCES

1. Knight, R.J. Jr. History, Distribution and Uses. In *The avocado: botany, production and uses*; Schaffer, B., Wolstenholme, B.N., Wiley, A.W., Eds.; CABI Publishing, 2002; pp. 1–14, doi:10.1079/9780851993577.0001.
2. Smith, C.E. Archeological Evidence for Selection in Avocado. *Econ. Bot.* **1966**, *20*, 169–175, doi:10.1007/BF02904012.
3. Barrientos-Priego, A.F.; López-López, L. Historia Y Genética Del Aguacate. In *El aguacate y su manejo integrado*; Télizd, D., Ed.; Mundi-Prensa: Mexico, 2000; pp. 33–51.
4. Scora, R.W.; Wolstenholme, B.N.; Lavi, U. Taxonomy and Botany. In *The avocado: botany, production and uses*; Schaffer, B., Wolstenholme, B.N., Wiley, A.W., Eds.; CABI Publishing, 2002; pp. 15–37, doi:10.1079/9780851993577.0015.
5. The United States Agency for International Development Avocado Production Manual (Persea Americana L.) Available online: <https://www.feedthefuture.gov> (accessed on 14 May 2024).
6. Diaz Diez, C.A.; Bernal Estrada, J.A. Generalidades Del Cultivo. In *Tecnología para el Cultivo del Aguacate*; Diaz Diez, C.A., Bernal Estrada, J.A., Eds.; Corporación colombiana de investigación agropecuaria - CORPOICA, 2005; pp. 11–83 ISBN 978-958-8311-74-6.
7. Alcaraz, M.L.; Hormaza, J.I. Optimization of Controlled Pollination in Avocado (Persea Americana Mill., Lauraceae). *Sci. Hortic.* **2014**, *79–85*, doi:10.1016/j.scienta.2014.10.022.
8. Salazar-López, N.J.; Domínguez-Avila, J.A.; Yahia, E.M.; Belmonte-Herrera, B.H.; Wall-Medrano, A.; Montalvo-González, E.; González-Aguilar, G.A. Avocado Fruit and By-Products as Potential Sources of Bioactive Compounds. *Food Res. Int.* **2020**, *138*, doi:10.1016/j.foodres.2020.109774.
9. Talavera, A.; Gonzalez-Fernandez, J.J.; Carrasco-Pancorbo, A.; Olmo-García, L.; Hormaza, J.. Avocado: Agricultural Importance and Nutraceutical Properties. In *Compendium of Crop Genome Designing for Nutraceuticals*; Kole, C., Ed.; Springer Singapore, 2023; pp. 1–19, doi:10.1007/978-981-19-3627-2\_40-1.
10. Paull, R.E.; Duarte, O. Avocado. In *Tropical fruits*; Paull, R. E. Duarte, O., Ed.; CABI Digital Library, 2010; Vol. 1, pp. 153–184, doi:10.1079/9781845936723.0153-3.
11. Bernal, J.A.; Díaz, C.A.; (Comps.) *Actualización Tecnológica y Buenas Prácticas Agrícolas (BPA) En El Cultivo de Aguacate*; Bernal Estrada, J.A., Díaz Díez, C.A., Eds.; 2nd Ed.; AGROSAVIA, 2020; ISBN 978-958-740-384-8.
12. Lahav, E.; Lavi, U. Avocado Genetics and Breeding. In *Breeding plantation tree crops: Tropical Species*; Jain, S.M., Priyadarshan, P.M., Eds.; Springer: New York, 2009; pp. 247–285, doi: 10.1007/978-0-387-71201-7\_8.
13. Wood, W. Avocado Cultivars. *South African Avocado Grow. Assoc. Yearb.* **1984**, *7*, 10–14.
14. FAO. Statistics Division of Food and Agriculture Organization of the United Nations (FAOSTAT). Available online: <https://www.fao.org/faostat/en/#data> (accessed on 10 May 2024).
15. Sommaruga, R.; Eldridge, H.M. Avocado Production: Water Footprint and Socio-Economic Implications. *EuroChoices* **2021**, 1–5, doi:10.1111/1746-692X.12289.
16. Organization for Economic Co-operation and Development; Food and Agriculture Organization of the United Nations *OECD-FAO Perspectivas Agrícolas 2021-2030*; OECD/FAO, 2021; ISBN 978-92-64-81384-7.
17. Colilles-Cascallar, E. El Aguacate En La Península Ibérica. In *Cultivo, poscosecha y procesado del aguacate*; Nmensy, A., Conesa, C., Hormaza, I., Lobo, G., Eds.; Biblioteca horticultura, 2021; pp. 19–26 ISBN 978-84-160931-5.
18. Ministerio de Agricultura, Pesca y Alimentación Anuario de Estadística. Superficies y Producciones de

- Cultivos Available online: <https://www.mapa.gob.es/es/estadistica> (accessed on 13 May 2024).
19. Market Intelligence Team. *2021 Industry Report: Avocado*; May 2021.
  20. Seelige, K. *Avocado in Europe. Practical Market Insights into Your Product*; May 2021.
  21. Pedreschi, R.; Ponce, E.; Hernández, I.; Fuentealba, C.; Urbina, A.; González-Fernández, J.J.; Hormaza, J.I.; Campos, D.; Chirinos, R.; Aguayo, E. Short vs. Long-Distance Avocado Supply Chains: Life Cycle Assessment Impact Associated to Transport and Effect of Fruit Origin and Supply Conditions Chain on Primary and Secondary Metabolites. *Foods* **2022**, *11*, 1807, doi:10.3390/foods11121807.
  22. WAO. World Avocado Organization; 2023; Available online: <http://www.avocadofruitoflife.com> (accessed on 14 May 2024).
  23. Bower, J.P.; Cutting, J.G. Avocado Fruit Development and Ripening Physiology. In *Horticultural Reviews*; Janick, J., Ed.; Timber Press: Portland, OR, 1988; Vol. 10, pp. 229–271.
  24. Montero-Calderon, M.; Cerdas-Araya, M. de M. Postharvest Physiology and Storage. In *Tropical and Subtropicals Fruits: Postharvest Physiology, Processing and Packaging*; Siddiq, M., Ed.; John Wiley & Sons, 2012; pp. 17–33, doi:10.1002/9781118324097.ch2.
  25. FAO. Food and Agriculture Organization; *Codex Standard for Avocado (Codex Stan 197-1995)*; 1995.
  26. Inoue, H. Postharvest Physiology of Avocado. *JIRCAS Int. Symp. Ser.* **1994**, 82–90.
  27. Blakey, R.J. Management of Avocado Postharvest Physiology, University of KwaZulu-Natal, 2011, doi:10.13140/RG.2.1.3652.7121.
  28. Kassim, A.; Workneh, T.S.; Bezuidenhout, C.N. A Review on Postharvest Handling of Avocado Fruit. *African J. Agric. Res.* **2013**, *8*, 2385–2402, doi:10.5897/AJAR12.1248.
  29. Defilippi, B.G.; Ejsmentewicz, T.; Covarrubias, M.P.; Gudenschwager, O.; Campos-Vargas, R. Changes in Cell Wall Pectins and Their Relation to Postharvest Mesocarp Softening of “Hass” Avocados (Persea Americana Mill.). *Plant Physiol. Biochem.* **2018**, 142–151, doi:10.1016/j.plaphy.2018.05.018.
  30. Cox, K.A.; McGhie, T.K.; White, A.; Woolf, A.B. Skin Colour and Pigment Changes during Ripening of “Hass” Avocado Fruit. *Postharvest Biol. Technol.* **2004**, *31*, 287–294, doi:10.1016/j.postharvbio.2003.09.008.
  31. Kassim, A.; Workneh, T.S.; Bezuidenhout, C.N. A Review on Postharvest Handling of Avocado Fruit. *African J. Agric. Res.* **2013**, *8*, 2385–2402, doi:10.5897/AJAR12.1248.
  32. Hofman, P.J.; Fuchs, Y.; Milne, D.L. Harvesting, Packing, Postharvest Technology, Transport and Processing. In *The avocado: botany, production and uses*; Schaffer, B., Wolstenholme, B.N., Whiley, A.W., Eds.; CABI Publishing, 2002; pp. 363–401, doi:10.1079/9780851993577.0363.
  33. Fonseca Duarte, P.; Alves Chaves, M.; Dellinghausen Borges, C.; Barboza Mendonça, C.R. Avocado: Characteristic, Health Benefits and Uses. *Cienc. Rural* **2016**, *46*, 747–754, doi:10.1590/0103-8478cr20141516.
  34. Jimenez, P.; Garcia, P.; Quitral, V.; Vasquez, K.; Parra-Ruiz, C.; Reyes-Farias, M.; Garcia-Diaz, D.F.; Robert, P.; Encina, C.; Soto-Covasich, J. Pulp, Leaf, Peel and Seed of Avocado Fruit: A Review of Bioactive Compounds and Healthy Benefits. *Food Rev. Int.* **2021**, *37*, 619–655, doi:10.1080/87559129.2020.1717520.
  35. USDA United States Department of Agriculture. FoodData Central Available online: <https://fdc.nal.usda.gov/fdc-app.html#/> (accessed on 13 May 2024).
  36. Villa-Rodríguez, J.A.; Molina-Corral, F.J.; Ayala-Zavala, J.F.; Olivas, G.I.; González-Aguilar, G.A. Effect of Maturity Stage on the Content of Fatty Acids and Antioxidant Activity of “Hass” Avocado. *Food Res. Int.* **2011**, *44*, 1231–1237, doi:10.1016/j.foodres.2010.11.012.
  37. Pedreschi, R.; Uarrota, V.; Fuentealba, C.; Alvaro, J.E.; Olmedo, P.; Defilippi, B.G.; Meneses, C.; Campos-

- Vargas, R. Primary Metabolism in Avocado Fruit. *Front. Plant Sci.* **2019**, *10*:795, doi:10.3389/fpls.2019.00795.
38. Cowan, A.K.; Wolstenholme, B.N. Avocado. *Encycl. Food Heal.* **2015**, 294–300, doi:10.1016/B978-0-12-384947-2.00049-0.
39. Grant, W.C. Influence of Avocados on Serum Cholesterol. *Proc. Soc. Exp. Biol. Med.* **1960**, *104*, 45–47, doi:http://dx.doi.org/10.3181/00379727-104-25722.
40. Pieterse, Z.; Johann, J.; Stonehouse, W. Avocados (Monounsaturated Fatty Acids), Weight Loss and Serum Lipids. *South African Avocado Grow. Assoc. Yearb.* **2003**, *26*, 65–71.
41. Pieterse, Z.; Jerling, J.C.; Oosthuizen, W.; Kruger, H.S.; Hanekom, S.M.; Smuts, C.M.; Schutte, A.E. Substitution of High Monounsaturated Fatty Acid Avocado for Mixed Dietary Fats during an Energy-Restricted Diet: Effects on Weight Loss, Serum Lipids, Fibrinogen, and Vascular Function. *Nutrition* **2005**, *21*, 67–75, doi:10.1016/j.nut.2004.09.010.
42. Cheng, F.W.; Rodríguez-ramírez, S.; Shamah-levy, T.; Pérez-tepayo, S.; Ford, N.A. Association Between Avocado Consumption and Diabetes in Mexican Adults: Results From the 2012, 2016, and 2018 Mexican National Health and Nutrition Surveys. *J. Acad. Nutr. Diet.* **2024**, doi:10.1016/j.jand.2024.04.012.
43. Lerman-garber, I.; Ichazo-cerro, S.; Zamora-gonzalez, J.; Cardoso-Saldaña, G.; Posadas-romero, C. Effect of a High-Monounsaturated Fat Diet Enriched with Avocado in NIDDM Patients. *Diabetes Care* **1994**, *17*, 311–315, doi:https://doi.org/10.2337/diacare.17.4.311.
44. Colquhoun, D.M.; Moores, D.; Somers, S.M.; Humphries, J.A. Comparison of the Effects on Lipoproteins and Apolipoproteins of a Diet High in Monounsaturated Fatty Acids, Enriched with Avocado, and a High-Carbohydrate Diet. *Am. J. Clin. Nutr.* **1992**, *56*, 671–677, doi:10.1093/ajcn/56.4.671.
45. Wang, L.; Bordi, P.L.; Fleming, J.A.; Hill, A.M.; Kris-Etherton, P.M. Effect of a Moderate Fat Diet with and without Avocados on Lipoprotein Particle Number, Size and Subclasses in Overweight and Obese Adults: A Randomized, Controlled Trial. *J. Am. Heart Assoc.* **2015**, *4*, e001355, doi:10.1161/JAHA.114.001355.
46. Park, E.; Edirisinghe, I.; Burton-Freeman, B. Avocado Fruit on Postprandial Markers of Cardio-Metabolic Risk: A Randomized Controlled Dose Response Trial in Overweight and Obese Men and Women. *Nutrients* **2018**, *10*, doi:10.3390/nu10091287.
47. Christiansen, B.A.; Bhatti, S.; Goudarzi, R.; Emami, S. Management of Osteoarthritis with Avocado/Soybean Unsaponifiables. *Cartilage* **2015**, *6*, 30–44, doi:10.1177/1947603514554992.
48. Frech, T.M.; Clegg, D.O. The Utility of Nutraceuticals in the Treatment of Osteoarthritis. *Curr. Rheumatol. Rep.* **2007**, *9*, 25–30, doi:10.1007/s11926-007-0018-x.
49. Maheu, E. Mazières, B.; Valat, J.P.; Loyau, G.; Le Loët, X.; Bourgeois, P.; Grouin, J.M.; Rozenberg, S. Symtomatic Efficacy of Avoc Avocado/Soybean Unsaponifiables in the Treatment of Osteoarthritis of the Knee and Hip: A Prospective, Randomized, Double-Blind, Placebo-Controlled, Multicenter Clinical Trial with a Six-Month Treatment Period and a Two-Month Followup Demonstrating a Persistent Effect. *Arthritis Rheum.* **1998**, *41*, 81–91, doi:10.1002/1529-0131(199801)41:1<81::AID-ART11>3.0.CO;2-9.
50. Tabeshpour, J.; Razavi, B.M.; Hosseinzadeh, H. Effects of Avocado (*Persea Americana*) on Metabolic Syndrome: A Comprehensive Systematic Review. *Phyther. Res.* **2017**, *31*, 819–837, doi:10.1002/ptr.5805.
51. Fulgoni, V.L.; Dreher, M.; Davenport, A.J. Avocado Consumption Is Associated with Better Diet Quality and Nutrient Intake, and Lower Metabolic Syndrome Risk in US Adults: Results from the National Health and Nutrition Examination Survey (NHANES) 2001–2008. *Nutr. J.* **2013**, *12*, 1–6, doi:10.1186/1475-2891-12-1.
52. Cervantes-Paz, B.; Yahia, E.M. Avocado Oil: Production and Market Demand, Bioactive Components,

- Implications in Health, and Tendencies and Potential Uses. *Compr. Rev. Food Sci. Food Saf.* **2021**, *20*, 4120–4158, doi:10.1111/1541-4337.12784.
53. Dreher, M.L.; Davenport, A.J. Hass Avocado Composition and Potential Health Effects. *Crit. Rev. Food Sci. Nutr.* **2013**, *53*, 738–750, doi:10.1080/10408398.2011.556759.
  54. Wang, M.; Zheng, Y.; Khuong, T.; Lovatt, C.J. Effect of Harvest Date on the Nutritional Quality and Antioxidant Capacity in “Hass” Avocado during Storage. *Food Chem.* **2012**, *135*, 694–698, doi:10.1016/j.foodchem.2012.05.022.
  55. Lu, Q.Y.; Arteaga, J.R.; Zhang, Q.; Huerta, S.; Go, V.L.W.; Heber, D. Inhibition of Prostate Cancer Cell Growth by an Avocado Extract: Role of Lipid-Soluble Bioactive Substances. *J. Nutr. Biochem.* **2005**, *16*, 23–30, doi:10.1016/j.jnutbio.2004.08.003.
  56. Ahmed, O.M.; Fahim, H.I.; Mohamed, E.E.; Abdel-Moneim, A. Protective Effects of Persea Americana Fruit and Seed Extracts against Chemically Induced Liver Cancer in Rats by Enhancing Their Antioxidant, Anti-Inflammatory, and Apoptotic Activities. *Environ. Sci. Pollut. Res.* **2022**, *29*, 43858–43873, doi:10.1007/s11356-022-18902-y.
  57. Ding, H.; Han, C.; Guo, D.; Chin, Y.W.; Ding, Y.; Kinghorn, A.D.; D’Ambrosio, S.M. Selective Induction of Apoptosis of Human Oral Cancer Cell Lines by Avocado Extracts via a ROS-Mediated Mechanism. *Nutr. Cancer* **2009**, *61*, 348–356, doi:10.1080/01635580802567158.
  58. Alkhalaf, M.I.; Alansari, W.S.; Ibrahim, E.A.; Elhalwagy, M.E.A. Anti-Oxidant, Anti-Inflammatory and Anti-Cancer Activities of Avocado (Persea Americana) Fruit and Seed Extract. *J. King Saud Univ. - Sci.* **2019**, *31*, 1358–1362, doi:10.1016/j.jksus.2018.10.010.
  59. Henning, S.M.; Guzman, J.B.; Thames, G.; Yang, J.; Tseng, C.H.; Heber, D.; Kim, J.; Li, Z. Avocado Consumption Increased Skin Elasticity and Firmness in Women - A Pilot Study. *J. Cosmet. Dermatol.* **2022**, *21*, 4028–4034, doi:10.1111/jocd.14717.
  60. Nayak, B.S.; Raju, S.S.; Chalapathi Rao, A.V. Wound Healing Activity of Persea Americana (Avocado) Fruit: A Preclinical Study on Rats. *J. Wound Care* **2008**, *17*, 123–126, doi:10.12968/jowc.2008.17.3.28670.
  61. Rosenblat, G.; Meretski, S.; Segal, J.; Tarshis, M.; Schroeder, A.; Zanin-Zhorov, A.; Lion, G.; Ingber, A.; Hochberg, M. Polyhydroxylated Fatty Alcohols Derived from Avocado Suppress Inflammatory Response and Provide Non-Sunscreen Protection against UV-Induced Damage in Skin Cells. *Arch. Dermatol. Res.* **2011**, *303*, 239–246, doi:10.1007/s00403-010-1088-6.
  62. Dreher, M.L.; Cheng, F.W.; Ford, N.A. A Comprehensive Review of Hass Avocado Clinical Traits, Observational Studies, and Biological Mechanisms. *Nutrients* **2021**, *13*, 4376.
  63. Kaniewski, D.; Van Campo, E.; Boiy, T.; Terral, J.F.; Khadari, B.; Besnard, G. Primary Domestication and Early Uses of the Emblematic Olive Tree: Palaeobotanical, Historical and Molecular Evidence from the Middle East. *Biol. Rev.* **2012**, *87*, 885–899, doi:10.1111/j.1469-185X.2012.00229.x.
  64. Polymerou-Kamilakis, A. The Culture of the Olive Tree (Mediterranean World). In *Olive Oil: Chemistry and Technology*; Boskou, D., Ed.; AOCS Press, 2006; pp. 1–12, doi:10.1016/B978-1-893997-88-2.50005.
  65. Breton, C.; Terral, J.F.; Pinatel, C.; Médail, F.; Bonhomme, F.; Bervillé, A. The Origins of the Domestication of the Olive Tree. *Comptes Rendus - Biol.* **2009**, *332*, 1059–1064, doi:10.1016/j.crv.2009.08.001.
  66. Terral, J.F.; Alonso, N.; Buxó I Capdevila, R.; Chatti, N.; Fabre, L.; Fiorentino, G.; Marival, P.; Jordá, G.P.; Pradat, B.; Rovira, N.; et al. Historical Biogeography of Olive Domestication (Olea Europaea L.) as Revealed by Geometrical Morphometry Applied to Biological and Archaeological Material. *J. Biogeogr.* **2004**, *31*, 63–77, doi:10.1046/j.0305-0270.2003.01019.x.
  67. Green, P.S. A Revision of Olea L. (Oleaceae). *Kew Bull.* **2002**, *57*, 91–140, doi:10.2307/4110824.
  68. Rallo, P.; Tenzer, I.; Gessler, C.; Baldoni, L.; Dorado, G.; Martín, A. Transferability of Olive Microsatellite Loci across the Genus Olea. *Theor. Appl. Genet.* **2003**, *107*, 940–946, doi:10.1007/s00122-003-1332-y.

69. Médail, F.; Quézel, P.; Besnard, G.; Khadari, B. Systematics, Ecology and Phylogeographic Significance of *Olea Europaea* L. Ssp. *Maroccana* (Greuter & Burdet) P. Vargas et AL., a Relictual Olive Tree in South-West Morocco. *Bot. J. Linn. Soc.* **2001**, *137*, 249–266, doi:10.1006/bojl.2001.0477.
70. Ghanbari, R.; Anwar, F.; Alkharfy, K.M.; Gilani, A.H.; Saari, N. Valuable Nutrients and Functional Bioactives in Different Parts of Olive (*Olea Europaea* L.)—A Review. *Int. J. Mol. Sci.* **2012**, *13*, 3291–3340, doi:10.3390/ijms13033291.
71. IOC International Olive Oil Council World Catalogue of Olive Varieties. In; 2000; pp. 1–360 Abaliable Online: <https://www.internationaloliveoil.org> (accessed on 29 May 2024).
72. Ilarioni, L.; Proietti, P. Olive Tree Cultivars. In *The Extra-Virgin Olive Oil Handbook*; Peri, C., Ed.; John Wiley & Sons, 2014; pp. 59–67, doi:10.1002/9781118460412.ch5.
73. Rallo, L.; Barranco, D.; Fernández-Escobar, R. Distribución Geográfica Del Olivar. In *El cultivo del Olivo*; Mundi-Prensa, 2008; pp. 1–845 ISBN 978-84-847632-9-1.
74. Ministerio de Industria Comercio y Turismo *La Balanza Comercial Agroalimentaria. Informes y Estadísticas.*; Spain, 2021.
75. Fabbri, A.; Rapoport, H.F. Anatomy and Morphology. In *The Olive: Botany and production*; Fabbri, A., Baldoni, L., Caruso, T., Famiani, F., Eds.; CAB International, 2023; pp. 33–65, doi:10.1079/9781789247350.0002.
76. Chiappetta, A.; Muzzalupo, I. Botanical Description. In *Olive Germplasm - The Olive Cultivation, Table Olive and Olive Oil Industry in Italy*; Muzzalupo, I., Ed.; IntechOpen, 2012; pp. 23–38, doi:10.5772/3314.
77. Besnard, G.; Terral, J.F.; Cornille, A. On the Origins and Domestication of the Olive: A Review and Perspectives. *Ann. Bot.* **2018**, *121*, 385–403, doi:10.1093/aob/mcx145.
78. Bianchi, G. Lipids and Phenols in Table Olives. *Eur. J. Lipid Sci. Technol.* **2003**, *105*, 229–242, doi:10.1002/ejlt.200390046.
79. Abaza, L.; Taamalli, A.; Nsir, H.; Zarrouk, M. Olive Tree (*Olea Europeae* L.) Leaves: Importance and Advances in the Analysis of Phenolic Compounds. *Antioxidants* **2015**, *4*, 682–698, doi:10.3390/antiox4040682.
80. Molina Alcaide, E.; Nefzaoui, A. Recycling of Olive Oil By-Products: Possibilities of Utilization in Animal Nutrition. *Int. Biodeterior. Biodegrad.* **1996**, *38*, 227–235, doi:10.1016/s0964-8305(96)00055-8.
81. Guinda, Á.; Rada, M.; Delgado, T.; Gutiérrez-Adán, P.; Castellano, J.M. Pentacyclic Triterpenoids from Olive Fruit and Leaf. *J. Agric. Food Chem.* **2010**, *58*, 9685–9691, doi:10.1021/jf102039t.
82. Hernández-Yera, M.; Peragón, J. Time Course Profile of Pentacyclic Triterpenes from Stem and Root of Cv. Picual Olive Tree (*Olea Europaea*, L.) along Ripening. *J. Plant Sci.* **2020**, *4*, 186–193, doi:10.25177/jps.4.1.ra.10611.
83. Lo Giudice, V.; Faraone, I.; Bruno, M.R.; Ponticelli, M.; Labanca, F.; Bisaccia, D.; Massarelli, C.; Milella, L.; Todaro, L. Olive Trees By-Products as Sources of Bioactive and Other Industrially Useful Compounds: A Systematic Review. *Molecules* **2021**, *26*, doi:10.3390/molecules26165081.
84. Kabera, J.N.; Semana, E.; Mussa, A.R.; He, X. Plant Secondary Metabolites: Biosynthesis, Classification, Function and Pharmacological Properties. *J. Pharm. Pharmacol.* **2014**, *2*, 377–392.
85. Talhaoui, N.; Taamalli, A.; Gómez-Caravaca, A.M.; Fernández-Gutiérrez, A.; Segura-Carretero, A. Phenolic Compounds in Olive Leaves: Analytical Determination, Biotic and Abiotic Influence, and Health Benefits. *Food Res. Int.* **2015**, *77*, 92–108, doi:10.1016/j.foodres.2015.09.011.
86. Bravo, L. Polyphenols: Chemistry, Dietary Sources, Metabolism, and Nutritional Significance. *Nutr. Rev.* **1998**, *56*, 317–333, doi:10.1111/j.1753-4887.1998.tb01670.x.
87. Bendini, A.; Cerretani, L.; Carrasco-pancorbo, A.; Gómez-caravaca, A.M.; Segura-carretero, A.;

- Fernández-gutiérrez, A.; Lercker, G. Phenolic Molecules in Virgin Olive Oils: A Survey of Their Sensory Properties, Health Effects, Antioxidant Activity and Analytical Methods. An Overview of the Last Decade. *Molecules* **2007**, *12*, 1679–1719, doi:https://doi.org/10.3390/12081679.
88. Andrés-Lacueva, C.; Medina-Rejon, A.; Llorach, R.; Urpi-Sarda, M.; Khan, N.; Chiva-Blanch, G.; Zamora-Ros, R.; Rotches-Ribalta, M.; Lamuela-Raventós, R.M. Phenolic Compounds: Chemistry and Occurrence in Fruits and Vegetables; In: *Fruit and Vegetable Phytochemicals: Chemistry, Nutritional Value, and Stability*, de la Rosa, L.A., Alvarez-Parrilla, E., González-Aguilar, G.A., Eds. 2009; pp. 53-88, doi:10.1002/9780813809397.ch2.
89. Xu, R.; Fazio, G.C.; Matsuda, S.P.T. On the Origins of Triterpenoid Skeletal Diversity. *Phytochemistry* **2004**, *65*, 261–291, doi:10.1016/j.phytochem.2003.11.014.
90. Jäger, S.; Trojan, H.; Kopp, T.; Laszczyk, M.N.; Scheffler, A. Pentacyclic Triterpene Distribution in Various Plants - Rich Sources for a New Group of Multi-Potent Plant Extracts. *Molecules* **2009**, *14*, 2016–2031, doi:10.3390/molecules14062016.
91. Jiménez-Herrera, R.; Pacheco-López, B.; Peragón, J. Water Stress, Irrigation and Concentrations of Pentacyclic Triterpenes and Phenols in *Olea Europaea* L. Cv. Picual Olive Trees. *Antioxidants* **2019**, *8*, doi:10.3390/antiox8080294.
92. Landa, B.B.; Pérez, A.G.; Luaces, P.; Montes-Borrego, M.; Navas-Cortés, J.A.; Sanz, C. Insights into the Effect of *Verticillium Dahliae* Defoliating-Pathotype Infection on the Content of Phenolic and Volatile Compounds Related to the Sensory Properties of Virgin Olive Oil. *Front. Plant Sci.* **2019**, *10*, 1–12, doi:10.3389/fpls.2019.00232.
93. López-Escudero, F.J.; Mercado-Blanco, J. *Verticillium* Wilt of Olive: A Case Study to Implement an Integrated Strategy to Control a Soil-Borne Pathogen. *Plant Soil* **2011**, *344*, 1–50, doi:10.1007/s11104-010-0629-2.
94. Navas-Cortés, J.A.; Landa, B.B.; Mercado-Blanco, J.; Trapero-Casas, J.L.; Rodríguez-Jurado, D.; Jiménez-Díaz, R.M. Spatiotemporal Analysis of Spread of Infections by *Verticillium Dahliae* Pathotypes within a High Tree Density Olive Orchard in Southern Spain. *Phytopathology* **2008**, *98*, 167–180, doi:10.1094/PHTO-98-2-0167.
95. Baroudy, F.; Habib, W.; Tanos, G.; Gerges, E.; Saab, C.; Choueiri, E.; Nigro, F. Long-Distance Spread of *Verticillium Dahliae* through Rivers and Irrigation Systems. *Plant Dis.* **2018**, *102*, 1559–1565, doi:10.1094/PDIS-08-17-1189-RE.
96. Mol, L. Effect of Plant Roots on the Germination of *Microsclerotia* of *Verticillium Dahliae*. *Eur. J. Plant Pathol.* **1995**, *101*, 679–685, doi:10.1007/bf01874872.
97. Hiemstra, J.A. Some General Features of *Verticillium* Wilts in Trees. In *A Compendium of Verticillium Wilts in Tree Species*; Hiemstra, J.A., Harris, D.C., Eds.; CPRO-DLO: Wageningen, 1998; p. 80 ISBN 9789073771253.
98. Keykhasaber, M.; Thomma, B.P.H.J.; Hiemstra, J.A. *Verticillium* Wilt Caused by *Verticillium Dahliae* in Woody Plants with Emphasis on Olive and Shade Trees. *Eur. J. Plant Pathol.* **2018**, *150*, 21–37, doi:10.1007/s10658-017-1273-y.
99. López-Escudero, F.J.; Mercado-Blanco, J.; Roca, J.M.; Valverde-Corredor, A.; Blanco-López, M.A. *Verticillium* Wilt of Olive in the Guadalquivir Valley (Southern Spain): Relations with Some Agronomical Factors and Spread of *Verticillium Dahliae*. *Phytopathol. Mediterr.* **2010**, *49*, 370–380, doi:10.14601/Phytopathol\_Mediterr-3154.
100. Jiménez-Díaz, R.M.; Olivares-García, C.; Landa, B.B.; Del Mar Jiménez-Gasco, M.; Navas-Cortés, J.A. Region-Wide Analysis of Genetic Diversity in *Verticillium Dahliae* Populations Infecting Olive in Southern Spain and Agricultural Factors Influencing the Distribution and Prevalence of Vegetative Compatibility Groups and Pathotypes. *Phytopathology* **2011**, *101*, 304–315, doi:10.1094/PHTO-07-10-0176.

101. Cardoni, M.; Mercado-Blanco, J. Confronting Stresses Affecting Olive Cultivation from the Holobiont Perspective. *Front. Plant Sci.* **2023**, *14*, 1–31, doi:10.3389/fpls.2023.1261754.
102. Martos-Moreno, C.; López-Escudero, F.J.; Blanco-López, M.Á. Resistance of Olive Cultivars to the Defoliating Pathotype of *Verticillium Dahliae*. *HortScience* **2006**, *41*, 1313–1316, doi:10.21273/hortsci.41.5.1313.
103. López-Escudero, F.J.; Del Río, C.; Caballero, J.M.; Blanco-López, M.A. Evaluation of Olive Cultivars for Resistance to *Verticillium Dahliae*. *Eur. J. Plant Pathol.* **2004**, *110*, 79–85, doi:10.1023/B:EJPP.0000010150.08098.2d.
104. Rallo, L.; Barranco, D.; Díez, C.M.; Rallo, P.; Suárez, M.P.; Trapero, C.; Pliego-Alfaro, F. Strategies for Olive (*Olea Europaea* L.) Breeding: Cultivated Genetic Resources and Crossbreeding. In *Advances in Plant Breeding Strategies: Fruits*; Al-Khayri, J.M., Jain, S.M., Johnson, D. V., Eds.; Springer Cham, 2018; Vol. 3, pp. 535–600, doi:10.1007/978-3-319-91944-7\_14.
105. Belaj, A.; Veral, M.G.; Sikaoui, H.; Moukhli, A.; Khadari, B.; Mariotti, R.; Baldoni, L. Olive Genetic Resources. In *The Olive Tree Genome*; Rugini, E., Baldoni, L., Muleo, R., Sebastiani, L., Eds.; Springer Cham, 2016; pp. 27–54, doi:10.1007/978-3-319-48887-5.
106. Rallo, L. Looking towards Tomorrow in Olive Growing: Challenges in Breeding. *Acta Hort.* **2014**, *1057*, 467–481, doi:10.17660/ActaHortic.2014.1057.59.
107. León, L.; Velasco, L.; de la Rosa, R. Initial Selection Steps in Olive Breeding Programs. *Euphytica* **2015**, *201*, 453–462, doi:10.1007/s10681-014-1232-z.
108. De la Rosa, R.; León, L. New Cultivars and Prospects in Olive Breeding. *Vida Rural* **2009**, *292*, 41–44.
109. Rallo, L. Breeding Oil and Table Olives for Mechanical Harvesting in Spain. *Horttechnology* **2014**, *24*, 295–300, doi:10.21273/horttech.24.3.295.
110. Leo, L.; Rosa, R. de la; Barranco, D.; Rallo, L. Breeding for Early Bearing in Olive. *Hortic. Sci.* **2007**, *42*, 499–502, doi:10.21273/HORTSCI.42.3.499.
111. Moreno-Alías, I.; López, R.; Luque, F.; Rapoport, H.F.; Hammami, S.; León, L.; De la Rosa, R. Overcoming Juvenility in an Olive Breeding Program. *Acta Hort* **2012**, *949*, 221–226, doi:10.17660/ActaHortic.2012.949.31.
112. León, L.; Beltrán, G.; Aguilera, M.P.; Rallo, L.; Barranco, D.; De la Rosa, R. Oil Composition of Advanced Selections from an Olive Breeding Program. *Eur. J. Lipid Sci. Technol.* **2011**, *113*, 870–875, doi:10.1002/ejlt.201000535.
113. Manai, H.; Haddada, F.M.; Trigui, A.; Daoud, D.; Zarrouk, M. Compositional Quality of Virgin Olive Oil from Two New Tunisian Cultivars Obtained through Controlled Crossings. *J. Sci. Food Agric.* **2007**, *87*, 600–606, doi:10.1002/jsfa.2732.
114. Serrano, A.; Rodríguez-Jurado, D.; Román, B.; Bejarano-Alcázar, J.; de la Rosa, R.; León, L. *Verticillium* Wilt Evaluation of Olive Breeding Selections under Semi-Controlled Conditions. *Plant Dis.* **2021**, *105*, 1781–1790, doi:10.1094/PDIS-08-20-1829-RE.
115. Arias-Calderón, R.; Rodríguez-Jurado, D.; Bejarano-Alcázar, J.; Belaj, A.; de la Rosa, R.; León, L. Evaluation of *Verticillium* Wilt Resistance in Selections from Olive Breeding Crosses. *Euphytica* **2015**, *206*, 619–629, doi:10.1007/s10681-015-1463-7.
116. León, L.; de la Rosa, R.; Arriaza, M. Prioritization of Olive Breeding Objectives in Spain: Analysis of a Producers and Researchers Survey. *Spanish J. Agric. Res.* **2021**, *19*, 1–8, doi:10.5424/sjar/2021194-18203.
117. Arias-Calderón, R.; Rodríguez-Jurado, D.; León, L.; Bejarano-Alcázar, J.; De la Rosa, R.; Belaj, A. Pre-Breeding for Resistance to *Verticillium* Wilt in Olive: Fishing in the Wild Relative Gene Pool. *Crop Prot.* **2015**, *75*, 25–33, doi:10.1016/j.cropro.2015.05.006.

118. Colella, C.; Miacola, C.; Amenduni, M.; D'Amico, M.; Bubici, G.; Cirulli, M. Sources of Verticillium Wilt Resistance in Wild Olive Germplasm from the Mediterranean Region. *Plant Pathol.* **2008**, *57*, 533–539, doi:10.1111/j.1365-3059.2007.01785.x.
119. Montes-Osuna, N.; Mercado-Blanco, J. Verticillium Wilt of Olive and Its Control: What Did We Learn during the Last Decade? *Plants* **2020**, *9*, 1–31, doi:10.3390/plants9060735.
120. Ramírez-Tejero, J.A.; Jiménez-Ruiz, J.; Serrano, A.; Belaj, A.; León, L.; de la Rosa, R.; Mercado-Blanco, J.; Luque, F. Verticillium Wilt Resistant and Susceptible Olive Cultivars Express a Very Different Basal Set of Genes in Roots. *BMC Genomics* **2021**, *22*, 229, doi:10.1186/s12864-021-07545-x.
121. Gharbi, Y.; Barkallah, M.; Bouazizi, E.; Gdoura, R.; Triki, M.A. Differential Biochemical and Physiological Responses of Two Olive Cultivars Differing by Their Susceptibility to the Hemibiotrophic Pathogen Verticillium Dahliae. *Physiol. Mol. Plant Pathol.* **2017**, *97*, 30–39, doi:10.1016/j.pmp.2016.12.001.
122. León, L.; De La Rosa, R.; Velasco, L.; Belaj, A. Using Wild Olives in Breeding Programs: Implications on Oil Quality Composition. *Front. Plant Sci.* **2018**, *9*, 1–9, doi:10.3389/fpls.2018.00232.
123. Diraman, H.; Karaman, H.T.; Sefer, F.; Ersoy, N.; Arsel, A.H. Using Nutritional Lipid and Sensorial Profiles for the Characterization of Turkish Olive (Memecik X Gemlik Cv) Hybrids Obtained from Controlled Crossbreeding. *JAOCs, J. Am. Oil Chem. Soc.* **2020**, *97*, 943–954, doi:10.1002/aocs.12363.
124. Pérez, A.G.; León, L.; Sanz, C.; de la Rosa, R. Fruit Phenolic Profiling: A New Selection Criterion in Olive Breeding Programs. *Front. Plant Sci.* **2018**, *9*, 1–14.
125. Yadav, S.P. The Wholeness in Suffix -Omics, -Omes, and the Word Om. *J. Biomol. Tech.* **2007**, *18*, 277.
126. Gosálvez, J.; Horcajadas, J.A. Introduction: Human Genome Projects: The Omics Starting Point. In *Reproductomics*; Horcajadas, J.A., Gosálvez, J., Eds.; Academic Press, 2018; pp. 17–29, doi:10.1016/B978-0-12-812571-7.00001-0.
127. Vailati-Riboni, M.; Palombo, V.; Loor, J.J. What Are Omics Sciences? In *Periparturient Diseases of Dairy Cows: A Systems Biology Approach*; Ametaj, B.N., Ed.; Springer Cham, 2017; pp. 1–276, doi:10.1007/978-3-319-43033-1\_1.
128. Fukusaki, E.; Kobayashi, A. Plant Metabolomics: Potential for Practical Operation. *J. Biosci. Bioeng.* **2005**, *100*, 347–354, doi:10.1263/jbb.100.347.
129. Wishart, D.S. Emerging Applications of Metabolomics in Drug Discovery and Precision Medicine. *Nat. Rev. Drug Discov.* **2016**, *15*, 473–484, doi:10.1038/nrd.2016.32.
130. Fiehn, O. Combining Genomics, Metabolome Analysis, and Biochemical Modelling to Understand Metabolic Networks. *Comp. Funct. Genomics* **2001**, *2*, 155–168, doi:10.1002/cfg.82.
131. Nicholson, J.K.; Lindon, J.C.; Holmes, E. “Metabonomics”: Understanding the Metabolic Responses of Living Systems to Pathophysiological Stimuli via Multivariate Statistical Analysis of Biological NMR Spectroscopic Data. *Xenobiotica* **1999**, *29*, 1181–1189, doi:10.1080/004982599238047.
132. Villas-Bôas, S.G.; Rasmussen, S.; Lane, G.A. Metabolomics or Metabolite Profiles? *Trends Biotechnol.* **2005**, *23*, 385–386, doi:10.1016/j.tibtech.2005.05.009.
133. Oliver, S.G.; Winson, M.K.; Kell, D.B.; Baganz, F. Systematic Functional Analysis of the Yeast Genome. *Trends Biotechnol.* **1998**, *16*, 373–378, doi:10.1016/S0167-7799(98)01214-1.
134. Steuer, A.E.; Brockbals, L.; Kraemer, T. Metabolomic Strategies in Biomarker Research—New Approach for Indirect Identification of Drug Consumption and Sample Manipulation in Clinical and Forensic Toxicology? *Front. Chem.* **2019**, *7*, doi:10.3389/fchem.2019.00319.
135. Dunn, W.B.; Bailey, N.J.C.; Johnson, H.E. Measuring the Metabolome: Current Analytical Technologies. *Analyst* **2005**, *130*, 606–625, doi:10.1039/b418288j.
136. Nalbantoglu, S. Metabolomics: Basic Principles and Strategies. *Mol. Med.* **2019**, 1–15,

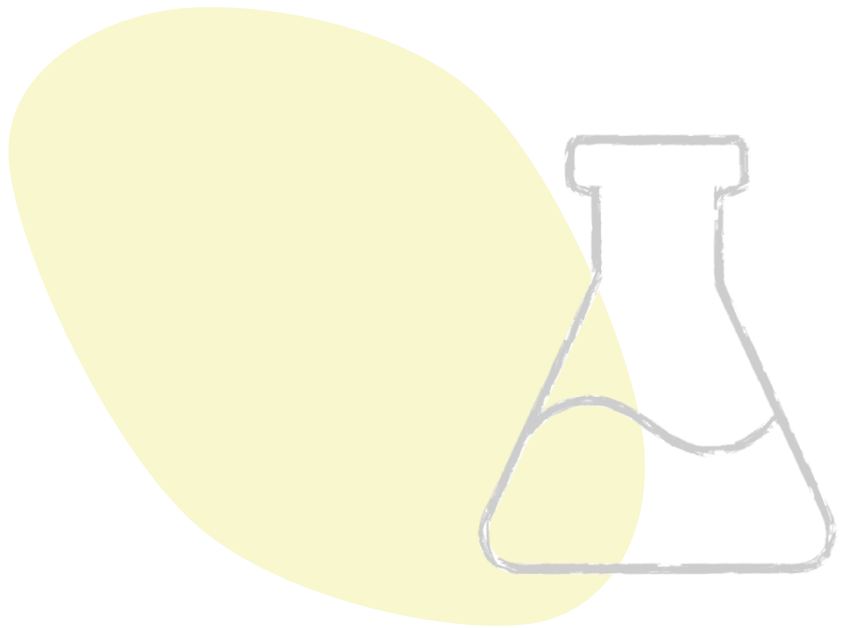
- doi:10.5772/intechopen.88563.
137. Klassen, A.; Tedesco Faccio, A.; Baptista Canuto, G.A.; Rocha da Cruz, P.L.; Caracho Ribeiro, H.; Maggi Tavares, M.F.; Sussulini, A. Metabolomics: Definitions and Significance in Systems Biology. In *Advances in Experimental Medicine and Biology*; Alessandra Sussulini, Ed.; Springer, Cham, 2017; Vol. 965, pp. 3–17, doi:10.1007/978-3-319-47656-8.
  138. Patel, M.K.; Pandey, S.; Kumar, M.; Haque, M.I.; Pal, S.; Yadav, N.S. Plants Metabolome Study: Emerging Tools and Techniques. *Plants* **2021**, *10*, 1–24, doi:10.3390/plants10112409.
  139. Oms-Oliu, G.; Odriozola-Serrano, I.; Martín-Belloso, O. Metabolomics for Assessing Safety and Quality of Plant-Derived Food. *Food Res. Int.* **2013**, *54*, 1172–1183, doi:10.1016/j.foodres.2013.04.005.
  140. Hamany Djande, C.Y.; Pretorius, C.; Tugizimana, F.; Piater, L.A.; Dubery, I.A. Metabolomics: A Tool for Cultivar Phenotyping and Investigation of Grain Crops. *Agronomy* **2020**, *10*, 1–30, doi:10.3390/agronomy10060831.
  141. Wishart, D.S. Metabolomics: Applications to Food Science and Nutrition Research. *Trends Food Sci. Technol.* **2008**, *19*, 482–493, doi:10.1016/j.tifs.2008.03.003.
  142. Fraga-Corral, M.; Carpena, M.; Garcia-Oliveira, P.; Pereira, A.G.; Prieto, M.A.; Simal-Gandara, J. Analytical Metabolomics and Applications in Health, Environmental and Food Science. *Crit. Rev. Anal. Chem.* **2020**, *52*, 712–734, doi:10.1080/10408347.2020.1823811.
  143. Díaz-Galiano, F.J.; Murcia-Morales, M.; Cutillas, V.; Fernández-Alba, A.R. Ions on the Move: The Combination of Ion Mobility and Food Metabolomics. *Trends Food Sci. Technol.* **2024**, *147*, doi:10.1016/j.tifs.2024.104446.
  144. Naz, S.; Vallejo, M.; García, A.; Barbas, C. Method Validation Strategies Involved in Non-Targeted Metabolomics. *J. Chromatogr. A* **2014**, *1353*, 99–105, doi:10.1016/j.chroma.2014.04.071.
  145. Karaman, I. Preprocessing and Pretreatment of Metabolomics Data for Statistical Analysis. In *Metabolomics: From Fundamentals to Clinical Applications*; Sussulini, A., Ed.; Springer Cham, 2017; pp. 145–161, doi:10.1007/978-3-319-47656-8\_6.
  146. Pinto, R.C. Chemometrics Methods and Strategies in Metabolomics. In *Metabolomics: From Fundamentals to Clinical Applications*; Sussulini, A., Ed.; Springer Cham, 2017; pp. 163–190, doi:10.1007/978-3-319-47656-8\_7.
  147. Puchades-Carrasco, L.; Pineda-Lucena, A. Metabolomics in Pharmaceutical Research and Development. *Curr. Opin. Biotechnol.* **2015**, *35*, 73–77, doi:10.1016/j.copbio.2015.04.004.
  148. Hall, R.D. Plant Metabolomics in a Nutshell: Potential and Future Challenges. *Annu. Plant Rev. Vol. 43 Biol. Plant Metabolomics* **2011**, *43*, 1–24, doi:10.1002/9781444339956.ch1.
  149. Hall, R.D. Plant Metabolomics: From Holistic Hope, to Hype, to Hot Topic. *New Phytol.* **2006**, *169*, 453–468, doi:10.1111/j.1469-8137.2005.01632.x.
  150. Gomez-Casati, D.F.; Zanol, M.I.; Busi, M. V. Metabolomics in Plants and Humans: Applications in the Prevention and Diagnosis of Diseases. *Biomed Res. Int.* **2013**, *2013*, doi:10.1155/2013/792527.
  151. Capozzi, F.; Bordoni, A. Foodomics: A New Comprehensive Approach to Food and Nutrition. *Genes Nutr.* **2013**, *8*, 1–4, doi:10.1007/s12263-012-0310-x.
  152. Levatte, M.; Keshteli, A.H.; Zarei, P.; Wishart, D.S. Applications of Metabolomics to Precision Nutrition. *Lifestyle Genomics* **2022**, *15*, 1–9, doi:10.1159/000518489.
  153. Jacobs, D.M.; van den Berg, M.A.; Hall, R.D. Towards Superior Plant-Based Foods Using Metabolomics. *Curr. Opin. Biotechnol.* **2021**, *70*, 23–28, doi:10.1016/j.copbio.2020.08.010.
  154. Wu, W.; Zhang, L.; Zheng, X.; Huang, Q.; Farag, M.A.; Zhu, R.; Zhao, C. Emerging Applications of Metabolomics in Food Science and Future Trends. *Food Chem. X* **2022**, *16*, 100500,

- doi:10.1016/j.fochx.2022.100500.
155. Cevallos-Cevallos, J.M.; Reyes-De-Corcuera, J.I.; Etxeberria, E.; Danyluk, M.D.; Rodrick, G.E. Metabolomic Analysis in Food Science: A Review. *Trends Food Sci. Technol.* **2009**, *20*, 557–566, doi:10.1016/j.tifs.2009.07.002.
  156. Hurtado-Fernández, E.; Carrasco-Pancorbo, A.; Fernández-Gutiérrez, A. Profiling LC-DAD-ESI-TOF MS Method for the Determination of Phenolic Metabolites from Avocado (*Persea Americana*). *J. Agric. Food Chem.* **2011**, *59*, 2255–2267, doi:10.1021/jf104276a.
  157. Figueroa, J.G.; Borrás-Linares, I.; Lozano-Sánchez, J.; Segura-Carretero, A. Comprehensive Characterization of Phenolic and Other Polar Compounds in the Seed and Seed Coat of Avocado by HPLC-DAD-ESI-QTOF-MS. *Food Res. Int.* **2018**, *105*, 752–763, doi:10.1016/j.foodres.2017.11.082.
  158. Figueroa, J.G.; Borrás-Linares, I.; Lozano-Sánchez, J.; Segura-Carretero, A. Comprehensive Identification of Bioactive Compounds of Avocado Peel by Liquid Chromatography Coupled to Ultra-High-Definition Accurate-Mass Q-TOF. *Food Chem.* **2018**, *245*, 707–716, doi:10.1016/j.foodchem.2017.12.011.
  159. López-Cobo, A.; Gómez-Caravaca, A.M.; Pasini, F.; Caboni, M.F.; Segura-Carretero, A.; Fernández-Gutiérrez, A. HPLC-DAD-ESI-QTOF-MS and HPLC-FLD-MS as Valuable Tools for the Determination of Phenolic and Other Polar Compounds in the Edible Part and by-Products of Avocado. *Lwt* **2016**, *73*, 505–513, doi:10.1016/j.lwt.2016.06.049.
  160. Younis, I.Y.; Khattab, A.R.; Selim, N.M.; Sobeh, M.; Elhawary, S.S.; Bishbishy, M.H.E. Metabolomics-Based Profiling of 4 Avocado Varieties Using HPLC-MS/MS and GC/MS and Evaluation of Their Antidiabetic Activity. *Sci. Rep.* **2022**, *12*, 1–15, doi:10.1038/s41598-022-08479-4.
  161. Di Stefano, V.; Avellone, G.; Bongiorno, D.; Indelicato, S.; Massenti, R.; Lo Bianco, R. Quantitative Evaluation of the Phenolic Profile in Fruits of Six Avocado (*Persea Americana*) Cultivars by Ultra-High-Performance Liquid Chromatography-Heated Electrospray-Mass Spectrometry. *Int. J. Food Prop.* **2017**, *20*, 1302–1312, doi:10.1080/10942912.2016.1208225.
  162. Martín-Torres, S.; Jiménez-Carvelo, A.M.; González-Casado, A.; Cuadros-Rodríguez, L. Authentication of the Geographical Origin and the Botanical Variety of Avocados Using Liquid Chromatography Fingerprinting and Deep Learning Methods. *Chemom. Intell. Lab. Syst.* **2020**, *199*, 103960, doi:10.1016/j.chemolab.2020.103960.
  163. Donetti, M.; Terry, L.A. Biochemical Markers Defining Growing Area and Ripening Stage of Imported Avocado Fruit Cv. Hass. *J. Food Compos. Anal.* **2014**, *34*, 90–98, doi:10.1016/j.jfca.2013.11.011.
  164. Villa-Rodríguez, J.A.; Yahia, E.M.; González-León, A.; Ifie, I.; Robles-Zepeda, R.E.; Domínguez-Avila, J.A.; González-Aguilar, G.A. Ripening of 'Hass' Avocado Mesocarp Alters Its Phytochemical Profile and the in Vitro Cytotoxic Activity of Its Methanolic Extracts. *South African J. Bot.* **2020**, *128*, 1–8, doi:10.1016/j.sajb.2019.09.020.
  165. Rodríguez-López, C.E.; Hernández-Brenes, C.; Treviño, V.; Díaz de la Garza, R.I. Avocado Fruit Maturation and Ripening: Dynamics of Aliphatic Acetogenins and Lipidomic Profiles from Mesocarp, Idioblasts and Seed. *BMC Plant Biol.* **2017**, *17*, 9–12, doi:10.1186/s12870-017-1103-6.
  166. Pedreschi, R.; Muñoz, P.; Robledo, P.; Becerra, C.; Defilippi, B.G.; van Eekelen, H.; Mumm, R.; Westra, E.; De Vos, R.C.H. Metabolomics Analysis of Postharvest Ripening Heterogeneity of "Hass" Avocados. *Postharvest Biol. Technol.* **2014**, *92*, 172–179, doi:10.1016/j.postharvbio.2014.01.024.
  167. Uarrotta, V.G.; Hernández, I.; Ponce, E.; Bauer, C.M.; Maraschin, M.; Pedreschi, R. Metabolic Profiling and Biochemical Analysis of Stored Hass Avocado Fruit by GC-MS and UHPLC-UV-VIS Revealed Oxidative Stress as the Main Driver of 'Blackspot' Physiological Disorder. *Int. J. Food Sci. Technol.* **2022**, *57*, 7896–7916, doi:10.1111/ijfs.16145.
  168. Núñez-Lillo, G.; Ponce, E.; Arancibia-Guerra, C.; Carpentier, S.; Carrasco-Pancorbo, A.; Olmo-García, L.; Chirinos, R.; Campos, D.; Campos-Vargas, R.; Meneses, C.; et al. A Multiomics Integrative Analysis

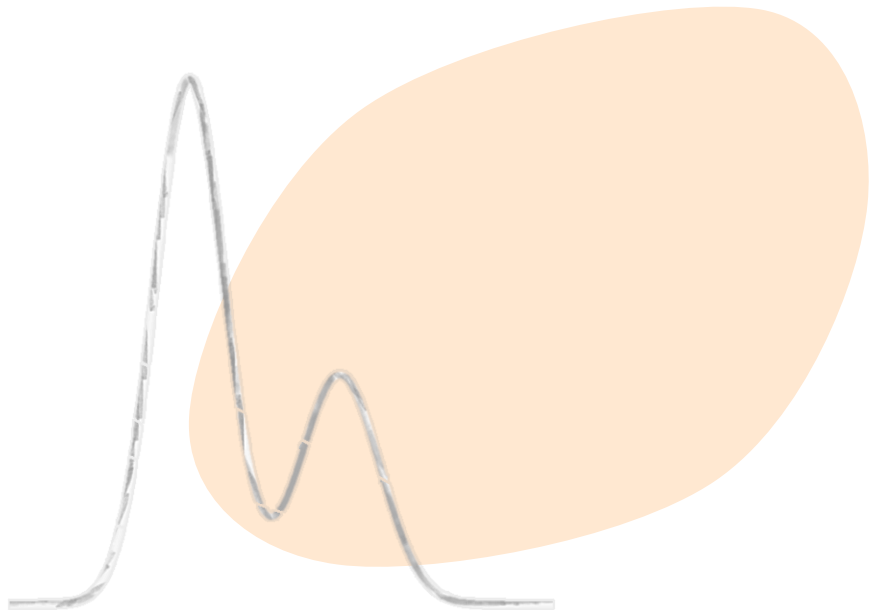
- of Color De-Synchronization with Softening of 'Hass' Avocado Fruit: A First Insight into a Complex Physiological Disorder. *Food Chem.* **2023**, *408*, doi:10.1016/j.foodchem.2022.135215.
169. Colombo, R.; Papetti, A. Avocado (*Persea Americana* Mill.) by-Products and Their Impact: From Bioactive Compounds to Biomass Energy and Sorbent Material for Removing Contaminants. A Review. *Int. J. Food Sci. Technol.* **2019**, *54*, 943–951, doi:10.1111/ijfs.14143.
170. Hatzakis, E.; Mazzola, E.P.; Shegog, R.M.; Ziegler, G.R.; Lambert, J.D. Perseoragin: A Natural Pigment from Avocado (*Persea Americana*) Seed. *Food Chem.* **2019**, *293*, 15–22, doi:10.1016/j.foodchem.2019.04.064.
171. Cincotta, F.; Merlino, M.; Conduro, C.; Miller, A.; Torre, M.; Verzera, A. Avocado Leaf-Waste Management: Drying Technology and Quality of Leaf Herbal Teas of Different Varieties Cultivated in the Mediterranean Area. *Int. J. Food Sci. Technol.* **2024**, *59*, 2516–2523, doi:10.1111/ijfs.16987.
172. Bhuyan, D.J.; Alsherbiny, M.A.; Perera, S.; Low, M.; Basu, A.; Devi, O.A.; Barooah, M.S.; Li, C.G.; Papoutsis, K. The Odyssey of Bioactive Compounds in Avocado (*Persea Americana*) and Their Health Benefits. *Antioxidants* **2019**, *8*, doi:10.3390/antiox8100426.
173. Ortega-Arellano, H.F.; Jimenez-Del-Rio, M.; Velez-Pardo, C. Neuroprotective Effects of Methanolic Extract of Avocado *Persea Americana* (Var. Colinred) Peel on Paraquat-Induced Locomotor Impairment, Lipid Peroxidation and Shortage of Life Span in Transgenic Knockdown Parkin *Drosophila Melanogaster*. *Neurochem. Res.* **2019**, *44*, 1986–1998, doi:10.1007/s11064-019-02835-z.
174. Lyu, X.; Agar, O.T.; Barrow, C.J.; Dunshea, F.R.; Suleria, H.A.R. Phenolic Compounds Profiling and Their Antioxidant Capacity in the Peel, Pulp, and Seed of Australian Grown Avocado. *Antioxidants* **2023**, *12*, 185, doi:10.3390/antiox12010185.
175. Wood, A.C.; Goodarzi, M.O.; Senn, M.K.; Gadgil, M.D.; Graca, G.; Allison, M.A.; Tzoulaki, I.; Mi, M.Y.; Greenland, P.; Ebbels, T.; et al. Associations between Metabolomic Biomarkers of Avocado Intake and Glycemia in the Multi-Ethnic Study of Atherosclerosis. *J. Nutr.* **2023**, *153*, 2797–2807, doi:10.1016/j.tjn.2023.07.013.
176. Thompson, S. V.; Bailey, M.A.; Taylor, A.M.; Kaczmarek, J.L.; Mysonhimer, A.R.; Edwards, C.G.; Reeser, G.E.; Burd, N.A.; Khan, N.A.; Holscher, H.D. Avocado Consumption Alters Gastrointestinal Bacteria Abundance and Microbial Metabolite Concentrations among Adults with Overweight or Obesity: A Randomized Controlled Trial. *J. Nutr.* **2021**, *151*, 753–762, doi:10.1093/jn/nxaa219.
177. Zuñiga-Martínez, B.S.; Domínguez-Avila, J.A.; Wall-Medrano, A.; Ayala-Zavala, J.F.; Hernández-Paredes, J.; Salazar-López, N.J.; Villegas-Ochoa, M.A.; González-Aguilar, G.A. Avocado Paste from Industrial Byproducts as an Unconventional Source of Bioactive Compounds: Characterization, in Vitro Digestion and in Silico Interactions of Its Main Phenolics with Cholesterol. *J. Food Meas. Charact.* **2021**, *15*, 5460–5476, doi:10.1007/s11694-021-01117-z.
178. Ingram, D.K.; Pistell, P.J.; Wang, Z.Q.; Yu, Y.; Massimino, S.; Davenport, G.M.; Hayek, M.; Roth, G.S. Characterization and Mechanisms of Action of Avocado Extract Enriched in Mannoheptulose as a Candidate Calorie Restriction Mimetic. *J. Agric. Food Chem.* **2021**, *69*, 7367–7376, doi:10.1021/acs.jafc.1c01995.
179. Olmo-García, L.; Polari, J.J.; Li, X.; Bajoub, A.; Fernández-Gutiérrez, A.; Wang, S.C.; Carrasco-Pancorbo, A. Deep Insight into the Minor Fraction of Virgin Olive Oil by Using LC-MS and GC-MS Multi-Class Methodologies. *Food Chem.* **2018**, *261*, 184–193, doi:10.1016/j.foodchem.2018.04.006.
180. Olmo-García, L.; Kessler, N.; Neuweger, H.; Wendt, K.; Olmo-Peinado, J.M.; Fernández-Gutiérrez, A.; Baessmann, C.; Carrasco-Pancorbo, A. Unravelling the Distribution of Secondary Metabolites in *Olea Europaea* L.: Exhaustive Characterization of Eight Olive-Tree Derived Matrices by Complementary Platforms (LC-ESI/APCI-MS and GC-APCI-MS). *Molecules* **2018**, *23*, 2419, doi:10.3390/molecules23102419.
181. Martakos, I.; Katsianou, P.; Koulis, G.; Efstratiou, E.; Nastou, E.; Nikas, S.; Dasenaki, M.; Pentogennis,

- M.; Thomaidis, N. Development of Analytical Strategies for the Determination of Olive Fruit Bioactive Compounds Using UPLC-HRMS and HPLC-DAD. Chemical Characterization of Kolovi Lesvos Variety as a Case Study. *Molecules* **2021**, *26*, 7182, doi:10.3390/molecules26237182.
182. Toumi, K.; Świątek, Ł.; Boguszewska, A.; Skalicka-Woźniak, K.; Bouaziz, M. Comprehensive Metabolite Profiling of Chemlali Olive Tree Root Extracts Using LC-ESI-QTOF-MS/MS, Their Cytotoxicity, and Antiviral Assessment. *Molecules* **2023**, *28*, 4829, doi:10.3390/molecules28124829.
183. Tóth, G.; Alberti, Á.; Sólyomváry, A.; Barabás, C.; Boldizsár, I.; Noszál, B. Phenolic Profiling of Various Olive Bark-Types and Leaves: HPLC-ESI/MS Study. *Ind. Crops Prod.* **2015**, *67*, 432–438, doi:10.1016/j.indcrop.2015.01.077.
184. Michel, T.; Khlif, I.; Kanakis, P.; Termentzi, A.; Allouche, N.; Halabalaki, M.; Skaltsounis, A.L. UHPLC-DAD-FLD and UHPLC-HRMS/MS Based Metabolic Profiling and Characterization of Different Olea Europaea Organs of Koroneiki and Chetoui Varieties. *Phytochem. Lett.* **2015**, *11*, 424–439, doi:10.1016/j.phytol.2014.12.020.
185. Abbattista, R.; Ventura, G.; Calvano, C.D.; Cataldi, T.R.I.; Losito, I. Bioactive Compounds in Waste By-Products from Olive Oil Production: Applications and Structural Characterization by Mass Spectrometry Techniques. *Foods* **2021**, *10*, 1236, doi:10.3390/foods10061236.
186. Bajoub, A.; Carrasco-Pancorbo, A.; Ajal, E.A.; Ouazzani, N.; Fernández-Gutiérrez, A. Potential of LC-MS Phenolic Profiling Combined with Multivariate Analysis as an Approach for the Determination of the Geographical Origin of North Moroccan Virgin Olive Oils. *Food Chem.* **2015**, *166*, 292–300, doi:10.1016/j.foodchem.2014.05.153.
187. Fayek, N.M.; Farag, M.A.; Saber, F.R. Metabolome Classification via GC/MS and UHPLC/MS of Olive Fruit Varieties Grown in Egypt Reveal Pickling Process Impact on Their Composition. *Food Chem.* **2021**, *339*, 127861, doi:10.1016/j.foodchem.2020.127861.
188. Olmo-García, L.; Wendt, K.; Kessler, N.; Bajoub, A.; Fernández-Gutiérrez, A.; Baessmann, C.; Carrasco-Pancorbo, A. Exploring the Capability of LC-MS and GC-MS Multi-Class Methods to Discriminate Virgin Olive Oils from Different Geographical Indications and to Identify Potential Origin Markers. *Eur. J. Lipid Sci. Technol.* **2019**, *121*, 1–13, doi:10.1002/ejlt.201800336.
189. Ghisoni, S.; Lucini, L.; Angilletta, F.; Rocchetti, G.; Farinelli, D.; Tombesi, S.; Trevisan, M. Discrimination of Extra-Virgin-Olive Oils from Different Cultivars and Geographical Origins by Untargeted Metabolomics. *Food Res. Int.* **2019**, *121*, 746–753, doi:10.1016/j.foodres.2018.12.052.
190. Sofo, A.; Fausto, C.; Mininni, A.N.; Dichio, B.; Lucini, L. Soil Management Type Differentially Modulates the Metabolomic Profile of Olive Xylem Sap. *Plant Physiol. Biochem.* **2019**, *139*, 707–714, doi:10.1016/j.plaphy.2019.04.036.
191. Martinelli, F.; Basile, B.; Morelli, G.; d'Andria, R.; Tonutti, P. Effects of Irrigation on Fruit Ripening Behavior and Metabolic Changes in Olive. *Sci. Hort.* **2012**, *144*, 201–207, doi:10.1016/j.scienta.2012.07.012.
192. Rosati, A.; Cafiero, C.; Paoletti, A.; Alfei, B.; Caporali, S.; Casciani, L.; Valentini, M. Effect of Agronomical Practices on Carpology, Fruit and Oil Composition, and Oil Sensory Properties, in Olive (*Olea Europaea* L.). *Food Chem.* **2014**, *159*, 236–243, doi:10.1016/j.foodchem.2014.03.014.
193. López-López, A.; Cortés-Delgado, A.; de Castro, A.; Sánchez, A.H.; Montañó, A. Changes in Volatile Composition during the Processing and Storage of Black Ripe Olives. *Food Res. Int.* **2019**, *125*, 108568, doi:10.1016/j.foodres.2019.108568.
194. Polari, J.J.; Garcá-Aguirre, D.; Olmo-García, L.; Carrasco-Pancorbo, A.; Wang, S.C. Interactions between Hammer Mill Crushing Variables and Malaxation Time during Continuous Olive Oil Extraction. *Eur. J. Lipid Sci. Technol.* **2018**, *120*, 1–7, doi:10.1002/ejlt.201800097.
195. Olmo-García, L.; Monasterio, R.P.; Sánchez-Arévalo, C.M.; Fernández-Gutiérrez, A.; Olmo-Peinado, J.M.; Carrasco-Pancorbo, A. Characterization of New Olive Fruit Derived Products Obtained by Means

- of a Novel Processing Method Involving Stone Removal and Dehydration with Zero Waste Generation. *J. Agric. Food Chem.* **2019**, *67*, 9295–9306, doi:10.1021/acs.jafc.9b04376.
196. Jllilat, A.; Ragone, R.; Gualano, S.; Santoro, F.; Gallo, V.; Varvaro, L.; Mastroilli, P.; Saponari, M.; Nigro, F.; D'Onghia, A.M. A Non-Targeted Metabolomics Study on *Xylella Fastidiosa* Infected Olive Plants Grown under Controlled Conditions. *Sci. Rep.* **2021**, *11*, 1070, doi:10.1038/s41598-020-80090-x.
197. Asteggiano, A.; Franceschi, P.; Zorzi, M.; Aigotti, R.; Bello, F.D.; Baldassarre, F.; Lops, F.; Carlucci, A.; Medana, C.; Ciccarella, G. HPLC-HRMS Global Metabolomics Approach for the Diagnosis of “Olive Quick Decline Syndrome” Markers in Olive Trees Leaves. *Metabolites* **2021**, *11*, 40, doi:10.3390/metabo11010040.
198. Drakopoulou, S.K.; Kritikou, A.S.; Baessmann, C.; Thomaidis, N.S. Untargeted 4D-Metabolomics Using Trapped Ion Mobility Combined with LC-HRMS in Extra Virgin Olive Oil Adulteration Study with Lower-Quality Olive Oils. *Food Chem.* **2024**, *434*, 137410, doi:10.1016/j.foodchem.2023.137410.
199. Baccouri, B.; Rajhi, I.; Theresa, S.; Najjar, Y.; Mohamed, S.N.; Willenberg, I. The Potential of Wild Olive Leaves (*Olea Europaea* L. Subsp. *Oleaster*) Addition as a Functional Additive in Olive Oil Production: The Effects on Bioactive and Nutraceutical Compounds Using LC–ESI–QTOF/MS. *Eur. Food Res. Technol.* **2022**, *248*, 2809–2823, doi:10.1007/s00217-022-04091-y.
200. Cavallo, P.; Dini, I.; Sepe, I.; Galasso, G.; Fedele, F.L.; Sicari, A.; Censi, S.B.; Gaspari, A.; Ritieni, A.; Lorito, M.; et al. An Innovative Olive Pâté with Nutraceutical Properties. *Antioxidants* **2020**, *9*, 1–13, doi:10.3390/antiox9070581.
201. Durante, M.; Blevé, G.; Selvaggini, R.; Veneziani, G.; Servili, M.; Mita, G. Bioactive Compounds and Stability of a Typical Italian Bakery Products “Taralli” Enriched with Fermented Olive Paste. *Molecules* **2019**, *24*, doi:10.3390/molecules24183258.
202. Rubió, L.; Macià, A.; Castell-Auví, A.; Pinent, M.; Blay, M.T.; Ardévol, A.; Romero, M.P.; Motilva, M.J. Effect of the Co-Occurring Olive Oil and Thyme Extracts on the Phenolic Bioaccessibility and Bioavailability Assessed by in Vitro Digestion and Cell Models. *Food Chem.* **2014**, *149*, 277–284, doi:10.1016/j.foodchem.2013.10.075.
203. Reboredo-Rodríguez, P.; Olmo-García, L.; Figueiredo-González, M.; González-Barreiro, C.; Carrasco-Pancorbo, A.; Cancho-Grande, B. Application of the INFOGEST Standardized Method to Assess the Digestive Stability and Bioaccessibility of Phenolic Compounds from Galician Extra-Virgin Olive Oil. *J. Agric. Food Chem.* **2021**, *69*, 11592–11605, doi:10.1021/acs.jafc.1c04592.
204. Soler, A.; Romero, M.P.; Macià, A.; Saha, S.; Furniss, C.S.M.; Kroon, P.A.; Motilva, M.J. Digestion Stability and Evaluation of the Metabolism and Transport of Olive Oil Phenols in the Human Small-Intestinal Epithelial Caco-2/TC7 Cell Line. *Food Chem.* **2010**, *119*, 703–714, doi:10.1016/j.foodchem.2009.07.017.
205. Kendall, M.; Batterham, M.; Callahan, D.L.; Jardine, D.; Prenzler, P.D.; Robards, K.; Ryan, D. Randomized Controlled Study of the Urinary Excretion of Biophenols Following Acute and Chronic Intake of Olive Leaf Supplements. *Food Chem.* **2012**, *130*, 651–659, doi:10.1016/j.foodchem.2011.07.101.
206. Kano, S.; Komada, H.; Yonekura, L.; Sato, A.; Nishiwaki, H.; Tamura, H. Absorption, Metabolism, and Excretion by Freely Moving Rats of 3,4-DHPEA-EDA and Related Polyphenols from Olive Fruits (*Olea Europaea*). *J. Nutr. Metab.* **2016**, *2016*, doi:10.1155/2016/9104208.
207. Conterno, L.; Martinelli, F.; Tamburini, M.; Fava, F.; Mancini, A.; Sordo, M.; Pindo, M.; Martens, S.; Masuero, D.; Vrhovsek, U.; et al. Measuring the Impact of Olive Pomace Enriched Biscuits on the Gut Microbiota and Its Metabolic Activity in Mildly Hypercholesterolaemic Subjects. *Eur. J. Nutr.* **2019**, *58*, 63–81, doi:10.1007/s00394-017-1572-2.
208. González-Domínguez, R.; Jáuregui, O.; Queipo-Ortuño, M.I.; Andrés-Lacueva, C. Characterization of the Human Exposome by a Comprehensive and Quantitative Large-Scale Multianalyte Metabolomics Platform. *Anal. Chem.* **2020**, *92*, 13767–13775, doi:10.1021/acs.analchem.0c02008.



## **EXPERIMENTAL PART, RESULTS AND DISCUSSION**





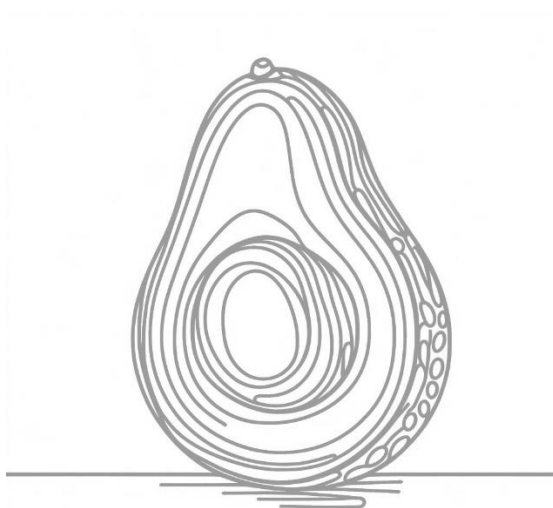
In the subsequent block, each chapter will be presented according to the section layout, general formatting, abbreviations, units, and other guidelines of the journal in which the respective studies have been published or are intended for publication. References within each chapter are independent and are cited using bracketed numbers.



# SECTION I

---

## METABOLOMIC APPROACHES APPLIED TO THE STUDY OF AVOCADO FRUIT



This section addresses two main topics related to the study of avocados. The first two studies investigate fruit maturation and ripening phenomena at a metabolic level using a targeted LC-MS approach ([Chapters 1 and 2](#)), while the subsequent chapters focus on differentiating and characterizing avocados based on their geographical origin, employing both targeted and non-targeted metabolomics approaches ([Chapters 3 and 4](#)).



# Chapter

# 1

## Prolonged on-tree maturation vs. cold storage of *Hass* avocado fruit: Changes in metabolites of bioactive interest at edible ripeness

Irene Serrano-García<sup>a</sup>, Elena Hurtado-Fernández<sup>b</sup>, José Jorge Gonzalez-Fernandez<sup>c</sup>, José Ignacio Hormaza<sup>c</sup>, Romina Pedreschi<sup>d</sup>, Patricia Reboredo-Rodríguez<sup>e</sup>, María Figueiredo-González<sup>e</sup>, Lucía Olmo-García<sup>a</sup>✉, Alegría Carrasco-Pancorbo<sup>a</sup>

<sup>a</sup> Department of Analytical Chemistry, Faculty of Sciences, University of Granada, Ave. Fuentenueva s/n, 18071, Granada, Spain

<sup>b</sup> Institute of General Organic Chemistry (IQOG-CSIC), Spanish National Research Council, C/ Juan de la Cierva 3, 28006, Madrid, Spain

<sup>c</sup> Institute for Mediterranean and Subtropical Horticulture (IHSM La Mayora-UMA-CSIC), 29750, Algarrobo-Costa, Málaga, Spain

<sup>d</sup> Pontificia Universidad Católica de Valparaíso, Facultad de Ciencias Agronómicas y de los Alimentos, Escuela de Agronomía, Calle San Francisco S/N, La Palma, Quillota 2260000, Chile

<sup>e</sup> Food and Health Omics. Department of Analytical and Food Chemistry, Faculty of Science, University of Vigo – Ourense Campus, 32004, Ourense, Spain.

✉ luciaolmo@ugr.es

**Food Chemistry, 394 (2022) 133447**

<https://doi.org/10.1016/j.foodchem.2022.133447>



**Abstract:** When the recipient of the product is relatively distant from the production area, it is necessary to use cold storage and controlled humidity to transport the avocado fruits. One of the main advantages of local avocado consumption lies on the possibility of prolonging on-tree maturation; this could foreseeably modify the metabolic profile of the fruit which arrives to the consumer. In this work, the effect of prolonged on tree maturation (during different time intervals) on the final composition of avocado fruit (at edible ripeness) was evaluated and compared with the impact of the same periods after prolonged cold storage. The quantitative evolution of nine bioactive metabolites (7 phenolic compounds, pantothenic and abscisic acids) over 40 days (10-days intervals) was studied by using a solid-liquid extraction protocol and a LC-MS methodology. The results were discussed both considering the quantitative evolution of each individual compound and the sum of all of them.

**Keywords:** Avocado, on-tree storage, ripening process, cold storage, metabolic profile, LC-MS

## 1. INTRODUCTION

The avocado (*Persea americana* Mill.) is native to Central America and Mexico, where it was domesticated and cultivated in pre-Columbian times. Traditionally, avocado genotypes have been divided into three ecological races or subspecies (West Indian, Mexican and Guatemalan) mainly related to their ecological and climatic preferences and botanical characteristics. Thus, the Mexican and Guatemalan subspecies are originated from highland regions in Central America (adapted to colder conditions) whereas the West Indian subspecies is originated from low-land regions with tropical climates (adapted to warmer conditions). The subspecies also differ in the fruit rate maturity and oil percentage [1]. The most common avocado variety in the international markets is *Hass* (a Guatemalan x Mexican hybrid), originated as a chance seedling in California in the 1920s and that shows a buttery flavour and a pear shape that changes from deep green to dark purplish black at the edible ripeness stage. In terms of fatty acids, avocado's average nutritional profile consists mainly of monounsaturated ( $\approx 73\%$ ), saturated ( $\approx 15\%$ ) and polyunsaturated fatty acids ( $\approx 12\%$ ), that are associated with a lower risk of cardiovascular diseases [2,3].

Avocado relevance in the international markets has increased exponentially in recent years and, in 2019, avocado world production was over 7 million tons. Most of the production is concentrated in a few countries (Mexico, Dominican Republic, Peru, Indonesia, Colombia, Brazil), Mexico being the largest world producer with about 32% of the total world production (more than 2 million tons) [4]. South America stands out in the global market with 23% of total world production in 2019 with the *Hass* variety as the main cultivar for the export market, mainly to the USA and Europe. European production represents only 1.5% of the world market share, with Spain standing out as the main producing country in Europe with 90% of the European avocado production [4]. Spanish production is destined mainly to France, the Netherlands, Germany and the United Kingdom, but it represents less than 10% of the total avocado consumption in Europe,

so fruit need to be imported from other countries, primarily Chile and Peru to satisfy the demand. These countries are quite distant from their destination markets, with travel times of up to 55 days, so ensuring that the fruit arrives at its final destination with the highest possible quality involves the use of cold storage and controlled atmosphere [5]. In contrast, for domestic and continental exports, land transport and cold storage (approximately for 30 days) at controlled temperature (4–5°C) and humidity (≈90%) is adequate.

On the other hand, the increasing popularity of avocado worldwide has forced to improve the distribution chain and harvest management of the fruit. The complexity of avocado fruit physiology is undeniable; in fact, the optimal strategy for identifying physiological maturity, which is not accompanied by external changes, is still unclear. Some of the most commonly used maturity indices to date are the oil concentration, fruit firmness, growth rate or dry matter (DM), which is related to oil content [6]. Portable near-infrared spectroscopy, characterized for being a non-destructive determination, is becoming a useful system to determine fruit DM, although the system has to be optimized for each variety of interest [7,8]. Avocado fruit development can be divided in two different, easily distinguishable processes: fruit maturation, which is the process of growing taking place while in the tree; and post-harvest ripening, comprising the softening of the mesocarp and improvement of organoleptic properties taking place only after the detachment of the fruit [9–11].

External pre-harvest (e.g., light intensity and temperature), at harvest (maturity stage or harvest stage) and postharvest (i.e., processing, handling, and storage) factors affect the final fruit composition. Carotenoids, sterols, phenolic compounds, carbohydrates, amino acids, proteins, vitamins, tannins, phytohormones and terpenoids, among others, have been determined in avocado, some of them predominantly in the mesocarp and others in the seed and peel [12]. The composition of a food and its quality is a well-recognized pairing. In this regard, the advent of sophisticated analytical techniques has opened up new frontiers and possibilities for scientists to dig deeper into the food composition. Qualitative and quantitative determinations of food metabolome offer insights into the content of the food analytes and details about some other valuable additional features (quality, authenticity, safety, health benefits, plant/fruit physiology...).

Many authors have reported that some of the bioactive compounds found in avocado participate in the mitigation of oxidative stress and inflammatory processes, reduce a platelet aggregation, regulate lipid and carbohydrate metabolism, exhibit anti-cancer and neuroprotective effects or help maintaining memory and brain health [3,13–15].

Maturation and ripening are very complex processes and different analytical platforms have been used to study the metabolic profile and composition changes in avocado over the harvest season, during ripening, and after prolonged cold and controlled atmosphere storage. [Table 1](#) gathers some interesting papers that have dealt with these topics (evolution of fruit composition over maturation and ripening), including different experimental designs, storage conditions, time

intervals (dates considered), analytical platforms and determinations carried out. This table is not intended to represent an exhaustive literature review, but rather a collection of several works that exemplify different experimental designs, determinations of interest, etc. As can be deduced from the just mentioned table, the selected examples focused on how some parameters of interest (DM, oil content, total soluble proteins, etc.) as well as some specific compounds (phenolic compounds, carotenoids, tocopherols, sugars, fatty acids, etc.) evolved during the harvest season of different varieties or over ripening. Other very valuable works regarding maturation over the harvest season and/or ripening could also be cited [16–21].

To the best of our knowledge, there is no study comparing the effect of prolonged on-tree maturation vs. cold storage over a 40-days period (at 10-days intervals) on the metabolic profile of *Hass* avocado fruit at ready-to-eat stage. To fill this gap, the aim of this work was to study the evolution of nine metabolites of interest in avocado fruit stored at 4°C for 10, 20, 30 and 40 days compared to fruit that remained on the tree during the same period of time. The monitored compounds were epicatechin, *p*-coumaric, ferulic, pantothenic and abscisic acids, and four hexoses of coumaric acid. Their quantitative evolution as well as how the permanence in the tree (prolonged on-tree maturation) or in cold storage affects the final composition of the fruit at ready-to-eat stage will be discussed in this contribution.

## 2. MATERIALS AND METHODS

### 2.1. Chemicals and reagents

Methanol (MeOH) was the solvent used for sample extraction and preparation of stock solution and was supplied by Prolabo (Paris, France). Standards of pantothenic, *p*-coumaric, ferulic and abscisic acids as well as epicatechin were acquired from Sigma-Aldrich (St. Louis, MO, USA). Moreover, *o*-coumaric acid from Sigma-Aldrich was used as internal standard (IS) to control the repeatability of the applied analytical methodology. Stock solution at a concentration of 200 mg L<sup>-1</sup> was first prepared by dissolving an appropriate amount of every metabolite in MeOH. Then, serial dilutions within the range from the quantification limit (LOQ) to 200 mg L<sup>-1</sup> were prepared. All the samples and solutions were filtered by using a nylon syringe filter Clarinet™ of 0.22 μm from Bonna-Agela Technologies (Wilmington, DE, USA) and stored in dark flasks at -20°C. Doubly deionized water with a conductivity of 18.2 MΩ was obtained by using a Milli-Q system (Millipore, Bedford, MA, USA). Acetic acid (AcH), used for the acidification of LC mobile phase A, was supplied by Panreac (Barcelona, Spain) and LC-MS grade acetonitrile (ACN) (phase B) by Lab-Scan (Dublin, Ireland). Mobile phases were filtered by using a nylon membrane filter 0.45 μm Nylaflo™ acquired from Pall Corporation (Ann Arbor, MI, USA). Reagents were of analytical or LC-MS grade and were used as received in the laboratory.

**Table 1.** Examples of interesting papers that have dealt with the evolution of avocado fruit composition over maturation and ripening

Aim of study	Samples	Period of study	Storage conditions	Chemical determinations / Determined compounds	Analytical platform/s	Ref.
To evaluate if ripening stage influences the content of specific compounds and determine <i>in vitro</i> cytotoxic activity	60 fruit batch. A sub-lot of 25 fruits for each RS	4 RS (0-, 4-, 8- and 12-days post-harvest)	14 days at 15°C	Seven phenolic compounds, carotenoids, tocopherols, phytosterols and cytotoxic activity	HPLC-DAD HPLC-FLD GC-FID	[22]
To appraise the metabolic changes that occur in four varieties during its main harvesting seasons in Southern Spain	3 or 4 pieces of fruit for each time point	Specific period for each variety of avocado (different harvesting dates)	1 week at 4-6°C and at room temperature until edible ripeness	Epicatechin, pantothenic, chlorogenic, <i>p</i> -coumaric, ferulic and abscisic acids	HPLC-ESI-IT MS	[23]
To compare the phenolic profiles of six varieties of avocado at two different RS	36 independent extracts	2 RS (unripe and ripe fruits)	-	Eighteen phenolic compounds	UHPLC-HESI-Q-Orbitrap MS	[24]
To evaluate the metabolic changes that occur in <i>cv. Reed</i> during the harvest season in Southern Spain	18 samples	9 dates over the harvest season between June and October (2011 season)	Samples were processed at edible ripeness	Ten different metabolites such as phenolic acids, flavonoids, a carbohydrate, an organic acid, a vitamin and a phytohormone	CE-MS HPLC-ESI-IT MS HPLC-ESI-QTOF MS	[25]
To establish a proper fruit biopsy sampling approach for <i>Hass</i> avocado and to explain the ripening heterogeneity	One hundred avocados from the same tree from a commercial orchard	-	5°C overnight before fruit biopsy. 5 RS (measured as loss of firmness, 0–5 hedonic scale)	Dry matter and total Ca <sup>2+</sup> , non-polar compounds (fatty acids and lipid-soluble isoprenoids), polar (C <sub>7</sub> and C <sub>6</sub> sugars) and semi-polar compounds	GC-TOF MS GC-Q MS HPLC-PDA-QTOF HPLC-PDA HPLC-FLD	[26]
To evaluate the application of UHPLC-TOF MS to study RS on avocado fruit	Fruit of 13 varieties at two different ripening degrees	2 RS (green and ready to eat)	Household conditions	Twenty different compounds (quinic acid, abscisic acid, benzoic acid, succinic acid, etc)	UHPLC-UV/ESI-TOF MS	[27]
To compare the effect of different pre-harvest conditions on the main bioactive compounds changes during ripening of imported avocado <i>cv. Hass</i> fruit	240 fruits from each country (Spain, Peru and Chile)	0, 1-, 2-, 4- and 7-days post-harvest in early, middle and late season	Day 0 at 5°C overnight Day 1, 2, 4 and 7 at 18-23°C	Perseitol, <i>D</i> -mannoheptulose, sucrose, fructose, glucose and five individual fatty acids	GC-FID HPLC-RID	[28]
To determinate changes in the concentrations and relationships between sugars, total soluble proteins and oil during <i>Hass</i> fruit ripening	Export grade <i>Hass</i> avocado fruit from commercial orchards near Tzaneen and Howick (South Africa)	5 or 6 RS (2, 5-, 8-, 11-, 13- and 15-days post-harvest or very similar intervals depending on the origin of the samples)	Ripened at 21 ± 2°C	Oil content, total soluble proteins, perseitol, <i>D</i> -mannoheptulose, sucrose, fructose and glucose	HPLC-RID	[29]

Aim of study	Samples	Period of study	Storage conditions	Chemical determinations / Determined compounds	Analytical platform/s	Ref.
To develop a method for sequential extraction and subsequent quantification of fatty acids and sugars on avocado mesocarp tissue	72 <i>Hass</i> fruits from Malaga (Spain)	3 RS (under-ripe, medium-ripe and eating-ripe)	Fruits arrived at lab 4 days after harvest. 12°C for 9 days in 3 L jars and then removed.	Dry matter, oil content, persectol, <i>D</i> -mannoheptulose, sucrose and five individual fatty acids	GC-FID HPLC-ELSD	[30]
To determine if exposure of fruit to sunlight could vary the biochemical compounds associated with maturity	Nine fruit per canopy and per cv. <i>Carmen</i> and cv. <i>Hass</i>	Study conducted during autumn, winter and spring seasons (February to January) during 2018/9 season	Fruits were sampled at two-week intervals and kept at 25°C for 7–10 days to allow ripening	Dry matter, oil content, persectol, <i>D</i> -mannoheptulose and total C <sub>7</sub> sugars	HPLC-RID	[31]
Dry matter, oil content and fatty acid composition of <i>Fuerte</i> and <i>Hass</i> fruits were examined with respect to the harvesting and post-harvest ripening period	<i>Fuerte</i> and <i>Hass</i> avocado fruits from Antalya (Turkey)	Fruits harvested in November, December, and January at one-month intervals. 3 RS (1-, 4-, and 8-days post-harvest)	Samples were kept for 8 days under ambient conditions (18-22°C) to ripen	Dry matter, oil content and seven individual fatty acids	GC-FID	[32]
To evaluate the effect of RS of <i>Hass</i> avocado on the content of hydrophilic and lipophilic compounds and their correlation with the antioxidant capacity	60 fruits in total (from Michoacan, Mexico). A sub-lot of 25 avocados for each RS	4 RS (0-, 4-, 8- and 12-days after arrival at lab)	14 days at 15°C	Respiration rate, ethylene production, dry matter, oil content, total phenolic content, flavonoid content and ten individual fatty acids	GC-MS GC-TCD GC-FID Spectrophotometry	[33]

Abbreviations used in the table in alphabetical order: CE (capillary electrophoresis); DAD (diode-array detector); ELSD (evaporative light scattering detector); ESI (electrospray ionization); FLD (Fluorescence detector); FID (flame ionization detector); GC (Gas chromatography); HESI (heated electrospray ionization); HPLC (high-performance liquid chromatography); IT (ion trap); PDA (photodiode-array detector); Q MS (quadrupole mass spectrometry); RID (refractive index detector); RS (ripening states); TCD (thermal conductivity detector); TOF MS (time of flight mass spectrometry); UHPLC (ultra-high-performance liquid chromatography); UV-VIS (ultraviolet-visible spectrophotometer).

## 2.2. Samples

The samples considered in the current study were obtained from the unique avocado germplasm collection maintained at the Institute for Mediterranean and Subtropical Horticulture (IHSM-UMA-CSIC) La Mayora in Malaga (Spain). A total of 45 samples were analyzed. *Hass* avocado harvest season in Spain lasts approximately from January to May. The specific time period considered in this research started at the end of February (27<sup>th</sup> February) and ended in almost mid-April (9<sup>th</sup> April), covering the most important production months in Spain, with five time-points being evaluated. Table 2 contains information about the samples considered in this study, including details about date of collection/harvest in the orchard, date of release from cold storage, number of days in cold storage, and number of replicates in each case. At the beginning of the study, a considerable number of avocados were harvested from La Mayora orchard. Some avocados were left directly at room temperature (simulating domestic ripening conditions) and left until they reached their ready-to-eat stage. The rest of the fruit was placed in the cold room (between  $4.41 \pm 0.84^{\circ}\text{C}$  and  $93.05 \pm 1.45\%$  of humidity). After 10, 20, 30 and 40 days, two events took place: a) fruits were harvested again from the orchard and left at room temperature; and b) the samples that had been in the storage chamber for a certain period of time were removed and placed at room temperature. No fruit was processed until the optimum ripeness stage for consumption was reached. Each sample consisted of different pieces of mesocarp from 4-5 avocado fruits. Each time-point in turn, as can be seen in the table, was composed of five different samples (five replicates). Fruits were peeled, chopped, lyophilized, crushed, homogenized and frozen at  $-20^{\circ}\text{C}$ .

DM was evaluated according to the AOAC 920.151 method [34] as soon as the fruit were detached from the tree.

**Table 2.** Details of the *Hass* avocado samples considered in this study

	Collection date*	Cold chamber output date*	Days in cold chamber	Number of biological replicates	DM <sup>†</sup>
t <sub>0</sub>	27/02	-	-	5	31
t <sub>1</sub> cold stored	27/02	08/03	10	5	
t <sub>1</sub> on-tree	08/03	-	-	5	32
t <sub>2</sub> cold stored	27/02	19/03	20	5	
t <sub>2</sub> on-tree	19/03	-	-	5	32
t <sub>3</sub> cold stored	27/02	29/03	30	5	
t <sub>3</sub> on-tree	29/03	-	-	5	33
t <sub>4</sub> cold stored	27/02	09/04	40	5	
t <sub>4</sub> on-tree	09/04	-	-	5	34

\*Dates are indicated as follows: "day of the month/month".

<sup>†</sup>The found DM values can be considered to be normal for what is usually found in *Hass* avocados in Spain in these dates of the harvest season. SD of DM measurements were close to 1 approx.

## 2.3. Extraction procedure

The applied sample extraction procedure was the one previously described by Hurtado-Fernández et al. [23]. Sample extracts were prepared by mixing 0.5 g of frozen, dried and

homogenized sample with 40 mL of pure MeOH and the proper amount of IS to obtain 25 mg L<sup>-1</sup> of it in the final extract. After 3 min of Vortex shaking, the tubes were introduced into an ultrasound bath for 30 min, with a final centrifugation step of 3 min at 5000 rpm. Once the two phases were separated, the supernatant was transferred to a flask. The solid residue was re-extracted by adding 20 mL of pure MeOH and applying the same procedure (2<sup>nd</sup> extraction cycle). Both supernatant were mixed and evaporated to dryness in a rotary evaporator. Finally, the residue was redissolved in 1 mL of pure MeOH. Two extracts were prepared for each sample.

Furthermore, to control instrument repeatability and to evaluate several parameters considered for the validation of the method, a representative quality control (QC) sample was prepared by mixing equivalent amounts of all the extracts.

#### 2.4. Liquid chromatography-Mass spectrometry analyses

Two different LC-MS platforms were used in this study. LC-MS system with a high-resolution MS analyzer was used with qualitative purposes, whereas the LC platform coupled to a low resolution MS was used to carry out the quantitation of the analytes of interest. The instrument used to analyze the total number of avocado extracts considered within this study (with quantitative purposes) was a 1260 Infinity Agilent (Agilent Technologies, Waldbronn, Germany) equipped with a Zorbax C<sub>18</sub> column (4.6 x 150 mm, 1.8 μm particle size) coupled to an Esquire 2000 Ion Trap (IT) mass spectrometer (Bruker Daltonics, Bremen, Germany) by means of an electrospray ionization (ESI) source. Some representative samples were analyzed with an Acquity UPLC™ H-Class system coupled to a QTOF SYNAPT G2 MS (Waters, Manchester, UK) through an ESI interface. The chromatographic conditions were the same in both platforms. The analytical column was set at 25°C and analytes were eluted with 0.5% AcH in water (mobile phase A) and pure acetonitrile (mobile phase B) using a flow rate of 0.8 mL/min. The following solvent gradient was applied: 0 min, 95% A and 5% B; 20.5 min, 30% A and 70% B; 22 min, 0% A and 100% B; at 23.5 min, the system returned to initial conditions and the column was re-equilibrated for 3 min. A volume of 10 μL was injected in each case (both for extracts and pure standards).

The low resolution MS was operated in negative mode and data were acquired in Full Scan mode for a mass range from 50 to 1000 *m/z*. Optimal parameters related to ESI source were the following: the nebulizer gas (nitrogen) was set at 30 psi, and the dry gas (nitrogen) flow rate and temperature were 9 L/min and 300°C, respectively. The capillary voltage was set at +3200 V and the end-plate offset at -500 V. These parameters were then transferred to the ESI-QTOF MS which operated both in negative and positive modes.

Agilent ChemStation (Agilent Technologies) and Esquire Control (Bruker Daltonics) were used to operate the LC and low resolution MS systems, respectively. The high resolution MS coupling was controlled with MassLynx (Waters). DataAnalysis 4.0 software (Bruker Daltonics, Bremen, Germany) was used for MS data processing. Microsoft Excel 2019 was used for quantitative data management and for representing the data graphically. Quantitative results were reported as mg

of analyte Kg<sup>-1</sup> in dry basis. Analysis of variance (one-way ANOVA) was performed using Statgraphics 19 (Statgraphics Technologies, Inc., The Plains, VA, USA). The significance of the differences at 5% ( $p < 0.05$ ) level between mean values was determined using the Tukey's test.

## 2.5. Validation studies

Pure standard solutions (both individual pure standards and mixtures of them), the QC and spiked extracts (with known added amounts of standards) were used for the validation of the method. Linearity, precision, trueness and possible matrix effect were evaluated.

Solutions of the five pure compounds (pantothenic, *p*-coumaric, ferulic and abscisic acids as well as epicatechin) were prepared in MeOH at ten different concentration levels over the range from the quantification limit to 200 mg L<sup>-1</sup> to establish external calibration curves and evaluate the linearity. Calibration curves were obtained for each standard by plotting the standard concentration as a function of the peak area and defining the least squares regression line. Each point of the calibration curve corresponded to the mean value from three independent injections ( $n=3$ ). When the pure standard of an analyte to be quantified was not commercially available, it was quantified in terms of the most similar molecule. Thus, hexoses of coumaric acid were quantified with *p*-coumaric acid external calibration curve; the other metabolites were quantified by using the equation of their own standard calibration curve. Specific calibration ranges were established for each compound.

Detection and quantification limits (LOD and LOQ) of each individual compound were calculated based on the signal/noise ratio (S/N) obtained at the lowest concentration level injected. Thus, the LOD and LOQ values were estimated by calculating the concentration that generated the S/N equal to 3 and 10, respectively.

The precision of the LC-MS method was evaluated in terms of repeatability (*intra*-day and *inter*-day) and expressed as coefficient of variation (%CV). The *intra*-day repeatability was obtained from seven injections of the QC carried out within the same sequence, whereas *inter*-day repeatability was obtained from the data from 14 injections of QC carried out on different sequences and, therefore, days. Trueness was expressed as recovery and was estimated by analyzing the samples before and after the addition of known concentrations of pure standards and calculating the difference between the obtained results. Different standard concentration levels within the linear range (low, medium and high) were used for the spiking experiments. Finally, matrix effect was evaluated by calculating a matrix effect coefficient [35] that compares the slope of the standard addition calibration in the QC and the external calibration in MeOH as follows:

$$\text{Matrix effect coefficient (\%)} = \left(1 - \frac{\text{slope of standard addition calibration line}}{\text{slope of external calibration line}}\right) \cdot 100$$

In general, a range of  $\pm 20\%$  has been established to consider that matrix effect is negligible.

### 3. RESULTS AND DISCUSSION

#### 3.1. Characterization of the metabolic profile of avocado mesocarp by LC-ESI-QTOF MS

A first qualitative exploration of the chromatographic profiles obtained was carried out. Avocado mesocarp is a quite complex matrix and the used LC-MS metabolic profiling approach made possible to detect a considerable number of compounds. Within the profile, a total of nine compounds were selected (see [Figure 1 Supplementary material](#)) taking into account: i) their relative abundance in the avocado mesocarp, ii) the possible fluctuation of their concentrations during the harvest season or the ripening process, and iii) the importance of some of these compounds in previous publications. Epicatechin, *p*-coumaric, ferulic, pantothenic and abscisic acids, and four hexoses of coumaric acid were the most relevant metabolites selected to be monitored in this study.

[Table 3](#) includes the retention time of each analyte, the detected *m/z* signals, and the peak assignment in positive and negative modes in LC-ESI-QTOF MS. MS signals for LC-ESI-IT MS in negative mode have also been reported in the table, since the quantitative analysis of the sample-set was carried out by using that coupling.

As stated, two hydroxycinnamic acids (*p*-coumaric acid and ferulic acid) and four hexoses of coumaric acid were selected to be quantified. Most hydroxycinnamic acids present in avocado are mainly conjugated with sugars or other small molecules such as quinic acid. Moreover, epicatechin (flavonoid), pantothenic acid (vitamin) and abscisic acid (phytohormone) were also appointed as analytes of interest and quantified by using their own pure standards. In elution order, the *m/z* signals detected for each metabolite were: Pantothenic acid gave a predominant MS signal at *m/z* 218.1032, epicatechin at *m/z* 289.0723, *p*-coumaric acid at *m/z* 163.0395 (together with another relevant signal at 119.0504 [M-H-44]<sup>-</sup>), ferulic acid at *m/z* 193.0505 and abscisic acid at *m/z* 263.1294 (in all these cases, the *pseudo*-molecular ion, [M-H]<sup>-</sup>, was the prevailing signal). In addition, coumaric acid hexose isomers I and II were tentatively identified, since their pure standards were not commercially available. Their identification was based on the following observations: a) the signals detected in TOF MS for these 2 compounds correspond to the *pseudo*-molecular ion (325.0932 and 325.0936 [M-H]<sup>-</sup>, respectively), the loss of a hexose moiety (145.0292 and 145.0298 [M-H-162(hexose)-18]<sup>-</sup>, for each isomer), and the typical signal of the *pseudo*-molecular ion of coumaric acid (163.0397 and 163.0403, apiece); b) they elute before *p*-coumaric acid (with a shorter retention time), which is logical, since the carbohydrate moiety confers these molecules a higher polarity; and c) other authors have previously considered the same tentative identification [25,36,37]. On the other hand, the MS signals that led to the identification of coumaric acid malonyl-hexose isomers I and II correspond to the *pseudo*-molecular ion 411.0910 and 411.0921 [M-H]<sup>-</sup>, the loss of a carboxylic acid moiety (367.1022 and 367.1030 [M-H-44 (CO<sub>2</sub>)]<sup>-</sup>), the loss of an hexose (-162) and malonyl group (-86) (145.0289 and 145.0287 [M-H-162-86 (hexose and malonyl)-18]<sup>-</sup>) and the typical signal of the *pseudo*-molecular ion of coumaric acid (163.0388

and 163.0393). The  $m/z$  signal of 367.1030 has also been assigned to the molecular formula  $C_{17}H_{20}O_9$  by other authors (as in our case), but they identified the substance as feruloylquinic acid [37]. The fact of detecting fragments typically related to *p*-coumaric acid, as well as the dimer of  $C_{18}H_{20}O_{11}$  ( $m/z$  823.1949), has led us to assign it the identity shown in Table 3 (coumaric acid malonyl-hexose isomer).

### 3.2. Analytical parameters of the LC-ESI-IT MS method

As previously stated, the applied method was validated considering linearity, LODs and LOQs, precision, trueness and matrix effect. Results were, in general, very satisfactory. The LODs ranged from 18.8 to 70.8  $\mu\text{g L}^{-1}$ , whilst the LOQs fluctuated between 62.5 and 123.2  $\mu\text{g L}^{-1}$ , for epicatechin and pantothenic acid, respectively. The *intra*-day repeatability did not exceed in any case the value of 7.26%, whilst the *inter*-day repeatability was always lower than 8.29% (both CV values corresponding to epicatechin). The trueness was found within the range from 97.7 to 113.0% (for pantothenic acid and epicatechin), and the matrix effect coefficients varied from -9.5 to 4.6%, for pantothenic and *p*-coumaric acids. Table 1 (Supplementary material) shows the analytical parameters of the LC-MS method used for the analysis of the avocado extracts.

### 3.3. Quantification of metabolites of interest by LC-ESI-IT MS

Concentration values found in the present study were the mean of five biological replicates extracted twice ( $n=10$ , 5 biological replicates  $\times$  2 analytical ones) and have been expressed in  $\text{mg Kg}^{-1}$  of dry weight (DW) with their corresponding standard deviation (Table 4).

Table 4 has been structured to give the quantitative values of each compound at the different time-points for both on-tree maturation and for avocados that were kept in cold storage. One-way ANOVA test followed by Turkey's test was applied to reveal whether there were significant differences in the concentration values among the different time-points belonging to the same strategy (on-tree or cold storage, respectively), or to determine whether there were quantitative differences at the same time-point as a consequence of the strategy considered (prolonged on-tree maturation vs. cold storage).

In order to evaluate in more detail, the results concerning each analyte, the graphs shown in Figure 1 were plotted. Each graph shows the evolution of each compound as the considered 10-day periods elapsed. The results for prolonged on-tree maturation are in one colour (green) and those for cold storage in a different one (orange). The magnitude of the standard deviations, in some cases, is substantial, which is perfectly normal considering that each value comes from a sample composed of five biological replicates (extracted twice).

**Table 3.** Peak assignment of the metabolites studied in this work found in the avocado samples

LC-ESI-QTOF MS				LC-ESI-IT MS		Molecular formula [M] generated	Assignment <sup>c</sup>
ESI(+) QTOF MS <sup>a</sup>	ESI(-) QTOF MS <sup>a</sup>	For experimental [M-H] <sup>-</sup>		Rt (min)	ESI(-) IT MS <sup>a</sup>		
		Error (ppm) <sup>b</sup>	mSigma value <sup>b</sup>				
220.1156 [M+H] <sup>+</sup> 242.0975 [M+Na] <sup>+</sup> 258.0636 [M+K] <sup>+</sup> 202.1050 [M+H-18] <sup>+</sup> 184.0952 [M+H-18-18] <sup>+</sup>	<u>218.1032</u> [M-H] <sup>-</sup> 146.0811 [M-H-28-44] <sup>-</sup> 459.1898 [2M-H+23] <sup>-</sup>	0.4	1.8	5.6	<u>218.0</u> [M-H] <sup>-</sup> 260.9 [M-H+44] <sup>-</sup> 437.1 [2M-H] <sup>-</sup>	C <sub>9</sub> H <sub>17</sub> NO <sub>5</sub>	Pantothenic acid*
<u>349.0791</u> [M+Na] <sup>+</sup> 365.0582 [M+K] <sup>+</sup>	<u>325.0932</u> [M-H] <sup>-</sup> 163.0397 [M-H-162] <sup>-</sup> 145.0292 [M-H-162-18] <sup>-</sup> 117.0337 [M-H-162-18-28] <sup>-</sup>	0.9	2.8	7.9	<u>325.0</u> [M-H] <sup>-</sup> 163.0 [M-H-162] <sup>-</sup> 145.0 [M-H-162-18] <sup>-</sup>	C <sub>15</sub> H <sub>18</sub> O <sub>8</sub>	Coumaric acid hexose I
<u>349.0793</u> [M+Na] <sup>+</sup> 365.0558 [M+K] <sup>+</sup>	<u>325.0936</u> [M-H] <sup>-</sup> 163.0403 [M-H-162] <sup>-</sup> 145.0298 [M-H-162-18] <sup>-</sup> 117.0335 [M-H-162-18-28] <sup>-</sup>	1.3	4.0	8.3	<u>325.0</u> [M-H] <sup>-</sup> 163.0 [M-H-162] <sup>-</sup> 145.1 [M-H-162-18] <sup>-</sup>	C <sub>15</sub> H <sub>18</sub> O <sub>8</sub>	Coumaric acid hexose II
<u>291.0856</u> [M+H] <sup>+</sup> 313.0650 [M+Na] <sup>+</sup> 165.0551 [M+H-126] <sup>+</sup>	<u>289.0723</u> [M-H] <sup>-</sup>	1.1	3.8	8.8	<u>289.0</u> [M-H] <sup>-</sup>	C <sub>15</sub> H <sub>14</sub> O <sub>6</sub>	Epicatechin*
413.1051 [M+H] <sup>+</sup> <u>435.0866</u> [M+Na] <sup>+</sup> 451.0609 [M+K] <sup>+</sup> 165.0521 [M+H-162-86] <sup>+</sup> 147.0425 [M+H-86-162-18] <sup>+</sup>	411.0910 [M-H] <sup>-</sup> 823.1943 [2M-H] <sup>-</sup> <u>367.1022</u> [M-H-44] <sup>-</sup> 205.0495 [M-H-44-162] <sup>-</sup> 163.0388 [M-H-162-86] <sup>-</sup> 145.0289 [M-H-180-86] <sup>-</sup>	1.6	8.2	9.4	410.9 [M-H] <sup>-</sup> <u>367.0</u> [M-H-44] <sup>-</sup> 205.0 [M-H-44-162] <sup>-</sup> 163.1 [M-H-162-86] <sup>-</sup> 145.1 [M-H-162-86-18] <sup>-</sup>	C <sub>18</sub> H <sub>20</sub> O <sub>11</sub>	Coumaric acid malonyl-hexose I
413.1044 [M+H] <sup>+</sup> <u>435.0858</u> [M+Na] <sup>+</sup> 451.0541 [M+K] <sup>+</sup> 165.0522 [M+H-162-86] <sup>+</sup> 147.0429 [M+H-162-86-18] <sup>+</sup>	411.0921 [M-H] <sup>-</sup> 823.1949 [2M-H] <sup>-</sup> <u>367.1030</u> [M-H-44] <sup>-</sup> 205.0500 [M-H-44-162] <sup>-</sup> 163.0393 [M-H-162-88] <sup>-</sup> 145.0287 [M-H-180-86] <sup>-</sup>	1.1	17.1	9.7	411.0 [M-H] <sup>-</sup> <u>367.0</u> [M-H-44] <sup>-</sup> 205.0 [M-H-44-162] <sup>-</sup> 163.0 [M-H-162-86] <sup>-</sup> 145.0 [M-H-162-86-18] <sup>-</sup>	C <sub>18</sub> H <sub>20</sub> O <sub>11</sub>	Coumaric acid malonyl-hexose II

LC-ESI-QTOF MS				LC-ESI-IT MS		Molecular formula [M] generated	Assignment <sup>c</sup>
ESI(+) QTOF MS <sup>a</sup>	ESI(-) QTOF MS <sup>a</sup>	For experimental [M-H] <sup>-</sup>		Rt (min)	ESI(-) IT MS <sup>a</sup>		
		Error (ppm) <sup>b</sup>	mSigma value <sup>b</sup>				
165.0477 [M+H] <sup>+</sup> 203.0017 [M+K] <sup>+</sup> <u>147.0433</u> [M+H-18] <sup>+</sup>	<u>163.0395</u> [M-H] <sup>-</sup> 119.0504 [M-H-44] <sup>-</sup>	0.0	0.0	10.4	<u>162.9</u> [M-H] <sup>-</sup> 119.1 [M-H-44] <sup>-</sup>	C <sub>9</sub> H <sub>8</sub> O <sub>3</sub>	<i>p</i> -Coumaric acid*
195.0949 [M+H] <sup>+</sup> 233.0128 [M+K] <sup>+</sup> <u>177.0539</u> [M+H-18] <sup>+</sup> 145.0271 [M+H-50] <sup>+</sup>	<u>193.0505</u> [M-H] <sup>-</sup> 178.0263 [M-H-15] <sup>-</sup> 134.0379 [M-H-15-44] <sup>-</sup>	0.4	2.1	11.0	<u>193.0</u> [M-H] <sup>-</sup> 178.0 [M-H-15] <sup>-</sup> 134.1 [M-H-15-44] <sup>-</sup>	C <sub>10</sub> H <sub>10</sub> O <sub>4</sub>	Ferulic Acid*
265.1436 [M+H] <sup>+</sup> 287.1254 [M+Na] <sup>+</sup> 303.0945 [M+K] <sup>+</sup> <u>247.1326</u> [M+H-18] <sup>+</sup> 201.1273 [247-46] <sup>+</sup> 187.1117 [247-60] <sup>+</sup> 163.0749 [M+H-102] <sup>+</sup>	<u>263.1294</u> [M-H] <sup>-</sup> 219.1390 [M-H-44] <sup>-</sup> 153.0922 [M-H-44-66] <sup>-</sup> 549.2435 [2M-H+23] <sup>-</sup>	1.1	4.2	13.6	<u>263.0</u> [M-H] <sup>-</sup> 219.3 [M-H-44] <sup>-</sup> 153.2 [M-H-44-66] <sup>-</sup>	C <sub>15</sub> H <sub>20</sub> O <sub>4</sub>	Abscisic acid*

<sup>a</sup> Different *m/z* values rather than [M+H]<sup>+</sup> / [M-H]<sup>-</sup> were detected in the MS spectra; when those ions were more intense than the corresponding [M+H]<sup>+</sup> / [M-H]<sup>-</sup>, they have been underlined. The mentioned different *m/z* values mainly correspond to in-source fragments (typical losses detected were -18 (H<sub>2</sub>O), -28 (CO), -44 (CO<sub>2</sub>), -162 (hexose)) and to sodium [M+23]<sup>+</sup> and potassium [M+49]<sup>+</sup> adducts, in negative and positive polarities, respectively.

<sup>b</sup> Values of error and mSigma did not exceed 1.6 and 17.1, apiece.

<sup>c</sup> (I, II) different isomers; (\*) identification confirmed by comparison with authentic standards.

**Table 4.** Quantitative results (mg Kg<sup>-1</sup>, dry weight) obtained for the determined metabolites in avocado mesocarp by using LC-ESI-IT MS

Time (days) (t <sub>a</sub> )	Tree	Cold storage	Tree	Cold storage	Tree	Cold storage
<i>p</i> -Coumaric acid*			coumaric acid hexose			
			I		II	
0 (t <sub>0</sub> )	36a <sup>Δ</sup> ± 6	36a <sup>Δ</sup> ± 6	165a <sup>Δ</sup> ± 36	165ab <sup>Δ</sup> ± 36	54ab <sup>Δ</sup> ± 14	54a <sup>Δ</sup> ± 14
10 (t <sub>1</sub> )	29a <sup>Δ</sup> ± 5	40a <sup>Δ</sup> ± 4	130a <sup>Δ</sup> ± 37	232a <sup>Δ</sup> ± 98	38ac <sup>Δ</sup> ± 6	54a <sup>Δ</sup> ± 16
20 (t <sub>2</sub> )	29a <sup>Δ</sup> ± 3	17b ± 2	164a <sup>Δ</sup> ± 26	94bc ± 23	65b <sup>Δ</sup> ± 17	31bc ± 10
30 (t <sub>3</sub> )	37a <sup>Δ</sup> ± 6	16b ± 5	231b <sup>Δ</sup> ± 40	137abc <sup>Δ</sup> ± 57	45ab <sup>Δ</sup> ± 12	40ab <sup>Δ</sup> ± 14
40 (t <sub>4</sub> )	11b <sup>Δ</sup> ± 2	4c ± 1	29c <sup>Δ</sup> ± 10	50c <sup>Δ</sup> ± 17	21c <sup>Δ</sup> ± 5	13c <sup>Δ</sup> ± 5
<i>ferulic acid</i> *			coumaric acid malonyl-hexose			
			I		II	
0 (t <sub>0</sub> )	6a <sup>Δ</sup> ± 2	6a <sup>Δ</sup> ± 2	15ab <sup>Δ</sup> ± 4	15a <sup>Δ</sup> ± 4	32ab <sup>Δ</sup> ± 9	32a <sup>Δ</sup> ± 9
10 (t <sub>1</sub> )	6.9a <sup>Δ</sup> ± 0.5	15b ± 3	10ac <sup>Δ</sup> ± 2	25b ± 9	18c <sup>Δ</sup> ± 4	37a ± 7
20 (t <sub>2</sub> )	3.1b <sup>Δ</sup> ± 0.8	11bc ± 2	16ab <sup>Δ</sup> ± 2	3c ± 1	38b <sup>Δ</sup> ± 5	8b ± 4
30 (t <sub>3</sub> )	7a <sup>Δ</sup> ± 2	12b <sup>Δ</sup> ± 3	23b <sup>Δ</sup> ± 9	5c ± 2	24ac <sup>Δ</sup> ± 8	11b <sup>Δ</sup> ± 4
40 (t <sub>4</sub> )	1.3b <sup>Δ</sup> ± 0.2	7ac ± 3	6c <sup>Δ</sup> ± 2	0.6c ± 0.2	15c <sup>Δ</sup> ± 5	1.1b ± 0.3
<i>epicatechin</i> *		<i>pantothenic acid</i> *		<i>abscisic acid</i> *		
0 (t <sub>0</sub> )	21a <sup>Δ</sup> ± 9	21a <sup>Δ</sup> ± 9	14ab <sup>Δ</sup> ± 3	14a <sup>Δ</sup> ± 3	12ab <sup>Δ</sup> ± 2	12a <sup>Δ</sup> ± 2
10 (t <sub>1</sub> )	2.2b <sup>Δ</sup> ± 0.8	17a ± 6	13.0ab <sup>Δ</sup> ± 0.4	11a <sup>Δ</sup> ± 3	16a <sup>Δ</sup> ± 5	17b <sup>Δ</sup> ± 2
20 (t <sub>2</sub> )	19a <sup>Δ</sup> ± 4	10a ± 3	11a <sup>Δ</sup> ± 3	14a <sup>Δ</sup> ± 3	12ab <sup>Δ</sup> ± 3	16b <sup>Δ</sup> ± 3
30 (t <sub>3</sub> )	32c <sup>Δ</sup> ± 6	21a <sup>Δ</sup> ± 10	14ab <sup>Δ</sup> ± 1	17a <sup>Δ</sup> ± 4	11.9ab <sup>Δ</sup> ± 0.7	15ab <sup>Δ</sup> ± 2
40 (t <sub>4</sub> )	7b <sup>Δ</sup> ± 2	16a ± 5	16b <sup>Δ</sup> ± 3	15a <sup>Δ</sup> ± 2	9b <sup>Δ</sup> ± 1	13ab ± 2

Concentrations are expressed as mean ± SD. n = 10; \*Compounds whose identity was confirmed by using pure standards; I and II are isomers of the same compound; Different letters in the same column (for each analyte) shows statistical differences ( $p \leq 0.05$ ) among the diverse time-points; different symbol (<sup>Δ</sup>) –meaning presence of the symbol in a column and absence of it in the other- at the same line shows statistical differences ( $p \leq 0.05$ ) when comparing on-tree maturation vs. cold storage.

It is difficult to compare the quantitative results in absolute terms with those reported in other works, as the concentrations of these compounds are highly dependent on the avocado variety, the harvest period, the ripening index, as well as other factors listed in the introduction. Moreover, some of these compounds have not been previously determined in avocado samples. As reported in the quantitative table, the average concentrations for avocado samples at  $t_0$  (the beginning of the study) were as follows:  $36 \pm 6$  mg Kg<sup>-1</sup> DW of *p*-coumaric acid,  $6 \pm 2$  mg Kg<sup>-1</sup> DW of ferulic acid,  $21 \pm 9$  mg Kg<sup>-1</sup> DW of epicatechin,  $14 \pm 3$  mg Kg<sup>-1</sup> DW of pantothenic acid, and  $12 \pm 2$  mg Kg<sup>-1</sup> DW of abscisic acid. As far as coumaric acid derivatives are concerned, the concentrations found were  $165 \pm 36$  and  $54 \pm 14$  mg Kg<sup>-1</sup> DW for coumaric acid hexose isomers I and II, respectively, and  $15 \pm 4$  and  $32 \pm 9$  mg Kg<sup>-1</sup> DW for coumaric acid malonyl-hexose I and II, apiece. In the following sub-sections the results will be analyzed with more detail by grouping the compounds by chemical families, paying attention to possible trends and comparing the effect of the two strategies considered in this research on the final fruit composition (at edible ripeness).

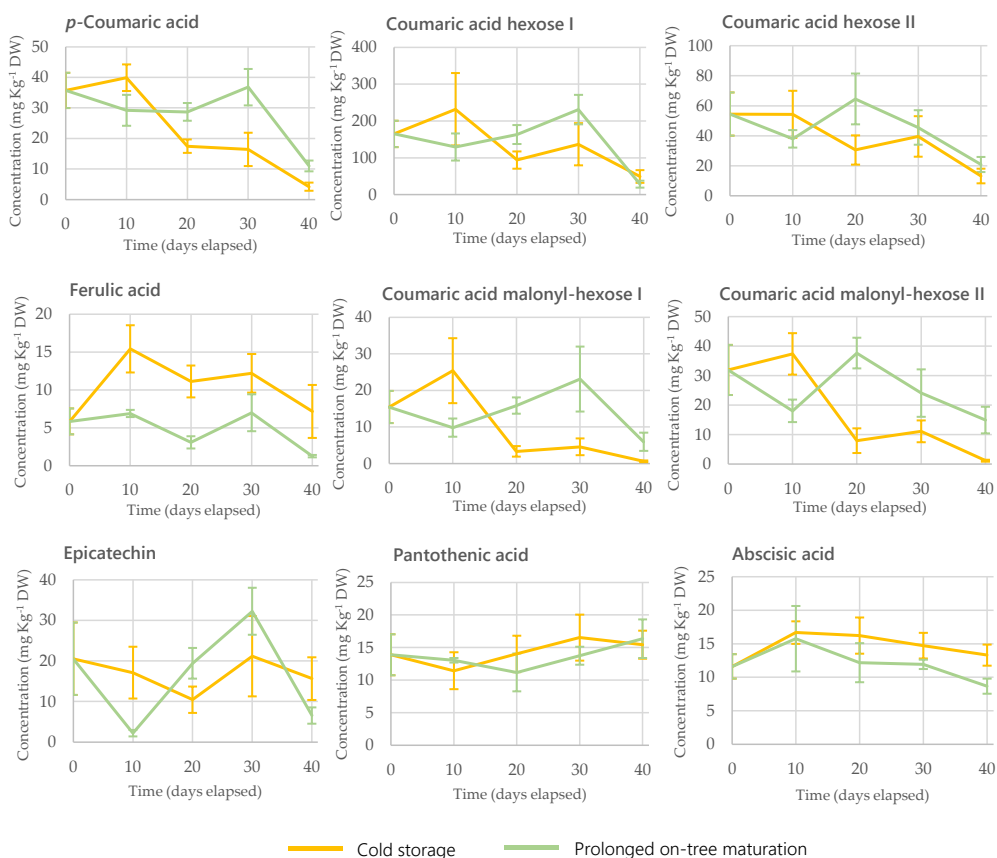


**Figure 1.** Effect of the two management strategies on the quantitative evolution of phenolic acids or related substances (*p*-coumaric and ferulic acid, and hexoses of coumaric acid), epicatechin (flavonoid), pantothenic acid (vitamin) and abscisic acid (phytohormone) over a period of 40 days

### 3.3.1. Phenolic acids and related compounds

The hydroxycinnamic acids are abundant in the plant cell walls and are characterized by their high antioxidant capacity [38]. They are usually accumulated in higher amounts in avocado pulp with other hydroxybenzoic acids and procyanidins [39,40]. In the current study, initial concentration levels of *p*-coumaric acid were notably higher than those of ferulic acid ( $36 \pm 6$  mg Kg<sup>-1</sup> DW and  $6 \pm 2$  mg Kg<sup>-1</sup> DW, respectively). These values were of the same order of magnitude as those previously described in *Hass* avocados and other varieties by different authors [23,25,37] although, as explained above, a comparison is difficult to make due to the diverse factors that affect the concentration of bioactive substances in this fruit. After 30 days on-tree maturation, levels of *p*-coumaric acid remained relatively stable, with a final significant decrease ( $p \leq 0.05$ ) of about 68% on the last time-point (40 days). On the contrary, for cold storage, a pronounced decline was observed (after an initial slight increase) for the concentrations of this metabolite over time. About 53% reduction in the levels of this phenolic acid was already observed after 20 days, reaching an 88% reduction at the last considered time-point. A comparable observation was reported in a previous study on avocado ripening process with a similar declining behaviour in *p*-coumaric acid (in that case the authors considered just two ripening stages) [37]. In general, the concentrations of this phenolic acid in the fruit at the ready-to-eat stage were higher when the avocados had remained on the tree for longer (except for the last time-point considered ( $t_4$ ), which falls within the late harvesting period of *Hass* in Spain.).

Ferulic acid showed a different behaviour than *p*-coumaric acid. The evolution of its concentration in avocados that remained longer in the tree was not clear, although the concentration after 40 days was significantly lower ( $1.3 \pm 0.2$  mg Kg<sup>-1</sup> DW) than the one at the initial time-point. After cold storage, ferulic acid concentrations increased significantly ( $p \leq 0.05$ ) during the first 30 days, reaching a value similar to the initial one at the end of the study (40-days' time-point) with  $7 \pm 3$  mg Kg<sup>-1</sup> DW.

From the metabolites considered within the current study, the isomers of coumaric acid hexose were those found at higher concentrations in the avocado mesocarp; levels of isomer I varied from  $165 \pm 36$  to  $29 \pm 10$  mg Kg<sup>-1</sup> DW for the on-tree longer maturation trial and from  $165 \pm 36$  to  $50 \pm 17$  mg Kg<sup>-1</sup> DW for the cold storage. An initial but non-significant increase was observed in cold storage, whereas the opposite trend was found in the tree. On successive days, the concentration of hexose (isomer I) progressively raised in the tree until the fourth time point (30 days) and then suddenly declined significantly. Coumaric acid hexose isomer II was found at more or less stable concentration levels in the tree for 30 days, and after that, the found amount decreased considerably ( $21 \pm 5$  mg Kg<sup>-1</sup> DW). In contrast, in the cold storage there was a relatively steady decline after the first 10 days for this analyte. There were only statistically significant differences in the concentration of this compound between on-tree vs. cold chamber at  $t_2$  (20 days). The protection exerted by the tree on the fruit could have led to a slightly superior stability compared to the fruits stored in a cold chamber.

The isomer I of coumaric acid malonyl-hexose exhibited a very similar behaviour to coumaric acid hexose I (both on-tree and cold storage). The same was evident for coumaric acid malonyl-hexose II when compared to coumaric acid hexose II.

Results from this section might reveal that the phenolic acids and related compounds accumulate during the early and mid *Hass* harvesting season in Spain (27<sup>th</sup> February to 29<sup>th</sup> March). However, for fruit harvested later (4<sup>th</sup> April), the amount of these compounds is lower. On the contrary, a decrease in the concentration of phenolic acids and related substances occurs when avocado fruit is stored under cold conditions for more than 10 days.

### **3.3.2. Other analytes of interest belonging to different chemical categories**

Epicatechin is a flavonoid that belongs to the flavan-3-ol family and it has been related with neuroprotective and antioxidant effects [12,15]. Its initial concentration was  $21 \pm 9$  mg Kg<sup>-1</sup> DW, similar to the value ( $15$  mg Kg<sup>-1</sup> DW) reported in a previous study for the same avocado variety [41]. Throughout the maturation process in the tree or softening in the cold chamber, the quantitative evolution of epicatechin was not clear, so it was not possible to establish a clear pattern. The evolution was similar in both cases, showing upward and downward fluctuations. However, only for fruit from extended tree maturation, some significant differences were observed during the period covered by this research (with a minimum concentration at 10 days,  $2.2 \pm 0.8$  mg Kg<sup>-1</sup> DW, and a maximum at 30 days after the beginning of the harvest season,  $32 \pm 6$  mg Kg<sup>-1</sup> DW).

For pantothenic acid (vitamin B<sub>5</sub>), the initial quantitative level was lower than the one for epicatechin, being present at a concentration of  $14 \pm 3$  mg Kg<sup>-1</sup> DW. This vitamin is a precursor of coenzyme A synthesis and it is distributed on animal and vegetal kingdoms. Its consumption is related, for instance, with certain beneficial effects on the skin status [42]. The quantitative variation of pantothenic acid over the considered period was not notable in any case (neither in the tree nor in cold storage under controlled conditions). The fact just described would allow hypothesizing that this vitamin's levels are not conditioned by the pre- and post-harvest management conditions.

Abscisic acid was initially found in amounts of  $12 \pm 2$  mg Kg<sup>-1</sup> DW. For samples collected after a longer time in the tree, its concentration did not vary significantly over the time span considered in this study. Literature describes that the abscisic acid accumulation on mesocarp depends on the presence of ethylene in the external environment, with the highest concentrations observed just after the peak production of this volatile plant hormone [43]. In addition, it has been reported that abscisic acid is also affected by the external stress and other factors [44]. The ethylene produced by the avocado fruit when is detached from the tree could induce a greater stimulation, production and preservation of abscisic acid. The fruits that were stored in cold chamber could, therefore, exhibit significant differences over the ripening due to the enzyme activity and the poorer air circulation. What was observed in the current study for cold stored fruit was an initial increase of abscisic acid concentration and a reversion to starting levels after 30 days. Higher concentrations

of this compound were determined in the fruit stored in the cold ripening chambers ( $t_4$ ) when compared with the avocados which were attached to the tree for a longer period.

Chirinos et al. have recently carried out a study in which they evaluated *Hass* avocado fruits from two harvests which were subjected to hydrothermal treatment or left untreated and then stored for 30 and 50 days in a controlled atmosphere (with subsequent ripening at  $\sim 20^\circ\text{C}$ ) [45]. Found amounts of abscisic acid at edible ripeness and some of the trends described for the concentration of this analyte are in good agreement with the results included in this contribution.

In addition, Hurtado-Fernández et al. conducted a study where *Hass* avocado metabolic composition was evaluated over the harvest season; in the samples analyzed by those authors, the initial concentration values were somewhat higher than those described here for epicatechin, but lower for pantothenic acid and abscisic acid [23]. This is perfectly reasonable considering the variability of avocado's composition between seasons and harvest periods.

### 3.4. Total content of metabolites in the evaluated samples

Total metabolite contents were calculated as the sum of the nine metabolites quantified at each time-point and for both strategies. Standard deviations were established as the square root of the quadratic sum of the corresponding standard deviation for each individual compound and expressed in  $\text{mg Kg}^{-1}$  DW. Summative calculations were also made for phenolic acids. Figure 2 shows the corresponding representations using bar diagrams; on the left-hand side (Figure 2a) the overall sums have been represented (at the different time-points for the two management strategies) and on the right-hand side (Figure 2b) the sum of the phenolic acids can be seen. As phenolic acids are, in any case, the most abundant group of metabolites considered in this work, both representations are very similar. Statistically significant variations were observed according to the different management strategies, monitoring the maximum total metabolites content after 10 days of storage in a cold chamber and after 30 days of prolonged on-tree maturation. Altogether, there was a constant increase in total metabolites content while the fruit were attached to the tree ( $t_0$ ,  $t_1$ ,  $t_2$  and  $t_3$ ). In contrast, in cold-stored avocados, there was an initial increase in overall content (at 10 days) but a continued decrease thereafter. In both cases, a significant and pronounced final decline was observed (at the 40-days' time-point).

In the introductory section, very interesting articles that focused either on the determination of different parameters/compounds over the harvesting season or during the softening of the fruit were cited. All these works made very relevant contributions [16,20,21,32,33,36,43], however, almost all of them addressed the determination of other compounds (fatty acids, sugars, volatile compounds...) or the measurement of other parameters (sensory attributes, antioxidant activity, dry matter, days to ripen, total phenolic compounds, etc.). To the best of our knowledge, no work has been published with this experimental design evaluating the quantitative evolution of the nine metabolites selected in this research (certainly related to nutritional quality of avocado). Thus, the

amount of these bioactive compounds that, depending on the pre- and post-harvest management of avocado, reach the consumer has not been described so far.

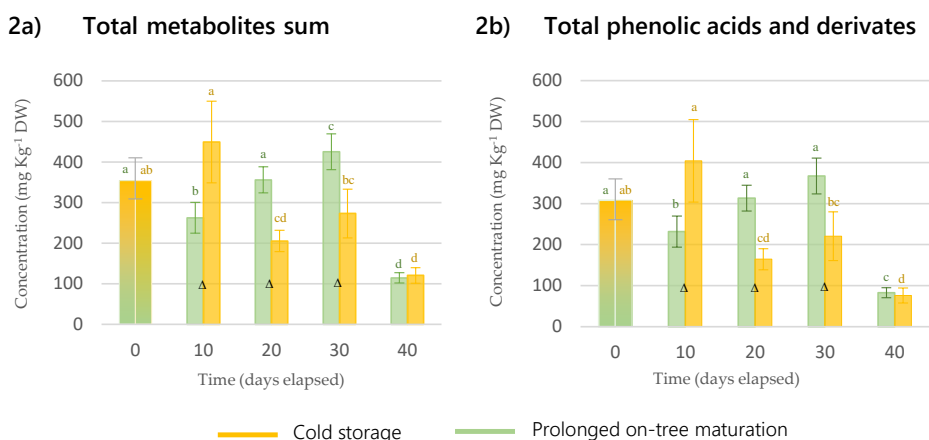


**Figure 2.** Bar diagram representing the sum (mg Kg<sup>-1</sup> DW) of all the avocado metabolites evaluated within this study (2a) and phenolic acids and derivatives (2b) for on-tree extended maturation and storage in a refrigerated chamber, at ten days intervals. Different letters on the same colour above the bars of the chart indicate statistically significant differences ( $p \leq 0.05$ ) after applying one-way ANOVA followed by Turkey's test to compare the concentration values among the different time-points belonging to the same strategy (on-tree or cold storage). The presence of the symbol ( $\Delta$ ) reveals statistically significant differences ( $p \leq 0.05$ ) when applying ANOVA followed by Turkey's test comparing the results of the two management strategies at the same time-point

Therefore, if the aim is to maximize the nutritional quality of the fruit, the optimum harvesting time for *Hass* avocados in Southern Spain (in the temporal interval evaluated here and under the conditions contemplated in this research) would be at the end of March. For continental exports, the optimum cold storage time for avocados picked at the end of February would be 10 days, after which the concentration of bioactive substances would decrease. All of the above means that the fruit could be harvested early in order to obtain economic benefits according to the needs of the market, while maintaining a high nutritional value. Moreover, early harvested fruit could remain in storage for up to 30 days without an unacceptable loss of metabolites of interest, although after 10 days the level of bioactives would be lower (for cold storage).

#### 4. CONCLUSIONS

The processes that take place in the avocado fruit during maturation and softening has been the subject of much research interest, but an experimental design such as the one envisaged here has not been described before. The perspective of this study was distinctive, as it focuses on finding out the effect of two different management strategies on the final composition of the avocado

fruit that reach the consumer and, thus, to some extent, on their potential health benefits. The effect of both harvest date and post-harvest management (cold storage) on the metabolic profile of *Hass* avocados grown in Spain between February and April (considering an interval of 40 days) was evaluated, taking into account nine metabolites of bioactive interest (and their summation). The two scenarios explored in this paper would be possible as long as domestic consumption or relatively short-distance exports are involved.

Our results indicate that the concentration of the most abundant metabolites of those evaluated (phenolic acids and related substances) rises over the early and mid *Hass* harvesting season in Spain (27th February-29th March). It is also possible to state that a drop in the concentration of phenolic acids and related substances occurs when avocado fruit is stored under cold conditions for more than 10 days, although it should be noted that up to about 30 days the fruit could be stored without a very significant decline in terms of bioactive substances. Pantothenic acid did not show drastic changes in any case, and for epicatechin it was not possible to establish a clear pattern. In the case of abscisic acid, higher concentrations were determined in avocados stored in the cold ripening chambers, probably due to the accumulation of ethylene in the environment that stimulates its synthesis. In an overall view, considering the evolution observed during the first 30 days of the study, the total content of bioactive compounds increases for avocados that remain longer on the tree, while it decreases for those avocados ripened in the chamber.

We firmly believe that this type of research is necessary, firstly, to delve further into "knowing what we eat" and secondly, to better understand the physiology and ripening phenomena of this interesting tropical fruit.

**Funding:** This work was supported by FPU grant to the first author from the Spanish Ministry of Science and Innovation (Grant number: FPU19/00700); LO-G is grateful to the Andalusian Regional Government for a contract for young doctors (Grant number: DOC\_01183). Additional funding was obtained by grant PID2019-109566RB-I00/AEI/10.13039/501100011033 funded by the Agencia Estatal de Investigación - Ministerio de Ciencia e Innovación, Spain. Funding for open access charge: Universidad de Granada / CBUA.

## References

1. Chen, H.; Morrell, P.L.; Ashworth, V.E.T.M.; De La Cruz, M.; Clegg, M.T. Tracing the Geographic Origins of Major Avocado Cultivars. *J. Hered.* **2009**, *100*, 56–65, doi:10.1093/jhered/esn068.
2. Dreher, M.L.; Davenport, A.J. Hass Avocado Composition and Potential Health Effects. *Crit. Rev. Food Sci. Nutr.* **2013**, *53*, 738–750, doi:10.1080/10408398.2011.556759.
3. Ramos-Aguilar, A.L.; Ornelas-Paz, J.; Tapia-Vargas, L.M.; Ruiz-Cruz, S.; Gardea-Béjar, A.A.; Yahia, E.M.; Ornelas-Paz, J. de J.; Pérez-Martínez, J.D.; Rios-Velasco, C.; Ibarra-Junquera, V. The Importance of the Bioactive Compounds of Avocado Fruit (*Persea Americana* Mill) on Human Health. *Biotecnia* **2019**, *27*, 154–162, doi:10.18633/biotecnia.v27i3.1047.

4. FAO. Statistics Division of Food and Agriculture Organization of the United Nations (FAOSTAT). Available online: <https://www.fao.org/faostat/en/#home> (accessed on 25 November 2021).
5. Hernández, I.; Uarrota, V.; Paredes, D.; Fuentealba, C.; Defilippi, B.G.; Campos-Vargas, R.; Meneses, C.; Hertog, M.; Pedreschi, R. Can Metabolites at Harvest Be Used as Physiological Markers for Modelling the Softening Behaviour of Chilean "Hass" Avocados Destined to Local and Distant Markets? *Postharvest Biol. Technol.* **2021**, *174*, doi:10.1016/j.postharvbio.2020.111457.
6. Ncama, K.; Magwaza, L.S.; Poblete-Echeverría, C.A.; Nieuwoudt, H.H.; Tesfay, S.Z.; Mditshwa, A. On-Tree Indexing of 'Hass' Avocado Fruit by Non-Destructive Assessment of Pulp Dry Matter and Oil Content. *Biosyst. Eng.* **2018**, *174*, 41–49, doi:10.1016/j.biosystemseng.2018.06.011.
7. Blakey, R.J. Evaluation of Avocado Fruit Maturity with a Portable Near-Infrared Spectrometer. *Postharvest Biol. Technol.* **2016**, *121*, 101–105, doi:10.1016/j.postharvbio.2016.06.016.
8. Burdon, J.; Lallu, N.; Haynes, G.; Francis, K.; Patel, M.; Laurie, T.; Hardy, J. Relationship between Dry Matter and Ripening Time in "Hass" Avocado. *Acta Hort.* **2015**, *1091*, 291–296, doi:10.17660/ActaHortic.2015.1091.36.
9. Lewis, C.E. The Maturity of Avocados—a General Review. *J. Sci. Food Agric.* **1978**, *29*, 857–866, doi:10.1002/jsfa.2740291007.
10. Schroeder, C.A. Growth and Development of the Avocado Fruit. *Calif. Avocado Soc.* **1958**, *42*, 114–118.
11. Rodríguez-López, C.E.; Hernández-Brenes, C.; Treviño, V.; Díaz de la Garza, R.I. Avocado Fruit Maturation and Ripening: Dynamics of Aliphatic Acetogenins and Lipidomic Profiles from Mesocarp, Idioblasts and Seed. *BMC Plant Biol.* **2017**, *17*, 9–12, doi:10.1186/s12870-017-1103-6.
12. Bhuyan, D.J.; Alsherbiny, M.A.; Perera, S.; Low, M.; Basu, A.; Devi, O.A.; Barooah, M.S.; Li, C.G.; Papoutsis, K. The Odyssey of Bioactive Compounds in Avocado (*Persea Americana*) and Their Health Benefits. *Antioxidants* **2019**, *8*, doi:10.3390/antiox8100426.
13. Salazar-López, N.J.; Domínguez-Avila, J.A.; Yahia, E.M.; Belmonte-Herrera, B.H.; Wall-Medrano, A.; Montalvo-González, E.; González-Aguilar, G.A. Avocado Fruit and By-Products as Potential Sources of Bioactive Compounds. *Food Res. Int.* **2020**, *138*, doi:10.1016/j.foodres.2020.109774.
14. Alkhalaf, M.I.; Alansari, W.S.; Ibrahim, E.A.; Elhalwagy, M.E.A. Anti-Oxidant, Anti-Inflammatory and Anti-Cancer Activities of Avocado (*Persea Americana*) Fruit and Seed Extract. *J. King Saud Univ. - Sci.* **2019**, *31*, 1358–1362, doi:10.1016/j.jksus.2018.10.010.
15. Ortega-Arellano, H.F.; Jimenez-Del-Rio, M.; Velez-Pardo, C. Neuroprotective Effects of Methanolic Extract of Avocado *Persea Americana* (Var. Colinred) Peel on Paraquat-Induced Locomotor Impairment, Lipid Peroxidation and Shortage of Life Span in Transgenic Knockdown Parkin *Drosophila Melanogaster*. *Neurochem. Res.* **2019**, *44*, 1986–1998, doi:10.1007/s11064-019-02835-z.
16. Arpaia, M.L.; Collin, S.; Sievert, J.; Obenland, D. Influence of Cold Storage Prior to and after Ripening on Quality Factors and Sensory Attributes of "Hass" Avocados. *Postharvest Biol. Technol.* **2015**, *110*, 149–157, doi:10.1016/j.postharvbio.2015.07.016.
17. Bower, J.P.; Cutting, J.G. Avocado Fruit Development and Ripening Physiology. In *Horticultural Reviews*; Janick, J., Ed.; John Wiley & Sons: Hoboken, NJ, USA, 1988; Vol. 10, pp. 229–271, doi:10.1002/9781118060834.ch7.
18. Ferreyra, R.; Defilippi, B.; Saavedra, J.; Sellés, G.; Robledo, P.; Arpaia, M.; Karlezi, D. Factores Precosecha Que Afectan La Postcosecha de La Palta Hass. *Boletín INIA* **2012**, *248*, 102.
19. Mpai, S.; Sivakumar, D. Influence of Growing Seasons on Metabolic Composition, and Fruit Quality of Avocado Cultivars at 'Ready-to-Eat Stage.' *Sci. Hortic.* **2020**, *265*, doi:10.1016/j.scienta.2019.109159.
20. Obenland, D.; Collin, S.; Sievert, J.; Negm, F.; Arpaia, M.L. Influence of Maturity and Ripening on Aroma Volatiles and Flavor in "Hass" Avocado. *Postharvest Biol. Technol.* **2012**, *71*, 41–50, doi:10.1016/j.postharvbio.2012.03.006.

21. Wang, M.; Zheng, Y.; Khuong, T.; Lovatt, C.J. Effect of Harvest Date on the Nutritional Quality and Antioxidant Capacity in “Hass” Avocado during Storage. *Food Chem.* **2012**, *135*, 694–698, doi:10.1016/j.foodchem.2012.05.022.
22. Villa-Rodríguez, J.A.; Yahia, E.M.; González-León, A.; Ifie, I.; Robles-Zepeda, R.E.; Domínguez-Avila, J.A.; González-Aguilar, G.A. Ripening of ‘Hass’ Avocado Mesocarp Alters Its Phytochemical Profile and the in Vitro Cytotoxic Activity of Its Methanolic Extracts. *South African J. Bot.* **2020**, *128*, 1–8, doi:10.1016/j.sajb.2019.09.020.
23. Hurtado-Fernández, E.; González-Fernández, J.J.; Hormaza, J.I.; Bajoub, A.; Fernández-Gutiérrez, A.; Carrasco-Pancorbo, A. Targeted LC-MS Approach to Study the Evolution over the Harvesting Season of Six Important Metabolites in Fruits from Different Avocado Cultivars. *Food Anal. Methods* **2016**, *9*, 3479–3491, doi:10.1007/s12161-016-0523-5.
24. Di Stefano, V.; Avellone, G.; Bongiorno, D.; Indelicato, S.; Massenti, R.; Lo Bianco, R. Quantitative Evaluation of the Phenolic Profile in Fruits of Six Avocado (Persea Americana) Cultivars by Ultra-High-Performance Liquid Chromatography-Heated Electrospray-Mass Spectrometry. *Int. J. Food Prop.* **2017**, *20*, 1302–1312, doi:10.1080/10942912.2016.1208225.
25. Contreras-Gutiérrez, P.K.; Hurtado-Fernández, E.; Gómez-Romero, M.; Hormaza, J.I.; Carrasco-Pancorbo, A.; Fernández-Gutiérrez, A. Determination of Changes in the Metabolic Profile of Avocado Fruits (Persea Americana) by Two CE-MS Approaches (Targeted and Non-Targeted). *Electrophoresis* **2013**, *34*, 2928–2942, doi:10.1002/elps.201200676.
26. Pedreschi, R.; Muñoz, P.; Robledo, P.; Becerra, C.; Defilippi, B.G.; van Eekelen, H.; Mumm, R.; Westra, E.; De Vos, R.C.H. Metabolomics Analysis of Postharvest Ripening Heterogeneity of “Hass” Avocados. *Postharvest Biol. Technol.* **2014**, *92*, 172–179, doi:10.1016/j.postharvbio.2014.01.024.
27. Hurtado-Fernández, E.; Pacchiarotta, T.; Gómez-Romero, M.; Schoenmaker, B.; Derks, R.; Deelder, A.M.; Mayboroda, O.A.; Carrasco-Pancorbo, A.; Fernández-Gutiérrez, A. Ultra High Performance Liquid Chromatography-Time of Flight Mass Spectrometry for Analysis of Avocado Fruit Metabolites: Method Evaluation and Applicability to the Analysis of Ripening Degrees. *J. Chromatogr. A* **2011**, *1218*, 7723–7738, doi:10.1016/j.chroma.2011.08.059.
28. Donetti, M.; Terry, L.A. Biochemical Markers Defining Growing Area and Ripening Stage of Imported Avocado Fruit Cv. Hass. *J. Food Compos. Anal.* **2014**, *34*, 90–98, doi:10.1016/j.jfca.2013.11.011.
29. Blakey, R.J.; Tesfay, S.Z.; Bertling, I.; Bower, J.P. Changes in Sugars, Total Protein, and Oil in “Hass” Avocado (Persea Americana Mill.) Fruit during Ripening. *J. Hortic. Sci. Biotechnol.* **2012**, *87*, 381–387, doi:10.1080/14620316.2012.11512880.
30. Meyer, M.D.; Terry, L.A. Development of a Rapid Method for the Sequential Extraction and Subsequent Quantification of Fatty Acids and Sugars from Avocado Mesocarp Tissue. *J. Agric. Food Chem.* **2008**, *56*, 7439–7445, doi:10.1021/jf8011322.
31. Shezi, S.; Magwaza, L.S.; Tesfay, S.Z.; Mditshwa, A. Biochemical Changes in Response to Canopy Position of Avocado Fruit (Cv. ‘Carmen’ and ‘Hass’) during Growth and Development and Relationship with Maturity. *Sci. Hortic.* **2020**, *265*, doi: 10.1016/j.scienta.2020.109227.
32. Ozdemir, F.; Topuz, A. Changes in Dry Matter, Oil Content and Fatty Acids Composition of Avocado during Harvesting Time and Post-Harvesting Ripening Period. *Food Chem.* **2004**, *86*, 79–83, doi:10.1016/j.foodchem.2003.08.012.
33. Villa-Rodríguez, J.A.; Molina-Corral, F.J.; Ayala-Zavala, J.F.; Olivas, G.I.; González-Aguilar, G.A. Effect of Maturity Stage on the Content of Fatty Acids and Antioxidant Activity of “Hass” Avocado. *Food Res. Int.* **2011**, *44*, 1231–1237, doi:10.1016/j.foodres.2010.11.012.
34. AOAC Association of Official Analytical Chemists. *Official Methods of Analysis of AOAC Int.* 2016, Latimer G.W, Ed. 20th ed.
35. Kmeňár, B.; Fodor, P.; Pareja, L.; Ferrer, C.; Martínez-Uroz, M.A.; Valverde, A.; Fernandez-Alba, A.R.

- Validation and Uncertainty Study of a Comprehensive List of 160 Pesticide Residues in Multi-Class Vegetables by Liquid Chromatography-Tandem Mass Spectrometry. *J. Chromatogr. A* **2008**, *1215*, 37–50, doi:10.1016/j.chroma.2008.10.121.
36. Campos, D.; Teran-hilares, F.; Chirinos, R.; Aguilar-galvez, A.; Garc, D.; Pacheco-avalos, A.; Pedreschi, R. Bioactive Compounds and Antioxidant Activity from Harvest to Edible Ripeness of Avocado Cv . Hass (Persea Americana) throughout the Harvest Seasons. *Int. J. Food Sci. Technol.* **2020**, *55*, 2208–2218, doi:10.1111/ijfs.14474.
  37. López-Cobo, A.; Gómez-Caravaca, A.M.; Pasini, F.; Caboni, M.F.; Segura-Carretero, A.; Fernández-Gutiérrez, A. HPLC-DAD-ESI-QTOF-MS and HPLC-FLD-MS as Valuable Tools for the Determination of Phenolic and Other Polar Compounds in the Edible Part and by-Products of Avocado. *LWT - Food Sci. Technol.* **2016**, *73*, 505–513, doi:10.1016/j.lwt.2016.06.049.
  38. Meyer, A.S.; Frankel, E.N. Antioxidant Activity of Hydroxycinnamic Acids on Human Low-Density Lipoprotein Oxidation. *Methods Enzymol.* **2001**, *335*, 256–265, doi:10.1016/S0076-6879(01)35248-5.
  39. Rodríguez-Carpena, J.G.; Morcuende, D.; Andrade, M.J.; Kylli, P.; Estevez, M. Avocado (Persea Americana Mill.) Phenolics, in Vitro Antioxidant and Antimicrobial Activities, and Inhibition of Lipid and Protein Oxidation in Porcine Patties. *J. Agric. Food Chem.* **2011**, *59*, 5625–5635, doi:10.1021/jf1048832.
  40. Rosero, J.C.; Cruz, S.; Osorio, C. Analysis of Phenolic Composition of Byproducts (Seeds and Peels) of Avocado (Persea Americana Mill.) Cultivated in Colombia. *Molecules* **2019**, *24*, 3209, doi:10.3390/molecules24173209.
  41. Hurtado-Fernández, E.; Pacchiarotta, T.; Mayboroda, O.A.; Fernández-Gutiérrez, A.; Carrasco-Pancorbo, A. Quantitative Characterization of Important Metabolites of Avocado Fruit by Gas Chromatography Coupled to Different Detectors (APCI-TOF MS and FID). *Food Res. Int.* **2014**, *62*, 801–811, doi:10.1016/j.foodres.2014.04.038.
  42. Djerassi, D. The Role of Vitamins in Aged Skin. *J. Appl. Cosmetol.* **1993**, *11*, 29–40.
  43. Meyer, M.D.; Chope, G.A.; Terry, L.A. Investigation into the Role of Endogenous Abscisic Acid during Ripening of Imported Avocado Cv. Hass. *J. Sci. Food Agric.* **2017**, *97*, 3656–3664, doi:10.1002/jsfa.8225.
  44. Bower, J.P.; Cutting, J.G.M.; Van Lelyveld, L.J. Long-Term Irrigation as Influencing Avocado Abscisic Acid Content and Fruit Quality. *South African Avocado Grow. Assoc. Yearb.* **1986**, *9*, 43–45.
  45. Chirinos, R.; Campos, D.; Martinez, S.; Llanos, S.; Betalleluz-Pallardel, I.; García-Ríos, D.; Pedreschi, R. The Effect of Hydrothermal Treatment on Metabolite Composition of Hass Avocados Stored in A. *Plants* **2021**, *10*, 2427, doi:10.3390/plants10112427.

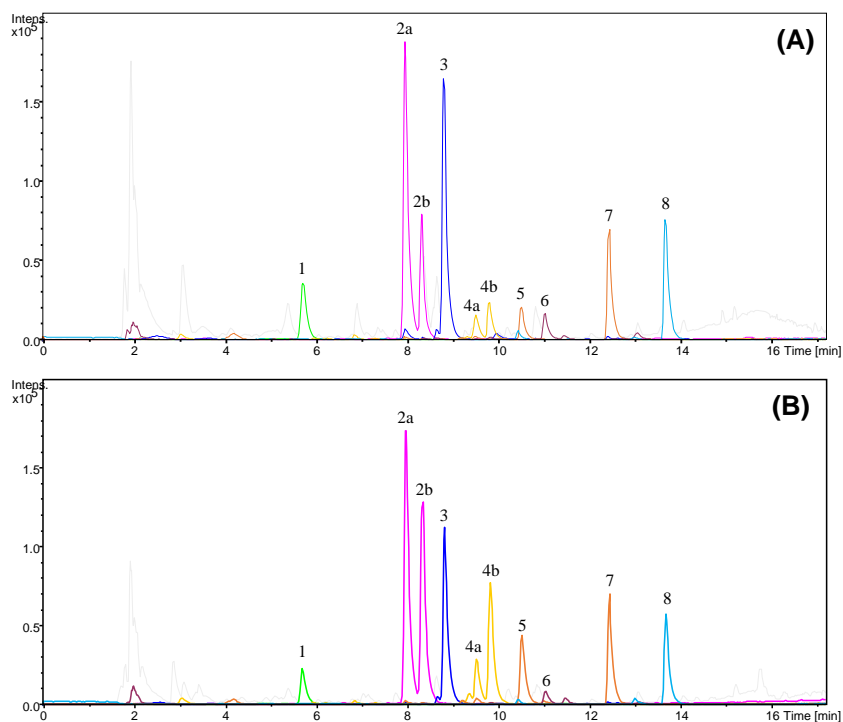


**Figure S1.** Profiles obtained for extracts of avocado samples at ready-to-eat stage after 30 days on (A) refrigerated storage and (B) prolonged on-tree maturation. Peaks identification: 1, pantothenic acid; 2, coumaric acid hexose I (2a) and II (2b); 3, epicatechin; 4, coumaric acid malonyl-hexose isomer I (4a) and II (4b); 5, *p*-coumaric acid; 6, ferulic acid; 7, *o*-coumaric acid (internal standard); 8, abscisic acid

**Table S1.** Analytical parameters of the LC-MS method used in the current study.

Compound	Rt (min)	Calibration curves	r <sup>2</sup>	LOD (µg L <sup>-1</sup> )	LOQ (µg L <sup>-1</sup> )	Lineal range (mg L <sup>-1</sup> )	Repeatability (% CV)		Trueness (%) <sup>c</sup>	Matrix effect coefficient (%) <sup>d</sup>
							Intra-day <sup>a</sup>	Inter-day <sup>b</sup>		
Pantothenic acid	5.6	y = 60676x - 7837.9	0.9861	70.8	235.8	LOQ - 15	4.36	5.83	97.7	-9.51
Epicatechin	8.8	y = 72604x + 52307	0.9934	18.8	62.5	LOQ - 25	7.26	8.29	113.0	1.39
		y = 30547x + 106	0.9999			25 - 100				-0.04
<i>p</i> -Coumaric acid	10.4	y = 25947x + 21083	0.9930	29.4	98.0	LOQ - 25	5.47	7.63	101.6	4.63
		y = 11175x + 447923	0.9899			25 - 200				-5.23
Ferulic acid	11.0	y = 25380x + 30965	0.9924	27.0	89.9	LOQ - 25	2.01	6.27	109.6	3.64
Abscisic acid	13.6	y = 91308x + 98537	0.9980	21.9	73.1	LOQ - 25	3.66	4.40	98.1	-0.28

Abbreviations used: Rt (Retention time); LOD (Limit of detection); LOQ (Limit of quantification).

<sup>a</sup> Coefficient of variation (%) corresponding to injections (n = 7) of the QC sample performed in the same sequence.

<sup>b</sup> Coefficient of variation (%) corresponding to injections (n = 14) of the QC sample carried out in sequences completed on different days.

<sup>c</sup> Trueness was measured by calculating the recovery (%), and it was estimated by analyzing samples before and after the addition of known concentrations of pure standards and calculating difference between the obtained results. The values included in this table are those obtained for an intermediate concentration level of all those tested.

<sup>d</sup> Matrix effect coefficient (%) = (1- (slope of the standard addition calibration line / slope of the calibration line with external standards)) · 100.

# Chapter

## Uncovering phytochemicals quantitative evolution in avocado fruit mesocarp during ripening: A targeted LC-MS metabolic exploration of *Hass*, *Fuerte* and *Bacon* varieties

Irene Serrano-García<sup>a</sup>, Carlos Saavedra Morillas<sup>a</sup>, María Gemma Beiro-Valenzuela<sup>a</sup>, Romina Monasterio<sup>a,b</sup>, Elena Hurtado-Fernández<sup>c</sup>, José Jorge Gonzalez-Fernandez<sup>d</sup>, José Ignacio Hormaza<sup>d</sup>, Romina Pedreschi<sup>e,f</sup>, Lucía Olmo-García<sup>a,✉</sup>, Alegría Carrasco-Pancorbo<sup>a</sup>

<sup>a</sup> *Department of Analytical Chemistry, Faculty of Sciences, University of Granada, Ave. Fuentenueva s/n, 18071, Granada, Spain*

<sup>b</sup> *Instituto de Biología Agrícola de Mendoza (IBAM), UNCuyo - CONICET, Facultad de Ciencias Agrarias, Chacras de Coria, Mendoza 5505, Argentina*

<sup>c</sup> *Department of Biological and Health Sciences, Faculty of Health Sciences, University of Loyola, Campus Sevilla, Avda. de las Universidades S/N, 41704 Dos Hermanas, Spain*

<sup>d</sup> *Institute for Mediterranean and Subtropical Horticulture (IHSM La Mayora-UMA-CSIC), 29750, Algarrobo-Costa, Málaga, Spain*

<sup>e</sup> *Escuela de Agronomía, Facultad de Ciencias Agronómicas y de los Alimentos, Pontificia Universidad Católica de Valparaíso, Calle San Francisco S/N, La Palma, Quillota, 2260000, Chile*

<sup>f</sup> *Millennium Institute Center for Genome Regulation (CRG), Santiago, 8331150, Chile*

✉ [luciaolmo@ugr.es](mailto:luciaolmo@ugr.es)

**Food Chemistry, 459 (2024) 140334**

<https://doi.org/10.1016/j.foodchem.2024.140334>



**Abstract:** Avocado ripening entails intricate physicochemical transformations resulting in desirable characteristics for consumption; however, its impact on specific metabolites and its cultivar dependence remains largely unexplored. This study employed LC-MS to quantitatively monitor 30 avocado pulp metabolites, including phenolic compounds, amino acids, nucleosides, vitamins, phytohormones, and related compounds, from unripe to overripe stages, in three commercial varieties (*Hass*, *Fuerte*, and *Bacon*). Multivariate statistical analysis revealed significant metabolic variations between cultivars, leading to the identification of potential varietal markers. Most monitored metabolites exhibited dynamic quantitative changes. Although phenolic compounds generally increased during ripening, exceptions such as epicatechin and chlorogenic acid were noted. Amino acids and derivatives displayed a highly cultivar-dependent evolution, with *Fuerte* demonstrating the highest concentrations and most pronounced fluctuations. In contrast to penstemide, uridine and abscisic acid levels consistently increased during ripening. Several compounds characteristic of the *Bacon* variety were delineated but require further research for identification and role elucidation.

**Keywords:** *Persea americana* Mill., phenolic compounds, amino acids, nucleosides, vitamins, phytohormones.

## 1. INTRODUCTION

The avocado (*Persea americana* Mill.) holds significant socio-economic importance and is highly valued both as fresh fruit and a versatile ingredient in various recipes. *P. americana* is a polymorphic species comprising several subspecies or horticultural races capable of hybridizing and producing a wide array of cultivars differing in botanical traits and edaphoclimatic preferences [1]. The global avocado industry is overwhelmingly dominated by *Hass*, accounting for 95% of commercial production due to its excellent pulp quality, higher yield, good and late on-tree storage, extended shelf life, high oil content and resistance to transport [2,3]. Other commercial hybrids include *Fuerte* and *Bacon* varieties, which are significant in Spain, the leading avocado producer in Europe [4]. Spain grows approximately 80% of *Hass*, 12% of *Fuerte*, 5% of *Bacon*, and 3% of other varieties [5].

Avocado fruit development comprises diverse physiological stages from cell division and enlargement during growth to lipid accumulation during maturation [6]. Unlike many other fruits, avocado maturation is primarily marked by the accumulation of lipids rather than carbohydrates and organic acids [2]. Both phases contribute to reach the fruit's physiological maturity, which is an essential indicator for determining the optimal harvesting time. The degree of maturity at harvest significantly impacts fruit quality and post-harvest ripening uniformity, thereby influencing consumer acceptance [7]. Avocado ripening occurs exclusively several days after harvest, marked by complex physiological and biochemical changes involving compound synthesis and degradation. As a climacteric fruit, avocado ripening is associated with an autocatalytic production

of ethylene and an increase in the rate of respiration, followed by a decrease as tissue senescence progresses to a state of over ripeness. Three distinct stages in respiration characterize the ripening process: pre-climacteric (minimum respiration), climacteric (peak respiration) and post-climacteric (decline in respiration) [8]. The most substantial changes occur during the pre-climacteric and climacteric stages, influencing fruit acceptability attributes such as texture, firmness, colour, flavour, and aroma. However, during the post-climacteric stage, fruit quality declines, rendering it more susceptible to pathogen attacks [6], partly attributed to the softening that takes place along ripening due to the activity of cell wall-degrading enzymes [9].

While fatty acids do not seem to act as respiratory substrates in avocado,  $C_7$  sugars, such as *D*-mannoheptulose and its polyol form perseitol, specific of avocado fruit in contrast to the more common  $C_6$  sugars, play an energetic role [10–12]. These  $C_7$  sugars have also been suggested to inhibit the ripening process while the fruit is still on the tree, as well as to contribute to the antioxidant capacity of the fruit [13,14]. Even though considerable research efforts have been dedicated to unravelling the physiological patterns of the aforementioned primary metabolites, the exploration of other minor yet equally crucial compounds has been somewhat neglected. For instance, there remains a dearth of knowledge regarding the impact of ripening on amino acid content, despite its significant influence on fruit flavour and quality [2]. A recent work has partially addressed this question, although it was not the main focus of the study [15]. Over the last decades, phenolic compounds have gained considerable scientific attention due to their health-promoting biological activity as well as their contribution to various aspects of fruit quality such as colour, flavour, bitterness, astringency, and oxidative stability [16,17]. While extensive information has been generated on the factors influencing phenolic content in avocado mesocarp, including genetic factors, geographical origin, harvesting time or growing conditions, studies specifically focusing on the relationship between ripening and phenolic compounds are limited, as illustrated in [Table 1](#). Most of these studies are relevant contributions but have often been restricted to a limited set of samples (typically covering only two ripening stages) or have not specifically aimed to unravel the complexities of climacteric ripening; instead, they assess the impact of post-harvest management on the concentrations of specific compounds in both green and ripe avocados. Villa-Rodríguez et al., considered 4 ripening stages but only reported total phenolic contents [18]. These same authors have recently carried out more detailed work analysing the dynamics of specific individual metabolites such as phenolic compounds, carotenoids, tocopherols, etc. at four different ripening stages [19]. However, such research is still restricted to a limited number of metabolites. In addition, most authors have focused on the *Hass* variety, largely overlooking possible cultivar-dependent factors.

**Table 1.** Studies assessing ripening dynamics in avocados listing the analytical methodologies used and the determinations made in each study. Papers are ordered by their published date

Cultivar	Ripening Stages	Sample Info	Methodology	Analytical Determinations	Observations	Ref.
<i>Hass</i>	Transport from orchard within 3 days (5-7 °C) RS1 (0 days after reception) RS2 (4 days) RS3 (8 days) RS4 (12 days)	60-fruit batch, a sub-batch of 25 avocados per RS (ripening at 15 °C)	GC-MS GC-TCD-FID UV-VIS	Respiration rate and ethylene production Physicochemical parameters Fatty acids content Total phenolic and flavonoid content Antioxidant capacity assays	First comprehensive study of climacteric ripening dynamics with several determinations and RS.	[18]
13 avocado varieties*	Unripe (at harvest time) Ripe (ready-to-eat stage)	Pulp of 3-4 pieces of fruit to compose a sample for each RS and variety	UHPLC-UV/ESI-TOF MS	Twenty metabolites including phenolic acids and related compounds, quinic acid, succinic acid, pantothenic acid, abscisic acid, and flavonoids	First comprehensive characterisation of C <sub>18</sub> avocado pulp profile Multivariate statistical analysis to discriminate varieties and RS	[20]
<i>Booth 7</i>	Unripe (1 day after harvest) 2 day-intervals for firmness Daily for ethylene production 3-d intervals for the rest of analysis	≈ 135 fruits	GC-PDHID	Fruit firmness and ethylene production Total phenolics and flavonoids assay Total antioxidant capacity Enzyme assays	The study primarily focused on investigating changes in preclimacteric stage avocado fruit treated with aqueous 1-methylcyclopropene and then ripened at 20°C	[21]
13 avocado varieties*	Unripe (at harvest time) Ripe (ready-to-eat stage)	Pulp of 3-4 pieces of fruit to compose a sample for each RS and variety	GC-FID/APCI-TOF MS	Analysis of 27 metabolites belonging to different chemical families	Evaluation of the potential of GC-APCI-MS in Food Metabolomics and comparison with GC-FID Multivariate statistical analysis to discriminate varieties and RS	[22]
13 avocado varieties*	Unripe (at harvest time) Ripe (ready-to-eat stage)	Pulp of 3-4 pieces of fruit to compose a sample for each RS and variety	GC-APCI-TOF MS	Non-targeted metabolic profiling	Multivariate statistical analysis to discriminate varieties and RS	[23]
<i>Hass</i>	Edible ripeness Over ripeness	≈ 10 kg of fruits	HPLC-DAD-ESI-QTOF-MS HPLC-FLD-MS	Phenolic and other polar compounds Flavan-3-ols	The main objective of this study was to evaluate the distribution of specific metabolites across the seed, peel, and pulp	[24]
<i>Bacon, Fuerte, Hass, Orotawa, Pinkerton, Rincon</i>	Unripe (at harvest time) Ripe (ready-to-eat stage)	Not specified	UHPLC-HESI-Q Orbitrap MS	Phenolic compounds (18) Total phenolics	Many compounds were not detected on the samples. Concentration of genticic and <i>p</i> -coumaric acid increased over ripening	[25]

Cultivar	Ripening Stages	Sample Info	Methodology	Analytical Determinations	Observations	Ref.
<i>Hass</i>	Transport from orchard within 3 days (5-7 °C) RS1 (0 days after reception) RS2 (4 days) RS3 (8 days) RS4 (12 days)	60-fruit batch, a sub-batch of 15 avocados per RS (ripening at 15 °C)	HPLC-DAD HPLC-FLD GC-FID	Individual phenolic compounds (7), carotenoids (6), tocopherols (3), phytosterols (3) Cytotoxic activity	Study and discussion of several individual metabolites throughout the climacteric period.	[19]
<i>Hass</i>	Unripe (0 days) Cold storage: 22 days and 37 days Edible ripeness: fruits after 22- and 37-days of storage	Ten independent fruits per sampling point	GC-TQ MS GC-FID HPLC-FLD UV/VIS UPLC-QTOF-PDA	Sugars and organic acids Fatty acids content and profile Tocopherols content Phytosterol content Total phenolics and antioxidant capacity Individual phenolic compounds	The primary objective of this study was to conduct a thorough phytochemical characterisation of <i>Hass</i> avocados throughout three harvest seasons, including from harvest, after cold storage and subsequent shelf life period to reach edible ripeness.	[26]
<i>Pinkerton</i>	Unripe (at harvest time) Ripe (ready-to-eat stage)	No specified	HPLC-PDA	Oil content and fatty acid composition Total phenolic and antioxidant activity Determination of phenolic compounds	This study mainly aimed to characterise the oil, bioactive properties and phytochemicals present in the pulp, seed, and peel of unripe and ripe avocado fruit dried using air, microwave or oven.	[27]
<i>Hass</i>	Unripe (at harvest time) Ripe (ready-to-eat stage)	≈ 400 fruits for the whole study	GC-MS UPLC-PDA	Fatty acids Polar metabolites (sugars, amino acids, etc.) Phenolic compounds Abscisic acid In-vitro hydrophilic and lipophilic antioxidant capacity	One of the first study paying attention to the composition of the amino acid and its relationship with softening phenomenon in avocado fruit	[15]

\*Avocado varieties info: *ColinV 33, Gem, Harvest, Hass, Hass Motril, Jiménez 1, Jiménez 2, Lamb Hass, Marvel, Nobel, Pinkerton, Sir Prize, Tacambaro*; Abbreviations in alphabetical order: APCI: Atmospheric pressure chemical ionisation; DAD: Diode array detector; ESI: Electrospray ionisation; FID: Flame ionisation detector; FLD: Fluorescence detector; GC: Gas chromatography; HESI: Heated electrospray ionisation source; HPLC: High pressure liquid chromatography; MS: Mass spectrometry; PDA: Photodiode array detector; PDHID: Discharge helium ionisation detector; Q: Quadrupole; RS: Ripening stage; TCD: Thermal conductivity detector; TOF: Time-of-flight; TQ: Triple quadrupole; UHPLC: Ultra-high pressure liquid chromatography; UV-VIS: Ultra violet-visible spectrophotometry.

The evident information gap highlighted above underscores the imperative for more comprehensive investigations. Consequently, employing liquid chromatography coupled with mass spectrometry (LC-MS), a total of 30 distinct metabolites including amino acids, nucleosides, vitamins, phytohormones, phenolic compounds, and related substances were meticulously identified and quantified in *Hass*, *Fuerte*, and *Bacon* avocado varieties at four ripening stages, ranging from green to slightly overripe fruits. The primary objectives of this study are as follows: (i) to assess the influence of ripening on the metabolic profile and the most notable compounds affected by this physiological process, (ii) to delineate the individual trends of the various metabolites across the diverse ripening stages, elucidating how their concentrations change over time, and (iii) to investigate whether the avocado variety directly influences metabolic evolution, examining if there are varietal differences in metabolite composition and ripening dynamics.

## 2. MATERIALS AND METHODS

### 2.1. Chemicals and reagents

LC-MS grade methanol (MeOH) and acetonitrile (ACN) were supplied by VWR Chemicals BDH® (Radnor, PA, EE.UU.). Ultra-pure water with a conductivity of 18.2 MΩ was obtained using a Milli-Q purification system from Millipore (Bedford, MA, USA). Acetic acid (ACh), used to acidify the mobile phase, was purchased from Sigma-Aldrich (St. Louis, MO, USA), as well as the pure standards of uridine (CAS 58-96-8), abscisic acid (CAS 14375-45-2), phenylalanine (CAS 150-30-1), pantothenic acid (CAS 137-08-6), tryptophan (CAS 54-12-6), ferulic acid (CAS 537-98-4), chlorogenic acid (CAS 327-97-9), epicatechin (CAS 490-46-0) and *p*-coumaric acid (CAS 501-98-4). Avocado extracts and pure standard solutions were filtered through a Acrodisc™ 0.22 μm syringe filters with nylon membrane, while mobile phases were filtered through Nylaflo™ 0.45 μm nylon membrane filter, both from Pall Corporation (Michigan, USA).

### 2.2. Plant material and avocado pre-treatment

Avocados fruits cv. *Bacon*, *Fuerte* and *Hass* were provided by The Institute for Mediterranean and Subtropical Horticulture “La Mayora” (IHSM La Mayora-CSIC-UMA). A total of 100 green fruits per variety were harvested at the end October for cv. *Bacon*, early November for cv. *Fuerte* and mid-March for cv. *Hass* during 2021-2022 season from the orchards of IHSM La Mayora-CSIC-UMA located in Algarrobo-Costa, Málaga (Spain). The choice of harvest time was based on ensuring similarity of dry matter (DM) content, which was measured according to the AOAC 920.151 method once the fruit was removed from the tree [28]. Unripe *Bacon* fruits displayed DM values around 27±2, while *Fuerte* and *Hass* avocados had DM values of 29±3 and 28±2, respectively. After the DM measurement, a total of 80 avocados per variety were selected and grouped into batches of 20 for the controlled ripening process. Unripe avocados (RS1, strongly firm) were processed immediately upon arrival in the laboratory in groups of four, to obtain five biological replicates of each stage (n=5, each consisting of 4 fruits). The remaining avocados were

kept in a well-ventilated place at 20-25 °C to simulate domestic handling for a total of two weeks. Avocados at the intermediate stage of ripening (RS2, firm but slightly softening) underwent processing 4-5 days after harvest, while processing of ripe (RS3, ready-to-eat stage) and overripe (RS4, overly soft texture) fruits started at 8-9 and 12-14 days, respectively. The handling of each biological replicate involved the following process: peeling, cutting, bagging, freezing, freeze-drying and grinding to homogenise the particle size. In total, 60 avocado samples (20 samples for each variety, comprising 5 samples × 4 ripeness stages) were obtained and stored at -23 °C until use.

### 2.3. Sample preparation and LC-MS analysis

A solid-liquid extraction protocol was used to extract the metabolites present in the avocado pulp matrix. A 0.25 g fraction of freeze-dried avocado powder was mixed with 20 mL of a MeOH:H<sub>2</sub>O (80:20, v/v) solution in a Falcon tube using a vortex. The mixture was then placed in an ultrasound-assisted bath for 30 minutes to ensure complete metabolite extraction. Subsequently, the Falcon tube was centrifuged for 5 minutes at 9000 rpm to separate the liquid phase from the remaining solid, and a second extraction cycle was performed following the same procedure. After pooling both supernatants, they were evaporated under vacuum conditions and resuspended in 1 mL MeOH/H<sub>2</sub>O (80:20, v/v). The liquid was filtered and transferred into an amber glass LC-vial.

External calibration curves, used for quantitative purposes, were prepared by diluting the required amount of each commercial standard in the appropriate volume of MeOH:H<sub>2</sub>O (80:20, v/v). A quality control (QC) sample, prepared from a solid portion of each avocado sample, was used to check the instrumental status over the sequences. All standard solutions and avocado extracts were stored at -23 °C until used.

Two distinct LC-MS platforms were used for sample analysis. An Elute series Ultra High Performance Liquid Chromatography (UHPLC) equipped with an electrospray source (ESI) and coupled to the compact QTOF high-resolution spectrometer from Bruker Datonics (Bremen, Germany) conducted the qualitative avocado characterisation based on its mass accuracy and its ability to perform MS/MS experiments. In addition, an InfinityAgilent 1260 series modular liquid chromatography system (Agilent Technologies, Waldbronn, Germany) coupled to a Bruker Esquire 2000 series Ion Trap (IT) mass spectrometer (LC-ESI-IT MS) by means of an ESI source was used for quantitative purposes. Both instruments were equipped with a Zorbax Eclipse Plus C<sub>18</sub> column (4.6 × 150 mm, 1.8 µm particle size) from Agilent Technologies. Chromatographic conditions were reproduced from the report of Serrano-García et al. [29]. To achieve the separation of the metabolites was necessary to use a mobile phase A consisting of Milli-Q ultra-pure water (0.5% acetic acid) and acetonitrile as mobile phase B, with a flow rate of 0.8 mL/min. A gradient elution was applied: 0 min, 95% A; 22 min, 25% A; 23 min, 0% A, 23.5 min; 0% A; and at 25 min return to initial conditions. Injection volume was 10 µL. ESI operated in negative polarity and *Full Scan* mode

(within the range  $m/z$  50-1000). Source parameters were adapted to the MS systems conditions as follows: 30 psi of nebuliser pressure, 9 L min<sup>-1</sup> and 300 °C of drying gas flow and temperature, respectively, and +3200 V capillary voltage on the IT MS system. In the QTOF MS system, the selected conditions were as follows: 3.0 Bar of nebuliser pressure, 9 L min<sup>-1</sup> and 220 °C of drying gas and +4500 V capillary voltage. Auto MS/MS fragmentation was carried out to facilitate compound identification. A predetermined absolute threshold of 1000 counts was chosen for precursor ion collection, alongside a cycle time of 1 second. Collision energy stepping factors varied within the range of 0.2% to 0.8%. The software controlling LC-IT MS comprised Agilent ChemStation and Bruker Esquire control, whilst LC-QTOF MS used Compass Hystar and Otof Control. Data treatment was done with Data Analysis 4.0 from Bruker Daltonics.

#### 2.4. Analytical parameters of the method

Pure standard solutions and QC samples were used to evaluate the main analytical parameters of the method such as the linearity, limits of detection (LOD) and quantification (LOQ) and repeatability *intra*- and *inter*- day. The external calibration curves were obtained by linear regression using the least squares method. Each point of the curves corresponded to the mean of three independent injections. Metabolites were quantified using the corresponding pure standard or, if not available, with a compound of the same chemical category. Thus, glycosylated and derived forms of coumaric acid were quantified with the *p*-coumaric acid standard. Also, the hexoses of dihydroxybenzoic acid, the glucoside of caffeic acid and unknown metabolites. The ferulic acid pure standard was used to quantify its glycosylated form. Phenylalanine calibration curves were used to quantify tyrosine, *N*-acetyl-tyrosine and *N*-acetyl-phenylalanine. Finally, using the tryptophan pure standard, the *N*-acetyl-tryptophan content was assessed. The other metabolites were quantified using their corresponding pure standard.

LOD and LOQ values were estimated using the lowest injected concentration of each standard and calculating the concentration generated with a signal-to-noise ratio (S/N) equal to 3 and 10, respectively. *Intra*-day and *inter*-day repeatability, expressed as coefficient of variation (% CV), were obtained from data of quality control injections performed on the same day or on different days.

#### 2.5. Statistical analysis

Quantitative data were expressed as mean  $\pm$  standard deviation (SD) ( $n=5$ ) and analysed using InfoStat 2020 software. Due to the non-normal distribution of the data, a non-parametric Kruskal-Wallis test was first performed. This was followed by pairwise comparisons using the Mann-Whitney test. Statistical significance was established with  $p$ -values less than  $\alpha = 0.05$ . SIMCA v14.1 software was used for the execution of an unsupervised principal component analysis (PCA) with a data matrix consisting of 60 samples (observations) and 30 variables (metabolites) expressed as concentration (mg kg<sup>-1</sup> DW). The heat map was performed in MetaboAnalyst 5.0 software with the

Euclidean distance measure and the ward clustering algorithm. Autoscaling was applied as a preprocessing step for compound normalisation.

### 3. RESULTS AND DISCUSSION

#### 3.1. Targeted metabolite characterisation

A targeted characterisation of the sample extracts was performed using LC-ESI-QTOF MS/MS. A total of 30 compounds were selected from the metabolic profile based on their predominance in the profile and/or potential relationship with the avocado ripening progression. Metabolite identification was based on the interpretation of the accurate mass information, predicted molecular formula (error  $\leq 5$  ppm), relative elution order and fragmentation patterns, which were compared with previous relevant reports [20,24,26,29], public MS/MS databases (*MassBank*, *MoNA*, *FoodDB*,...) and *in-silico* fragmentation MetFrag tool [30]. Table 2 lists the selected metabolites, which include a wide range of metabolite groups, such as nucleosides, amino acids and related compounds, phenolic compounds, vitamins, phytohormones and iridoids. It should be noted that while several compounds could not be reliably annotated, they were included in any case due to their relevance within the metabolic profile.

##### 3.1.1. Amino acids, nucleosides, and related compounds

Seven metabolites were tentatively classified within the group of nucleosides, amino acids, and *N*-acetyl-amino acid derivatives. Briefly, the chromatographic peaks at 2.7, 2.9, 4.9 and 6.4 min were identified as uridine (exhibiting a predominant signal at  $m/z$  243.0622 [M-H]<sup>-</sup>), tyrosine ( $m/z$  180.0665 [M-H]<sup>-</sup>), phenylalanine ( $m/z$  164.0718 [M-H]<sup>-</sup>) and tryptophan ( $m/z$  203.0826 [M-H]<sup>-</sup>), respectively, based on the comparison with their pure standards. The peak appearing at 6.7 min with an MS signal at  $m/z$  222.0770 [M-H]<sup>-</sup> and main fragments at  $m/z$  180, 163, 119, 107 and 58 was tentatively assigned as *N*-acetyl-tyrosine, according to the predicted molecular formula provided considering the accurate mass and the fragmentation pattern. Similarly, the peak eluting at 9.6 min and mass spectrum dominated by the signal  $m/z$  206.0824 [M-H]<sup>-</sup> was tentatively assigned to *N*-acetyl-phenylalanine. Lastly, the peak with a retention time of 10.3 min and molecular formula C<sub>13</sub>H<sub>14</sub>N<sub>2</sub>O<sub>3</sub> was consistent with *N*-acetyl-tryptophan, according to ion descriptors, relative elution order and fragmentation pattern. This latter compound is being described for the first time in avocado.

##### 3.1.2. Phenolic compounds and derivatives

Fifteen phenolic compounds constituted the largest chemical group of metabolites quantified in avocado pulp. The different annotated compounds will be described in order of appearance in the chromatographic profiles.

**Table 2.** Overview of compounds identified (or with a tentative identity assigned) in the avocado samples under study

Proposed Compound	Chemical Family	Formula	Rt (min)	$m/z_{exp}$	$m/z_{theo}$	$\Delta m/z$ (ppm)	mSigma	Main MS/MS fragments (% relative abundance)
Uridine	Nucleoside	C <sub>9</sub> H <sub>12</sub> N <sub>2</sub> O <sub>6</sub>	2.7	243.0622	243.0623	0.1	5.1	110.03 (100), 82.03 (43), 122.02 (13), 152.03 (9)
Tyrosine	Amino acid	C <sub>9</sub> H <sub>11</sub> NO <sub>3</sub>	2.9	180.0665	180.0666	0.7	10.7	119.05 (100), 163.04 (62), 93.03 (23), 106.04 (20)
Unknown 1	-	C <sub>14</sub> H <sub>26</sub> O <sub>11</sub>	3.0	369.1402	369.1402	0.2	4.7	59.02 (100), 73.03 (80.7), 101.02(69), 161.05 (57), 237.09 (29)
Isotachoside	Phenolic compound	C <sub>13</sub> H <sub>18</sub> O <sub>8</sub>	4.2	301.0931	301.0929	-0.8	9.2	123.01 (100), 138.03 (20), 124.01 (7), 139.04 (5)
Dihydroxybenzoic acid hexose I	Phenolic compound	C <sub>13</sub> H <sub>16</sub> O <sub>9</sub>	4.2	315.0722	315.0722	-0.2	4.0	108.02 (100), 152.01 (92), 315.07 (55), 109.03 (27), 153.02 (25)
Tachioside	Phenolic compound	C <sub>13</sub> H <sub>18</sub> O <sub>8</sub>	4.5	301.0929	301.0929	0.1	12.0	123.01 (100), 138.03 (35), 124.01 (8), 139.04 (5)
Phenylalanine	Amino acid	C <sub>9</sub> H <sub>11</sub> NO <sub>2</sub>	4.9	164.0718	164.0717	-0.7	5.1	103.05 (100), 72.01 (60), 147.04 (46)
Dihydroxybenzoic acid hexose II	Phenolic compound	C <sub>13</sub> H <sub>16</sub> O <sub>9</sub>	5.0	315.0723	315.0722	-0.5	4.8	153.02 (100), 109.03 (97), 315.07 (60), 152.01 (29), 108.02 (14)
Unknown 2	-	C <sub>13</sub> H <sub>22</sub> O <sub>10</sub>	5.0	337.1138	337.1140	0.6	3.9	193.07 (100), 57.03 (74), 101.02 (54), 161.05 (6)
Pantothenic acid	Vitamin	C <sub>9</sub> H <sub>17</sub> NO <sub>5</sub>	5.2	218.1036	218.1034	-0.9	8.2	146.08 (100), 71.05 (97), 88.04 (77)
Unknown 3	-	C <sub>15</sub> H <sub>26</sub> O <sub>11</sub>	5.6	381.1401	381.1402	0.3	18.2	237.10 (100), 59.01 (71), 57.03 (71), 125.03 (24), 279.11 (12), 161.04 (5)
Tryptophan	Amino acid	C <sub>11</sub> H <sub>12</sub> N <sub>2</sub> O <sub>2</sub>	6.4	203.0826	203.0826	-0.1	0.9	116.05 (100), 74.03 (41), 142.07 (24)
Penstemide	Iridoid	C <sub>21</sub> H <sub>32</sub> O <sub>10</sub>	6.5	443.1922	443.1923	0.1	3.6	443.19 (100), 59.01 (7), 101.02 (6), 113.02 (4)
Caffeic acid glucoside	Phenolic compound	C <sub>15</sub> H <sub>18</sub> O <sub>9</sub>	6.5	341.0878	341.0878	0.1	6.6	161.02 (100), 133.03 (12), 179.03 (10), 59.01 (4)
<i>N</i> -acetyl-tyrosine	Amino acid derivative	C <sub>11</sub> H <sub>13</sub> NO <sub>4</sub>	6.7	222.0770	222.0772	0.8	2.7	180.07 (100), 58.03 (61), 119.05 (58), 107.05 (52), 163.04 (40)
Chlorogenic acid	Phenolic compound	C <sub>16</sub> H <sub>18</sub> O <sub>9</sub>	7.2	353.0879	353.0878	-0.2	4.3	191.06 (100), 89.02 (8)
Coumaric acid hexose	Phenolic compound	C <sub>15</sub> H <sub>18</sub> O <sub>8</sub>	7.5	325.0932	325.0929	-0.8	8.5	145.03 (100), 163.04 (9), 119.04 (7), 59.01 (6)
Ferulic acid hexose	Phenolic compound	C <sub>16</sub> H <sub>20</sub> O <sub>9</sub>	7.9	355.1032	355.1021	0.7	8.3	175.04 (100), 193.05 (20), 160.02 (17), 355.10 (11), 134.04 (9), 59.01 (8)
Epicatechin	Phenolic compound	C <sub>15</sub> H <sub>14</sub> O <sub>6</sub>	8.3	289.0718	289.0718	0.0	6.8	109.03 (100), 123.05 (92), 245.08 (85), 203.07 (77)
Unknown 4	-	C <sub>20</sub> H <sub>28</sub> O <sub>11</sub>	8.4	443.1558	443.1554	-1.0	1.9	299.11 (100), 281.10 (78), 57.03 (72), 341.12 (51)
Coumaric acid malonyl-hexose I	Phenolic compound	C <sub>18</sub> H <sub>20</sub> O <sub>11</sub>	8.7	411.0931	411.0933	0.3	11.2	145.03 (100), 163.04 (10), 367.10 (8)
Unknown 5	-	C <sub>17</sub> H <sub>28</sub> O <sub>10</sub>	8.8	391.1606	391.1610	0.9	1.6	247.12 (100), 57.04 (91), 101.03 (44), 161.04 (35), 113.02 (25)
Coumaric acid malonyl-hexose II	Phenolic compound	C <sub>18</sub> H <sub>20</sub> O <sub>11</sub>	9.0	411.0932	411.0933	0.2	9.8	145.03 (100), 163.04 (41), 367.10 (20)
Coumaric acid malonyl-hexose III	Phenolic compound	C <sub>18</sub> H <sub>20</sub> O <sub>11</sub>	9.3	411.0932	411.0933	0.2	6.2	145.03 (100), 163.04 (9), 367.10 (9)
Coumaric acid derivative	Phenolic compound	C <sub>21</sub> H <sub>26</sub> O <sub>12</sub>	9.4	469.1350	469.1351	0.3	2.6	145.03(100), 163.04 (63), 323.10 (54), 367.10 (34)
<i>N</i> -acetyl-phenylalanine	Amino acid derivative	C <sub>11</sub> H <sub>13</sub> NO <sub>3</sub>	9.6	206.0824	206.0823	-0.5	5.0	117.04 (100), 91.05 (67), 145.03 (62), 164.08 (61), 58.03 (46), 147.05 (44), 103.05 (40)
<i>p</i> -Coumaric acid	Phenolic compound	C <sub>9</sub> H <sub>8</sub> O <sub>3</sub>	9.9	163.0400	163.0401	0.3	5.3	119.05 (100), 93.03 (11)
<i>N</i> -acetyl-tryptophan	Amino acid derivative	C <sub>13</sub> H <sub>14</sub> N <sub>2</sub> O <sub>3</sub>	10.3	245.0934	245.0932	-0.9	3.9	74.03 (100), 203.08 (67), 116.05 (60), 98.02 (42), 142.07 (28)
Ferulic Acid	Phenolic compound	C <sub>10</sub> H <sub>10</sub> O <sub>4</sub>	10.4	193.0505	193.0506	0.9	3.4	134.04 (100), 178.03 (9)
Abscisic acid	Phytohormone	C <sub>15</sub> H <sub>20</sub> O <sub>4</sub>	13.0	263.1291	263.1289	-0.8	1.4	153.09 (100), 204.12 (69), 219.14 (46)

The prevalent ion detected in the MS spectra of coumaric acid malonyl-hexose I, II and III was [M-H-44]<sup>-</sup>, corresponding to a  $m/z$  signal of 367.

More than 95% of the compounds displayed a score of 100.0.

The peaks at 4.2 and 4.5 min, with the molecular formula  $C_{13}H_{18}O_8$ , were tentatively identified as phenolic glycosides known as isotachioside (4-hydroxy-2-methoxyphenyl-1- $O$ - $\beta$ -glucopyranoside) and tachioside (4-hydroxy-3-methoxyphenyl-1- $O$ - $\beta$ -D-glucopyranoside), respectively. This identification was based, among other reasons, on the 0.9215 score predicted by MetFrag from MS data and the fragmentation pattern. While these compounds have been previously described in other plant matrices, to the best of our knowledge, this is the first time to be reported in avocado. The mass spectra of the peaks detected at 4.2 and 5.0 min showed a common precursor ion at  $m/z$  315.072  $[M-H]^-$ , and fragment ions at  $m/z$  108, 109, 152 and 153 (in order from lowest to highest  $m/z$  value), which were consistent with isomeric molecules of dihydroxybenzoic acid hexose. The caffeic acid glucoside observed at 6.5 min was identified based on the exact mass and the fragments at  $m/z$  161 and 179, caused from the neutral loss of the glycosidic moiety. The identity of the chromatographic peaks of chlorogenic, *p*-coumaric and ferulic acids was corroborated by comparing retention times and MS spectra with their respective pure standards. Several coumaric acid derivatives and one ferulic acid derivative were detected in the  $C_{18}$  metabolic profile of avocado pulp. The peak eluting at 7.5 min was identified as coumaric acid hexose ( $C_{15}H_{18}O_8$ ). The glycosidic form of ferulic acid was detected at  $m/z$  355.1032 (7.9 min). The identity of epicatechin (a flavonoid) at 8.3 min ( $m/z$  289.0718  $[M-H]^-$ ) was corroborated with its pure standard. In addition, three distinct chromatographic peaks were detected at 8.7, 9.0 and 9.3 min, respectively, which coincided with isomers of coumaric acid malonyl-hexose; the  $m/z$  411  $[M-H]^-$  signal was observed without high intensity in the mass spectrum, while  $m/z$  367  $[M-H-44]^-$  was the predominant signal. Another coumaric acid derivative was detected at 9.4 min, although the complete structure of the molecule remains partially elucidated.

### 3.1.3. Other interesting metabolites detected within the profile

The presence of pantothenic acid (also known as vitamin B5) was confirmed at 5.2 min (*pseudo*-molecular ion at  $m/z$  218.1036) by comparison with the pure standard. Similarly, abscisic acid (a phytohormone), which appeared in the profile at 13.0 min ( $m/z$  263.1291  $[M-H]^-$ ) was also identified. Following a previously published report, the mass spectrum of the peak with a retention time of 6.5 min at  $m/z$  433.1922  $[M-H]^-$  was tentatively noted as pensternide [24]; it showed slight fragmentation with fragments at  $m/z$  113, 101 and 59. Five other compounds with  $m/z$  369.1402 ( $C_{14}H_{26}O_{11}$ ),  $m/z$  337.1138 ( $C_{13}H_{22}O_{10}$ ),  $m/z$  381.1401 ( $C_{15}H_{26}O_{11}$ ),  $m/z$  443.1558 ( $C_{20}H_{28}O_{11}$ ) and  $m/z$  391.1606 ( $C_{17}H_{28}O_{10}$ ) could not be tentatively identified, but they were included in the analysis because they appeared to exhibit a rather evident evolution throughout ripening. Further experiments are already underway in the lab to gather more information about these compounds.

**Table 3.** Quantitative results of LC-MS analysis of avocado pulp at four different ripening stages for *Hass*, *Fuerte* and *Bacon* varieties

Compound	Unripe (RS1)			Medium (RS2)			Edible ripeness (RS3)			Overripe (RS4)		
	<i>Bacon</i>	<i>Fuerte</i>	<i>Hass</i>	<i>Bacon</i>	<i>Fuerte</i>	<i>Hass</i>	<i>Bacon</i>	<i>Fuerte</i>	<i>Hass</i>	<i>Bacon</i>	<i>Fuerte</i>	<i>Hass</i>
<b>Amino acids, nucleosides and related compounds</b>												
<i>N</i> -acetyl-phenylalanine	131±42 <sup>abB</sup>	326±77 <sup>abC</sup>	33±8 <sup>aA</sup>	126±34 <sup>abB</sup>	390±32 <sup>bcC</sup>	28±10 <sup>aA</sup>	172±32 <sup>bbB</sup>	323±67 <sup>acC</sup>	32±8 <sup>aA</sup>	91±17 <sup>abB</sup>	244±56 <sup>acC</sup>	29±1 <sup>aA</sup>
<i>N</i> -acetyl-tryptophan	17±3 <sup>aA</sup>	60±14 <sup>abB</sup>	21±4 <sup>aA</sup>	17±2 <sup>aA</sup>	61±11 <sup>abB</sup>	21±3 <sup>aA</sup>	18±1 <sup>aA</sup>	65±15 <sup>acC</sup>	27±5 <sup>abB</sup>	15±1 <sup>aA</sup>	58±14 <sup>acC</sup>	22±2 <sup>abB</sup>
<i>N</i> -acetyl-tyrosine	17±6 <sup>aA</sup>	52±16 <sup>abB</sup>	21±6 <sup>aA</sup>	23±6 <sup>aA</sup>	135±42 <sup>bbB</sup>	27±10 <sup>aA</sup>	59±13 <sup>caC</sup>	250±39 <sup>ccC</sup>	114±43 <sup>cbB</sup>	43±4 <sup>baA</sup>	259±34 <sup>cbB</sup>	59±22 <sup>baA</sup>
Phenylalanine	7±2 <sup>bbB</sup>	14±4 <sup>bcC</sup>	3.6±0.2 <sup>baA</sup>	22±5 <sup>cbB</sup>	30±7 <sup>ccC</sup>	2.3±0.7 <sup>abaA</sup>	3.2±0.4 <sup>aaA</sup>	2.7±0.6 <sup>aaA</sup>	2.5±0.4 <sup>aaA</sup>	3.2±0.8 <sup>baA</sup>	3±1 <sup>aA</sup>	2.4±0.5 <sup>aaA</sup>
Tryptophan	2.8±0.6 <sup>bbB</sup>	2.3±0.4 <sup>bbB</sup>	1.7±0.2 <sup>baA</sup>	4±1 <sup>ccC</sup>	3.1±0.4 <sup>cbB</sup>	1.6±0.3 <sup>baA</sup>	5±1 <sup>cbB</sup>	1.4±0.3 <sup>baA</sup>	1.2±0.1 <sup>aaA</sup>	1.7±0.3 <sup>baA</sup>	1.8±0.5 <sup>abaA</sup>	1.4±0.2 <sup>abaA</sup>
Tyrosine	6±1 <sup>aA</sup>	15±5 <sup>abB</sup>	4.1±0.2 <sup>aaA</sup>	18±5 <sup>bbB</sup>	36±10 <sup>bcC</sup>	3.2±1 <sup>aA</sup>	6±1 <sup>abB</sup>	110±28 <sup>ccC</sup>	3.4±0.8 <sup>aaA</sup>	5.6±0.7 <sup>aaA</sup>	126±16 <sup>ccC</sup>	9±3 <sup>bbB</sup>
Uridine	27±9 <sup>abB</sup>	14±3 <sup>aaA</sup>	25±5 <sup>abB</sup>	24±9 <sup>abB</sup>	14±5 <sup>aA</sup>	29±4 <sup>abB</sup>	58±10 <sup>bbB</sup>	29±7 <sup>baA</sup>	49±13 <sup>bbB</sup>	63±13 <sup>bbB</sup>	15±3 <sup>aA</sup>	59±15 <sup>bbB</sup>
<b>Iridoid</b>												
Penstemide	38±6 <sup>bbB</sup>	51±13 <sup>bbB</sup>	27±2 <sup>caA</sup>	34±4 <sup>bbB</sup>	43±4 <sup>bcC</sup>	18±5 <sup>baA</sup>	23±4 <sup>abB</sup>	17±5 <sup>aaB</sup>	11±3 <sup>aaA</sup>	20±2 <sup>abB</sup>	17±2 <sup>abB</sup>	13±3 <sup>baA</sup>
<b>Phenolics and related compounds</b>												
Caffeic acid glucoside	n.d	n.d	n.d	2.0±0.6 <sup>aaA</sup>	2.3±0.7 <sup>aaA</sup>	14±3 <sup>abB</sup>	106±28 <sup>bcC</sup>	27±7 <sup>cbB</sup>	18±4 <sup>aaA</sup>	80±11 <sup>bbB</sup>	17±4 <sup>baA</sup>	22±7 <sup>aaA</sup>
Chlorogenic acid	31±6 <sup>abB</sup>	4.5±0.6 <sup>baA</sup>	38±8 <sup>cbB</sup>	37±12 <sup>abC</sup>	5±2 <sup>bbB</sup>	2.3±0.6 <sup>baA</sup>	26±8 <sup>abB</sup>	0.8±0.2 <sup>aaA</sup>	1.2±0.4 <sup>aaA</sup>	55±9 <sup>bcC</sup>	0.6±0.1 <sup>aaA</sup>	1.1±0.2 <sup>bbB</sup>
Coumaric acid derivative	n.d	n.d	n.d	1.4±0.2 <sup>aaA</sup>	n.d	3.6±0.9 <sup>abB</sup>	58±4 <sup>bbB</sup>	6±1 <sup>aA</sup>	48±7 <sup>bcC</sup>	112±19 <sup>ccC</sup>	9±1 <sup>baA</sup>	50±13 <sup>bbB</sup>
Coumaric acid hexose	n.d	1.3±0.2 <sup>aA</sup>	n.d	3±1 <sup>aA</sup>	8±3 <sup>bbB</sup>	262±55 <sup>acC</sup>	2448±388 <sup>baA</sup>	1981±306 <sup>caA</sup>	2226±351 <sup>caA</sup>	2919±374 <sup>bcB</sup>	2213±361 <sup>cbB</sup>	1299±214 <sup>baA</sup>
Coumaric acid malonyl-hexose I	0.6±0.1 <sup>aaA</sup>	n.d	0.7±0.1 <sup>aaA</sup>	0.7±0.2 <sup>aaA</sup>	n.d	7±2 <sup>bbB</sup>	3.2±0.8 <sup>baA</sup>	24±6 <sup>bbB</sup>	47±13 <sup>ccC</sup>	4.6±0.7 <sup>caA</sup>	27±2 <sup>abB</sup>	45±11 <sup>ccC</sup>
Coumaric acid malonyl-hexose II	0.9±0.1 <sup>aaA</sup>	1.5±0.3 <sup>abB</sup>	1.3±0.1 <sup>abB</sup>	0.9±0.2 <sup>aaA</sup>	1.8±0.6 <sup>abB</sup>	74±21 <sup>bcC</sup>	43±12 <sup>baA</sup>	280±72 <sup>bbB</sup>	467±96 <sup>ccC</sup>	59±10 <sup>baA</sup>	330±47 <sup>bbB</sup>	439±74 <sup>cbB</sup>
Coumaric acid malonyl-hexose III	0.6±0.2 <sup>aaA</sup>	n.d	0.8±0.2 <sup>aaA</sup>	0.8±0.2 <sup>aaA</sup>	1.3±0.2 <sup>abB</sup>	29±10 <sup>bcC</sup>	10±3 <sup>baA</sup>	92±27 <sup>bbB</sup>	176±53 <sup>ccC</sup>	15±3 <sup>caA</sup>	84±15 <sup>bbB</sup>	133±38 <sup>ccC</sup>
Dihydroxybenzoic acid hexose I	17±4 <sup>abB</sup>	8±2 <sup>aaA</sup>	61±12 <sup>acC</sup>	17±4 <sup>abB</sup>	6±1 <sup>aA</sup>	51±9 <sup>acC</sup>	17±5 <sup>abB</sup>	8±1 <sup>aA</sup>	59±4 <sup>acC</sup>	20±3 <sup>abB</sup>	8±2 <sup>aaA</sup>	55±9 <sup>acC</sup>
Dihydroxybenzoic acid hexose II	14±2 <sup>abB</sup>	10±2 <sup>aaA</sup>	66±5 <sup>acC</sup>	16±4 <sup>abB</sup>	7.6±0.7 <sup>aaA</sup>	60±10 <sup>acC</sup>	13±4 <sup>abB</sup>	8±1 <sup>aA</sup>	61±5 <sup>acC</sup>	15±3 <sup>abB</sup>	7±2 <sup>aaA</sup>	60±8 <sup>acC</sup>
Epicatechin	4±1 <sup>abA</sup>	4±1 <sup>baA</sup>	28±6 <sup>cbB</sup>	6±2 <sup>bbB</sup>	3±1 <sup>abA</sup>	3±1 <sup>aA</sup>	2.4±0.7 <sup>abB</sup>	0.7±0.2 <sup>aaA</sup>	1.7±0.4 <sup>abB</sup>	6±2 <sup>bbB</sup>	1.0±0.3 <sup>aaA</sup>	6±2 <sup>bbB</sup>
Ferulic acid	0.16±0.04 <sup>aaA</sup>	n.d	0.17±0.07 <sup>abB</sup>	0.19±0.5 <sup>aaA</sup>	0.3±0.1 <sup>aaA</sup>	2.3±0.8 <sup>bbB</sup>	4±1 <sup>baA</sup>	2.8±0.8 <sup>baA</sup>	9.3±0.9 <sup>ebB</sup>	3.1±0.9 <sup>baA</sup>	3.4±0.4 <sup>baA</sup>	8±1 <sup>cbB</sup>
Ferulic acid hexose	n.d	n.d	n.d	0.5±0.2 <sup>aaA</sup>	0.7±0.2 <sup>aaA</sup>	8±3 <sup>abB</sup>	143±25 <sup>ccC</sup>	37±11 <sup>baA</sup>	65±18 <sup>bbB</sup>	59±17 <sup>baA</sup>	57±13 <sup>baA</sup>	59±14 <sup>baA</sup>
Isotachioside	27±6 <sup>bcC</sup>	14±4 <sup>bbB</sup>	8±1 <sup>baA</sup>	30±6 <sup>bcC</sup>	14±2 <sup>bbB</sup>	5.2±0.5 <sup>aaA</sup>	16±5 <sup>acC</sup>	9±2 <sup>abB</sup>	5.2±0.7 <sup>aaA</sup>	26±3 <sup>bcC</sup>	8±1 <sup>bbB</sup>	5.0±0.7 <sup>aaA</sup>
<i>p</i> -Coumaric acid	n.d	n.d	n.d	n.d	n.d	8±3 <sup>a</sup>	22±5 <sup>aaA</sup>	20±4 <sup>aaA</sup>	44±12 <sup>bbB</sup>	29±5 <sup>abB</sup>	23±4 <sup>aaA</sup>	31±3 <sup>bbB</sup>
Tachioside	30±6 <sup>abB</sup>	42±3 <sup>acC</sup>	6±1 <sup>aA</sup>	29±4 <sup>abB</sup>	47±4 <sup>ccC</sup>	5.6±0.9 <sup>aaA</sup>	25±6 <sup>abB</sup>	43±5 <sup>ccC</sup>	7.9±0.4 <sup>baA</sup>	42±5 <sup>bbB</sup>	42±4 <sup>abB</sup>	7.5±0.6 <sup>baA</sup>
<b>Phytohormone</b>												
Absciscic acid	0.15±0.04 <sup>aaA</sup>	5±2 <sup>abB</sup>	3.7±0.6 <sup>abB</sup>	3±1 <sup>baA</sup>	5.5±0.9 <sup>abB</sup>	7±2 <sup>abB</sup>	8±2 <sup>caA</sup>	11±4 <sup>baB</sup>	17±1 <sup>cbB</sup>	5±1 <sup>baA</sup>	9±3 <sup>baB</sup>	14±2 <sup>bbB</sup>
<b>Vitamin</b>												
Pantothenic acid	18±3 <sup>bbB</sup>	12±3 <sup>aaA</sup>	11±2 <sup>aaA</sup>	15.9±0.9 <sup>abB</sup>	12±2 <sup>aaA</sup>	10±2 <sup>aaA</sup>	14±2 <sup>abB</sup>	10.5±0.5 <sup>aaA</sup>	13±1 <sup>abB</sup>	14±2 <sup>abB</sup>	10±2 <sup>aaA</sup>	12±2 <sup>abB</sup>

Compound	Unripe (RS1)			Medium (RS2)			Edible ripeness (RS3)			Overripe (RS4)		
	Bacon	Fuerte	Hass	Bacon	Fuerte	Hass	Bacon	Fuerte	Hass	Bacon	Fuerte	Hass
<b>Not identified metabolites</b>												
Unknown 1 ( <i>m/z</i> 369)	48±9 <sup>aAB</sup>	38±5 <sup>bA</sup>	55±3 <sup>bb</sup>	46±10 <sup>aA</sup>	39±6 <sup>bA</sup>	36±6 <sup>aA</sup>	38±10 <sup>aA</sup>	26±7 <sup>aA</sup>	32±5 <sup>aA</sup>	53±6 <sup>aC</sup>	24±3 <sup>aA</sup>	39±7 <sup>bB</sup>
Unknown 2 ( <i>m/z</i> 337)	n.d	n.d	n.d	n.d	n.d	n.d	53±11 <sup>ab</sup>	2.5±0.8 <sup>aA</sup>	2.9±0.7 <sup>aA</sup>	58±12 <sup>aC</sup>	3±1 <sup>aA</sup>	9±2 <sup>bB</sup>
Unknown 3 ( <i>m/z</i> 381)	722±72 <sup>ab</sup>	5.0±0.6 <sup>aA</sup>	4.9±0.7 <sup>aA</sup>	791±112 <sup>ab</sup>	5.1±0.4 <sup>aA</sup>	6.0±0.7 <sup>aA</sup>	906±211 <sup>abc</sup>	8±2 <sup>bA</sup>	20±4 <sup>bb</sup>	1269±197 <sup>bc</sup>	7.4±0.4 <sup>bA</sup>	31±4 <sup>cb</sup>
Unknown 4 ( <i>m/z</i> 443)	5±1 <sup>a</sup>	n.d	n.d	7±1 <sup>b</sup>	n.d	n.d	23±6 <sup>cC</sup>	13±5 <sup>ab</sup>	3±1 <sup>aA</sup>	31±9 <sup>cb</sup>	22±3 <sup>bb</sup>	6±2 <sup>bA</sup>
Unknown 5 ( <i>m/z</i> 391)	28±6 <sup>ab</sup>	n.d	2.2±0.2 <sup>aA</sup>	32±10 <sup>aC</sup>	2.0±0.6 <sup>bA</sup>	3.7±0.7 <sup>bb</sup>	40±13 <sup>aC</sup>	3.0±0.9 <sup>bA</sup>	7±1 <sup>cb</sup>	98±18 <sup>bc</sup>	3±1 <sup>bA</sup>	11±2 <sup>db</sup>

Data are expressed in mg kg<sup>-1</sup> dry weight as mean ± standard deviation (n = 5); Different small letters indicate a statistical difference (p≤0.05) between the ripeness stages of the same variety; Different capital letters indicate a statistical difference (p≤0.05) at the same ripeness stage between *Bacon*, *Fuerte* and *Hass* varieties; n.d: not detected.

### 3.2. Quantitative data

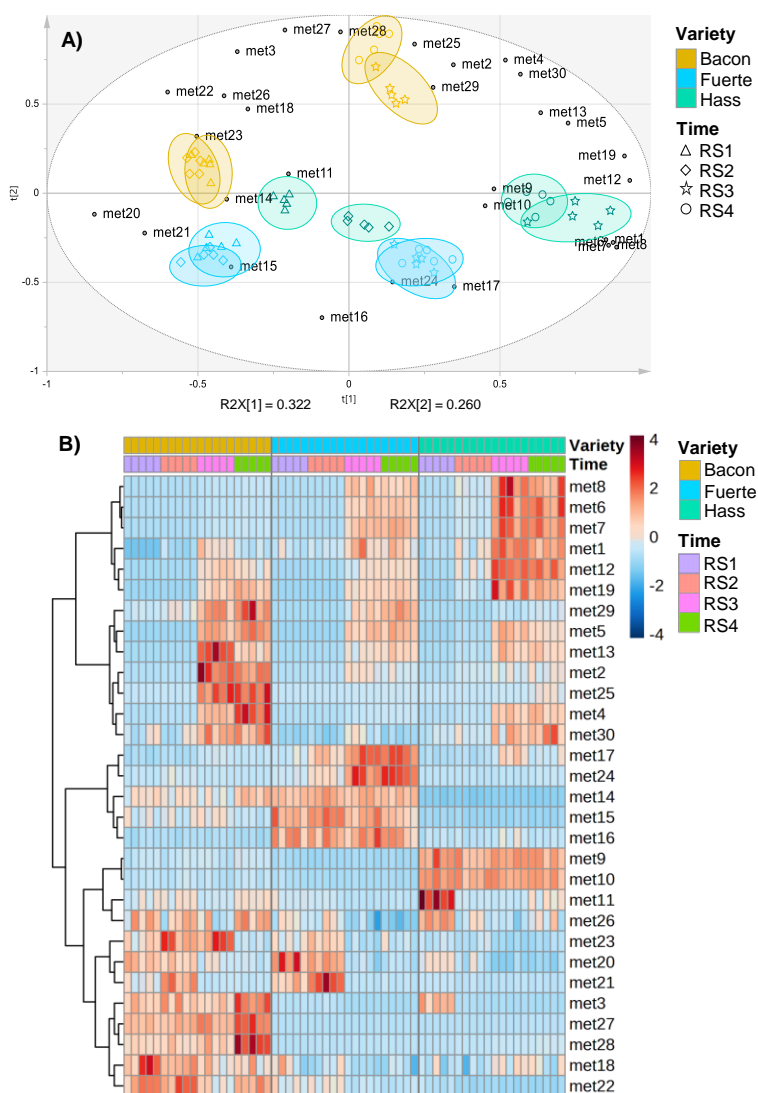
After qualitatively characterising the acquired profiles, we proceeded to define the analytical parameters of the employed methodology. Table 1 of Supplementary material summarises the data extracted for each analytical parameter, including calibration functions, correlation coefficients, quantitative ranges, LODs and LOQs, as well as repeatability. Adequate figures were obtained for  $R^2$  (with values above 0.990 in all cases). The LODs ranged from 5.2 to 35.2  $\mu\text{g L}^{-1}$  and the LOQs from 17.3 to 117.2  $\mu\text{g L}^{-1}$ . *Intra*-day repeatability did not exceed 9.05% and *inter*-day repeatability 10.28%, indicating a correct operating procedure. After checking the methodological reliability, quantification was carried out.

Table 3 summarises the quantitative data obtained through external calibration curves. Despite the absence of pure standards in some cases, preventing absolute quantification, this approach enabled a meaningful comparison of metabolite evolution during climacteric ripening and a thorough assessment against the three evaluated cultivars. Additionally, statistical analyses, essential for drawing significant conclusions, are presented in the same table. Compounds not detected at certain ripening stages were not subjected to pair testing, assuming significance at subsequent stages if the compound was determined in the subsequent level. Consequently, statistically significant differences ( $p \leq 0.05$ ) were not only observed between ripening stages within the same variety but also among the three varieties at corresponding stages. With this initial perspective guiding us, the upcoming sections will delve into untangling these nuances.

#### 3.2.1. Unsupervised exploration of the correlation between the concentrations of the different phytochemicals determined, ripening stages and varieties

The quantitative data set obtained by LC-MS was first examined by applying principal component analysis (PCA). This initial step allowed to assess the overall quality of the data, explore the biological diversity, and identify the main sources of variance and possible natural clustering of the samples. The first two principal components (PC1 and PC2) were considered for the illustration shown in Figure 1A. For better understanding, the scores plot and the loading plot were merged, resulting in the biplot figure. PC1 accounted for 32.2% of the overall variance in the model, followed by PC2 at 26.0%. The inclusion of the third principal component (PC3) contributed an additional 19.5%, resulting in a cumulative variance coverage of 77.7%. This indicates that the first three principal components captured a significant portion of the variability present in the data, allowing for a meaningful interpretation of the results.

The PCA biplot shows clear metabolic differences both with regard to the ripening process of the fruit and the avocado variety examined. The first component (PC1), which explains the largest proportion of the variance, appeared to have a strong influence on the differences in the metabolic profile according to the ripening stage. In general, unripe (RS1) and medium-ripe (RS2) avocados were situated at negative scores of PC1, while ripe (RS3) and overripe (RS4) fruits were situated at positive scores.



**Figure 1.** Two-dimensional (2D) principal component analysis biplot using the first two principal components (A) and heat map (B) obtained from the LC-MS quantitative data set. Ripening stage: RS1- Unripe, RS2- Medium, RS3- Edible ripeness, RS4- Overripe. Meaning of dots: met1-Abscisic acid; met2- Caffeic acid glucoside, met3- Chlorogenic acid, met4- Coumaric acid derivative, met5- Coumaric acid hexose, met6- Coumaric acid malonyl-hexose I, met7- Coumaric acid malonyl-hexose II, met8- Coumaric acid malonyl-hexose III, met9- Dihydroxybenzoic acid hexose I, met10- Dihydroxybenzoic acid hexose II, met11- Epicatechin, met12- Ferulic acid, met13- Ferulic acid hexose, met14- Tachioside, met15- *N*-acetyl-phenylalanine, met16- *N*-acetyl-tryptophan, met17- *N*-acetyl-tyrosine, met18- Pantothenic acid, met19- *p*-Coumaric acid, met20- Penstemide, met21- Phenylalanine, met22- Isotachioside, met23- Tryptophan, met24- Tyrosine, met25- Unknown 2 (*m/z* 337), met26- Unknown 1 (*m/z* 369), met27- Unknown 3 (*m/z* 381), met28- Unknown 5 (*m/z* 391), met29- Unknown 4 (*m/z* 443), met30- Uridine

Notably, early ripening stages RS1 and RS2, especially in *Bacon* and *Fuerte*, displayed closely clustered chemical profiles. However, *Hass* samples RS1 and RS2 exhibited a somewhat less compact grouping. Similarly, the ripe and overripe avocados (RS3 and RS4) manifested overlapping profiles, with *Bacon* and *Hass* presenting the most distinctive metabolic characteristics during the transition from climacteric to post-climacteric stages. The second component (PC2) appeared to facilitate the differentiation of avocado varieties, with *Bacon* situated at positive scores, while *Fuerte* and *Hass* were predominantly situated in the negative zone along its axis.

After verifying the differentiation of the phytochemical profile, possible correlations between cultivar- and ripening-associated metabolites were studied by correlation analysis and interactive visual heat mapping (Figure 1B). Several key metabolites were preliminarily highlighted as playing a pivotal role in cultivar distinction. Two of the most significant metabolites for varietal discrimination were the two hexose isomers of dihydroxybenzoic acid (characteristic of *Hass* fruits due to their high content). On the other hand, low tachioside concentrations occurred to be typical for the same variety. Two of the compounds that could not be annotated ( $m/z$  381 and 391), isotachioside, chlorogenic acid, pantothenic acid and tryptophan, showed remarkably high concentrations in avocado cv. *Bacon* exclusively. Fruits of cv. *Fuerte* stood out for their tyrosine, *N*-acetyl-tyrosine, *N*-acetyl-phenylalanine and *N*-acetyl-tryptophan contents. In relation to metabolic evolution during ripening, several compounds correlated positively with the time elapsed. Among them, the most influential were coumaric acid hexose, *p*-coumaric acid, ferulic acid hexose and ferulic acid. In addition, abscisic acid, unknown 4 ( $m/z$  443) and uridine were also correlated. In contrast, penstemide was the most negatively correlated metabolite.

### 3.2.2. Evolution of metabolites concentration during avocado fruit ripening

In the preceding section, our aim was to delve into the dataset's structure through a general examination using statistical analysis of the quantitative LC-MS data. The subsequent phase involved providing an intricate account of the overarching evolution, categorised by "chemical categories," alongside a detailed portrayal of the individual patterns exhibited by each metabolite throughout all stages of fruit ripening.

As expected, some compounds displayed consistent trends across the three varieties, while others exhibited distinctive behaviour patterns. To enhance clarity and comprehension, this section has been partitioned into two subsections, each complemented by Figures 2 and 3.

#### 3.2.2.1. Delving into phenolic compounds quantitative evolution over time

Plant phenols are generally located in the vacuole and are derived from the shikimate, pentose phosphate and phenylpropanoid pathways [31]. These secondary metabolites, which include, among others, phenolic acids, flavonoids and lignans, are found in both free and conjugated forms (primarily as  $\beta$ -glycosides). Phenolic compounds play many essential roles in plants, influencing sensory attributes such as flavour, taste, and colour, while also playing a crucial role in plant defence mechanisms [32].

The category of phenolic compounds exhibited a significant ( $p \leq 0.05$ ) response to the ripening process, as demonstrated in the preceding section. Notably, only the isomers of dihydroxybenzoic acid hexose showed no substantial changes. This finding aligns with the observations of López-Cobo et al., who also found no significant variation in the concentration of one of the isomers of this compound in *Hass* fruit pulp between the optimal time of consumption and the stage of overripening [24]. However, it is worth noting that López-Cobo's study focused solely on these two ripening stages, contrasting with the more comprehensive examination of four ripening stages in our investigation. While these metabolites (isomers of dihydroxybenzoic acid hexose) do not seem to be directly correlated with ripening phenomena, they do play a significant role in distinguishing varietal characteristics. The concentration found in *Hass* avocados was three times higher (ranging from 51-61 mg kg<sup>-1</sup> DW) than in *Bacon* and *Fuerte* varieties at all ripening stages.

Moving beyond this specific compound, most other phenolic compounds (elaborated upon later) exhibited a significant ( $p \leq 0.05$ ) increase in content during fruit softening. Several showed a steady increase from RS1 to RS4, while others progressively increased from RS1 to RS3 and subsequently decreased with senescence, though not always significantly. This latter pattern was particularly evident in *Hass* avocados. This trend aligns with the findings of Villa-Rodríguez et al., who reported the highest total phenolic content in mature fruit and the lowest in unripe fruit for *Hass* avocados [18]. The authors also emphasised the negative impact of the senescence stage on the phenolic content of *Hass* avocados. Similarly, Zhang et al. documented a trend of total phenolic accumulation during ripening in the avocado cv. *Booth 7* [21]. It is essential to take into account the large number of metabolites that are quantified individually in this work; no such research has been carried out so comprehensively so far, only a rather partial comparison with literature results will be possible.

The overall increase of many phenolic compounds during fruit softening would be related to the enzyme phenylalanine ammonia lyase (PAL), which is one of the key players in the initiation of phenolic biosynthesis. This pivotal enzyme operates within the phenylpropanoid pathway of plant metabolism and is responsible for catalysing the deamination of phenylalanine, leading to the formation of *trans*-cinnamic acid [33]. PAL activity is subject to stresses and increases as part of a plant defence response against diseases, insect attacks, and the stress commonly encountered by many fleshy fruits during ripening [17,33]. Indeed, fruit softening is a clear way to increase fruit vulnerability. Moreover, the induction of PAL activity by ethylene has been suggested on several occasions [17,34], which is particularly relevant in climacteric fruits such as avocado.

Looking deeper into the individual phenolic metabolites shown in [Figure 2](#), *p*-coumaric and ferulic acids (two simple hydroxycinnamic acids), showed a significant increase in concentration ( $p \leq 0.05$ ) as the avocado ripened. Previous reports have described these same trends [20,22,25,35]. Within the phenolic compounds category, the most substantial concentrations were observed for compounds derived from coumaric acid. Notably, all these compounds exhibited a parallel increase in concentration as the fruit ripened, at least up to the ready-to-eat stage (RS3). Several

coumaric acid derivatives have been previously described by Pedreschi et al., who also observed the described increase as the avocado fruit ripened [15].

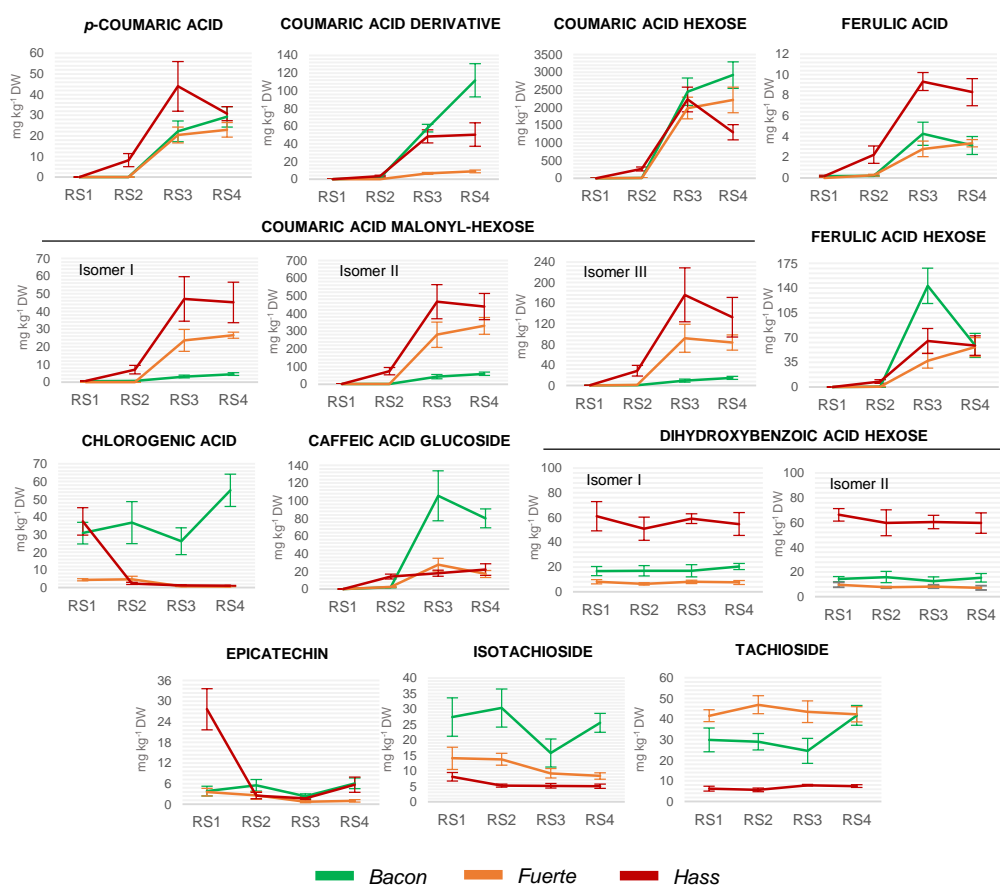


**Figure 2.** Graphical depictions of individual trends observed during ripening for the fifteen phenolic compounds and related substances determined in the avocado pulp of *Hass*, *Fuerte* and *Bacon* samples

Despite a common general trend, certain varietal differences were observed. For example, even though the isomer II of coumaric acid malonyl-hexose was the most abundant in all three varieties, its evolution was much less pronounced in *Bacon* than in *Hass* and *Fuerte*. Something similar occurred with the coumaric acid derivative in *Fuerte* fruits, which exhibited a less pronounced increase compared to *Bacon* avocados. The coumaric acid hexose, which was the most predominant compound, evolved in a rather similar way and with a very comparable content regardless of the variety up to the ready-to-eat stage. From that point onwards, the levels found in ripe avocados were maintained in *Bacon* and *Fuerte* fruits (even showing a slight increase), while in *Hass* it decreased significantly in the overripe stage.

The remaining glycosidic forms of phenolic acids, namely ferulic acid hexose and caffeic acid glucoside, exhibited dominance in *Bacon* (compared to the other varieties) as the fruit ripened, although the observed increase was shared across all varieties. Specifically, ferulic acid hexose in *Bacon* reached its peak only up to the edible ripeness, but experienced a significant decline, reaching mean values comparable to the other two varieties ( $57\text{--}59\text{ mg kg}^{-1}\text{ DW}$ ) in the post-climacteric stage. In contrast, the decrease of caffeic acid glucoside in *Bacon* at overripe fruits was less pronounced and did not reach statistical significance. As previously highlighted, the rate at which metabolic changes unfolded within each fruit was a significant differentiator between the varieties tested.

Chlorogenic acid showed a distinctive evolution depending on the variety observed. For example, cv. *Bacon* and *Hass* showed similar concentrations in unripe avocados (RS1) with  $31\pm 6$  and  $38\pm 8\text{ mg kg}^{-1}\text{ DW}$ , respectively. However, a significant decrease in the concentration of this compound in RS2 characterised *Hass* fruits. This is similar to what was also observed by Di Stefano and Hurtado-Fernández and their respective collaborators [20,22,25]. Di Stefano and co-authors also studied *Bacon* and *Fuerte* varieties, describing a decrease in chlorogenic acid in *Bacon* and an increase in *Fuerte* from unripe to ripe fruit (considering only 2 ripening stages) [25]. In this research, chlorogenic acid in *Fuerte* showed a quantitative evolution comparable to *Hass*, although with lower overall values. However, in avocados cv. *Bacon*, the concentration of this compound was maintained or even increased significantly as they matured, with contents of up to  $55\text{ mg kg}^{-1}\text{ DW}$  in the overripe stage. This distinctive characteristic of high chlorogenic acid contents in *Bacon* fruits aligns with findings by Hurtado-Fernández and co-authors, who exclusively analysed ripe avocados from several varieties [36]. It is noteworthy that although chlorogenic acid was determined in all studied samples, its accumulation predominantly occurs in the avocado peel rather than the pulp [10,37].

Epicatechin showed a decrease in *Hass* avocados, particularly from early to medium ripeness. Its concentration also decreased overall in *Fuerte* and exhibited some fluctuations in *Bacon*. This reduction from green to ripe *Hass* fruit is in agreement with data reported by Hurtado-Fernández et al. [20]. Also Di Stefano and collaborators observed a decreasing trend of epicatechin with fruit ripening (for all the varieties they studied except *Hass*) [25]. Villa-Rodríguez and colleagues reported that epicatechin reached its maximum contents in RS4, finding  $126.6\text{ mg kg}^{-1}$  for *Hass* samples from Mexico, a value significantly higher than those determined for the samples considered in this work [19]. The highest observed concentrations of this flavon-3-ol were  $28\pm 6\text{ mg kg}^{-1}\text{ DW}$ , found in the green *Hass* fruit (RS1). Epicatechin is involved in the regulation of the lipoxygenase activity in avocado, making it an important factor in modulating the fruit's resistance to post-harvest attack [38]. Epicatechin is additionally associated with the browning of mesocarp tissue [39]. Finally, both peaks, tentatively identified as isotachioside and tachioside (glycosidic phenols), showed a closer similarity to the glycosidic isomers of dihydroxybenzoic acid. Although significant differences were detected during ripening in both *Bacon* and *Hass* varieties, no

pronounced overall trend was observed. Both substances exhibited notable concentrations in RS1 and RS2 avocados; for instance, in RS1 for *Bacon* isotachioside and tachioside, respectively, were found at  $27\pm 6$  and  $30\pm 6$  mg kg<sup>-1</sup> DW, and in *Fuerte* the concentration levels were  $14\pm 4$  and  $42\pm 3$  mg kg<sup>-1</sup> DW, for the same analytes.

### **3.2.2.2. Quantitative progression of the remaining considered metabolites (amino acids and related compounds, nucleosides, iridoids, phytohormones, vitamins, and unidentified substances)**

Plant amino acid metabolism plays a fundamental role, serving as the basis for protein synthesis, respiration processes and the synthesis of various other metabolites [2]. For instance, phenylalanine is the primary precursor in the phenylpropanoid biosynthesis pathway. In addition, free amino acids are important for the synthesis or enhanced activity of several enzymes that operate during climacteric ripening. Amino acids and derivatives can also influence fruit aroma, taste and quality [40]. While avocado fruit is relatively rich in protein, the role of free amino acids in postharvest avocado ripening has received minimal attention over the years. Significant differences were observed in both variety and ripeness stage for the amino acids and *N*-acetyl-amino acid derivatives group, although a discernible general pattern could not be defined. In contrast to phenolic compounds, the individual trends within this group exhibited a high level of heterogeneity.

In terms of total amino acids and derivatives contents, *Fuerte* fruits consistently exhibited the highest amounts, both in green and ripe avocados, while *Hass* fruits displayed the lowest contents. *Bacon* fruits showed significantly higher levels of tryptophan concentration exclusively. Examining the individual compounds of this category (Figure 3), the steadiest evolution was observed for tyrosine and *N*-acetyl-tyrosine levels, which underwent a strong increase, particularly in *Fuerte*. Tyrosine levels in *Fuerte* at RS4 were  $126\pm 6$  mg kg<sup>-1</sup> DW and *N*-acetyl-tyrosine levels were  $259\pm 34$  mg kg<sup>-1</sup> DW, respectively. The distinct increasing trend observed was not replicated in *Hass* and *Bacon* varieties, although a partial resemblance was noted for *N*-acetyl-tyrosine, albeit to a lesser extent.

Phenylalanine exhibited a positive evolution in the early stages of climacteric ripening in *Fuerte* and *Bacon*, with a notable reduction upon reaching maturity for consumption. In contrast, *Hass* fruits showed a minimal reduction over time. Tryptophan increased significantly ( $p\leq 0.05$ ) in *Bacon* fruits during climacteric ripening, rising from  $2.8\pm 0.6$  to  $5\pm 1$  mg kg<sup>-1</sup> DW, with the highest levels reached at the edible ripeness stage. This metabolite did not show significant and consistent changes in *Hass* and *Fuerte*. There were no significant changes in the contents of *N*-acetyl-tryptophan for any of the varieties analysed. Although there were alterations in the levels of *N*-acetyl-phenylalanine in *Bacon* and *Fuerte*, the progression was not distinctly evident. In *Fuerte* fruits, both metabolites stood out, implying that they could potentially serve as specific markers for this cultivar, as previously mentioned. The cultivar-dependent behaviour of amino acids and

derivatives may be associated with the unique requirements of each variety, as these compounds are essential for providing foundational components necessary for protein synthesis, respiration, and the biosynthesis of various secondary metabolites.

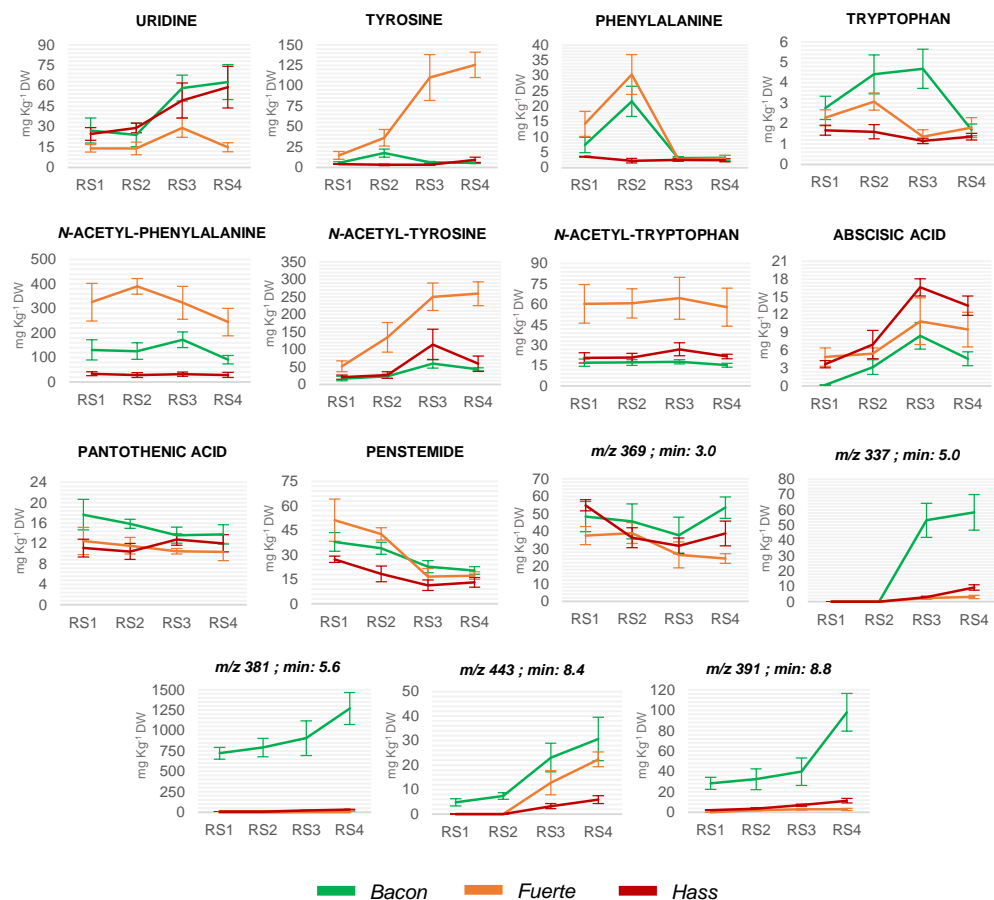


**Figure 3.** Quantitative evolution patterns observed over ripening for amino acids, nucleosides and related compounds, iridoids, phytohormones, vitamins, and the five not fully annotated substances determined in the avocado pulp of *Hass*, *Fuerte* and *Bacon* varieties

Regarding nucleosides, we observed consistently elevated and statistically significant ( $p \leq 0.05$ ) levels of uridine as fruits ripened across all three varieties. Notably, in the case of *Fuerte*, a distinct and significant decline was observed as it approached senescence. Nucleosides serve as crucial precursors for nucleotide synthesis, which in turn are fundamental building blocks of nucleic acids like DNA and RNA. These molecules play pivotal roles in the storage, transfer, and expression of genetic information [41]. It is documented that in avocado fruit, the expression of numerous genes undergoes alterations through ripening under the influence of the phytohormone ethylene [42]. Therefore, if the number of specific mRNAs increased with ripening, the documented rise in uridine as fruit ripened could be consequence of the increased demand for precursors.

Penstemide, identified as the only iridoid compound, showed a steady decline in all varieties, reaching its highest levels in green fruit and dropping to the lowest levels at the overripe stage. Iridoids are secondary plant metabolites and comprise the predominant category of monoterpenoids with acyclopentan-[C]-pyran skeleton. Even though cytotoxic properties have been attributed to penstemide [43], there are currently no available reports providing evidence of the impact of iridoids on the climacteric ripening process of fruits.

Pantothenic acid (a water-soluble B<sub>5</sub>-vitamin) is the main precursor for the biosynthesis of coenzyme A (CoA) which is an essential cofactor for the respiratory pathway but also plays a key role in fatty acid synthesis/oxidation and the synthesis of many secondary metabolites [44]. Nevertheless, this metabolite showed a minimal significant reduction in *Bacon* during fruit ripening, remained stable in *Fuerte*, and showed irregular fluctuations in *Hass* without a discernible pattern. Considering these results, pantothenic acid content would not be correlated with the climacteric ripening, despite its role in supporting concurrent biosynthetic pathways. Interestingly, Serrano-García and co-authors observed that this vitamin was also not altered by a prolonged on tree fruit maturation or storage in cold chambers, although displayed comparable ranges (9-15 mg kg<sup>-1</sup> DW) to those observed in the present study for *Hass* fruits at edible ripeness [45].

Abscisic acid (ABA) demonstrated consistent behaviour throughout the study. A progressive increase in ABA content was observed in the avocado fruit mesocarp during softening, mirroring a similar pattern to ethylene biosynthesis and the respiration rate up to a specific threshold. In all three varieties studied, the highest ABA concentration in the pulp occurred just after the climacteric peak at RS3, with values ranging from 8 to 17 mg kg<sup>-1</sup> DW depending on the cultivar. Subsequently, ABA levels declined with senescence. Slightly higher ready-to-eat ABA values of 19.6-26.8 mg kg<sup>-1</sup> DW were reported by Chirinos et al., for *Hass* fruits obtained at different harvest dates and subjected to different storage conditions; the small differences observed could be related to variations in maturation rates and overall shelf life [46]. Previous results have already suggested a link between ABA and ethylene metabolism [47]. In fact, recent developments seem to indicate that the ripening of climacteric fruits is not only due to ethylene, but to an interaction with other phytohormones, so that ABA, auxin, jasmonates, brassinosteroids and cytokinins may act as signalling molecules that stimulate the ripening of these climacteric fruits by inducing the expression of ripening-related genes [48]. At the molecular level, the biosynthetic pathway of ABA in plants typically incorporates carotenoids as precursors, leading to the production of xanthoxin. Subsequently, xanthoxin is converted into ABA-aldehyde, and further transformation results in ABA, which represents the biologically active form of the hormone. Indeed, the impact of ripening on carotenoid content in avocado pulp has been previously documented with a consistent reduction, a fact that could be partially attributed to the requirement of carotenoids for ABA synthesis [19,49].

As previously highlighted, unknowns 2, 3 and 5 at *m/z* 337, 381, and 391 appear distinctly associated with *Bacon* fruits, exhibiting significantly higher concentrations in this variety regardless

of the ripening stage. Notably, in *Bacon* avocados, the concentration of these compounds increases with ripeness, although a minor elevation on a different concentration scale is also observed in the other two varieties. A similar, albeit less pronounced, trend is observed for the unknown 4 ( $m/z$  443), with its concentration displaying a comparable increase across all three varieties. Conversely, the concentration of the unidentified compound with  $m/z$  369 remained relatively unchanged in *Bacon* but decreased significantly ( $p \leq 0.05$ ) in *Hass* and *Fuerte* as the fruits ripened. Considering the demonstrated relevance of these substances, especially in distinguishing the *Bacon* variety, it is imperative to further investigate and elucidate their structure, ultimately assigning them a name. Ongoing analyses in this direction are currently being conducted in our laboratory.

#### 4. CONCLUSIONS

A powerful LC-MS method has been applied to quantify thirty relevant individual metabolites throughout the entire avocado ripening process, spanning from unripe to overripe stages, in three commercially significant avocado varieties (*Hass*, *Fuerte*, and *Bacon*). The aim was to explore the dynamic metabolic transformations occurring during ripening, while considering the influence of the variety. Noteworthy metabolic differences were observed between unripe and ripe fruits, as well as among the evaluated genotypes. The phenolic compound group exhibited a consistent increase over time during ripening, while the behaviour of amino acids and related compounds was predominantly cultivar dependent. Abscisic acid, uridine, and penstamide displayed consistent trends across all three varieties. Additionally, the abundance of several unidentified compounds was found to be characteristic of the *Bacon* variety, with these analytes showing an increase with fruit ripening. Future research efforts integrating multi-omics methods will provide a more comprehensive understanding of the physicochemical processes underlying avocado ripening dynamics. This work, along with future studies, aims to deepen our insight into the biosynthetic pathways of key metabolites and their variation among commercially available avocado cultivars.

**Funding:** This research has been partially financed by Grants PID2021-128508OB-I00 and PID2022-141851OB-I00 funded by MCIN/AEI/10.13039/501100011033 and “FEDER Una manera de hacer Europa”, by Grant PID2019-109566RB-I00 funded by MCIN/AEI /10.13039/501100011033, and the Millennium Science Initiative Program – ICN2021\_044. Authors are grateful for the financial support received from the Spanish Government (FPU19/00700) (I.S-G.), and from “UE-NextGenerationUE” (R.P.M.). Funding for open access charge: Universidad de Granada / CBUA.

#### References

1. Talavera, A.; Gonzalez-Fernandez, J.J.; Carrasco-Pancorbo, A.; Olmo-García, L.; Hormaza, J.. Avocado: Agricultural Importance and Nutraceutical Properties. In *Compendium of Crop Genome Designing for Nutraceuticals*; Kole, C., Ed.; Springer Singapore, 2023; pp. 1–19, doi:10.1007/978-981-19-3627-2.

2. Pedreschi, R.; Uarrotta, V.; Fuentealba, C.; Alvaro, J.E.; Olmedo, P.; Defilippi, B.G.; Meneses, C.; Campos-Vargas, R. Primary Metabolism in Avocado Fruit. *Front. Plant Sci.* **2019**, *10*, 795, doi:10.3389/fpls.2019.00795.
3. Crane, J.H.; Douhan, G.; Faber, B.A.; Arpaia, M.L.; Bender, G.S.; Balerdi, C.F.; Barrientos-Priego, A.F. Cultivars and Rootstocks. In *The avocado: botany, production and uses*; Schaffer, B., Wolstenholme, B.N., Whiley, A.W., Eds.; CAB International, 2013; pp. 200–233, doi:10.1079/9781845937010.0200.
4. FAO. Statistics Division of Food and Agriculture Organization of the United Nations (FAOSTAT). Available online: <https://www.fao.org/faostat/en/#home> (accessed on 7 June 2023).
5. Cascallar, E.C. 1.2 El Aguacate En La Península Ibérica. In *Cultivo, Poscosecha y Procesado Del Aguacate*; Namesny, A., Conesa, C., Hormaza, I., Lobo, G., Eds.; 2020; pp. 19–26 ISBN 9788416909315.
6. Kassim, A.; Workneh, T.S.; Bezuidenhout, C.N. A Review on Postharvest Handling of Avocado Fruit. *African J. Agric. Res.* **2013**, *8*, 2385–2402, doi:10.5897/AJAR12.1248.
7. Núñez-Lillo, G.; Ponce, E.; Arancibia-Guerra, C.; Carpentier, S.; Carrasco-Pancorbo, A.; Olmo-García, L.; Chirinos, R.; Campos, D.; Campos-Vargas, R.; Meneses, C.; et al. A Multiomics Integrative Analysis of Color De-Synchronization with Softening of ‘Hass’ Avocado Fruit: A First Insight into a Complex Physiological Disorder. *Food Chem.* **2023**, *408*, doi:10.1016/j.foodchem.2022.135215.
8. Hurtado-Fernandez, E.; Fernandez-Gutierrez, A.; Carrasco-Pancorbo, A. Avocado Fruit—Persea Americana. In *Exotic Fruits Reference Guide*; Rodrigues, S., Silva, E. de O., Brito, E.S. de, Eds.; 2016; pp. 37–48, doi: 10.1016/B978-0-12-803138-4.00001-0.
9. Defilippi, B.G.; Ejsmentewicz, T.; Covarrubias, M.P.; Gudenschwager, O.; Campos-Vargas, R. Changes in Cell Wall Pectins and Their Relation to Postharvest Mesocarp Softening of “Hass” Avocados (Persea Americana Mill.). *Plant Physiol. Biochem.* **2018**, *128*, 142–151, doi:10.1016/j.plaphy.2018.05.018.
10. Beiro-Valenzuela, M.G.; Serrano-García, I.; Monasterio, R.P.; Moreno-Tovar, M.V.; Hurtado-Fernández, E.; González-Fernández, J.J.; Hormaza, J.I.; Pedreschi, R.; Olmo-García, L.; Carrasco-Pancorbo, A. Characterization of the Polar Profile of Bacon and Fuerte Avocado Fruits by Hydrophilic Interaction Liquid Chromatography-Mass Spectrometry: Distribution of Non-Structural Carbohydrates, Quinic Acid, and Chlorogenic Acid between Seed, Mesocarp, and Exocar. *J. Agric. Food Chem.* **2023**, *71*, 5674–5685, doi:10.1021/acs.jafc.2c08855.
11. Tesfay, S.Z.; Bertling, I.; Bower, J.P. D-Mannoheptulose and Perseitol in “Hass” Avocado: Metabolism in Seed and Mesocarp Tissue. *South African J. Bot.* **2012**, *79*, 159–165, doi:10.1016/j.sajb.2011.10.006.
12. Blakey, R.J.; Tesfay, S.Z.; Bertling, I.; Bower, J.P. Changes in Sugars, Total Protein, and Oil in “Hass” Avocado (Persea Americana Mill.) Fruit during Ripening. *J. Hortic. Sci. Biotechnol.* **2012**, *87*, 381–387, doi:10.1080/14620316.2012.11512880.
13. Tesfay, S.Z.; Bertling, I.; Bower, J.P. Anti-Oxidant Levels in Various Tissues during the Maturation of “Hass” Avocado (Persea Americana Mill.). *J. Hortic. Sci. Biotechnol.* **2010**, *85*, 106–112, doi:10.1080/14620316.2010.11512639.
14. Cowan, A.K. Metabolic Control of Avocado Fruit Growth: 3-Hydroxy-3-Methylglutaryl Coenzyme a Reductase, Active Oxygen Species and the Role of C7 Sugars. *South African J. Bot.* **2004**, *70*, 75–82, doi:10.1016/S0254-6299(15)30309-4.
15. Pedreschi, R.; Ponce, E.; Hernández, I.; Fuentealba, C.; Urbina, A.; González-Fernández, J.J.; Hormaza, J.I.; Campos, D.; Chirinos, R.; Aguayo, E. Short vs. Long-Distance Avocado Supply Chains: Life Cycle Assessment Impact Associated to Transport and Effect of Fruit Origin and Supply Conditions Chain on Primary and Secondary Metabolites. *Foods* **2022**, *11*, 1807, doi:10.3390/foods11121807.
16. Gómez-Maqueo, A.; Escobedo-Avellaneda, Z.; Welti-Chanes, J. Phenolic Compounds in Mesoamerican Fruits—Characterization, Health Potential and Processing with Innovative Technologies. *Int. J. Mol. Sci.* **2020**, *21*, 1–41, doi:10.3390/ijms21218357.

17. Tomás-Barberán, F.A.; Espín, J.C. Phenolic Compounds and Related Enzymes as Determinants of Quality in Fruits and Vegetables. *J. Sci. Food Agric.* **2001**, *81*, 853–876, doi:10.1002/jsfa.885.
18. Villa-Rodríguez, J.A.; Molina-Corral, F.J.; Ayala-Zavala, J.F.; Olivas, G.I.; González-Aguilar, G.A. Effect of Maturity Stage on the Content of Fatty Acids and Antioxidant Activity of “Hass” Avocado. *Food Res. Int.* **2011**, *44*, 1231–1237, doi:10.1016/j.foodres.2010.11.012.
19. Villa-Rodríguez, J.A.; Yahia, E.M.; González-León, A.; Ifie, I.; Robles-Zepeda, R.E.; Domínguez-Avila, J.A.; González-Aguilar, G.A. Ripening of ‘Hass’ Avocado Mesocarp Alters Its Phytochemical Profile and the in Vitro Cytotoxic Activity of Its Methanolic Extracts. *South African J. Bot.* **2020**, *128*, 1–8, doi:10.1016/j.sajb.2019.09.020.
20. Hurtado-Fernández, E.; Pacchiarotta, T.; Gómez-Romero, M.; Schoenmaker, B.; Derks, R.; Deelder, A.M.; Mayboroda, O.A.; Carrasco-Pancorbo, A.; Fernández-Gutiérrez, A. Ultra High Performance Liquid Chromatography-Time of Flight Mass Spectrometry for Analysis of Avocado Fruit Metabolites: Method Evaluation and Applicability to the Analysis of Ripening Degrees. *J. Chromatogr. A* **2011**, *1218*, 7723–7738, doi:10.1016/j.chroma.2011.08.059.
21. Zhang, Z.; Huber, D.J.; Rao, J. Antioxidant Systems of Ripening Avocado (*Persea Americana* Mill.) Fruit Following Treatment at the Prelimacteric Stage with Aqueous 1-Methylcyclopropene. *Postharvest Biol. Technol.* **2013**, *76*, 58–64, doi:10.1016/j.postharvbio.2012.09.003.
22. Hurtado-Fernández, E.; Pacchiarotta, T.; Mayboroda, O.A.; Fernández-Gutiérrez, A.; Carrasco-Pancorbo, A. Quantitative Characterization of Important Metabolites of Avocado Fruit by Gas Chromatography Coupled to Different Detectors (APCI-TOF MS and FID). *Food Res. Int.* **2014**, *62*, 801–811, doi:10.1016/j.foodres.2014.04.038.
23. Hurtado-Fernández, E.; Pacchiarotta, T.; Mayboroda, O.A.; Fernández-Gutiérrez, A.; Carrasco-Pancorbo, A. Metabolomic Analysis of Avocado Fruits by GC-APCI-TOF MS: Effects of Ripening Degrees and Fruit Varieties. *Anal. Bioanal. Chem.* **2015**, *407*, 547–555, doi:10.1007/s00216-014-8283-9.
24. López-Cobo, A.; Gómez-Caravaca, A.M.; Pasini, F.; Caboni, M.F.; Segura-Carretero, A.; Fernández-Gutiérrez, A. HPLC-DAD-ESI-QTOF-MS and HPLC-FLD-MS as Valuable Tools for the Determination of Phenolic and Other Polar Compounds in the Edible Part and by-Products of Avocado. *LWT - Food Sci. Technol.* **2016**, *73*, 505–513, doi:10.1016/j.lwt.2016.06.049.
25. Di Stefano, V.; Avellone, G.; Bongiorno, D.; Indelicato, S.; Massenti, R.; Lo Bianco, R. Quantitative Evaluation of the Phenolic Profile in Fruits of Six Avocado (*Persea Americana*) Cultivars by Ultra-High-Performance Liquid Chromatography-Heated Electrospray-Mass Spectrometry. *Int. J. Food Prop.* **2017**, *20*, 1302–1312, doi:10.1080/10942912.2016.1208225.
26. Campos, D.; Teran-Hilares, F.; Chirinos, R.; Aguilar-Galvez, A.; García-Ríos, D.; Pacheco-Avalos, A.; Pedreschi, R. Bioactive Compounds and Antioxidant Activity from Harvest to Edible Ripeness of Avocado Cv. Hass (*Persea Americana*) throughout the Harvest Seasons. *Int. J. Food Sci. Technol.* **2020**, *55*, 2208–2218, doi:10.1111/ijfs.14474.
27. Babiker, E.E.; Mohamed Ahmed, I.A.; Uslu, N.; Özcan, M.M.; Al Juhaimi, F.; Ghafoor, K.; Almusallam, I.A. Influence of Drying Methods on Bioactive Properties, Fatty Acids and Phenolic Compounds of Different Parts of Ripe and Unripe Avocado Fruits. *J. Oleo Sci.* **2021**, *70*, 589–598, doi:10.5650/jos.ess20343.
28. AOAC Association of Official Analytical Chemists. Official Methods of Analysis of AOAC Int. 2016, Latimer G.W, Ed. 20th ed.
29. Serrano-García, I.; Domínguez-García, J.; Hurtado-Fernandez, E.; González-Fernández, J.J.; Hormaza, I.; Beiro-Valenzuela, M.G.; Monasterio, R.; Pedreschi, R.; Olmo-García, L.; Carrasco-Pancorbo, A. Assessing the RP-LC-MS-Based Metabolic Profile of Hass Avocados Marketed in Europe from Different Geographical Origins (Peru, Chile, and Spain) over the Whole Season. *Plants* **2023**, *12*, 3004, doi:https://doi.org/10.3390/plants12163004.

30. Ruttkies, C.; Schymanski, E.L.; Wolf, S.; Hollender, J.; Neumann, S. MetFrag Relaunched: Incorporating Strategies beyond in Silico Fragmentation. *J. Cheminform.* **2016**, *8*, 3, doi:10.1186/s13321-016-0115-9.
31. Lin, D.; Xiao, M.; Zhao, J.; Li, Z.; Xing, B.; Li, X.; Kong, M.; Li, L.; Zhang, Q.; Liu, Y.; et al. An Overview of Plant Phenolic Compounds and Their Importance in Human Nutrition and Management of Type 2 Diabetes. *Molecules* **2016**, *21*, 1374, doi:10.3390/molecules21101374.
32. Balasundram, N.; Sundram, K.; Samman, S. Phenolic Compounds in Plants and Agri-Industrial by-Products: Antioxidant Activity, Occurrence, and Potential Uses. *Food Chem.* **2006**, *99*, 191–203, doi:10.1016/j.foodchem.2005.07.042.
33. Bajguz, A.; Piotrowska-Niczyporuk, A. Biosynthetic Pathways of Hormones in Plants. *Metabolites* **2023**, *13*, 1–36, doi:10.3390/metabo13080884.
34. Li, X.; Li, B.; Li, M.; Fu, X.; Zhao, X.; Min, D.; Li, F.; Zhang, X. Ethylene Pretreatment Induces Phenolic Biosynthesis of Fresh-Cut Pitaya Fruit by Regulating Ethylene Signaling Pathway. *Postharvest Biol. Technol.* **2022**, *192*, 112028, doi:10.1016/j.postharvbio.2022.112028.
35. Contreras-Gutiérrez, P.K.; Hurtado-Fernández, E.; Gómez-Romero, M.; Hormaza, J.I.; Carrasco-Pancorbo, A.; Fernández-Gutiérrez, A. Determination of Changes in the Metabolic Profile of Avocado Fruits (*Persea Americana*) by Two CE-MS Approaches (Targeted and Non-Targeted). *Electrophoresis* **2013**, *34*, 2928–2942, doi:10.1002/elps.201200676.
36. Hurtado-Fernández, E.; González-Fernández, J.J.; Hormaza, J.I.; Bajjoub, A.; Fernández-Gutiérrez, A.; Carrasco-Pancorbo, A. Targeted LC-MS Approach to Study the Evolution over the Harvesting Season of Six Important Metabolites in Fruits from Different Avocado Cultivars. *Food Anal. Methods* **2016**, *9*, 3479–3491, doi:10.1007/s12161-016-0523-5.
37. Ramos-Aguilar, A.L.; Ornelas-Paz, J.; Tapia-Vargas, L.M.; Gardea-Bejar, A.A.; Yahia, E.M.; Ornelas-Paz, J. de J.; Perez-Martinez, J.D.; Rios-Velasco, C.; Escalante-Minakata, P. Metabolomic Analysis and Physical Attributes of Ripe Fruits from Mexican Creole (*Persea Americana* Var. *Drymifolia*) and “Hass” Avocados. *Food Chem.* **2021**, *354*, doi:10.1016/j.foodchem.2021.129571.
38. Guetsky, R.; Kobiler, I.; Wang, X.; Perlman, N.; Gollop, N.; Avila-Quezada, G.; Hadar, I.; Prusky, D. Metabolism of the Flavonoid Epicatechin by Laccase of *Colletotrichum Gloeosporioides* and Its Effect on Pathogenicity on Avocado Fruits. *Phytopathology* **2005**, *95*, 1341–1348, doi:10.1094/PHYTO-95-1341.
39. Tesfay, S.Z.; Bertling, I.; Bower, J.P. Seasonal Trends of Specific Phenols in “Hass” Avocado Tissues. *Acta Hort.* **2011**, *911*, 349–354, doi:10.17660/ActaHortic.2011.911.40.
40. Mandrioli, R.; Mercolini, L.; Raggi, M.A. Recent Trends in the Analysis of Amino Acids in Fruits and Derived Foodstuffs. *Anal. Bioanal. Chem.* **2013**, *405*, 7941–7956, doi:10.1007/s00216-013-7025-8.
41. Domínguez-Álvarez, J.; Mateos-Vivas, M.; Rodríguez-Gonzalo, E.; García-Gómez, D.; Bustamante-Rangel, M.; Delgado Zamarreño, M.M.; Carabias-Martínez, R. Determination of Nucleosides and Nucleotides in Food Samples by Using Liquid Chromatography and Capillary Electrophoresis. *TrAC - Trends Anal. Chem.* **2017**, *92*, 12–31, doi:10.1016/j.trac.2017.04.005.
42. McGarvey, D.J.; Sirevåg, R.; Christoffersen, R.E. Ripening-Related Gene from Avocado Fruit: Ethylene-Inducible Expression of the mRNA and Polypeptide. *Plant Physiol.* **1992**, *98*, 554–559, doi:10.1104/pp.98.2.554.
43. Wysokinska, H.; Skrzypek, Z.; Kunert-Radek, J. Studies on Iridoids of Tissue Cultures of *Penstemon Serrulatus*: Isolation and Their Antiproliferative Properties. *J. Nat. Prod.* **1992**, *55*, 58–63.
44. Webb, M.E.; Smith, A.G.; Abell, C. Biosynthesis of Pantothenate. *Nat. Prod. Rep.* **2004**, *21*, 695–721, doi:10.1039/b316419p.
45. Serrano-García, I.; Hurtado-Fernández, E.; Gonzalez-Fernandez, J.J.; Hormaza, J.I.; Pedreschi, R.; Reboredo-Rodríguez, P.; Figueiredo-González, M.; Olmo-García, L.; Carrasco-Pancorbo, A. Prolonged

- On-Tree Maturation vs. Cold Storage of Hass Avocado Fruit: Changes in Metabolites of Bioactive Interest at Edible Ripeness. *Food Chem.* **2022**, *394*, doi:10.1016/j.foodchem.2022.133447.
46. Chirinos, R.; Campos, D.; Martinez, S.; Llanos, S.; Betalleluz-Pallardel, I.; García-Ríos, D.; Pedreschi, R. The Effect of Hydrothermal Treatment on Metabolite Composition of Hass Avocados Stored in A. *Plants* **2021**, *10*, 2427, doi:https://doi.org/10.3390/plants10112427.
47. Meyer, M.D.; Chope, G.A.; Terry, L.A. Investigation into the Role of Endogenous Abscisic Acid during Ripening of Imported Avocado Cv. Hass. *J. Sci. Food Agric.* **2017**, *97*, 3656–3664, doi:10.1002/jsfa.8225.
48. Vincent, C.; Mesa, T.; Munné-Bosch, S. Hormonal Interplay in the Regulation of Fruit Ripening and Cold Acclimation in Avocados. *J. Plant Physiol.* **2020**, *251*, 153225, doi:10.1016/j.jplph.2020.153225.
49. Ashton, O.B.O.; Wong, M.; McGhie, T.K.; Vather, R.; Wang, Y.; Requejo-Jackman, C.; Ramankutty, P.; Woolf, A.B. Pigments in Avocado Tissue and Oil. *J. Agric. Food Chem.* **2006**, *54*, 10151–10158, doi:10.1021/jf061809j.

**Table S1.** Analytical parameters of the LC-MS method used in the present study.

Compound	Rt (min)	Calibration curves	R <sup>2</sup>	Lineal range (mg L <sup>-1</sup> )	LOD <sup>a</sup> (µg L <sup>-1</sup> )	LOQ <sup>a</sup> (µg L <sup>-1</sup> )	Repeatability (% CV)	
							Intra-day <sup>b</sup>	Inter-day <sup>c</sup>
Uridine	2.7	f(x)= 105563.83x + 7808.15	0.999	LOQ – 4.02	35.2	117.2	7.93	9.11
		f(x)= 53300.90x + 255748.78	0.997	4.02 – 32.17				
Phenylalanine	4.9	f(x)= 45365.21x - 2981.85	0.998	LOQ – 13.40	20.5	68.3	7.11	10.25
		f(x)= 23896.02x + 295581.5	0.997	13.40 – 53.62				
Pantothenic acid	5.2	f(x)= 262291.52x + 9129.10	0.999	LOQ – 13.40	31.3	104.2	8.75	10.28
Tryptophan	6.4	f(x)= 215977.70x - 12770.41	0.997	LOQ – 6.70	19.1	63.6	7.23	8.94
Chlorogenic acid	7.2	f(x)= 216198.40x - 9704.88	0.993	LOQ – 2.68	30.2	100.7	7.96	9.85
		f(x)= 98912.37x + 446674.79	0.996	2.68 – 42.90				
Epicatechin	8.3	f(x)= 571067.88x - 8043.94	0.999	LOQ – 2.68	11.1	37.0	7.93	10.18
		f(x)= 266924.29x + 970085.83	0.996	2.68 – 21.45				
<i>p</i> -Coumaric acid	9.9	f(x)= 81338.63x - 1708.04	0.999	LOQ – 1.41	14.6	48.6	7.51	9.59
		f(x)= 50869.28x + 64969.78	0.996	1.41 – 22.62				
		f(x)= 19891.17x + 904704.61	0.990	22.62 - 180.97				
		f(x)= 8794.72x + 3075255.5	0.984	180.97 – 723.86				
Ferulic acid	10.4	f(x)= 117813.37x + 22969.69	0.993	LOQ – 5.36	8.1	27.0	9.05	10.11
		f(x)= 29014.72x + 582382.83	0.966	5.36 – 42.9				
Abscisic acid	13.0	f(x)= 814918.03x + 16787.59	0.999	LOQ – 2.01	5.2	17.3	7.89	9.76
		f(x)= 390324.10x + 1027474.35	0.996	2.01 – 16.09				

<sup>a</sup> Calculated as the concentration that generates a signal to noise ratio equal to 3 (LOD) and 10 (LOQ).

<sup>b</sup> RSD (%) of peak area for 7 injections of the QC sample carried out within the same sequence.

<sup>c</sup> RSD (%) of peak area for 13 injections of the QC sample from different sequences carried out over several days.

Abbreviations: LOD, Limit of detection; LOQ, Limit of quantification.



# Chapter

# 3

## Assessing the RP-LC-MS-based metabolic profile of *Hass* avocados marketed in Europe from different geographical origins (Peru, Chile, and Spain) over the whole season

Irene Serrano-García<sup>1</sup>, Joel Domínguez-García<sup>1</sup>, Elena Hurtado-Fernández<sup>2</sup>,  
José Jorge Gonzalez-Fernandez<sup>3</sup>, José Ignacio Hormaza<sup>3</sup>, María Beiro-  
Valenzuela<sup>1</sup>, Romina Monasterio<sup>1,4</sup>, Romina Pedreschi<sup>5,6</sup>, Lucía Olmo-García<sup>1</sup>✉,  
Alegria Carrasco-Pancorbo<sup>1</sup>

<sup>1</sup> Department of Analytical Chemistry, Faculty of Sciences, University of Granada, Ave. Fuentenueva S /N, 18071 Granada, Spain; [iserrano@ugr.es](mailto:iserrano@ugr.es) (I.S.-G.); [jdogar99@correo.ugr.es](mailto:jdogar99@correo.ugr.es) (J.D.-G.); [gembav@ugr.es](mailto:gembav@ugr.es) (M.G.B.-V.); [rmonasterio@ugr.es](mailto:rmonasterio@ugr.es) (R.M.); [alegriac@ugr.es](mailto:alegriac@ugr.es) (A.C.-P.)

<sup>2</sup> Department of Biological and Health Sciences, Faculty of Health Sciences, University of Loyola, Campus Sevilla, Avda. de las Universidades S/N, 41704 Dos Hermanas, Sevilla, Spain; [emhurtado@uloyola.es](mailto:emhurtado@uloyola.es)

<sup>3</sup> Institute for Mediterranean and Subtropical Horticulture (IHSM La Mayora-UMA-CSIC), 29750 Algarrobo -Costa, Málaga, Spain; [jorgegonzalez-fernandez@eelm.csic.es](mailto:jorgegonzalez-fernandez@eelm.csic.es) (J.J.G.-F.); [ihormaza@eelm.csic.es](mailto:ihormaza@eelm.csic.es) (J.I.H.)

<sup>4</sup> Instituto de Biología Agrícola de Mendoza (IBAM), UNCuyo-CONICET, Facultad de Ciencias Agrarias, Chacras de Coria, 5505 Mendoza, Argentina

<sup>5</sup> Pontificia Universidad Católica de Valparaíso, Escuela de Agronomía, Facultad de Ciencias Agronómicas y de los Alimentos, Calle San Francisco S/N, La Palma, 2260000 Quillota, Chile; [romina.pedreschi@pucv.cl](mailto:romina.pedreschi@pucv.cl)

<sup>6</sup> Millennium Institute Center for Genome Regulation (CRG), 8331150 Santiago, Chile.

✉ [luciaolmo@ugr.es](mailto:luciaolmo@ugr.es)

**Plants, 12 (2023) 3004**

<https://doi.org/10.3390/plants12163004>



**Abstract:** Spain dominates avocado production in Europe, with the *Hass* variety being the most prominent. Despite this, Spanish production satisfies less than 10% of the overall avocado demand in Europe. Consequently, the European avocado market heavily relies on imports from overseas, primarily sourced from Peru and Chile. Herein, a comprehensive characterization of the metabolic profile of *Hass* avocado fruits from Spain, Peru, and Chile, available in the European market throughout the year, was carried out. The determination of relevant substances was performed using high- and low-resolution RP-LC-MS. Remarkable quantitative differences regarding phenolic compounds, amino acids, and nucleosides were observed. Principal component analysis revealed a natural clustering of avocados according to geographical origin. Moreover, a specific metabolic pattern was established for each avocado-producing country using supervised partial least squares discriminant analysis. Spanish fruits exhibited high levels of coumaric acid malonyl-hexose II, coumaric acid hexose II, and ferulic acid hexose II, together with considerably low levels of pantothenic acid and uridine. Chilean avocado fruits presented high concentrations of abscisic acid, uridine, ferulic acid, succinic acid, and tryptophan. Fruits from Peru showed high concentrations of dihydroxybenzoic acid hexose, alongside very low levels of p-coumaric acid, ferulic acid, coumaric acid malonyl-hexose I, and ferulic acid hexose II.

**Keywords:** *Hass*; avocado mesocarp; geographical origin; phenolic compounds; pantothenic acid; abscisic acid; amino acids; nucleosides

## 1. INTRODUCTION

The avocado (*Persea americana* Mill.) is a subtropical evergreen fruit tree crop native to Mesoamerica. Of the at least eight botanical varieties or subspecies usually recognized, three of them, known as horticultural races, present agronomic importance: West Indian, Guatemalan, and Mexican [1,2]. They are sexually intercompatible but exhibit different botanical traits and edaphoclimatic preferences [3]. Most commercial avocado varieties currently grown in subtropical and Mediterranean climates are inter-racial Mexican × Guatemalan hybrids. An example is *Hass*, the most widespread, cultivated, and marketed variety worldwide [4], which originated as a chance seedling in California ninety years ago [5]. *Hass* is also the most important cultivated variety in Spain, with more than 80% of the acreage and continuing to gain share over other varieties that are still grown, such as *Fuerte* or *Bacon*. *Hass* avocado presents a great environmental plasticity, a long harvesting period, and a hard skin that hides damages and bruises during handling. In addition, it shows a long post-harvest life and good adaptation to pre-ripening, thereby enhancing fruit storage. For consumers, it offers good organoleptic attributes and easy identification of the ideal moment of consumption due to the change in the fruit skin color from green to dark violet/black as the fruit ripens [6].

Among the major tropical fruits, avocados have experienced the fastest growth in global output and international trade over the last decades. The predictions for 2030 project that global

avocado production will reach 12 Mt, more than three times its level in 2010, and that avocado will become the most traded tropical fruit in international markets. According to the Food and Agriculture Organization of the United Nations, a total of 69 countries distributed around the world produced avocados in 2021 [7]. Mexico ranked first, followed by Colombia, Peru, Indonesia, and the Dominican Republic. Spain is far from the top growing countries, although it is of great importance as the main producer in the Mediterranean area, together with Israel and Morocco. Avocado commercial cultivation started in Spain in the 1950s, but the main expansion took place in the 1970s [8]. Avocado cultivation in Spain is concentrated in the Southern Mediterranean coast (provinces of Malaga and Granada) as well as in the Canary Islands, with recent increasing expansion to the East (Valencian Community) and West (provinces of Huelva and Cadiz) of the country. The production in Spain reached close to 117,000 tons of fruit/year in 2021 [7]. More than 90% of the European Union's avocado production comes from Spain, although Spanish production, which in the case of *Hass* is concentrated between November and March, only covers about 10% of the total European consumption. Therefore, most of the *Hass* avocado volume marketed in Europe is imported from South America and Africa, with Peru and Chile as the main suppliers. Peru dominates the summer supply, whereas Chilean avocados are traditionally covering the gap between Peruvian and Spanish productions in autumn. Thus, having in the market a single variety (*Hass*) from very different geographical and edaphoclimatic origins results in a lack of homogeneity of the avocados available in Europe.

The avocado fruit is principally composed of monounsaturated and polyunsaturated fatty acids, but also carbohydrates, proteins, and fiber [9,10]. It also contains some relevant vitamins and minerals [11]. The minor fraction of avocado includes mainly phenolic compounds, carotenoids, and terpenoids and has been extensively studied for its biological activity and its relationship with beneficial health effects [9–11]. Nevertheless, the compositional profile of the avocado fruit depends on a huge number of factors, such as the variety, climatic conditions, orchard location, or pre- and post-harvest biotic and abiotic stresses [3,12]. All this may lead to the presumption that avocado fruits of the same variety, grown in different countries with different edaphoclimatic conditions and subjected to distinct pre- and post-harvest treatments (depending on whether or not they are exported), will have a different compositional profile. Several works have assessed a correlation between some nutritional components of the avocado and the producing region. Landahl and co-authors and Donetti and Terry determined fatty acids and C<sub>7</sub> sugars, among other parameters, in *Hass* avocados grown in Chile, Peru, and Spain [13,14]. Both works described that the composition of fatty acids varied significantly according to the geographical origin; Donetti and Terry suggested oleic acid as a potential marker to distinguish fruit origin [14]. With the same objective, Tan and collaborators analyzed *Hass* avocado oils from Mexico, Australia, the United States, and New Zealand [15]. Moreover, the impact of orchard altitude and fruit maturity on the fatty acid content of *Hass* avocado fruits from Colombia was evaluated by Carvalho and Velásquez [16]. In the same country, Henao-Rojas and colleagues analyzed physical, chemical, and nutritional parameters associated with the quality of *Hass* avocado in eight localities of the department of

Antioquia [17]. Other studies combined the lipid chromatographic fingerprint with powerful chemometrics tools to classify avocado samples according to their geographical origin and botanical variety [18,19]. In addition, Muñoz and co-authors approached for the first time the evaluation of the isotopic composition of five light bio-elements (C, N, S, H, and O), together with the mineral content, in avocado samples from eight producing regions [20]. In contrast, metabolomic approaches focused on the determination of other types of compounds (phenolic substances, organic acids, amino acids, etc.) have been little exploited for this purpose. They have previously been used for other goals, such as the comprehensive characterization of avocado tissues [21–25], varietal discrimination [26,27], and assessment of the impact of fruit transport (short- and long-distance) on certain primary and secondary metabolites [28,29].

To the best of our knowledge, no work has been published that evaluates the metabolic profile of *Hass* avocados from different origins in the same market over a whole year, including domestic production and imported fruit. Therefore, the aim of the present study was multiple: 1) to provide a detailed analysis of the metabolic profile (RP-LC-MS-based) of *Hass* avocados marketed in the European market from three different origins, and 2) to find some compounds that could act as potential origin markers, grouping *Hass* avocado fruits according to their geographical provenance (Spain, Peru, and Chile).

## 2. RESULTS AND DISCUSSION

### 2.1. Qualitative characterization of the metabolic profile of avocado cv. *Hass* by LC-MS

An in-depth qualitative characterization of the metabolic profiles of *Hass* fruits from Spain, Chile, and Peru was carried out using LC-QTOF MS (MS and MS/MS data). Among all the compounds detected, we focused on those with the highest intensity in the chromatographic profiles of the samples from the different geographical origins, selecting 27 substances. Of these, 22 could be identified (at least tentatively), and 5 remained unknown (see Table 1). Table 1 includes the compound annotation, chemical family, retention time (Rt), experimental and theoretical  $m/z$  of the pseudo-molecular ion, fragments observed in MS/MS analyses, and the calculated molecular formula. Peak identification was achieved by considering accurate MS data, relative retention times, and MS/MS fragmentation patterns. The use of pure standards together with information from previously published reports [21–25,30,31] and several databases (FooDB-[www.foodb.ca](http://www.foodb.ca) (accessed on 5th August 2023), MassBank Europe Mass Spectral DataBase-[www.massbank.eu](http://www.massbank.eu) (accessed on 5th August 2023), MassBank of North America-[www.mona.fiehnlab.ucdavis.edu](http://www.mona.fiehnlab.ucdavis.edu) (accessed on 5th August 2023), etc.) was essential to support the identifications described in the present work.

**Table 1.** Peak assignment of the metabolites found in the *Hass* avocado samples from Spain, Chile, and Peru

Compound	Family	Molecular Formula	Rt (min)	<i>m/z</i> experim	<i>m/z</i> theor	Error (ppm)	mSigma Value	MS/MS
Uridine	Nucleoside	C <sub>9</sub> H <sub>12</sub> N <sub>2</sub> O <sub>6</sub>	2.7	243.0610	243.0623	0.7	6.9	199.9 [M-H-43] <sup>-</sup>
Tyrosine	Amino acid	C <sub>9</sub> H <sub>11</sub> NO <sub>3</sub>	3.0	180.0662	180.0666	2.5	18.2	162.9 [M-H-17] <sup>-</sup>
Succinic acid	Organic acid	C <sub>4</sub> H <sub>6</sub> O <sub>4</sub>	3.2	117.0192	117.0193	1.0	8.8	-
Dihydroxybenzoic acid hexose	Phenolic acid derivative	C <sub>13</sub> H <sub>16</sub> O <sub>9</sub>	4.9	315.0715	315.0722	2.0	3.6	152.9 [M-H-162] <sup>-</sup>
Phenylalanine	Amino acid	C <sub>9</sub> H <sub>11</sub> NO <sub>2</sub>	4.9	164.0720	164.0717	-1.7	16.6	146.9 [M-H-17] <sup>-</sup>
Unknown 1	-	C <sub>13</sub> H <sub>22</sub> O <sub>10</sub>	5.0	337.1139	337.1140	0.3	12.1	-
Pantothenic acid	Vitamin	C <sub>9</sub> H <sub>17</sub> NO <sub>5</sub>	5.2	218.1028	218.1034	2.7	17.9	145.9 [M-H-28-44] <sup>-</sup>
Hydroxybenzoic acid hexose	Phenolic acid derivative	C <sub>13</sub> H <sub>16</sub> O <sub>8</sub>	6.3	299.0770	299.0772	0.7	52.8	-
Tryptophan	Amino acid	C <sub>11</sub> H <sub>12</sub> N <sub>2</sub> O <sub>2</sub>	6.5	203.0818	203.0826	4.1	2.1	159.0 [M-H-44] <sup>-</sup> 115.9 [M-H-28-44] <sup>-</sup>
<i>N</i> -acetyl-tyrosine	Amino acid derivative	C <sub>11</sub> H <sub>13</sub> NO <sub>4</sub>	6.6	222.0772	222.0772	-0.2	7.3	179.9 [M-H-42] <sup>-</sup> 162.9 [M-H-42-17] <sup>-</sup>
Chlorogenic acid	Phenolic acid	C <sub>16</sub> H <sub>18</sub> O <sub>9</sub>	7.1	353.0887	353.0878	-2.4	25.1	191.0 [M-H-caffeic moiety] <sup>-</sup>
Coumaric acid hexose I	Phenolic acid derivative	C <sub>15</sub> H <sub>18</sub> O <sub>8</sub>	7.5	325.0934	325.0929	-1.5	6.6	162.9 [M-H-162] <sup>-</sup> 145.0 [M-H-162-18] <sup>-</sup>
Coumaric acid hexose II	Phenolic acid derivative	C <sub>15</sub> H <sub>18</sub> O <sub>8</sub>	7.8	325.0917	325.0929	3.6	6.5	162.9 [M-H-162] <sup>-</sup> 145.0 [M-H-162-18] <sup>-</sup>
Ferulic acid hexose I	Phenolic acid derivative	C <sub>16</sub> H <sub>20</sub> O <sub>9</sub>	7.8	355.1033	355.1035	0.3	21.4	192.9 [M-H-162] <sup>-</sup>
Unknown 2	-	C <sub>16</sub> H <sub>22</sub> O <sub>8</sub>	7.8	341.1242	341.1242	0.0	4.8	298.8 [M-H-42] <sup>-</sup> 280.9 [M-H-162] <sup>-</sup>
Ferulic acid hexose II	Phenolic acid derivative	C <sub>16</sub> H <sub>20</sub> O <sub>9</sub>	8.1	355.1027	355.1035	2.2	22.1	192.9 [M-H-162] <sup>-</sup>
Epicatechin	Flavonoid	C <sub>15</sub> H <sub>14</sub> O <sub>6</sub>	8.3	289.0711	289.0718	2.3	8.5	244.9 [M-H-44] <sup>-</sup>
<i>N</i> -acetyl-leucine	Amino acid derivative	C <sub>8</sub> H <sub>15</sub> NO <sub>3</sub>	8.6	172.0974	172.0979	2.8	22.1	-
Coumaric acid malonyl-hexose I	Phenolic acid derivative	C <sub>17</sub> H <sub>20</sub> O <sub>9</sub>	9.0	367.1021	367.1035	3.8	3.4	162.9 [M-H-162-86] <sup>-</sup> 144.9 [M-H-180-86] <sup>-</sup>

Compound	Family	Molecular Formula	Rt (min)	$m/z$ experim	$m/z$ theoret	Error (ppm)	mSigma Value	MS/MS
Coumaric acid malonyl-hexose II	Phenolic acid derivative	C <sub>17</sub> H <sub>20</sub> O <sub>9</sub>	9.3	367.1027	367.1035	2.1	14.9	162.9 [M-H-162-86] <sup>-</sup> 145.0 [M-H-180-86] <sup>-</sup>
<i>N</i> -acetyl-phenylalanine	Amino acid derivative	C <sub>11</sub> H <sub>13</sub> NO <sub>3</sub>	9.4	206.0817	206.0823	2.5	27.1	163.9 [M-H-42] <sup>-</sup> 146.9 [M-H-42-17] <sup>-</sup>
<i>p</i> -Coumaric acid	Phenolic acid	C <sub>9</sub> H <sub>8</sub> O <sub>3</sub>	9.9	163.0395	163.0401	1.5	6.2	118.9 [M-H-44] <sup>-</sup> 177.8 [M-H-15] <sup>-</sup>
Ferulic Acid	Phenolic acid	C <sub>10</sub> H <sub>10</sub> O <sub>4</sub>	10.4	193.0498	193.0506	4.3	17.2	133.9 [M-H-15-44] <sup>-</sup>
Unknown 3	-	C <sub>9</sub> H <sub>16</sub> O <sub>4</sub>	11.4	187.0976	187.0976	0.0	10.9	-
Unknown 4	-	C <sub>14</sub> H <sub>24</sub> O <sub>6</sub>	12.3	287.1492	287.1500	0.1	19.4	227.0 [M-H-60] <sup>-</sup> 209.0 [M-H-18] <sup>-</sup>
Abscisic acid	Phytohormone	C <sub>15</sub> H <sub>20</sub> O <sub>4</sub>	12.9	263.1286	263.1289	1.2	3.9	219.0 [M-H-44] <sup>-</sup> 153.0 [M-H-44-66] <sup>-</sup>
Unknown 5	-	C <sub>9</sub> H <sub>16</sub> O <sub>3</sub>	13.6	171.1020	171.1027	4.1	5.4	152.9 [M-H-18] <sup>-</sup> 127.0 [M-H-44] <sup>-</sup>

When MS/MS information is not included for some compounds, it is because clean fragmentation spectra were not obtained (due to low concentration or difficult cleavage of their labile bonds). Some of the different  $m/z$  values observed in the MS/MS spectra correspond to typical losses of -17 (NH<sub>3</sub>), -18 (H<sub>2</sub>O), -28 (CO), -42 (C<sub>2</sub>H<sub>2</sub>O), -43 (CHNO), -44 (CO<sub>2</sub>), and -162 (hexose). The prevalent ion detected in the MS spectra of coumaric acid malonyl-hexose I and II was [M-H-44]<sup>-</sup>, corresponding to a  $m/z$  signal of 367.

Different chemical compounds such as amino acids and derivatives, nucleosides, organic acids, phenolic compounds, vitamins, and phytohormones were identified in the chromatographic profiles. As usual in negative polarity, the predominant ion observed was the  $[M-H]^-$  (i.e., the *pseudo*-molecular ion). In elution order, uridine (nucleoside) at  $m/z$  243.0610 was the most polar compound monitored and eluted at 2.7 min. Tyrosine with  $m/z$  180.0662 (amino acid) and succinic acid with  $m/z$  117.0192 (organic acid) were the next to elute, and their identity was corroborated with the pure standard of each. The signal  $m/z$  315.0715 at 4.9 min was tentatively assigned to dihydroxybenzoic acid hexose, which has already been reported by different authors [30,32]. The MS/MS analyses showed a fragment with  $m/z$  152.9  $[M-H-162]^-$ , corresponding to the loss of a hexose moiety. The peaks of phenylalanine (amino acid) with  $m/z$  164.0720 and pantothenic acid (vitamin) with a predominant MS signal at  $m/z$  218.1028 were annotated using their pure standard, whereas the signal with  $m/z$  299.0770 at 6.3 min was tentatively assigned to hydroxybenzoic acid hexose [30]. Both hydroxybenzoic acid derivatives (with  $R_t$  4.9 and 6.3 min, respectively) had the same relative elution order as that observed in the study just cited, a fact that reinforces the assignment given.

Tryptophan (amino acid), with a main MS signal at  $m/z$  203.0818, eluted at 6.5 min, followed by the  $m/z$  222.0772, which was tentatively assigned as *N*-acetyl-tyrosine. The MS/MS analysis revealed a fragmentation pattern giving a primary fragment of  $m/z$  179.9  $[M-H-42]^-$ , which would be a plausible fragmentation with the suggested identity (breakage by the linkage between the acetyl group and the tyrosine moiety). Moreover, predicted MS/MS spectra coming from the available databases also support the attributed annotation. Chlorogenic acid (phenolic acid) with  $m/z$  353.0887 was corroborated using its pure standard. Note that the term 'chlorogenic acids' embraces a large group of naturally occurring substances; in this research, we focus on the determination of an outstanding compound of this chemical class, which is assigned the trivial name of chlorogenic acid (CAS number 327-97-9). Coumaric acid hexose isomers I and II (two hydroxycinnamic acid derivatives), with MS signals at  $m/z$  325.0934 and 325.0917, respectively, were previously described in avocado mesocarp by Serrano-García and co-authors [28]. In this and other cases, when several isomers of a substance are found, they are indicated with I and II, respectively. Two additional hydroxycinnamic acid derivatives (ferulic acid hexose isomers I and II) were detected at 7.8 and 81 min, respectively, giving the prevailing MS signals with  $m/z$  355.1033 and 355.1027, apiece. Both compounds were also previously identified by Campos, Hurtado-Hernandez, López-Cobo, and their respective co-authors [22,30,32]. The signal of epicatechin at  $m/z$  289.0718 ( $[M-H]^-$ ) was detected at 8.3 min, and another amino acid derivative (*N*-acetyl-leucine) was identified at 8.6 min with  $m/z$  172.0974. The coumaric acid-derived compounds previously reported by Serrano-García and collaborators were detected herein, yielding  $m/z$  signals of 367.1021 and 367.1027, respectively [28]. The next compound found, following the chromatographic elution order, was annotated as *N*-acetyl-phenylalanine, bearing in mind its prevalent MS signal ( $m/z$  206.0817), the MS/MS experimental data and the MS/MS spectra found in the consulted databases. The fragment observed with  $m/z$  163.9  $[M-H-42]^-$  would correspond

to the release of the phenylalanine moiety. Finally, the identification of *p*-coumaric acid (phenolic acid), ferulic acid (phenolic acid), and abscisic acid (ABA) (phytohormone) with MS signals of  $m/z$  163.0395, 193.0498, and 263.1286, respectively, was based on the use of their pure standards.

Five other unknown compounds with MS signals of  $m/z$  337.1139, 341.1242, 187.0976, 287.1492, and 171.1020 were detected within the profiles with considerable intensity, but it was not possible to assign an identity to them. We believe, in any case, that this is not a negative aspect of the work and that the complete elucidation of the identity of these substances is beyond the scope of the present contribution.

Figure 1 includes examples of the metabolic profiles of avocado extracts from three different geographical origins (Spain, Chile, and Peru), displaying the Extracted Ion Chromatograms of the most abundant substances. The profiles turned out to be quite similar from a qualitative point of view regardless of their origin; however, interesting quantitative differences were observed among origins. They will be discussed in the next sections of this article.

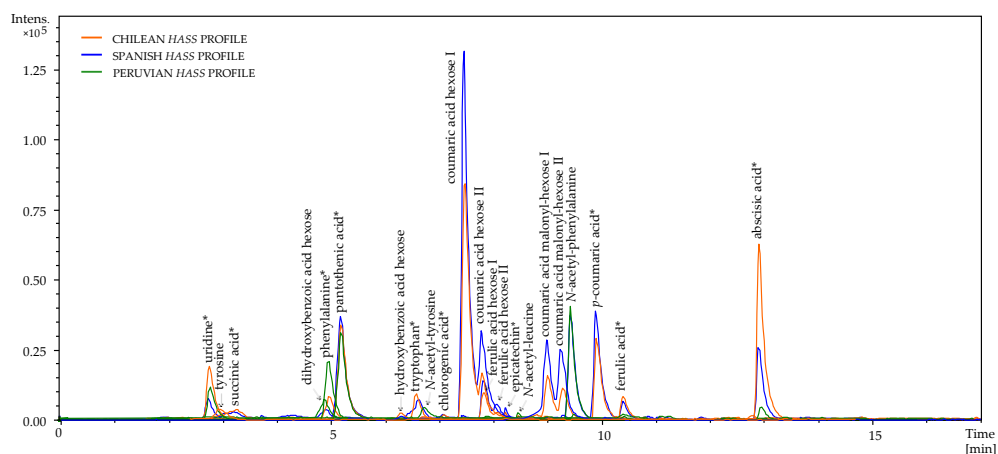


**Figure 1.** Extracted Ion Chromatograms (EIC) of the most abundant substances within the metabolic profiles obtained from *Hass* avocado extracts from Spain, Chile, and Peru. \*Corroborated with the pure standard

## 2.2. Analytical parameters of the method

The analytical performance of the applied method was tested considering linearity, the limits of detection (LODs), the limits of quantification (LOQs), and precision (*intra*- and *inter*-day). The obtained results were satisfactory for every parameter (see Table S1).  $R^2$  was higher than 0.994 for all the calibration curves, which shows the excellent linearity in each established range and, therefore, the reliability of the quantifications performed. The *intra*-day repeatability ranged between 7.15 and 9.30% (CV values for succinic and ferulic acids, respectively), and *inter*-day repeatability varied from 7.83 to 14.63%, for ABA and succinic acid, apiece. These data show the

good precision of the method used. LODs and LOQs ranged between 7.7 and 118.7  $\mu\text{g L}^{-1}$  and 23.6 and 395.4  $\mu\text{g L}^{-1}$  for ABA and succinic acid, respectively.

### 2.3. Quantitative LC-MS results

For quantitative purposes, all avocado extracts considered in this study were analyzed using the LC-ESI-IT MS analytical platform. Initially, the results of each and every sample from the different locations were evaluated in detail, and a heat map considering all samples and compounds was generated (Figure 2). This representation revealed some similarities in the compositional profiles of samples coming from the same geographical origin during the whole sampling period considered in each case. In fact, they were clustered together according to the country of provenance. Nevertheless, as the main aim of this work was to identify the typical compositional patterns of the avocados of each geographical origin, we decided to perform a different type of quantitative data assessment. Therefore, to facilitate the visualization and understanding of the data, the concentrations found for each identified compound were aggregated according to geographical origin to describe what could be considered the “average C18 LC-MS-based metabolic profile” for each country. The results were expressed as  $\text{mg kg}^{-1}$  of dry weight (DW) together with the associated standard deviation (SD), as shown in Table 2 and in Figure S1. The SD values were considerably high given the design of this study, which covered relatively wide time intervals for sampling (up to 6 months) and a significant number of horticultural replicates ( $n = 5$ ) for each time point. Compounds were classified into six families: amino acids (or related compounds) and nucleosides, flavonoids, organic acids, phytohormones, phenolic acids and related compounds, and vitamins.

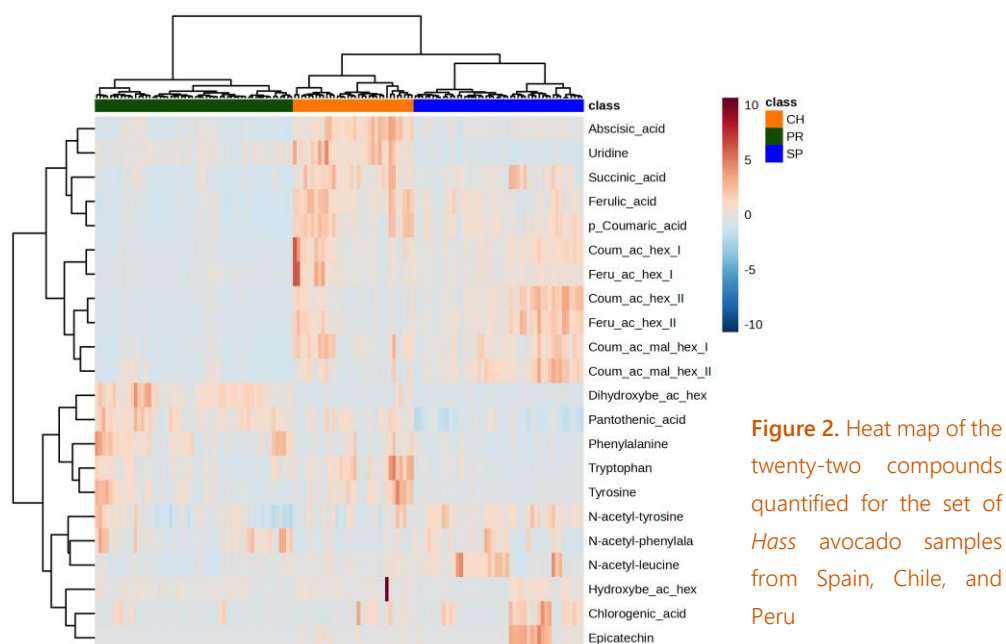


Figure 2. Heat map of the twenty-two compounds quantified for the set of *Hass* avocado samples from Spain, Chile, and Peru

**Table 2.** Summary of the quantitative results obtained for the avocado samples obtained from Spain, Chile, and Peru. The values are expressed as mg kg<sup>-1</sup> of dry weight (global SD is indicated for each value)

Chemical Class	Compound	Spain		Chile		Peru	
		Mean	SD	Mean	SD	Mean	SD
<b>Amino acids and nucleotides</b>							
	<i>N</i> -acetyl-leucine	3.35	2.37	1.99	0.42	1.24	0.50
	<i>N</i> -acetyl-phenylalanine	16.76	9.02	10.24	2.77	19.31	11.84
	<i>N</i> -acetyl-tyrosine	13.33	2.77	9.96	2.45	24.25	15.84
	Phenylalanine	5.42	2.33	11.05	6.30	18.11	7.30
	Tryptophan	1.58	0.66	5.98	3.49	2.65	0.94
	Tyrosine	2.62	0.76	9.18	5.85	5.74	3.80
	Uridine	18.68	6.85	96.72	10.14	41.46	6.71
<b>Flavonoids</b>							
	Epicatechin	27.82	17.48	7.11	6.51	0.05	0.03
<b>Organic acids</b>							
	Succinic acid	836.34	170.16	1295.68	263.90	383.93	139.43
<b>Phytohormones</b>							
	Abscisic acid	11.22	3.87	30.81	7.77	7.89	3.42
<b>Phenolic acids and related compounds</b>							
	Chlorogenic acid	1.89	1.49	1.14	0.76	0.55	0.37
	Coumaric acid hexose I	165.16	37.33	212.37	30.49	18.67	14.09
	Coumaric acid hexose II	49.08	33.63	22.62	18.89	3.99	3.73
	Coumaric acid malonyl-hexose I	44.70	18.38	49.52	28.71	8.62	7.21
	Coumaric acid malonyl-hexose II	51.54	21.28	26.95	13.58	12.51	10.56
	Dihydroxybenzoic acid hexose	6.18	0.94	9.25	4.21	35.96	11.30
	Ferulic Acid	8.08	2.46	13.57	3.56	3.06	1.40
	Ferulic acid hexose I	10.78	3.20	19.25	18.29	1.74	1.56
	Ferulic acid hexose II	6.35	3.59	3.99	3.33	0.37	0.23
	Hydroxybenzoic acid hexose	1.94	1.67	3.40	3.10	3.12	2.38
	<i>p</i> -Coumaric acid	52.54	20.80	75.40	34.52	11.29	10.48
<b>Vitamins</b>							
	Pantothenic acid	20.15	4.84	30.26	4.04	35.14	6.13

Some notable compositional differences were observed among the avocado samples according to their geographical origin. Regarding amino acids and nucleotides, uridine stood out above the others, ranging from  $18.68 \pm 6.85$  mg kg<sup>-1</sup> DW in Spanish fruits to  $96.72 \pm 10.14$  mg kg<sup>-1</sup> DW in Chilean avocado samples. Peruvian fruits, in general terms, exhibited higher contents of amino acids and related compounds than Chilean or Spanish fruits, especially for phenylalanine ( $18.11 \pm 7.30$  mg kg<sup>-1</sup> DW) and *N*-acetyl-tyrosine (mean values of  $24.25 \pm 15.84$  mg kg<sup>-1</sup> DW). Tyrosine content was higher in Chilean ( $9.18 \pm 5.85$  mg kg<sup>-1</sup> DW) than in Spanish ( $2.62 \pm 0.76$  mg kg<sup>-1</sup> DW) fruits, similar to the observations in a previous work [29].

Flavonoids are synthesized by plants in response, among other factors, to microbial infections and external stresses [33]. Epicatechin was the only flavonoid quantified in the present study, and its highest content was found in Spanish fruits ( $27.82 \pm 17.48$  mg kg<sup>-1</sup> DW). This average concentration is similar to previous results for fruits of the same variety reported by Hurtado-Fernández and colleagues and Serrano-García and co-authors [28,34]. High standard deviation

values for this compound were observed for all geographical origins. This is probably because fruits from the same origin but harvested at different times of the season were analyzed. Fruits from Peru showed by far the lowest flavonoid content ( $0.05 \pm 0.03 \text{ mg kg}^{-1} \text{ DW}$ ).

Furthermore, organic acids are not only involved in important pathways of plant anabolism and catabolism but also play an essential role in the organoleptic properties, quality, microbial stability, and consistency of plant foods [35]. Succinic acid was quantified in the present work, and it had been previously reported in avocado mesocarp [22,23,29,30,32]. The concentration of this organic acid fluctuated from  $1295.68 \pm 263.90 \text{ mg kg}^{-1} \text{ DW}$  in Chilean avocados to  $383.93 \pm 139.43 \text{ mg kg}^{-1} \text{ DW}$  in Peruvian avocados. Lower concentrations have been previously reported by Hurtado-Fernández et al. [32], and higher concentrations have been found by Campos and Ramos-Aguilar and their respective collaborators [23,30]. As in the present work, Pedreschi and co-authors reported similar succinic acid contents and found higher amounts of this analyte in Chilean than in Spanish *Hass* avocados [29].

As far as ABA is concerned, the highest average concentrations were found in the Chilean fruits ( $30.81 \pm 7.77 \text{ mg Kg}^{-1} \text{ DW}$ ), while the Spanish and Peruvian fruits were more similar ( $11.22 \pm 3.87 \text{ mg kg}^{-1} \text{ DW}$  and  $7.89 \pm 3.42 \text{ mg kg}^{-1} \text{ DW}$ , respectively). The differences in ABA contents could be associated with the role of this phytohormone during fruit softening and the sensitivity to external stresses and other factors. Pantothenic acid, also called vitamin B5, ranged from  $20.15 \pm 4.84 \text{ mg kg}^{-1} \text{ DW}$  for Spanish fruits to  $35.14 \pm 6.13 \text{ mg kg}^{-1} \text{ DW}$  for Peruvian ones. Its mean concentration in Chilean fruits was  $30.26 \pm 4.04 \text{ mg kg}^{-1} \text{ DW}$ . Similar concentration levels of both compounds (ABA and pantothenic acid) have been previously observed by Serrano-García et al. in *Hass* avocados from Spain [28].

Phenolic acids and related compounds conformed the category with the highest number of compounds. The avocado mesocarp, together with its peel and seed, is an important source of phenolic compounds, and its extracts show valuable antioxidant activities [36]. *p*-Coumaric acid and its derivatives were the most abundant phenolic compounds found in the pulp. This is consistent with what has been observed in a recent study [28]. Avocados from Chile showed the highest levels of *p*-coumaric and ferulic acids, with  $75.40 \pm 34.52 \text{ mg kg}^{-1} \text{ DW}$  and  $13.57 \pm 3.56 \text{ mg kg}^{-1} \text{ DW}$ , respectively, although not significantly higher than the contents of avocados from Spain with  $52.54 \pm 20.80 \text{ mg kg}^{-1} \text{ DW}$  and  $8.08 \pm 2.46 \text{ mg kg}^{-1} \text{ DW}$ . Peru was undoubtedly the origin with the lowest mean concentration of phenolic compounds.

As noted above, the compounds structurally related to *p*-coumaric acid were more prominent than those from ferulic acid. Coumaric acid hexose isomer I was greater in fruits from Chile ( $212.37 \pm 30.49 \text{ mg kg}^{-1} \text{ DW}$ ), whereas coumaric acid hexose isomer II was higher in avocados from Spain ( $49.08 \pm 33.63 \text{ mg kg}^{-1} \text{ DW}$ ). With regard to coumaric acid malonyl-hexoses, isomer I was found at relatively similar concentrations in samples from Chile and Spain ( $49.52 \pm 28.71 \text{ mg kg}^{-1} \text{ DW}$  and  $44.70 \pm 18.37 \text{ mg kg}^{-1} \text{ DW}$ , respectively), but the contents of isomer II were significantly higher

in Spanish avocados, with  $51.54 \pm 21.28 \text{ mg kg}^{-1} \text{ DW}$ . The two hexoses of ferulic acid showed lower concentrations in all origins. Ferulic acid hexose I was the most prevalent but in no case showed as high amounts as the coumaric acid derivatives.

For the two hexoses related to hydroxybenzoic acid, the same pattern (among the countries) was observed, both appearing in much higher concentrations in Peruvian avocados. The amount of dihydroxybenzoic acid hexose found in Peru ( $35.96 \pm 11.30 \text{ mg kg}^{-1} \text{ DW}$ ) was much higher than in Chile or Spain ( $9.25 \pm 4.21 \text{ mg kg}^{-1} \text{ DW}$  and  $6.18 \pm 0.94 \text{ mg kg}^{-1} \text{ DW}$ , respectively). Several isomers of hydroxybenzoic acid derivatives have been previously quantified in Spanish and Chilean *Hass* avocados [29]; however, as the results of that study did not specify the pure standard with respect to which the quantification was carried out, it is not possible to make a direct comparison with our concentration values. Nonetheless, Chilean avocados exhibited higher amounts of these isomers (especially of what the authors called isomer 3) than Spanish ones, which was also observed in our study. Chlorogenic acid was the compound with the lowest concentration within this family, and its maximum content was  $1.89 \pm 1.49 \text{ mg kg}^{-1} \text{ DW}$  (Spain). In a previous work, Hurtado-Fernández and colleagues quantified chlorogenic acid in avocado cv. *Hass*, but it was found only in green unripe fruits [32]. Chlorogenic and neochlorogenic acids are dominant in the avocado peel and seed but not in the pulp, which is consistent with our results [24,25].

Figure 3 aims to summarize, in percentage terms, the composition of avocados from each country. For this purpose, the compounds have been grouped into families (as shown in Table 2), their concentrations have been added up, and the percentage represented by each class (with respect to the total metabolites considered in this study) has been calculated. Succinic acid has not been considered in this representation, as it has a magnitude that would prevent any distribution from being correctly seen in the figures.

The average metabolic profile of the Spanish fruits was characterized by 77% phenolic acids and related compounds, 12% nucleosides and amino acids, 5% flavonoids, 4% vitamins, and 2% phytohormones. The average composition of Chilean avocados did not differ much from that just described, with the following percentages: 67% phenolic acids and related compounds, 22% nucleosides and amino acids, 5% vitamins, 5% phytohormones, and 1% flavonoids. The samples from Chile had (in percentage terms) less phenolic acids and more amino acids and nucleosides and phytohormones than the Spanish avocados. The compositional profiles of the samples from Peru were different from those just described, with the following mean distribution in decreasing order of the percentages: 44% amino acids and nucleosides, 39% phenolic acids and derivatives, 14% vitamins, and 3% phytohormones. The content of epicatechin (flavonoids) was very low and accounted for practically none of the total metabolites determined. Therefore, the compositional pattern of the Peruvian samples was more in balance than the others regarding the phenolic acid and amino acid-nucleoside families' percentage content. Pantothenic acid also constituted a higher percentage of the total in avocados from Peru than in those from Chile and Spain.

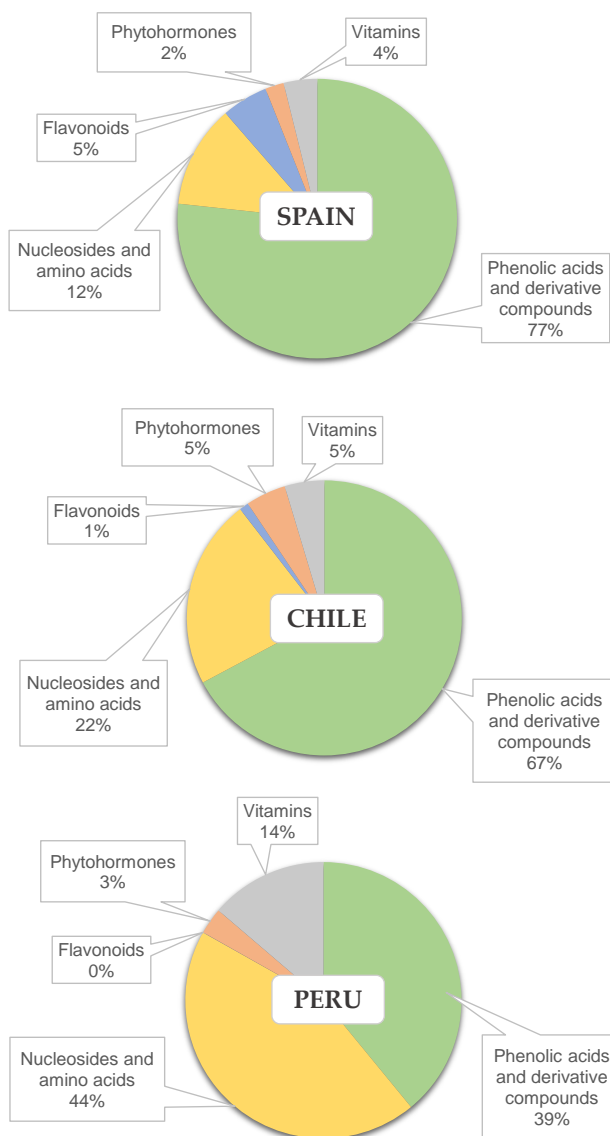


**Figure 3.** Pie charts of the percentages (%) represented by each chemical family in *Hass* avocados metabolic profiles from Spain, Chile, and Peru

**2.4. Preliminary results to select potential markers linked to the geographical origin of avocado cv. *Hass***

PCA was carried out to explore the natural grouping of the samples as well as to point out some possible markers that could be linked to the geographical origin of the avocado fruits. The PCA scores plot (Figure 4A) and biplot (Figure 4B) obtained using the LC-MS quantitative data set were displayed in a two-dimensional (2D) plot using the first two principal components, which covered 33.4% (PC1) and 17.1% (PC2) of the total variance, respectively. The accumulated variance

explains 71.6%, reaching 5PC's. Different pre-treatment methods were tested in our data set, i.e., mean centering, auto scaling, pareto scaling, and range scaling, before setting up the best one for this particular case. After several evaluations and the exploration of the nature of the data, auto scaling was the pre-treatment used. The aim of such a strategy is to compare metabolites based on correlation and become all metabolites with equal importance [37].

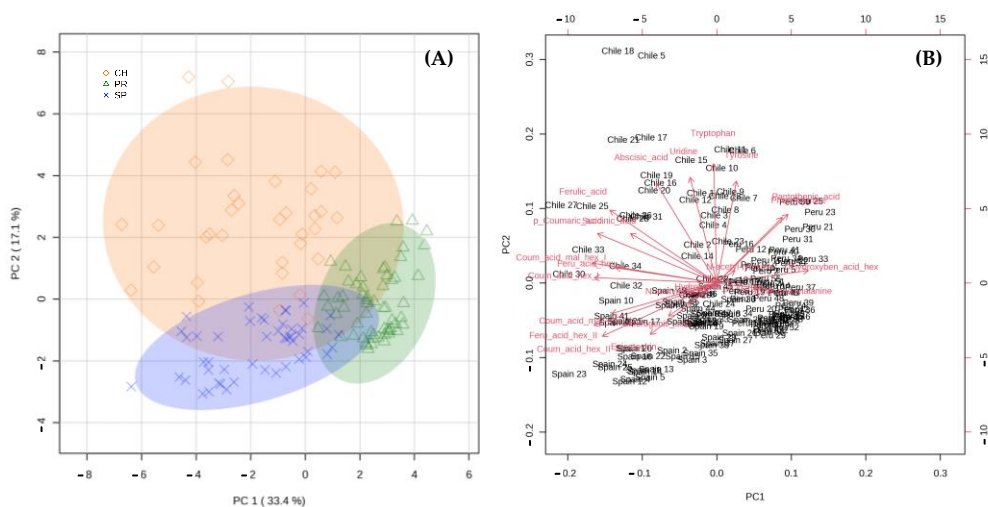


**Figure 4.** Principal component analysis scores plot (A) and biplot (B) obtained using the LC-MS quantitative data set in a two-dimensional (2D) plot using the first two principal components (2PCs)

As seen in the PCA scores plot (Figure 4A), Chile was the origin whose samples showed the greatest deviation or heterogeneity between them, whereas those from Peru and Spain were closer to each other in the representation, indicating a greater homogeneity of avocados of these two origins. In addition, it is possible to observe a certain natural grouping of the samples according to the country of origin, suggesting that the metabolite profiling of fruits could enable distinguishing between *Hass* avocados from Peru, Chile, and Spain.

This work was aimed at describing the typical profiles of avocados from different origins rather than “discriminating” the samples, but using statistical tools to pinpoint the most characteristic features of each origin proved to be very meaningful. Observations in both the PCA and previous sections of this work indicate that some compounds could be useful in defining the distinctive characteristics of the fruits of each origin. By checking the PCA biplot (Figure 4B), it is possible to state that the values of coumaric acid malonyl-hexose II, coumaric acid hexose II, ferulic acid hexose II, epicatechin, and chlorogenic acid were found to be significant in Spanish avocados. Moreover, some phenolic acids and derivatives, as well as uridine, tryptophan, tyrosine, and ABA were important in defining the Chilean avocado’s metabolic pattern versus those of the other origins. Similarly, pantothenic acid, phenylalanine, *N*-acetyl-phenylalanine, and dihydroxybenzoic acid hexose could be considered as markers to identify Peruvian *Hass* avocado fruits.

To further explore this direction, PLS-DA analysis was used, where a model was built to separate the samples from each country from the rest of the extracts that comprised the sample set. Figure 5 shows the results achieved by applying this strategy, showing from left to right the scores plots, the compounds with the highest VIP in each model (together with their relative concentration in each class of the model), and the quality parameters of the model obtained after cross-validation (accuracy,  $R^2$ , and  $Q^2$ ).

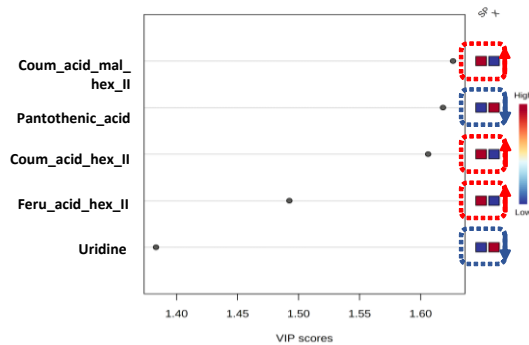
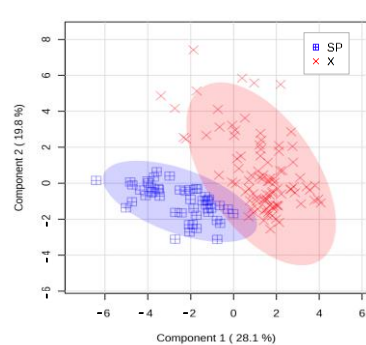
Thus, the most important features to distinguish avocados from Spain were the following: high levels of coumaric acid malonyl-hexose II, coumaric acid hexose II, and ferulic acid hexose II, together with considerably low levels of pantothenic acid and uridine. Chilean avocado fruits were distinguished from avocados from other countries by their remarkably high concentrations of ABA, uridine, ferulic acid, succinic acid, and tryptophan. As far as avocados from Peru are concerned, it is possible to describe their characteristic pattern as follows: high concentrations of dihydroxybenzoic acid hexose, alongside very low levels of *p*-coumaric acid, ferulic acid, coumaric acid malonyl-hexose I, and ferulic acid hexose II.

### 3. MATERIALS AND METHODS

#### 3.1. Chemicals and reagents

All reagents were of analytical or LC-MS grade and were used as received in the laboratory. Double deionized water with a conductivity of 18.2 M $\Omega$ , obtained using a Milli-Q system (Millipore, Bedford, USA), was used to prepare phase mobile A. Acetic acid, used for the acidification of mobile phase A, was supplied by Panreac (Barcelona, Spain). LC-MS grade acetonitrile (mobile phase B) from Lab-Scan (Dublin, Ireland) was also used. The entire volume of the prepared mobile phase was filtered through a 0.45  $\mu$ m Nylaflo<sup>TM</sup> nylon membrane filter, which was supplied by Pall Corporation (Michigan, USA).

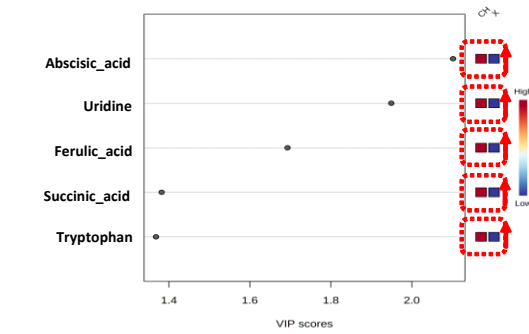
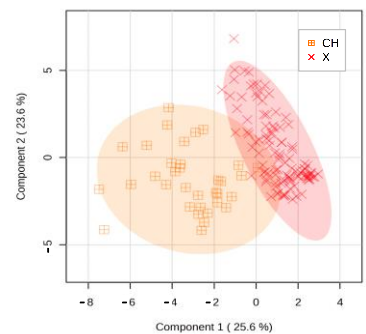
Methanol was the solvent selected for the preparation of the working solutions and the metabolite extraction; it was provided by Prolabo (Paris, France). The pure standards used were uridine, succinic acid, phenylalanine, pantothenic acid, tryptophan, chlorogenic acid, epicatechin, *p*-coumaric acid, ferulic acid, and abscisic acid, all of which were supplied by Sigma-Aldrich (St. Louis, USA).  $\beta$ -Estradiol, provided by Sigma-Aldrich, was used as an internal standard (IS) to assess the reproducibility of the analytical process. Stock solutions of each analyte were prepared in methanol. Prior to injection, each extract or standard mixture was filtered with a 0.22  $\mu$ m Clarinet<sup>TM</sup> nylon syringe filter (purchased from Bonna-Agela Technologies (Wilmington, DE, USA)) and stored in amber vials at -23 °C.



PLS-DA (SP) cross validation details:

Measure	1 comp	2 comp	3 comp
Accuracy	0.90800	0.98667	0.99333
R <sup>2</sup>	0.61156	0.75668	0.81089
Q <sup>2</sup>	0.58418	0.73101	0.77577

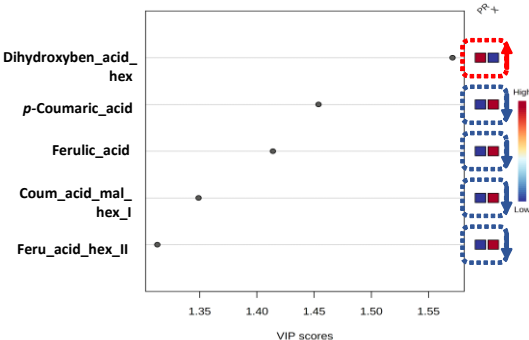
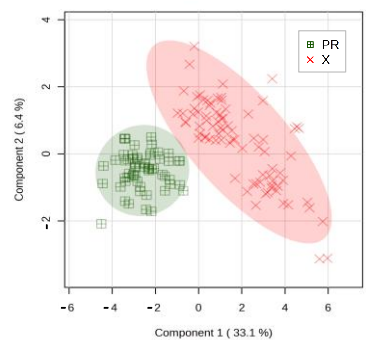
*SPAIN*



PLS-DA (CH) cross validation details:

Measure	1 comp	2 comp	3 comp
Accuracy	0.95829	0.97962	0.99429
R <sup>2</sup>	0.67271	0.78205	0.82665
Q <sup>2</sup>	0.6418	0.74594	0.77819

*CHILE*



PLS-DA (PR) cross validation details:

Measure	1 comp	2 comp	3 comp	4 comp
Accuracy	0.96267	1.0	1.0	1.0
R <sup>2</sup>	0.70007	0.84944	0.86249	0.87261
Q <sup>2</sup>	0.68924	0.79975	0.82486	0.8352

*PERU*

**Figure 5.** Two-dimensional partial least square analysis scores plot (right column), compounds with the highest VIPs in each model (center column), and quality parameters of the model (left column) obtained using the LC-MS quantitative data set. The latter parameters were obtained after cross-validation (accuracy, R<sup>2</sup>, and Q<sup>2</sup>)

### 3.2. Samples

Spanish avocado fruits were provided by the Institute for Mediterranean and Subtropical Horticulture (IHSM La Mayora-UMA-CSIC) located in Algarrobo-Costa, Málaga. Approximately, 240–250 fruits of *Hass* avocado from Spain ( $n = 48$ ) were harvested between January and July covering the early, mid, and late *Hass* avocado harvesting seasons in Spain. During this period, samples were taken approximately every 3 weeks, considering a total of 10 different samplings (dates of reception or time points). Spanish avocados' dry matter (DM) ranged from 25% at the beginning of the season to 32% in the last months of fruit harvesting. All DM measures were performed on unripe fruits according to the AOAC 920.151 method [38]. Avocado fruits from Chile and Peru, covering the periods of time in which there is no domestic *Hass* production in Spain, were provided by the avocado supplier company Trops, which imports avocado from those countries to supply the European market when no *Hass* from Spain is available. Regarding avocados from Peru, about 290–300 fruits ( $n = 59$ ) were received between June and September (every 1–1.5 weeks, collecting a total of 12 sampling points). About 160–170 Chilean avocado fruits were received between October and November (approximately every week for a total of 6 samplings,  $n = 34$ ). DM of Chilean avocados ranged from 23% to 27%, while Peruvian avocados varied from 24% to 30%, as they covered a longer period. Fruits from Chile and Peru were imported in controlled atmosphere by transoceanic transport and were received in optimal conditions. To ensure the representativeness of the sampling, for each geographical origin, each sample was composed of mesocarp aliquots taken from 5 different fruits; in addition, at each sampling point (each date of reception), about 5 samples were taken.

Avocado fruits were ripened under ambient conditions (20 °C–25 °C) until they reached the “ready-to-eat” stage. Ripe avocados were peeled and cut in half to remove the pit. Once the mesocarp was separated, it was cut into strips, sampled, freeze-dried, crushed, homogenized, and frozen at –26 °C.

A quality control (QC) avocado extract was prepared by mixing an equivalent volume of each extract from all the avocado samples under study and was utilized for instrument control and method validation.

### 3.3. Extraction procedure

Sample extracts were prepared in duplicate following the solid–liquid extraction protocol described by Serrano-García and collaborators with certain modifications [28]. IS was added before starting the sample preparation to assure the repeatability of the whole analytical protocol. A portion of 0.25 g of freeze-dried sample was extracted twice with 20 mL of pure methanol. Both extraction steps consisted of 2 min of vortex shaking, ultrasound bath for 30 min, and centrifugation (5 min at 9000 rpm). After phase separation, the supernatants were mixed and evaporated, and the residue was redissolved in 1 mL of methanol and filtered using a 0.22 µm pore size nylon syringe filter.

### 3.4. LC-MS and statistical analyses

Qualitative studies were performed using an Acquity UPLC™ H-Class system coupled to a high-resolution (HR) MS detector (QTOF SYNAPT G2 MS (Waters, Manchester, UK)). The analytical platform used for quantitative analyses was a 1260 Infinity Agilent (Agilent Technologies, Waldbronn, Germany) coupled with an Esquire 2000 Ion Trap (IT) low-resolution (LR) mass spectrometer (Bruker Daltonics, Bremen, Germany). Both instruments worked with an electrospray (ESI) interface. Identical chromatographic conditions were applied to both LC systems. The column used was a Zorbax Eclipse Plus C18 column (4.6 × 150 mm, 1.8 μm particle size) and was thermostated at 25 °C. Analytes were eluted with 0.5% acetic acid in water (mobile phase A) and pure acetonitrile (mobile phase B) applying the following gradient: 0 min, 95% A and 5% B; 22 min, 25% A and 75% B; 23 min, 0% A and 100% B; 23.5 min, 0% A and 100%; 25 min, initial conditions. The flow rate was set at 0.8 mL min<sup>-1</sup>, and an injection volume of 10 μL was used both for extracts and pure standards.

Data from both MS analyzers were acquired in full scan mode in a mass range from 50 to 1000 *m/z* and negative polarity. The ionization source in the IT MS worked under the following conditions: 30 psi for the nebulizer gas (nitrogen), 9 L min<sup>-1</sup> for dry gas (nitrogen) flow rate, and 300 °C as dry gas temperature. The capillary voltage was set at +3200 V and the end-plate offset at -500 V. For HR MS analyses, all these parameters were transferred and adapted to the ESI-QTOF MS system. The ionization source in the HR MS system operated at +2100 V, 100 °C in the capillary, and 100 L h<sup>-1</sup> of cone gas flow at 500 °C. The AutoMS data acquisition mode, based on the fragmentation of the prevalent precursor ion per scan, was used to acquire the MS/MS spectra.

MassLynx (Waters), Agilent ChemStation (Agilent Technologies), and Esquire Control (Bruker Daltonics) were the software used for instrument control. DataAnalysis 4.0 software (Bruker Daltonics, Bremen, Germany) was used for data processing, and Microsoft Excel v2204 for data representation. MetaboAnalyst v5.0 was the software applied to carry out supervised and unsupervised statistics (principal components analysis (PCA) and partial least squares-discriminant analyses (PLS-DA)). Auto scaling normalization was selected as a pre-processing step. In the first stage, the natural clustering of the samples was studied by performing a PCA with a data matrix composed of 22 variables (the quantified compounds) and 141 samples (the total sample set comprising the samples from Peru, Chile, and Spain). Subsequently, three different two-class models were built using PLS-DA (one for each geographical origin versus the rest of the samples) to show the characteristic compositional patterns of each producing region. Full cross-validation was performed to evaluate the predictive power of the obtained models. The Hierarchical Clustering Heatmap, used for intuitive visualization of the entire data set, was completed using a Euclidean distance measure and Ward clustering method.

### 3.5. Analytical parameters of the method

Pure standards solutions and QC extracts were used to establish the figures of merit of the applied analytical method. The linear calibration ranges, LODs, LOQs, and repeatability were established for the 10 analytes that were available as pure standards. Solutions of uridine, succinic acid, phenylalanine, pantothenic acid, tryptophan, chlorogenic acid, epicatechin, *p*-coumaric acid, ferulic acid, and ABA were prepared in pure methanol at 10 different concentrations levels. The concentration range for each compound was defined by considering the previously described concentration levels for that substance in avocado mesocarp samples, as well as the results of our preliminary studies with the sample set of this research. Calibration curves were obtained for each standard by least squares regression, each point on the line being the mean value of three separate injections ( $n = 3$ ). In case the pure commercial standard was not available or could not be obtained, the analyte was quantified with another compound of the same chemical family (assuming that they would be expected to exhibit similar responses). Four coumaric acid-derived compounds, hydroxybenzoic acid hexose, and dihydroxybenzoic acid hexose were quantified in terms of the *p*-coumaric acid pure standard. Two ferulic acid derivatives (ferulic acid hexoses) were quantified with its aglycone standard (ferulic acid). Tyrosine, *N*-acetyl-tyrosine, *N*-acetyl-phenylalanine, and *N*-acetyl-leucine were quantified with the phenylalanine pure standard.

LOD and LOQ of each individual compound were estimated by calculating the concentration that generated the signal-to-noise ratio (obtained at the lowest concentration level of those tested) equal to 3 and 10, respectively. Precision was evaluated in terms of repeatability. Intra-day repeatability was expressed as a coefficient of variation (% CV) from 7 injections of the QC extracts performed within the same sequence. Inter-day repeatability was obtained from 18 injections of the same QC extract performed in different sequences and days.

## 4. CONCLUSIONS

Since self-sufficiency in avocado consumption in Europe is currently unattainable, imports of avocados from other continents are necessary. In this work, a comprehensive characterization of the metabolic profile of *Hass* avocados marketed in Europe and originating from Spain, Chile, and Peru was carried out by LC-MS. A total of 22 compounds from different categories were determined, their concentrations were compared between samples, and the relative proportions of each of these chemical classes (as a percentage) in the total metabolic profile were established. Finally, PCA and PLS-DA were applied to the data analysis.

The levels of epicatechin, coumaric acid malonyl-hexose II, coumaric acid hexose II, and ferulic acid hexose II were higher in Spanish avocados. Chilean avocados stood out in terms of uridine, tryptophan, ABA, succinic acid, and several phenolic acids content. Peruvian avocados exhibited notable concentrations of *N*-acetyl-phenylalanine, phenylalanine, pantothenic acid, and dihydroxybenzoic acid hexose. Thus, the obtained results, with the help of statistical models,

defined avocado fruit compositional patterns for each geographical origin. It might help to obtain comparative nutritional information on the avocados available in the market (domestic or not) throughout the year.

**Funding:** This research has been partially financed by Grant PID2021-128508OB-I00 funded by MCIN/AEI/10.13039/501100011033 and “FEDER Una manera de hacer Europa”, and also by Grant PID2019-109566RB-I00 funded by MCIN/AEI /10.13039/501100011033. The authors are also grateful for the support they received from: the Millennium Science Initiative Program-ICN2021\_044; the Special Research Programme of the University of Granada (PPJIA2022.39); the Spanish Government (FPU19/00700) (I.S.-G.), and “UE-NextGenerationUE” (R.P.M.).

**Acknowledge:** The authors are grateful to Trops for supplying the *Hass* avocado samples imported from Peru and Chile used in this work.

## References

1. Pliego-Alfaro, F.; Palomo-Ríos, E.; Mercado, J.A.; Pliego, C.; Barceló-Muñoz, A.; López-Gómez, R.; Hormaza, J.I.; Litz, R.E. 12.1 *Persea Americana* Avocado. In *Biotechnology of fruit and nut crops*; Litz, R.E., Pliego-Alfaro, F., Hormaza, J.I., Eds.; CABI, 2020; pp. 258–281, doi:10.1079/9781780648279.0258.
2. Schaffer, B.; Wolstenholme, B.N.; Whiley, A.W. 1. Introduction. In *The avocado: botany, production and uses*; Schaffe, B., Wolstenholme, B.N., Whiley, A.W., Eds.; CABI, 2013; pp. 1–8 doi:10.1079/9781845937010.0001.
3. Hurtado-Fernández, E.; Fernández-Gutiérrez, A.; Carrasco-Pancorbo, A. Avocado Fruit—*Persea Americana*. *Exot. Fruits Ref. Guid.* **2018**, 37–48, doi:10.1016/B978-0-12-803138-4.00001-0.
4. Cowan, A.K.; Wolstenholme, B.N. Avocado. *Encycl. Food Heal.* **2015**, 294–300, doi:10.1016/B978-0-12-384947-2.00049-0.
5. Crane, J.H.; Douhan, G.; Faber, B.A.; Arpaia, M.L.; Bender, G.S.; Balerdi, C.F.; Barrientos-Priego, A.F. 8. Cultivars and Rootstocks. In *The avocado: botany, production and uses*; 2013; pp. 200–233.
6. Marín-Obispo, L.M.; Villarreal-Lara, R.; Rodríguez-Sánchez, D.G.; Del Follo-Martínez, A.; Barquera, M. de la C.E.; Jaramillo-De la Garza, J.S.; de la Garza, R.I.D.; Hernández-Brenes, C. Insights into Drivers of Liking for Avocado Pulp (*Persea Americana*): Integration of Descriptive Variables and Predictive Modeling. *Foods* **2021**, 10, 99, doi:10.3390/foods10010099.
7. FAO. Statistics Division of Food and Agriculture Organization of the United Nations (FAOSTAT). Available online: <https://www.fao.org/faostat/en/#home> (accessed on 5 August 2023).
8. Farré, J.M.; Pliego, F. Avocado in Spain. *South African Avocado Grow. Assoc. Yearb.* **1987**, 10, 27–28.
9. Talavera, A.; Gonzalez-Fernandez, J.J.; Carrasco-Pancorbo, A.; Olmo-García, L.; Hormaza, J.I. Avocado: Agricultural Importance and Nutraceutical Properties. In *Compendium of Crop Genome Designing for Nutraceuticals*; Kole, C., Ed.; Springer Singapore, 2023; pp. 1–19, doi:10.1007/978-981-19-3627-2\_40-1.
10. Jimenez, P.; Garcia, P.; Quitral, V.; Vasquez, K.; Parra-Ruiz, C.; Reyes-Farias, M.; Garcia-Diaz, D.F.; Robert, P.; Encina, C.; Soto-Covasich, J. Pulp, Leaf, Peel and Seed of Avocado Fruit: A Review of Bioactive Compounds and Healthy Benefits. *Food Rev. Int.* **2021**, 37, 619–655, doi:10.1080/87559129.2020.1717520.
11. Bhuyan, D.J.; Alsherbiny, M.A.; Perera, S.; Low, M.; Basu, A.; Devi, O.A.; Barooah, M.S.; Li, C.G.; Papoutsis, K. The Odyssey of Bioactive Compounds in Avocado (*Persea Americana*) and Their Health

- Benefits. *Antioxidants* **2019**, *8*, 426, doi:10.3390/antiox8100426.
12. Mpai, S.; Sivakumar, D. Influence of Growing Seasons on Metabolic Composition, and Fruit Quality of Avocado Cultivars at 'Ready-to-Eat Stage.' *Sci. Hort.* **2020**, *265*, 109159, doi:10.1016/j.scienta.2019.109159.
  13. Landahl, S.; Meyer, M.D.; Terry, L.A. Spatial and Temporal Analysis of Textural and Biochemical Changes of Imported Avocado Cv. Hass during Fruit Ripening. *J. Agric. Food Chem.* **2009**, *57*, 7039–7047, doi:10.1021/jf803669x.
  14. Donetti, M.; Terry, L.A. Biochemical Markers Defining Growing Area and Ripening Stage of Imported Avocado Fruit Cv. Hass. *J. Food Compos. Anal.* **2014**, *34*, 90–98, doi:10.1016/j.jfca.2013.11.011.
  15. Tan, C.X.; Tan, S.S.; Tan, S.T. Influence of Geographical Origins on the Physicochemical Properties of Hass Avocado Oil. *JAOCS, J. Am. Oil Chem. Soc.* **2017**, *94*, 1431–1437, doi:10.1007/s11746-017-3042-7.
  16. Carvalho, C.P.; Velásquez, M.A. Fatty Acid Content of Avocados (*Persea Americana* Mill. Cv. Hass) in Relation to Orchard Altitude and Fruit Maturity Stage. *Agron. Colomb.* **2015**, *33*, 220–227, doi:10.15446/agron.colomb.v33n2.49902.
  17. Henao-Rojas, J.C.; Lopez, J.H.; Osorio, N.W.; Ramírez-Gil, J.G. Fruit Quality in Hass Avocado and Its Relationships with Different Growing Areas under Tropical Zones. *Rev. Ceres* **2019**, *66*, 341–350, doi:10.1590/0034-737X201966050003.
  18. Martín-Torres, S.; Jiménez-Carvelo, A.M.; González-Casado, A.; Cuadros-Rodríguez, L. Authentication of the Geographical Origin and the Botanical Variety of Avocados Using Liquid Chromatography Fingerprinting and Deep Learning Methods. *Chemom. Intell. Lab. Syst.* **2020**, *199*, doi:10.1016/j.chemolab.2020.103960.
  19. Jiménez-Carvelo, A.M.; Martín-Torres, S.; Ortega-Gavilán, F.; Camacho, J. PLS-DA vs Sparse PLS-DA in Food Traceability. A Case Study: Authentication of Avocado Samples. *Talanta* **2021**, *224*, doi:10.1016/j.talanta.2020.121904.
  20. Muñoz-Redondo, J.M.; Bertoldi, D.; Tonon, A.; Ziller, L.; Camin, F.; Moreno-Rojas, J.M. Multi-Element and Stable Isotopes Characterization of Commercial Avocado Fruit (*Persea Americana* Mill) with Origin Authentication Purposes. *Food Control* **2022**, *137*, doi:10.1016/j.foodcont.2022.108975.
  21. Hurtado-Fernández, E.; Carrasco-Pancorbo, A.; Fernández-Gutiérrez, A. Profiling LC-DAD-ESI-TOF MS Method for the Determination of Phenolic Metabolites from Avocado (*Persea Americana*). *J. Agric. Food Chem.* **2011**, *59*, 2255–2267, doi:10.1021/jf104276a.
  22. López-Cobo, A.; Gómez-Caravaca, A.M.; Pasini, F.; Caboni, M.F.; Segura-Carretero, A.; Fernández-Gutiérrez, A. HPLC-DAD-ESI-QTOF-MS and HPLC-FLD-MS as Valuable Tools for the Determination of Phenolic and Other Polar Compounds in the Edible Part and by-Products of Avocado. *LWT - Food Sci. Technol.* **2016**, *73*, 505–513, doi:10.1016/j.lwt.2016.06.049.
  23. Ramos-Aguilar, A.L.; Ornelas-Paz, J.; Tapia-Vargas, L.M.; Gardea-Bejar, A.A.; Yahia, E.M.; Ornelas-Paz, J. de J.; Perez-Martinez, J.D.; Rios-Velasco, C.; Escalante-Minakata, P. Metabolomic Analysis and Physical Attributes of Ripe Fruits from Mexican Creole (*Persea Americana* Var. *Drymifolia*) and "Hass" Avocados. *Food Chem.* **2021**, *354*, doi:10.1016/j.foodchem.2021.129571.
  24. Figueroa, J.G.; Borrás-Linares, I.; Lozano-Sánchez, J.; Segura-Carretero, A. Comprehensive Characterization of Phenolic and Other Polar Compounds in the Seed and Seed Coat of Avocado by HPLC-DAD-ESI-QTOF-MS. *Food Res. Int.* **2018**, *105*, 752–763, doi:10.1016/j.foodres.2017.11.082.
  25. Figueroa, J.G.; Borrás-Linares, I.; Lozano-Sánchez, J.; Segura-Carretero, A. Comprehensive Identification of Bioactive Compounds of Avocado Peel by Liquid Chromatography Coupled to Ultra-High-Definition Accurate-Mass Q-TOF. *Food Chem.* **2018**, *245*, 707–716, doi:10.1016/j.foodchem.2017.12.011.
  26. Hurtado-Fernández, E.; González-Fernández, J.J.; Hormaza, J.I.; Bajoub, A.; Fernández-Gutiérrez, A.;

- Carrasco-Pancorbo, A. Targeted LC-MS Approach to Study the Evolution over the Harvesting Season of Six Important Metabolites in Fruits from Different Avocado Cultivars. *Food Anal. Methods* **2016**, *9*, 3479–3491, doi:10.1007/s12161-016-0523-5.
27. Di Stefano, V.; Avellone, G.; Bongiorno, D.; Indelicato, S.; Massenti, R.; Lo Bianco, R. Quantitative Evaluation of the Phenolic Profile in Fruits of Six Avocado (*Persea Americana*) Cultivars by Ultra-High-Performance Liquid Chromatography-Heated Electrospray-Mass Spectrometry. *Int. J. Food Prop.* **2017**, *20*, 1302–1312, doi:10.1080/10942912.2016.1208225.
28. Serrano-García, I.; Hurtado-Fernández, E.; Gonzalez-Fernandez, J.J.; Hormaza, J.I.; Pedreschi, R.; Reboredo-Rodríguez, P.; Figueiredo-González, M.; Olmo-García, L.; Carrasco-Pancorbo, A. Prolonged On-Tree Maturation vs. Cold Storage of Hass Avocado Fruit: Changes in Metabolites of Bioactive Interest at Edible Ripeness. *Food Chem.* **2022**, *394*, 133447, doi:10.1016/j.foodchem.2022.133447.
29. Pedreschi, R.; Ponce, E.; Hernández, I.; Fuentealba, C.; Urbina, A.; González-Fernández, J.J.; Hormaza, J.I.; Campos, D.; Chirinos, R.; Aguayo, E. Short vs. Long-Distance Avocado Supply Chains: Life Cycle Assessment Impact Associated to Transport and Effect of Fruit Origin and Supply Conditions Chain on Primary and Secondary Metabolites. *Foods* **2022**, *11*, 1807, doi:10.3390/foods11121807.
30. Campos, D.; Teran-Hilares, F.; Chirinos, R.; Aguilar-Galvez, A.; García-Ríos, D.; Pacheco-Avalos, A.; Pedreschi, R. Bioactive Compounds and Antioxidant Activity from Harvest to Edible Ripeness of Avocado Cv. Hass (*Persea Americana*) throughout the Harvest Seasons. *Int. J. Food Sci. Technol.* **2020**, *55*, 2208–2218, doi:10.1111/ijfs.14474.
31. Fan, S.; Qi, Y.; Shi, L.; Giovani, M.; Zaki, N.A.A.; Guo, S.; Suleria, H.A.R. Screening of Phenolic Compounds in Rejected Avocado and Determination of Their Antioxidant Potential. *Processes* **2022**, *10*, doi:10.3390/pr10091747.
32. Hurtado-Fernández, E.; Pacchiarotta, T.; Gómez-Romero, M.; Schoenmaker, B.; Derks, R.; Deelder, A.M.; Mayboroda, O.A.; Carrasco-Pancorbo, A.; Fernández-Gutiérrez, A. Ultra High Performance Liquid Chromatography-Time of Flight Mass Spectrometry for Analysis of Avocado Fruit Metabolites: Method Evaluation and Applicability to the Analysis of Ripening Degrees. *J. Chromatogr. A* **2011**, *1218*, 7723–7738, doi:10.1016/j.chroma.2011.08.059.
33. Panche, A.N.; Diwan, A.D.; Chandra, S.R. Flavonoids: An Overview. *J. Nutr. Sci.* **2016**, *5*, doi:10.1017/jns.2016.41.
34. Hurtado-Fernández, E.; Pacchiarotta, T.; Mayboroda, O.A.; Fernández-Gutiérrez, A.; Carrasco-Pancorbo, A. Quantitative Characterization of Important Metabolites of Avocado Fruit by Gas Chromatography Coupled to Different Detectors (APCI-TOF MS and FID). *Food Res. Int.* **2014**, *62*, 801–811, doi:10.1016/j.foodres.2014.04.038.
35. Pereira, C.; Barros, L.; Carvalho, A.M.; Ferreira, I.C.F.R. Use of UFLC-PDA for the Analysis of Organic Acids in Thirty-Five Species of Food and Medicinal Plants. *Food Anal. Methods* **2013**, *6*, 1337–1344, doi:10.1007/s12161-012-9548-6.
36. Rodríguez-Carpena, J.G.; Morcuende, D.; Andrade, M.J.; Kylli, P.; Estevez, M. Avocado (*Persea Americana* Mill.) Phenolics, in Vitro Antioxidant and Antimicrobial Activities, and Inhibition of Lipid and Protein Oxidation in Porcine Patties. *J. Agric. Food Chem.* **2011**, *59*, 5625–5635, doi:10.1021/jf1048832.
37. van den Berg, R.A.; Hoefsloot, H.C.J.; Westerhuis, J.A.; Smilde, A.K.; van der Werf, M.J. Centering, Scaling, and Transformations: Improving the Biological Information Content of Metabolomics Data. *BMC Genomics* **2006**, *7*, 1–15, doi:10.1186/1471-2164-7-142.
38. AOAC Association of Official Analytical Chemists. Official Methods of Analysis of AOAC Int. 2016, Latimer G.W, Ed. 20th ed.

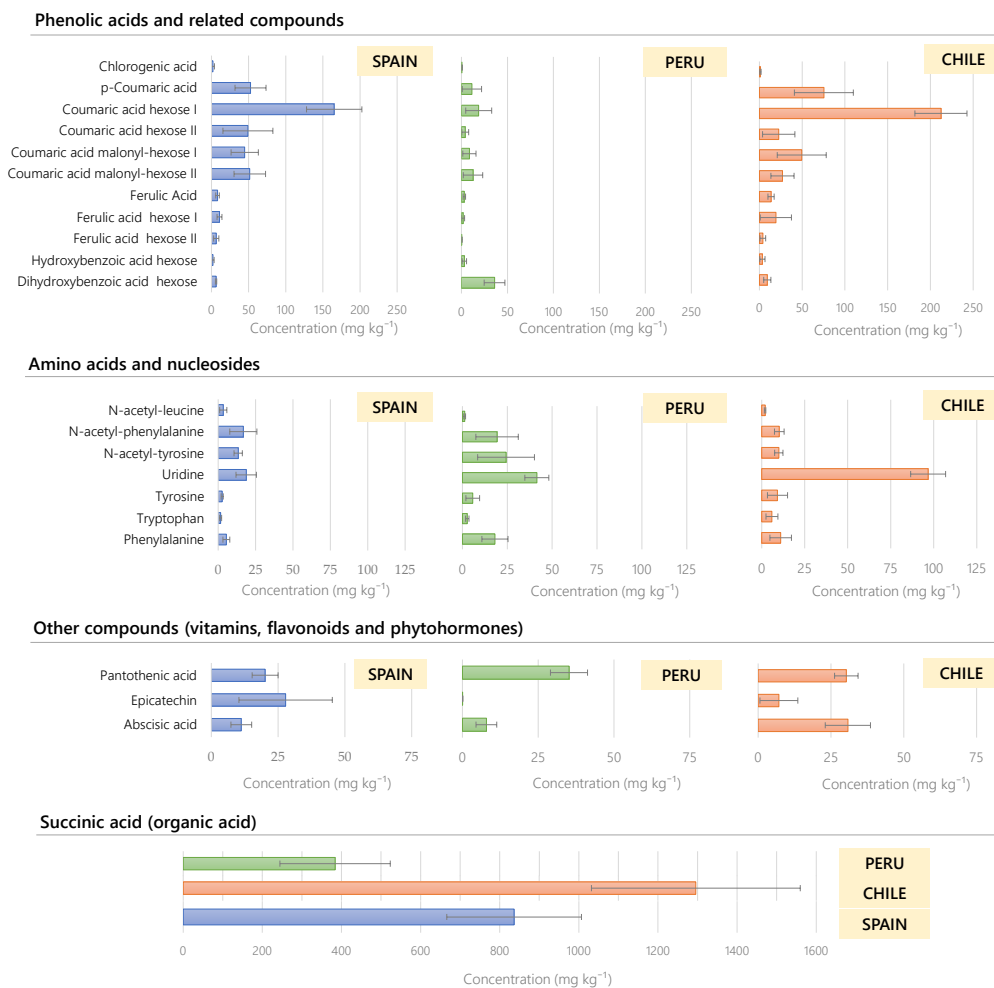


**Figure S1.** Bar diagrams of the twenty-two compounds quantified in *Hass* avocados from Chile, Peru, and Spain. Compounds are grouped by chemical families and results are expressed as the mean of each geographical origin in mg kg<sup>-1</sup> with associated standard deviations (SD)

**Table S1.** Analytical parameters of the LC-MS method used in the current study.

Compound	Rt (min)	Calibration curves	R <sup>2</sup>	LOD (µg L <sup>-1</sup> )	LOQ (µg L <sup>-1</sup> )	Lineal range (mg L <sup>-1</sup> )	Repeatability (% CV)	
							Intra-day <sup>a</sup>	Inter-day <sup>b</sup>
Uridine	2.7	y = 7087.8 + 15744.5x	0.9910	40.2	133.8	LOQ - 16.1 16.1 – 64.3	8.90	9.23
		y = 157088.5 + 6364.1x	0.9945					
Succinic acid	3.2	y = 1887.9 + 1302.5x	0.9939	118.4	395.4	LOQ – 20.1 20.1 – 643.4	7.15	14.63
		y = 29928.5 + 577.6x	0.9910					
Phenylalanine	4.9	y = -184.1 + 35428.7x	0.9992	20.1	67.1	LOQ – 1.7 1.7 – 26.8	7.53	12.45
		y = 19534.4 + 31628.4x	0.9983					
Pantothenic acid	5.2	y = 250.3 + 66086.8x	0.9984	35.4	118.0	LOQ – 0.8 0.8 – 26.8	9.25	10.08
		y = 28703.0 + 54982.3x	0.9968					
Tryptophan	6.4	y = 1557.6 + 58178.7x	0.9973	22.5	75.0	LOQ – 0.8 0.8 – 13.4	7.85	10.34
		y = -3198.1 + 62650.8x	0.9997					
Chlorogenic acid	7.1	y = -152.6 + 28634.7x	0.9962	62.1	206.7	LOQ – 1.3 1.3 – 10.7	8.26	10.83
		y = 11441.8 + 22052.8x	0.9956					
Epicatechin	8.3	y = 21437.4 + 65579.4x	0.9905	13.6	45.2	LOQ – 10.7 10.7 – 85.8	7.73	10.38
		y = 894997.8 + 25710.0x	0.9944					
<i>p</i> -Coumaric acid	9.9	y = 87289.2 + 23255.4x	0.9983	17.8	59.1	LOQ – 90.5 90.5 – 723.9	7.21	9.51
		y = 1837252.8 + 6750.0x	0.9911					
Ferulic acid	10.4	y = 5700.8 + 37765.4x	0.9928	13.8	46.1	LOQ – 5.4 5.4 – 21.5	9.30	10.30
		y = 124533.4 + 15519.3x	0.9954					
Abscisic acid	12.9	y = 7005.9 + 125830.9x	0.9988	7.1	23.6	LOQ – 4.0 4.0 – 32.2	6.76	7.83
		y = 366668.8 + 57711.5x	0.9909					

Abbreviations used: Rt (Retention time); LOD (Limit of detection); LOQ (Limit of quantification).

a: coefficient of variation (%) corresponding to injections (n = 7) of the QC sample performed in the same sequence.

b: coefficient of variation (%) corresponding to injections (n = 18) of the QC sample carried out in sequences carried out on different days.



# Chapter

## Comprehensive LC-IMS-MS characterisation of avocado fruits from different Iberian regions: Integrating ion mobility as a valuable descriptor in non-targeted metabolomics

Irene Serrano-García<sup>a</sup>, Lucía Olmo-García<sup>a</sup>, Romina Pedreschi<sup>b,c</sup>, José Jorge Gonzalez-Fernandez<sup>d</sup>, José Ignacio Hormaza<sup>d</sup>, Alegría Carrasco-Pancorbo<sup>a</sup>

<sup>a</sup> *Department of Analytical Chemistry, Faculty of Sciences, University of Granada, Ave. Fuentenueva s/n, 18071, Granada, Spain*

<sup>b</sup> *Escuela de Agronomía, Facultad de Ciencias Agronómicas y de los Alimentos, Pontificia Universidad Católica de Valparaíso, Calle San Francisco S/N, La Palma, Quillota, 2260000, Chile*

<sup>c</sup> *Millennium Institute Center for Genome Regulation (CRG), Santiago, 8331150, Chile*

<sup>d</sup> *Institute for Mediterranean and Subtropical Horticulture (IHSM La Mayora-UMA-CSIC), 29750, Algarrobo-Costa, Málaga, Spain*

 luciaolmo@ugr.es

***Food Chemistry (to be submitted)***



**Abstract:** This study explores the influence of geographic origin on the metabolic profile of *Hass* avocado fruits by analysing their compositional profiles across eight Iberian regions using an advanced UHPLC-TimsTOF MS/MS analytical platform. A comprehensive profiling of the methanolic extracts was performed to construct a metabolic library incorporating the ion mobility descriptor. By applying unsupervised chemometrics-assisted non-targeted metabolomics, avocado fruits clustered according to geographical proximity, with the most significant metabolic differences observed between the northern and southern regions. Despite this general trend, each region exhibited distinct metabolic patterns, even between neighbouring areas. To further delineate the region-specific metabolic compositions, multiple two-class orthogonal partial least squares discriminant analysis (OPLS-DA) models were designed to identify the most influential variables in the projections, resulting in the identification of origin-specific biomarkers characteristic of avocados from each growing area. This research offers valuable information on how regional edaphoclimatic factors impact avocado quality and compositional diversity.

**Keywords:** *Persea americana* Mill., *Hass* avocado mesocarp, geographical origin, plant metabolomics, Spanish avocado, phenolic compounds

## 1. INTRODUCTION

Although native to Mexico and Central America, the avocado (*Persea americana* Mill.) has gained prominence in Spain as a compelling alternative to traditional crops such as olives, mandarins, and vines. While avocado was introduced in Spain in the 16th century, it was not until the 1970s that commercial production reached a significant volume. Three commercial horticultural avocado races are known, including Mexican (*P. americana* var. *drymifolia*), Guatemalan (*P. americana* var. *guatemalensis*) and West Indian (*P. americana* var. *americana*) [1]. Avocado thrives in tropical, semitropical, and subtropical climates, although the great genetic diversity, facilitated by the ease of hybridisation between races, allows the crop to adapt to different environmental and agronomic conditions [1,2]. The *Hass* avocado, an inter-racial hybrid with approximately 40% of its genome derived from the Guatemalan race introgressed into a Mexican race background, according to recent genome sequencing data [3], remains the most widely recognised and commercially promoted cultivar [4].

With around 19,520 hectares under cultivation and a production of 105,930 tonnes in 2022 [5], Spain maintains its position as Europe's leading avocado producer and supplier while partially covering the country's needs. The key avocado-producing regions are concentrated along the Mediterranean and Atlantic coastal region of Andalusia, which contribute to about 75-80% of the country's total production, mainly in the provinces of Malaga and Granada. However, rising global demand, likely driven by the widely recognised health benefits associated with avocados [6], along with the effects of climate change [7], is leading to the expansion of avocado cultivation to previously mostly unexploited regions of the Iberian Peninsula. Thus, in the last decade, avocado

cultivation has expanded significantly to the Algarve in Portugal and the Valencian Community in eastern Spain, as well as to specific areas in the coastal northern regions. In addition, avocado is also grown in the Canary Islands, with more than 2,000 hectares, although production is largely limited to supplying local markets [8].

Avocado fruit is rich in fatty acids, carbohydrates, phenolic compounds, pigments, vitamins, sterols, and other phytochemicals. However, its quality and nutritional composition are significantly affected by several pre- and post-harvest factors [6,9]. Among these decisive factors, the geographical area of cultivation, closely linked to climatic conditions, emerges as one of the most influential aspects. Climatic stress induces significant changes in avocado crop physiology and phenology, which are also reflected in plant transcriptomics, proteomics and metabolomics [10]. Temperature and relative humidity influence flowering and fruit setting processes [11]. Fruit development and ripening are also temperature-sensitive, with accelerated development rates and shorter production cycles under elevated temperatures [7,12]. Water availability is another critical constraint. Drought conditions during early fruit development increase the risk of fruit physiological disorders such as pulp spot and vascular blackening [13]. Conversely, excessive water over a short period can harm plant roots and promote the development of root diseases [14]. However, these issues are often alleviated by the implementation of crop irrigation strategies [15]. Additionally, factors such as light conditions, wind, or crop altitude may also impact tree vigour, fruit quality, and overall crop yield [16,17].

Plant metabolism alterations in response to environmental adaptations are often accompanied by the synthesis and accumulation of both growth-related primary metabolites and defence-related secondary metabolites [10]. This responsiveness presumably modulates fruit compositional profiles consistently as a function of geographic provenance, even when comparing the same avocado variety. Several studies have shown that oil content and fatty acid composition of avocado flesh are influenced by geographic origin and climate [17–23]. Indeed, oleic acid has been suggested as a potential biochemical marker for distinguishing the origin of *Hass* avocado fruits [18]. Lipid chromatographic fingerprinting has also been used to efficiently classify avocado fruits according to their provenance [24,25] and stable isotopes and elemental profiles have proven to be valuable tools for distinguishing Spanish avocados [26]. Recent research has explored whether specific compounds in avocado flesh -such as phenolic acids, flavonoids, vitamins, organic acids, and amino acids- are influenced by the geographical origin of the fruit as well as by soil and climatic conditions and, consequently, if they can be used to trace the fruit's origin. Using a targeted metabolomics approach, Serrano-García and co-authors defined the quantitative metabolic profiles of *Hass* mesocarp grown in Peru, Chile, and Spain, and pointed out promising origin-specific biomarkers [27]. Additionally, Méndez-Hernandez et al. evaluated disparities in terms of total phenolic compounds and flavonoids between the same variety grown in different locations on the island of Tenerife (Spain) [8].

Even though chemometrics-assisted non-targeted metabolomics represents a powerful tool for food traceability [28–31], its applicability to the study of avocado provenance remains largely unexplored. Most metabolomic analyses rely on liquid chromatography high-resolution mass spectrometry (LC-HRMS) due to its superior sensitivity, selectivity, and peak reproducibility. Recently, ion mobility spectrometry (IMS) coupled to HRMS has gained considerable attention in metabolomics because of its ability to provide ion structural information through an additional dimension of separation. IMS technology is based on the gas-phase three-dimensional ion size and charge, which are translated into a single Collision Cross Section (CCS) value [32]. Integrating CCS value with other metabolite identification criteria (such as retention time, mass accuracy, fragmentation pattern, and isotopic pattern) enhances the reliability of metabolite annotation; this approach may be particularly useful in non-targeted metabolomics studies, where most biomarkers are unknown. To the best of our knowledge, no previous studies have applied LC-IMS-MS to avocado mesocarp metabolomics. Bearing this in mind, the present work aims to: (i) comprehensively characterise the metabolites in avocado mesocarp to provide a complete experimental CCS library using UHPLC-TimsTOF MS/MS, (ii) investigate whether there are differences in the metabolic profile of *Hass* avocados grown in different regions of the Iberian Peninsula with varying climatic conditions and (iii) describe the characteristic compositional patterns of avocado fruits from each geographic region.

## 2. MATERIALS AND METHODS

### 2.1. Chemicals and reagents

Ultrapure water was obtained using a Milli-Q purification system from Millipore (Bedford, MA, USA). LC-MS grade acetonitrile and methanol were provided by VWR International EuroLab S.L.U. (Barcelona, Spain). Acetic acid (AcH) and analytical standards of quinic acid, uridine, succinic acid, phenylalanine, pantothenic acid, tryptophan, chlorogenic acid, epicatechin, *p*-coumaric acid, ferulic acid and abscisic acid were purchased from Sigma-Aldrich (St. Louis, MO, USA). Acrodisc™ 0.22 µm nylon syringe filters, and 0.45 µm Nylaflo™ nylon membranes (used to filter the mobile phases) were supplied by Pall Corporation (Michigan, USA).

### 2.2. Plant material and sampling information

The plant material consisted of a representative sample set comprising 480 avocados cv. *Hass* from eight different geographical origins in the Iberian Peninsula (Spain and Portugal). Between March and April of the 2021-2022 season, a total of 50-60 fruits were harvested from each avocado producing regions of the Iberian Peninsula considered in this study. Avocado fruits from Galicia and Asturias (in north-western Spain) were provided by Vivazplant and Aguacastur, respectively; those from Valencia (in eastern Spain) by AVA-ASAJA (Asociación Valenciana de Agricultores); fruits from Granada (Motril and Jete), Cadiz, and Malaga (in the southern region of Spain) were supplied by Huerta Tropical, ASAJA (Asociación Agraria de Jóvenes Agricultores)-Cádiz and IHSM

La Mayora, respectively; avocados from Algarve (on the southern coast of Portugal) were procured by Nuno Neto. Table 1 provides information on the location coordinates (region, elevation, latitude, and longitude) of the different sampling points, along with meteorological conditions (precipitation, relative humidity, solar irradiation, and temperatures) in these production areas over a one-year period from June 2021 until the harvesting time in April 2022. Given the significant impact of climatic conditions on avocado phenology, detailed month by month climatic data are presented in Figure S1.

**Table 1.** Location and meteorological conditions (precipitation, relative humidity, solar irradiation and temperatures) of the considered sampling points.

Region	Elevation (m)	Latitude	Longitude	Temperature (°C)			RH (%)	ASR (MJ/m <sup>2</sup> )	Rainfall (mm)
				Max.	Mean	Min.			
Asturias	300	43°25'44.03"N	5°24'28.07"W	25.2	12.4	2.9	86.9	128.8	1414.4
Cadiz	11	36°43'46.0"N	6°05'18.1"W	30.7	17.5	5.8	71.0	192.6	437.6
Pontevedra (Galicia)	19	41°55'16.9"N	8°47'26.5"W	27.5	15.1	5.3	77.0	159.2	942.0
Granada	139 (Jete)	36°47'50"N	3°40'05"W	27.4	17.5	8.4	73.2	184.5	230.8
	45 (Motril)	36°46' 51"N	3°30'17"W						
Malaga	35	36°45'23.9"N	4°02'33.3"W	30.3	18.0	7.5	60.7	184.7	232.8
Algarve	68	37°10'18.1"N	7°34'39.1"W	28.3	17.1	8.5	70.1	186.6	444.2
Valencia	14	39°11'44"N	0°23'35"W	29.8	17.1	7.8	77.1	154.6	908.5

RH: Relative humidity, ASR: Accumulated Solar Radiation (calculated as the sum of total accumulated radiation over the considered months), Rainfall (calculated as the sum of total accumulated precipitation over the considered months).

After harvesting, avocado fruits were transported to the laboratory within 1-2 days and left to ripen at room temperature (20-25 °C) until they reached optimal ripeness (ready to eat stage; 4-14 N mesocarp firmness). Fruits were processed in batches of five pieces to ensure multiple biological replicates, resulting in a total of 8-10 samples per origin (n=8-10, with five fruits per replicate). Preparation of each sample consisted of peeling, slicing, bagging, freezing, freeze-drying, and careful grinding to ensure sample homogenisation. All prepared avocado samples were stored at -23 °C until use.

### 2.3. Metabolite extraction from the avocado samples

Metabolites were extracted from the avocado samples following the solid-liquid protocol outlined by Serrano-García and co-authors [27]. Initially, 0.25 g of freeze-dried avocado sample was subjected to extraction using 20 mL of pure MeOH. The extraction process involved a 3-min vortex shake, followed by 30-min ultrasound bath, and concluded with a 5 min centrifugation at 9000 rpm. Subsequently, the liquid phase was transferred to a glass flask, while the residual avocado solid phase was subjected to a second extraction cycle applying the same procedure. The resulting supernatants from both extractions were combined, evaporated, and redissolved in 1 mL of pure MeOH. The solution was then filtered by using a nylon syringe filter (0.22 µm pore size) before being transferred into an LC amber vial. All vials were stored at -23 °C until analysis. A

quality control (QC) sample was prepared by taking equivalent volumes of each and every extract that made up the sample set.

#### 2.4. UHPLC-TimsTOF MS/MS methodology and system stability assurance

Analyses of the samples under study were conducted using an Elute series of Ultra High-Performance Liquid Chromatography (UHPLC) equipped with a Vacuum Insulated Probe Heated ElectroSpray Ionisation source (VIP-HESI) and coupled to a trapped ion mobility -time of flight (timsTOF) Pro 2 high-resolution spectrometer from Bruker Daltonics (Bremen, Germany). This analytical platform is powered by the latest parallel accumulation serial fragmentation (PASEF®) technology based on data-dependent acquisition attending to the auto MS/MS mode. The UHPLC was furnished with an Intensity Solo 2 C18 column (2.1 × 100 mm, 1.8 μm particle size) from Bruker Daltonics. The column temperature was maintained at 35 °C, while the autosampler kept the extracts refrigerated at 4 °C throughout the analytical sequence. Each analysis involved injecting a sample volume of 2 μL. The mobile phases were Milli-Q water with 0.5 % acetic acid (phase A) and pure acetonitrile (phase B), and the optimum flow rate was 0.4 mL/min. A gradient elution was applied as follows: 0.0 min, 95 % A; 14.0 min, 46 % A; 14.5 min, 1 % A, 17.0 min; 1 % A; 17.1 min, 95 % A and at 20.0 min, 95 % A. The VIP-HESI source operated in negative polarity and *Full Scan* mode ( $m/z$  20-1300), with specific settings such as +4500 V of capillary, 4.0 bar of nebuliser pressure, 8.0 L/min and 200 °C of drying gas, and 4.0 L/min and 450 °C of sheath gas. TIMS operated with nitrogen (N<sub>2</sub>) as the drift gas, with both accumulation and ramp times set at 100 ms. The ion mobility was scanned from 0.10 V·s/cm<sup>2</sup> to 1.50 V·s/cm<sup>2</sup>.

External calibration of the system (TIMS and HRMS) was performed at the beginning of each sequence by using both sodium formate and ESI-L Low Concentration Tuning Mix (Agilent Technologies, Waldbronn, Germany) solutions. Additional internal calibration was implemented and used for data processing by infusion of the calibrant solution at the beginning of each analysis. The QC sample was analysed every 10 samples to evaluate the stability of the instrument response and correct potential time/intensity shifts. Additionally, pure solvent (MeOH) injections were performed at the same intervals to clean the column and prevent contamination. The samples were injected in a randomised sequence to minimise carryover effects and reduce the risk of analysis bias. Control software included Compass Hystar and timsControl provided by Bruker Corporation.

#### 2.5. Data processing and metabolite identification

Data processing was performed utilising MetaboScape 2023 software, with the T-Rex 4D (LC-TIMS-QTOF MS) algorithm. This algorithm automatically recalibrated the acquired MS data and conducted molecular feature selection, peak alignment, filtering, and scaling. The criteria for feature extraction included a minimum presence of 80% in samples per origin, an intensity threshold of 10000 counts, a minimum 4D peak size of 100 points, and recursive features defined at 75 points. The retention time range considered for the data treatment, spanning from 0.4

minutes to 12 minutes, was selected based on the elution area of polar and semi-polar metabolites. Ion deconvolution utilised an EIC correlation of 0.8, with  $[M-H]^-$  as the primary ion,  $[M+Cl]^-$  as the seed ion, and  $[M-H-H_2O]^-$  and  $[2M-H]^-$  as the common ions. The Within-Batch Correction tool was applied to mitigate potential drifts during the sequences. Features extracted from analytical blanks were automatically excluded if the sample/solvent ratio exceeded 3.0. In total, 1955 features comprised the variables considered in the study.

Once the feature table was generated, the extracted ions were firstly characterised by the tools integrated within the data processing software. Among these tools, SmartFormula determines the molecular formula based on its accurate mass and isotopic distribution with a maximum mass error of 5 ppm. The study primarily focused on molecular formulas composed of carbon, hydrogen, nitrogen, oxygen, and phosphorus, reflecting the common metabolite families present in avocado mesocarp. Besides, molecular descriptors and fragmentation patterns were compared to established analyte lists and MS/MS spectral libraries, such as the Bruker Sumner MetaboBASE Plant Library or public available online metabolic databases (MassBank, MoNA, HMDB...). Moreover, the Compound Crawler tool included into MetaboScape was used to search for molecular structures corresponding to specified molecular formulas across local (AnalyteDB) and online public databases (ChEBI, ChemSpider, and PubChem). This software also incorporates MetFrag, which performs the *in silico* fragmentation of potential structures and compares them with the acquired HRMS/MS spectra. Additionally, a CCS prediction tool was used to compare the expected CCS values of the candidate compounds with the experimental CCS values.

## 2.6. Statistical analyses

Chemometric analyses, including principal component analysis (PCA), hierarchical clustering analysis (HCA), and orthogonal partial least squares discriminant analysis (OPLS-DA), were conducted using SIMCA v14.1 software. Before the analyses, the X-data matrix was standard normalised and scaled using unit variance. Unsupervised PCA reduced data dimensionality and provided initial exploratory insights. It also served to detect outliers and, to some extent (considering the QC samples), to test the repeatability of the system. HCA, represented by a dendrogram and calculated with Ward's distance and sorted by size, was used to elucidate similarities among observations. Supervised OPLS-DA models were employed to individually characterise the metabolic patterns of each origin by comparing one region against all others. The most important variables in the projection (VIP) were selected for metabolite identification as potential origin descriptors (markers). Model quality was evaluated through the goodness of fit ( $R^2X$ ,  $R^2Y$ ) and predictive ability ( $Q^2$ ) parameters, while cross-validation included F and *p*-value from the ANOVA test.

### 3. RESULTS AND DISCUSSION

#### 3.1. Qualitative metabolic characterisation of avocado mesocarp by integrating the ion mobility descriptor

The non-targeted LC-IMS-HRMS/MS approach uncovered a large number of peaks in avocado mesocarp, underlining the great complexity of the matrix. In the initial phase of this study, we focused on thoroughly characterising these metabolic profiles, based on previously published data on avocado and considering compounds identified in other plants. Compound annotation was carried out by interpreting high resolution MS and MS/MS spectra, taking into account the relative elution order and using commercial standards when available. In addition, relevant literature and open access databases such as MassBank, MoNA, HMDB, etc. were consulted. Several characteristic functional groups or substitutions exhibited consistent MS fragmentations, enabling the identification of various conjugated forms. A mass difference of 132.0423 Da ( $C_5H_8O_4$ ) indicated the presence of a pentose moiety, while 162.0528 Da ( $C_6H_{10}O_5$ ) suggested a hexose, and 146.0579 Da ( $C_6H_{10}O_4$ ) indicated a deoxyhexose. Additionally, a difference of 308.1107 Da ( $C_{12}H_{20}O_9$ ) corresponded to a rutoside or deoxyhexose-hexose conjugate, and 324.1056 Da ( $C_{12}H_{20}O_{10}$ ) matched a di-hexose structure. A malonyl group was identified by a mass difference of 86.0004 Da ( $C_3H_2O_3$ ), and malonyl-hexose by a difference of 248.0532 Da ( $C_9H_{12}O_8$ ). Moreover, a mass difference of 144.0423 Da ( $C_6H_8O_4$ ), along with neutral losses of 102.0317 Da ( $C_4H_6O_3$ ) and 62.0004 Da ( $CH_2O_3$ ), was consistent with a 3-hydroxy-3-methylglutaryl (HMG) substitution [33,34].

Table 2 provides a detailed list of compounds arranged by their order of elution, including their calculated molecular formulas, experimental  $m/z$  values, mass errors, mSigma scores,  $^{TIMS}CCS_{N_2}$  values, and the main MS/MS fragments associated with each peak. Relevant studies that support the proposed identifications are also referenced, though the table is not intended to serve as an exhaustive literature review for each compound. The integration of ion mobility in this study represents a significant advancement, enabling the generation of an experimental  $^{TIMS}CCS_{N_2}$  library, which will enhance reliable metabolite characterisation in future avocado metabolomics research. More than one hundred primary and secondary metabolites were identified, at least tentatively, which can be classified into different chemical groups as outlined below.

**Sugars and their derivatives** eluted early in the metabolic profile, a behaviour attributed to their polar nature. Identified compounds include the non-structural C7 carbohydrates *D*-mannoheptulose ( $C_7H_{14}O_7$ ; 137.0 Å<sup>2</sup>) and its sugar alcohol form, perseitol ( $C_7H_{16}O_7$ ; 136.0 Å<sup>2</sup>), along with the C6 monosaccharides glucose or fructose ( $C_6H_{12}O_6$ ; 127.0 Å<sup>2</sup>) and the disaccharide sucrose ( $C_{12}H_{22}O_{11}$ ; 166.2 Å<sup>2</sup>).

Several common **organic acids**, such as quinic acid ( $C_7H_{12}O_6$ ; 132.4 Å<sup>2</sup>), malic acid ( $C_4H_6O_5$ ; 118.8 Å<sup>2</sup>) and succinic acid ( $C_4H_6O_4$ ; 112.4 Å<sup>2</sup>) also eluted in the initial part of the chromatogram. Interestingly, a substance with a molecular formula equivalent to the dimer of quinic acid ( $C_{14}H_{24}O_{12}$ ; 183.5 Å<sup>2</sup>) was also detected at 1.02 min. Other organic acids identified included two

isomers of citric acid ( $C_6H_8O_7$ ). These were detected by TIMS, showing two distinct peaks on the mobilogram at 124.3  $\text{\AA}^2$  and 132.6  $\text{\AA}^2$ , together with a characteristic fragmentation pattern at  $m/z$  111.01. In addition, the peak at  $m/z$  205.0353  $[M-H]^-$  with a molecular formula of  $C_7H_{10}O_7$  (133.4  $\text{\AA}^2$ ) was consistent with methyl citric acid based on the MS and MS/MS data. Meanwhile, the peak at  $m/z$  175.0612  $[M-H]^-$ , which appeared at min 2.99, was identified as isopropylmalic acid ( $C_7H_{12}O_5$ ; 127.6  $\text{\AA}^2$ ).

Avocado extracts contained various **nitrogenous substances**. In the category of **amino acids and derivatives**, glutamine ( $C_5H_{10}N_2O_3$ ; 123.8  $\text{\AA}^2$ ), pyroglutamic acid hexoside ( $C_{11}H_{17}NO_8$ ; 156.6  $\text{\AA}^2$ ) and its aglycone ( $C_5H_7NO_3$ ; 120.7  $\text{\AA}^2$ ), tyrosine ( $C_9H_{11}NO_3$ ; 140.7  $\text{\AA}^2$ ), hexose-leucine ( $C_6H_{13}NO_2$ ; 127.1  $\text{\AA}^2$ ), phenylalanine ( $C_9H_{11}NO_2$ ; 136.0  $\text{\AA}^2$ ), *N*-acetyl-tyrosine ( $C_{11}H_{13}NO_4$ ; 149.0  $\text{\AA}^2$ ), tryptophan ( $C_{11}H_{12}N_2O_2$ ; 148.1  $\text{\AA}^2$ ), *N*-acetyl-leucine ( $C_8H_{15}NO_3$ ; 137.2  $\text{\AA}^2$ ), *N*-acetyl-phenylalanine ( $C_{11}H_{13}NO_3$ ; 144.2  $\text{\AA}^2$ ) and *N*-acetyl-tryptophan ( $C_{13}H_{14}N_2O_3$ ; 156.1  $\text{\AA}^2$ ) were identified. Additionally, **nucleosides, nucleotides, and their analogues** were also detected, including uridine ( $C_9H_{12}N_2O_6$ ; 148.3  $\text{\AA}^2$ ), guanosine ( $C_{10}H_{13}N_5O_5$ ; 158.9  $\text{\AA}^2$ ) and adenosine ( $C_{10}H_{13}N_5O_4$ ; 161.8  $\text{\AA}^2$ ), along with adenosine monophosphate ( $C_{10}H_{14}N_5O_7P$ ; 171.1  $\text{\AA}^2$ ) and succinyladenosine ( $C_{14}H_{17}N_5O_8$ ; 189.2  $\text{\AA}^2$ ). We confirmed the identity of pantothenic acid ( $C_9H_{17}NO_5$ ; 114.2  $\text{\AA}^2$ ), a water-soluble **vitamin**, using its pure standard. Furthermore, its glycosylated form ( $C_{15}H_{27}NO_{10}$ ; 178.3  $\text{\AA}^2$ ) was also identified, eluting at 2.07 min.

**Phenolic compounds** were the most abundant group identified in avocado mesocarp, with a significant presence of **phenolic acids and their derivatives**. Among the hydroxybenzoic acids and derivatives, some of the most prominent metabolites were gallic acid ( $C_7H_6O_5$ ; 121.5  $\text{\AA}^2$ ) and its glycosylated form ( $C_{13}H_{16}O_{10}$ ; 166.1  $\text{\AA}^2$ ). Several dihydroxybenzoic acid derivatives were identified within the profiles, distinguished by their characteristic fragmentation at  $m/z$  153.02, 152.01, 109.03 and 108.02. These conjugates included two molecules bound to a hexose moiety ( $C_{13}H_{16}O_9$ ; 169.2 and 163.9  $\text{\AA}^2$ ), one attached to a pentose ( $C_{12}H_{14}O_8$ ; 162.3  $\text{\AA}^2$ ) and another with both hexose and pentose moieties ( $C_{18}H_{24}O_{13}$ ; 187.4  $\text{\AA}^2$ ). Moreover, 4-hydroxybenzoic acid ( $C_7H_6O_3$ ; 117.3  $\text{\AA}^2$ ), along with two hexose-bound isomers of hydroxybenzoic acid ( $C_{13}H_{16}O_8$ ; 166.7  $\text{\AA}^2$  and 162.2  $\text{\AA}^2$ ) and other two isomers containing hexose-pentose sugar moieties ( $C_{18}H_{24}O_{12}$ ; 181.4  $\text{\AA}^2$  and 183.6  $\text{\AA}^2$ ) were identified based on MS/MS data. Other noteworthy compounds included two isomers of vanillic acid hexose ( $C_{14}H_{18}O_9$ ; 174.7  $\text{\AA}^2$  and 175.5  $\text{\AA}^2$ ), one of vanillic acid hexoside-pentoside ( $C_{19}H_{26}O_{13}$ ; 187.5  $\text{\AA}^2$ ), vanillin ( $C_8H_8O_3$ ; 124.7  $\text{\AA}^2$ ), syringic acid ( $C_9H_{10}O_5$ ; 135.2  $\text{\AA}^2$ ) and syringic acid glycoside ( $C_{15}H_{20}O_{10}$ ; 185.9  $\text{\AA}^2$ ).

Hydroxycinnamic acids and their derivatives were the most abundant subgroup among the phenolic acids. They comprised several *O*-caffeoylquinic acids ( $C_{16}H_{18}O_9$ ); these were mass isomers identified as neochlorogenic acid (2.42 min; 168.3  $\text{\AA}^2$ ), chlorogenic acid (3.25 min, pure standard; 182.9  $\text{\AA}^2$ ) and cryptochlorogenic acid (3.40 min; 181.9  $\text{\AA}^2$ ) according to the elution order previously described in literature.

**Table 2.** Qualitative characterisation of *Hass* avocado mesocarp metabolites detected by using UHPLC-TimsTOF MS/MS

No.	Putative compound name	Molecular formula	Rt (min)	$m/z$ <sup>exp</sup> *	Error (ppm)	mSigma	<sup>TIMS</sup> CCSN <sub>2</sub> (Å <sup>2</sup> )	Main fragments via MS/MS*	Ref.
1	Perseitol	C <sub>7</sub> H <sub>16</sub> O <sub>7</sub>	0.84	211.0824	0.545	1.1	136.0	193.07; 131.04; 119.04; 101.03; 89.02	[35] <sup>a</sup>
2	D-mannoheptulose	C <sub>7</sub> H <sub>14</sub> O <sub>7</sub>	0.97	209.0667	-0.145	10.6	137.0	89.03; 85.03; 73.03; 71.02; 59.02; 57.04	[35] <sup>a</sup>
3	Quinic acid	C <sub>7</sub> H <sub>12</sub> O <sub>6</sub>	0.97	191.0562	0.491	1.3	132.4	127.04; 93.04; 85.03	standard
4	Glucose / Fructose	C <sub>6</sub> H <sub>12</sub> O <sub>6</sub>	0.97	179.0561	-0.207	8.3	127.0	59.02	[35] <sup>a</sup>
5	Glutamine	C <sub>5</sub> H <sub>10</sub> N <sub>2</sub> O <sub>3</sub>	1.00	145.0619	0.092	12.7	123.8	127.05	[36] <sup>a</sup>
6	Quinic acid dimer	C <sub>14</sub> H <sub>24</sub> O <sub>12</sub>	1.02	383.1196	0.400	16.3	183.5	191.06	[37] <sup>a</sup>
7	Sucrose	C <sub>12</sub> H <sub>22</sub> O <sub>11</sub>	1.08	341.1089	-0.300	7.7	166.2	119.04; 101.03; 89.03	[35] <sup>a</sup>
8	Malic acid	C <sub>4</sub> H <sub>6</sub> O <sub>5</sub>	1.10	133.0142	0.100	7.1	118.8	115.00; 71.01	[38] <sup>a</sup>
9	Adenosine monophosphate	C <sub>10</sub> H <sub>14</sub> N <sub>5</sub> O <sub>7</sub> P	1.19	346.0559	0.350	5.3	171.1	211.00; 134.05; 96.97; 78.96	[39] <sup>a</sup>
10	Citric acid (is. 1)	C <sub>6</sub> H <sub>8</sub> O <sub>7</sub>	1.20	191.0198	0.577	3.2	124.3	111.01; 87.02	[40] <sup>a</sup>
11	Citric acid (is. 2)	C <sub>6</sub> H <sub>8</sub> O <sub>7</sub>	1.20	191.0198	0.613	3.1	132.6	111.01	[40] <sup>a</sup>
12	Pyroglutamic acid hexoside	C <sub>11</sub> H <sub>17</sub> NO <sub>8</sub>	1.21	290.0883	0.468	13.9	156.6	200.06; 128.04	[41]
13	L-5-Oxoproline	C <sub>5</sub> H <sub>7</sub> NO <sub>3</sub>	1.24	128.0353	0.143	4.5	120.7	72.01; 52.02; 42.62	[36] <sup>a</sup>
14	Uridine	C <sub>9</sub> H <sub>12</sub> N <sub>2</sub> O <sub>6</sub>	1.25	243.0623	0.091	1.5	148.3	152.04; 110.02; 82.04	standard
15	Tyrosine	C <sub>9</sub> H <sub>11</sub> NO <sub>3</sub>	1.28	180.0666	0.064	6.4	140.7	163.03; 119.05; 93.03; 72.01	[27] <sup>a</sup>
16	Succinic acid	C <sub>4</sub> H <sub>6</sub> O <sub>4</sub>	1.31	117.0193	-0.045	6.9	112.4	99.01; 73.03; 55.02	standard
17	Guanosine	C <sub>10</sub> H <sub>13</sub> N <sub>5</sub> O <sub>5</sub>	1.34	282.0846	-0.840	27.4	158.9	150.04; 133.02; 108.03	[39] <sup>a</sup>
18	Adenosine	C <sub>10</sub> H <sub>13</sub> N <sub>5</sub> O <sub>4</sub>	1.36	266.0895	0.019	9.2	161.8	134.05	[40] <sup>a</sup>
19	Hexose-leucine	C <sub>6</sub> H <sub>13</sub> NO <sub>2</sub>	1.39	292.1402	0.303	25.7	163.0	130.09	[41]
20	Methyl citric acid	C <sub>7</sub> H <sub>10</sub> O <sub>7</sub>	1.47	205.0353	-0.529	3.0	133.4	143.03; 111.01	[42]
21	Gallic acid hexoside	C <sub>13</sub> H <sub>16</sub> O <sub>10</sub>	1.49	331.0670	-0.160	17.6	166.1	169.01; 168.01; 149.99; 125.02	[43] <sup>a</sup>
22	Dihydroxybenzoic acid hexoside (is.1)	C <sub>13</sub> H <sub>16</sub> O <sub>9</sub>	1.76	315.0723	0.587	1.3	169.2	153.02; 152.01; 109.03; 108.02	[27] <sup>a</sup>
23	Phenylalanine	C <sub>9</sub> H <sub>11</sub> NO <sub>2</sub>	1.85	164.0717	-0.029	5.5	136.0	147.04; 103.06; 91.05; 72.01	standard
24	Pantothenic acid	C <sub>9</sub> H <sub>17</sub> NO <sub>5</sub>	1.96	218.1035	0.428	2.3	144.2	146.08; 116.08; 99.05; 88.04; 71.05	standard
25	Succinyladenosine	C <sub>14</sub> H <sub>17</sub> N <sub>5</sub> O <sub>8</sub>	2.04	382.1005	-0.032	5.7	189.2	266.09; 250.06; 206.07; 134.05; 115.01	[44]
26	Dihydroxybenzoic acid hexoside (is.2)	C <sub>13</sub> H <sub>16</sub> O <sub>9</sub>	2.05	315.0722	0.001	18.1	163.9	153.02; 109.03	[27] <sup>a</sup>
27	Pantothenic acid hexoside	C <sub>15</sub> H <sub>27</sub> NO <sub>10</sub>	2.07	380.1563	0.105	22.1	178.3	218.10; 146.08	[44]
28	Dihydrophasic acid dihexoside	C <sub>27</sub> H <sub>42</sub> O <sub>15</sub>	2.08	605.2448	-0.490	2.8	244.7	443.19	[40] <sup>a</sup>
29	Caffeic acid glucoside (is. 1)	C <sub>15</sub> H <sub>18</sub> O <sub>9</sub>	2.16	341.0878	-0.052	20.8	182.1	179.04; 161.03; 135.04	[45] <sup>a</sup>
30	Dihydroxybenzoic acid hexoside-pentoside	C <sub>18</sub> H <sub>24</sub> O <sub>13</sub>	2.23	447.1146	0.295	8.0	187.4	315.07; 153.02; 152.01; 108.02	[44]
31	Hydroxybenzoic acid hexoside (is. 1)	C <sub>13</sub> H <sub>16</sub> O <sub>8</sub>	2.26	299.0775	0.974	4.1	166.7	179.04; 137.03; 93.03	[27] <sup>a</sup>
32	Hydroxytyrosol glucoside	C <sub>14</sub> H <sub>20</sub> O <sub>8</sub>	2.30	315.1087	0.493	1.9	169.6	153.06; 123.04	[38] <sup>a</sup>
33	Syringic acid glycoside	C <sub>15</sub> H <sub>20</sub> O <sub>10</sub>	2.36	359.0984	0.004	2.2	185.9	197.05; 182.02; 138.03; 123.01	[38] <sup>a</sup>

No.	Putative compound name	Molecular formula	Rt (min)	$m/z$ <sub>exp</sub> *	Error (ppm)	mSigma	<sup>TIMS</sup> CCSN <sub>2</sub> (Å <sup>2</sup> )	Main fragments via MS/MS*	Ref.
34	Vanillic acid hexoside (is. 1)	C <sub>14</sub> H <sub>18</sub> O <sub>9</sub>	2.39	329.0891	0.435	18.0	174.7	167.03; 123.05	[45] <sup>a</sup>
35	Neochlorogenic acid	C <sub>16</sub> H <sub>18</sub> O <sub>9</sub>	2.42	353.0879	0.160	2.3	168.3	191.06; 179.03; 135.05	[46] <sup>a</sup>
36	Gallic acid	C <sub>7</sub> H <sub>6</sub> O <sub>5</sub>	2.44	169.0142	-0.102	8.2	121.5	125.02; 55.01; 41.00	[40] <sup>a</sup>
37	Dihydroxybenzoic acid pentoside	C <sub>12</sub> H <sub>14</sub> O <sub>8</sub>	2.45	285.0617	0.434	3.4	162.3	153.02; 152.02; 108.02	[47]
38	Vanillic acid hexoside (is. 2)	C <sub>14</sub> H <sub>18</sub> O <sub>9</sub>	2.54	329.0878	0.140	18.5	175.5	167.03; 123.05	[45] <sup>a</sup>
39	Hydroxybenzoic acid hexoside-pentoside (is.1)	C <sub>18</sub> H <sub>24</sub> O <sub>12</sub>	2.55	431.1194	-0.305	5.4	181.4	137.03; 93.03	[44]
40	Caffeic acid glucoside (is. 2)	C <sub>15</sub> H <sub>18</sub> O <sub>9</sub>	2.56	341.0879	0.285	18.4	172.6	179.04; 135.04	[45] <sup>a</sup>
41	Dihydrophaseic acid hexoside (is. 1)	C <sub>21</sub> H <sub>32</sub> O <sub>10</sub>	2.67	443.1923	-0.000	8.2	197.4	281.14	[40] <sup>a</sup>
42	<i>N</i> -acetyl-tyrosine	C <sub>11</sub> H <sub>13</sub> NO <sub>4</sub>	2.67	222.0772	0.297	2.5	149.0	180.07; 163.04; 119.05; 108.05; 58.03	[27] <sup>a</sup>
43	Tryptophan	C <sub>11</sub> H <sub>12</sub> N <sub>2</sub> O <sub>2</sub>	2.70	203.0825	-0.386	6.4	148.1	142.07; 130.07; 116.05; 74.02	standard
44	Tyrosol glucoside	C <sub>14</sub> H <sub>20</sub> O <sub>7</sub>	2.72	299.1136	0.064	0.3	159.5	137.06; 119.04; 89.02; 59.02	[45] <sup>a</sup>
45	Caffeic acid glucoside (is. 3)	C <sub>15</sub> H <sub>18</sub> O <sub>9</sub>	2.74	341.0880	0.417	18.3	181.6	179.04; 161.03; 133.03	[45] <sup>a</sup>
46	Vanillic acid hexoside-pentoside	C <sub>19</sub> H <sub>26</sub> O <sub>13</sub>	2.77	461.1299	-0.364	4.7	187.5	167.04; 123.04	[44]
47	Dihydrophaseic acid hexoside (is. 2)	C <sub>21</sub> H <sub>32</sub> O <sub>10</sub>	2.82	443.1924	0.325	10.1	198.3	281.14; 237.15	[40] <sup>a</sup>
48	Coumaric acid dihexoside	C <sub>21</sub> H <sub>28</sub> O <sub>13</sub>	2.91	487.1456	-0.168	17.5	176.2	325.09; 307.08 163.04; 145.03; 119.05	[48]
49	Hydroxybenzoic acid hexoside (is. 2)	C <sub>13</sub> H <sub>16</sub> O <sub>8</sub>	2.94	299.0774	0.569	1.8	162.2	137.03; 93.03	[27] <sup>a</sup>
50	Isopropylmalic acid	C <sub>7</sub> H <sub>12</sub> O <sub>5</sub>	2.99	175.0612	-0.285	4.5	127.6	115.04; 113.06; 85.07	[44]
51	Tyrosol-hexoside-pentoside	C <sub>19</sub> H <sub>28</sub> O <sub>11</sub>	3.01	431.1559	0.116	3.8	186.0	299.11; 161.05; 149.05; 137.06; 113.03	[45] <sup>a</sup>
52	Penstemide	C <sub>21</sub> H <sub>32</sub> O <sub>10</sub>	3.01	443.1923	0.022	4.0	193.5	113.03; 101.03; 59.01	[45] <sup>a</sup>
53	4-Hydroxybenzoic acid	C <sub>7</sub> H <sub>6</sub> O <sub>3</sub>	3.10	137.0245	0.561	5.6	117.3	108.03; 93.03; 65.04	[49] <sup>a</sup>
54	Hydroxybenzoic acid hexoside-pentoside (is.2)	C <sub>18</sub> H <sub>24</sub> O <sub>12</sub>	3.19	431.1194	-0.256	3.3	183.6	299.11; 137.02; 93.03	[44]
55	Catechin	C <sub>15</sub> H <sub>14</sub> O <sub>6</sub>	3.25	289.0719	0.378	2.0	155.2	245.08; 203.07; 151.04; 123.05; 109.04	[40] <sup>a</sup>
56	Chlorogenic acid	C <sub>16</sub> H <sub>18</sub> O <sub>9</sub>	3.25	353.0878	-0.008	4.6	182.9	191.06	standard
57	Epicatechin glucoside	C <sub>21</sub> H <sub>24</sub> O <sub>11</sub>	3.33	451.1244	-0.320	10.8	189.8	289.07; 271.06; 245.08; 203.07	[50] <sup>a</sup>
58	Cryptochlorogenic acid	C <sub>16</sub> H <sub>18</sub> O <sub>9</sub>	3.40	353.0879	0.140	19.3	181.9	191.06; 173.05; 135.05	[46] <sup>a</sup>
59	Coumaric acid hexoside (is.1)	C <sub>15</sub> H <sub>18</sub> O <sub>8</sub>	3.44	325.0932	0.887	5.3	178.7	145.03; 117.03; 89.03; 59.01	[27] <sup>a</sup>
60	Sinapic acid hexoside (is. 1)	C <sub>17</sub> H <sub>22</sub> O <sub>10</sub>	3.47	385.1141	0.286	6.5	205.0	223.06; 208.04; 179.08; 164.04; 149.02	[40] <sup>a</sup>
61	Coumaric acid-hexoside-pentoside (is.1)	C <sub>20</sub> H <sub>26</sub> O <sub>12</sub>	3.56	457.1352	0.212	10.4	205.0	163.04; 145.03; 119.05	[45] <sup>a</sup>
62	6,7-Dihydroxycoumarin (Esculetin)	C <sub>9</sub> H <sub>6</sub> O <sub>4</sub>	3.62	177.0194	0.032	7.7	124.7	149.03; 133.03; 121.03; 105.03; 89.04	[43] <sup>a</sup>
63	Coumaric acid-hexoside-pentoside (is.2)	C <sub>20</sub> H <sub>26</sub> O <sub>12</sub>	3.63	457.1350	-0.142	2.2	187.2	163.04; 145.03; 119.05	[45] <sup>a</sup>
64	Coumaric acid hexoside (is.2)	C <sub>15</sub> H <sub>18</sub> O <sub>8</sub>	3.67	325.0931	0.779	1.9	178.1	145.03; 117.03; 89.03; 59.02	[27] <sup>a</sup>
65	Coumaric acid-hexoside-pentoside (is.3)	C <sub>20</sub> H <sub>26</sub> O <sub>12</sub>	3.70	457.1350	-0.289	3.5	200.2	163.04; 145.03; 119.05	[45] <sup>a</sup>
66	Caffeic acid	C <sub>9</sub> H <sub>8</sub> O <sub>4</sub>	3.75	179.0350	-0.038	7.5	129.7	135.05	[49] <sup>a</sup>
67	Dihydrophaseic acid (is.1)	C <sub>15</sub> H <sub>22</sub> O <sub>5</sub>	3.79	281.1397	0.952	0.6	176.6	237.15; 219.14; 171.12; 153.09; 139.08; 111.05	[40] <sup>a</sup>
68	Ferulic acid hexoside (is.1)	C <sub>16</sub> H <sub>20</sub> O <sub>9</sub>	3.83	355.1037	0.617	1.4	187.6	193.05; 175.04; 160.02; 134.04; 89.02; 59.02	[27] <sup>a</sup>

No.	Putative compound name	Molecular formula	Rt (min)	$m/z$ <sub>exp</sub> *	Error (ppm)	mSigma	TIM <sup>MS</sup> CCS <sub>N2</sub> (Å <sup>2</sup> )	Main fragments via MS/MS*	Ref.
69	Coumaric acid rutinoside	C <sub>21</sub> H <sub>28</sub> O <sub>12</sub>	3.84	471.1509	0.192	9.8	207.5	163.04; 145.03; 119.05	[45] <sup>a</sup>
70	Syringic acid	C <sub>9</sub> H <sub>10</sub> O <sub>5</sub>	3.91	197.0454	-0.925	10.1	135.2	182.02; 166.99; 138.03; 123.01; 95.01; 67.02	[40] <sup>a</sup>
71	Sinapic acid hexoside (is. 2)	C <sub>17</sub> H <sub>22</sub> O <sub>10</sub>	3.93	385.1142	0.324	16.3	195.5	223.06; 205.05; 190.03; 179.08; 164.04	[40] <sup>a</sup>
72	Ferulic acid hexoside (is.2)	C <sub>16</sub> H <sub>20</sub> O <sub>9</sub>	4.04	355.1035	0.235	2.0	187.7	193.05; 175.04; 160.02; 134.04; 89.03; 59.01	[27] <sup>a</sup>
73	Epicatechin	C <sub>15</sub> H <sub>14</sub> O <sub>6</sub>	4.06	289.0716	-0.326	0.7	155.0	245.08; 203.07; 151.04; 123.04; 109.03	standard
74	<i>N</i> -acetyl-leucine	C <sub>8</sub> H <sub>15</sub> NO <sub>3</sub>	4.09	172.0979	-0.185	6.8	137.2	130.09	[27] <sup>a</sup>
75	Ferulic acid rutinoside	C <sub>22</sub> H <sub>30</sub> O <sub>13</sub>	4.10	501.1611	-0.483	8.0	214.9	193.05; 175.04	[51]
76	Sinapic acid hexoside (is. 3)	C <sub>17</sub> H <sub>22</sub> O <sub>10</sub>	4.14	385.1140	-0.030	1.5	195.6	223.06; 205.05; 190.03; 164.05; 149.02	[40] <sup>a</sup>
77	Dihydrophaseic acid (is.2)	C <sub>15</sub> H <sub>22</sub> O <sub>5</sub>	4.20	281.1396	0.500	9.3	164.0	237.15; 219.14; 171.12; 153.09; 139.08; 111.05	[40] <sup>a</sup>
78	Methyl(epi)catechin hexoside (is. 1)	C <sub>22</sub> H <sub>26</sub> O <sub>11</sub>	4.25	465.1400	-0.792	3.7	204.4	303.09; 285.08; 179.03; 137.03; 125.03	[52]
79	Caffeoylshikimic acid	C <sub>16</sub> H <sub>16</sub> O <sub>8</sub>	4.32	335.0773	0.272	2.6	180.3	179.03; 161.03; 135.04	[53]
80	Coumaric acid isomer	C <sub>9</sub> H <sub>8</sub> O <sub>3</sub>	4.40	163.0400	-0.070	0.7	127.0	119.05; 93.04	MS/MS Lib. <sup>b</sup>
81	Vanillin	C <sub>8</sub> H <sub>8</sub> O <sub>3</sub>	4.61	151.0400	-0.137	5.9	124.7	136.02; 108.02; 92.03	[40] <sup>a</sup>
82	<i>N</i> -acetyl-phenylalanine	C <sub>11</sub> H <sub>13</sub> NO <sub>3</sub>	4.67	206.0822	-0.099	1.1	144.2	164.07; 147.04; 103.05; 91.06	[27] <sup>a</sup>
83	Methyl(epi)catechin hexoside (is. 2)	C <sub>22</sub> H <sub>26</sub> O <sub>11</sub>	4.69	465.1401	-0.285	4.2	196.3	303.09; 285.98; 179.03; 137.03; 125.03	[52]
84	Coumaric acid malonyl-hexoside (is. 1)	C <sub>18</sub> H <sub>20</sub> O <sub>11</sub>	4.75	411.0933	-0.036	0.9	185.3	367.10; 325.09; 307.08; 163.04; 145.03	[27] <sup>a</sup>
85	<i>p</i> -Coumaric acid	C <sub>9</sub> H <sub>8</sub> O <sub>3</sub>	4.83	163.0401	0.231	3.9	127.1	119.05; 93.04	standard
86	<i>p</i> -Coumaroyl malic acid	C <sub>13</sub> H <sub>12</sub> O <sub>7</sub>	4.87	279.0510	0.163	15.0	167.8	163.04; 119.05	[54] <sup>a</sup>
87	Coumaric acid malonyl-hexoside (is. 2)	C <sub>18</sub> H <sub>20</sub> O <sub>11</sub>	5.00	411.0935	0.403	3.1	178.2	367.10; 163.04; 145.03	[27] <sup>a</sup>
88	Ferulic acid isomer	C <sub>10</sub> H <sub>10</sub> O <sub>4</sub>	5.09	193.0506	-0.629	8.3	136.6	178.03; 149.06; 134.04	MS/MS Lib. <sup>b</sup>
89	3'- <i>O</i> -methylcatechin	C <sub>16</sub> H <sub>16</sub> O <sub>6</sub>	5.12	303.0875	0.483	2.1	167.7	285.08; 137.03; 125.03	[43] <sup>a</sup>
90	Scopoletin	C <sub>10</sub> H <sub>8</sub> O <sub>4</sub>	5.24	191.0350	0.221	8.2	132.0	176.01; 148.02; 120.02; 104.03	[43] <sup>a</sup>
91	Ferulic acid	C <sub>10</sub> H <sub>10</sub> O <sub>4</sub>	5.34	193.0506	-0.153	0.1	136.6	178.03; 134.04	standard
92	<i>N</i> -acetyl-tryptophan	C <sub>13</sub> H <sub>14</sub> N <sub>2</sub> O <sub>3</sub>	5.35	245.0934	0.819	9.2	156.1	203.08; 142.07; 116.05; 98.02; 74.02	[55] <sup>a</sup>
93	Sinapic acid	C <sub>11</sub> H <sub>12</sub> O <sub>5</sub>	5.40	223.0612	-0.041	0.8	145.8	208.04; 193.01; 164.04; 121.03; 93.03	[40] <sup>a</sup>
94	Hydroxyabscisic acid glucoside	C <sub>21</sub> H <sub>30</sub> O <sub>10</sub>	5.41	441.1764	-0.241	4.3	194.1	330.13	[45] <sup>a</sup>
95	Dihydroquercetin (taxifolin)	C <sub>15</sub> H <sub>12</sub> O <sub>7</sub>	5.51	303.0510	0.012	16.0	162.8	285.04; 175.04; 151.00; 125.02	[43] <sup>a</sup>
96	2-Hydroxysebacic acid	C <sub>10</sub> H <sub>18</sub> O <sub>5</sub>	5.64	217.1081	-0.120	12.8	142.3	199.09; 171.10; 155.11	[56]
97	Abscisic acid hexose ester	C <sub>21</sub> H <sub>30</sub> O <sub>9</sub>	5.69	425.1816	-0.254	5.8	193.1	287.13; 263.13; 219.14; 153.10	[40] <sup>a</sup>
98	<i>p</i> -Coumaroyl tyrosine	C <sub>18</sub> H <sub>17</sub> NO <sub>5</sub>	6.11	326.1035	0.457	4.6	164.4	282.12; 206.05; 180.07; 163.04; 145.03; 119.05	[43] <sup>a</sup>
99	Syringaresinol-β-D-glucoside	C <sub>28</sub> H <sub>36</sub> O <sub>13</sub>	6.29	579.2082	-0.167	7.4	215.4	417.16; 181.05	[53]
100	2-Hydroxy-2-phenylacetic acid	C <sub>8</sub> H <sub>8</sub> O <sub>3</sub>	6.41	151.0400	-0.101	7.0	125.0	136.02; 121.03; 92.03	[43] <sup>a</sup>
101	Hydroxyheptanoic acid	C <sub>7</sub> H <sub>14</sub> O <sub>3</sub>	6.54	145.0870	-0.264	5.3	131.9	127.08; 99.08	-
102	Azelaic acid	C <sub>9</sub> H <sub>16</sub> O <sub>4</sub>	6.57	187.0975	-0.308	1.8	136.8	125.10	[41]
103	Oxododecanedioic acid (is.1)	C <sub>12</sub> H <sub>20</sub> O <sub>5</sub>	6.60	243.1238	0.092	2.6	150.4	225.11; 207.11; 181.13	[56]

No.	Putative compound name	Molecular formula	Rt (min)	$m/z$ <sup>*</sup> <sub>exp</sub>	Error (ppm)	mSigma	<sup>TIMS</sup> CCS <sub>N2</sub> (Å <sup>2</sup> )	Main fragments via MS/MS*	Ref.
104	Oxododecanedioic acid (is. 2)	C <sub>12</sub> H <sub>20</sub> O <sub>5</sub>	6.78	243.1238	0.177	10.8	150.5	225.11; 207.10; 181.13	[56]
105	Abscisic acid	C <sub>15</sub> H <sub>20</sub> O <sub>4</sub>	7.75	263.1291	0.741	6.2	164.9	219.04; 204.11; 153.10	standard
106	Sebacic acid	C <sub>10</sub> H <sub>18</sub> O <sub>4</sub>	8.05	201.1133	0.167	10.1	141.4	183.10; 139.11	[56]
107	Syringaresinol	C <sub>22</sub> H <sub>26</sub> O <sub>8</sub>	8.18	417.1552	-0.625	5.2	210.1	402.13; 387.11; 181.05; 166.03	[57]
108	4-Methoxycinnamic acid	C <sub>10</sub> H <sub>10</sub> O <sub>3</sub>	8.32	177.0558	0.216	7.2	134.7	145.03; 117.03; 89.04	[40] <sup>a</sup>
109	9-Oxononanoic acid	C <sub>9</sub> H <sub>16</sub> O <sub>3</sub>	8.93	171.1026	-0.333	8.1	140.5	153.09; 127.11; 99.08; 71.05	MS/MS Lib. <sup>b</sup>
110	Undecanedioic acid	C <sub>11</sub> H <sub>20</sub> O <sub>4</sub>	9.46	215.1288	-0.290	8.9	146.1	197.12; 153.13	[56]
111	Trihydroxyoctadecadienoic acid	C <sub>18</sub> H <sub>32</sub> O <sub>5</sub>	9.82	327.2177	0.204	16.9	179.4	171.10	[41]
112	Methyl 4-methoxycinnamate	C <sub>11</sub> H <sub>12</sub> O <sub>3</sub>	10.04	191.0713	0.087	8.2	142.5	163.04; 145.03; 119.05; 117.03	-
113	Trihydroxypalmitic acid	C <sub>16</sub> H <sub>32</sub> O <sub>5</sub>	10.37	303.2179	0.515	3.5	171.5	-	[40] <sup>a</sup>
114	Trihydroxyoctadecenoic acid	C <sub>18</sub> H <sub>34</sub> O <sub>5</sub>	10.41	329.2334	0.133	3.5	181.4	229.14; 211.14; 171.01	[40] <sup>a</sup>
115	Dodecanedioic acid	C <sub>12</sub> H <sub>22</sub> O <sub>4</sub>	10.80	229.1445	-0.373	4.3	150.9	211.13; 185.16; 167.14	MS/MS Lib. <sup>b</sup>

Abbreviation: is, isomer. <sup>\*</sup> $m/z$  values correspond to [M-H]<sup>-</sup>. <sup>\*</sup>The fragments observed during MS/MS experiments have been described with only 2 decimal digits to contain the dimension of the table. <sup>a</sup>previously described in *Persea americana* Mill. <sup>b</sup>MSMS\_Public\_EXP\_Neg\_VS17 spectral library.

All compounds listed in the table have confidence level 2 annotations (putatively annotated compounds) [58], except for those confirmed by comparison with a pure standard (confidence level 1). Molecular formula calculation, structure database search, *in silico* fragmentation, CCS prediction and spectral library search were performed using MetaboScape.

Caffeic acid ( $C_9H_8O_4$ ;  $129.7 \text{ \AA}^2$ ) and three isomeric glycosylated forms ( $C_{15}H_{18}O_9$ ;  $182.1 \text{ \AA}^2$ ,  $172.6 \text{ \AA}^2$  and  $181.6 \text{ \AA}^2$ ) were also found within the profiles. A similar observation was made with sinapic acid ( $C_{11}H_{12}O_5$ ;  $145.8 \text{ \AA}^2$ ), which showed three glycosylated conjugates ( $C_{17}H_{22}O_{10}$ ;  $205.0 \text{ \AA}^2$ ,  $195.5 \text{ \AA}^2$ ,  $195.6 \text{ \AA}^2$ ). Based on molecular descriptors, caffeoylshikimic acid with a molecular formula of  $C_{16}H_{16}O_8$  ( $180.3 \text{ \AA}^2$ ) eluted at 4.32 minutes. Ferulic acid ( $C_{10}H_{10}O_4$ ;  $136.6 \text{ \AA}^2$ ) and *p*-coumaric acid ( $C_9H_8O_3$ ;  $127.1 \text{ \AA}^2$ ) were identified by comparison with pure standards. Besides, an isomer of ferulic acid was detected at 5.09 minutes, while an isomer of *p*-coumaric acid was found at 4.40 minutes.

The metabolic profile of avocado also contained a large diversity of coumaric acid conjugates. These included, for instance, coumaric acid rutinoid ( $C_{21}H_{28}O_{12}$ ;  $207.5 \text{ \AA}^2$ ) and coumaric acid dihexose ( $C_{21}H_{28}O_{13}$ ;  $176.2 \text{ \AA}^2$ ). Two coumaric acid compounds attached to a hexose moiety ( $C_{15}H_{18}O_8$ ;  $178.7 \text{ \AA}^2$  and  $178.1 \text{ \AA}^2$ ) were also identified, along with three coumaric acid-hexoside-pentoside isomers ( $C_{20}H_{26}O_{12}$ ;  $205.0 \text{ \AA}^2$ ,  $187.2 \text{ \AA}^2$  and  $200.2 \text{ \AA}^2$ ) and two malonyl-hexose coumaric acid isomers ( $C_{18}H_{20}O_{11}$ ;  $185.3 \text{ \AA}^2$  and  $178.2 \text{ \AA}^2$ ). The profile also included 4-methoxycinnamic acid ( $C_{10}H_{10}O_3$ ;  $134.7 \text{ \AA}^2$ ) and methyl 4-methoxycinnamate ( $C_{11}H_{12}O_3$ ;  $142.5 \text{ \AA}^2$ ). Two other peaks were annotated as *p*-coumaroyl malic acid ( $C_{13}H_{12}O_7$ ;  $167.8 \text{ \AA}^2$ ) and *p*-coumaroyl tyrosine ( $C_{18}H_{17}NO_5$ ;  $164.4 \text{ \AA}^2$ ) based on the MS/MS spectra. Only two glycosylated forms of ferulic acid ( $C_{16}H_{20}O_9$ ;  $187.6 \text{ \AA}^2$  and  $187.7 \text{ \AA}^2$ ) and one conjugated with a rutinoid moiety, *i.e.*, ferulic acid rutinoid ( $C_{22}H_{30}O_{13}$ ;  $214.9 \text{ \AA}^2$ ), were preliminarily identified in the profiles of avocado extracts.

Although it has been described in previous works that relatively high concentrations of **flavonoids** may be found in avocado seeds and peels [43,46,50,59], they were comparatively scarce in the mesocarp. Catechin ( $C_{15}H_{14}O_6$ ;  $155.2 \text{ \AA}^2$ ) eluted before its isomer, epicatechin ( $155.0 \text{ \AA}^2$ ), as confirmed by comparison with pure standards. A peak at 3.3 minutes corresponded to epicatechin glucoside ( $C_{21}H_{24}O_{11}$ ;  $189.8 \text{ \AA}^2$ ), identified by its relative elution time and the main fragment observed at  $m/z$  289.07, corresponding to the flavonoid aglycone. Another peak, which eluted at 5.12 min with an  $m/z$  of 303.0875  $[M-H]^-$  ( $C_{16}H_{16}O_6$ ), was tentatively identified as 3'-O-methylcatechin ( $167.7 \text{ \AA}^2$ ). Two glycosylated derivatives of this compound were detected at 4.25 and 4.69 minutes, respectively, with molecular formula of  $C_{22}H_{26}O_{11}$  (and CCS values of  $204.4 \text{ \AA}^2$  and  $196.3 \text{ \AA}^2$ ). Additionally, the flavanone taxifolin ( $C_{15}H_{12}O_7$ ;  $162.8 \text{ \AA}^2$ ), previously described in avocado fruit, was detected at 5.51 min.

Three other phenolic compounds (derivatives of those commonly known as simple phenols), probably related to hydroxytyrosol and tyrosol, were putatively annotated: hydroxytyrosol glycoside ( $C_{14}H_{20}O_8$ ;  $169.6 \text{ \AA}^2$ ), tyrosol glycoside ( $C_{14}H_{20}O_7$ ;  $159.5 \text{ \AA}^2$ ) and tyrosol-hexoside-pentoside ( $C_{19}H_{28}O_{11}$ ;  $186.0 \text{ \AA}^2$ ). The avocado mesocarp also contained **lignans**, including syringaresinol ( $C_{22}H_{26}O_8$ ;  $210.1 \text{ \AA}^2$ ) and its glycosylated form ( $C_{28}H_{36}O_{13}$ ;  $215.4 \text{ \AA}^2$ ). Within the **coumarin class**, 6,7-dihydroxycoumarin ( $C_9H_6O_4$ ;  $124.7 \text{ \AA}^2$ ) and scopoletin ( $C_{10}H_8O_4$ ;  $132.0 \text{ \AA}^2$ ) were detected. Penstemide ( $C_{21}H_{32}O_{10}$ ;  $193.5 \text{ \AA}^2$ ), previously reported in avocado mesocarp, was the only **iridoid** found. Moreover, a compound with  $m/z$  151.0400  $[M-H]^-$  ( $C_8H_8O_3$ ) was tentatively identified as 2-hydroxy-2-phenylacetic acid ( $125.0 \text{ \AA}^2$ ).

As far as **sesquiterpenoids** are concerned, the presence of abscisic acid ( $C_{15}H_{20}O_4$ ; 164.9  $\text{\AA}^2$ ) was verified using the commercial standard. The metabolic profile also included derivatives such as hydroxyabscisic acid glucoside ( $C_{21}H_{30}O_{10}$ ; 194.1  $\text{\AA}^2$ ) and abscisic acid hexose ester ( $C_{21}H_{30}O_9$ ; 193.1  $\text{\AA}^2$ ), which have been previously reported in avocado fruit. Additionally, two isomeric forms of dihydrophaseic acid ( $C_{15}H_{22}O_5$ ; 176.6  $\text{\AA}^2$  and 164.0  $\text{\AA}^2$ ) were detected at 3.79 and 4.20 minutes, respectively. Two simple glycosylated forms of dihydrophaseic acid ( $C_{21}H_{32}O_{10}$ ; 197.4  $\text{\AA}^2$  and 198.3  $\text{\AA}^2$ ) and one diglycosylated form ( $C_{27}H_{42}O_{15}$ ; 244.7  $\text{\AA}^2$ ) were also annotated, based on their elution times and fragmentation patterns.

In the analytical window where compounds of lower polarity eluted, some **fatty acids and certain derivatives** were detected in the following elution order: 2-hydroxysebacic acid ( $C_{10}H_{18}O_5$ ; 142.3  $\text{\AA}^2$ ), hydroxyheptanoic acid ( $C_7H_{14}O_3$ ; 131.9  $\text{\AA}^2$ ), azelaic acid ( $C_9H_{16}O_4$ ; 136.8  $\text{\AA}^2$ ), two isomers of oxododecanedioic acid ( $C_{12}H_{20}O_5$ ; 150.4  $\text{\AA}^2$  and 150.5  $\text{\AA}^2$ ), sebacic acid ( $C_{10}H_{18}O_4$ ; 141.4  $\text{\AA}^2$ ), 9-oxononanoic acid ( $C_9H_{16}O_3$ ; 140.5  $\text{\AA}^2$ ), undecanedioic acid ( $C_{11}H_{20}O_4$ ; 146.1  $\text{\AA}^2$ ), trihydroxyoctadecadienoic acid ( $C_{18}H_{32}O_5$ ; 179.4  $\text{\AA}^2$ ), trihydroxypalmitic acid ( $C_{16}H_{32}O_5$ ; 171.5  $\text{\AA}^2$ ), trihydroxyoctadecenoic acid ( $C_{18}H_{34}O_5$ ; 181.4  $\text{\AA}^2$ ) and dodecanedioic acid ( $C_{12}H_{22}O_4$ ; 150.9  $\text{\AA}^2$ ).

### 3.2. Exploring avocado metabolomics data by applying unsupervised multivariate statistics

Since plant metabolism is dynamically regulated in response to abiotic factors, qualitative and quantitative variations in fruit composition can be expected to occur in different geographic regions, influenced by the unique climates and edaphic conditions of each area. Although several works have examined the postharvest quality of avocados in relation to various growing conditions and locations [23,60–62], few have specifically explored metabolic differences in avocados from different growing regions. Existing studies typically focus on samples from different countries, which often introduces substantial environmental variability. Donetti & Terry, for instance, found differences in primary metabolites of the mesocarp of *Hass* avocado fruits from Spain, Chile, and Peru [18], whereas Pedreschi et al. found differences in primary and secondary metabolites in avocados from Chile and Spain [36]. This study aims to fill the gap of comprehensively addressing metabolic differences across multiple locations within a single country.

The metabolomics data, including all extracted features, were initially subjected to unsupervised exploratory methods such as PCA and HCA (Figure 1). Prior to assessing the clustering capability, PCA incorporating both sample extracts and quality control samples ( $n=77$ ) was evaluated in order to detect any possible systematic errors. This examination confirmed the good repeatability of the analytical methodology, as evidenced by the cluster of QC samples located near the centre of the model. Furthermore, an additional PCA model was constructed excluding the QC samples ( $n=66$ ) (Figure S2). The comparison between the two PCA models (with and without QC samples) revealed a consistent clustering of the samples, with minimal influence of QC samples on the plots. Moreover, no outliers were identified in the set of samples analysed,

and metabolic variations between replicates were attributed to inherent biological variability between specimens.

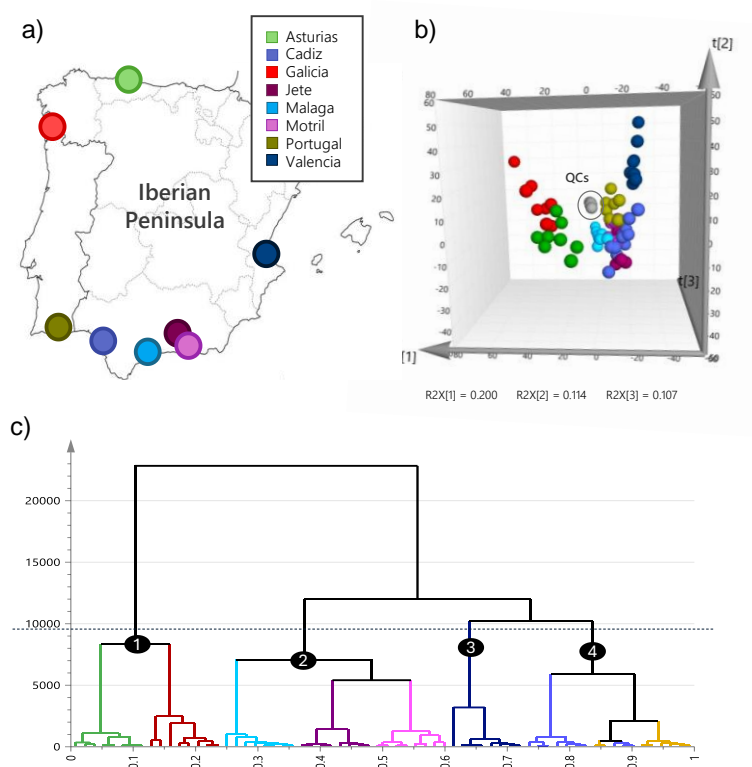


**Figure 1.** (a) Map of the Iberian Peninsula indicating sampling locations with colour coding, (b) PCA scores plot illustrating the distribution of samples, including QC samples, based on the first three principal components, and (c) HCA shown as a dendrogram to depict the relationships between the samples.

The PCA scores plot constructed using the first three principal components (PCs), provides a comprehensive overview of the metabolic variation among avocado samples from different regions. These three PCs collectively explained 42.1% of the total variance, revealing clear regional trends. PC1, which captured 20.0% of the data variation, played a key role in distinguishing the avocado samples from Galicia and Asturias from those of other regions. PC2 and PC3, accounting for 11.4% and 10.7% of the variance respectively, further reinforced the differentiation among regions, particularly highlighting the distinct metabolic profile of avocado from Valencia. These associations were further validated by HCA, which delineated two primary groups: one comprising the northern Spanish regions, Galicia and Asturias, and the other encompassing the remaining locations. Within the first group, Galicia and Asturias, though clustered distinctly, subtle metabolic variations among samples from the same region were observed, suggesting that even within geographically close areas, microclimatic and edaphoclimatic factors could influence avocado metabolism. These regions, characterised by the lowest average temperatures and highest annual

precipitation, likely exhibit this unique metabolic profile as a result of their specific climatic conditions. The second main group, which included the remaining locations, showed further subdivision. Samples from the Malaga province clustered closely with samples from Jete and Motril, both located in the Granada province, reflecting their geographical proximity and similar climatic conditions, although the latter two showed more similar metabolomic profiles to each other. In contrast, samples from Valencia showed greater resemblance to samples from Cadiz and Portugal although maintaining a distinct cluster. Interestingly, some Cadiz samples mixed within samples of the Portugal cluster, suggesting closer metabolic similarities between these regions.

These results highlight that avocados have distinct metabolic signatures shaped by their geographic origin, with varying degrees of differentiation influenced by factors such as orchard proximity and local climatic conditions.

### 3.3. Establishing the compositional metabolic patterns of *Hass* avocado based on growth location

Both unsupervised PCA and HCA plots provided compelling evidence of distinct metabolic differences among the analysed avocado samples from different regions. Consequently, the next step involved constructing multiple supervised two-group OPLS-DA models to differentiate each region by comparing one provenance (group 1) against all other locations (group 2). The scores plots, as well as the quality and cross-validation parameters obtained for the eight OPLS-DA models built to define the characteristic metabolic patterns per origin, are presented in [Figure S3](#) and [Table S1](#), respectively. The OPLS-DA models were highly robust, with quality parameters ( $R^2$  and  $Q^2$ ) consistently above 0.82 in all cases, with minimal differences between these values, suggesting a low likelihood of overfitting. Moreover, cross-validation ANOVA, evaluated using F and  $p$ -values, confirmed the statistical significance of the models.

After building the OPLS-DA discriminant models, the ten to twelve main variables with the highest VIP values were selected (always with VIP above 1.90) for each region. This selection aimed to identify potential biomarkers specific to each origin. This process facilitated the characterisation of typical avocado compositional patterns, identifying compounds that were either positively correlated (indicating higher concentrations) or negatively correlated (suggesting lower concentrations) within each category, as summarised in [Table 3](#). It is important to note that, despite efforts to tentatively annotate most of these biomarkers, compound identification remains one of the most challenging aspects of non-targeted metabolomics, with some ambiguities still persisting. [Figure 2](#) illustrates a box-and-whisker plot that highlights the intensity levels of the top four discriminant features for each origin, offering valuable insights into the observed variation of these features. Notably, Cadiz stands out as the only region where several potential markers exhibited significantly lower concentrations compared to other areas of the Iberian Peninsula. In contrast, for the other regions, the most important features were primarily distinguished by their higher concentrations within the discriminated category.

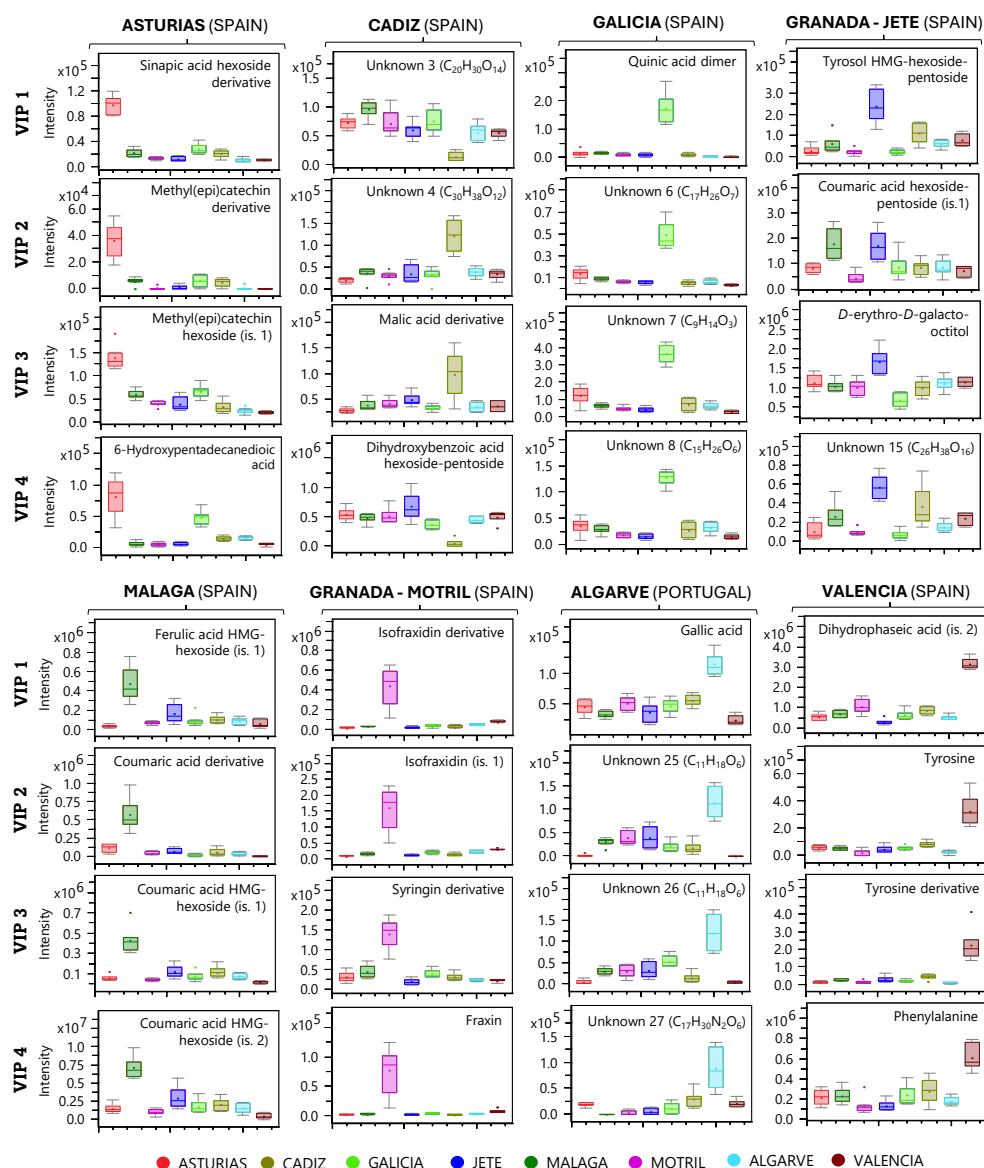


**Figure 2.** Box and whisker plots of the four metabolites with the highest VIP scores obtained from two-class OPLS-DA models to describe the typical metabolic patterns of the eight different avocado cultivation regions.

**Asturias:** All compounds with higher VIP values for the Asturias region exhibited a positive correlation. The most significant compound, with a molecular formula  $C_{22}H_{26}O_{11}$ , was tentatively identified as a derivative of sinapic acid hexoside ( $217.8 \text{ \AA}^2$ ). This identification was based on characteristic fragmentation patterns, specifically at  $m/z$  223.06 (sinapic acid moiety,  $C_{11}H_{12}O_5$ ) and 385.11 (glycosylated form of sinapic acid,  $C_{17}H_{22}O_{10}$ ), respectively. However, the 80 Da mass difference remains unassigned, requiring further investigation. The compound eluting at 2.6 min

( $C_{17}H_{24}O_{11}$ ;  $180.7 \text{ \AA}^2$ ) was identified as oleoside 11-methyl ester, previously reported in avocado [43]. Additionally, two glycosylated flavonoids were labelled as isomers of methyl(epi)catechin hexose ( $C_{22}H_{26}O_{11}$ ; with CCS values of  $204.4 \text{ \AA}^2$  and  $196.3 \text{ \AA}^2$ , respectively) through the neutral loss of the hexose moiety ( $162.05 \text{ Da}$ ). These flavonoids have been previously described in bean by-products [52]. Another derivative of methyl(epi)catechin was consistent with the signal at  $m/z$  611.1769 [M-H]<sup>-</sup> ( $C_{31}H_{32}O_{13}$ ;  $230.3 \text{ \AA}^2$ ), based on its main fragmentation at  $m/z$  303.09 corresponding to methyl(epi)catechin moiety ( $C_{16}H_{16}O_6$ ). The peak with molecular formula  $C_{15}H_{28}O_5$  ( $170.0 \text{ \AA}^2$ ) eluting at 7.81 min, could potentially represent a hydroxy fatty acid, such as 6-hydroxypentadecanedioic acid. Interestingly, the intensity of this compound was also prominent in fruits from Galicia, as illustrated in Figure 2, emphasising a significant similarity between the metabolic profiles of both regions in this regard. The identification of a coumaric acid ester, specifically osmanthuside A ( $C_{23}H_{26}O_9$ ;  $197.3 \text{ \AA}^2$ ), was supported by its fragmentation pattern and the CCS value, both of which closely matched the data available in the HMDB. Another compound, potentially derived from coumaric acid ( $C_{28}H_{36}O_{12}$ ;  $222.2 \text{ \AA}^2$ ) was identified taking into account the characteristic signals typically observed in HRMS/MS spectra for this phenolic acid; this compound was also suggested as a potential marker for this origin. The peak at  $m/z$  519.1715 [M-H]<sup>-</sup> ( $C_{22}H_{32}O_{14}$ ) exhibited a primary fragment at  $m/z$  151.04 ( $C_8H_8O_3$ ), suggesting it could be a derivative of vanillin. Indole-3-acetyl-L-glutamic acid ( $C_{15}H_{16}N_2O_5$ ) was identified by comparing the MS and MS/MS spectra with public spectral libraries, displaying a total score of 930.13 (Figure S4). However, two significant biomarkers with molecular formulas  $C_{25}H_{30}O_{12}$  (unknown 1;  $208.6 \text{ \AA}^2$ ) and  $C_{17}H_{24}O_{11}$  (unknown 2;  $188.1 \text{ \AA}^2$ ) remained unidentified.

**Cadiz:** The metabolites that contributed most to differentiate the Cadiz samples from the others showed both positive and negative correlations. In other words, certain markers were at higher relative concentrations in the Cadiz samples, whereas others were found in lower quantities compared to the samples from the other production areas evaluated. Among the negatively correlated compounds, dihydroxybenzoic acid hexoside-pentoside ( $C_{18}H_{24}O_{13}$ ) was previously described by Mekky et al. in other plant material [44], while dihydrocaffeic acid glucoside ( $C_{15}H_{20}O_9$ ) was identified in avocado fruit by Velderrain-Rodríguez and co-authors [50]. According to public spectral libraries, the peak at  $m/z$  327.1085 [M-H]<sup>-</sup> ( $C_{15}H_{20}O_8$ ) was identified as 3-(4-hydroxyphenyl)-3-oxopropyl beta-D-glucopyranoside, with a score of 980.22 (Figure S4). Two additional unidentified metabolites with molecular formula  $C_{20}H_{30}O_{14}$  (unknown 3;  $206.9 \text{ \AA}^2$ ) and  $C_{16}H_{24}O_{10}$  (unknown 5;  $187.9 \text{ \AA}^2$ ), respectively, were also relevant, though their tentative identities remain undetermined.

The positively correlated compounds included in Table 3 were six. The peak at  $m/z$  267.0722 [M-H]<sup>-</sup> was likely related to malic acid, as indicated by its characteristic fragments at  $m/z$  133.01 ( $C_4H_6O_5$ ) and 115.00 ( $C_4H_4O_4$ ). Coumaric acid di-hexose ( $C_{21}H_{28}O_{13}$ ) showed two successive hexose losses ( $162.05 \text{ Da}$ ), resulting in the release of coumaric acid aglycone. The compound at  $m/z$  621.2545 ( $C_{31}H_{42}O_{13}$ ) was proposed as a coumaric acid derivative, supported by its typical

fragments at  $m/z$  163.04 ( $C_9H_8O_3$ ) and 119.05 ( $C_8H_8O$ ). Another compound, eluting at 9.12 min with a molecular formula of  $C_{25}H_{26}O_{10}$  (and CCS value of 215.2  $\text{\AA}^2$ ), was identified as a derivative of methoxycinnamic acid based on its fragmentation pattern and relative retention time. Moreover, tyrosol-hexoside-pentoside ( $C_{19}H_{28}O_{11}$ ) and an unidentified compound with the molecular formula  $C_{30}H_{38}O_{12}$  (unknown 4) were also positively correlated with avocados from the Cadiz region.

**Galicia:** Galician avocados were characterised by elevated levels of quinic acid ( $C_7H_{12}O_6$ ) and their derivatives, including the dimer ( $C_{14}H_{24}O_{12}$ ), and a derivative with molecular formula  $C_{28}H_{20}O_5$ , which showed a distinctive fragment in  $m/z$  191.06 (indicative of the quinic acid moiety). Two other compounds with molecular formulas  $C_{17}H_{26}O_7$  (unknown 6; min 8.73) and  $C_{15}H_{24}O_6$  (unknown 9; min 6.84), respectively, displayed similar fragmentation patterns, suggesting a potential link to the sesquiterpenoid dihydrophaseic acid ( $C_{15}H_{22}O_5$ ). Also, one peak was identified as an isomer of oxododecanedioic acid (isomer 2), which has been previously documented in *Melastoma dodecandrum* Lour. [56]. The remaining markers included substances with the following molecular formulas:  $C_9H_{14}O_3$  (unknown 7; 143.4  $\text{\AA}^2$ ),  $C_{15}H_{26}O_6$  (unknown 8; 167.9  $\text{\AA}^2$ ),  $C_{16}H_{26}O_6$  (unknown 10; 174.0  $\text{\AA}^2$ ),  $C_{16}H_{28}O_7$  (unknown 11; 178.8  $\text{\AA}^2$ ),  $C_8H_{14}O_3$  (unknown 12; 140.6  $\text{\AA}^2$ ),  $C_{30}H_{44}O_{16}$  (unknown 13; 235.1  $\text{\AA}^2$ ) and  $C_{13}H_{24}O_6$  (unknown 14; 158.5  $\text{\AA}^2$ ).

**Jete (Granada):** High levels of coumaric acid hexoside-pentoside ( $C_{20}H_{26}O_{12}$ ) and the sugar *D*-erythro-*D*-galacto-octitol ( $C_8H_{18}O_8$ ) characterised the avocado fruits grown in Jete. The most significant classifier was tyrosol HMG-hexoside-pentoside ( $C_{25}H_{36}O_{15}$ ). Such annotation was supported by the characteristic loss of the HMG moiety  $[M-H-144.04]^-$  which produced a MS signal at  $m/z$  431.16, corresponding to tyrosol-hexoside-pentoside ( $C_{19}H_{28}O_{11}$ ). This metabolite has not been previously described and further research is needed to confirm its identity. Other remarkable classifiers included those with molecular formulas of:  $C_{26}H_{38}O_{16}$  (unknown 15; 221.8  $\text{\AA}^2$ ),  $C_{21}H_{34}O_{11}$  (unknown 16; 202.5  $\text{\AA}^2$ ),  $C_{20}H_{34}O_{15}$  (unknown 17; 205.2  $\text{\AA}^2$ ),  $C_{26}H_{42}O_{13}$  (unknown 18; 220.7  $\text{\AA}^2$ ),  $C_{20}H_{28}O_{12}$  (unknown 19; 191.8  $\text{\AA}^2$ ),  $C_{21}H_{36}O_{11}$  (unknown 20; 201.3  $\text{\AA}^2$ ) and  $C_{18}H_{28}O_9$  (unknown 21; 185.4  $\text{\AA}^2$ ), though their structures remain undetermined. Another compound of relevance was annotated as a derivative of coumaric acid ( $C_{13}H_{13}NO_4$ ), based on its fragmentation pattern (with MS signals at  $m/z$  163.04 ( $C_9H_8O_3$ ) and 119.05 ( $C_8H_8O$ )).

**Motril (Granada):** The metabolic profile of fruit from Motril was distinguished by a high relative abundance of several hydroxycoumarins and their derivatives. Among them, two isomers of isofraxidin ( $C_{11}H_{10}O_5$ ; 142.3  $\text{\AA}^2$  and 142.0  $\text{\AA}^2$ ) and fraxin ( $C_{16}H_{18}O_{10}$ ; 181.6  $\text{\AA}^2$ ) were annotated based on public spectral libraries data, with total scores of 967.38 and 837.90, respectively (Figure S4). The peaks at  $m/z$  443.1194  $[M-H]^-$  ( $C_{19}H_{24}O_{12}$ ; 200.9  $\text{\AA}^2$ ) and 589.1772  $[M-H]^-$  ( $C_{25}H_{34}O_{16}$ ; 217.1  $\text{\AA}^2$ ) were tentatively identified as isofraxidin derivatives, based on the signal at  $m/z$  221.05 ( $C_{11}H_{10}O_5$ ) and other fragments consistent with isofraxidin. Furthermore, the compound at  $m/z$  515.1768  $[M-H]^-$  was annotated as a derivative of syringin based on the data reported for *Viscum album* L. [34]. Feruloylsucrose, with molecular formula  $C_{22}H_{30}O_{14}$  (212.8  $\text{\AA}^2$ ), was annotated by the interpretation of its HRMS/MS spectra. The compound with molecular formula  $C_{12}H_{15}NO_4$  (unknown 22) could

not be identified. The unknown 23 ( $C_{13}H_{22}O_{10}$ ; 169.7  $\text{\AA}^2$ ) had previously been detected in avocado mesocarp, although its exact identity remains unresolved [27]. This metabolite, which produces a prominent fragment at  $m/z$  193.08, has also been detected in the aerial parts of selected *Potentilla* species, where it has been classified as a polyphenolic derivative [63]. In addition to the above, perseitol ( $C_7H_{16}O_7$ ), syringaresinol ( $C_{22}H_{26}O_8$ ), the unidentified compound 24 ( $C_{17}H_{26}O_9$ ), and sinapic acid glucoside isomer 3 ( $C_{17}H_{22}O_{10}$ ; min 4.14) also contributed to defining the typical compositional profile of avocados cultivated in Motril.

**Malaga:** Almost all compounds with high VIP values in the "Malaga vs. the rest" model were associated with ferulic and *p*-coumaric acids, exhibiting a positive correlation. Among these, two potential isomeric derivatives of ferulic acid ( $C_{22}H_{28}O_{13}$ ; 203.5  $\text{\AA}^2$  and 198.1  $\text{\AA}^2$ ) were putatively annotated as ferulic acid HMG-hexoside isomers. These identifications were based on high resolution MS/MS spectra, which revealed an ion  $[M-H-144.04]^-$  at  $m/z$  355.10 and a fragment  $[M-H-144.04-162.05]^-$  at  $m/z$  193.05, indicating the presence of the HMG group and a sugar moiety attached to the aglycone. A previous study on *Herniaria polygama* suggested a comparable structure containing 2-hydroxy-4-methoxycinnamic acid as the aglycone [33]. Similarly, four coumaric acid derivatives were identified as coumaric acid HMG-hexoside isomers ( $C_{21}H_{26}O_{12}$ ; with CCS values of 217.8  $\text{\AA}^2$ , 196.4  $\text{\AA}^2$ , 209.1  $\text{\AA}^2$  and 191.6  $\text{\AA}^2$ , respectively) based on their distinctive pattern of consecutive losses (the same as describe above for ferulic acid derivatives), with coumaric acid as the aglycone. Another coumaric acid derivative with molecular formula  $C_{22}H_{28}O_{12}$  (211.7  $\text{\AA}^2$ ) was also significant for distinguishing Malaga samples, although its full structure has not yet been fully elucidated. The classifier with  $m/z$  413.1451  $[M-H]$ , annotated as dicrotalic acid (benzyl)hexoside, had been previously described in *Prunus cerasifera* L. by Sottile and co-authors [64]. The compound with molecular formula  $C_{25}H_{40}O_{12}$  was annotated as zizyvoside I; it had been previously found in *Arum palaestinum* leaves by Abu-Reidah and collaborators [53]. The peak at  $m/z$  365.1455  $[M-H]^-$  was identified as a propyl HMG-hexoside in Faustrime fruit [65]. The latter two substances had VIP values of 2.39 and 2.27, respectively. Coumaric acid rutinoid ( $C_{21}H_{28}O_{12}$ ) and one isomer of coumaric acid ( $C_9H_8O_3$ ) also played a key role in differentiating the Malaga samples from others, with both compounds showing higher relative abundances in avocados from this region.

**Algarve (Portugal):** Gallic acid ( $C_7H_6O_5$ ) emerged as the most influential metabolite that defines the compositional profile of avocados from Portugal. The following compounds, in decreasing VIP order, have not been identified, but are two isomers with the molecular formula  $C_{11}H_{18}O_6$ , which share the same fragmentation pattern and have very similar CCS values (unknowns 25 and 26). A distinctive feature of this origin is the prevalence of nitrogenous compounds, including several markers such as: unknown 27 ( $C_{17}H_{30}N_2O_6$ ; 181.6  $\text{\AA}^2$ ), unknown 29 ( $C_{14}H_{23}NO_4$ ; 167.1  $\text{\AA}^2$ ), unknown 30 ( $C_{12}H_{13}NO_5$ ; 163.1  $\text{\AA}^2$ ) and unknown 31 ( $C_9H_{15}NO_5$ ; 143.1  $\text{\AA}^2$ ). A tentative identification as malic acid derivative was made for the substance with  $m/z$  434.0939  $[M-H]^-$  ( $C_{16}H_{21}NO_{13}$ ), taking into account the observed fragments at  $m/z$  133.01 ( $C_4H_6O_5$ ) and 115.00

(C<sub>4</sub>H<sub>4</sub>O<sub>4</sub>). Based on the study of high-resolution spectra and relative retention time, the compound corresponding to the molecular formula C<sub>14</sub>H<sub>15</sub>NO<sub>6</sub> was putatively annotated as *p*-coumaroyl-glutamic acid (160.1 Å<sup>2</sup>). Another compound of interest, with the molecular formula C<sub>12</sub>H<sub>16</sub>O<sub>5</sub>, could not be identified (unknown 28). Finally, the peak at *m/z* 293.1243 [M-H]<sup>-</sup>, annotated as methyl glucopyranosyloxy pentanoic acid, was recognised based on a prior characterisation of *Pistacia lentiscus* leaves [66].

**Valencia:** Avocados grown in Valencia possess a distinct metabolic profile, marked by elevated levels of dihydrophaseic acid isomer 2 (C<sub>15</sub>H<sub>22</sub>O<sub>5</sub>; 4.20 min) and higher concentrations of key amino acids, such as tyrosine and phenylalanine, compared to other production areas. Valencia fruit also displayed elevated peak intensities of the substance with *m/z* 550.2139 [M-H]<sup>-</sup>, (C<sub>23</sub>H<sub>37</sub>NO<sub>14</sub>), which may be a tyrosine derivative, fact supported by the observed fragment at *m/z* 180.07 (C<sub>9</sub>H<sub>11</sub>NO<sub>3</sub>). Similar to what was observed for the Malaga fruit, a peak with molecular formula C<sub>15</sub>H<sub>26</sub>O<sub>10</sub> (3.72 min) was identified as propyl HMG-hexoside, which had identical fragmentation pattern and a retention time very close to that of the isomer 1 detected in the Malaga samples. Additionally, oxododecanedioic acid (isomer 1) (C<sub>12</sub>H<sub>20</sub>O<sub>5</sub>; 150.5 Å<sup>2</sup>) was a distinguishing feature of Valencia avocados, similar to how isomer 2 was characteristic of Galicia fruits. Glucose/fructose (C<sub>6</sub>H<sub>12</sub>O<sub>6</sub>; 127.0 Å<sup>2</sup>) was also markedly abundant in this provenance. Further research to achieve the complete structural elucidation of other significant compounds pointed out in the statistical model would be highly valuable. These would include: C<sub>23</sub>H<sub>38</sub>O<sub>17</sub> (unknown 32), C<sub>13</sub>H<sub>22</sub>O<sub>9</sub> (unknown 33), C<sub>16</sub>H<sub>30</sub>O<sub>12</sub> (unknown 34), C<sub>21</sub>H<sub>38</sub>O<sub>9</sub> (unknown 35), C<sub>17</sub>H<sub>32</sub>O<sub>12</sub> (unknown 36), and C<sub>15</sub>H<sub>42</sub>O<sub>11</sub> (unknown 37).

The distinct metabolic signatures identified in this study highlight the significant influence of geographic origin and local climatic conditions on avocado composition. The biomarkers uncovered offer valuable insights into the unique compositional patterns of each region, providing a molecular-level understanding of how environmental factors shape the fruit's metabolome. However, some compounds remain incompletely characterised, requiring further research for full structural elucidation. This additional investigation could deepen our understanding of region-specific metabolic profiles and improve the precision of these biomarkers for tracing the geographic origin of avocados.

Furthermore, future research should seek to build upon these findings by examining the dynamic changes in the avocado metabolome over time, considering factors such as fruit maturation, post-harvest processing, and storage conditions. Additionally, investigating the impact of specific agricultural practices -such as irrigation, fertilisation, and pest management- on the avocado's metabolic profile could offer valuable insights into how these practices affect fruit quality and composition. Ultimately, integrating these findings with sensory analysis and consumer preference studies could pave the way for tailored agricultural strategies that enhance both the nutritional value and market appeal of avocados from different regions.

**Table 3.** VIP Metabolites pointed out by the OPLS-DA models for geographical differentiation based on avocado mesocarp metabolic profiles

Compound	VIP	Rel. conc.	Molecular formula	Rt (min)	$m/z$ <sub>exp</sub> [M-H] <sup>-</sup>	Error (ppm)	mSigma	TIM <sup>5</sup> CCS <sub>N2</sub> (Å <sup>2</sup> )	Main fragments via MS/MS*	Annot. conf. level	Ref.
<b>ASTURIAS</b>											
Sinapic acid hexoside derivative	2.39	↑	C <sub>22</sub> H <sub>26</sub> O <sub>11</sub>	3.92	465.1399	-0.667	5.4	217.8	385.11; 223.06; 205.05; 59.01	3	-
Methyl(epi)catechin derivative	2.35	↑	C <sub>31</sub> H <sub>32</sub> O <sub>13</sub>	7.09	611.1769	-0.253	8.6	230.3	303.09; 285.08; 163.04; 145.03; 137.03	3	-
Methyl(epi)catechin hexoside (is. 1)	2.22	↑	C <sub>22</sub> H <sub>26</sub> O <sub>11</sub>	4.25	465.1400	-0.792	3.7	204.4	303.09; 285.08; 179.03; 137.03; 125.03	2	[52]
6-Hydroxypentadecanedioic acid	2.14	↑	C <sub>15</sub> H <sub>28</sub> O <sub>5</sub>	7.81	287.1865	0.019	1.5	170.0	185.12; 129.06	2	-
Osmanthuside A	2.12	↑	C <sub>23</sub> H <sub>26</sub> O <sub>9</sub>	6.81	445.1503	-0.163	3.3	197.3	307.08; 163.04; 145.03; 137.07; 119.05	2	-
Unknown 1	2.12	↑	C <sub>25</sub> H <sub>30</sub> O <sub>12</sub>	5.90	521.1661	-0.714	2.9	208.6	503.15; 473.14; 307.08; 163.04; 145.03	4	-
Coumaric acid derivative	2.09	↑	C <sub>28</sub> H <sub>36</sub> O <sub>12</sub>	6.87	563.2133	0.119	2.3	222.2	381.12; 163.04; 145.03; 119.05	3	-
Vanillin derivative	2.03	↑	C <sub>22</sub> H <sub>32</sub> O <sub>14</sub>	4.58	519.1715	-0.767	4.0	213.0	307.10; 151.04; 59.01	3	-
Oleoside 11-methylester	2.02	↑	C <sub>17</sub> H <sub>24</sub> O <sub>11</sub>	2.60	403.1246	0.059	1.1	180.7	223.06; 208.04; 138.03; 59.02	2	[43] <sup>a</sup>
Unknown 2	2.01	↑	C <sub>17</sub> H <sub>24</sub> O <sub>11</sub>	4.21	403.1245	-0.357	7.7	188.1	259.08; 161.05; 125.02 113.02; 101.03; 59.01	4	-
Indole-3-acetyl-L-glutamic acid	2.00	↑	C <sub>15</sub> H <sub>16</sub> N <sub>2</sub> O <sub>5</sub>	5.01	303.0986	-0.008	4.1	160.8	156.05; 146.05; 128.04; 102.06	2	MS/MS Lib. <sup>b</sup>
Methyl(epi)catechin hexoside (is. 2)	1.99	↑	C <sub>22</sub> H <sub>26</sub> O <sub>11</sub>	4.69	465.1401	-0.285	4.2	196.3	303.09; 285.08; 179.03; 137.03; 125.03	2	[52]
<b>CADIZ</b>											
Unknown 3	2.15	↓	C <sub>20</sub> H <sub>30</sub> O <sub>14</sub>	1.61	493.1561	-0.441	5.1	206.9	327.11; 195.07; 165.06; 117.02; 73.03	4	-
Unknown 4	2.13	↑	C <sub>30</sub> H <sub>38</sub> O <sub>12</sub>	6.97	589.2287	-0.116	8.4	227.5	531.28; 443.19; 163.04; 145.03; 119.05	4	-
Malic acid derivative	2.03	↑	C <sub>9</sub> H <sub>16</sub> O <sub>9</sub>	1.02	267.0722	-0.016	15.0	149.2	133.01; 115.00; 71.02; 59.01	3	-
Dihydroxybenzoic acid hexoside-pentoside	2.02	↓	C <sub>18</sub> H <sub>24</sub> O <sub>13</sub>	2.23	447.1146	0.295	8.0	187.4	315.07; 153.02; 152.01; 108.02	2	[44]
Coumaric acid derivative	2.02	↑	C <sub>31</sub> H <sub>42</sub> O <sub>13</sub>	5.13	621.2545	-0.280	7.6	240.9	163.05; 119.05	3	-
Unknown 5	2.02	↓	C <sub>16</sub> H <sub>24</sub> O <sub>10</sub>	2.81	375.1297	0.026	4.2	187.9	153.06; 138.03; 123.01; 113.02; 101.03; 59.01	4	-
Methoxycinnamic derivative	2.00	↑	C <sub>25</sub> H <sub>26</sub> O <sub>10</sub>	9.12	485.1448	-0.963	8.7	215.2	307.08; 177.06; 145.03; 96.97	3	-
3-(4-hydroxyphenyl)-3-oxopropyl beta-D-glucopyranoside	1.96	↓	C <sub>15</sub> H <sub>20</sub> O <sub>8</sub>	2.96	327.1085	0.038	7.4	173.7	147.04; 113.02; 101.02; 85.03; 71.01; 59.01	2	MS/MS Lib. <sup>b</sup>
Coumaric acid di-hexoside	1.95	↑	C <sub>21</sub> H <sub>28</sub> O <sub>13</sub>	2.91	487.1456	-0.168	17.5	176.2	325.09; 307.08 163.04; 145.03; 119.05	2	[48]
Dihydrocaffeic acid glucoside	1.95	↓	C <sub>15</sub> H <sub>20</sub> O <sub>9</sub>	2.08	343.1036	0.453	6.2	168.5	181.05; 163.04; 135.05; 93.04; 59.02	2	[50] <sup>a</sup>
Tyrosol-hexoside-pentoside	1.90	↑	C <sub>19</sub> H <sub>28</sub> O <sub>11</sub>	3.01	431.1559	0.116	3.8	186.0	299.11; 161.05; 149.05; 137.06; 113.03	2	[45] <sup>a</sup>
<b>GALICIA</b>											
Quinic acid dimer	2.11	↑	C <sub>14</sub> H <sub>24</sub> O <sub>12</sub>	1.02	383.1196	0.400	16.3	183.5	191.06	2	[37] <sup>a</sup>
Unknown 6	2.10	↑	C <sub>17</sub> H <sub>26</sub> O <sub>7</sub>	8.73	341.1607	0.251	18.3	179.5	281.14; 263.13; 237.15; 219.14; 195.14	4	-
Unknown 7	2.08	↑	C <sub>9</sub> H <sub>14</sub> O <sub>3</sub>	9.90	169.0869	-0.961	7.4	143.4	125.10; 97.07; 80.03; 71.05; 55.02; 41.00	4	-
Unknown 8	2.08	↑	C <sub>15</sub> H <sub>26</sub> O <sub>6</sub>	6.61	301.1657	0.311	15.0	167.9	221.15; 197.15; 179.14; 153.13; 125.10; 73.03	4	-
Unknown 9	2.08	↑	C <sub>15</sub> H <sub>24</sub> O <sub>6</sub>	6.84	299.1501	0.326	14.8	167.4	281.14; 237.15; 219.14; 195.14; 71.05; 57.04	4	-
Quinic acid	2.06	↑	C <sub>7</sub> H <sub>12</sub> O <sub>6</sub>	0.96	191.0562	0.635	8.8	132.5	127.04; 85.03	1	Standard
Quinic acid derivative	2.06	↑	C <sub>28</sub> H <sub>20</sub> O <sub>5</sub>	1.24	435.1235	-0.286	6.6	196.0	191.06	3	-
Unknown 10	2.03	↑	C <sub>16</sub> H <sub>26</sub> O <sub>6</sub>	9.75	313.1658	0.449	15.8	174.0	253.15; 235.14; 211.13; 191.14; 167.15	4	-
Unknown 11	2.03	↑	C <sub>16</sub> H <sub>28</sub> O <sub>7</sub>	9.51	331.1764	-0.118	7.6	178.8	289.17; 271.16; 229.15; 211.13; 169.12; 59.01	4	-

Compound	VIP	Rel. conc.	Molecular formula	Rt (min)	m/z <sub>exp</sub> [M-H] <sup>-</sup>	Error (ppm)	mSigma	TIMS <sup>2</sup> CCS <sub>N2</sub> (Å <sup>2</sup> )	Main fragments via MS/MS*	Annot. conf. level	Ref.
<b>GALICIA</b>											
Oxododecanedioic acid (is. 2)	2.02	1	C <sub>12</sub> H <sub>20</sub> O <sub>5</sub>	6.78	243.1238	0.177	10.8	150.5	225.11; 207.10; 181.13	2	[56]
Unknown 12	2.02	1	C <sub>8</sub> H <sub>14</sub> O <sub>3</sub>	8.98	157.0870	-0.166	5.7	140.6	113.10; 95.09; 57.03	4	-
Unknown 13	2.02	1	C <sub>30</sub> H <sub>44</sub> O <sub>16</sub>	5.17	659.2558	0.194	5.5	235.1	437.18; 389.16; 225.08; 195.07; 59.02	4	-
Unknown 14	2.01	1	C <sub>13</sub> H <sub>24</sub> O <sub>6</sub>	4.98	275.1502	0.548	0.7	158.5	257.14; 211.13; 183.14; 155.14; 125.10; 72.99	4	-
<b>JETE (GRANADA)</b>											
Tyrosol HMG-hexoside-pentoside	2.34	1	C <sub>25</sub> H <sub>36</sub> O <sub>15</sub>	4.24	575.1979	-0.509	2.5	212.6	513.18; 473.17; 431.16; 299.11; 161.05; 149.05; 137.06	2	-
Coumaric acid hexoside-pentoside (is. 1)	2.30	1	C <sub>20</sub> H <sub>26</sub> O <sub>12</sub>	3.56	457.1352	0.212	10.4	205.0	163.04; 145.03; 119.05	2	[45] <sup>a</sup>
<i>D</i> -erythro- <i>D</i> -galacto-octitol	2.28	1	C <sub>8</sub> H <sub>18</sub> O <sub>8</sub>	0.80	241.0931	0.969	4.3	143.9	223.08; 101.03; 89.02; 59.02	2	[67] <sup>a</sup>
Unknown 15	2.25	1	C <sub>26</sub> H <sub>38</sub> O <sub>16</sub>	4.50	605.2086	-0.179	7.3	221.8	503.18; 461.16; 443.16; 149.05; 57.04	4	-
Unknown 16	2.13	1	C <sub>21</sub> H <sub>34</sub> O <sub>11</sub>	2.82	461.2026	-0.448	17.9	202.5	401.18; 383.17; 221.12; 163.08; 151.08; 59.01	4	-
Coumaric acid derivative	2.11	1	C <sub>13</sub> H <sub>13</sub> NO <sub>4</sub>	4.84	246.0772	-0.029	11.4	157.2	163.04; 119.05	3	-
Unknown 17	2.10	1	C <sub>20</sub> H <sub>34</sub> O <sub>15</sub>	2.37	513.1823	-0.339	9.8	205.2	411.15; 369.14; 351.13; 237.10; 161.05; 99.04	4	-
Unknown 18	2.09	1	C <sub>26</sub> H <sub>42</sub> O <sub>13</sub>	6.12	561.2550	-0.536	3.9	220.7	311.10; 251.08; 221.07; 191.06; 149.05; 89.02	4	-
Unknown 19	2.06	1	C <sub>20</sub> H <sub>28</sub> O <sub>12</sub>	3.15	459.1507	-0.184	3.3	191.8	191.06; 147.05; 89.02; 59.02	4	-
Unknown 20	2.03	1	C <sub>21</sub> H <sub>36</sub> O <sub>11</sub>	4.45	463.2183	-0.289	8.3	201.3	403.20; 379.16; 223.13; 179.06; 119.04; 89.02; 59.01	4	-
Unknown 21	2.00	1	C <sub>18</sub> H <sub>28</sub> O <sub>9</sub>	7.19	387.1662	0.398	3.8	185.4	225.11; 181.12; 207.10; 163.11; 89.03; 59.02	4	-
<b>MOTRIL (GRANADA)</b>											
Isofraxidin derivative	2.65	1	C <sub>19</sub> H <sub>24</sub> O <sub>12</sub>	3.74	443.1194	-0.274	4.4	200.9	221.05; 206.02; 191.01; 163.00; 135.01; 59.01	3	-
Isofraxidin (is.1)	2.63	1	C <sub>11</sub> H <sub>10</sub> O <sub>5</sub>	4.51	221.0455	0.119	5.6	142.3	206.02; 191.01; 163.00; 147.01; 135.01; 107.02	2	MS/MS Lib. <sup>b</sup>
Syringin derivative	2.63	1	C <sub>23</sub> H <sub>32</sub> O <sub>13</sub>	4.34	515.1768	-0.377	8.3	208.1	306.07; 209.08; 194.07; 57.04	3	[34]
Fraxin	2.61	1	C <sub>16</sub> H <sub>18</sub> O <sub>10</sub>	2.62	369.0823	-1.041	15.6	181.6	354.06; 207.03; 192.01; 191.00; 163.01	2	MS/MS Lib. <sup>b</sup>
Feruloylsucrose	2.52	1	C <sub>22</sub> H <sub>30</sub> O <sub>14</sub>	2.99	517.1562	-0.134	9.4	212.8	193.05; 175.06	2	[53]
Unknown 22	2.47	1	C <sub>12</sub> H <sub>15</sub> NO <sub>4</sub>	3.61	236.0927	-0.586	6.2	154.3	98.02; 72.05	4	-
Isofraxidin derivative	2.45	1	C <sub>25</sub> H <sub>34</sub> O <sub>16</sub>	4.03	589.1772	-0.300	11.7	217.1	307.11; 221.05; 206.02; 191.01; 163.00; 59.01	3	-
Unknown 23	2.45	1	C <sub>13</sub> H <sub>22</sub> O <sub>10</sub>	1.90	337.1141	0.301	2.6	169.7	193.08; 161.05; 125.03; 101.02; 57.04	4	-
Unknown 24	2.38	1	C <sub>17</sub> H <sub>26</sub> O <sub>9</sub>	4.00	373.1505	0.206	6.7	174.9	358.13; 281.11; 211.10; 196.07; 59.01	4	-
Isofraxidin (is. 2)	2.37	1	C <sub>11</sub> H <sub>10</sub> O <sub>5</sub>	5.50	221.0455	0.171	10.7	142.0	206.02; 191.00; 163.00; 147.01; 135.01; 107.02	2	MS/MS Lib. <sup>b</sup>
Perseitol	2.34	1	C <sub>7</sub> H <sub>16</sub> O <sub>7</sub>	0.84	211.0824	0.545	1.1	136.0	193.07; 131.04; 119.04; 101.03; 89.02	2	[35] <sup>a</sup>
Syringaresinol	2.32	1	C <sub>22</sub> H <sub>26</sub> O <sub>8</sub>	8.18	417.1552	-0.625	5.2	210.1	402.13; 387.11; 181.05; 166.03	2	[57]
Sinapic acid hexoside (is. 3)	2.30	1	C <sub>17</sub> H <sub>22</sub> O <sub>10</sub>	4.14	385.1140	-0.030	1.5	195.6	223.06; 205.05; 190.03; 164.05; 149.02	2	[40] <sup>a</sup>
<b>MALAGA</b>											
Ferulic acid HMG-hexoside (is.1)	2.60	1	C <sub>22</sub> H <sub>28</sub> O <sub>13</sub>	5.51	499.1457	-0.066	3.9	203.5	437.14; 397.11; 355.10; 193.05; 175.04; 134.04	2	[33]
Coumaric acid derivative	2.59	1	C <sub>22</sub> H <sub>28</sub> O <sub>12</sub>	6.45	483.1505	-0.483	4.1	211.7	407.13; 367.10; 325.09; 163.04; 145.03; 119.05	3	-
Coumaric acid HMG-hexoside (is.1)	2.57	1	C <sub>21</sub> H <sub>26</sub> O <sub>12</sub>	5.03	469.1349	-0.451	3.0	217.8	407.13; 367.10; 325.09; 163.04; 145.03; 119.05	2	[68]
Coumaric acid HMG-hexoside (is.2)	2.55	1	C <sub>21</sub> H <sub>26</sub> O <sub>12</sub>	5.21	469.1352	0.086	12.5	196.4	407.13; 367.10; 325.09; 163.04; 145.03; 119.05	2	[68]
Coumaric acid HMG-hexoside (is.3)	2.50	1	C <sub>21</sub> H <sub>26</sub> O <sub>12</sub>	5.21	469.1352	0.139	9.9	209.1	407.13; 367.10; 325.09; 163.04; 145.03; 119.05	2	[68]

Compound	VIP	Rel. conc.	Molecular formula	Rt (min)	$m/z$ <sub>exp</sub> [M-H] <sup>-</sup>	Error (ppm)	mSigma	TIMS <sup>2</sup> CCS <sub>N2</sub> (Å <sup>2</sup> )	Main fragments via MS/MS*	Annot. conf. level	Ref.
<b>MALAGA</b>											
Dicrotic acid (benzyl)hexoside	2.43	†	C <sub>19</sub> H <sub>26</sub> O <sub>10</sub>	5.71	413.1451	-0.916	9.5	194.2	269.10; 161.05; 101.02; 59.01	2	[64]
Coumaric acid HMG-hexoside (is. 4)	2.40	†	C <sub>21</sub> H <sub>26</sub> O <sub>12</sub>	5.45	469.1352	0.139	9.9	191.6	407.13; 367.10; 325.09; 163.04; 145.03; 119.05	2	[68]
Zizyvoside I	2.39	†	C <sub>25</sub> H <sub>40</sub> O <sub>12</sub>	5.73	531.2443	-0.669	21.6	211.8	429.21; 387.20; 125.03; 99.05; 57.04	2	[53]
Ferulic acid HMG-hexoside (is. 2)	2.33	†	C <sub>22</sub> H <sub>28</sub> O <sub>13</sub>	5.67	499.1454	-0.445	7.3	198.1	437.14; 397.11; 355.10; 193.05; 175.04; 134.03	2	[33]
Coumaric acid isomer	2.31	†	C <sub>9</sub> H <sub>8</sub> O <sub>3</sub>	4.40	163.0400	-0.070	0.7	127.0	119.05; 93.04	2	MS/MS Lib. <sup>b</sup>
Propyl HMG-hexoside (is. 1)	2.27	†	C <sub>15</sub> H <sub>26</sub> O <sub>10</sub>	3.40	365.1455	0.716	2.2	181.4	221.10; 161.04; 125.02; 113.03; 101.03	2	[65]
Coumaric acid rutinoside	2.25	†	C <sub>21</sub> H <sub>28</sub> O <sub>12</sub>	3.84	471.1509	0.192	9.8	207.5	163.04; 145.03; 119.05	2	[45] <sup>a</sup>
<b>ALGARVE (PORTUGAL)</b>											
Gallic acid	2.69	†	C <sub>7</sub> H <sub>6</sub> O <sub>5</sub>	2.44	169.0142	-0.102	8.2	121.5	125.02; 55.01; 41.00	2	[40] <sup>a</sup>
Unknown 25 (isomer)	2.65	†	C <sub>11</sub> H <sub>18</sub> O <sub>6</sub>	3.37	245.1031	-0.016	11.1	149.3	227.09; 183.10; 165.10; 139.08; 127.08; 121.11; 59.02	4	-
Unknown 26 (isomer)	2.63	†	C <sub>11</sub> H <sub>18</sub> O <sub>6</sub>	3.60	245.1031	-0.022	8.2	148.6	227.09; 183.10; 165.10; 139.08; 127.08; 121.11; 59.01	4	-
Unknown 27	2.52	†	C <sub>17</sub> H <sub>30</sub> N <sub>2</sub> O <sub>6</sub>	3.57	357.2030	-0.237	17.7	181.6	325.18; 263.17; 220.17; 58.03; 42.00	4	-
Unknown 28	2.46	†	C <sub>12</sub> H <sub>16</sub> O <sub>5</sub>	4.55	239.0925	0.119	11.4	148.6	195.10; 141.06; 59.02	4	-
Unknown 29	2.34	†	C <sub>14</sub> H <sub>23</sub> NO <sub>4</sub>	10.12	268.1555	0.252	1.8	167.1	236.13; 150.09; 107.04	4	-
Malic acid derivative	2.26	†	C <sub>16</sub> H <sub>21</sub> NO <sub>13</sub>	1.40	434.0939	-0.360	12.5	197.5	133.01; 115.00; 71.01	3	-
<i>p</i> -coumaroyl-glutamic acid	2.17	†	C <sub>14</sub> H <sub>15</sub> NO <sub>6</sub>	3.49	292.0827	0.106	16.9	160.1	163.04; 145.03; 128.04; 119.05; 102.06	2	[69]
Unknown 30	2.16	†	C <sub>12</sub> H <sub>13</sub> NO <sub>5</sub>	3.08	250.0722	0.390	0.4	163.1	188.07; 176.07; 161.07; 146.06; 119.05; 93.04; 42.00	4	-
Unknown 31	2.09	†	C <sub>9</sub> H <sub>15</sub> NO <sub>5</sub>	2.89	216.0877	0.042	6.8	143.1	154.09; 116.07; 59.02	4	-
Methyl glucopyranosyloxy pentanoic acid	2.05	†	C <sub>12</sub> H <sub>22</sub> O <sub>8</sub>	3.17	293.1243	0.414	1.8	162.3	131.07; 59.02	2	[66]
<b>VALENCIA</b>											
Dihydrophaseic acid (is. 2)	2.31	†	C <sub>15</sub> H <sub>22</sub> O <sub>5</sub>	4.20	281.1396	0.500	9.3	164.0	237.15; 219.14; 171.12; 153.09; 139.08; 111.05	2	[40] <sup>a</sup>
Tyrosine	2.29	†	C <sub>9</sub> H <sub>9</sub> NO <sub>3</sub>	1.28	180.0666	0.064	6.4	140.7	163.03; 119.05; 93.03; 72.01	2	[27] <sup>a</sup>
Tyrosine derivative	2.23	†	C <sub>23</sub> H <sub>37</sub> NO <sub>14</sub>	1.29	550.2139	-0.400	9.5	209.7	369.14; 237.10; 180.07	3	-
Phenylalanine	2.20	†	C <sub>9</sub> H <sub>9</sub> NO <sub>2</sub>	1.85	164.0717	-0.029	5.5	136.0	147.04; 103.06; 91.05; 72.01	1	Standard
Unknown 32	2.15	†	C <sub>23</sub> H <sub>38</sub> O <sub>17</sub>	1.87	585.2034	-0.436	3.7	226.5	187.03; 143.04; 111.01; 67.02	4	-
Unknown 33	2.14	†	C <sub>13</sub> H <sub>22</sub> O <sub>9</sub>	2.36	321.1193	0.645	6.3	164.3	177.08; 159.06; 57.03	4	-
Propyl HMG-hexoside (is. 2)	2.12	†	C <sub>15</sub> H <sub>26</sub> O <sub>10</sub>	3.72	365.1452	-0.192	3.8	181.4	221.10; 161.04; 125.02; 113.02; 101.03	2	[65]
Oxododecanedioic acid (is. 1)	2.10	†	C <sub>12</sub> H <sub>20</sub> O <sub>5</sub>	6.60	243.1238	0.092	2.6	150.4	225.11; 207.11; 181.13	2	[56]
Unknown 34	2.09	†	C <sub>16</sub> H <sub>30</sub> O <sub>12</sub>	2.08	413.1665	0.069	4.7	190.5	353.15; 221.10; 161.044; 101.03	4	-
Unknown 35	2.03	†	C <sub>21</sub> H <sub>38</sub> O <sub>9</sub>	6.00	433.2440	-0.594	5.9	200.4	397.15; 352.22; 59.02	4	-
Unknown 36	2.02	†	C <sub>17</sub> H <sub>32</sub> O <sub>12</sub>	2.48	427.1818	-0.706	1.8	195.7	367.16; 221.10; 161.04; 59.01	4	-
Unknown 37	2.01	†	C <sub>15</sub> H <sub>42</sub> O <sub>11</sub>	7.15	517.2651	-0.664	2.6	210.9	415.23; 161.04; 101.03; 57.04	4	-
Glucose/Fructose	1.93	†	C <sub>6</sub> H <sub>12</sub> O <sub>6</sub>	0.97	179.0561	-0.207	8.3	127.0	59.02	2	[35] <sup>a</sup>

Abbreviations: †, high content; ‡, low content; is, isomer; HMG, 3-hydroxy-3-methylglutaryl. \*The fragments observed during MS/MS experiments have been described with only 2 decimal digits to contain the dimension of the table. <sup>a</sup> previously described in *Persea americana* Mill. <sup>b</sup> MSMS\_Public\_EXP\_Neg\_VS17 spectral library. The annotation confidence levels follow the criteria outlined by Sumner et al. [58]: 1- compound identified by comparison with pure standard; 2- putatively annotated compound; 3- putatively characterised compound class, 4- unknown compound. For each origin, the displayed markers are listed in decreasing order of VIP. Those markers without identity (unknown substances) are numbered in order of appearance in the table to facilitate their recognition in the discussion.

## 4. CONCLUSIONS

In this study, the mesocarp metabolic profile of avocados from eight different regions of the Iberian Peninsula was analysed using an advanced UPLC-IMS-HRMS/MS method. This comprehensive analytical approach enabled the identification of more than one hundred primary and secondary metabolites, with phenolic compounds emerging as the most prevalent chemical family in the avocado mesocarp. The integration of ion mobility spectrometry significantly increased the confidence in metabolite annotation by incorporating the CCS value as an additional descriptor. This advancement not only strengthens the reliability of our findings but also lays a robust foundation for future research in the field of avocado fruit metabolomics. While this study focused on avocados from the Iberian Peninsula, the developed approach could be applied to other avocado-producing regions worldwide.

Our results demonstrated the effectiveness of chemometrics-assisted non-targeted metabolomics as a robust and powerful tool for tracing the geographical origin of avocado fruits. Through the application of this approach, we observed significant metabolic similarities between avocados from Asturias and Galicia, in contrast to the distinct profiles of those from Malaga, Granada, Valencia, Cadiz, and Algarve. Despite these similarities between fruits from certain areas, all samples from different origins could be effectively distinguished on the basis of their unique metabolic profile. Therefore, by employing multiple two-class supervised OPLS-DA models, which demonstrated very satisfactory cross-validation parameters, we defined not only compositional patterns typical for each region but also identified origin-specific biomarkers that are characteristic of avocado from each growing area.

The implications of these findings are substantial for the avocado industry. By providing producers with a deeper understanding of the compositional profile of their avocados, this research will allow them to better assess the influence of soil, climatic conditions, and other environmental factors on the composition of the fruit. Such insights are crucial for optimising agricultural practices and improving the quality of the produce. Moreover, this knowledge could also be instrumental in differentiating Spanish avocados, including those from various regions, from the imported counterparts. This differentiation could be used to boost the market competitiveness of locally grown avocados, enabling producers to potentially command premium prices by highlighting the unique compositional attributes of their products.

**Funding:** This research has been partially financed by Grants PID2021-128508OB-I00 and PID2022-141851OB-I00 funded by MCIN/AEI/10.13039/501100011033 and “FEDER Una manera de hacer Europa”, and the Millennium Science Initiative Program – ICN2021\_044. I.S.-G. is grateful for the financial support received from the Spanish Government (FPU19/00700).

**Acknowledge:** The authors of this study express their deep gratitude to the companies that generously contributed by providing avocado samples from various regions: Vivazplant,

Aguacastur, Asociación Valenciana de Agricultores (AVA-ASAJA), ASAJA (Asociación Agraria de Jóvenes Agricultores)-Cádiz, Nuno Neto and Huerta Tropical.

## References

- Chanderbali, A.S.; Albert, V.A.; Ashworth, V.E.T.M.; Clegg, M.T.; Litz, R.E.; Soltis, D.E.; Soltis, P.S. *Persea Americana* (Avocado): Bringing Ancient Flowers to Fruit in the Genomics Era. *BioEssays* **2008**, *30*, 386–396, doi:10.1002/bies.20721.
- Wolstenholme, B.N. Ecology: Climate and Soils. In *The avocado: botany, production and uses*; Schaffer, B., Wolstenholme, B.N., Whiley, A.W., Eds.; 2nd Ed. CAB International, 2013; pp. 86–117, doi:10.1079/9781845937010.0086.
- Rendón-Anaya, M.; Ibarra-Laclette, E.; Méndez-Bravo, A.; Lan, T.; Zheng, C.; Carretero-Paulet, L.; Perez-Torres, C.A.; Chacón-López, A.; Hernandez-Guzmán, G.; Chang, T.H.; et al. The Avocado Genome Informs Deep Angiosperm Phylogeny, Highlights Introgressive Hybridization, and Reveals Pathogen-Influenced Gene Space Adaptation. *Proc. Natl. Acad. Sci. U. S. A.* **2019**, *116*, 17081–17089, doi:10.1073/pnas.1822129116.
- Lahav, E.; Lavi, U. Avocado Genetics and Breeding. In *Breeding plantation tree crops: Tropical Species*; Jain, S.M., Priyadarshan, P.M., Eds.; Springer: New York, 2009; pp. 247–285, doi:10.1007/978-0-387-71201-7\_8.
- FAO. Statistics Division of Food and Agriculture Organization of the United Nations (FAOSTAT). Available online: <https://www.fao.org/faostat/en/#home> (accessed on 1 February 2024).
- Talavera, A.; Gonzalez-Fernandez, J.J.; Carrasco-Pancorbo, A.; Olmo-García, L.; Hormaza, J. Avocado: Agricultural Importance and Nutraceutical Properties. In *Compendium of Crop Genome Designing for Nutraceuticals*; Kole, C., Ed.; Springer Singapore, 2023; pp. 1–19, doi:10.1007/978-981-19-3627-2\_40-1.
- Howden, M.; Newett, S.; Deuter, P. Climate Change-Risks and Opportunities for the Avocado Industry. In: *New Zeal. Aust. Avocado Grow. Conf.* Holland, P., Ed.; Tauranda, New Zealand, 2005, 1-28.
- Méndez Hernández, C.; Grycz, A.; Rios Mesa, D.; Rodríguez Galdón, B.; Rodríguez-Rodríguez, E.M. The Quality Evaluation of Avocado Fruits (*Persea Americana* Mill.) of Hass Produced in Different Localities on the Island of Tenerife, Spain. *Foods* **2024**, *13*, 1058, doi:10.3390/foods13071058.
- Hurtado-Fernández, E.; Fernández-Gutiérrez, A.; Carrasco-Pancorbo, A. Avocado Fruit—*Persea Americana*. In *Exotic Fruits Reference Guide*; Rodrigues, S., Silva, E. de O., Brito, E.S. de, Eds.; 2018; pp. 37–48, doi:10.1016/B978-0-12-803138-4.000.
- Ahuja, I.; de Vos, R.C.H.; Bones, A.M.; Hall, R.D. Plant Molecular Stress Responses Face Climate Change. *Trends Plant Sci.* **2010**, *15*, 664–674, doi:10.1016/j.tplants.2010.08.002.
- Hormaza, J.I.; Garner, L.C.; Lovatt, C.J. Reproductive Biology. In *Avocado: Botany, Production and Uses (3rd Edition)*; Carrillo, D., Shaffer, B., Wolstenholme, N., Whiley, A.W., Eds.; CAB International (*in press*).
- Ramírez-Gil, J.G.; Henao-Rojas, J.C.; Diaz-Diez, C.A.; Peña-Quifones, A.J.; León, N.; Parra-Coronado, A.; Bernal-Estrada, J.A. Phenological Variations of Avocado Cv. Hass and Their Relationship with Thermal Time under Tropical Conditions. *Heliyon* **2023**, *9*, e19642, doi:10.1016/j.heliyon.2023.e19642.
- Bower, J.P.; Cutting, J.G.M.; Wolstenholme, B.N. Effect of Pre- and Post-Harvest Water Stress on the Potential for Fruit Quality Defects in Avocado (*Persea Americana* Mill.). *South African J. Plant Soil* **1989**, *6*, 219–222, doi:10.1080/02571862.1989.10634516.
- Gustafson, C.D. Avocado Water Relations. *Calif. Avocado Soc.* **1976**, *60*, 57–72.
- Lahav, E.; Whiley, A.W.; Turner, D.W. Irrigation and Mineral Nutrition. In *The avocado: botany, production and uses (2nd Edition)*; Schaffer, B., Wolstenholme, B.N., Whiley, A.W., Eds.; CABI Digital

- Library, 2013; pp. 301–341, doi:10.1079/9781845937010.0301.
16. Schaffer, B.; Gil, P.M.; Mickelbart, M. V; Whiley, A.W. Ecophysiology. In *The avocado: botany, production and uses (2nd Edition)*; Schaffer, B., Wolstenholme, B.N., Whiley, A.W., Eds.; CABI Digital Library, 2013; pp. 168–199, doi:10.1079/9781845937010.0168.
  17. Fischer, G.; Parra-Coronado, A.; Balaguera-López, H.E. Altitude as a Determinant of Fruit Quality with Emphasis on the Andean Tropics of Colombia. A Review. *Agron. Colomb.* **2022**, *40*, 212–227, doi:10.15446/agron.colomb.v40n2.101854.
  18. Donetti, M.; Terry, L.A. Biochemical Markers Defining Growing Area and Ripening Stage of Imported Avocado Fruit Cv. Hass. *J. Food Compos. Anal.* **2014**, *34*, 90–98, doi:10.1016/j.jfca.2013.11.011.
  19. Henao-Rojas, J.C.; Lopez, J.H.; Osorio, N.W.; Ramírez-Gil, J.G. Fruit Quality in Hass Avocado and Its Relationships with Different Growing Areas under Tropical Zones. *Rev. Ceres* **2019**, *66*, 341–350, doi:10.1590/0034-737X201966050003.
  20. Carvalho, C.P.; Velásquez, M.A. Fatty Acid Content of Avocados (*Persea Americana* Mill. Cv. Hass) in Relation to Orchard Altitude and Fruit Maturity Stage. *Agron. Colomb.* **2015**, *33*, 220–227, doi:10.15446/agron.colomb.v33n2.49902.
  21. Landahl, S.; Meyer, M.D.; Terry, L.A. Spatial and Temporal Analysis of Textural and Biochemical Changes of Imported Avocado Cv. Hass during Fruit Ripening. *J. Agric. Food Chem.* **2009**, *57*, 7039–7047, doi:10.1021/jf803669x.
  22. Méndez Hernández, C.; Ríos Mesa, D.; Rodríguez-Galdón, B.; Rodríguez-Rodríguez, E.M. Study of Environmental Factors on the Fat Profile of Hass Avocados. *J. Food Compos. Anal.* **2023**, *123*, 105544, doi:10.1016/j.jfca.2023.105544.
  23. Ferreyra, R.; Sellés, G.; Saavedra, J.; Ortiz, J.; Zúñiga, C.; Troncoso, C.; Rivera, S.A.; González-Agüero, M.; Defilippi, B.G. Identification of Pre-Harvest Factors That Affect Fatty Acid Profiles of Avocado Fruit (*Persea Americana* Mill) Cv. “Hass” at Harvest. *South African J. Bot.* **2016**, *104*, 15–20, doi:10.1016/j.sajb.2015.10.006.
  24. Martín-Torres, S.; Jiménez-Carvelo, A.M.; González-Casado, A.; Cuadros-Rodríguez, L. Authentication of the Geographical Origin and the Botanical Variety of Avocados Using Liquid Chromatography Fingerprinting and Deep Learning Methods. *Chemom. Intell. Lab. Syst.* **2020**, *199*, 103960, doi:10.1016/j.chemolab.2020.103960.
  25. Jiménez-Carvelo, A.M.; Martín-Torres, S.; Ortega-Gavilán, F.; Camacho, J. PLS-DA vs Sparse PLS-DA in Food Traceability. A Case Study: Authentication of Avocado Samples. *Talanta* **2021**, *224*, 121904, doi:10.1016/j.talanta.2020.121904.
  26. Muñoz-Redondo, J.M.; Bertoldi, D.; Tonon, A.; Ziller, L.; Camin, F.; Moreno-Rojas, J.M. Multi-Element and Stable Isotopes Characterization of Commercial Avocado Fruit (*Persea Americana* Mill) with Origin Authentication Purposes. *Food Control* **2022**, *137*, doi:10.1016/j.foodcont.2022.108975.
  27. Serrano-García, I.; Domínguez-García, J.; Hurtado-Fernández, E.; González-Fernández, J.J.; Hormaza, J.I.; Beiro-Valenzuela, M.G.; Monasterio, R.; Olmo-García, L.; Carrasco-Pancorbo, A.; Pedreschi, R. Assessing the RP-LC-MS-Based Metabolic Profile of Hass Avocados Marketed in Europe from Different Geographical Origins (Peru, Chile, and Spain) over the Whole Season. *Plants* **2023**, *12*, 3004, doi:doi.org/10.3390/plants12163004.
  28. Olmo-García, L.; Wendt, K.; Kessler, N.; Bajoub, A.; Fernández-Gutiérrez, A.; Baessmann, C.; Carrasco-Pancorbo, A. Exploring the Capability of LC-MS and GC-MS Multi-Class Methods to Discriminate Virgin Olive Oils from Different Geographical Indications and to Identify Potential Origin Markers. *Eur. J. Lipid Sci. Technol.* **2019**, *121*, 1800336, doi:10.1002/ejlt.201800336.
  29. Pan, Y.; Gu, H.W.; Lv, Y.; Yin, X.L.; Chen, Y.; Long, W.; Fu, H.; She, Y. Untargeted Metabolomic Analysis of Chinese Red Wines for Geographical Origin Traceability by UPLC-QTOF-MS Coupled with Chemometrics. *Food Chem.* **2022**, *394*, 133473, doi:10.1016/j.foodchem.2022.133473.

30. Putri, S.P.; Irifune, T.; Yusianto; Fukusaki, E. GC/MS Based Metabolite Profiling of Indonesian Specialty Coffee from Different Species and Geographical Origin. *Metabolomics* **2019**, *15*, 126, doi:10.1007/s11306-019-1591-5.
31. Drakopoulou, S.K.; Damalas, D.E.; Baessmann, C.; Thomaidis, N.S. Trapped Ion Mobility Incorporated in LC-HRMS Workflows as an Integral Analytical Platform of High Sensitivity: Targeted and Untargeted 4D-Metabolomics in Extra Virgin Olive Oil. *J. Agric. Food Chem.* **2021**, *69*, 15728–15737, doi:10.1021/acs.jafc.1c04789.
32. Chouinard, C.D.; Nagy, G.; Smith, R.D.; Baker, E.S. Ion Mobility-Mass Spectrometry in Metabolomic, Lipidomic, and Proteomic Analyses. In *Comprehensive Analytical Chemistry*; Donald, W.A., Prell, J.S., Eds.; Elsevier, 2019; Vol. 83, pp. 123–159, doi:10.1016/bs.coac.2018.11.001.
33. Kolodziejczyk-Czepas, J.; Kozachok, S.; Pecio, Ł.; Marchyshyn, S.; Oleszek, W. Determination of Phenolic Profiles of *Herniaria Polygama* and *Herniaria Incana* Fractions and Their in Vitro Antioxidant and Anti-Inflammatory Effects. *Phytochemistry* **2021**, *190*, 112861, doi:10.1016/j.phytochem.2021.112861.
34. Szurpnicka, A.; Wrońska, A.K.; Bus, K.; Kozińska, A.; Jabczyńska, R.; Szterk, A.; Lubelska, K. Phytochemical Screening and Effect of *Viscum Album* L. on Monoamine Oxidase A and B Activity and Serotonin, Dopamine and Serotonin Receptor 5-HT<sub>1A</sub> Levels in *Galleria Mellonealla* (Lepidoptera). *J. Ethnopharmacol.* **2022**, *298*, 115604, doi:10.1016/j.jep.2022.115604.
35. Beiro-Valenzuela, M.G.; Serrano-García, I.; Monasterio, R.P.; Moreno-Tovar, M.V.; Hurtado-Fernández, E.; González-Fernández, J.J.; Hormaza, J.I.; Pedreschi, R.; Olmo-García, L.; Carrasco-Pancorbo, A. Characterization of the Polar Profile of Bacon and Fuerte Avocado Fruits by Hydrophilic Interaction Liquid Chromatography-Mass Spectrometry: Distribution of Non-Structural Carbohydrates, Quinic Acid, and Chlorogenic Acid between Seed, Mesocarp, and Exocar. *J. Agric. Food Chem.* **2023**, *71*, 5674–5685, doi:10.1021/acs.jafc.2c08855.
36. Pedreschi, R.; Ponce, E.; Hernández, I.; Fuentealba, C.; Urbina, A.; González-Fernández, J.J.; Hormaza, J.I.; Campos, D.; Chirinos, R.; Aguayo, E. Short vs. Long-Distance Avocado Supply Chains: Life Cycle Assessment Impact Associated to Transport and Effect of Fruit Origin and Supply Conditions Chain on Primary and Secondary Metabolites. *Foods* **2022**, *11*, 1807, doi:10.3390/foods11121807.
37. Trujillo-Mayol, I.; Casas-Forero, N.; Pastene-Navarrete, E.; Silva, F.L.; Alarcón-Enos, J. Fractionation and Hydrolyzation of Avocado Peel Extract: Improvement of Antibacterial Activity. *Antibiotics* **2021**, *10*, 23, doi:10.3390/antibiotics10010023.
38. Campos, D.; Teran-Hilares, F.; Chirinos, R.; Aguilar-Galvez, A.; García-Ríos, D.; Pacheco-Avalos, A.; Pedreschi, R. Bioactive Compounds and Antioxidant Activity from Harvest to Edible Ripeness of Avocado Cv. Hass (*Persea Americana*) throughout the Harvest Seasons. *Int. J. Food Sci. Technol.* **2020**, *55*, 2208–2218, doi:10.1111/ijfs.14474.
39. Ge, Y.; Zang, X.; Liu, Y.; Wang, L.; Wang, J.; Li, Y.; Ma, W. Multi-Omics Analysis to Visualize Ecotype-Specific Heterogeneity of the Metabolites in the Mesocarp Tissue of Three Avocado (*Persea Americana* Mill.) Ecotypes. *Horticulturae* **2021**, *7*, doi:10.3390/horticulturae7050094.
40. Hurtado-Fernández, E.; Pacchiarotta, T.; Gómez-Romero, M.; Schoenmaker, B.; Derks, R.; Deelder, A.M.; Mayboroda, O.A.; Carrasco-Pancorbo, A.; Fernández-Gutiérrez, A. Ultra High Performance Liquid Chromatography-Time of Flight Mass Spectrometry for Analysis of Avocado Fruit Metabolites: Method Evaluation and Applicability to the Analysis of Ripening Degrees. *J. Chromatogr. A* **2011**, *1218*, 7723–7738, doi:10.1016/j.chroma.2011.08.059.
41. Rodríguez-Pérez, C.; Quirantes-Piné, R.; Fernández-Gutiérrez, A.; Segura-Carretero, A. Comparative Characterization of Phenolic and Other Polar Compounds in Spanish Melon Cultivars by Using High-Performance Liquid Chromatography Coupled to Electrospray Ionization Quadrupole-Time of Flight Mass Spectrometry. *Food Res. Int.* **2013**, *54*, 1519–1527, doi:10.1016/j.foodres.2013.09.011.
42. Jiménez-Sánchez, C.; Lozano-Sánchez, J.; Gabaldón-Hernández, J.A.; Segura-Carretero, A.; Fernández-Gutiérrez, A. RP-HPLC-ESI-QTOF/MS<sup>2</sup> Based Strategy for the Comprehensive Metabolite

- Profiling of Sclerocarya Birrea (Marula) Bark. *Ind. Crops Prod.* **2015**, *71*, 214–234, doi:10.1016/j.indcrop.2015.01.068.
43. Lyu, X.; Agar, O.T.; Barrow, C.J.; Dunshea, F.R.; Suleria, H.A.R. Phenolic Compounds Profiling and Their Antioxidant Capacity in the Peel, Pulp, and Seed of Australian Grown Avocado. *Antioxidants* **2023**, *12*, 185, doi:10.3390/antiox12010185.
  44. Mekky, R.H.; Contreras, M.D.M.; El-Gindi, M.R.; Abdel-Monem, A.R.; Abdel-Sattar, E.; Segura-Carretero, A. Profiling of Phenolic and Other Compounds from Egyptian Cultivars of Chickpea (*Cicer Arietinum* L.) and Antioxidant Activity: A Comparative Study. *RSC Adv.* **2015**, *5*, 17751–17767, doi:10.1039/c4ra13155j.
  45. López-Cobo, A.; Gómez-Caravaca, A.M.; Pasini, F.; Caboni, M.F.; Segura-Carretero, A.; Fernández-Gutiérrez, A. HPLC-DAD-ESI-QTOF-MS and HPLC-FLD-MS as Valuable Tools for the Determination of Phenolic and Other Polar Compounds in the Edible Part and by-Products of Avocado. *Lwt* **2016**, *73*, 505–513, doi:10.1016/j.lwt.2016.06.049.
  46. Figueroa, J.G.; Borrás-Linares, I.; Lozano-Sánchez, J.; Segura-Carretero, A. Comprehensive Characterization of Phenolic and Other Polar Compounds in the Seed and Seed Coat of Avocado by HPLC-DAD-ESI-QTOF-MS. *Food Res. Int.* **2018**, *105*, 752–763, doi:10.1016/j.foodres.2017.11.082.
  47. Gil-Martínez, L.; Aznar-Ramos, M.J.; del Carmen Razola-Díaz, M.; Mut-Salud, N.; Falcón-Piñeiro, A.; Baños, A.; Guillamón, E.; Gómez-Caravaca, A.M.; Verardo, V. Establishment of a Sonotrode Extraction Method and Evaluation of the Antioxidant, Antimicrobial and Anticancer Potential of an Optimized *Vaccinium Myrtillus* L. Leaves Extract as Functional Ingredient. *Foods* **2023**, *12*, 1288, doi:10.3390/foods12081688.
  48. Shang, Y.F.; Zhang, T.H.; Thakur, K.; Zhang, J.G.; Cespedes-Acuña, C.L.A.; Wei, Z.J. HPLC-MS/MS Targeting Analysis of Phenolics Metabolism and Antioxidant Activity of Extractions from *Lycium Barbarum* and Its Meal Using Different Methods. *Food Sci. Technol.* **2022**, *42*, e71022, doi:10.1590/fst.71022.
  49. Hurtado-Fernández, E.; Carrasco-Pancorbo, A.; Fernández-Gutiérrez, A. Profiling LC-DAD-ESI-TOF MS Method for the Determination of Phenolic Metabolites from Avocado (*Persea Americana*). *J. Agric. Food Chem.* **2011**, *59*, 2255–2267, doi:10.1021/jf104276a.
  50. Velderrain-Rodríguez, G.R.; Salvia-Trujillo, L.; Martín-Belloso, O. Lipid Digestibility and Polyphenols Bioaccessibility of Oil-in-Water Emulsions Containing Avocado Peel and Seed Extracts as Affected by the Presence of Low Methoxyl Pectin. *Foods* **2021**, *2193*, doi:10.3390/foods10092193.
  51. Zheleva-Dimitrova, D.; Voynikov, Y.; Gevrenova, R.; Balabanova, V. A Comprehensive Phytochemical Analysis of *Sideritis Scardica* Infusion Using Orbitrap UHPLC-HRMS. *Molecules* **2024**, *29*, 204, doi:10.3390/molecules29010204.
  52. Abu-Reidah, I.M.; Arráez-Román, D.; Warad, I.; Fernández-Gutiérrez, A.; Segura-Carretero, A. UHPLC/MS2-Based Approach for the Comprehensive Metabolite Profiling of Bean (*Vicia Faba* L.) by-Products: A Promising Source of Bioactive Constituents. *Food Res. Int.* **2017**, *93*, 87–96, doi:10.1016/j.foodres.2017.01.014.
  53. Abu-Reidah, I.M.; Ali-Shtayeh, M.S.; Jamous, R.M.; Arráez-Román, D.; Segura-Carretero, A. Comprehensive Metabolite Profiling of *Arum Palaestinum* (Araceae) Leaves by Using Liquid Chromatography-Tandem Mass Spectrometry. *Food Res. Int.* **2015**, *70*, 74–86, doi:10.1016/j.foodres.2015.01.023.
  54. Fan, S.; Qi, Y.; Shi, L.; Giovani, M.; Zaki, N.A.A.; Guo, S.; Suleria, H.A.R. Screening of Phenolic Compounds in Rejected Avocado and Determination of Their Antioxidant Potential. *Processes* **2022**, *10*, 1747, doi:10.3390/pr10091747.
  55. Serrano-García, I.; Saavedra Morillas, C.; Beiro-Valenzuela, M.G.; Monasterio, R.; Hurtado-Fernández, E.; González-Fernández, J.J.; Hormaza, J.I.; Pedreschi, R.; Olmo-García, L.; Carrasco-Pancorbo, A.

- Uncovering Phytochemicals Quantitative Evolution in Avocado Fruit Mesocarp during Ripening: A Targeted LC-MS Metabolic Exploration of Hass, Fuerte and Bacon Varieties. *Food Chem.* **2024**, *459*, 140334, doi:10.1016/j.foodchem.2024.140334.
56. Wang, J.; Jia, Z.; Zhang, Z.; Wang, Y.; Liu, X.; Wang, L.; Lin, R.; Schmidt, T.J. Analysis of Chemical Constituents of *Melastoma Dodecandrum* Lour. by UPLC-ESI-Q-Exactive Focus-MS/MS. *Molecules* **2017**, *22*, 476, doi:10.3390/molecules22030476.
57. Olmo-García, L.; Kessler, N.; Neuweiger, H.; Wendt, K.; Olmo-Peinado, J.M.; Fernández-Gutiérrez, A.; Baessmann, C.; Carrasco-pancorbo, A. Unravelling the Biochemical Distribution of Secondary Metabolites in Olea Matrices by Complementary Platforms ( LC-ESI / APCI-MS and GC-APCI-MS ) (Supplementary Material). *Molecules* **2018**, *23*, 2419, doi:10.3390/molecules23102419.
58. Sumner, L.W.; Amberg, A.; Barrett, D.; Beale, M.H.; Beger, R.; Daykin, C.A.; Fan, T.W.-M.; Fiehn, O.; Goodacre, R.; Griffin, J.L.; et al. Proposed Minimum Reporting Standards for Chemical Analysis. *Metabolomics* **2007**, *3*, 211–221, doi:10.1007/s11306-007-0082-2.
59. Figueroa, J.G.; Borrás-Linares, I.; Lozano-Sánchez, J.; Segura-Carretero, A. Comprehensive Identification of Bioactive Compounds of Avocado Peel by Liquid Chromatography Coupled to Ultra-High-Definition Accurate-Mass Q-TOF. *Food Chem.* **2018**, *245*, 707–716, doi:10.1016/j.foodchem.2017.12.011.
60. Arpaia, M.L. Preharvest Factors Influencing Postharvest Quality of Tropical and Subtropical Fruit. *HortScience* **1994**, *29*, 982–985, doi:10.21273/hortsci.29.9.982.
61. Hernández, I.; Fuentealba, C.; Olaeta, J.A.; Lurie, S.; Defilippi, B.G.; Campos-Vargas, R.; Pedreschi, R. Factors Associated with Postharvest Ripening Heterogeneity of “Hass” Avocados (*Persea Americana* Mill). *Fruits* **2016**, *71*, 259–268, doi:10.1051/fruits/2016016.
62. Rivera, S.A.; Ferreyra, R.; Robledo, P.; Selles, G.; Arpaia, M.L.; Saavedra, J.; Defilippi, B.G. Identification of Preharvest Factors Determining Postharvest Ripening Behaviors in ‘Hass’ Avocado under Long Term Storage. *Sci. Hortic.* **2017**, *216*, 29–37, doi:10.1016/j.scienta.2016.12.024.
63. Augustynowicz, D.; Lemieszek, M.K.; Strawa, J.W.; Wiater, A.; Tomczyk, M. Anticancer Potential of Acetone Extracts from Selected *Potentilla* Species against Human Colorectal Cancer Cells. *Front. Pharmacol.* **2022**, *13*, 1027315, doi:10.3389/fphar.2022.1027315.
64. Sottile, F.; Napolitano, A.; Badalamenti, N.; Bruno, M.; Tundis, R.; Loizzo, M.R.; Piacente, S. A New Bloody Pulp Selection of Myrobalan (*Prunus Cerasifera* L.): Pomological Traits, Chemical Composition, and Nutraceutical Properties. *Foods* **2023**, *12*, 1107, doi:10.3390/foods12051107.
65. Cannavacciuolo, C.; Pagliari, S.; Giustra, C.M.; Carabetta, S.; Guidi Nissim, W.; Russo, M.; Branduardi, P.; Labra, M.; Campone, L. LC-MS and GC-MS Data Fusion Metabolomics Profiling Coupled with Multivariate Analysis for the Discrimination of Different Parts of Fastrime Fruit and Evaluation of Their Antioxidant Activity. *Antioxidants* **2023**, *12*, 565, doi:10.3390/antiox12030565.
66. Rodríguez-Pérez, C.; Quirantes-Piné, R.; Amessis-Ouchemoukh, N.; Khodir, M.; Segura-Carretero, A.; Fernández-Gutierrez, A. A Metabolite-Profilng Approach Allows the Identification of New Compounds from *Pistacia Lentiscus* Leaves. *J. Pharm. Biomed. Anal.* **2013**, *77*, 167–174, doi:10.1016/j.jpba.2013.01.026.
67. Charlson, A.J.; Richtmyer, N.K. The Isolation of an Octulose and an Octitol from Natural Sources: O-Glycero-O-Manno-Octulose and O-Erythro-T-Galacto-Octitol from the Avocado and O-Glycero-O-Manno-Octulose from *Sedum* Species. *J. Am. Chem. Soc.* **1960**, *82*, 3428–3434.
68. Song, D.; Chou, G.X.; Zhong, G.Y.; Wang, Z.T. Two New Phenylpropanoid Derivatives from *Codonopsis Tangshen* Oliv. *Helv. Chim. Acta* **2008**, *91*, 1984–1988, doi:10.1002/hlca.200890213.
69. Hashim, Y.; Toume, K.; Mizukami, S.; Kitami, T.; Taniguchi, M.; Teklemichael, A.A.; Tayama, Y.; Huy, N.T.; Lami, J.N.; Bodi, J.M.; et al. Phenylpropanoid-Conjugated Iridoid Glucosides from Leaves of *Morinda Morindoides*. *J. Nat. Med.* **2022**, *76*, 281–290, doi:10.1007/s11418-021-01567-1.

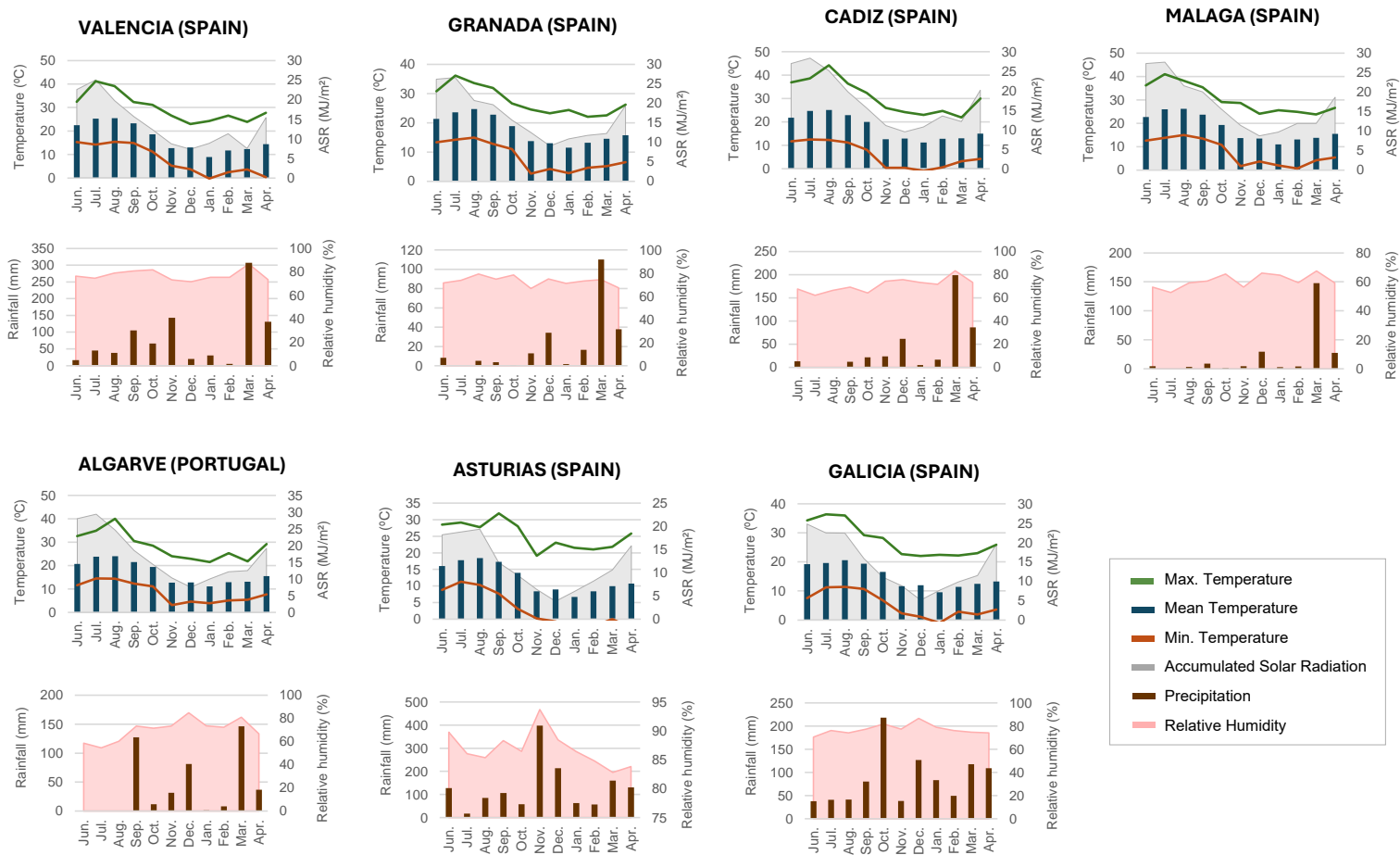
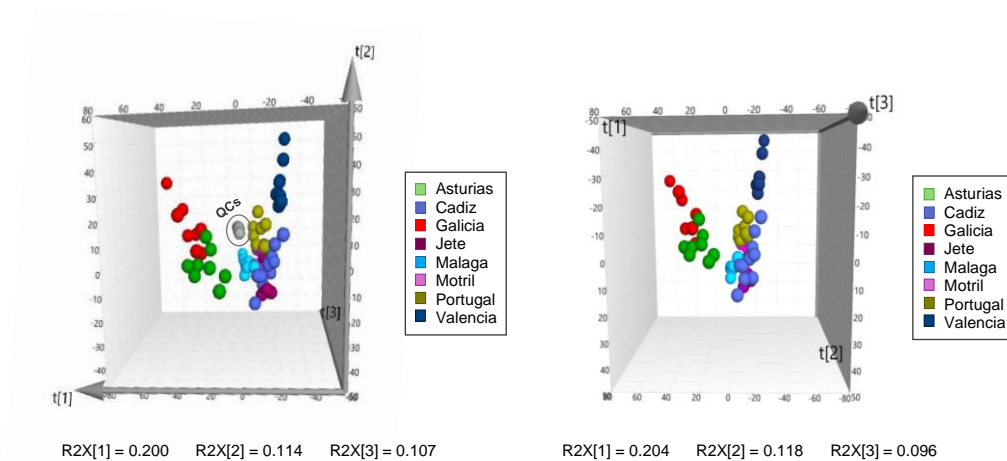


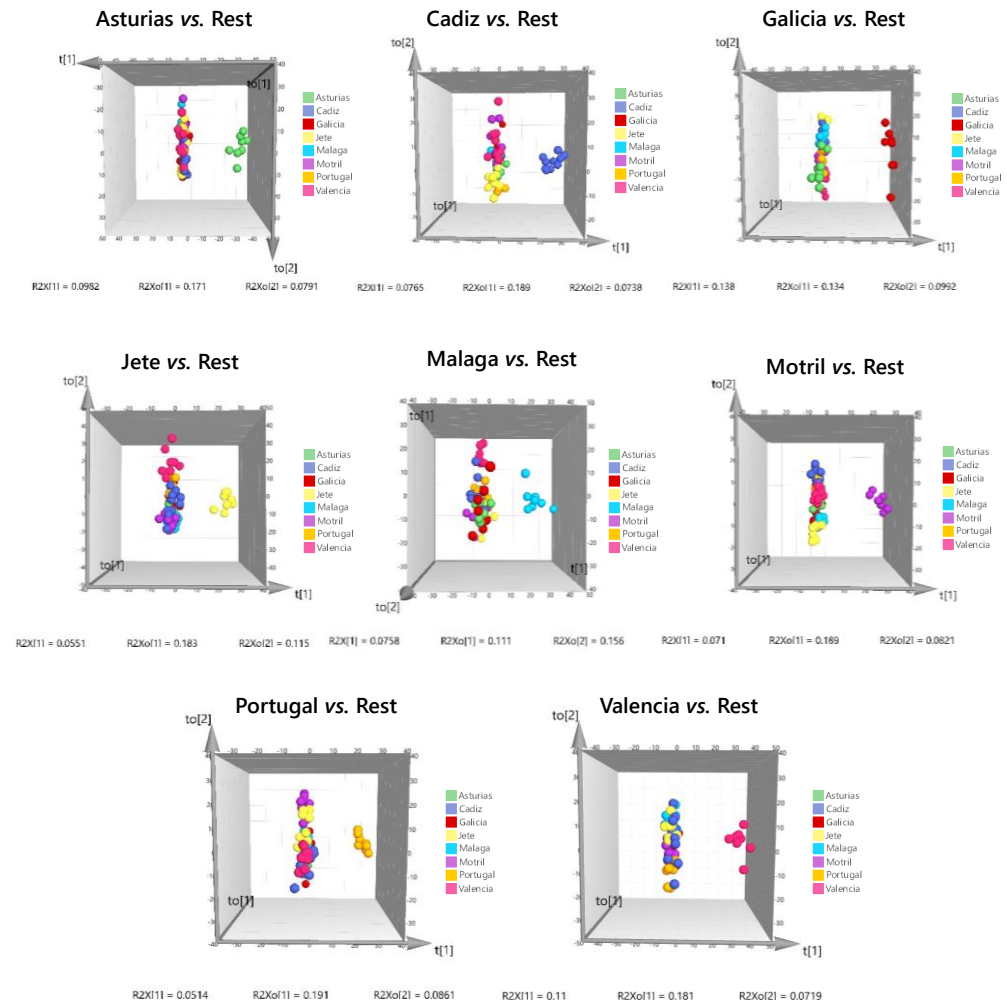
Figure S1. Monthly climate data at the sampling points of Hass avocado cultivated from June 2021 until the harvesting period in April 2022



**Figure S2.** Comparison of the PCA scores plot generated with the first three principal components (PCs) including the QC samples (n=77) (left side) and without including the QC samples (n=66) (right side)

**Table S1.** Quality and cross-validation parameters obtained for the eight OPLS-DA models built to define the characteristic metabolic patterns per origin

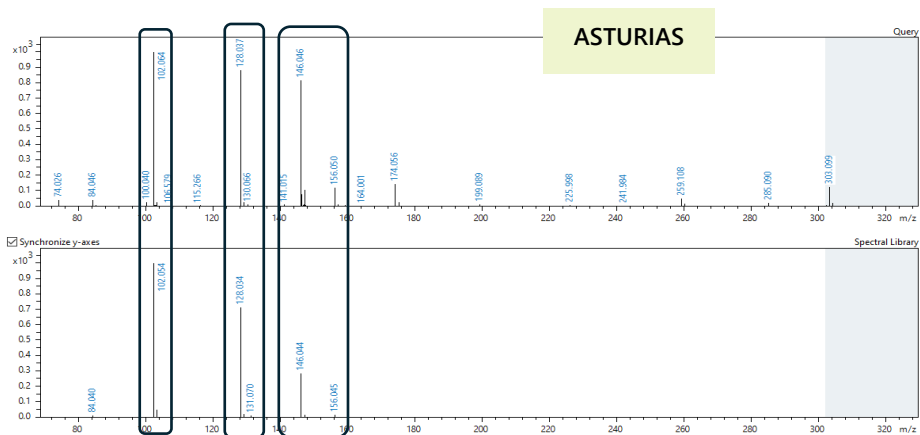
OPLS-DA Model	A	N	R <sup>2</sup> X (cum)	R <sup>2</sup> Y (cum)	Q <sup>2</sup> (cum)	Cross-Validated ANOVA	
						F	p-values
Asturias vs. Rest	1+3+0	66	0.391	0.978	0.929	92.65	$8.19 \times 10^{-30}$
Cadiz vs. Rest	1+4+0	66	0.479	0.956	0.840	28.83	$2.32 \times 10^{-18}$
Galicia vs. Rest	1+3+0	66	0.411	0.987	0.955	156.66	$1.32 \times 10^{-35}$
Jete vs. Rest	1+3+0	66	0.413	0.944	0.877	51.00	$3.43 \times 10^{-23}$
Malaga vs. Rest	1+2+0	66	0.342	0.896	0.820	44.70	$3.70 \times 10^{-20}$
Motril vs. Rest	1+4+0	66	0.479	0.972	0.901	49.96	$5.67 \times 10^{-24}$
Portugal vs. Rest	1+4+0	66	0.467	0.966	0.871	37.17	$6.74 \times 10^{-21}$
Valencia vs. Rest	1+3+0	66	0.416	0.973	0.925	88.44	$2.77 \times 10^{-29}$

**Figure S3.** Three-dimensional OPLS-DA scores plot depicting the discrimination of each specific region from the rest of the sampling points

**INDOLE-3-ACETYL-L-GLUTAMIC ACID**

Score: 930.13

MF: C<sub>15</sub>H<sub>16</sub>N<sub>2</sub>O<sub>5</sub>



**3-(4-HYDROXYPHENYL)-3-OXOPROPYL BETA-D-GLUCOPYRANOSIDE**

Score: 980.22

MF: C<sub>15</sub>H<sub>20</sub>O<sub>8</sub>

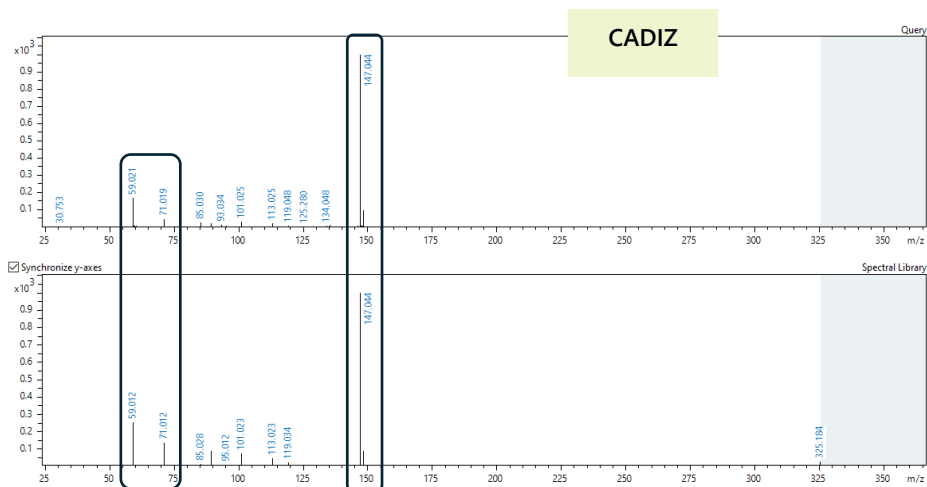


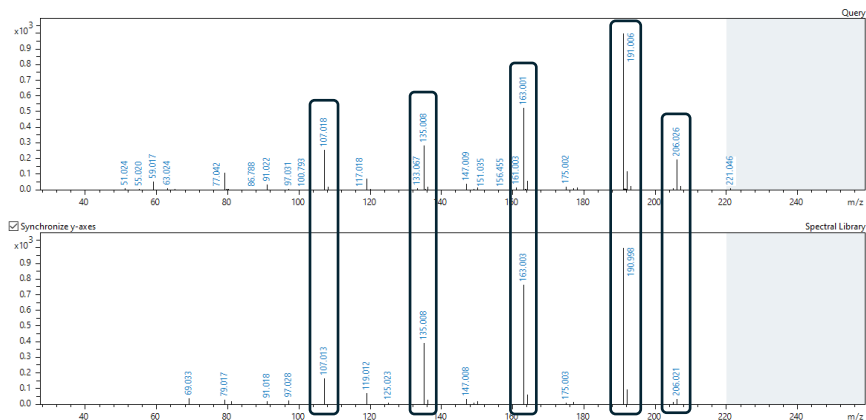
**Figure S4.** Potential markers tentatively annotated by the public MS/MS spectral libraries

**ISOFRAXIDIN**

Score: 967.38

MF: C<sub>11</sub>H<sub>10</sub>O<sub>5</sub>

MOTRIL



**FRAXIN**

Score: 837.90

MF: C<sub>16</sub>H<sub>18</sub>O<sub>10</sub>

MOTRIL

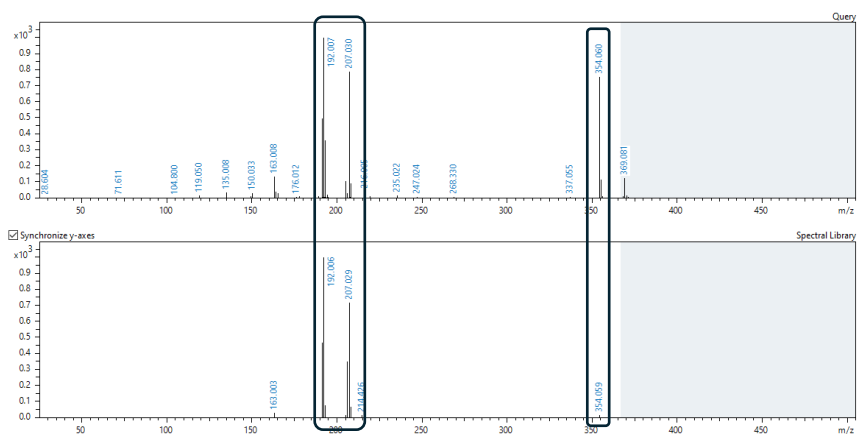


Figure S4 (cont.). Potential markers tentatively annotated by the public MS/MS spectral libraries.



## SECTION II

---

# METABOLOMIC APPROACHES APPLIED TO THE STUDY OF OLIVE-RELATED MATRICES



The work presented in this section focuses on the study of olive-related matrices and is framed within olive breeding programs. The first chapter explores a previously undervalued subspecies using a targeted LC-MS approach ([Chapter 5](#)), while the subsequent chapters address one of the most devastating diseases affecting olive crops (verticillium wilt), employing both targeted and non-targeted metabolomic approaches ([Chapters 6 and 7](#)).



## Chapter

# Fruit phenolic and triterpenic composition of progenies of *Olea europaea* subsp. *cuspidata*, an interesting phytochemical source to be included in olive breeding programs

Irene Serrano-García<sup>1</sup>, Lucía Olmo-García<sup>1</sup>✉, Daniel Polo-Megías<sup>1</sup>, Alicia Serrano<sup>2</sup>, Lorenzo León<sup>2</sup>, Raúl de la Rosa<sup>2</sup>, Ana María Gómez-Caravaca<sup>1</sup>, Alegría Carrasco-Pancorbo<sup>1</sup>

<sup>1</sup> Department of Analytical Chemistry, Faculty of Sciences, University of Granada, Ave. Fuentenueva s/n, 18071, Granada, Spain; iserrano@ugr.es (I.S.-G.); danielpm@ugr.es (D.P.-M.); anagomez@ugr.es (A.M.G.-C.); alegriac@ugr.es (A.C.-P.)

<sup>2</sup> IFAPA Centro Alameda del Obispo, Ave. Menéndez Pidal s/n, 14004, Córdoba, Spain; alicia.serrano.gomez@juntadeandalucia.es (A.S.); lorenzo.leon@juntadeandalucia.es (L.L.); raul.rosa@juntadeandalucia.es (R.d.l.R.)

✉ luciaolmo@ugr.es

**Plants, 11 (2022) 1791**

<https://doi.org/10.3390/plants11141791>



**Abstract:** *Olea europaea* subsp. *cuspidata* has a relatively low commercial value due to the low size and pulp to stone ratio of its drupes compared to commercial olive cultivars. Nevertheless, this subspecies could represent a valid source of useful traits for olive breeding. In the current work, the drupe metabolic composition (secoiridoids, flavonoids, simple phenols, triterpenic acids, etc.) of a progeny of 27 *cuspidata* genotypes coming from free pollination and their female parent was evaluated by applying a powerful LC-MS method. A total of 62 compounds were detected within the profiles; 60 of them were annotated and 27 quantified. From a quantitative point of view, the genotypes from the progeny of *cuspidata* showed quite different metabolic profiles to olive common cultivars (“Arbequina”, “Frantoio”, “Koroneiki” and “Picual”) used as controls. *Cuspidata* drupes were richer in terms of several bioactive compounds such as rutin, hydroxytyrosol glucoside, a few interesting secoiridoids and the compounds of *m/z* 421 and 363. The relationships among several secondary metabolites determined in the progeny inferred from the results of both PCA and cross-correlation analysis were explained according to metabolic biosynthesis pathways in olive drupes. These outcomes underlined the potential of *cuspidata* genetic resources as a source of potentially interesting variability in olive breeding programs.

**Keywords:** breeding programs; *cuspidata*; olive drupe; metabolic profile; LC-MS

## 1. INTRODUCTION

The genus *Olea* belongs to the family *Oleaceae* and is divided into three different subgenera: *Olea*, *Tetrapilus* and *Paniculatae* [1]. Six subspecies have been defined for *Olea europaea* L., which is popularly known as “The Olive Complex”. The subsp. *europaea* (diploid), which can be found throughout the whole Mediterranean basin, is represented by two botanical varieties: cultivated olive (*Olea europaea* subsp. *europaea* var. *europaea*) and wild olive (*Olea europaea* subsp. *europaea* var. *sylvestris*). Additionally, five more non-cultivated sbsp. have been described: *laperrinei* (diploid), *cuspidata* (diploid), *guanchica* (diploid), *maroccana* (polyploid 6n) and *cerasiformis* (polyploid 4n) [2–4]. The geographical origin and domestication of olive tree remain unclear. It is usually accepted that olive tree domestication began in the Northern Levant approximately six thousand years ago [5]. Different paleobotanic and genetic investigations have hypothesized that the current cultivars arose from one or multiple random hybridizations between wild and domesticated Mediterranean genotypes. Both wild and cultivated olive trees have coexisted in human civilizations [4,6].

Nowadays, the cultivated olive tree is considered the most emblematic tree of the Mediterranean basin and is of undeniable economic importance. Spain tops the list of major olive-producing countries with an annual production of almost 10 million tonnes, followed by Italy and Greece with productions of approximately 1.9 and 1.1 million [7]. Meanwhile, *Olea europaea* subsp. *cuspidata*, also called *Olea ferruginea* Royle (the wild non-Mediterranean olive), has a wide continental distribution from Austral Africa to China. Its presence has also been reported in

Australia, north of New Zealand and Hawaii [2]. It has been hypothesized that the subsp. *cuspidata* ancestors contributed to the origin of cultivated olive. The African olive (subsp. *cuspidata*) is not of a great economic importance due to its little drupe size (diameter generally <8 mm). Nevertheless, it could represent a valid source of useful traits for cultivated olive, such as adaptability to semi-arid to *meso*-humid climate conditions and resistance to abiotic or biotic stresses [8]. Its wood is used to make furniture or as vegetable hedge, while leaves and other plant organs are locally used for the treatment of various diseases [9–11]. Both subspecies (*europaea* and *cuspidata* subsp.) are sexually compatible either in nature or in experimental crosses, which could be particularly interesting for the introgression of some agronomic traits, phytochemical features and/or resistance to biotic and abiotic stresses in breeding programs.

Olive breeding initiatives have been developed in several countries around the world (Argentina, Australia, Croatia, France, Greece, Iran, Israel, Italy, Jordan, Lebanon, Montenegro, Morocco, Portugal, Spain, Tunisia, Turkey, Uruguay, and USA) [12,13]. Breeding programs are focused on improving agronomic traits such as early bearing, productivity, oil content and composition [14–16]. Tolerance to abiotic and biotic stresses such as *Verticillium dahliae* or *Xylella fastidiosa* are also important objectives for olive breeding programs [17]. Pérez and collaborators proposed a high-throughput methodology to include the phenolic composition as a selection criterion in olive breeding programs [18]. The high correlation between fruit and the content of oil phenolic components and the high genotypic variance described for these compounds suggest the usefulness of the analysis of fruit phenolic compounds in olive breeding programs to select olive genotypes of potential interest in terms of oil phenolic composition.

The metabolic profile of wild olives has not been explored and is practically unknown; on the contrary, there is a lot of research focused on the study of the minor fraction of common cultivated olives. The minor fraction of olive fruit represents approximately 1 to 3% of the total olive composition and contains, among others, phenolic compounds, pentacyclic triterpenes, tocopherols and phytosterols [19]. The phenolic fraction is very complex and its profile is conditioned by many factors (cultivar, ripening stage, season, etc.); it comprises secoiridoids, simple phenols, phenolic acids, flavonoids and lignans. The potent antioxidant activity, beneficial health effects and influence on sensory characteristics of olive oil are some of the properties that have been ascribed to these compounds [20,21]. Pentacyclic triterpenes are mainly found in the stem bark and in the surface cuticular waxes of olive leaves and fruits. The most studied ones are the maslinic, oleanolic and ursolic acids and the alcohols erythrodiol and uvaol. Numerous health-promoting properties have been attributed to them [22–24]. Tocopherols and phytosterols are mainly present in olive oil and their intake is related, among other factors, to the protective capacity against oxidative stress and the regulation of cholesterol, respectively [25,26]. The assessment of the mentioned minor compounds in olive cultivars (in particular, phenolic compounds and triterpenes) has been traditionally addressed by studying each family of compounds separately (i.e., by using targeted approaches). [Table 1](#) includes some of the most

comprehensive reports describing olive fruit's minor components. Information about the cultivar, analytical platform(s) used, determined compounds, etc., has been gathered within the table; when the studies considered more than one olive-derived matrix, it has been pointed out.

**Table 1.** Examples of comprehensive reports describing minor components of olive fruit

Olive Cultivar	Matrix/ces considered	Analytical platform/s used	Total number of determined analytes	Compounds detected in drupes	Ref.
Frantoio and Correggilo	Olive oil, pulp and mill waste	RPLC-DAD/FLD RPLC-ESI-TQ MS	79	5 simple phenols, 5 organic acids, 12 flavonoids, 25 secoiridoids and 4 unknown compounds	[27]
Koroneiki	Olive drupes, fruit paste, unrefined oil and "final" oil	LC-PDA/ESI-LTQ-Orbitrap XL hybrid MS	52	4 simple phenols and derivatives, 25 secoiridoids and derivatives, 3 phenolic acid derivatives, 7 flavonoids, 2 triterpenes and 1 lactone	[28]
Anyvalik, Domat and Gemlik	Olive fruit and olive oil	HPLC-DAD	20	12 phenolic acids, 3 simple phenols, oleuropein, and 4 flavonoids	[29]
Arbequina, Picual, Sikitita, Arbosana, Changlot Real and Koroneiki	Olive fruit	HPLC-DAD/TOF-MS	57	18 secoiridoids, 14 flavonoids, 11 simple phenols, 9 oleosides and 5 elenolic acid glucosides	[30]
Istrska belica	Olive fruit, stones, paste, oil, pomace, and wastewater	UPLC-DAD/ESI-QTOF-HRMS	80	5 simple phenols, 4 cinnamic acids, 12 flavonoids and 24 secoiridoids	[31]
Arauco	Olive drupes and oil	GC-MS HPLC-DAD/FLD	10	3 tocopherols, squalene, 3 simple phenols and derivatives, 3 secoiridoids and 2 lignans	[32]
Picudo	Olive leaf, stem, seed, fruit skin and pulp, different types of olive oils	LC-ESI/APCI-QTOF MS GC-APCI-QTOF MS	142 in LC-MS 58 in GC-MS	12 phenolic acids and aldehydes, 4 organic acids and coumarins, 9 simple phenols and derivatives, 32 secoiridoids and derivatives, 14 flavonoids, 4 lignans, 6 pentacyclic triterpenes, 2 tocopherols and 5 sterols	[33]

APCI: Atmospheric pressure chemical ionization; DAD: Diode array detector; ESI: Electrospray ionization; FLD: Fluorescence detector; GC: Gas chromatography; HRMS: High-resolution mass spectrometry; HPLC: High-performance liquid chromatography; LC: Liquid chromatography; LTQ: Linear ion trap quadrupole; MS: Mass spectrometry; PDA: Photodiode array detector; Q: Quadrupole; RPLC: Reverse-phase liquid chromatography; TOF: Time of flight; TQ: Triple quadrupole; UPLC: Ultra-performance liquid chromatography

To date, there are only few studies dealing with the characterization of different olive oils obtained from wild olives from various origins (Pakistan, Tunisia, Algerian or Portugal) [34–39]. Dabbou and co-authors, for instance, observed that oleasters could be potentially interesting, since they produced oils with good quality characteristics in terms of minor compounds (phenols and volatiles) compared to the "Chemlali Sfax" cultivar [38]. Similarly, Bouarroudj and colleagues highlighted the high potential of Algerian oleaster oils as phytochemical and genetic resources to

improve the quality of olive oil [37]. Another thorough study has suggested that the use of wild germplasm in olive breeding programs will not have a negative impact on olive oil composition in terms of fatty acids, tocopherol content and tocopherol and phytosterol profiles, given that the selection of these compounds is conducted starting from early generations [15]. Unfortunately, the potential of *cuspidata* olive drupes regarding their phytochemical composition has not yet been deciphered and their differences with cultivated olives have been scarcely studied.

Therefore, the objective of the present work was: i) to perform an in-depth characterization of the metabolic profile of *cuspidata* samples; ii) to compare their compositional profiles regarding phenolic and triterpenic substances (qualitatively and quantitatively) with that of four olive common cultivars (“Arbequina”, “Frantoio”, “Koroneiki” and “Picual”); and iii) to evaluate whether the subsp. *cuspidata* could represent a valid source of useful traits for cultivated olive, proving eventually the potential of this subspecies to be included in breeding programs.

## 2. RESULTS AND DISCUSSION

### 2.1. Characterization of the metabolic profile of progenies from *Olea europaea* subsp. *cuspidata* by LC-MS

As stated in the Materials and Methods (see [Section 3](#)), liquid chromatography (LC) coupled with high-resolution mass spectrometry (HRMS) was used to perform a qualitative profiling of the extracts of the subsp. *cuspidata* fruit samples. A total of 62 compounds were detected within the profiles; a combination of accurate mass and isotopic distribution was used to calculate the theoretical elemental formula of the detected metabolites. The identity of some compounds was verified by using the commercial or isolated pure standards available in-house; for some other metabolites, however, we just provided a tentative identification based on a combination of experimental data (HRMS data and *in-source* fragmentation patterns), the expertise of our research group and the information previously described in the literature regarding olive fruit characterization [28,30,31,33]. [Table 2](#) shows the qualitative exploration of progenies from *Olea europaea* subsp. *cuspidata*. Each row of the table includes the identity assigned to each analyte, to which chemical class it might belong, its molecular formula, retention time, experimental and theoretical *m/z* signals, error (ppm) and mSigma value, as well as the *in-source* fragments detected in MS.

Secoiridoids (40) made up the most numerous group of compounds, followed by flavonoids (10), pentacyclic triterpenes (5), simple phenols or related analytes (3) and organic acids (2). It should be noted that a large part of the identified compounds corresponded to glycosylated derivatives and isomers, especially in the case of secoiridoids. As far as secoiridoids are concerned, 22 analytes were structurally related to hydroxytyrosol (oleuropein derivatives), 3 to tyrosol (ligstroside derivatives) and 12 resulted to be oleoside-type and elenolic acid derivatives.

**Table 2.** First qualitative exploration of progenies from *Olea europaea* subsp. *cuspidata*

Compound	Family	Molecular Formula	Rt (min)	$m/z_{exp}$	$m/z_{theo}$	Error (ppm)	mSigma	In-Source Fragment/s	Quantified Peak Number	Standard (Quantified in Terms of)
quinic acid	organic acid	C <sub>7</sub> H <sub>12</sub> O <sub>6</sub>	0.90	191.0550	191.0561	5.6	7.5	-	1	quinic acid
citric acid	organic acid	C <sub>6</sub> H <sub>8</sub> O <sub>7</sub>	0.95	191.0190	191.0197	4.0	3.9	-	-	-
dehydro oleuropein aglycone (A)	secoiridoids	C <sub>16</sub> H <sub>24</sub> O <sub>10</sub>	0.98	375.1292	375.1297	1.4	63.7	133.0133	-	-
acyclodihydroelenolic acid hexoside (A)	secoiridoids	C <sub>17</sub> H <sub>28</sub> O <sub>11</sub>	1.00	407.1536	407.1559	5.6	0.27	815.3155	-	-
oleoside/secologanoside (A)	secoiridoids	C <sub>16</sub> H <sub>22</sub> O <sub>11</sub>	1.00	389.1087	389.1089	0.5	17.9	345.1180	-	-
elenolic acid glucoside (A)	secoiridoids	C <sub>17</sub> H <sub>24</sub> O <sub>11</sub>	1.01	403.1232	403.1246	3.4	22	223.0591	-	-
dehydro oleuropein aglycone (B)	secoiridoids	C <sub>16</sub> H <sub>24</sub> O <sub>10</sub>	1.22	375.1296	375.1297	0.2	19.8	133.0139	-	-
oleoside/secologanoside (B)	secoiridoids	C <sub>16</sub> H <sub>22</sub> O <sub>11</sub>	1.34	389.1083	389.1089	1.7	10.2	345.1183	-	-
hydroxytyrosol glucoside	simple phenols	C <sub>14</sub> H <sub>20</sub> O <sub>8</sub>	1.34	315.1081	315.1085	1.4	11.9	153.0549	2	hydroxytyrosol
acyclodihydroelenolic acid hexoside (B)	secoiridoids	C <sub>17</sub> H <sub>28</sub> O <sub>11</sub>	1.60	407.1558	407.1559	0.3	10	815.3151	3	oleuropein
dehydro acyclodihydroelenolic acid hexoside	secoiridoids	C <sub>17</sub> H <sub>26</sub> O <sub>10</sub>	1.62	389.1454	389.1453	-0.2	5.8	-	-	-
oleoside/secologanoside (C)	secoiridoids	C <sub>16</sub> H <sub>22</sub> O <sub>11</sub>	2.36	389.1074	389.1089	4.0	6.1	345.1178	4	oleuropein
elenolic acid glucoside (B)	secoiridoids	C <sub>17</sub> H <sub>24</sub> O <sub>11</sub>	2.45	403.1234	403.1246	3.0	15.4	223.0601	-	-
oxydized hydroxytyrosol	simple phenols	C <sub>8</sub> H <sub>8</sub> O <sub>3</sub>	3.10	151.0395	151.0401	3.5	7.1	-	-	-
elenolic acid glucoside (C)	secoiridoids	C <sub>17</sub> H <sub>24</sub> O <sub>11</sub>	3.52	403.1246	403.1246	1.5	8.3	223.0598	5	oleuropein
$\beta$ - hydroxy verbascoside	secoiridoids	C <sub>29</sub> H <sub>36</sub> O <sub>16</sub>	4.22	639.1929	639.1931	0.3	11.2	-	6	verbascoside
oleuropein glucoside (A)	secoiridoids	C <sub>31</sub> H <sub>42</sub> O <sub>18</sub>	4.61	701.2293	701.2298	0.8	8.2	-	-	-
rutin (A)	flavonoids	C <sub>27</sub> H <sub>30</sub> O <sub>16</sub>	4.77	609.1463	609.1461	-0.3	14.9	-	-	-
phenylethyl primeveroside	simple phenols	C <sub>19</sub> H <sub>28</sub> O <sub>10</sub>	4.96	415.1606	415.1610	0.8	6.6	-	-	-
hydroxy decarboxymethyl oleuropein aglycone	secoiridoids	C <sub>17</sub> H <sub>20</sub> O <sub>7</sub>	5.14	335.1147	335.1136	-3.1	13.1	-	-	-
demethyl oleuropein	secoiridoids	C <sub>24</sub> H <sub>30</sub> O <sub>13</sub>	5.73	525.1608	525.1614	1.1	5.4	1051.3298	7	oleuropein
rutin (B)	flavonoids	C <sub>27</sub> H <sub>30</sub> O <sub>16</sub>	5.81	609.1440	609.1461	3.4	11.2	301.0351	8	rutin
hydroxyoleuropein	secoiridoids	C <sub>25</sub> H <sub>32</sub> O <sub>14</sub>	6.21	555.1720	555.1719	-0.1	7.6	393.1195	-	-
neonuzhenide	secoiridoids	C <sub>31</sub> H <sub>42</sub> O <sub>18</sub>	6.30	701.2292	701.2298	0.9	5.2	-	9	oleuropein
luteolin 7-O-glucoside	flavonoids	C <sub>21</sub> H <sub>20</sub> O <sub>11</sub>	6.48	447.0932	447.0933	0.1	6.9	285.0406	10	luteolin 7-O-glucoside
verbascoside	secoiridoids	C <sub>29</sub> H <sub>36</sub> O <sub>15</sub>	6.84	623.1979	623.1981	0.3	37.1	-	11	verbascoside
luteolin rutinoside	flavonoids	C <sub>27</sub> H <sub>30</sub> O <sub>15</sub>	7.12	593.1516	593.1512	-0.6	19.1	-	-	-
methoxy oleuropein (A)	secoiridoids	C <sub>26</sub> H <sub>34</sub> O <sub>14</sub>	7.28	569.1878	569.1876	-0.4	7.5	389.1071	12	oleuropein

Compound	Family	Molecular Formula	Rt (min)	m/z <sub>exp</sub>	m/z <sub>theo</sub>	Error (ppm)	mSigma	In-Source Fragment/s	Quantified Peak Number	Standard (Quantified in Terms of)
demethyl ligstroside	secoiridoids	C <sub>24</sub> H <sub>30</sub> O <sub>12</sub>	7.43	509.1666	509.1664	-0.2	10.2	347.1122	13	verbascoside
luteolin glucoside (A)	flavonoids	C <sub>21</sub> H <sub>20</sub> O <sub>11</sub>	7.67	447.0937	447.0933	-1.0	17.6	-	-	-
dihydro oleuropein	secoiridoids	C <sub>25</sub> H <sub>36</sub> O <sub>13</sub>	7.71	543.2082	543.2083	0.2	21.1	525.1972 513.1981	14	oleuropein
dehydro nuzhenide	secoiridoids	C <sub>31</sub> H <sub>40</sub> O <sub>16</sub>	7.78	667.2244	667.2244	-0.1	11.0	310.0872	15	oleuropein
nuzhenide	secoiridoids	C <sub>31</sub> H <sub>42</sub> O <sub>17</sub>	7.80	685.2350	685.2349	-0.2	13.7	523.1806	-	-
luteolin glucoside (B)	flavonoids	C <sub>21</sub> H <sub>20</sub> O <sub>11</sub>	7.97	447.0931	447.0933	0.4	6.1	285.0388	16	luteolin 7-O-glucoside
apigenin 7-O-glucoside	flavonoids	C <sub>21</sub> H <sub>20</sub> O <sub>10</sub>	8.08	431.0981	431.0984	0.7	11.7	-	-	-
oleuropein glucoside (B)	secoiridoids	C <sub>31</sub> H <sub>42</sub> O <sub>18</sub>	8.12	701.2232	701.2298	-0.5	6.9	-	-	oleuropein
10-hydroxyoleuropein aglycon (A)	secoiridoids	C <sub>19</sub> H <sub>22</sub> O <sub>9</sub>	8.19	393.1189	393.1191	0.6	21.8	-	-	-
caffeoyl 6-secologanoside	secoiridoids	C <sub>25</sub> H <sub>28</sub> O <sub>14</sub>	8.34	551.1385	551.1406	3.8	9.8	-	17	verbascoside
methoxy oleuropein (B)	secoiridoids	C <sub>26</sub> H <sub>34</sub> O <sub>14</sub>	8.85	569.1876	569.1876	-0.1	18.7	389.1069	-	-
luteolin glucoside (C)	flavonoids	C <sub>21</sub> H <sub>20</sub> O <sub>11</sub>	8.92	447.0923	447.0933	2.1	7.2	-	-	-
oleuropein	secoiridoids	C <sub>25</sub> H <sub>32</sub> O <sub>13</sub>	9.93	539.1768	539.1770	0.5	6.2	377.1232 307.0821	18	oleuropein
fraxamoside	secoiridoids	C <sub>25</sub> H <sub>30</sub> O <sub>13</sub>	10.50	537.1605	537.1614	1.7	31.3	-	-	-
10-hydroxyoleuropein aglycon (B)	secoiridoids	C <sub>19</sub> H <sub>22</sub> O <sub>9</sub>	10.88	393.1180	393.1191	2.9	19.8	-	-	-
lucidumoside C (A)	secoiridoids	C <sub>27</sub> H <sub>36</sub> O <sub>14</sub>	11.48	583.2031	583.2032	0.2	5.3	1167.4106 537.1594 403.1223	19	oleuropein
luteolin	flavonoids	C <sub>15</sub> H <sub>10</sub> O <sub>6</sub>	11.59	285.0398	285.0405	2.4	3.0	-	-	-
elenolic acid glucoside (D)	secoiridoids	C <sub>17</sub> H <sub>24</sub> O <sub>11</sub>	11.70	403.1241	403.1246	1.3	11.8	223.0591 361.1276	-	-
ligstroside	secoiridoids	C <sub>25</sub> H <sub>32</sub> O <sub>12</sub>	11.91	523.1820	523.1821	0.2	5.5	291.0858 259.0969	20	oleuropein
elenolic acid glucoside (E)	secoiridoids	C <sub>17</sub> H <sub>24</sub> O <sub>11</sub>	11.95	403.1246	403.1246	0.7	24.4	223.0594	-	-
hydroxyoleuropein	secoiridoids	C <sub>26</sub> H <sub>36</sub> O <sub>13</sub>	12.03	555.2084	555.2083	-0.1	6.8	539.1779	-	-
apigenin	flavonoids	C <sub>15</sub> H <sub>10</sub> O <sub>5</sub>	12.19	269.0442	269.0455	5	15.4	-	-	-
lucidumoside C (B)	secoiridoids	C <sub>27</sub> H <sub>36</sub> O <sub>14</sub>	12.44	583.2026	583.2032	1.1	11.6	-	-	-
unknown 1	-	C <sub>19</sub> H <sub>24</sub> O <sub>7</sub>	12.60	363.1440	363.1449	2.5	8.7	-	21	oleuropein
oleuropein aglycone (A)	secoiridoids	C <sub>19</sub> H <sub>22</sub> O <sub>8</sub>	12.71	377.1230	377.1242	3.3	14.5	345.0969 307.0814 275.0918	22	oleuropein
compound related to oleuropein aglycone	secoiridoids	C <sub>20</sub> H <sub>26</sub> O <sub>8</sub>	12.71	393.1542	393.1555	3.3	9.3	-	-	-

Compound	Family	Molecular Formula	Rt (min)	$m/z_{exp}$	$m/z_{theo}$	Error (ppm)	mSigma	In-Source Fragment/s	Quantified Peak Number	Standard (Quantified in Terms of)
compound related to oleuropein aglycone	secoiridoids	C <sub>20</sub> H <sub>26</sub> O <sub>8</sub>	13.10	393.1552	393.1555	0.9	6.6	-	-	-
oleuropein aglycone (B)	secoiridoids	C <sub>19</sub> H <sub>22</sub> O <sub>8</sub>	13.29	377.1230	377.1242	3.2	10.7	345.0964 307.0809 275.0917	23	oleuropein
unknown 2	-	C <sub>21</sub> H <sub>26</sub> O <sub>9</sub>	13.58	421.1494	421.1504	2.5	9.7	-	24	oleuropein
monohydroxylated derivative of maslinic acid	pentacyclic triterpenes	C <sub>30</sub> H <sub>48</sub> O <sub>5</sub>	14.27	487.3420	487.3429	1.9	7.2	-	-	-
maslinic acid	pentacyclic triterpenes	C <sub>30</sub> H <sub>48</sub> O <sub>4</sub>	15.78	471.3479	471.348	0.2	0.2	393.3158	25	maslinic acid
betulinic acid	pentacyclic triterpenes	C <sub>30</sub> H <sub>48</sub> O <sub>3</sub>	17.48	455.3529	455.3531	0.4	11.4	-	26	betulinic acid
betulinic/oleanolic acid isomer	pentacyclic triterpenes	C <sub>30</sub> H <sub>48</sub> O <sub>3</sub>	17.65	455.3531	455.3531	0.0	6.1	-	-	-
oleanolic acid	pentacyclic triterpenes	C <sub>30</sub> H <sub>48</sub> O <sub>3</sub>	17.82	455.3528	455.3531	0.6	12.3	-	27	oleanolic acid

In many of the genotypes evaluated, the compounds annotated as oleuropein, verbascoside, elenolic acid glucoside (isomer C), demethyl oleuropein, lucidumoside C, ligstroside and oleoside/secologanoside (isomer C) were the peaks with the highest relative intensity in the profiles. Similarly, several oleuropein-, ligstroside-, and elenolic acid-derived compounds, such as oleuropein aglycone isomers, demethyl ligstroside and acyclodihydroelenolic acid hexoside (isomer B), were found to be relevant in the chromatographic profile of the *cuspidata* samples. The presence of oleuropein and ligstroside aglycones in the drupes is the consequence of the overexpression of the  $\beta$ -glucosidase enzyme, which is involved in the ripening mechanism [28]. In this case, two isomers of oleuropein aglycon and some of its derivatives (dehydro oleuropein aglycone A and B, hydroxy decarboxymethyl oleuropein aglycone, and 10-hydroxy oleuropein aglycon A and B) were detected in *cuspidata* samples, while ligstroside aglycones were not detected.

The second most numerous group of compounds was flavonoids. In this category, we found the following substances: rutins A and B, luteolin 7-O-glucoside, luteolin rutinoside, luteolin glucoside isomers A, B and C, apigenin 7-O-glucoside, luteolin and apigenin. Luteolin 7-O-glucoside and luteolin glucoside isomer B ( $m/z$  447.0937) and, in particular, rutin ( $m/z$  609.1463) were the most abundant ones.

Within the category of pentacyclic triterpenes, five compounds were identified: maslinic acid ( $m/z$  471.3479), betulinic acid ( $m/z$  455.3529), oleanolic acid ( $m/z$  455.3528), an isomer with  $m/z$  455.3531 and a monohydroxylated derivative of maslinic acid. These compounds have been previously reported by other authors in olive fruit tissues of subspecies *europaea* [23,33].

Substances belonging to the chemical classes of simple phenols and organic acids were also found in the LC-MS profiles of *cuspidata* genotypes. Regarding simple phenols (or similar compounds), three compounds were identified: hydroxytyrosol glucoside ( $m/z$  315.1081), oxydized hydroxytyrosol ( $m/z$  151.0395) and phenylethyl primeveroside ( $m/z$  415.1606). Organic acids were the most polar analytes of all those detected in the profiles, eluting at the beginning of the chromatogram. Within this category, quinic and citric acids were found in the samples. Only the first one ( $m/z$  191.0550) was remarkable due to its intensity in the profile.

Three other substances, which were found in the profiles with high relative intensities, could not be identified with confidence. The peak with  $m/z$  537.1605 ( $C_{25}H_{30}O_{13}$ ) was tentatively assigned to fraxamoside, considering that its presence has been recently described in Greek olives by Kritikou and co-authors [40]. The MS/MS analysis described in their work agreed with some of our *in-source* fragments ( $m/z$  323.0811 and 221.0273), which suggests that it could be the same compound they described. The second unknown peak was the one with  $m/z$  363.1440, which could be a compound related to ligstroside aglycone (the predicted molecular formula was  $C_{19}H_{24}O_7$ ), and the third one was the peak with  $m/z$  421.1494 and molecular formula  $C_{21}H_{26}O_9$ . Our hypothesis regarding the latter one is that it could be a secoiridoid derivative (oleuropein aglycone +  $C_2H_4O$

or ligstroside aglycone acetate). Some experiments are already in progress to be able to assign an identity to them in the near future.

## 2.2. Application of LC-MS for the quantitative evaluation of samples under study

From the identified compounds, a total of 27 metabolites were quantitatively assessed in the samples under study by using LC coupled to low-resolution (LR) MS (Figure 1). The choice of the compounds to be quantified was mainly based on: (1) the compounds having a higher prevalence (in terms of area and intensity; i.e., they are more abundant) in the chromatographic profiles, and (2) having an appropriate pure standard to perform a proper quantification. We decided to quantify three flavonoids (luteolin glucoside (isomer B), luteolin 7-*O*-glucoside and rutin (isomer B)), one organic acid (quinic acid), three pentacyclic triterpenes (betulinic, oleanolic and maslinic acids), sixteen secoiridoids (caffeoyl 6-secologanoside, dihydro oleuropein, dehydro nuzhenide,  $\beta$ -hydroxy verbascoside, neonuzhenida, methoxy oleuropein (isomer A), oleuropein aglycone isomers A and B, demethyl ligstroside, acyclodihydroelenolic acid hexoside (B), oleoside/secologanoside (isomer C), ligstroside, lucidumoside C (isomer A), demethyl oleuropein, elenolic acid glucoside (isomer C), verbascoside and oleuropein), one simple phenol (hydroxytyrosol glucoside) and two unknown compounds, with  $m/z$  of 363 and 421, respectively. Most of the secoiridoids and the two unknown compounds were quantified in terms of oleuropein.  $\beta$ -hydroxy verbascoside, verbascoside, caffeoyl 6-secologanoside and demethyl ligstroside were quantified by using the calibration curve obtained with the pure standard of verbascoside. This seemed appropriate because a relatively low area was found for the latter compounds in the samples under study. Hydroxytyrosol glucoside was quantified with the hydroxytyrosol standard, and luteolin glucoside in terms of its isomer luteolin 7-*O*-glucoside.

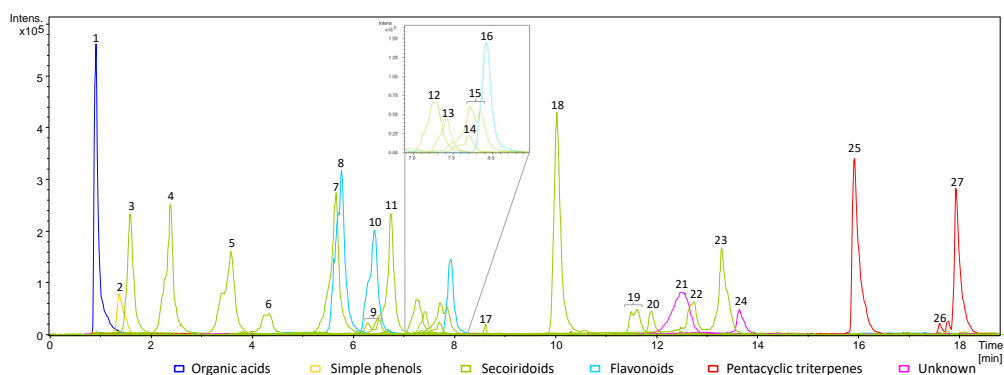


**Figure 1.** Example of the profile obtained for the extract of one cuspidata sample (316-6-G14) including the chromatograms of the extracted ions of the quantified metabolites. Colors have been used to indicate belonging to the different chemical categories of each numbered peak: organic acids (dark blue), simple phenols (yellow), secoiridoids (green), flavonoids (light blue), pentacyclic triterpenes (red) and unknown compounds (pink)

### 2.3. Comparison between *cuspidata* and cultivars fruits: Evaluating the potential of *cuspidata* phytochemical source to be included in olive breeding programs

#### 2.3.1. Fruit weight, oil content and total compounds of wild and cultivated olives

As expected, a highly significant correlation was found between fruit weight and oil content ( $r=0.80$ ,  $p<0.001$ ), with most *cuspidata* genotypes and their female parents, in the lower range of values for these two traits, respect to the four cultivars analyzed (Figure 2, upper left). The oil yield ranged from 10 to 45% approx. (fruit dry weight (%)) in *cuspidata* fruit, although most genotypes exhibited values between 10 and 25%. Similar contents were reported by Joshi and Gulfranz et al., ranging from about 20 to 28% for *Olea ferruginea* Royle in the north-west of India and from 33 to 39% in Pakistan, respectively [41,42]. Another study described lower values of oil yield by mill extraction for *Olea ferruginea* Royle from Pakistan, within the range from 11.1 to 12.5% [34]. A few *cuspidata* genotypes showed values for these two traits close to the ones obtained for the cultivars, which indicates that potentially interesting values for these attributes can be recovered in a single generation.

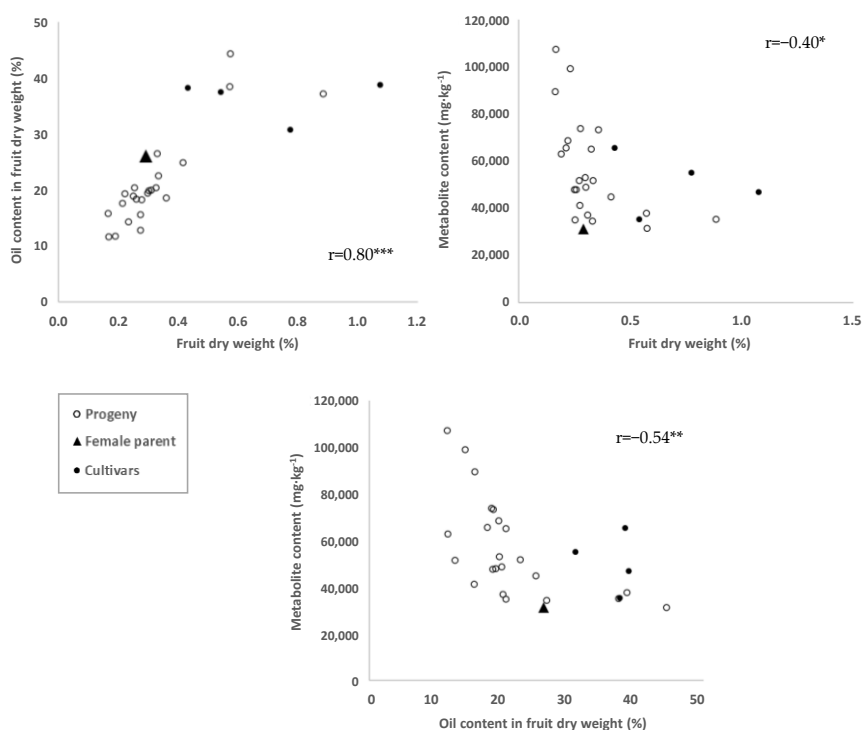


**Figure 2.** Evaluation of the relationships between fruit weight (g), oil content (%) and total metabolite content (mg·kg<sup>-1</sup>). \*, \*\*, \*\*\*: significant at  $p < 0.05$ , 0.01, 0.001, respectively

The relationship between fruit weight or oil content and total metabolite content (right and lower parts of Figure 2) was not so clear, even though a significant negative correlation was

observed in both cases. Similar results were obtained also for either individual components or different chemical categories (data not shown). Higher contents of some others minor compounds such as tocopherols, associated with concomitant lower values for fruit size and oil content has been also reported in non-cultivated olive plant materials [15]. Additionally, this negative relationship is always found with lower values for phenolic and other minor components as fruit size and oil content increase during fruit ripening [30,43].

### 2.3.2. Quantitative evaluation of the selected individual compounds and principal component analysis to explore the natural clustering of the samples

Table 3 presents a summary of the quantitative data. The quantitative data for each and every compound quantified in the progeny, the female parent and the cultivars have been included in Table S1 (Supplementary material). Two independent replicates of each *cuspidata* genotype and cultivar samples ( $n = 28 \times 2$  (*cuspidata*) and  $n = 4 \times 2$  (cultivars), respectively), injected twice, were used to obtain the final quantitative values.

As observed in Table 3, most of the 27 compounds selected to be quantified were determined in all the genotypes of the *cuspidata* progeny, with the exception of methoxy oleuropein, demethyl ligstroside, ligstroside and demethyl oleuropein, which were quantified in 27 samples; luteolin 7-O-glucoside and  $\beta$ -hydroxy verbascoside, which were determined in 26 samples; and verbascoside, which was only quantified in 18 wild olive fruit extracts. Metabolites that were not found in all samples of *O. europaea* subsp. *europaea* were  $\beta$ -hydroxy verbascoside, verbascoside and the unknown compound with  $m/z$  363, quantified in three of the four cultivars; methoxy oleuropein (A) and demethyl oleuropein, determined in two cultivars ("Arbequina" and "Frantoio"); and neonuzhenide and demethyl ligstroside, which were only quantified in "Frantoio".

The main differences between the pulp of *cuspidata* and *europaea* samples appeared to be associated with flavonoids, particularly rutin. It was the most abundant flavonoid in both types of samples, but its concentration in *cuspidata* was five times higher than in the cultivars. The organic acids and pentacyclic triterpenes exhibited similar concentrations in the two types of samples and simple phenols were higher in *cuspidata* pulp, but not by much. Although, in the secoiridoid family, verbascoside and oleuropein were the predominant metabolites for both progeny and conventional olives, some differences were observed.

Substances such as demethyl ligstroside, oleoside/secologanoside (C), ligstroside, lucidumoside C (A), demethyl oleuropein and elenolic acid glucoside (C) were consistently more abundant in wild olives, whereas, for instance, dihydro oleuropein, oleuropein aglycone (isomers A and B) and acyclodihydroelenolic acid hexoside (B) were, on average, more abundant in cultivars.

Figure 3 shows the quantitative distribution of some compounds in the samples of progeny, the female parent of open pollination progeny and the cultivars. In all cases, the x-axis shows the concentration in  $\text{g}\cdot\text{kg}^{-1}$  and the y-axis the frequency (the number of samples that exhibited concentrations in a given range); letters (to facilitate interpretation) indicate in which group the

female parent or the different cultivars fell. The range of variability for the *cuspidata* progeny markedly expands the value of their corresponding female parents for total metabolite contents, achieving, therefore, a huge improvement in one single generation. Cultivars showed intermediate ranges of total metabolite concentration, while the highest values were found for some *cuspidata* samples.

**Table 3.** Summary of the quantitative data obtained for the metabolites quantified in the *cuspidata* progeny and female parent, and the cultivars ("Arbequina", "Frantoio", "Koroneiki" and "Picual"). The compounds are ordered in the table by chemical classes and increasing concentrations in the progeny.

The N column indicates the number of times each compound was quantified in each group

Family	Compound	<i>cuspidata</i>			Cultivars		
		N	Mean*	C.V. (%)	N	Mean*	C.V. (%)
Flavonoids			7195	45		1750	53
	Luteolin glucoside (is B)	28	243	73	4	48	99
	Luteolin 7-O-glucoside	26	500	56	4	420	73
	Rutin (is B)	28	6452	50	4	1282	48
Organic acids	Quinic acid	28	12,316	24	4	13,024	19
			13,187	31		12,612	29
Pentacyclic triterpenes	Betulinic acid	28	43	76	4	15	43
	Oleanolic acid	28	3588	46	4	2804	38
	Maslinic acid	28	9556	27	4	9794	27
			19,950	85		23,233	54
Secoiridoids	Caffeoyl 6-secologanoside	28	127	119	4	261	71
	Dihydro oleuropein	28	151	56	4	755	79
	Dehydro nuzhenide	28	187	126	4	72	130
	$\beta$ -hydroxy verbascoside	26	231	125	3	84	108
	Neonuzhenide	28	241	68	1	322	M
	Methoxy oleuropein (is A)	27	267	84	2	30	4
	Oleuropein aglycone (is A)	28	418	136	4	1056	88
	Oleuropein aglycone (is B)	28	562	109	4	2014	51
	Demethyl ligstroside	27	994	127	1	592	M
	Acyclodihydroelenolic acid hexoside (is B)	28	1023	57	4	1499	23
	Oleoside/secologanoside (is C)	28	1123	66	4	314	89
	Ligstroside	27	1241	161	4	1012	84
	Lucidumoside C (is A)	28	1297	117	4	457	66
	Demethyl oleuropein	27	1797	103	2	639	99
	Elenolic acid glucoside (is C)	28	2012	57	4	1248	72
	Verbascoside	18	2044	76	3	2047	85
Oleuropein	28	6237	155	4	10831	88	
Simple phenols	Hydroxytyrosol glucoside	28	2196	73	4	1434	29
			1009	64		212	137
Unknowns	Unknown 1 ( <i>m/z</i> 363)	28	483	83	3	41	80
	Unknown 2 ( <i>m/z</i> 421)	28	526	93	4	171	89
			55,853	37		52,265	25
<b>Total</b>							

\*Mean is expressed as mg·kg<sup>-1</sup> of dry weight; is: isomer; M: not calculable

When the oleuropein histogram was studied in detail, it was noted that most of the wild progeny clustered together with their female parents in the lowest range of concentration,

although some exceptional genotypes showing high oleuropein contents were also obtained among the *cuspidata* progeny. Oleuropein aglycone (isomers A and B) prevailed in cultivars, especially in “Picual” and “Frantoio”; although there were some *cuspidata* samples that were richer than the cultivars, the most common situation was that the greatest number of genotypes fell into the lower concentration ranges (together with the female parent). Rutin showed a histogram quite different from those just discussed. “Arbequina”, “Frantoio”, “Koroneiki” and “Picual” exhibited the lowest concentrations; the female parent of the progeny, however, showed concentrations at least three times higher than those of the cultivars. Eleven genotypes had rutin levels equal to or higher than those of the female parent (reaching values of up to 14.1 g·kg<sup>-1</sup>) and all were substantially richer than the cultivars. The quinic acid content of the progeny appeared to be comparable to that of the cultivars ranging from 10.3 to 14.3 g·kg<sup>-1</sup> for 18 of the genotypes studied.

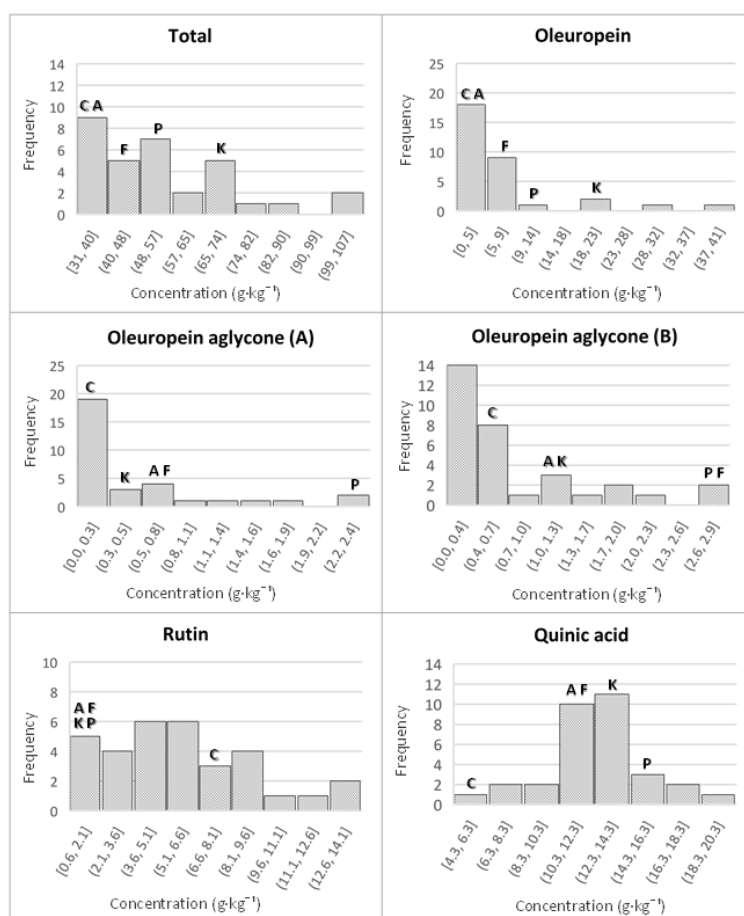


**Figure 3.** Histograms for total metabolite content and five specific compounds analyzed in the progeny (g·kg<sup>-1</sup>). The ranges in which the female parent and cultivars fall are indicated with letters as follows: female parent of the open pollination progeny -C; “Arbequina” cultivar -A; “Frantoio” cultivar -F; “Koroneiki” cultivar -K; “Picual” cultivar -P

Some of the details just mentioned were also revealed in the principal component analysis (PCA), which was used to perform a preliminary exploratory analysis of the variability between and within the groups of samples evaluated (Figure 4). The PCA scores plots obtained using the entire LC-MS quantitative data set are displayed in a two-dimensional plot using the first two principal components (left of Figure 4), which covered 24.0% and 15.0% of the total variance, respectively. The graph shows a quite clear separation among the cultivars and the genotypes from the progeny, although the *cuspidata* samples were spread over several areas of the plot, which would mean that a relatively wide range of variability was observed over the entire progeny. The right part of Figure 4 shows the loading plots of the PCA model. The meaning of the numbers assigned to each compound is shown in the figure caption; these were assigned considering the relative abundance (in decreasing order) in the progeny samples.

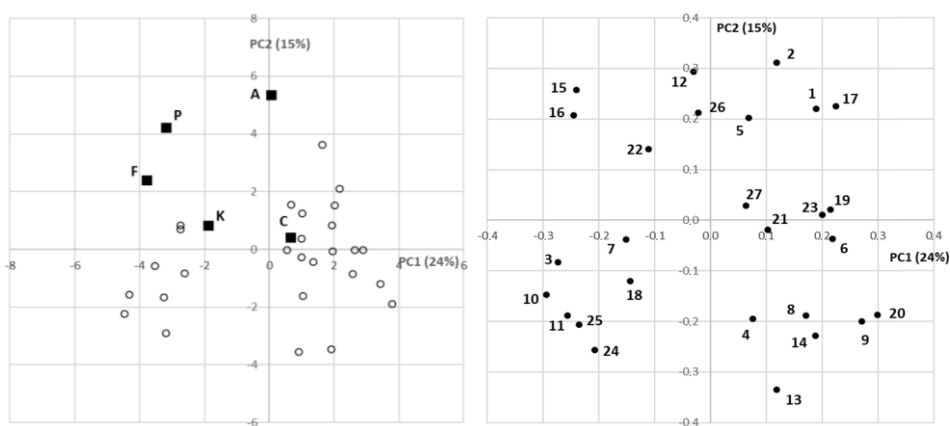


**Figure 4.** Scores (left) and loading (right) plots from PCA. Meaning of letters in the scores plot: female parent of the open pollination progeny -C; "Arbequina" cultivar -A; "Frantoio" cultivar -F; "Koroneiki" cultivar -K; "Picual" cultivar -P. Meaning of numbers in the loading plot: 1-quinic acid; 2-maslinic acid; 3-oleuropein; 4-rutin (B); 5-oleanolic acid; 6-hydroxytyrosol glucoside; 7-verbascoside; 8-elenolic acid glucoside (C); 9-demethyl oleuropein; 10-ligstroside; 11-lucidumoside C (A); 12-acyclodihydroelenolic acid hexoside (B); 13-oleoside/secologanoside (C); 14-demethyl ligstroside; 15-oleuropein aglycone (B); 16-oleuropein aglycone (A); 17-luteolin 7-*O*-glucoside; 18-unknown 2 (*m/z* 421); 19-unknown 1 (*m/z* 363); 20-methoxy oleuropein (A); 21-neonuzhenide; 22-dihydro oleuropein; 23-luteolin glucoside (B); 24- $\beta$ -hydroxy verbascoside; 25-dehydro nuzhenide; 26-caffeoyl 6-secologanoside; 27-betulinic acid

PC1 correlated positively, mainly, with hydroxytyrosol glucoside, unknown 1 (*m/z* 363), neonuzhenide, luteolin glucoside (B) and betulinic acid, and negatively with oleuropein and verbascoside. PC2 was positively related to oleanolic acid, acyclodihydroelenolic acid hexoside (B) and caffeoyl 6-secologanoside, among other compounds.

In view of the loading plot, it can be stated that five secoiridoids are able to define a fairly typical pattern for samples of *O. europaea* subsp. *europaea*, with these substances being the

following: dihydro oleuropein, acyclodihydroelenolic acid hexoside (B), caffeoyl 6-secologanoside and isomers A and B of oleuropein aglycone.

### 2.3.3. Quantitative results structured by chemical classes

In this section, we intend to discuss the results considering the different families of metabolites that were determined, i.e., flavonoids, organic acids, triterpenes, secoiridoids, simple phenols and unknowns. For this purpose, Figure 5 shows a graph describing the compositional pattern of each sample according to the percentage that each family of compounds represents with respect to the total concentration of metabolites (with all values normalized to the maximum metabolite concentration found for each sample).

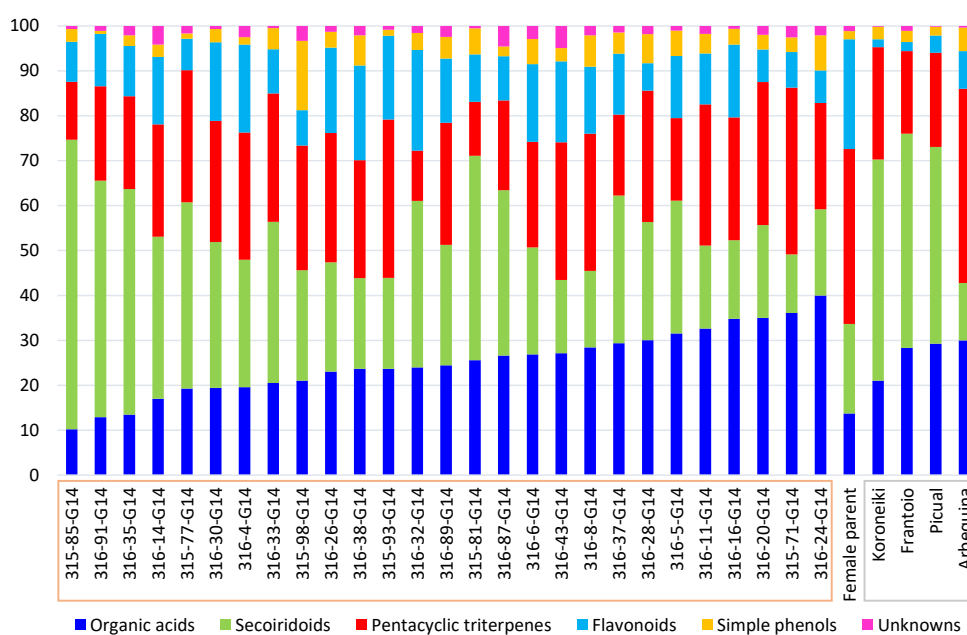


**Figure 5.** Description of the compositional pattern of each sample according to the percentage that each family of compounds represents with respect to the total concentration of metabolites (with all values normalized to the maximum metabolite concentration found for each sample). All the samples of the progeny are on the left side of the graphic (G-14) and the female parent in between the progeny and cultivars

“Koroneiki”, “Frantoio” and “Picual” seem to have a percentage distribution of the different chemical classes quite comparable to each other. “Arbequina” was not found to have a very similar compositional distribution to the other cultivars, showing the highest percentage of simple phenols (5.3%), pentacyclic acids (43.3%) and flavonoids (8.4%).

The relative abundance of the different families of compounds in the female parent is not comparable with any of the cultivars. A great content of flavonoids (6.1-22.4%) was observed in the progeny, although none of the evaluated *cuspidata* genotypes exceeded the percentage of

flavonoids found in the female parent (24.4%). Simple phenols and pentacyclic triterpenes ranged from 0.7 to 15.4% and 11.2 to 37.2%, respectively, in the wild olive extracts. Organic acids and secoiridoids showed the highest overall and maximum percentages in the genotypes of the progeny, ranging from 10.2 to 40.0% and 13.0 to 64.5%, respectively. It would be possible to establish a hypothetical correlation between these two families, since, in general, the lower the percentage of quinic acid in a sample, the higher the percentage of secoiridoids found.

#### **2.3.4. Preliminary exploration of metabolic pathways: Cross-correlation of the secondary metabolites determined in the progeny**

The metabolic biosynthesis pathways in olive matrices are exceptionally complex. A great diversity in the structures and dynamic transformations of compounds are found during development, ripening, harvesting or olive oil extraction. Different pathways, including the shikimate, phenylpropanoid, mevalonate and flavonoid pathways, have been described as the basis for producing several precursors of phenolic compounds. Briefly, the shikimate pathway consists of the condensation of phosphoenolpyruvic acid and erythrose-4-phosphate to synthesize 3-dehydroquinic acid, which is transformed into shikimic acid. The final metabolite known as chorismic acid is synthesized in subsequent reactions and is a key branch point for the formation of L-Phenylalanine, which is the substrate of phenylpropanoid and flavonoid pathways [44]. Secoiridoids, the main iridoids found in Oleaceae, are biosynthesized by the mevalonate pathway from deoxylorganic acid. The connection of secoiridoids to the shikimate pathway is provided by two simple phenols (tyrosol and hydroxytyrosol) synthesized in the phenylpropanoid pathway [45–47]. For example, oleuropein is synthesized from hydroxytyrosol, which in turn is also related to ligstroside.

A cross-correlation for the metabolites determined in the progeny is shown in [Table 4](#); it was carried out to evaluate whether a certain metabolic relationship could be established between some of the compounds under study in the present investigation. This table shows a positive significant correlation ( $p < 0.001$ ) between luteolin glucoside and luteolin 7-O-glucoside, as well as oleuropein aglycones A and B, respectively. A balance in the synthesis of isomeric compounds could be the most plausible reason for these correlations. Likewise, a dynamic interconversion between some secoiridoids could be the cause of the significant positive correlation ( $p < 0.001$ ) highlighted for some compounds in the cross-correlation table. The correlation noted in this table between dimethyl oleuropein and the unknown  $m/z$  363 leads us to think that this compound could be a secoiridoid. Since its predicted molecular formula is  $C_{19}H_{24}O_7$ , we hypothesize that it is a substance possibly related to ligstroside aglycone (perhaps with one less double bond).

In addition, quinic acid showed strong and inverse correlations ( $p < 0.001$ ) with oleuropein and lucidumoside C (isomer A). Both quinic and shikimic acids have been described as precursors in the biosynthesis of several aromatic natural products in the shikimate pathway [48]. In this pathway, a reversible reduction of 3-dehydroquinic acid by quinic acid dehydrogenase occurs to

produce quinic acid as a secondary metabolite [44]. Thus, a high content of quinic acid in olive fruit would lead to a lower amount of chorismic acid and L-phenylalanine and, consequently, a lesser amount of hydroxytyrosol. The biosynthesis of secoiridoids is interrelated with simple phenols, such as hydroxytyrosol, and their low availability could lead to a reduced formation of oleuropein and lucidumoside C. All these significant correlations among metabolites could be also inferred from the previously shown loading plot of PCA. Subsequent studies should, however, test this hypothesis.

### 3. MATERIALS AND METHODS

#### 3.1. Plant materials

The used materials included olive fruits from 27 *cuspidata* genotypes coming from free pollination and their corresponding female parent. In addition, fruit samples from the cultivars "Arbequina", "Frantoio", "Picual" and "Koroneki" were also included in the experiment for comparison. The genotype acting as the female parent belongs to the wild olive Germplasm Bank preserved at the Institute of Agricultural and Fishery Research and Training, Córdoba, Spain [49]. Fruit samples (around 1 kg) were randomly collected for each plant on a common date (mid-October).

#### 3.2. Chemicals and reagents

All the reagents were of analytical grade or LC-MS and used as received in the laboratory. Ethanol (EtOH) (in aqueous mixtures) was the solvent used for metabolite extraction and was supplied by Prolabo (Paris, France). Mobile phases were prepared using doubly deionized water with a conductivity of 18.2 M $\Omega$  obtained by using a Milli-Q system (Millipore, Bedford, USA) (phase A) and LC-MS-grade acetonitrile (ACN) from Prolabo (Paris, France) (phase B) acidified with acetic acid (AcH), supplied by Sigma-Aldrich (St. Louis, Missouri, USA). Pure standards of organic acids (quinic acid), phenolic compounds (vanillin, *p*-coumaric acid, ferulic acid, hydroxytyrosol, tyrosol, rutin, oleuropein, luteolin, luteolin 7-*O*-glucoside, verbascoside, apigenin, apigenin 7-*O*-glucoside and pinoresinol) and pentacyclic triterpenes (maslinic, betulinic and oleanolic acids, erythrodiol and uvaol) were acquired from Sigma-Aldrich (St. Louis, USA). A stock solution was prepared by dissolving an appropriate amount of each metabolite in EtOH/H<sub>2</sub>O (80:20 v/v) and then different dilutions were prepared to obtain diverse concentration ranges for each individual compound. All the sample extracts and standard solutions were filtered through Clarinet™ 0.22  $\mu$ m nylon syringe filters acquired from Bonna-Agela Technologies (Wilmington, DE, USA). Mobile phases were filtered through a Nylaflo™ 0.45  $\mu$ m nylon membrane filter supplied by Pall Corporation (Michigan, USA). All the solutions were stored in dark flasks at -23 °C.

**Table 4.** Cross-correlation of secondary metabolites quantified in the progeny. Significant correlations at  $p < 0.001$  are highlighted

Maslinic acid	Oleuropein	Rutin (B)	Oleanolic acid	Hydroxytyrosol glucoside	Verbascoide	Elenolic acid glucoside (C)	Demethyl oleuropein	Ligstroside	Lucidumoside C (A)	Acylodihydroelenolic acid hexoside (B)	Oleoside/secologanoside (C)	Demethyl ligstroside	Oleuropein aglycone (B)	Oleuropein aglycone (A)	Luteolin 7-O-glucoside	Unknown 2 (m/z 421)	Unknown 1 (m/z 363)	Methoxy oleuropein (A)	Neonuzhenide	Dihydro oleuropein	Luteolin glucoside (B)	$\beta$ -hydroxy verbascoide	Dehydro nuzhenide	Caffeoyl 6-secologanoside	Betulinic acid		
0.20	<b>-0.61</b>	-0.28	0.18	0.28	-0.14	0.27	0.20	-0.58	<b>-0.69</b>	0.28	-0.30	0.09	-0.09	-0.13	0.22	-0.23	0.31	0.19	0.07	0.04	0.04	-0.20	-0.32	0.10	-0.22	Quinic acid	
	-0.48	0.09	0.69	0.00	-0.27	-0.45	-0.14	-0.34	-0.38	0.22	-0.31	-0.10	0.07	-0.01	0.53	-0.15	0.12	-0.05	-0.01	-0.15	0.17	-0.29	-0.32	0.14	0.44	Maslinic acid	
		-0.27	-0.43	-0.42	0.00	-0.17	-0.39	0.65	0.62	-0.14	-0.06	-0.29	0.28	0.35	-0.48	0.05	-0.38	-0.41	-0.03	0.23	-0.33	0.05	0.12	0.12	-0.14	Oleuropein	
			0.04	-0.14	-0.06	-0.17	-0.01	-0.01	0.11	-0.36	0.29	0.01	-0.43	-0.38	0.22	0.25	0.05	0.10	0.04	-0.43	0.42	0.08	0.17	-0.25	0.44	Rutin (B)	
				0.06	-0.24	-0.38	-0.24	-0.21	-0.16	0.24	-0.22	-0.19	-0.09	-0.02	0.13	0.18	0.27	-0.03	-0.26	-0.39	0.08	0.07	-0.06	0.07	0.41	Oleanolic acid	
					-0.17	0.28	0.37	-0.45	-0.46	0.01	0.40	0.15	-0.26	-0.25	0.15	-0.20	0.44	0.42	0.03	-0.12	0.20	-0.15	-0.20	-0.21	0.41	Hydroxytyrosol glucoside	
						0.02	-0.08	0.16	-0.04	-0.04	0.01	-0.18	0.52	0.18	-0.11	0.12	-0.42	-0.33	-0.05	0.48	-0.33	0.61	0.63	0.19	-0.32	Verbascoide	
							0.57	-0.25	-0.15	-0.04	0.28	0.39	-0.41	-0.43	0.01	-0.26	0.14	0.55	0.34	0.00	0.07	-0.13	-0.12	-0.06	-0.35	Elenolic acid glucoside (C)	
								-0.50	-0.47	-0.29	0.41	<b>0.77</b>	-0.38	-0.49	0.20	-0.40	0.15	<b>0.85</b>	0.06	0.03	0.16	-0.37	-0.36	-0.09	-0.14	Demethyl oleuropein	
									0.64	-0.11	-0.12	-0.34	0.16	0.15	-0.56	0.22	-0.41	-0.56	-0.24	0.05	-0.38	0.33	0.38	-0.13	-0.13	Ligstroside	
										-0.13	0.16	-0.37	0.07	0.35	-0.43	0.45	-0.24	-0.39	0.02	-0.24	-0.13	0.32	0.41	0.00	-0.03	Lucidumoside C (A)	
											-0.42	-0.30	0.31	0.27	0.09	0.08	0.19	-0.24	-0.19	0.29	-0.10	-0.07	-0.15	0.07	-0.11	Acylodihydroelenolic acid hexoside (B)	
												0.17	-0.46	-0.35	0.00	0.14	0.40	0.39	0.11	-0.30	0.12	0.01	0.09	-0.31	0.01	Oleoside/secologanoside (C)	
													-0.27	-0.39	0.17	-0.25	0.20	0.69	-0.02	0.04	0.11	-0.27	-0.23	-0.16	-0.02	Demethyl ligstroside	
														<b>0.79</b>	-0.11	0.01	-0.50	-0.56	-0.14	0.66	-0.30	0.14	0.18	0.30	-0.10	Oleuropein aglycone (B)	
															-0.14	0.12	-0.43	-0.56	-0.24	0.23	-0.19	0.16	0.20	0.24	-0.14	Oleuropein aglycone (A)	
																-0.38	0.15	0.10	0.32	-0.16	<b>0.71</b>	-0.41	-0.42	0.09	0.18	Luteolin 7-O-glucoside	
																	0.10	-0.25	-0.22	-0.12	-0.15	0.37	0.46	-0.09	0.20	Unknown 2 (m/z 421)	
																		<b>0.34</b>	0.19	-0.20	0.23	-0.34	-0.38	0.13	0.05	Unknown 1 (m/z 363)	
																			0.24	-0.13	0.15	-0.44	-0.44	0.07	0.17	Methoxy oleuropein (A)	
																				0.13	0.17	-0.30	-0.25	0.30	-0.07	Neonuzhenide	
																						-0.32	-0.08	-0.01	0.19	-0.18	Dihydro oleuropein
																							-0.37	-0.29	-0.04	0.28	Luteolin glucoside (B)
																								<b>0.98</b>	-0.20	-0.14	$\beta$ -hydroxy verbascoide
																									-0.25	-0.08	Dehydro nuzhenide
																										-0.14	Caffeoyl 6-secologanoside

### 3.3. Fruit weight and oil content

From each sample, three subsamples of around 25 g were randomly selected to produce dried samples sizes suitable for NMR sample holder. Fruit fresh weight was measured and, after drying in a forced-air oven at 105 °C for 42 h to ensure dehydration, oil content was determined using an NMR fat analyzer (Minispec MQone, Bruker Optik GmbH, Ettlingen, Germany) and expressed as a percentage on a dry weight basis [50].

### 3.4. Extraction and LC-MS analysis of fruit metabolites

A representative sample of 50 fruits were destoned and the pulp was chopped, lyophilized and crushed to a fine powder and frozen at -23 °C. The applied metabolite-extraction procedure was the one previously reported by Olmo-García and colleagues [33,51], with a few modifications. Briefly, sample extracts were prepared by mixing 0.2 g of freeze-dried and homogenized pulp with 10 mL of EtOH/H<sub>2</sub>O (60:40, v/v) in a 15 mL falcon tube. After 1 min of vortex shaking, the tube was put into an ultrasound bath for 30 min and centrifuged for 5 min at 8000 rpm. Once the two phases were separated, the supernatant was transferred to a flask. The pellet was re-extracted twice by adding 10 mL of EtOH/H<sub>2</sub>O (80:20, v/v), applying, in both cases, the same procedure as in the first extraction. The use of EtOH/H<sub>2</sub>O mixtures in varying proportions ensured the effective extraction of the compounds of interest belonging to different chemical classes. All the supernatants (coming from the 3 extraction cycles) were mixed and about 1 mL of sample extract was placed in an HPLC vial after being filtered with a nylon syringe filter of 0.22 µm.

Two different LC-MS platforms were used in this study. The LC-MS system with a HRMS analyzer was used for qualitative purposes, whereas the LC platform coupled to an LR-MS was used to carry out the quantitation of the analytes of interest. For qualitative purposes, the used LC-MS platform consisted of an Acquity UPLC™ H-Class system coupled to a quadrupole-time-of-flight (QTOF) SYNAPT G2 MS (Waters, Manchester, UK). This instrument provided an accurate mass and the isotopic pattern which allowed us to predict the molecular formulae of the detected compounds, which greatly facilitates compound annotation and the identification of unknown peaks in complex matrices. Thus, the analysis of samples with HRMS helped us to describe the qualitative profiles of the samples under study. Afterwards, quantitative analyses were performed on a 1260 Infinity Agilent (Agilent Technologies, Waldbronn, Germany) coupled to an Esquire 2000 ion trap (IT) mass spectrometer (Bruker Daltonics, Bremen, Germany), which allowed us to quantify the targeted compounds by using standard calibration curves. Both MS instruments were equipped with an electrospray (ESI) interface. The selected column was an analytical Zorbax Extend C<sub>18</sub> column (4.6 × 100 mm; 1.8 µm particle size) working at 40 °C. Water with 1% AcH (v/v) (phase A) and ACN with 1% AcH (v/v) (phase B) were used as mobile phases. A solvent gradient was applied for the separation of analytes and the mobile phase composition changed as follows: 0 min, 90% A and 10% B; 10 min, 75% A and 25% B; 12 min, 40% A and 60% B; 14 min, 20%A and 80%B; 18 min, 0%A and 100%B. At 20 min, the system returned to the initial conditions and the

column was re-equilibrated for 3 min. The flow rate was kept constant at 1 mL/min and the injection volume was set at 10  $\mu$ L. The IT MS data were acquired in full-scan mode for a mass range from 50 to 1000  $m/z$  and the system was operated in the negative polarity mode. As far as the ESI source is concerned, the operating parameters were as follows: the nebulizer gas (nitrogen) was set at 30 psi, the dry gas flow rate was fixed at 9 L/min and dry gas temperature at 300 °C, the capillary voltage was set at +3200 V and the end-plate offset at -500 V. For HRMS analyses, these parameters were transferred to the ESI-QTOF MS system.

To operate the LC and the LR-MS systems, the Agilent ChemStation (Agilent Technologies) and Esquire Control (Bruker Daltonics) were used, respectively. The HRMS platform was controlled by means of MassLynx (Waters). The data processing was performed by using DataAnalysis v 4.0 software (Bruker Daltonics, Bremen, Germany) and Microsoft Excel v 2204.

### 3.5. Statistical analysis

The variability for the metabolites quantified in the *cuspidata* progeny and the cultivars ("Arbequina", "Frantoio", "Koroneiki" and "Picual") was studied. Correlations between fruit weight, oil content and total metabolite content as well as the cross-correlation for the metabolites quantified in the progeny were evaluated. Principal component analysis (PCA) was performed to test the relations among the different phenolic and triterpenic compounds as well as samples' grouping by genotype. Statistix (Analytical Software, Tallahassee, FL, USA) and Unscrambler (CAMO A/S, Trondheim, Norway) were used for the statistical analysis.

## 4. CONCLUSIONS

This contribution presents the first in-depth characterization (qualitatively and quantitatively) of fruit samples from *Olea europaea* subsp. *cuspidata*. By means of a powerful LC-MS method, about 60 compounds were identified and the most representative ones were quantified. The metabolic profiles of a progeny bred through the open pollination of *cuspidata* were compared with those of a sample of cultivars, showing that the genotypes from the progeny, overall, were richer in bioactive compounds than the cultivars and, particularly, in terms of the concentrations of rutin, hydroxytyrosol glucoside, several interesting secoiridoids and the compounds of  $m/z$  421 and 363. These results suggest that the inclusion of *cuspidata* could be very interesting for the introgression of potentially interesting compounds in breeding programs. Studies such as this one make it possible to take advantage of the potential of food metabolomics for the identification and maintenance of olive genetic diversity.

**Funding:** This research was funded by FEDER/Junta de Andalucía-Consejería de Transformación Económica, Industria, Conocimiento y Universidades, Proyecto P20\_00263; FEDER/Junta de Andalucía-Consejería de Economía y Conocimiento, Proyecto B-AGR-416-UGR18; Andalusian Institute of Agricultural and Fisheries Research and Training (IFAPA), grant number AVA2019.027,

and European Regional Development Fund. I.S.-G. is grateful to the Spanish Ministry of Science and Innovation for the support received through the FPU grant (Grant number: FPU19/00700).

## References

- Green, P.S. A Revision of *Olea* L. (Oleaceae). *Kew Bull.* **2002**, *57*, 91–140, doi:10.2307/4110824.
- Besnard, G.; Henry, P.; Wille, L.; Cooke, D.; Chapuis, E. On the Origin of the Invasive Olives (*Olea Europaea* L., Oleaceae). *Heredity.* **2007**, *99*, 608–619, doi:10.1038/sj.hdy.6801037.
- Kassa, A.; Konrad, H.; Geburek, T. Molecular Diversity and Gene Flow within and among Different Subspecies of the Wild Olive (*Olea Europaea* L.): A Review. *Flora* **2019**, *250*, 18–26, doi:10.1016/j.flora.2018.11.014.
- Kaniewski, D.; Van Campo, E.; Boiy, T.; Terral, J.F.; Khadari, B.; Besnard, G. Primary Domestication and Early Uses of the Emblematic Olive Tree: Palaeobotanical, Historical and Molecular Evidence from the Middle East. *Biol. Rev.* **2012**, *87*, 885–899, doi:10.1111/j.1469-185X.2012.00229.x.
- Besnard, G.; Khadari, B.; Navascués, M.; Fernández-Mazuecos, M.; Bakkali, A. El; Arrigo, N.; Baali-Cherif, D.; Brunini-Bronzini de Caraffa, V.; Santoni, S.; Vargas, P.; et al. The Complex History of the Olive Tree: From Late Quaternary Diversification of Mediterranean Lineages to Primary Domestication in the Northern Levant. *Proc. R. Soc. B Biol. Sci.* **2013**, *280*, 20122833, doi:10.1098/rspb.2012.2833.
- Breton, C.; Tersac, M.; Bervillé, A. Genetic Diversity and Gene Flow between the Wild Olive (*Oleaster*, *Olea Europaea* L.) and the Olive: Several Plio-Pleistocene Refuge Zones in the Mediterranean Basin Suggested by Simple Sequence Repeats Analysis. *J. Biogeogr.* **2006**, *33*, 1916–1928, doi:10.1111/j.1365-2699.2006.01544.x.
- FAO Statistics Division of Food and Agriculture Organization of the United Nations (FAOSTAT). Available online: <http://www.fao.org/faostat/es/#data/QC> (accessed on 10 December 2021).
- Hannachi, H.; Sommerlatte, H.; Breton, C.; Msallem, M.; El Gazzah, M.; Ben El Hadj, S.; Bervillé, A. *Oleaster* (Var. *Sylvestris*) and Subsp. *Cuspidata* Are Suitable Genetic Resources for Improvement of the Olive (*Olea Europaea* Subsp. *Europaea* Var. *Europaea*). *Genet. Resour. Crop Evol.* **2009**, *56*, 393–403, doi:10.1007/s10722-008-9374-2.
- Long, H.S.; Tilney, P.M.; Van Wyk, B.E. The Ethnobotany and Pharmacognosy of *Olea Europaea* Subsp. *Africana* (Oleaceae). *South African J. Bot.* **2010**, *76*, 324–331, doi:10.1016/j.sajb.2009.12.005.
- Aerts, R.; Negussie, A.; Maes, W.; November, E.; Hermy, M.; Muys, B. Restoration of Dry Afromontane Forest Using Pioneer Shrubs as Nurse-Plants for *Olea Europaea* Ssp. *Cuspidata*. *Restor. Ecol.* **2007**, *15*, 129–138, doi:10.1111/j.1526-100X.2006.00197.x.
- Caceres, M.E.; Pupilli, F.; Sarri, V.; Mencuccini, M.; Ceccarelli, M. Floral Biology in *Olea Europaea* Subsp. *Cuspidata*: A Comparative Structural and Functional Characterization. *Flora* **2016**, *222*, 27–36, doi:10.1016/j.flora.2016.03.006.
- Rallo, L.; Barranco, D.; Díez, C.M.; Rallo, P.; Suárez, M.P.; Trapero, C.; Pliego-Alfaro, F. Strategies for Olive (*Olea Europaea* L.) Breeding: Cultivated Genetic Resources and Crossbreeding. In *Advances in Plant Breeding Strategies: Fruits*; Al-Khayri, J.M., Jain, S.M., Johnson, D.V., Eds.; Springer International Publishing, 2018; Vol. 3, pp. 535–600, doi:10.1007/978-3-319-91944-7\_14.
- Rallo, L. Looking towards Tomorrow in Olive Growing: Challenges in Breeding. *Acta Hort.* **2014**, *1057*, 467–481, doi:10.17660/ActaHortic.2014.1057.59.
- Diraman, H.; Karaman, H.T.; Sefer, F.; Ersoy, N.; Arsel, A.H. Using Nutritional Lipid and Sensorial Profiles for the Characterization of Turkish Olive (Memecik X Gemlik Cv) Hybrids Obtained from Controlled Crossbreeding. *J. Am. Oil Chem. Soc.* **2020**, *97*, 943–954, doi:10.1002/aocs.12363.

15. León, L.; De La Rosa, R.; Velasco, L.; Belaj, A. Using Wild Olives in Breeding Programs: Implications on Oil Quality Composition. *Front. Plant Sci.* **2018**, *9*, 1–9, doi:10.3389/fpls.2018.00232.
16. De la Rosa, R.; Arias-Calderón, R.; Velasco, L.; León, L. Early Selection for Oil Quality Components in Olive Breeding Progenies. *Eur. J. Lipid Sci. Technol.* **2016**, *118*, 1160–1167, doi:10.1002/ejlt.201500425.
17. Arias-Calderón, R.; Rodríguez-Jurado, D.; León, L.; Bejarano-Alcázar, J.; De la Rosa, R.; Belaj, A. Pre-Breeding for Resistance to Verticillium Wilt in Olive: Fishing in the Wild Relative Gene Pool. *Crop Prot.* **2015**, *75*, 25–33, doi:10.1016/j.cropro.2015.05.006.
18. Pérez, A.G.; León, L.; Sanz, C.; de la Rosa, R. Fruit Phenolic Profiling: A New Selection Criterion in Olive Breeding Programs. *Front. Plant Sci.* **2018**, *9*, 241, doi:10.3389/fpls.2018.00241 Olive.
19. Ghanbari, R.; Anwar, F.; Alkharfy, K.M.; Gilani, A.H.; Saari, N. Valuable Nutrients and Functional Bioactives in Different Parts of Olive (*Olea Europaea* L.)-A Review. *Int. J. Mol. Sci.* **2012**; *13*, 3291–3340, doi:10.3390/ijms13033291.
20. Servili, M.; Selvaggini, R.; Esposito, S.; Taticchi, A.; Montedoro, G.F.; Morozzi, G. Health and Sensory Properties of Virgin Olive Oil Hydrophilic Phenols: Agronomic and Technological Aspects of Production That Affect Their Occurrence in the Oil. *J. Chromatogr. A* **2004**, *1054*, 113–127, doi:10.1016/j.chroma.2004.08.070.
21. Romani, A.; Ieri, F.; Urciuoli, S.; Noce, A.; Marrone, G.; Nediani, C.; Bernini, R. Health Effects of Phenolic Compounds Found in Extra-Virgin Olive Oil, By-Products, and Leaf of *Olea Europaea* L. *Nutrients* **2019**, *11*, doi:10.3390/nu11081776.
22. Sultana, N.; Ata, A. Oleanolic Acid and Related Derivatives as Medicinally Important Compounds. *J. Enzyme Inhib. Med. Chem.* **2008**, *23*, 739–756, doi:10.1080/14756360701633187.
23. Guinda, Á.; Rada, M.; Delgado, T.; Gutiérrez-Adánez, P.; Castellano, J.M. Pentacyclic Triterpenoids from Olive Fruit and Leaf. *J. Agric. Food Chem.* **2010**, *58*, 9685–9691, doi:10.1021/jf102039t.
24. Sánchez-Quesada, C.; López-Biedma, A.; Warleta, F.; Campos, M.; Beltrán, G.; Gaforio, J.J. Bioactive Properties of the Main Triterpenes Found in Olives, Virgin Olive Oil, and Leaves of *Olea Europaea* L. *J. Agric. Food Chem.* **2013**, *61*, 12173–12182, doi:10.1021/jf403154e.
25. Azadmard-Damirchi, S.; Dutta, P.C. Phytosterols Classes in Olive Oils and Their Analysis by Common Chromatographic Methods. In *Olives and Olive Oil in Health and Disease Prevention*; Preedy, V.R., Watson, R.R., Eds.; Elsevier Inc., 2010; pp. 249–258, doi:10.1016/B978-0-12-374420-3.00027-9.
26. Shahidi, F.; De Camargo, A.C. Tocopherols and Tocotrienols in Common and Emerging Dietary Sources: Occurrence, Applications, and Health Benefits. *Int. J. Mol. Sci.* **2016**, *17*, 1–29, doi:10.3390/ijms17101745.
27. Obied, H.K.; Bedgood Jr, D.R.; Prenzler, P.D.; Robards, K. Chemical Screening of Olive Biophenol Extracts by Hyphenated Liquid Chromatography. *Anal. Chim. Acta* **2007**, *603*, 176–189, doi:10.1016/j.aca.2007.09.044.
28. Kanakis, P.; Termentzi, A.; Michel, T.; Gikas, E.; Halabalaki, M.; Skaltsounis, A.L. From Olive Drupes to Olive Oil: An HPLC-Orbitrap-Based Qualitative and Quantitative Exploration of Olive Key Metabolites. *Planta Med.* **2013**, *79*, 1576–1587, doi:10.1055/s-0033-1350823.
29. Dagdelen, A.; Tümen, G.; Özcan, M.M.; Dündar, E. Phenolics Profiles of Olive Fruits (*Olea Europaea* L.) and Oils from Ayvalik, Domat and Gemlik Varieties at Different Ripening Stages. *Food Chem.* **2013**, *136*, 41–45, doi:10.1016/j.foodchem.2012.07.046.
30. Talhaoui, N.; Gómez-Caravaca, A.M.; León, L.; De La Rosa, R.; Fernández-Gutiérrez, A.; Segura-Carretero, A. Pattern of Variation of Fruit Traits and Phenol Content in Olive Fruits from Six Different Cultivars. *J. Agric. Food Chem.* **2015**, *63*, 10466–10476, doi:10.1021/acs.jafc.5b04315.
31. Jerman Klen, T.; Golc Wondra, A.; Vrhovšek, U.; Mozetič Vodopivec, B. Phenolic Profiling of Olives and Olive Oil Process-Derived Matrices Using UPLC-DAD-ESI-QTOF-HRMS Analysis. *J. Agric. Food Chem.*

- 2015, 63, 3859–3872, doi:10.1021/jf506345q.
32. Bodoira, R.; Torres, M.; Pierantozzi, P.; Taticchi, A.; Servili, M.; Maestri, D. Oil Biogenesis and Antioxidant Compounds from “ Arauco ” Olive ( *Olea Europaea* L.) Cultivar during Fruit Development and Ripening. *Eur. J. Lipid Sci. Technol.* **2015**, 377–388, doi:10.1002/ejlt.201400234.
  33. Olmo-García, L.; Kessler, N.; Neuweger, H.; Wendt, K.; Olmo-Peinado, J.M.; Fernández-Gutiérrez, A.; Baessmann, C.; Carrasco-Pancorbo, A. Unravelling the Distribution of Secondary Metabolites in *Olea Europaea* L.: Exhaustive Characterization of Eight Olive-Tree Derived Matrices by Complementary Platforms (LC-ESI/APCI-MS and GC-APCI-MS). *Molecules* **2018**, 23, 2419, doi:10.3390/molecules23102419.
  34. Anwar, P.; Bendini, A.; Gulfranz, M.; Qureshi, R.; Valli, E.; Di Lecce, G.; Naqvi, S.M.S.; Gallina Toschi, T. Characterization of Olive Oils Obtained from Wild Olive Trees (*Olea Ferruginea* Royle) in Pakistan. *Food Res. Int.* **2013**, 54, 1965–1971, doi:10.1016/j.foodres.2013.09.029.
  35. Baccouri, B.; Guerfel, M.; Zarrouk, W.; Taamalli, W.; Daoud, D.; Zarrouk, M. Wild Olive (*Olea Europaea* L.) Selection for Quality Oil Production. *J. Food Biochem.* **2011**, 35, 161–176, doi:10.1111/j.1745-4514.2010.00373.x.
  36. Baccouri, B.; Zarrouk, W.; Baccouri, O.; Guerfel, M.; Nouairi, I.; Krichene, D.; Daoud, D.; Zarrouk, M. Composition, Quality and Oxidative Stability of Virgin Olive Oils from Some Selected Wild Olives (*Olea Europaea* L. Subsp. *Oleaster*). *Grasas Y Aceites* **2008**, 59, 346–351, doi:10.3989/gya.2008.v59.i4.528.
  37. Bouarroudj, K.; Tamendjari, A.; Larbat, R. Quality, Composition and Antioxidant Activity of Algerian Wild Olive (*Olea Europaea* L. Subsp. *Oleaster*) Oil. *Ind. Crops Prod.* **2016**, 83, 484–491, doi:10.1016/j.indcrop.2015.12.081.
  38. Dabbou, S.; Dabbou, S.; Selvaggini, R.; Urbani, S.; Taticchi, A.; Servili, M.; Hammami, M. Comparison of the Chemical Composition and the Organoleptic Profile of Virgin Olive Oil from Two Wild and Two Cultivated Tunisian *Olea Europaea*. *Chem. Biodivers.* **2011**, 8, 189–202, doi:10.1002/cbdv.201000086.
  39. Rodrigues, N.; Pinho, T.; Casal, S.; Peres, A.M.; Baptista, P.; Pereira, J.A. Chemical Characterization of *Oleaster*, *Olea Europaea* Var. *Sylvestris* (Mill.) Lehr., Oils from Different Locations of Northeast Portugal. *Appl. Sci.* **2020**, 10, 6414, doi:10.3390/APP10186414.
  40. Kritikou, E.; Kalogiouri, N.P.; Kolyvira, L.; Thomaidis, N.S. Target and Suspect HRMS Metabolomics for the 13 Varieties of Olive Leaves and Drupes from Greece. *Molecules* **2020**, 25, 4889, doi:10.3390/molecules25214889.
  41. Joshi, S. *Olea Ferruginea* Royle, Indian Olive: An Underutilised Fruit Tree Crop of North-West Himalaya. *Fruits* **2012**, 67, 121–126, doi:10.1051/fruits/2012003.
  42. Gulfranz, M.; Kasuar, R.; Arshad, G.; Mehmood, S.; Minhas, N.; Asad, M.J.; Ahmad, A.; Siddique, F. Isolation and Characterization of Edible Oil from Wild Olive. *African J. Biotechnol.* **2009**, 8, 3734–3738, doi:10.5897/AJB2009.000-9373.
  43. Pérez, A.G.; León, L.; Pascual, M.; de la Rosa, R.; Belaj, A.; Sanz, C. Analysis of Olive (*Olea Europaea* L.) Genetic Resources in Relation to the Content of Vitamin E in Virgin Olive Oil. *Antioxidants* **2019**, 8, 242, doi:10.3390/antiox8080242.
  44. Santos-Sánchez, N.F.; Salas-Coronado, R.; Hernández-Carlos, B.; Villanueva-Cañongo, C. Shikimic Acid Pathway in Biosynthesis of Phenolic Compounds. In *Plant Physiological Aspects of Phenolic Compounds*; M. Soto-Hernández, García-Mateos, R., Palma-Tenango, M., Eds.; IntechOpen, 2019; pp. 1–15, doi:10.5772/intechopen.83815.
  45. Obied, H.K.; Prenzler, P.D.; Ryan, D.; Servili, M.; Taticchi, A.; Esposto, S.; Robards, K. Biosynthesis and Biotransformations of Phenol-Conjugated Oleosidic Secoiridoids from *Olea Europaea* L. *Nat. Prod. Rep.* **2008**, 25, 1167–1179, doi:10.1039/b719736e.

46. Dini, I.; Graziani, G.; Fedele, F.L.; Sicari, A.; Vinale, F.; Castaldo, L.; Ritieni, A. An Environmentally Friendly Practice Used in Olive Cultivation Capable of Increasing Commercial Interest in Waste Products from Oil Processing. *Antioxidants* **2020**, *9*, 466, doi:10.3390/antiox9060466.
47. Ryan, D.; Antolovich, M.; Prenzler, P.; Robards, K.; Lavee, S. Biotransformations of Phenolic Compounds in *Olea Europaea* L. *Sci. Hortic.* **2002**, *92*, 147–176, doi:10.1016/S0304-4238(01)00287-4.
48. Hiroya, K.; Ogasawara, K. A Concise Enantio- and Diastereo-Controlled Synthesis of (2) -Quinic Acid and (2) -Shikimic Acid. *Chem. Commun.* **1998**, *4*, 2033–2034, doi:10.1039/A805775C.
49. Belaj, A.; Ninot, A.; Gómez-Gálvez, F.J.; El Riachy, M.; Gurbuz-Veral, M.; Torres, M.; Lazaj, A.; Klepo, T.; Paz, S.; Ugarte, J.; et al. Utility of EST-SNP Markers for Improving Management and Use of Olive Genetic Resources: A Case Study at the Worldwide Olive Germplasm Bank of Córdoba. *Plants* **2022**, *11*, 921, doi:10.3390/plants11070921.
50. Del Río, C.; Romero, A.M. Whole, Unmilled Olives Can Be Used to Determine Their Oil Content by Nuclear Magnetic Resonance. *Horttechnology* **1999**, *9*, 675–680, doi:10.21273/HORTTECH.9.4.675.
51. Olmo-García, L.; Polari, J.J.; Li, X.; Bajoub, A.; Fernández-Gutiérrez, A.; Wang, S.C.; Carrasco-Pancorbo, A. Deep Insight into the Minor Fraction of Virgin Olive Oil by Using LC-MS and GC-MS Multi-Class Methodologies. *Food Chem.* **2018**, *261*, 184–193, doi:10.1016/j.foodchem.2018.04.006.

Table S1. Quantitative data for each and every compound quantified in the progeny, the female parent and the cultivars (mg·kg<sup>-1</sup>).

Sample	Acyclohydrocinnelic acid hexoside (B)	Caffeoyl 6-secologanoside	Dehydro nuzhenide	Dihydro oleuropein	Demethyl ligstroside	Flenolic acid glucoside (C)	Ligstroside	Lucidumside C (A)	Methoxy oleuropein (A)	Neonuzhenide	Oleoside/secologanoside (C)	Oleuropein	Demethyl oleuropein	Oleuropein aglycone (A)	Oleuropein aglycone (B)	Verbascoside	β-hydroxy verbascoside	Quinic acid	Hydroxytyrosin glucoside	Masilinic acid	Oleanolic acid	Betulinic acid	Rutin (B)	Luteolin glucoside (B)	Luteolin 7-O-glucoside	Unknown 1 (m/z 363)	Unknown 2 (m/z 421)
315-71-G14 a	1672.0	140.4	13.2	185.1	318.2	994.0	29.1	68.6	209.0	126.9	100.9	178.8	515.7	66.5	114.4	n.d	n.d	13136.8	1194.7	9897.9	3553.0	72.8	2855.3	10.4	n.d	821.4	106.1
315-71-G14 b	1544.0	129.6	12.2	170.9	293.8	918.0	26.9	63.4	193.0	117.1	93.1	165.2	476.3	61.5	105.6	n.d	n.d	12131.2	1103.3	9140.1	3281.0	67.2	2636.7	9.6	n.d	758.6	97.9
315-77-G14 a	2272.2	49.9	253.7	75.7	616.6	2225.2	1397.5	3825.4	208.0	153.9	1098.0	7806.8	1480.7	2249.1	1910.1	1316.4	197.6	12584.7	793.4	13772.2	5414.2	37.4	3824.4	301.5	451.3	131.0	954.5
315-77-G14 b	2102.8	46.1	234.3	69.9	569.4	2054.8	1290.5	3532.6	192.0	142.1	1014.0	7209.2	1367.3	2076.9	1763.9	1215.6	182.4	11621.3	732.6	12717.8	4999.8	34.6	3531.6	278.5	416.7	121.0	881.5
315-81-G14 a	670.7	61.3	166.4	72.8	2548.5	6233.6	486.6	1990.2	606.2	788.2	2087.9	7761.1	3718.3	13.5	31.2	1743.7	165.3	16384.1	3690.3	6379.2	1272.7	21.8	6038.1	257.9	476.2	235.0	117.5
315-81-G14 b	619.3	56.7	153.6	67.2	2353.5	5756.4	449.4	1837.8	559.8	727.8	1928.1	7166.9	3433.7	12.5	28.8	1810.3	152.7	15129.9	3407.7	5890.8	1175.3	20.2	5575.9	238.1	439.8	217.0	108.5
315-85-G14 a	1912.2	281.8	400.3	346.1	377.4	3407.4	5368.5	5209.4	97.7	165.3	2099.4	42973.9	572.9	1744.8	2293.8	4270.5	431.5	11380.6	3152.7	11043.7	3314.9	54.1	9663.9	132.1	138.3	122.4	662.4
315-85-G14 b	1765.8	260.2	369.7	319.7	348.6	3146.6	4957.5	4810.6	90.3	152.7	1938.6	39684.1	529.1	1611.2	2118.2	3943.5	398.5	10509.4	2911.3	10198.3	3061.1	49.9	8924.1	121.9	127.7	113.1	611.6
315-93-G14 a	311.9	346.3	39.9	167.4	810.0	968.1	265.1	210.0	177.8	115.4	280.7	1167.7	986.8	115.4	617.6	n.q	35.4	7721.6	447.1	9248.0	2228.3	17.7	5438.2	136.2	511.6	54.1	214.2
315-93-G14 b	288.1	319.7	36.9	154.6	748.0	893.9	244.9	194.0	164.2	106.6	259.3	1078.3	911.2	106.6	570.4	n.q	32.6	7130.4	412.9	8540.0	2057.7	16.3	5021.8	125.8	472.4	49.9	197.8
315-98-G14 a	1215.5	79.0	62.9	263.1	953.5	2874.0	76.9	112.3	685.2	250.6	2501.8	590.6	4093.7	223.6	370.2	n.q	87.3	12340.3	9056.7	11711.3	4502.3	71.9	4133.2	128.9	358.7	1407.9	539.7
315-98-G14 b	1122.5	73.0	58.1	242.9	880.5	2654.0	71.1	103.7	632.8	231.4	2310.2	545.4	3780.3	206.4	341.8	n.q	80.7	11395.7	8363.3	10814.7	4157.7	66.3	3816.8	119.1	331.3	1300.1	498.3
316-11-G14 a	841.2	59.3	57.2	109.2	579.2	1374.6	37.4	79.3	620.8	127.9	422.2	319.2	2020.3	61.3	167.4	443.0	69.7	11557.4	1527.5	2963.4	61.7	17.7	3643.5	114.4	261.0	549.0	86.3
316-11-G14 b	776.8	54.7	52.8	100.8	534.8	1269.4	34.6	73.3	194.0	118.1	389.8	294.8	1865.7	56.7	154.6	409.0	64.3	10672.6	1410.5	7530.8	2736.6	16.3	3364.5	105.6	241.0	507.0	79.7
316-14-G14 a	774.7	765.3	62.4	100.9	316.1	1925.7	382.6	2523.6	453.4	726.8	1444.3	8243.5	1647.0	243.3	220.4	n.q	67.6	9378.0	1496.3	9509.0	4267.3	43.5	7150.7	457.5	674.8	1591.9	706.0
316-14-G14 b	715.3	706.7	57.6	93.1	291.9	1778.3	353.4	2330.4	418.6	671.2	1333.7	7612.5	1521.0	224.7	203.6	n.q	62.4	8660.0	1381.7	8781.0	3940.7	40.1	6603.3	422.5	623.2	1470.1	652.0
316-16-G14 a	277.6	70.7	67.6	51.0	889.0	2664.0	38.5	87.3	345.2	367.0	685.2	485.6	2331.2	15.0	48.9	995.1	84.2	16948.7	1721.9	9935.3	3370.0	19.8	6709.8	372.2	797.5	248.5	62.4
316-16-G14 b	256.4	65.3	62.4	47.0	821.0	2460.0	35.5	80.7	318.8	339.0	632.8	448.4	2152.8	13.8	45.1	918.9	77.8	15651.3	1590.1	9174.7	3112.0	18.2	6196.2	343.8	736.5	229.5	57.6
316-20-G14 a	1387.1	241.2	25.0	46.8	125.8	2635.9	n.d	106.1	247.5	176.8	209.0	134.5	1661.6	43.7	113.0	n.d	n.d	12158.4	1132.3	7503.2	3550.9	9.4	2022.4	119.6	380.6	528.2	149.7
316-20-G14 b	1280.9	222.8	23.0	43.2	116.2	2434.1	n.d	97.9	228.5	163.2	193.0	132.5	1534.4	40.3	104.4	n.d	n.d	11227.6	1045.7	6928.8	3279.1	8.6	1867.6	110.4	351.4	488.7	138.3
316-24-G14 a	423.2	59.3	76.9	38.5	973.3	1941.3	70.7	245.4	199.6	193.4	681.1	1426.6	1523.3	43.7	115.4	532.4	139.3	16948.7	3326.3	6694.2	3311.8	21.8	2639.0	178.8	263.1	647.8	228.8
316-24-G14 b	390.8	54.7	71.1	35.5	898.7	1792.7	65.3	226.6	184.4	178.6	628.9	1317.4	1406.7	40.3	106.6	491.6	128.7	15651.3	3071.7	6181.8	3058.2	20.2	2437.0	165.2	242.9	598.2	211.2
316-26-G14 a	677.9	17.7	82.0	226.7	633.2	1146.9	343.1	610.4	188.2	522.0	545.9	2571.4	561.5	262.0	234.0	854.7	65.5	8238.3	1267.5	8309.0	1975.6	14.6	5881.1	184.0	713.3	296.3	166.4
316-26-G14 b	626.1	16.3	75.8	209.3	584.8	1059.1	316.9	563.6	173.8	482.0	504.1	2374.6	518.5	242.0	216.0	789.3	60.5	7607.7	1170.5	7673.0	1824.4	13.4	5430.9	170.0	658.7	273.7	153.6
316-28-G14 a	800.6	340.0	605.2	229.8	241.2	1151.1	569.8	1250.8	126.9	214.2	672.8	5774.0	443.0	1574.3	2053.6	4323.5	773.2	19207.2	4125.9	12111.6	6577.8	41.5	3156.8	263.1	477.3	190.1	988.8
316-28-G14 b	739.4	314.0	558.8	212.2	222.8	1062.9	526.2	1155.0	117.1	197.8	621.2	5332.0	409.0	1453.7	1896.4	3992.5	714.0	17736.8	3810.1	11184.4	6074.2	38.3	2915.2	242.9	440.7	175.5	913.2
316-30-G14 a	664.4	8.3	479.3	121.7	595.8	1515.0	6297.0	2240.8	44.7	212.5	1385.0	7884.8	123.7	269.3	967.0	4489.9	499.1	13940.6	2124.3	13565.2	5757.4	57.2	12385.1	47.8	142.6	83.2	394.1
316-30-G14 b	613.6	7.7	442.7	112.3	550.2	1399.0	5815.0	2069.2	41.3	196.3	1279.0	7281.2	114.3	248.7	893.4	4146.1	460.9	12873.4	1961.7	12526.8	5316.6	52.8	11436.9	44.2	131.6	76.8	363.9
316-32-G14 a	893.2	68.6	227.7	332.7	2294.8	2699.3	596.8	1227.0	741.4	264.1	2089.0	6150.4	5978.9	227.7	230.8	2003.7	322.3	15780.0	2479.9	5829.1	1502.5	34.3	14375.2	133.1	234.0	401.4	628.0
316-32-G14 b	824.8	63.4	210.3	307.3	2119.2	2492.7	551.2	1133.0	684.6	243.9	1929.0	5679.6	5521.2	210.3	213.2	1850.3	297.7	14572.0	2290.1	5382.9	1387.5	31.7	13274.8	122.9	216.0	370.6	580.0
316-33-G14 a	891.1	97.7	55.1	281.8	6868.9	3214.0	350.4	175.4	1013.8	100.9	1619.0	1962.1	8392.2	70.7	182.0	72.7	60.3	14484.4	3310.7	14317.0	8952.6	61.3	5752.2	376.4	838.1	180.9	158.0
316-33-G14 b	822.9	90.3	50.9	260.2	6343.1	2968.0	323.6	162.0	936.2	93.1	1495.0	1811.9	7749.8	65.3	168.0	667.3	55.7	13375.6	3057.3	13221.0	5370.4	56.7	5311.8	346.6	773.9	167.1	146.0
316-35-G14 a	1997.5	120.6	777.8	183.0	988.8	3949.2	3667.4	3822.3	209.0	326.5	2620.3	21083.9	1103.2	614.0	422.2	2083.9	329.2	12047.1	12047.1	12178.1	6201.7	78.0	9954.0	567.1	n.q	335.9	1545.1
316-35-G14 b	1844.5	111.4	718.2	169.0	913.2	3646.8	3386.6	3529.7	193.0	301.5	2419.7	21737.0	1018.8	290.0	389.8	3240.7	861.3	11124.9	1947.3	11245.9	5782.3	72.0	9192.0	51.9	n.q	310.1	1426.9
316-37-G14 a	619.7	42.6	184.0	291.1	1546.2	2549.6	94.6	164.3	117.7	167.4	760.1	1070.0	3214.0	128.9	431.5	3592.5	242.3	10482.2	1680.3	5331.1	1087.6	8.5	3931.5	175.7	735.1	235.0	281.8
316-37-G14 b	572.3	39.4	170.0	268.9	1427.8	2354.4	87.4	151.7	201.1	154.6	701.9	988.0	2968.0	119.1	398.5	3317.5	223.7	9679.8	1551.7	4922.9	1004.4	7.9	3630.5	162.3	678.9	217.0	260.2
316-38-G14 a	2352.0	30.2	167.4	142.5	462.7	2121.2	183.0	183.0	141.4	120.6	590.6	1767.7	365.0	641.6	555.3	810.0	153.9	12549.3	3570.7	9913.5	3949.2	68.6	9370.7	791.3	1034.6	607.2	484.5
316-38-G14 b	2172.0	27.8	154.6	131.5	427.3	1958.8	169.0	845.0	130.6	111.4	545.4	1632.3	337.0	592.4	512.7	748.0	142.1	11588.7	3297.3	9154.5	3646.8	63.4	8653.3	730.7	955.4	560.8	447.5

Sample	Acylodihydroelenolic acid hexoside (B)	Caffeoyl 6-secologanoside	Dehydro nuzhenide	Dihydro oleuropein	Demethyl ligstroside	Elenolic acid glucoside (C)	Ligstroside	Lucidumoside C (A)	Methoxy oleuropein	Neonuzhenide	Oleoside/secologanoside (C)	Oleuropein	Demethyl oleuropein	Oleuropein aglycone (A)	Oleuropein aglycone (B)	Verbascoside	$\beta$ -hydroxy verbascoside	Quinic acid	Hydroxytyrosol glucoside	Maslinic acid	Oleanoic acid	Betulinic acid	Rutin (B)	Luteolin glucoside (B)	Luteolin 7-O-glucoside	Unknown 1 (m/z 363)	Unknown 2 (m/z 421)
316-43-G14 a	1483.8	23.9	96.7	100.5	1211.4	1297.7	236.0	671.7	298.4	130.2	1007.6	1055.4	629.1	71.7	339.0	n.q	98.8	14592.6	1580.5	10180.7	6180.6	101.9	9291.7	183.0	218.6	976.4	1681.4
316-43-G14 b	1370.2	22.1	89.3	92.9	1118.6	1198.3	218.0	620.3	275.6	120.2	930.4	974.6	580.9	66.3	313.0	n.q	91.2	13475.4	1459.5	9401.3	5707.4	94.1	8580.3	169.0	201.8	901.6	1552.6
316-4-G14 a	1124.0	19.8	997.2	94.6	237.1	1171.9	2619.3	2796.0	42.6	130.0	1838.4	5150.1	99.8	1261.3	1588.4	5065.9	1197.8	14070.6	1159.4	14302.4	5970.5	40.6	13887.6	74.2	118.5	316.1	1486.9
316-4-G14 b	1038.0	18.2	920.8	87.4	218.9	1082.1	2418.7	2582.0	39.4	120.0	1697.6	4755.9	92.2	1164.7	1466.8	4678.1	1106.2	12993.4	1070.6	13207.6	5513.5	37.4	12824.4	68.6	109.5	291.9	1373.1
316-5-G14 a	785.0	164.3	114.5	208.0	1724.0	2222.1	934.8	244.4	252.7	222.5	411.8	3819.2	1882.0	146.6	196.5	1227.0	111.3	14338.8	2556.9	6699.4	1646.0	22.0	5211.5	471.0	596.8	251.6	226.7
316-5-G14 b	725.0	151.7	105.7	192.0	1592.0	2051.9	863.2	225.6	233.3	205.5	380.2	3526.8	1738.0	135.4	181.5	1133.0	102.7	13241.2	2361.1	6186.6	1520.0	20.4	4812.5	435.0	551.2	232.4	209.3
316-6-G14 a	1282.1	54.1	29.1	88.4	736.2	1706.3	162.2	144.5	295.3	153.9	1702.2	2568.3	2565.2	144.5	183.0	n.q	32.2	13385.3	2780.4	8735.4	2941.6	27.0	7096.6	520.9	1016.9	1207.2	232.9
316-6-G14 b	1183.9	49.9	26.9	81.6	679.8	1575.7	149.8	133.5	272.7	142.1	1571.8	2371.7	2368.8	133.5	169.0	n.q	29.8	12360.7	2567.6	8066.6	2716.4	25.0	6553.4	481.1	939.1	1114.8	215.1
316-87-G14 a	1344.5	136.2	196.5	184.0	480.4	1349.7	2358.3	2056.7	101.9	205.3	987.8	7722.6	163.2	608.3	453.4	471.0	162.2	13384.3	1112.6	7924.3	2107.7	22.9	4799.7	41.6	104.0	639.5	1646.0
316-87-G14 b	1241.5	125.8	181.5	170.0	443.6	1246.3	2177.7	1899.3	94.1	189.5	912.2	7131.4	150.8	561.7	418.6	435.0	149.8	12359.7	1027.4	7317.7	1946.3	21.1	4432.3	38.4	96.0	590.5	1520.0
316-89-G14 a	432.6	82.1	37.7	71.7	907.7	2055.7	71.7	807.9	228.8	304.7	2664.0	3621.6	2701.4	72.8	211.1	n.q	36.4	13049.5	2572.5	11150.8	3291.0	40.6	6181.6	403.4	1050.2	1063.5	230.8
316-89-G14 b	399.4	75.9	34.9	66.3	838.3	1898.3	66.3	746.1	211.2	281.3	2460.0	3344.4	2494.6	67.2	194.9	n.q	33.6	12050.5	2375.5	10297.2	3039.0	37.4	5708.4	372.6	969.8	982.1	213.2
316-8-G14 a	848.5	73.8	14.6	151.6	359.8	872.4	84.2	151.8	131.0	213.2	737.2	545.9	1578.4	294.3	506.4	n.q	6.2	10953.3	2681.6	9193.9	2541.3	26.0	4781.0	294.3	675.9	639.5	163.2
316-8-G14 b	783.5	68.2	13.4	140.0	332.2	805.6	77.8	140.2	121.0	196.8	680.8	504.1	1457.6	271.7	467.6	n.q	5.8	10114.7	2476.4	8490.1	2346.7	24.0	4415.0	271.7	624.1	590.5	150.8
316-91-G14 a	1729.2	213.2	75.9	141.4	115.9	2159.7	7662.3	5360.2	29.0	335.9	978.5	31830.4	85.3	1055.4	1223.8	1880.0	241.2	13067.2	693.5	15041.7	6189.9	41.6	10599.7	531.3	685.2	298.4	793.4
316-91-G14 b	1596.8	196.8	70.1	130.6	107.1	1994.3	7075.7	4949.8	26.8	310.1	903.5	29393.6	78.7	974.6	1130.2	1736.0	222.8	12066.8	640.5	13890.3	5716.1	38.4	9788.3	490.7	632.8	275.6	732.6
Female parent a	106.1	38.3	74.9	86.3	n.d	149.3	447.1	657.2	n.d	190.3	470.0	3442.8	n.d	209.0	586.4	n.q	35.4	4461.8	585.4	9584.9	2920.8	167.4	7060.2	321.3	567.7	7.7	363.9
Female parent b	97.9	35.3	69.1	79.7	n.d	137.9	412.9	606.8	n.d	175.7	434.0	3179.2	n.d	193.0	541.6	n.q	32.6	4120.2	540.6	8851.1	2697.2	154.6	6519.8	296.7	524.3	7.1	336.1
Arbequina a	1610.7	142.5	14.3	65.5	n.d	93.6	18.7	97.7	30.4	n.d	94.6	245.4	199.3	676.9	1313.3	742.9	n.d	10776.5	1889.3	11799.7	3741.2	18.7	2064.0	118.5	829.8	36.4	92.5
Arbequina b	1487.3	131.5	13.3	60.5	n.d	86.4	17.3	90.3	28.0	n.d	87.4	226.6	184.1	625.1	1212.7	686.1	n.d	9951.5	1744.7	10896.3	3454.8	17.3	1906.0	109.5	766.2	33.6	85.5
Frantoio a	2046.3	235.0	215.2	1548.3	615.6	2076.5	1367.3	351.5	32.2	334.8	254.8	6979.1	1129.2	795.4	3065.3	4177.9	188.2	12606.5	1109.5	6806.5	1382.9	5.4	603.1	16.6	266.2	80.1	412.8
Frantoio b	1889.7	217.0	198.8	1429.7	568.4	1917.5	1262.7	324.5	29.8	309.2	235.2	6444.9	1042.8	734.6	2830.7	3858.1	173.8	11641.5	1024.5	6285.5	1277.1	5.0	556.9	15.4	245.8	73.9	381.2
Koroneiki a	1309.1	152.9	60.3	927.5	n.d	1980.8	2086.9	642.6	n.d	n.d	751.8	23432.9	n.d	395.1	1044.0	1464.0	70.7	14005.1	1840.4	12990.2	3669.5	19.0	1068.9	10.4	106.1	n.d	118.5
Koroneiki b	1208.9	141.1	55.7	856.5	n.d	1829.2	1927.1	593.4	n.d	n.d	694.2	21639.1	n.d	364.9	964.0	1352.0	65.3	12932.9	1699.6	11995.8	3388.5	17.6	987.1	9.6	97.9	n.d	109.5
Picalu a	1268.6	556.3	7.9	598.9	n.d	1040.8	735.1	810.0	n.d	n.d	204.8	14391.9	n.d	2524.6	2954.1	n.q	1.9	16782.4	1124.0	9137.8	2866.7	17.7	1594.0	54.6	545.9	12.5	85.3
Picalu b	1171.4	513.7	7.3	553.1	n.d	961.2	678.9	748.0	n.d	n.d	189.2	13290.1	n.d	2331.4	2727.9	n.q	1.7	15497.6	1038.0	8438.2	2647.3	16.3	1472.0	50.4	504.1	11.5	78.7

SD values have not been included to contain the size of the table. Coefficient of variation (%) were below 4.3% in every case.

# Chapter

## Characterization of the metabolic profile of olive tissues (roots, stems and leaves): relationship with cultivars' resistance/susceptibility to the soil fungus *Verticillium dahliae*

Irene Serrano-García<sup>1</sup>, Lucía Olmo-García<sup>1✉</sup>, Olga Monago-Maraña<sup>2</sup>, Iván Muñoz Cabello de Alba<sup>1</sup>, Lorenzo León<sup>3</sup>, Raúl de la Rosa<sup>3,4</sup>, Alicia Serrano<sup>5</sup>, Ana María Gómez-Caravaca<sup>1</sup>, Alegría Carrasco-Pancorbo<sup>1</sup>

<sup>1</sup>Department of Analytical Chemistry, Faculty of Sciences, University of Granada, Ave. Fuentenueva s/n, E-18071 Granada, Spain; [iserrano@ugr.es](mailto:iserrano@ugr.es) (I.S.-G.); [ivanfenty@correo.ugr.es](mailto:ivanfenty@correo.ugr.es) (I.M.C.d.A.); [anagomez@ugr.es](mailto:anagomez@ugr.es) (A.M.G.-C.); [alegriac@ugr.es](mailto:alegriac@ugr.es) (A.C.-P.)

<sup>2</sup>Department of Analytical Sciences, Faculty of Sciences, Universidad Nacional de Educación a Distancia (UNED), Avda. Esparta s/n, Ctra. de Las Rozas-Madrid, E-28232 Madrid, Spain; [olgamonago@ccia.uned.es](mailto:olgamonago@ccia.uned.es)

<sup>3</sup>Instituto de Investigación y Formación Agraria y Pesquera (IFAPA), Centro Alameda del Obispo, Ave. Menéndez Pidal s/n, E-14004 Córdoba, Spain; [lorenzo.leon@juntadeandalucia.es](mailto:lorenzo.leon@juntadeandalucia.es) (L.L.); [raul.rosa@juntadeandalucia.es](mailto:raul.rosa@juntadeandalucia.es) (R.d.I.R.)

<sup>4</sup>Instituto de Agricultura Sostenible-CSIC, Ave. Menéndez Pidal s/n, E-14004 Córdoba, Spain; [raul.rosa@ias.csic.es](mailto:raul.rosa@ias.csic.es) (present address)

<sup>5</sup>Department of Experimental Biology, The University Institute of Research on Olive and Olive Oils (INUO), University of Jaén, Campus Las Lagunillas s/n, 23071 Jaén, Spain; [segoalicia@gmail.com](mailto:segoalicia@gmail.com)

✉ [Luciaolmo@ugr.es](mailto:Luciaolmo@ugr.es)

**Antioxidants, 12 (2023) 2120**

<https://doi.org/10.3390/antiox12122120>



**Abstract:** Verticillium wilt of olive (VWO) is one of the most widespread and devastating olive diseases in the world. Harnessing host resistance to the causative agent is considered one of the most important measures within an integrated control strategy of the disease. Aiming to understand the mechanisms underlying olive resistance to VWO, the metabolic profiles of olive leaves, stems and roots from 10 different cultivars with varying levels of susceptibility to this disease were investigated by liquid chromatography coupled to mass spectrometry (LC-MS). The distribution of 56 metabolites among the three olive tissues was quantitatively assessed and the possible relationship between the tissues' metabolic profiles and resistance to VWO was evaluated by applying unsupervised and supervised multivariate analysis. Principal component analysis (PCA) was used to explore the data, and separate clustering of highly resistant and extremely susceptible cultivars was observed. Moreover, partial least squares discriminant analysis (PLS-DA) models were built to differentiate samples of highly resistant, intermediate susceptible/resistant, and extremely susceptible cultivars. Root models showed the lowest classification capability, but metabolites from leaf and stem were able to satisfactorily discriminate samples according to the level of susceptibility. Some typical compositional patterns of highly resistant and extremely susceptible cultivars were described, and some potential resistance/susceptibility metabolic markers were pointed out.

**Keywords:** *Olea europaea* L.; verticillium wilt; plant metabolomics; LC-MS profiling; secondary metabolites; phenolic compounds; triterpenic compounds

## 1. INTRODUCTION

*Olea europaea* L. is one of the oldest trees that mankind has cultivated. Its derived products, mainly table olives and oil, are consumed practically all over the world, mainly due to its important nutraceutical properties [1]. As a result, olive trees have gained great relevance worldwide, and are considered a very valuable crop providing important economic and ecological benefits [2,3]. However, they are susceptible to various abiotic and biotic stresses. Among them, verticillium wilt of olive (VWO), a disease caused by the soil-born fungus *Verticillium dahliae*, currently represents the main phytosanitary limitation in many olive-growing areas. This fungus enters the olive tree through the roots and spreads to the trunk, branches and leaves, where it blocks the flow of water and nutrients through the xylem vessels, causing plant wilting and, eventually, the death of the infected tree [4]. Thus, VWO can severely affect the growth and yield of olives, leading to significant economic losses [5]. *V. dahliae* can persist in soil for years, making it difficult to control once established [6]. In the absence of effective preventive or curative chemical fungicides, integrated approaches involving the use of multiple before and after planting practices need to be implemented to reduce the incidence of the disease [6–8]. One of the most important practices is the use of resistant cultivars. Although a wide genetic variability has been reported in the olive germplasm [9], very few cultivars have shown a high level of resistance to VWO [10]. Therefore,

several breeding efforts have been developed to produce new cultivars with a high level of resistance to VWO combined with good agronomic characteristics [10–13].

To improve the efficiency of those breeding programs, it would be of interest to uncover the genetic and metabolic pathways involved in VWO resistance [6,14]. In this sense, all plants develop a defence strategy upon pathogen attack, which triggers a set of multi-component responses, including the production of signalling molecules such as reactive oxygen species, induction of the antioxidant system, activation of pathways that generate anti-fungal secondary metabolites and others [15]. Moreover, a higher resistance of some olive cultivars to VWO infection has been correlated with enhanced enzymatic activities related to cell-wall reinforcement and the up-regulation of plant hormones involved in the induction of innate systemic resistance [16]. The functional traits of olive roots (biomass allocation, dry matter content and root system architecture) have been also associated with the resistance level to VWO [17], and a differential basal set of genes and diverse transcriptomic responses have been found in roots of resistant and susceptible cultivars [14,18]. Therefore, the evidence suggests that there are distinct biochemical and physiological differences between susceptible and resistant cultivars. These differences exist at the genome, transcriptome and metabolome levels, and can be constitutive (basal) or induced by the fungus–plant interaction [16].

Secondary metabolites are not directly involved in the growth and development of plants, but are synthesized for specific ecological roles, such as defence against pathogens or abiotic constraints [19,20]. The exact mechanisms by which secondary metabolites confer resistance to *V. dahliae* are not yet fully understood. However, it has been proposed that these compounds may act by inhibiting the growth and development of the fungus, by modulating the plant's immune response, or by enhancing the plant's tolerance to stress [19,21]. Some olive secondary metabolites, such as rutin, oleuropein, luteolin-7-glucoside and hydroxytyrosol have shown in vitro antifungal activity against *V. dahliae* [22,23].

The accumulation of phenolic compounds in different olive organs after *V. dahliae* inoculation has been repeatedly reported [21,22,24,25]. Even though most of the cited reports focused on the total phenolic and total o-diphenols content (determined by colorimetric methods), some information has also been gathered about the role of specific compounds on olive defence against this soil-borne fungus. For example, Báidez and collaborators found that infected stem tissues presented higher levels of oleuropein, rutin and luteolin 7-glucoside than the tissues from healthy plants [22]. Contrastingly, Markakis and co-workers found a negative correlation among oleuropein content and relative fungus DNA quantity in infected roots. On the contrary, the same authors described an increase in the verbascoside concentration in roots after *V. dahliae* infection, showing an opposite behaviour of the two major root metabolites [26]. Recently, Cardoni and co-authors found only minor significant changes in the metabolic profile of roots after *V. dahliae* inoculation [27].

In addition to the induced changes in secondary metabolites, the study of the basal composition of olive tissues is relevant to understanding the mechanisms underlying resistance/susceptibility to VWO [27]. A positive association has been found between total basal polyphenol content in olive leaves, stems and roots and the resistance level of the cultivar [24,25]. However, little information is available on the correlation between the basal content of specific metabolites and the cultivar's resistance to *V. dahliae* infection. A negative association between the root content of verbascoside, maslinic acid and methoxypinoresinol glucoside and the tolerance level to VWO of 'Picual', 'Hojiblanca' and 'Lechín de Sevilla' cultivars has been recently reported [27]. The same authors also described higher concentrations of oleuropein, oleuropein aglycone, ligstroside and elenolic acid glucoside in roots of VWO-tolerant varieties ('Changlot Real', 'Empeltre' and 'Frantoio'). Nonetheless, a thorough metabolomic analysis of various plant tissues in cultivars exhibiting a broad range of responses to VWO has yet to be conducted.

Metabolomics represents a powerful tool to explore the metabolic profiles of cultivars showing varying levels of resistance/susceptibility to VWO and to assess the distribution of secondary metabolites among different olive tissues involved in *V. dahliae* infection and spread through the plant. These kinds of analytical approaches have also been proven to be effective in achieving the phenolic characterization of olive leaves of cultivars resistant to *Xylella*, both at a baseline level and after inoculation [28,29]. Thus, the main goals of this work were: (i) to carry out the metabolic profiling of leaves, stems, and roots from 10 olive cultivars showing varying levels of resistance to VWO; (ii) to establish the metabolite distribution in the different tissues affected by the fungus infection; and (iii) to find possible metabolite correlations with resistance/susceptibility to *V. dahliae*.

## 2. MATERIALS AND METHODS

### 2.1. Chemicals and standards

Deionized water (resistivity 18.2 MΩ cm) was produced with a Millipore Milli-Q system (Bedford, MA, USA). Gradient grade ethanol and LC-MS grade acetonitrile were supplied by Prolabo (Paris, France). Acetic acid and pure standards of olive secondary metabolites (quinic, maslinic, betulinic and oleanolic acids, hydroxytyrosol, tyrosol, luteolin 7-O-glucoside, rutin, verbascoside and oleuropein) were purchased from Sigma-Aldrich (St. Louis, MO, USA).

### 2.2. Plant material and samples pre-treatment

One year old plants from 10 different cultivars ('Arbequina', 'Empeltre', 'Frantoio', 'Hojiblanca', 'Jabali', 'Koroneiki', 'Leccino', 'Mastoidis', 'Menya' and 'Picual') were obtained by vegetative propagation of semi-hardwood stem cuttings from the World Olive Germplasm Bank of the Centro IFAPA 'Alameda del Obispo' in Cordoba, Spain [9]. These cultivars were selected as having different levels of resistance/susceptibility to VWO [6,10], from highly resistant to extremely susceptible:

'Frantoio' and 'Empeltre', highly resistant (HR); 'Koroneiki and 'Leccino', resistant (R); 'Arbequina' and 'Picual', moderately susceptible (MS); 'Hojiblanca' and 'Menya', susceptible (S); 'Jabali' and 'Mastoidis', extremely susceptible (ES). Roots, stems and leaves were sampled from three plants (biological replicates) from each olive cultivar to get a total number of 90 samples. Plant tissues were washed with water and dried at room temperature in the dark until constant weight. Afterwards, all the samples were ground, sieved through a 0.5 mm metal sieve to obtain a standard particle size and stored at  $-20\text{ }^{\circ}\text{C}$ .

### 2.3. Secondary metabolites extraction and LC-MS analysis

The extraction of the fraction of olive secondary metabolites was carried out by applying a previously reported ultrasound-assisted solid–liquid extraction protocol [30] with slight modifications. First, 100 mg of tissue powder was subjected to two consecutive extraction steps with ethanol–water mixtures (60:40 for the first step and 80:20 for the second one) followed by a third step with pure ethanol. Leaf samples required a volume of 10 mL of the extractant agent in each extraction step, whereas roots and stems were extracted with 5 mL of solvent per cycle. Each extraction cycle involved 30 min of ultrasound extraction, centrifugation at  $8603 \times g$  for 10 min and upper phase separation. Finally, 1 mL aliquots of the combined supernatants were filtered with  $0.22\text{ }\mu\text{m}$  Clarinert<sup>®</sup> nylon syringe filters (Agela Technologies, Torrance, CA, USA) and transferred to amber glass HPLC vials.

External calibration curves ( $0.1\text{--}500\text{ mg L}^{-1}$ ) of commercially available standards were prepared in ethanol–water (80:20, v/v) and used for the quantification of the analytes of interest. Standard solutions and quality controls (QC) of each matrix, which were prepared by mixing a portion of solid powder from all the samples included in the study (per tissue type), were used to assess the main analytical parameters of the method as well as to assess the performance of the analytical system during the analysis sequence. All the stock solutions and plant extracts were stored at  $-20\text{ }^{\circ}\text{C}$  until analysis.

LC-MS analyses were conducted on two different systems. First, the qualitative characterization of samples' metabolic profiles was carried out on a Waters Acquity UPLC H–Class system coupled to a QTOF SYNAPT G2 mass spectrometer (Waters, Manchester, UK). Second, an Agilent 1260 LC system (Agilent Technologies, Waldbronn, Germany) coupled to a Bruker Daltonics Esquire 2000 IT mass spectrometer (Bruker Daltonik, Bremen, Germany) was used for quantitative purposes.

Chromatographic and MS detection conditions were adapted from those presented in a previous report [31]. Regardless of the employed LC-MS system, metabolite separation was carried out on a Zorbax Extend C18 column ( $100 \times 4.6\text{ mm}$ ,  $1.8\text{ }\mu\text{m}$  particle size, Agilent Technologies) operated at  $40\text{ }^{\circ}\text{C}$ , with a sample injection volume of  $10\text{ }\mu\text{L}$ . A mobile phase gradient of water (Phase A) and acetonitrile (Phase B)—both acidified with 1% acetic acid—was applied for the elution of compounds at a flow rate of  $1\text{ mL min}^{-1}$ : 0–10 min, 10–25% B; 10–12 min, 25–60% B; 12–14 min, 60–80% B; 14–18 min, 80–100% B (kept for 2 min), 20–21 min, 100–10% B (kept for 3 min of

equilibration time). The LC flow was diverted (1:4) to the electrospray interface, and source parameters were accordingly selected, depending on the MS instrument used as analyser: +3.2 kV of capillary voltage, 30 psi of nebulizer pressure, 300 °C and 9 L min<sup>-1</sup> of drying gas temperature and gas flow, respectively, on the ESI-IT-MS spectrometer, and +2.1 kV of capillary voltage, 100 °C of source temperature, 50 L h<sup>-1</sup> of cone gas flow, 500 °C and 1000 L h<sup>-1</sup> of desolvation temperature and gas flow, apiece, on the ESI-QTOF-MS platform. Full scan spectra (50–1200 Da) were recorded in negative polarity with both detectors.

#### 2.4. Data treatment

Instrument control and chromatographic data treatment were carried out with the software ChemStation B.04.03 (Agilent Technologies, Waldbronn, Germany), Esquire Control and Data Analysis 4.0 (Bruker Daltonik, Bremen, Germany), and MassLynx 4.4 (Waters). Quantitative data were expressed as mean  $\pm$  standard deviation ( $n = 3$ ) in mg kg<sup>-1</sup> of dry weight (DW). Analysis of variance (one-way ANOVA) was conducted using the statistical software InfoStat 2020. Statistical significance was defined as  $p$ -values less than  $\alpha = 0.05$  using the Tukey's post hoc test. Graphical representations were performed with the software Excel 2021 (v.18.0). In order to explore the variation in data between varieties with different resistance to VWO, PCA was applied using The Unscrambler, version 6.11 (CAMO Software AS, Oslo, Norway). After that, to evaluate the possibility of discriminating samples according to the level of VWO resistance, PLS-DA was employed as a classification algorithm [32] using Matlab R2007b (The MathWorks, Inc., Natick, MA, USA) with the PLS\_Toolbox 5.51 (Eigenvector Research Inc. Wenatchee, WA, USA). In both cases, data were scaled before the analysis.

### 3. RESULTS AND DISCUSSION

#### 3.1. Qualitative characterization of plant tissue metabolic profiles

In a first stage of this work, the metabolic profiles of roots, stems and leaves from the sampled olive cultivars were comprehensively characterised. The powerful multi-class LC-MS method applied to the analysis of the prepared extracts allowed the monitoring of diverse chemical families in a single run (organic acids, pentacyclic triterpenes and phenolic compounds) [31]. The accurate  $m/z$  and isotopic distribution obtained with the QTOF MS analyser enabled the prediction of the molecular formula of the compounds. Metabolite identification was carried out by comparison with commercial standards (when available), as well as with an in-house built database of *Olea europaea* L. secondary metabolites and existing literature (see Table 1), considering high-resolution MS (HRMS) data, retention time (Rt) and elution order of the detected peaks.

**Table 1.** List of metabolites detected in root, stem and leaf extracts by LC-ESI-QTOF MS profiling

Rt/ min	Experimental m/z*	Error/ mDa	iFIT	Molecular Formula	Name of the Compound	Chemical Family	References	Quantified in:		
								Leaf	Stem	Root
0.8	191.0557	0.1	418.2	C <sub>7</sub> H <sub>12</sub> O <sub>6</sub>	quinic acid	organic acids	standard	x	x	x
1.0	389.1083	-0.1	266.9	C <sub>16</sub> H <sub>22</sub> O <sub>11</sub>	oleoside	secoiridoids and derivatives	[33,34]	x	x	x
1.3	315.1078	-0.2	373.2	C <sub>14</sub> H <sub>20</sub> O <sub>8</sub>	hydroxytyrosol glucoside	simple phenols and derivatives	[28,30,35,36]	x	x	
1.4	153.0551	-0.1	260.2	C <sub>8</sub> H <sub>10</sub> O <sub>4</sub>	hydroxytyrosol	simple phenols and derivatives	standard	x		
1.8	465.1035	0.2	277.6	C <sub>21</sub> H <sub>22</sub> O <sub>12</sub>	dihydroquercetin 3-O-glucoside	flavonoids	[28]		x	
2.3	389.1082	-0.2	527.9	C <sub>16</sub> H <sub>22</sub> O <sub>11</sub>	secologanoside	secoiridoids and derivatives	[28,33,34]	x	x	x
2.4	625.1977	-0.3	376.0	C <sub>25</sub> H <sub>38</sub> O <sub>18</sub>	unknown 1	unknown	-	x	x	x
3.0	305.0670	-0.28	313.2	C <sub>15</sub> H <sub>14</sub> O <sub>7</sub>	galocatechin	flavonoids	[30,37,38]	x		
3.0	449.1086	0.2	122.6	C <sub>21</sub> H <sub>22</sub> O <sub>11</sub>	cyanidin O-glucoside	flavonoids	[30,39]		x	
3.5	403.1236	-0.4	479.2	C <sub>17</sub> H <sub>24</sub> O <sub>11</sub>	elenolic acid glucoside (isomer 1)	secoiridoids and derivatives	[28,33,36,40]	x	x	x
3.9	377.1447	-0.1	337.0	C <sub>16</sub> H <sub>26</sub> O <sub>10</sub>	aldehydic form of decarboxymethyl elenolic acid glucoside	secoiridoids and derivatives	[41]	x	x	
3.9	537.1974	0.2	275.9	C <sub>26</sub> H <sub>34</sub> O <sub>12</sub>	cycloolivil glucoside (isomer 1)	lignans	[38,42,43]			x
4.7	403.1239	-0.1	458.3	C <sub>17</sub> H <sub>24</sub> O <sub>11</sub>	elenolic acid glucoside (isomer 2)	secoiridoids and derivatives	[28,33,36,40]	x	x	x
4.8	537.1976	0.4	125.2	C <sub>26</sub> H <sub>34</sub> O <sub>12</sub>	cycloolivil glucoside (isomer 2)	lignans	[43]			x
5.1	415.1607	0.3	529.8	C <sub>19</sub> H <sub>28</sub> O <sub>10</sub>	phenylethyl primeveroside	simple phenols and derivatives	[30]		x	
5.6	525.1604	-0.4	639.1	C <sub>24</sub> H <sub>30</sub> O <sub>13</sub>	demethyl oleuropein	secoiridoids and derivatives	[33,38,41]	x	x	
5.7	609.1453	-0.3	427.3	C <sub>27</sub> H <sub>30</sub> O <sub>16</sub>	rutin	flavonoids	standard	x	x	
5.8	359.1341	-0.1	513.8	C <sub>16</sub> H <sub>24</sub> O <sub>9</sub>	7-deoxyloganic acid	iridoid	[37,38,43]			x
6.1	555.1711	-0.3	302.3	C <sub>25</sub> H <sub>32</sub> O <sub>14</sub>	hydroxy oleuropein	secoiridoids and derivatives	[28,30,36,38]		x	x
6.2	303.0506	0.1	166.6	C <sub>15</sub> H <sub>12</sub> O <sub>7</sub>	taxifolin	flavonoids	[30,35,44,45]		x	
6.2	463.0874	-0.3	393.1	C <sub>21</sub> H <sub>20</sub> O <sub>12</sub>	quercetin O-glucoside (isomer 1)	flavonoids	[30,38,45]		x	
6.3	375.1444	0.0	113.0	C <sub>20</sub> H <sub>24</sub> O <sub>7</sub>	cycloolivil	lignans	[39,42,43]		x	
6.4	701.2291	-0.2	570.0	C <sub>31</sub> H <sub>42</sub> O <sub>18</sub>	neonuzhenide/oleuropein glucoside (isomer 1)	secoiridoids and derivatives	[28,38]	x	x	x
6.4	447.0923	-0.4	308.2	C <sub>21</sub> H <sub>20</sub> O <sub>11</sub>	luteolin 7-O-glucoside (isomer 1)	flavonoids	standard	x	x	
6.7	511.3484	0.2	161.5	C <sub>25</sub> H <sub>52</sub> O <sub>10</sub>	unknown 2	unknown	-	x	x	x
6.8	623.1977	0.1	450.0	C <sub>29</sub> H <sub>36</sub> O <sub>15</sub>	verbascoside	simple phenols and derivatives	standard	x	x	x
7.4	577.1561	0.4	403.9	C <sub>27</sub> H <sub>30</sub> O <sub>14</sub>	apigenin O-rutinoside	flavonoids	[38,40]	x		
7.5	623.1975	-0.1	323.9	C <sub>29</sub> H <sub>36</sub> O <sub>15</sub>	isoverbascoside	simple phenols and derivatives	[33,34,38]			x

Rt/ min	Experimental m/z*	Error/ mDa	iFIT	Molecular Formula	Name of the Compound	Chemical Family	References	Quantified in:		
								Leaf	Stem	Root
7.8	447.0925	-0.2	407.7	C <sub>21</sub> H <sub>20</sub> O <sub>11</sub>	luteolin O-glucoside (isomer 2)	flavonoids	[36,38]	x	x	
7.9	535.1810	-0.6	257.2	C <sub>26</sub> H <sub>32</sub> O <sub>12</sub>	hydroxypinoresinol glucoside	lignans	[28,38,42,43]		x	x
7.9	701.2290	-0.3	275.2	C <sub>31</sub> H <sub>42</sub> O <sub>18</sub>	neonuzhenide/oleuropein glucoside (isomer 2)	secoiridoids and derivatives	[28,36,38]		x	x
8.0	463.0882	0.5	380.5	C <sub>21</sub> H <sub>20</sub> O <sub>12</sub>	quercetin O-glucoside (isomer 2)	flavonoids	[30,34]		x	
8.0	431.0976	-0.2	395.2	C <sub>21</sub> H <sub>20</sub> O <sub>10</sub>	apigenin 7-O-glucoside	flavonoids	standard	x		
8.1	565.1923	0.2	283.0	C <sub>27</sub> H <sub>34</sub> O <sub>13</sub>	methoxypinoresinol glucoside	lignans	[42]		x	x
8.2	607.1666	0.3	187.2	C <sub>28</sub> H <sub>32</sub> O <sub>15</sub>	diosmin	flavonoids	[37,38]	x		
8.3	287.0551	-0.5	351.0	C <sub>15</sub> H <sub>12</sub> O <sub>6</sub>	dihydrokaempferol	flavonoids	[30]		x	
8.3	701.2288	-0.5	333.7	C <sub>31</sub> H <sub>42</sub> O <sub>18</sub>	neonuzhenide/oleuropein glucoside (isomer 3)	secoiridoids and derivatives	[28]	x		
8.6	461.1080	-0.4	50.3	C <sub>22</sub> H <sub>22</sub> O <sub>11</sub>	chrysoeriol O-glucoside	flavonoids	[30,37,40]	x		
8.7	577.1921	0.0	165.0	C <sub>28</sub> H <sub>34</sub> O <sub>13</sub>	acetoxypinoresinol glucoside	lignans	[38,42]		x	x
8.8	447.0924	-0.3	329.7	C <sub>21</sub> H <sub>20</sub> O <sub>11</sub>	luteolin O-glucoside (isomer 3)	flavonoids	[28,30,36]	x	x	
9.0	463.0881	0.4	412.2	C <sub>21</sub> H <sub>20</sub> O <sub>12</sub>	quercetin O-glucoside (isomer 3)	flavonoids	[30,34]		x	
9.2	491.1769	0.4	370.4	C <sub>21</sub> H <sub>32</sub> O <sub>13</sub>	unknown 3	unknown	-			x
9.5	701.2296	-0.3	43.1	C <sub>31</sub> H <sub>42</sub> O <sub>18</sub>	neonuzhenide/oleuropein glucoside (isomer 4)	secoiridoids and derivatives	[28]	x	x	x
9.8	539.1762	-0.2	646.3	C <sub>25</sub> H <sub>32</sub> O <sub>13</sub>	oleuropein	secoiridoids and derivatives	standard	x	x	x
10.3	555.2076	-0.2	352.7	C <sub>26</sub> H <sub>36</sub> O <sub>13</sub>	11-hydroxyiridodial glucoside pentaacetate	iridoid	[46]		x	x
10.8	539.1764	-0.1	513.6	C <sub>25</sub> H <sub>32</sub> O <sub>13</sub>	oleuroside	secoiridoids and derivatives	[33,38]	x	x	
11.5	583.2023	-0.4	211.3	C <sub>27</sub> H <sub>36</sub> O <sub>14</sub>	lucidumoside C	secoiridoids and derivatives	[28,30,43]	x	x	x
11.8	523.1817	0.1	60.1	C <sub>25</sub> H <sub>32</sub> O <sub>12</sub>	ligstroside	secoiridoids and derivatives	[28,30,38]	x	x	x
11.5	651.2283	-0.6	374.7	C <sub>31</sub> H <sub>40</sub> O <sub>15</sub>	unknown 4	unknown	-		x	
12.7	415.1392	-0.1	448.8	C <sub>22</sub> H <sub>24</sub> O <sub>8</sub>	acetoxypinoresinol	lignans	[33]		x	x
12.7	377.1235	-0.1	350.2	C <sub>19</sub> H <sub>22</sub> O <sub>8</sub>	oleuropein aglycone (isomer 1)	secoiridoids and derivatives	[30,38]	x	x	
13.3	377.1239	0.3	54.8	C <sub>19</sub> H <sub>22</sub> O <sub>8</sub>	oleuropein aglycone (isomer 2)	secoiridoids and derivatives	[30,38]	x	x	
15.7	471.3467	-0.7	607.4	C <sub>30</sub> H <sub>48</sub> O <sub>4</sub>	maslinic acid	pentacyclic triterpenes	standard	x	x	x
16.4	617.3840	-0.2	101.8	C <sub>39</sub> H <sub>54</sub> O <sub>6</sub>	unknown 5	unknown	-	x	x	
17.5	455.3527	0.2	241.1	C <sub>30</sub> H <sub>48</sub> O <sub>3</sub>	betulinic acid	pentacyclic triterpenes	standard	x	x	x
17.8	455.3526	0.1	282.5	C <sub>30</sub> H <sub>48</sub> O <sub>3</sub>	oleanolic acid	pentacyclic triterpenes	standard	x	x	x

Rt, retention time; \* m/z values correspond to [M-H]<sup>-</sup>.

The list of compounds found in the investigated samples is presented in [Table 1](#). It includes the detected  $m/z$  of the  $[M-H]^-$  ion, the mass error (difference between detected and theoretically calculated  $m/z$  signals), the iFIT value (which gives an idea of the concordance between the experimental and theoretical isotopic patterns), the calculated molecular formula and the identity assigned to each detected peak. Some reports in which the compounds were previously described are cited under the reference heading, and the kind of plant tissue where the compound was quantified in a subsequent step of the project is marked in the appropriate column. It is worth noting that [Table 1](#) lists a good number of examples of very meritorious works in the field, but by no means does it pretend to be a comprehensive review by citing all the references reporting each compound. More than 50 compounds belonging to several chemical classes were, at least, tentatively annotated: 1 organic acid (quinic acid), 3 pentacyclic triterpenes (maslinic, betulinic and oleanolic acids) and 47 phenolic compounds. The last class of metabolites, one of the most ubiquitously distributed in the plant kingdom, gathered the largest number of compounds, which can be classified into 5 subfamilies: 7 lignans (cycloolivil, and two isomers of its glycosidic form, acetoxypinoresinol, acetoxypinoresinol glucoside, hydroxypinoresinol glucoside and methoxypinoresinol glucoside), 16 flavonoids (dihydroquercetin 3-*O*-glucoside, gallocatechin, cyanidin *O*-glucoside, rutin, taxifolin, three isomers of quercetin *O*-glucoside, three isomers of luteolin *O*-glucoside, apigenin *O*-rutinoside, apigenin 7-*O*-glucoside, diosmin, dihydrokaempferol and chrysoeriol *O*-glucoside), 5 simple phenols and glucoside derivatives (hydroxytyrosol and its glycosidic form, verbascoside, isoverbascoside and phenylethyl  $\beta$ -primeveroside (which has been included in this subfamily because of its structural similarity), 2 iridoids (7-deoxyloganic acid and 11-hydroxyiridodial glucoside pentaacetate) and 17 secoiridoids and related compounds. The group of secoiridoids was the most abundant subfamily of phenolic compounds and comprised lucidumoside C, ligstroside, 4 isomers of a compound with molecular formula  $C_{31}H_{42}O_{18}$ , which could be either neonuzhenide or oleuropein glucoside, several oleuropein related compounds (oleuropein, demethyl oleuropein, hydroxy oleuropein, two isomers of oleuropein aglycone, and oleuroside) and 5 derivatives of elenolic acid (two isomers of elenolic acid glucoside, the aldehydic form of decarboxymethyl elenolic acid glucoside, oleoside and secologanoside). The latter two are mass isomers whose identity was assigned based on the relative retention times described in previous reports [33,34]. As seen in [Table 1](#), a large proportion of the identified compounds were glycosylated derivatives and isomers with hexoses attached in different positions that could not be determined on the basis of the HRMS data exclusively, when the pure standards were not available.

Some other compounds could not be confidently annotated but are presented in [Table 1](#) because of their relevance within the profiles (in terms of peak area). The compound with  $m/z$  625.1977 eluting at 2.4 min (unknown 1) presented  $C_{25}H_{38}O_{18}$  as the calculated molecular formula. Interestingly, it produced two major in-source fragments, corresponding to  $C_{17}H_{24}O_{11}$  (elenolic acid glucoside) and  $C_{23}H_{34}O_{16}$  (elenolic acid diglucoside), which suggest that it might be an elenolic acid diglucoside derivative ( $+C_2O_2H_4$ ). The molecular formula calculated for unknown 3 (Rt: 9.2

min and  $m/z$  491.1769) was  $C_{27}H_{32}O_{13}$ . Such metabolite has not been described before in any olive matrix to the best of our knowledge; nevertheless, it could correspond to a phenolic glycoside, such as 3,4,5-trimethoxyphenyl 2-*O*-( $\alpha$ -L-fucopyranosyl)- $\beta$ -D-glucopyranoside from *Walsura yunnanensis* [47]. In the same way, unknown 4 (Rt: 11.5 min and  $m/z$  651.2283), with a calculated molecular formula of  $C_{31}H_{40}O_{15}$  could be annotated as martynoside, a verbascoside derivative previously isolated from *Buddleja globosa* hope [48]. Regarding unknown 5 (Rt: 16.4 min and  $m/z$  617.3840), with a calculated molecular formula of  $C_{39}H_{54}O_6$ , as it eluted in the chromatogram area of triterpenic acids, it may be some kind of derivative, such as the ester caffeoyl-oleanolic acid that was isolated from *Dioclea lasiophylla* by David and coauthors [49]. Another unidentified compound (unknown 2), presenting a major signal with  $m/z$  511.3484 (calculated molecular formula:  $C_{25}H_{52}O_{10}$ ), eluted at 6.7 min, but no plausible identity could be suggested for this metabolite.

### 3.2. Quantitative analysis of the targeted metabolites

In a subsequent stage, the prepared extracts were studied from a quantitative point of view, to assess the abundance and distribution of the most relevant metabolites in the three different plant tissues under investigation (leaves, stems and roots) and to seek out differences in the metabolic profiles of the evaluated cultivars. Firstly, serial dilutions of a standard solution containing 10 pure standards of some of the detected analytes were injected into the LC-IT MS system and the main analytical parameters of the quantitative method (linear dynamic range, limits of detection and quantification and repeatability) were assessed to ensure the quality of the obtained results (Table S1). Limits of detection and quantification were found between 2.0–171.3  $\mu\text{g L}^{-1}$  and 6.7–571.0  $\mu\text{g L}^{-1}$  for betulinic acid and tyrosol, respectively. The intra-day repeatability, expressed as coefficient of variation (%CV), presented values between 0.3 and 7.1% for quinic acid and hydroxytyrosol, respectively, and the inter-day repeatability was, in all cases, less than 10.6%, which indicates that the applied methodology exhibited very satisfactory precision.

After evaluating the basic quality parameters of the method, all the prepared extracts were injected into the LC-IT MS system and quantitative data were generated for 56 analytes (28 compounds in roots, 44 in stems and 34 in leaves). The area of compounds lacking an available pure standard was compared to the external calibration curve of a different compound belonging to the same metabolite subfamily or presenting a chemical structure of a similar molecular weight. In this way, luteolin 7-*O*-glucoside was used to quantify all the flavonoids except for rutin and apigenin *O*-rutinoside, which were quantified with the rutin calibration curve; hydroxytyrosol was used to quantify its glycosidic derivative and oleuropein was used to quantify the rest of phenolic compounds and unknowns. Even though no absolute quantification was performed, this strategy enabled the fair comparison of metabolite profusion in the three olive matrices, as well as among the different cultivars.

### 3.2.1. Metabolites distribution throughout plant tissues

If we focus on the total amount of the quantified compounds, the leaf was the tissue presenting the greatest concentration of the targeted metabolites, the root was the olive organ that had the lowest concentration of this type of compounds and the stem was the matrix with the richest profile in terms of the number of detected molecules. The latter had been observed by Tóth and co-workers, who detected 41 metabolites in olive barks by LC-MS and just 32 of them in leaves [35]. Secoiridoids were the most abundant chemical family and oleuropein was the compound most concentrated in all samples, as widely reported before [35,36,38,44,50,51], except for in 'Hojiblanca' and 'Picual' roots, where a higher content of verbascoside was found. This finding is in accordance with the results from Cardoni and collaborators [27], and those from Mechri and collaborators, who found a higher concentration of verbascoside in roots of well-watered 'Chétoui' olive trees [52].

In order to facilitate the evaluation of the results, most of the quantified compounds were grouped into five main groups: simple phenols and glycoside derivatives, secoiridoids and related compounds, flavonoids, lignans and triterpenic acids, as presented in Figure 1. Compounds not belonging to any of the mentioned chemical families are not included in the graphics but will be addressed individually in subsequent discussions. Figure 1 shows the distribution of the different groups of metabolites among the three analysed tissues for each cultivar. The sum concentration of all the compounds belonging to a given group is expressed as a percentage of the total amount found in the three matrices of each olive cultivar, which is normalized to 100. In this way, it is possible to depict several general tendencies, although, in some cases, great variability can be observed depending on the cultivar.

As far as simple phenols and glycoside derivatives were concerned, they were found in all three evaluated matrices. Roots were the matrix with the highest percentage of these types of compounds (40–70%), except for 'Empeltre', in which leaves were the richest plant organ with around 70% of the total. In the rest of the cultivars, leaves accounted for 20–40%, while the remaining 5–15% was found in stems. It is worth noticing that the distribution of individual metabolites belonging to this group was also diverse (Table 1); verbascoside and isoverbascoside were the only simple phenol glycosides found in roots; phenylethyl primeveroside was just detected in stems and hydroxytyrosol in leaves. Secoiridoids and related compounds were mostly found in leaves (45–60%), followed by stems (20–35%) and roots (10–30%). As previously mentioned, oleuropein was the secoiridoid found at the highest rates, ranging from 6736 mg kg<sup>-1</sup> (in 'Hojiblanca' roots) to 74,453 mg kg<sup>-1</sup> DW (in 'Mastoidis' leaves). Triterpenic acids was the other family of metabolites distributed throughout the three studied tissues. Between 65 and 75% of these compounds were found in leaves, followed by roots and stems with 5–20%, each. Oleanolic acid was the compound found at the highest concentration in leaves (10,152–15,670 mg kg<sup>-1</sup> DW) and stems (1064–3775 mg kg<sup>-1</sup> DW), while maslinic acid was the most concentrated in roots (2181–3897 mg kg<sup>-1</sup> DW). No flavonoids were detected in roots, which agrees with previous works in

which they were not found [27,38,53] or were reported at very low concentration levels [50,51]. Flavonoids were mostly found in leaves (80–90%), with minor amounts quantified in stems (510 to 1267 mg kg<sup>-1</sup> DW). Moreover, as seen in Table 1, just the three isomers of luteolin *O*-glucoside and rutin were common to both matrices; quercetin *O*-glucoside, dihydroquercetin 3-*O*-glucoside, cyanidin *O*-glucoside, dihydrokaempferol and taxifolin were absent from leaves, and apigenin 7-*O*-glucoside, apigenin *O*-rutinoside, diosmin and gallocatechin were not found in stems. A comparable trend was observed for lignans. They were distributed homogeneously amongst roots (45–65%) and stems (35–55%) but were missing in leaves. Most of them were found in both matrices except for cyclooolivil, which was only found in stems, and its glycosylated form, which appeared just in roots. Acetoxypinoresinol glucoside was the most abundant lignan in most cultivars, with contents ranging from 494 to 1588 mg kg<sup>-1</sup> DW in stems, and 262 to 1001 mg kg<sup>-1</sup> DW in roots. The absence of this family of compounds in olive leaves has been widely documented in other works dealing with the LC-MS phenolic profiling of leaves [38,54,55], while other authors have reported very low levels of lignans in this olive tissue [30,36,56].

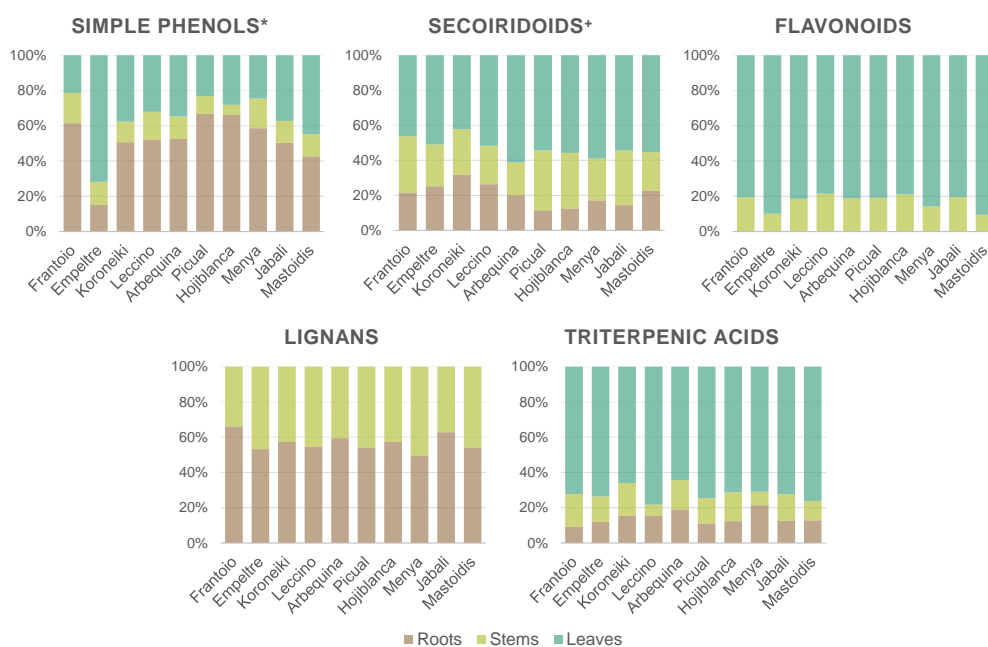


**Figure 1.** Metabolite distribution (percentage of total amount) throughout the three analysed tissues (roots, stems and leaves) of 10 different olive cultivars (sorted by resistance to VWO: from highly resistant (HR, left) to extremely susceptible (ES, right)). Contents expressed in a normalized way. \* and glycoside derivatives \*and related compounds

Regarding the rest of the metabolites not belonging to any of the major groups, different behaviours can be pointed out. Quinic acid was quantified in the three matrices and presented the highest content in leaves (4439–7815 mg kg<sup>-1</sup> DW), followed by stems (1469–2710 mg kg<sup>-1</sup> DW) and roots (239–377 mg kg<sup>-1</sup> DW). With respect to iridoids, they were not found in leaves and the

highest content of these compounds was observed in roots, as previously described by Michel and collaborators for 7-deoxyloganic acid [38]. Finally, five unknown compounds were semi-quantified because of their high relative intensity in the profiles (the oleuropein calibration curve was used to quantify all of them). The highest contents were found for unknowns 2 and 5 in olive leaves. As already mentioned, no tentative identity was proposed for unknown 2, but unknown 5 could be an oleanolic acid derivative and its high relative abundance in leaves could support this hypothesis.

### **3.2.2. Assessment of differences in the metabolic profiles of the 10 cultivars under study**

It is widely recognized that the genetic origin is one of the main factors affecting the profile of secondary metabolites of olive-related matrices such as olive oil or olive leaves [28,36,45]. In this project, 10 different olive cultivars belonging to different resistance/susceptibility response categories to VVO, according to a previous evaluation of disease parameters, were studied [6,10]. Two cultivars belonging to each pre-existing category were chosen: 'Frantoio' and 'Empeltre' (HR); 'Koroneiki and 'Leccino' (R); 'Arbequina' and 'Picual' (MS); 'Hojiblanca' and 'Menya' (S); 'Jabali' and 'Mastoidis' (ES). Thus, in a subsequent step, the generated quantitative data were re-evaluated with the final aim of finding possible links between the resistance to *V. dahliae* and the metabolic profiles of leaves, stems and roots of the cultivars under investigation. To facilitate the visualization of the results, [Figure 2](#) presents the sum concentrations per compound class in the three olive tissues of each cultivar, following the same strategy of metabolite grouping as in [Figure 1](#). It is important to note that the results shown are the average of three biological replicates ( $n = 3$ ). Thus, the magnitude of the error bars illustrating the standard deviation makes complete sense if we have in mind the variability among different plant individuals. In general terms, the abundance of each group of metabolites in the different cultivars followed the same trend in the three plant tissues, i.e., the cultivar that exhibited the highest concentration of a specific group of compounds in one matrix also ranked among the richest ones in the other two matrices. This can be clearly observed for secoiridoids and related compounds, flavonoids, lignans and simple phenol and glycoside derivatives (except for roots). This indicates that the prevalence of secondary metabolites in the different tissues of the plant seems to be somehow proportional and is cultivar-dependent.

As discussed in the previous section, secoiridoids were the most abundant family of metabolites for all the evaluated cultivars. Indeed, they were one order of magnitude more abundant than the rest of groups of compounds, on average. Therefore, taking into account the contribution of all the quantified molecules, the general trend followed by secoiridoids is applicable to the total content of secondary metabolites. In this way, it is possible to deduce from [Figure 2](#) that 'Empeltre' (HR) and 'Mastoidis' (ES) were the richest cultivars in terms of secoiridoids and, thus, in terms of secondary metabolites, while 'Picual' (MS), 'Hojiblanca' (S), 'Arbequina' (MS) and 'Frantoio' (HR) were among the cultivars with the lowest content of this fraction of compounds. These general observations suggest that the total amount of secondary metabolites does not correlate with the resistance/susceptibility of these olive cultivars to the fungus *V. dahliae*. This

finding contrasts with the conclusions achieved by Gharbi and collaborators, that reported a higher total polyphenol content in roots and stems of 'Sayali' (resistant) compared to 'Chemlali' (extremely susceptible) olive trees [24]. However, it is important to note that a direct comparison of our results may not be entirely feasible. This discrepancy arises from the fact that these authors employed a colorimetric method to assess phenolic content in olive tissues and examined two olive cultivars that are not within the scope of our current study. Our working hypothesis suggests that the key factor contributing to a more effective protective response against the pathogen in resistant cultivars is likely linked to the compositional profile of plant organs rather than simply the total concentration of some families of metabolites.

In the case of secoiridoids, some cultivars stood out for presenting high amounts of specific metabolites, such as secologanoside in the three tissues of 'Jabali' (ES), or ligstroside in all 'Leccino' (R) samples (Table S2). Regarding simple phenols and glycoside derivatives, the highest contents were found in 'Empeltre' (HR) in leaves, and 'Leccino' and 'Empeltre' in stems (Figure 2). However, the prevalence of this family of metabolites in roots was completely different, and 'Empeltre' stood out for its low concentration. As far as flavonoids were concerned, 'Jabali' (ES) was the richest cultivar, followed by 'Leccino' in stems and 'Empeltre' in leaves, while 'Menya' (S) was among the cultivars with the lowest flavonoid content in both tissues. The compounds with the highest weight in the flavonoid profile were luteolin 7-O-glucoside in leaves, dihydrokaempferol in 'Hojiblanca' (S) stems and taxifolin in 'Leccino' (R) stems (Table S2). As seen in Figure 2, the contents of lignans were more homogeneous among the evaluated cultivars, although 'Menya' (S) could be pointed out as the richest variety in terms of this family of compounds in stems, while 'Picual' (MS) was the poorest in roots (statistical significance  $p < 0.05$ ). Finally, triterpenic acids trends varied a lot from one kind of matrix to the others. For example, 'Leccino' and 'Menya' presented very low contents of these metabolites in stems, but they were among the richest cultivars in the other two matrices (Figure 2). 'Arbequina' (MS) stems presented a particular profile characterised by very similar amounts of maslinic and oleanolic acids, unlike the rest of the cultivars in which oleanolic acid was prevalent, as commented in Section 3.2.1.

Few prior studies have addressed the distribution of secondary metabolites across various olive plant tissues, and none of them have conducted such an investigation quantitatively. Consequently, there is no existing data to compare with our results.

### **3.3. Relationship between cultivars metabolic profiles and resistance/susceptibility to the soil fungus *Verticillium dahliae***

To further investigate the possible relationship between tissues' metabolic profiles and resistance to VWO, the quantitative results were evaluated by applying unsupervised and supervised multivariate analysis. In this way, 28 compounds in roots, 44 in stems and 34 in leaves were used as variables in the three data matrices (with 30 samples each) that were built for statistical analysis.



**Figure 2.** Sum concentration of the main metabolite classes in the three analysed tissues (leaves (A), stems (B) and roots (C)) of 10 different olive cultivars sorted by resistance to VVO: from HR (left) to ES (right). Error bars show the standard deviation of three biological replicates ( $n = 3$ ). Lower case letters indicate Tukey's post hoc test differences ( $p < 0.05$ ) among different cultivars. \* and glycoside derivatives \*and related compounds

Initially, principal component analysis (PCA) was performed to check the natural clustering of samples from each tissue type. **Figure 3** shows the obtained PCA scores plots for the two principal components (PCs) showing the best grouping of the samples for each olive tissue.

In the leaf samples, the first two PCs covered 52% of the variance, and discriminated between HR (blue colour) and ES (green colour) cultivars along the PC2. The rest of the categories (MS, S and R), coloured in red, were mixed in the central cluster (**Figure 3A**). Scores values for PC2 were high for the ES category, which means that compounds with positive loadings (**Figure S1A**) such as elenolic acid glucoside (isomers 1 and 2), unknown 1, hydroxytyrosol glucoside and neonuzhenide/oleuropein glucoside (isomer 3) were positively related to ES cultivars. The negative loadings (**Figure S1A**) corresponded to unknown 5, betulinic acid, oleuropein aglycone (isomer 2), oleanolic acid, neonuzhenide/oleuropein glucoside (isomer 4), maslinic acid and quinic acid, among others. According to scores for PC2, these metabolites were positively related to the HR category. The loading plot also revealed the importance of unknown 2 for the separation of some leaf samples with intermediate susceptibility (**Figure S1A**).

In stem samples, the first two PCs explained 40% of the variance. However, PC4, explaining only 9% of the variance, was responsible for a moderately good separation among HR, intermediate susceptibility/resistance (MS, S and R) and ES categories (**Figure 3B**). In this case, the loading plot (**Figure S1B**) indicated that the main compounds affecting the separation were oleanolic acid, quinic acid, acetoxypinoresinol, unknown 5 and oleuropein aglycone (isomer 1) (positive loadings showing a positive relation with the HR category), and neonuzhenide/oleuropein glucoside (isomer 2), unknown 2, elenolic acid glucoside (isomer 2), hydroxytyrosol glucoside, cyanidin *O*-glucoside, quercetin *O*-glucoside (isomers 1 and 3), and the aldehydic form of decarboxymethyl elenolic acid glucoside (negative loadings showing a positive relation with ES cultivars).

Lastly, in root samples, the first two PCs covered 53% of the variance, but good separation among cultivars from different resistance categories could barely be found (data not shown). PC5, explaining just 6% of the variance, provided a slightly better separation between the HR and ES categories (**Figure 3C**). The loading plot (**Figure S1C**) showed that compounds such as acetoxypinoresinol, acetoxypinoresinol glucoside, oleanolic acid, betulinic acid, hydroxypinoresinol glucoside and maslinic acid presented a positive relation with HR cultivars and some samples from the intermediate susceptibility categories (which were quite mixed in this case). On the contrary, negative loadings showed as main compounds: isoverbacoside, hydroxyoleuropein, lucidumoside C and unknown 3, with a positive relation to ES cultivars and a negative one to the HR category. Overall, none of the quantitative data from the three studied olive tissues pointed out any clear potential marker for cultivars with intermediate resistance.

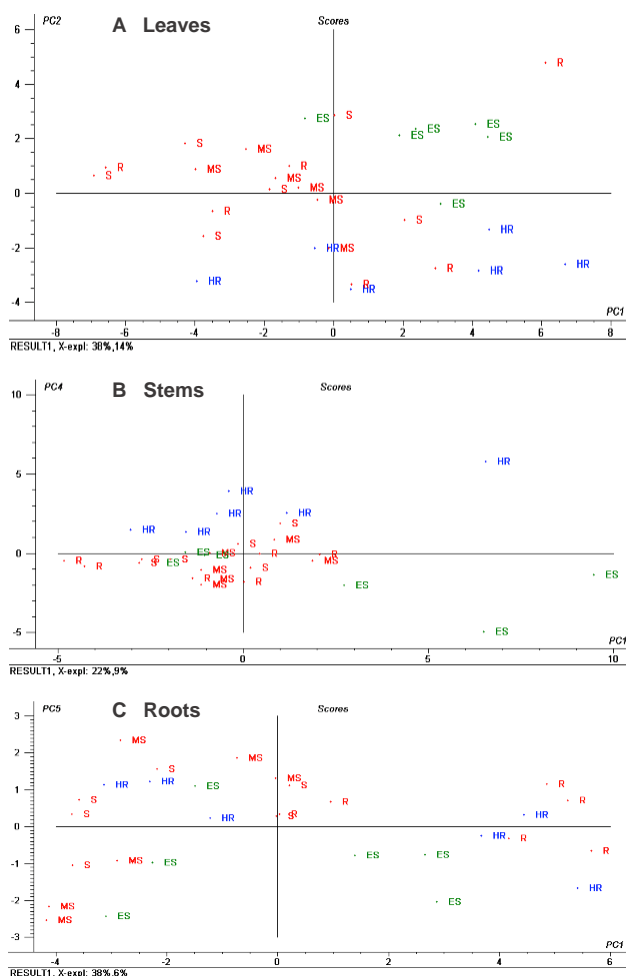


**Figure 3.** Principal component analysis (PCA) scores plots representing the two principal components (PCs) showing best samples' grouping for each olive tissue: **(A)** leaves (PC1 vs. PC2), **(B)** stems (PC1 vs. PC4) and **(C)** roots (PC1 vs. PC5)

In a later stage, supervised partial least squares discriminant analysis (PLS-DA) was performed to discriminate samples belonging to olive cultivars showing different resistance/susceptibility to VVO. This time, cultivars were grouped in the three classes inferred from the previous unsupervised analysis: HR (class 1), MS + S + R (class 2) and ES (class 3). The full cross-validation parameters of the models built for each olive tissue type are displayed in [Table 2](#). Confusion matrices showing correctly and wrongly classified samples from the cross-validation subset can be also found in [Table 2](#). As already seen in the PCA plots ([Figure 3](#)), the metabolites from the matrix showing less capability to discriminate samples among resistance categories were those from the roots. The root PLS-DA model presented the lowest accuracy and the highest error rate. In fact, it showed the worst classification capacity, with 10 samples assigned to a wrong class ([Table 2](#)). On

the other hand, both leaf and stem models presented very satisfactory correct classification rates, showing accuracy values of 90 and 93% for cross-validation, and only 3 and 2 wrongly classified samples, respectively. Interestingly, in both tissues, HR and ES categories were well-classified and those samples wrongly classified corresponded to cultivars with intermediate susceptibility (class 2). This might be due to the fact that the latter was the broader class, which, as mentioned before, gathered together three intermediate resistance categories (MS, S and R), presenting very diverse metabolic profiles.

**Table 2.** Cross-validation confusion matrices and validation parameters for the PLS-DA classification models. Class 1: highly resistant cultivars; class 2: resistant, moderately susceptible and susceptible cultivars; class 3: extremely susceptible cultivars

Real/Predicted	Leaves			Stems			Roots		
	Class 1	Class 2	Class 3	Class 1	Class 2	Class 3	Class 1	Class 2	Class 3
Class 1	6	0	0	6	0	0	5	0	1
Class 2	2	15	1	2	16	0	5	9	4
Class 3	0	0	6	0	0	6	0	0	6
Components	3			4			3		
Error rate	0.06			0.04			0.28		
Accuracy	0.90			0.93			0.70		

The variables' influence in each class of the three PLS-DA models is depicted in [Figure S2](#), which shows the joint representation of the regression coefficient of each metabolite and its variable importance on the projection (VIP) value. Compounds with VIP values higher than 1 could be pointed out as potential markers for each class (in this case a VIP value > 1.2–1.5 was considered). It is possible to see that they correspond to minimum and maximum regression coefficients, which give an idea of the importance of each variable in the prediction. Thus, the information retrieved from these graphs can be used to describe typical compositional patterns of cultivars belonging to distinct categories of resistance/susceptibility for each studied olive tissue ([Table 3](#)). As expected, some of these potential markers were also the variables influencing the most sample clustering in the PCA models ([Figures 3 and S1](#)), such as maslinic acid, oleuropein aglycone (isomer 2), hydroxytyrosol glucoside and elenolic acid glucoside (isomers 1 and 2) in leaves; quinic acid, acetoxypinoresinol, unknown 5 and neonuzhenide/oleuropein glucoside (isomer 2) in stems; and betulinic acid in roots. It is also worth noting that some metabolites appeared as markers of the same category in different olive tissues, which reinforces their discriminating role in the metabolic profiles. For example, low levels of elenolic acid glucoside (isomer 2) were characteristic features of HR cultivars both in leaves and stems, showing high VIP values and negative regression coefficients. A high content of 11-hydroxyiridodial glucoside pentaacetate was characteristic of stems and roots of cultivars with medium susceptibility to VWO, while the opposite behaviour was typical from the same tissues from ES cultivars. In the same way, high levels of maslinic acid were found in leaves and stems of ES cultivars, while cultivars with medium susceptibility were characterized by low levels of this triterpenic acid.

**Table 3.** Compositional patterns of cultivars belonging to different resistance/susceptibility categories as pointed out by the PLS-DA models built for each olive tissue type

Highly Resistant Cultivars			Medium Susceptibility Cultivars *			Extremely Susceptible Cultivars					
	Metabolite	Regression Coefficient	VIP Value	Metabolite	Regression Coefficient	VIP Value	Metabolite	Regression Coefficient	VIP Value		
Leaves	↑	Maslinic acid	0.057	1.60	Gallocatechin	0.121	3.78	Lucidumoside C	0.064	1.43	
		Oleuropein aglycone (is 2)	0.055	1.92				Oleuroside	0.060	1.44	
								Neonuzhenide/oleuropein glucoside (is 3)	0.060	2.05	
								Hydroxytyrosol glucoside	0.057	1.87	
								Elenolic acid glucoside (is 2)	0.038	1.71	
								Maslinic acid <sup>+</sup>	0.035	1.82	
								Elenolic acid glucoside (is 1)	0.019	1.11	
		↓	Lucidumoside C	-0.002	1.35	Luteolin 7-O-glucoside (is 1)	-0.066	1.65	Oleuropein aglycone (is 2)	-0.001	1.49
			Oleuroside	-0.007	1.61	Chrysoeriol O-glucoside	-0.070	2.03	Aldehydic form of DEA glucoside	-0.004	1.37
			Neonuzhenide/oleuropein glucoside (is 3)	-0.030	2.83	Oleuropein aglycone (is 1)	-0.077	2.05			
			Hydroxytyrosol glucoside	-0.032	2.62	Demethyl oleuropein	-0.084	2.19			
			Elenolic acid glucoside (is 1)	-0.040	1.53	Maslinic acid <sup>+</sup>	-0.092	2.96			
			Elenolic acid glucoside (is 2) <sup>+</sup>	-0.045	2.54						
			Aldehydic form of DEA glucoside <sup>+</sup>	-0.053	1.49						
Stems	↑	Unknown 4	0.058	3.39	11-Hydroxyiridodial glucoside pentaacetate <sup>+</sup>	0.096	2.12	Oleuroside	0.094	4.04	
		Quinic acid	0.051	2.49				Metoxypinoresinol glucoside	0.067	2.14	
		Demethyl oleuropein	0.042	1.94				Oleuropein	0.060	3.34	
		Oleanolic acid	0.036	2.70				Neonuzhenide/oleuropein glucoside (is 2)	0.057	1.65	
		Acetoxypinoresinol	0.029	1.64				Betulinic acid	0.045	1.68	
		Unknown 5	0.022	2.06				Maslinic acid <sup>+</sup>	0.023	1.63	
		↓	Neonuzhenide/oleuropein glucoside (is 2)	-0.029	2.55	Betulinic acid	-0.059	2.21	11-Hydroxyiridodial glucoside pentaacetate <sup>+</sup>	-0.085	1.90
			Aldehydic form of DEA glucoside <sup>+</sup>	-0.038	1.54	Maslinic acid <sup>+</sup>	-0.063	1.92			
			Elenolic acid glucoside (is 2) <sup>+</sup>	-0.042	2.40	Metoxypinoresinol glucoside	-0.086	2.71			
			Unknown 2	-0.045	2.96	Oleuropein	-0.112	4.08			
						Oleuroside	-0.130	5.18			

Highly Resistant Cultivars			Medium Susceptibility Cultivars *			Extremely Susceptible Cultivars			
	Metabolite	Regression Coefficient	VIP Value	Metabolite	Regression Coefficient	VIP Value	Metabolite	Regression Coefficient	VIP Value
Roots	† Cycloolivil glucoside (is 2)	0.082	5.69	11-Hydroxyiridodial glucoside pentaacetate <sup>+</sup>	0.110	2.56	Acetoxypinoresinol glucoside	0.109	3.04
	Betulinic acid	0.047	1.94	Hydroxypinoresinol glucoside	0.092	1.92	Unknown 1	0.083	1.74
	Elenolic acid glucoside (is 1)	0.034	1.42	Betulinic acid	0.052	1.70			
	‡ Verbascoside	-0.047	1.75	Acetoxypinoresinol glucoside	-0.110	2.20	Cycloolivil glucoside (is 2)	-0.015	1.67
				Cycloolivil glucoside (is 2)	-0.067	2.56	Oleanolic acid	-0.076	2.17
							Hydroxypinoresinol glucoside	-0.088	2.78
							Betulinic acid	-0.099	3.06
						11-Hydroxyiridodial glucoside pentaacetate <sup>+</sup>	-0.113	3.85	

\* including resistant, moderately susceptible and susceptible cultivars; <sup>+</sup> markers of a given category matching in several olive tissues. Abbreviations: †, high content; ‡, low content; is, isomer; DEA, decarboxymethyl elenolic acid.

When just one tissue is considered, contrasting trends of some metabolites in different categories can be observed. This means that it is the synergistic effect of several metabolites (described as compositional pattern) which could be linked to the level of resistance to VWO. For example, low levels of maslinic acid were found in leaves of cultivars belonging to the medium susceptibility class, while high levels were typical of HR cultivars when accompanied by a high concentration of oleuropein aglycone (isomer 2), and low contents of lucidumoside C, oleuroside, neonuzhenide/oleuropein glucoside (isomer 3), hydroxytyrosol glucoside and elenolic acid glucoside (isomers 1 and 2). On the contrary, high leaf levels of maslinic acid and the aforementioned metabolites (lucidumoside C, oleuroside, neonuzhenide/oleuropein glucoside (isomer 3), hydroxytyrosol glucoside and elenolic acid glucoside (isomers 1 and 2)), together with low levels of oleuropein aglycone (isomer 2) were typical from ES cultivars. In stems, neonuzhenide/oleuropein glucoside (isomer 2) could be pointed out as a specific marker with a contrary trend in the extreme categories: low content in HR cultivars (negative regression coefficient) and high concentration in ES samples (positive regression coefficient). Moreover, stems from ES cultivars presented low concentrations of 11-hydroxyiridodial glucoside pentaacetate and high levels of oleuropein, oleuroside, metoxypinoresinol glucoside and two triterpenic acids (betulinic and maslinic), exactly the opposite pattern shown by samples from the medium susceptibility categories. Finally, in roots, high concentrations of cycloolivil glucoside (isomer 2) and betulinic acid were characteristic of HR cultivars, while a high content of betulinic acid and low cycloolivil glucoside (isomer 2) concentration were typical from medium susceptibility cultivars, and low levels of both metabolites were representative of the ES category. 11-hydroxyiridodial glucoside pentaacetate and hydroxypinoresinol glucoside were also useful to discriminate cultivars from the medium susceptibility class, where they were found at high concentrations (positive correlation coefficients), and ES cultivars, which presented low levels of these two compounds (negative correlation coefficients).

The description of these compositional patterns in cultivars displaying varying levels of resistance or susceptibility to VWO stands out as a major accomplishment of this research. This information holds the potential for categorising olive cultivars in the future based on the metabolic profiles of their leaves, stems or roots. Furthermore, it is noteworthy to highlight the impressive results generated through the statistical analysis, particularly given the significant diversity among the samples under study, which encompassed 10 different olive cultivars classified into 5 resistance/susceptibility categories. Extending this study with additional cultivars and replicates in future projects presents a promising prospect for future research.

#### 4. CONCLUSIONS

In this work, the metabolic profiles of leaves, stems and roots of 10 different olive cultivars with different degrees of resistance/susceptibility to VWO were studied by applying a multiclass LC-MS method (using both high- and low-resolution analysers with qualitative and quantitative purposes,

respectively). A total of 56 compounds belonging to several chemical classes (organic acids, simple phenols, secoiridoids, flavonoids, lignans, triterpenic acids, etc.) were identified in the profiles. From them, 28 were quantified in roots, 44 in stems and 34 in leaves, and their distribution among the three tissues was established. In general, although no flavonoids were found in roots and no lignans were detected in leaves, the prevalence of the chemical families found commonly throughout the different plant organs seemed to be consistent and cultivar-dependent. PCA and PLS-DA were also performed on the quantitative data matrices of the evaluated olive tissues to investigate the possible relationship between the metabolite content and the cultivar's susceptibility level, trying to gain a deeper understanding of the metabolic processes underlying olive resistance to VWO. The models for both leaves and stems exhibited highly commendable correct classification rates, achieving accuracy values of 90% and 93% for cross-validation, respectively. Our findings revealed that cultivars showing similar susceptibility levels shared common compositional patterns. This discovery holds the potential to facilitate the identification of optimal genitor candidates in future breeding programs, aiming to develop cultivars with heightened resistance to VWO while maintaining favourable agronomic characteristics. Furthermore, the models, constructed using the information from various olive tissues, consistently underscored certain compounds as potential markers of resistance and susceptibility, suggesting their possible involvement in the plant's defence mechanisms against *V. dahliae*. For instance, the levels of elenolic acid glucoside (isomer 2) and the aldehydic form of decarboxymethyl elenolic acid glucoside in leaves and stems exhibited an inverse correlation with VWO resistance. A similar negative correlation was established for VWO susceptibility and the contents of 11-hydroxyiridodial glucoside pentaacetate in stems and roots. In addition, high concentrations of maslinic acid in leaves and stems were linked to higher susceptibility to VWO. In this way, a targeted quantification of such specific metabolites could serve as a valuable tool for predicting resistance/susceptibility of new genotypes from crossbreeding.

**Funding:** This research was funded by FEDER/Junta de Andalucía-Consejería de Transformación Económica, Industria, Conocimiento y Universidades (Proyecto P20\_00263) and FEDER/Junta de Andalucía-Consejería de Economía y Conocimiento (Proyecto B-AGR-416-UGR18). The work was also supported by the grant RYC2021-032996-I funded by MCIN/AEI/10.13039/501100011033 and by "European Union NextGenerationEU/PRTR" (L.O.-G.) and the grant FPU19/00700 from the Spanish Ministerio de Ciencia, Innovación y Universidades (I.S.-G.).

## References

1. Martínez-González, M.A.; Salas-Salvadó, J.; Estruch, R.; Corella, D.; Fitó, M.; Ros, E. Benefits of the Mediterranean Diet: Insights From the PREDIMED Study. *Prog. Cardiovasc. Dis.* **2015**, *58*, 50–60, doi:10.1016/j.pcad.2015.04.003.
2. International Olive Council World Olive Oil Consumption Statistics. Available online: <https://www.internationaloliveoil.org/wp-content/uploads/2022/12/IOC-Olive-Oil-Dashboard-2.html#consumption> (accessed on 10 September 2023).

3. European Commission Market Situation for Olive Oil and Table Olives. Available online: [https://agriculture.ec.europa.eu/data-and-analysis/markets/price-data/price-monitoring-sector/olive-oil\\_en#marketsituation](https://agriculture.ec.europa.eu/data-and-analysis/markets/price-data/price-monitoring-sector/olive-oil_en#marketsituation) (accessed on 10 September 2023).
4. Keykhasaber, M.; Thomma, B.P.H.J.; Hiemstra, J.A. Verticillium Wilt Caused by Verticillium Dahliae in Woody Plants with Emphasis on Olive and Shade Trees. *Eur. J. Plant Pathol.* **2018**, *150*, 21–37, doi:10.1007/s10658-017-1273-y.
5. Montes-Osuna, N.; Mercado-Blanco, J. Verticillium Wilt of Olive and Its Control: What Did We Learn during the Last Decade? *Plants* **2020**, *9*, 1–31, doi:10.3390/plants9060735.
6. López-Escudero, F.J.; Mercado-Blanco, J. Verticillium Wilt of Olive: A Case Study to Implement an Integrated Strategy to Control a Soil-Borne Pathogen. *Plant Soil* **2011**, *344*, 1–50, doi:10.1007/s11104-010-0629-2.
7. Mulero-Aparicio, A.; Varo, A.; Agustí-Brisach, C.; López-Escudero, F.J.; Trapero, A. Biological Control of Verticillium Wilt of Olive in the Field. *Crop Prot.* **2020**, *128*, doi:10.1016/j.cropro.2019.104993.
8. Santos-Rufo, A.; Rodríguez-Jurado, D. Unravelling the Relationships among Verticillium Wilt, Irrigation, and Susceptible and Tolerant Olive Cultivars. *Plant Pathol.* **2021**, *70*, 2046–2061, doi:10.1111/ppa.13442.
9. Belaj, A.; Ninot, A.; Gómez-Gálvez, F.J.; El Riachy, M.; Gurbuz-Veral, M.; Torres, M.; Lazaj, A.; Klepo, T.; Paz, S.; Ugarte, J.; et al. Utility of EST-SNP Markers for Improving Management and Use of Olive Genetic Resources: A Case Study at the Worldwide Olive Germplasm Bank of Córdoba. *Plants* **2022**, *11*, 921, doi:10.3390/plants11070921.
10. Serrano, A.; Rodríguez-Jurado, D.; Ramírez-Tejero, J.A.; Luque, F.; López-Escudero, F.J.; Belaj, A.; Román, B.; León, L. Response to Verticillium Dahliae Infection in a Genetically Diverse Set of Olive Cultivars. *Sci. Hortic.* **2023**, *316*, doi:10.1016/j.scienta.2023.112008.
11. Díaz-Rueda, P.; Aguado, A.; Romero-Cuadrado, L.; Capote, N.; Colmenero-Flores, J.M. Wild Olive Genotypes as a Valuable Source of Resistance to Defoliating Verticillium Dahliae. *Front. Plant Sci.* **2021**, *12*, 662060, doi:10.3389/fpls.2021.662060.
12. Ostos, E.; García-Lopez, M.T.; Porras, R.; Lopez-Escudero, F.J.; Trapero-Casas, A.; Michailides, T.J.; Moral, J. Effect of Cultivar Resistance and Soil Management on Spatial–Temporal Development of Verticillium Wilt of Olive: A Long-Term Study. *Front. Plant Sci.* **2020**, *11*, 1–12, doi:10.3389/fpls.2020.584496.
13. Arias-Calderón, R.; Rodríguez-Jurado, D.; León, L.; Bejarano-Alcázar, J.; De la Rosa, R.; Belaj, A. Pre-Breeding for Resistance to Verticillium Wilt in Olive: Fishing in the Wild Relative Gene Pool. *Crop Prot.* **2015**, *75*, 25–33, doi:10.1016/j.cropro.2015.05.006.
14. Ramírez-Tejero, J.A.; Jiménez-Ruiz, J.; Serrano, A.; Belaj, A.; León, L.; de la Rosa, R.; Mercado-Blanco, J.; Luque, F. Verticillium Wilt Resistant and Susceptible Olive Cultivars Express a Very Different Basal Set of Genes in Roots. *BMC Genomics* **2021**, *22*, 229, doi:10.1186/s12864-021-07545-x.
15. Pusztahelyi, T.; Holb, I.J.; Pócsi, I. Secondary Metabolites in Fungus-Plant Interactions. *Front. Plant Sci.* **2015**, *6*, 1–23, doi:10.3389/fpls.2015.00573.
16. Gharbi, Y.; Barkallah, M.; Bouazizi, E.; Gdoura, R.; Triki, M.A. Differential Biochemical and Physiological Responses of Two Olive Cultivars Differing by Their Susceptibility to the Hemibiotrophic Pathogen Verticillium Dahliae. *Physiol. Mol. Plant Pathol.* **2017**, *97*, 30–39, doi:10.1016/j.pmp.2016.12.001.
17. Cardoni, M.; Mercado-Blanco, J.; Villar, R. Functional Traits of Olive Varieties and Their Relationship with the Tolerance Level towards Verticillium Wilt. *Plants* **2021**, *10*, 1079, doi:10.3390/plants10061079.
18. Leyva-Pérez, M. de la O.; Jiménez-Ruiz, J.; Gómez-Lama Cabanás, C.; Valverde-Corredor, A.; Barroso, J.B.; Luque, F.; Mercado-Blanco, J. Tolerance of Olive (*Olea Europaea*) Cv Frantoio to Verticillium Dahliae Relies on Both Basal and Pathogen-Induced Differential Transcriptomic Responses. *New*

- Phytol.* **2018**, *217*, 671–686, doi:10.1111/nph.14833.
19. Kaur, S.; Samota, M.K.; Choudhary, M.; Choudhary, M.; Pandey, A.K.; Sharma, A.; Thakur, J. How Do Plants Defend Themselves against Pathogens-Biochemical Mechanisms and Genetic Interventions. *Physiol. Mol. Biol. Plants* **2022**, *28*, 485–504, doi:10.1007/s12298-022-01146-y.
  20. Zaynab, M.; Fatima, M.; Abbas, S.; Sharif, Y.; Umair, M.; Zafar, M.H.; Bahadar, K. Role of Secondary Metabolites in Plant Defense against Pathogens. *Microb. Pathog.* **2018**, *124*, 198–202, doi:10.1016/j.micpath.2018.08.034.
  21. Trabelsi, R.; Sellami, H.; Gharbi, Y.; Cheffi, M.; Chaari, A.; Baucher, M.; El Jaziri, M.; Triki, M.A.; Gdoura, R. Response of Olive Tree (*Olea Europaea* L.Cv. Chemlali) to Infection with Soilborne Fungi. *J. Plant Dis. Prot.* **2017**, *124*, 153–162, doi:10.1007/s41348-016-0062-8.
  22. Báidez, A.G.; Gómez, P.; Del Río, J.A.; Ortuño, A. Dysfunctionality of the Xylem in *Olea Europaea* L. Plants Associated with the Infection Process by *Verticillium Dahliae* Kleb. Role of Phenolic Compounds in Plant Defense Mechanism. *J. Agric. Food Chem.* **2007**, *55*, 3373–3377, doi:10.1021/jf063166d.
  23. Drais, M.I.; Pannucci, E.; Caracciolo, R.; Bernini, R.; Romani, A.; Santi, L.; Varvaro, L. Antifungal Activity of Hydroxytyrosol Enriched Extracts from Olive Mill Waste against *Verticillium Dahliae*, the Cause of *Verticillium* Wilt of Olive. *Phytopathol. Mediterr.* **2021**, *60*, 139–147, doi:10.36253/phyto-12019.
  24. Gharbi, Y.; Barkallah, M.; Bouazizi, E.; Hibar, K.; Gdoura, R.; Triki, M.A. Lignification, Phenols Accumulation, Induction of PR Proteins and Antioxidant-Related Enzymes Are Key Factors in the Resistance of *Olea Europaea* to *Verticillium* Wilt of Olive. *Acta Physiol. Plant.* **2017**, *39*, doi:10.1007/s11738-016-2343-z.
  25. Gharbi, Y.; Barkallah, M.; Bouazizi, E.; Cheffi, M.; Gdoura, R.; Triki, M.A. Differential Fungal Colonization and Physiological Defense Responses of New Olive Cultivars Infected by the Necrotrophic Fungus *Verticillium Dahliae*. *Acta Physiol. Plant.* **2016**, *38*, doi:10.1007/s11738-016-2261-0.
  26. Markakis, E.A.; Tjamos, S.E.; Antoniou, P.P.; Roussos, P.A.; Paplomatas, E.J.; Tjamos, E.C. Phenolic Responses of Resistant and Susceptible Olive Cultivars Induced by Defoliating and Nondefoliating *Verticillium Dahliae* Pathotypes. *Plant Dis.* **2010**, *94*, 1156–1162, doi:10.1094/PDIS-94-9-1156.
  27. Cardoni, M.; Olmo-García, L.; Serrano-García, I.; Carrasco-Pancorbo, A.; Mercado-Blanco, J. The Roots of Olive Cultivars Differing in Tolerance to *Verticillium Dahliae* Show Quantitative Differences in Phenolic and Triterpenic Profiles. *J. Plant Interact.* **2023**, *18*, 1-14 doi:10.1080/17429145.2023.2206840.
  28. Vergine, M.; Pavan, S.; Negro, C.; Nicoli, F.; Greco, D.; Sabella, E.; Aprile, A.; Ricciardi, L.; De Bellis, L.; Luvisi, A. Phenolic Characterization of Olive Genotypes Potentially Resistant to *Xylella*. *J. Plant Interact.* **2022**, *17*, 462–474, doi:10.1080/17429145.2022.2049381.
  29. Luvisi, A.; Aprile, A.; Sabella, E.; Vergine, M.; Nicoli, F.; Nutricati, E.; Miceli, A.; Negro, C.; De Bellis, L. *Xylella Fastidiosa* Subsp. *Pauca* (CoDiRO Strain) Infection in Four Olive (*Olea Europaea* L.) Cultivars: Profile of Phenolic Compounds in Leaves and Progression of Leaf Scorch Symptoms. *Phytopathol. Mediterr.* **2017**, *56*, 259–273, doi:10.14601/Phytopathol\_Mediterr-20578.
  30. Olmo-García, L.; Kessler, N.; Neuweger, H.; Wendt, K.; Olmo-Peinado, J.M.; Fernández-Gutiérrez, A.; Baessmann, C.; Carrasco-Pancorbo, A. Unravelling the Distribution of Secondary Metabolites in *Olea Europaea* L.: Exhaustive Characterization of Eight Olive-Tree Derived Matrices by Complementary Platforms (LC-ESI/APCI-MS and GC-APCI-MS). *Molecules* **2018**, *23*, 2419, doi:10.3390/molecules23102419.
  31. Serrano-García, I.; Olmo-García, L.; Polo-Megías, D.; Serrano, A.; León, L.; de la Rosa, R.; Gómez-Caravaca, A.M.; Carrasco-Pancorbo, A. Fruit Phenolic and Triterpenic Composition of Progenies of *Olea Europaea* Subsp. *Cuspidata*, an Interesting Phytochemical Source to Be Included in Olive Breeding Programs. *Plants* **2022**, *11*, 1791, doi:10.3390/plants11141791.
  32. Barker, M.; Rayens, W. Partial Least Squares for Discrimination. *J. Chemom.* **2003**, *17*, 166–173, doi:10.1002/cem.785.

33. Klen, T.J.; Wondra, A.G.; Vrhovšek, U.; Vodopivec, B.M. Phenolic Profiling of Olives and Olive Oil Process-Derived Matrices Using UPLC-DAD-ESI-QTOF-HRMS Analysis. *J. Agric. Food Chem.* **2015**, *63*, 3859–3872, doi:10.1021/jf506345q.
34. Garcia-Aloy, M.; Groff, N.; Masuero, D.; Nisi, M.; Franco, A.; Battelini, F.; Vrhovsek, U.; Mattivi, F. Exploratory Analysis of Commercial Olive-Based Dietary Supplements Using Untargeted and Targeted Metabolomics. *Metabolites* **2020**, *10*, 516, doi:10.3390/metabo10120516.
35. Tóth, G.; Alberti, Á.; Sólyomváry, A.; Barabás, C.; Boldizsár, I.; Noszál, B. Phenolic Profiling of Various Olive Bark-Types and Leaves: HPLC-ESI/MS Study. *Ind. Crops Prod.* **2015**, *67*, 432–438, doi:10.1016/j.indcrop.2015.01.077.
36. Olmo-García, L.; Bajoub, A.; Benlamaalam, S.; Hurtado-Fernández, E.; Bagur-González, M.G.; Chigr, M.; Mbarki, M.; Fernández-Gutiérrez, A.; Carrasco-Pancorbo, A. Establishing the Phenolic Composition of *Olea Europaea* L. Leaves from Cultivars Grown in Morocco as a Crucial Step Towards Their Subsequent Exploitation. *Molecules* **2018**, *23*, 2524, doi:10.3390/molecules23102524.
37. Abbattista, R.; Ventura, G.; Calvano, C.D.; Cataldi, T.R.I.; Losito, I. Bioactive Compounds in Waste By-Products from Olive Oil Production: Applications and Structural Characterization by Mass Spectrometry Techniques. *Foods* **2021**, *10*, 1236, doi:10.3390/foods10061236.
38. Michel, T.; Khlif, I.; Kanakis, P.; Termentzi, A.; Allouche, N.; Halabalaki, M.; Skaltsounis, A.L. UHPLC-DAD-FLD and UHPLC-HRMS/MS Based Metabolic Profiling and Characterization of Different *Olea Europaea* Organs of Koroneiki and Chetoui Varieties. *Phytochem. Lett.* **2015**, *11*, 424–439, doi:10.1016/j.phytol.2014.12.020.
39. Ghanbari, R.; Anwar, F.; Alkharfy, K.M.; Gilani, A.H.; Saari, N. Valuable Nutrients and Functional Bioactives in Different Parts of Olive (*Olea Europaea* L.)-A Review. *Int. J. Mol. Sci.* **2012**, *13*, 3291–3340, doi:10.3390/ijms13033291.
40. Talhaoui, N.; Gómez-Caravaca, A.M.; León, L.; De la Rosa, R.; Segura-Carretero, A.; Fernández-Gutiérrez, A. Determination of Phenolic Compounds of “Sikitita” Olive Leaves by HPLC-DAD-TOF-MS. Comparison with Its Parents “Arbequina” and “Picual” Olive Leaves. *LWT - Food Sci. Technol.* **2014**, *58*, 28–34, doi:10.1016/j.lwt.2014.03.014.
41. Contreras, M.D.M.; Gomez-Cruz, I.; Romero, I.; Castro, E. Olive Pomace-Derived Biomasses Fractionation through a Two-Step Extraction Based on the Use of Ultrasound: Chemical Characteristics. *Foods* **2021**, *10*, 111.
42. Al-Warhi, T.; Elmaidomy, A.H.; Maher, S.A.; Abu-Baih, D.H.; Selim, S.; Albqmi, M.; Al-Sanea, M.M.; Alnusaire, T.S.; Ghoneim, M.M.; Mostafa, E.M.; et al. The Wound-Healing Potential of *Olea Europaea* L. Cv. Arbequina Leaves Extract: An Integrated In Vitro, In Silico, and In Vivo Investigation. *Metabolites* **2022**, *12*, doi:10.3390/metabo12090791.
43. Ammar, S.; Contreras, M. del M.; Gargouri, B.; Segura-Carretero, A.; Bouaziz, M. RP-HPLC-DAD-ESI-QTOF-MS Based Metabolic Profiling of the Potential *Olea Europaea* by-Product “Wood” and Its Comparison with Leaf Counterpart. *Phytochem. Anal.* **2017**, *28*, 217–229, doi:10.1002/pca.2664.
44. Hashmi, M.A.; Khan, A.; Hanif, M.; Farooq, U.; Perveen, S. Traditional Uses, Phytochemistry, and Pharmacology of *Olea Europaea* (Olive). *Evidence-based Complement. Altern. Med.* **2015**, *2015*, 1–29, doi:10.1155/2015/541591.
45. Zhang, C.; Xin, X.; Zhang, J.; Zhu, S.; Niu, E.; Zhou, Z.; Liu, D. Comparative Evaluation of the Phytochemical Profiles and Antioxidant Potentials of Olive Leaves from 32 Cultivars Grown in China. *Molecules* **2022**, *27*, doi:10.3390/molecules27041292.
46. Sánchez-Lucas, R. The Effect of Increasing Temperature on Olive Trees (*Olea Europaea* L. Subsp. *Europaea*) Biology: An Integrated Morphological, Phenological and Biomolecular Study, University of Cordoba, Córdoba, Spain, 2019.
47. Luo, X.D.; Wu, D.G.; Cai, X.H.; Kennelly, E.J. New Antioxidant Phenolic Glycosides from Walsura

- Yunnanensis. *Chem. Biodivers.* **2006**, *3*, 224–230, doi:10.1002/cbdv.200690026.
48. Torres-Vega, J.; Gómez-Alonso, S.; Pérez-Navarro, J.; Alarcón-Enos, J.; Pastene-Navarrete, E. Polyphenolic Compounds Extracted and Purified from *Buddleja Globosa* Hope (Buddlejaceae) Leaves Using Natural Deep Eutectic Solvents and Centrifugal Partition Chromatography. *Molecules* **2021**, *26*, 1–20, doi:10.3390/molecules26082192.
  49. David, J.M.; Barreiros, A.L.B.S.; David, J.P. Antioxidant Phenylpropanoid Esters of Triterpenes from *Dioclea Lasiophylla*. *Pharm. Biol.* **2004**, *42*, 36–38, doi:10.1080/13880200490505447.
  50. Vidović, N.; Pasković, I.; Lukić, I.; Žurga, P.; Germek, V.M.; Grozić, K.; Cukrov, M.; Marčelić, Š.; Ban, D.; Talhaoui, N.; Palcic, I.; Rubinic, V.; Ban, S.G. Biophenolic Profile Modulations in Olive Tissues as Affected by Manganese Nutrition. *Plants* **2021**, *10*, 1–17, doi:10.3390/plants10081724.
  51. Ben Brahim, S.; Priego-Capote, F.; Bouaziz, M. Use of High-Performance Liquid Chromatography/Electrospray Ionization Mass Spectrometry for Structural Characterization of Bioactive Compounds in the Olive Root Bark and Wood of Chemlali Cultivar. *ACS Omega* **2022**, *7*, 33873–33883, doi:10.1021/acsomega.2c02746.
  52. Mechri, B.; Tekaya, M.; Attia, F.; Hammami, M.; Chehab, H. Drought Stress Improved the Capacity of *Rhizophagus Irregularis* for Inducing the Accumulation of Oleuropein and Mannitol in Olive (*Olea Europaea*) Roots. *Plant Physiol. Biochem.* **2020**, *156*, 178–191, doi:10.1016/j.plaphy.2020.09.011.
  53. Skodra, C.; Michailidis, M.; Dasenaki, M.; Ganopoulos, I.; Thomaidis, N.S.; Tanou, G.; Molassiotis, A. Unraveling Salt-Responsive Tissue-Specific Metabolic Pathways in Olive Tree. *Physiol. Plant.* **2021**, *173*, 1643–1656.
  54. Liu, S.; Liu, H.; Zhang, L.; Ma, C.; Abd El-Aty, A.M. Edible Pentacyclic Triterpenes: A Review of Their Sources, Bioactivities, Bioavailability, Self-Assembly Behavior, and Emerging Applications as Functional Delivery Vehicles. *Crit. Rev. Food Sci. Nutr.* **2022**, 1–17, doi:10.1080/10408398.2022.2153238.
  55. Machała, P.; Liudvytska, O.; Kicel, A.; Dziedzic, A.; Olszewska, M.A.; Żbikowska, H.M. Valorization of the Photo-Protective Potential of the Phytochemically Standardized Olive (*Olea Europaea* L.) Leaf Extract in UVA-Irradiated Human Skin Fibroblasts. *Molecules* **2022**, *27*, doi:10.3390/molecules27165144.
  56. Cittan, M.; Çelik, A. Development and Validation of an Analytical Methodology Based on Liquid Chromatography–Electrospray Tandem Mass Spectrometry for the Simultaneous Determination of Phenolic Compounds in Olive Leaf Extract. *J. Chromatogr. Sci.* **2018**, *56*, 336–343, doi:10.1093/chromsci/bmy003.



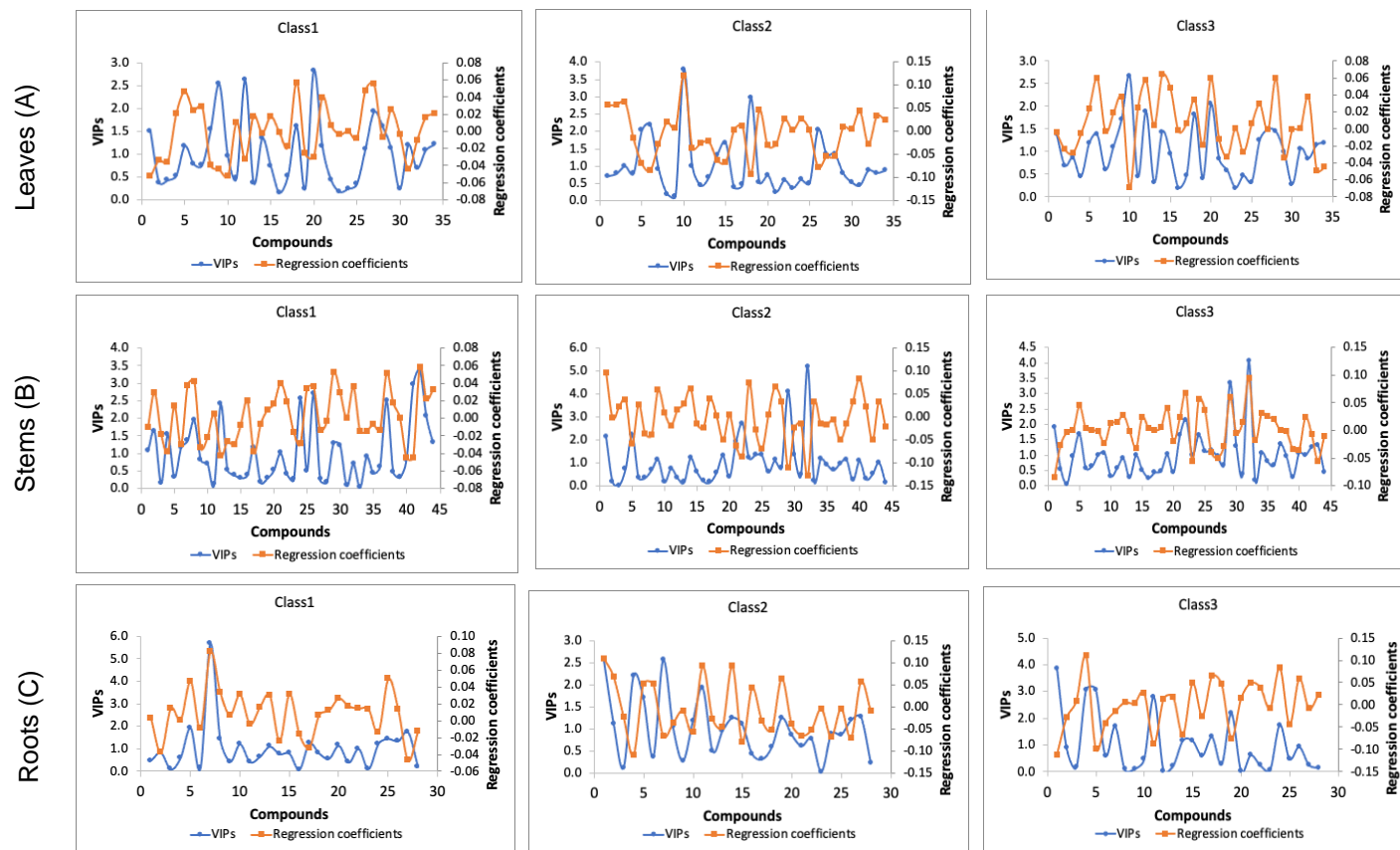


**Figure S2.** Representation of the regression coefficients and variable importance on the projection (VIP) values of each metabolite quantified in the three olive tissues under study: leaves (A), stems (B) and roots (C). Class 1: high resistant cultivars; class 2: resistant, moderately susceptible, and susceptible cultivars; class 3: extremely susceptible cultivars. \*Compound numbers at the end of the document

\*Compound numbers in Figure S1 and S2.

LEAVES		STEMS		ROOTS	
Code	Compound name	Code	Compound name	Code	Compound name
C1	Aldehydic form of decarboxymethyl elenolic acid glucoside	C1	11-Hydroxyiridodial glucoside pentaacetate	C1	11-Hydroxyiridodial glucoside pentaacetate
C2	Apigenin 7-O-glucoside	C2	Acetoxypinoresinol	C2	7-deoxyloganin acid
C3	Apigenin O-rutinoside	C3	Acetoxypinoresinol glucoside	C3	Acetoxypinoresinol
C4	Betulinic acid	C4	Aldehydic form of decarboxymethyl elenolic acid glucoside	C4	Acetoxypinoresinol glucoside
C5	Chrysoeriol O-glucoside	C5	Betulinic acid	C5	Betulinic acid
C6	Demethyl oleuropein	C6	Cyanidin O-glucoside	C6	Cycloolivil glucoside (isomer 1)
C7	Diosmin	C7	Cycloolivil	C7	Cycloolivil glucoside (isomer 2)
C8	Elenolic acid glucoside (isomer 1)	C8	Demethyl oleuropein	C8	Elenolic acid glucoside (isomer 1)
C9	Elenolic acid glucoside (isomer 2)	C9	Dihydrokaempferol	C9	Elenolic acid glucoside (isomer 2)
C10	Gallocatechin	C10	Dihydroquercetin 3-O-glucoside	C10	Hydroxy oleuropein
C11	Hydroxytyrosol	C11	Elenolic acid glucoside (isomer 1)	C11	Hydroxypinoresinol glucoside
C12	Hydroxytyrosol glucoside	C12	Elenolic acid glucoside (isomer 2)	C12	Ligstroside
C13	Ligstroside	C13	Hydroxy oleuropein	C13	Lucidumoside C
C14	Lucidumoside C	C14	Hydroxypinoresinol glucoside	C14	Maslinic acid
C15	Luteolin 7-O-glucoside (isomer 1)	C15	Hydroxytyrosol glucoside	C15	Metoxypinoresinol glucoside
C16	Luteolin O-glucoside (isomer 2)	C16	Ligstroside	C16	Neonuzhenide/oleuropein glucoside (isomer 1)
C17	Luteolin O-glucoside (isomer 3)	C17	Lucidumoside C	C17	Neonuzhenide/oleuropein glucoside (isomer 2)
C18	Maslinic acid	C18	Luteolin 7-O-glucoside (isomer 1)	C18	Neonuzhenide/oleuropein glucoside (isomer 4)
C19	Neonuzhenide/oleuropein glucoside (isomer 1)	C19	Luteolin O-glucoside (isomer 2)	C19	Oleanolic acid
C20	Neonuzhenide/oleuropein glucoside (isomer 3)	C20	Luteolin O-glucoside (isomer 3)	C20	Oleoside
C21	Neonuzhenide/oleuropein glucoside (isomer 4)	C21	Maslinic acid	C21	Secologanoside
C22	Oleanolic acid	C22	Metoxypinoresinol glucoside	C22	Oleuropein
C23	Oleoside	C23	Neonuzhenide/oleuropein glucoside (isomer 1)	C23	Quinic acid
C24	Secologanoside	C24	Neonuzhenide/oleuropein glucoside (isomer 2)	C24	Unknown 1
C25	Oleuropein	C25	Neonuzhenide/oleuropein glucoside (isomer 4)	C25	Unknown 2
C26	Oleuropein aglycone (isomer 1)	C26	Oleanolic acid	C26	Unknown 3
C27	Oleuropein aglycone (isomer 2)	C27	Oleoside	C27	Verbascoside
C28	Oleurosides	C28	Secologanoside	C28	Isoverbascoside
C29	Quinic acid	C29	Oleuropein		
C30	Rutin	C30	Oleuropein aglycone (isomer 1)		
C31	Unknown 1	C31	Oleuropein aglycone (isomer 2)		
C32	Unknown 2	C32	Oleurosides		
C33	Unknown 5	C33	Phenylethyl primeveroside		
C34	Verbascoside	C34	Quercetin O-glucoside (isomer 1)		
		C35	Quercetin O-glucoside (isomer 2)		

LEAVES	STEMS	ROOTS
Code Compound name	Code Compound name	Code Compound name
	C36 Quercetin <i>O</i> -glucoside (isomer 3)	
	C37 Quinic acid	
	C38 Rutin	
	C39 Taxifolin	
	C40 Unknown 1	
	C41 Unknown 2	
	C42 Unknown 4	
	C43 Unknown 5	
	C44 Verbascoside	

**Table S1.** Analytical parameters of the LC-IT MS method.

Compound	Calibration curve	R <sup>2</sup>	Dynamic linear range / mg l <sup>-1</sup>	LOD <sup>a</sup> / µg l <sup>-1</sup>	LOQ <sup>a</sup> / µg l <sup>-1</sup>	Intra-day repeatability <sup>b</sup> (area RSD / %)	Inter-day repeatability <sup>c</sup> (area RSD / %)
Quinic acid	y = 6212.5 + 36428.1x	0.9983	LOQ – 18.7	24.4	81.3	0.33	0.49
	y = 512246.7 + 17005.7x	0.9948	18.7 – 150.0				
Hydroxytyrosol	y = 8449.0 + 31061.1x	0.9976	LOQ – 52.0	47.3	157.6	7.08	10.62
	y = -583.7 + 10334.9x	0.9997	LOQ – 25.0				
Tyrosol	y = 107822.0 + 6833.5x	0.9898	25.0 – 100.0	171.3	571.0	5.70	8.56
	y = -36097.3 + 169422.6x	0.9992	LOQ – 12.0				
Rutin	y = 1067657.8 + 107842.2x	0.9911	12.0 – 96.0	28.4	94.6	5.23	7.85
	y = 56511.5 + 411020.5x	0.9966	LOQ – 8.0				
Luteolin-7-O-glucoside	y = 2348016.3 + 193405.8x	0.9924	8.0 – 64.0	18.7	62.3	1.66	2.49
	y = 53328.5 + 111178.1x	0.9955	LOQ – 52				
Verbascoside	y = 514056.1 + 183004.9x	0.9942	LOQ – 62.5	25.4	84.6	2.25	3.37
	y = 10361638.0 + 48313.3x	0.9954	62.5 – 500.0				
Oleuropein	y = 166450.8 + 197117.1x	0.9899	LOQ – 12.5	14.9	49.5	3.59	5.38
	y = 2244039.3 + 54184.3x	0.9933	12.5 – 100.0				
Maslinic acid	y = 70030.7 + 930415.0x	0.9916	LOQ – 2.5	2.0	6.7	1.36	2.05
	y = 1436593.5 + 396367.1x	0.9902	2.5 – 10.0				
Betulinic acid	y = 251665.6 + 430573.6x	0.9913	LOQ – 9.0	5.8	19.2	1.96	2.94
	y = 2409833.3 + 151759.4x	0.9949	9.0 – 72.0				

<sup>a</sup> Calculated as the concentration that generates a signal to noise ratio equal to 3 (LOD) and 10 (LOQ).

<sup>b</sup> RSD (relative standard deviation) of peak area for 6 injections of the quality control sample carried out within the same sequence.

<sup>c</sup> RSD of peak area for 20 injections of the quality control sample from different sequences carried out over 3 days.

Abbreviations: LOD, Limit of detection; LOQ, Limit of quantification.

**Table S2.** Quantitative results obtained by LC-IT MS. Data expressed as mg kg<sup>-1</sup> of olive tissue (DW) ± standard deviation.

<b>a) Leaves</b>	<i>Arbequina</i>	<i>Empeltre</i>	<i>Frantoio</i>	<i>Hojiblanca</i>	<i>Jabali</i>	<i>Koroneiki</i>	<i>Leccino</i>	<i>Mastoidis</i>	<i>Menya</i>	<i>Pical</i>
<i>Aldehydic form of decarboxymethyl elenolic acid glucoside</i>	771±156 <sup>ab</sup>	741±132 <sup>ab</sup>	240±77 <sup>a</sup>	1095±670 <sup>abc</sup>	1891±374 <sup>c</sup>	957±558 <sup>abc</sup>	648±133 <sup>ab</sup>	438±35 <sup>ab</sup>	1274±411 <sup>bc</sup>	1239±287 <sup>abc</sup>
<i>Apigenin-7-O-glucoside</i>	138±21 <sup>a</sup>	193±34 <sup>a</sup>	234±80 <sup>a</sup>	250±198 <sup>a</sup>	422±82 <sup>a</sup>	80±43 <sup>a</sup>	1025±364 <sup>b</sup>	236±23 <sup>a</sup>	353±109 <sup>a</sup>	246±81 <sup>a</sup>
<i>Apigenin-O-rutinoside</i>	436±61 <sup>ab</sup>	404±50 <sup>ab</sup>	270±76 <sup>ab</sup>	411±196 <sup>ab</sup>	564±165 <sup>bc</sup>	142±51 <sup>a</sup>	854±251 <sup>c</sup>	288±39 <sup>ab</sup>	445±113 <sup>ab</sup>	328±58 <sup>ab</sup>
<i>Betulinic acid</i>	113±33 <sup>ab</sup>	234±19 <sup>b</sup>	165±25 <sup>ab</sup>	151±77 <sup>ab</sup>	149±57 <sup>ab</sup>	118±57 <sup>ab</sup>	181±49 <sup>ab</sup>	197±20 <sup>ab</sup>	96±31 <sup>a</sup>	137±56 <sup>ab</sup>
<i>Chrysoeriol-O-glucoside</i>	82±20 <sup>a</sup>	209±54 <sup>a</sup>	205±85 <sup>a</sup>	81±59 <sup>a</sup>	173±30 <sup>a</sup>	129±85 <sup>a</sup>	117±51 <sup>a</sup>	167±17 <sup>a</sup>	65±9 <sup>a</sup>	103±35 <sup>a</sup>
<i>Demethyl oleuropein</i>	510±182 <sup>a</sup>	1053±69 <sup>ab</sup>	826±329 <sup>ab</sup>	445±270 <sup>a</sup>	2021±1240 <sup>b</sup>	591±217 <sup>a</sup>	316±127 <sup>a</sup>	598±101 <sup>a</sup>	329±201 <sup>a</sup>	587±472 <sup>a</sup>
<i>Diosmin</i>	222±84 <sup>a</sup>	682±195 <sup>b</sup>	114±34 <sup>a</sup>	127±12 <sup>a</sup>	308±105 <sup>a</sup>	231±123 <sup>a</sup>	147±83 <sup>a</sup>	259±79 <sup>a</sup>	57±21 <sup>a</sup>	133±50 <sup>a</sup>
<i>Elenolic acid glucoside (isomer 1)</i>	506±67 <sup>a</sup>	358±30 <sup>a</sup>	334±127 <sup>a</sup>	297±12 <sup>a</sup>	510±120 <sup>a</sup>	464±306 <sup>a</sup>	398±157 <sup>a</sup>	680±111 <sup>a</sup>	596±147 <sup>a</sup>	314±48 <sup>a</sup>
<i>Elenolic acid glucoside (isomer 2)</i>	227±9 <sup>a</sup>	303±71 <sup>a</sup>	158±54 <sup>a</sup>	338±191 <sup>a</sup>	609±49 <sup>abc</sup>	904±478 <sup>bc</sup>	281±68 <sup>a</sup>	1035±182 <sup>c</sup>	381±103 <sup>ab</sup>	485±176 <sup>ab</sup>
<i>Gallocatechin</i>	46±13 <sup>a</sup>	48±6 <sup>ab</sup>	30±9 <sup>a</sup>	59±19 <sup>ab</sup>	29±7 <sup>a</sup>	40±16 <sup>a</sup>	37±5 <sup>a</sup>	51±6 <sup>ab</sup>	59±9 <sup>ab</sup>	80±14 <sup>b</sup>
<i>Hydroxytyrosol</i>	577±107 <sup>ab</sup>	725±38 <sup>ab</sup>	726±243 <sup>ab</sup>	354±123 <sup>a</sup>	714±61 <sup>ab</sup>	585±304 <sup>ab</sup>	786±134 <sup>ab</sup>	880±54 <sup>b</sup>	479±132 <sup>ab</sup>	492±156 <sup>ab</sup>
<i>Hydroxytyrosol glucoside</i>	1241±141 <sup>ab</sup>	1347±254 <sup>ab</sup>	450±102 <sup>a</sup>	649±509 <sup>ab</sup>	3678±1037 <sup>c</sup>	2872±2071 <sup>bc</sup>	1760±563 <sup>abc</sup>	2845±114 <sup>bc</sup>	1209±434 <sup>ab</sup>	811±187 <sup>ab</sup>
<i>Ligstroside</i>	3991±728 <sup>ab</sup>	8608±1434 <sup>c</sup>	2085±808 <sup>a</sup>	2136±368 <sup>a</sup>	3320±920 <sup>ab</sup>	3393±2351 <sup>ab</sup>	3732±1531 <sup>ab</sup>	6372±1012 <sup>bc</sup>	3507±1139 <sup>ab</sup>	2292±959 <sup>a</sup>
<i>Lucidumoside C</i>	89±16 <sup>a</sup>	100±14 <sup>a</sup>	177±57 <sup>abc</sup>	88±37 <sup>a</sup>	212±92 <sup>abc</sup>	116±54 <sup>ab</sup>	110±38 <sup>a</sup>	264±62 <sup>c</sup>	253±14 <sup>bc</sup>	107±41 <sup>a</sup>
<i>Luteolin-7-O-glucoside (isomer 1)</i>	1263±353 <sup>ab</sup>	1726±427 <sup>ab</sup>	1430±677 <sup>ab</sup>	720±660 <sup>a</sup>	2674±432 <sup>b</sup>	1175±899 <sup>ab</sup>	768±414 <sup>a</sup>	1347±128 <sup>ab</sup>	586±464 <sup>a</sup>	1265±498 <sup>ab</sup>
<i>Luteolin-O-glucoside (isomer 2)</i>	403±145 <sup>a</sup>	530±175 <sup>a</sup>	375±181 <sup>a</sup>	411±356 <sup>a</sup>	508±71 <sup>a</sup>	454±343 <sup>a</sup>	129±61 <sup>a</sup>	447±34 <sup>a</sup>	183±35 <sup>a</sup>	450±197 <sup>a</sup>
<i>Luteolin-O-glucoside (isomer 3)</i>	86±17 <sup>ab</sup>	144±45 <sup>ab</sup>	59±18 <sup>a</sup>	62±45 <sup>a</sup>	94±26 <sup>ab</sup>	145±87 <sup>ab</sup>	39±18 <sup>a</sup>	189±23 <sup>b</sup>	83±23 <sup>ab</sup>	111±38 <sup>ab</sup>
<i>Maslinic acid</i>	1274±254 <sup>a</sup>	4768±186 <sup>c</sup>	3368±288 <sup>bc</sup>	2039±984 <sup>ab</sup>	3292±925 <sup>bc</sup>	2047±892 <sup>ab</sup>	2342±784 <sup>ab</sup>	3430±26 <sup>bc</sup>	1580±539 <sup>ab</sup>	2559±908 <sup>ab</sup>
<i>Neonuzhenide/oleuropein glucoside (isomer 1)</i>	48±19 <sup>a</sup>	58±5 <sup>a</sup>	29±10 <sup>a</sup>	72±51 <sup>a</sup>	174±83 <sup>a</sup>	177±148 <sup>a</sup>	180±112 <sup>a</sup>	62±11 <sup>a</sup>	615±405 <sup>a</sup>	57±19 <sup>a</sup>
<i>Neonuzhenide/oleuropein glucoside (isomer 3)</i>	416±56 <sup>ab</sup>	501±29 <sup>ab</sup>	228±84 <sup>a</sup>	272±178 <sup>a</sup>	686±122 <sup>bc</sup>	438±240 <sup>ab</sup>	489±159 <sup>ab</sup>	899±88 <sup>c</sup>	407±152 <sup>ab</sup>	393±114 <sup>ab</sup>
<i>Neonuzhenide/oleuropein glucoside (isomer 4)</i>	163±44 <sup>a</sup>	157±15 <sup>a</sup>	520±204 <sup>b</sup>	191±83 <sup>a</sup>	106±21 <sup>a</sup>	75±35 <sup>a</sup>	257±100 <sup>ab</sup>	242±26 <sup>a</sup>	214±120 <sup>a</sup>	245±113 <sup>a</sup>
<i>Oleanolic acid</i>	10152±2241 <sup>a</sup>	15255±632 <sup>a</sup>	15670±1969 <sup>a</sup>	13431±5751 <sup>a</sup>	11844±2796 <sup>a</sup>	10749±4897 <sup>a</sup>	15636±3204 <sup>a</sup>	14196±504 <sup>a</sup>	12239±3635 <sup>a</sup>	14957±3449 <sup>a</sup>
<i>Oleoside/secologanoside (isomer 1)</i>	626±95 <sup>abc</sup>	1095±135 <sup>d</sup>	382±108 <sup>a</sup>	566±151 <sup>abc</sup>	682±55 <sup>abc</sup>	625±179 <sup>abc</sup>	673±55 <sup>abc</sup>	893±52 <sup>cd</sup>	818±198 <sup>bcd</sup>	523±138 <sup>ab</sup>
<i>Oleoside/secologanoside (isomer 2)</i>	1666±402 <sup>ab</sup>	3515±316 <sup>c</sup>	1005±360 <sup>a</sup>	1465±781 <sup>ab</sup>	2347±313 <sup>abc</sup>	1502±702 <sup>ab</sup>	1990±229 <sup>ab</sup>	1551±28 <sup>ab</sup>	2580±942 <sup>bc</sup>	1541±101 <sup>ab</sup>
<i>Oleuropein</i>	49364±4286 <sup>abc</sup>	70692±5619 <sup>bc</sup>	28663±12486 <sup>a</sup>	31231±10647 <sup>a</sup>	40919±6365 <sup>ab</sup>	42112±21892 <sup>ab</sup>	46581±7692 <sup>abc</sup>	74453±5306 <sup>c</sup>	50140±13178 <sup>abc</sup>	29239±9434 <sup>a</sup>
<i>Oleuropein aglycone (isomer 1)</i>	203±83 <sup>a</sup>	640±160 <sup>b</sup>	263±41 <sup>a</sup>	124±47 <sup>a</sup>	124±71 <sup>a</sup>	101±61 <sup>a</sup>	190±86 <sup>a</sup>	572±205 <sup>b</sup>	74±12 <sup>a</sup>	164±86 <sup>a</sup>
<i>Oleuropein aglycone (isomer 2)</i>	95±12 <sup>ab</sup>	391±59 <sup>d</sup>	325±50 <sup>cd</sup>	130±62 <sup>abc</sup>	78±32 <sup>a</sup>	99±59 <sup>ab</sup>	280±132 <sup>bcd</sup>	317±123 <sup>cd</sup>	71±20 <sup>a</sup>	104±9 <sup>ab</sup>
<i>Oleurosides</i>	2147±277 <sup>bc</sup>	2567±106 <sup>c</sup>	999±477 <sup>a</sup>	1102±426 <sup>ab</sup>	1928±214 <sup>abc</sup>	1093±561 <sup>ab</sup>	1666±476 <sup>abc</sup>	4349±403 <sup>d</sup>	1469±458 <sup>abc</sup>	1309±327 <sup>ab</sup>
<i>Quinic acid</i>	5802±590 <sup>abc</sup>	7815±328 <sup>c</sup>	6357±1190 <sup>abc</sup>	4992±1146 <sup>ab</sup>	5916±463 <sup>abc</sup>	5826±1589 <sup>abc</sup>	7229±1019 <sup>bc</sup>	5549±350 <sup>abc</sup>	4769±251 <sup>ab</sup>	4439±574 <sup>a</sup>
<i>Rutin</i>	287±132 <sup>a</sup>	578±159 <sup>a</sup>	166±25 <sup>a</sup>	145±130 <sup>a</sup>	461±144 <sup>a</sup>	493±368 <sup>a</sup>	142±52 <sup>a</sup>	368±60 <sup>a</sup>	188±70 <sup>a</sup>	240±162 <sup>a</sup>
<i>Unknown 1</i>	120±60 <sup>a</sup>	42±14 <sup>a</sup>	29±7 <sup>a</sup>	56±10 <sup>a</sup>	107±46 <sup>a</sup>	260±242 <sup>a</sup>	81±58 <sup>a</sup>	265±43 <sup>a</sup>	113±51 <sup>a</sup>	24±15 <sup>a</sup>
<i>Unknown 2</i>	423±39 <sup>ab</sup>	258±47 <sup>a</sup>	440±59 <sup>ab</sup>	488±127 <sup>b</sup>	402±64 <sup>ab</sup>	409±99 <sup>ab</sup>	351±70 <sup>ab</sup>	461±80 <sup>ab</sup>	545±66 <sup>b</sup>	458±80 <sup>ab</sup>

<b>a) Leaves</b>	<i>Arbequina</i>	<i>Empeltre</i>	<i>Frantoio</i>	<i>Hojiblanca</i>	<i>Jabali</i>	<i>Koroneiki</i>	<i>Leccino</i>	<i>Mastoidis</i>	<i>Menya</i>	<i>Pical</i>
<i>Unknown 5</i>	763±155 <sup>ab</sup>	958±39 <sup>b</sup>	813±218 <sup>ab</sup>	588±248 <sup>ab</sup>	386±97 <sup>a</sup>	546±200 <sup>ab</sup>	935±279 <sup>b</sup>	823±46 <sup>ab</sup>	585±170 <sup>ab</sup>	569±190 <sup>ab</sup>
<i>Verbascoide</i>	2638±1403 <sup>a</sup>	12863±4150 <sup>b</sup>	1204±221 <sup>a</sup>	3506±3379 <sup>a</sup>	3025±853 <sup>a</sup>	3676±2519 <sup>a</sup>	4118±1928 <sup>a</sup>	2137±1623 <sup>a</sup>	706±316 <sup>a</sup>	2216±1177 <sup>a</sup>

Lower case letters indicate Tukey's post hoc test differences ( $p < 0.05$ ) among different cultivars. Means with a common letter are not significantly different ( $p > 0.05$ )

<b>b) Stems</b>	<i>Arbequina</i>	<i>Empeltre</i>	<i>Frantoio</i>	<i>Hojiblanca</i>	<i>Jabali</i>	<i>Koroneiki</i>	<i>Leccino</i>	<i>Mastoidis</i>	<i>Menya</i>	<i>Pical</i>
<i>11-Hydroxyiridodial glucoside pentaacetate</i>	15±3 <sup>a</sup>	81±23 <sup>bcd</sup>	36±4 <sup>ab</sup>	27±4 <sup>ab</sup>	18±5 <sup>a</sup>	94±20 <sup>cd</sup>	105±47 <sup>d</sup>	7±1 <sup>a</sup>	51±17 <sup>abc</sup>	22±8 <sup>a</sup>
<i>Acetoxipinoresinol</i>	112±26 <sup>bcd</sup>	143±57 <sup>d</sup>	70±27 <sup>abc</sup>	96±17 <sup>abcd</sup>	44±8 <sup>ab</sup>	50±8 <sup>abc</sup>	57±4 <sup>abc</sup>	69±14 <sup>abc</sup>	116±25 <sup>cd</sup>	31±6 <sup>a</sup>
<i>Acetoxipinoresinol glucoside</i>	1052±133 <sup>bc</sup>	1172±189 <sup>cd</sup>	613±118 <sup>ab</sup>	996±179 <sup>abc</sup>	779±207 <sup>abc</sup>	1102±131 <sup>bcd</sup>	637±24 <sup>ab</sup>	1268±85 <sup>cd</sup>	1588±365 <sup>d</sup>	494±80 <sup>a</sup>
<i>Aldehydic form of decarboxymethyl elenolic acid glucoside</i>	286±9 <sup>a</sup>	397±11 <sup>ab</sup>	220±54 <sup>a</sup>	678±66 <sup>c</sup>	1114±236 <sup>d</sup>	747±11 <sup>c</sup>	168±30 <sup>a</sup>	245±18 <sup>a</sup>	294±36 <sup>a</sup>	640±126 <sup>bc</sup>
<i>Betulinic acid</i>	76±18 <sup>ab</sup>	128±15 <sup>abc</sup>	176±52 <sup>cd</sup>	133±28 <sup>bc</sup>	211±29 <sup>d</sup>	222±19 <sup>d</sup>	58±16 <sup>a</sup>	184±10 <sup>cd</sup>	118±23 <sup>abc</sup>	81±15 <sup>ab</sup>
<i>Cyanidin-O-glucoside</i>	18±3 <sup>a</sup>	23±6 <sup>a</sup>	16±3 <sup>a</sup>	101±15 <sup>b</sup>	88±33 <sup>b</sup>	13±1 <sup>a</sup>	92±38 <sup>b</sup>	16±1 <sup>a</sup>	6±2 <sup>a</sup>	76±6 <sup>b</sup>
<i>Cycloolivil</i>	80±7 <sup>ab</sup>	137±21 <sup>ab</sup>	273±171 <sup>ab</sup>	74±16 <sup>a</sup>	101±4 <sup>ab</sup>	108±9 <sup>ab</sup>	296±148 <sup>b</sup>	81±19 <sup>abc</sup>	173±61 <sup>ab</sup>	87±13 <sup>ab</sup>
<i>Demethyl oleuropein</i>	42±10 <sup>abc</sup>	128±38 <sup>d</sup>	76±23 <sup>abcd</sup>	32±9 <sup>ab</sup>	96±17 <sup>cd</sup>	70±15 <sup>abcd</sup>	93±40 <sup>bcd</sup>	37±5 <sup>abc</sup>	87±13 <sup>abcd</sup>	28±4 <sup>a</sup>
<i>Dihydrokaempferol</i>	163±10 <sup>bc</sup>	116±21 <sup>b</sup>	60±3 <sup>a</sup>	278±27 <sup>e</sup>	200±23 <sup>cd</sup>	59±7 <sup>a</sup>	188±31 <sup>cd</sup>	45±7 <sup>a</sup>	31±5 <sup>a</sup>	229±12 <sup>de</sup>
<i>Dihydroquercetin 3-O-glucoside</i>	62±12 <sup>ab</sup>	43±4 <sup>ab</sup>	84±32 <sup>abc</sup>	20±4 <sup>a</sup>	142±43 <sup>cd</sup>	103±3 <sup>bcd</sup>	177±56 <sup>d</sup>	76±4 <sup>abc</sup>	51±7 <sup>ab</sup>	76±21 <sup>abc</sup>
<i>Elenolic acid glucoside (isomer 1)</i>	308±22 <sup>a</sup>	555±74 <sup>b</sup>	328±55 <sup>a</sup>	383±20 <sup>ab</sup>	558±15 <sup>b</sup>	419±42 <sup>ab</sup>	427±143 <sup>ab</sup>	397±36 <sup>ab</sup>	481±93 <sup>ab</sup>	345±30 <sup>a</sup>
<i>Elenolic acid glucoside (isomer 2)</i>	81±11 <sup>a</sup>	182±48 <sup>abc</sup>	71±26 <sup>a</sup>	92±21 <sup>ab</sup>	278±31 <sup>cde</sup>	237±36 <sup>bcd</sup>	402±125 <sup>e</sup>	352±53 <sup>de</sup>	315±53 <sup>cde</sup>	196±33 <sup>abc</sup>
<i>Hydroxy oleuropein</i>	126±42 <sup>ab</sup>	146±33 <sup>ab</sup>	94±42 <sup>a</sup>	158±31 <sup>ab</sup>	148±28 <sup>ab</sup>	133±67 <sup>ab</sup>	80±30 <sup>a</sup>	174±40 <sup>ab</sup>	221±62 <sup>b</sup>	119±18 <sup>ab</sup>
<i>Hydroxypinoresinol glucoside</i>	105±11 <sup>a</sup>	125±34 <sup>a</sup>	90±18 <sup>a</sup>	146±11 <sup>a</sup>	66±10 <sup>a</sup>	77±4 <sup>a</sup>	356±110 <sup>b</sup>	148±18 <sup>a</sup>	106±27 <sup>a</sup>	368±28 <sup>b</sup>
<i>Hydroxytyrosol glucoside</i>	1273±222 <sup>bc</sup>	1472±278 <sup>c</sup>	767±32 <sup>ab</sup>	373±126 <sup>a</sup>	1545±428 <sup>c</sup>	1610±379 <sup>c</sup>	1301±162 <sup>bc</sup>	1350±94 <sup>bc</sup>	954±138 <sup>abc</sup>	1010±47 <sup>abc</sup>
<i>Ligstroside</i>	957±169 <sup>a</sup>	2885±388 <sup>bc</sup>	1345±151 <sup>abc</sup>	1402±32 <sup>abc</sup>	1623±509 <sup>abc</sup>	1311±343 <sup>ab</sup>	2916±1403 <sup>c</sup>	1905±431 <sup>abc</sup>	1599±127 <sup>abc</sup>	2145±464 <sup>abc</sup>
<i>Lucidumoside C</i>	242±117 <sup>abc</sup>	200±33 <sup>ab</sup>	108±54 <sup>a</sup>	247±30 <sup>abc</sup>	216±74 <sup>ab</sup>	246±143 <sup>abc</sup>	103±33 <sup>a</sup>	357±105 <sup>bc</sup>	485±123 <sup>c</sup>	147±37 <sup>ab</sup>
<i>Luteolin-7-O-glucoside (isomer 1)</i>	36±16 <sup>a</sup>	12±1 <sup>a</sup>	51±36 <sup>ab</sup>	21±14 <sup>a</sup>	97±35 <sup>b</sup>	32±0 <sup>a</sup>	10±5 <sup>a</sup>	5±3 <sup>a</sup>	11±2 <sup>a</sup>	53±27 <sup>ab</sup>
<i>Luteolin-O-glucoside (isomer 2)</i>	7±2 <sup>a</sup>	7±4 <sup>a</sup>	40±35 <sup>a</sup>	32±8 <sup>a</sup>	102±16 <sup>b</sup>	2±1 <sup>a</sup>	5±2 <sup>a</sup>	n.d	4±0 <sup>a</sup>	20±3 <sup>a</sup>
<i>Luteolin-O-glucoside (isomer 3)</i>	14±6 <sup>ab</sup>	8±1 <sup>ab</sup>	23±10 <sup>b</sup>	8±6 <sup>ab</sup>	21±3 <sup>b</sup>	11±2 <sup>ab</sup>	4±1 <sup>a</sup>	n.d	9±1 <sup>ab</sup>	20±10 <sup>b</sup>
<i>Maslinic acid</i>	488±69 <sup>ab</sup>	1041±121 <sup>bc</sup>	984±499 <sup>abc</sup>	710±153 <sup>ab</sup>	1385±349 <sup>c</sup>	680±184 <sup>ab</sup>	351±101 <sup>a</sup>	497±104 <sup>ab</sup>	364±65 <sup>a</sup>	772±162 <sup>abc</sup>
<i>Metoxypinoresinol glucoside</i>	137±13 <sup>bc</sup>	114±1 <sup>abc</sup>	135±7 <sup>bc</sup>	89±17 <sup>a</sup>	133±28 <sup>bc</sup>	130±17 <sup>abc</sup>	106±13 <sup>ab</sup>	150±8 <sup>c</sup>	119±20 <sup>abc</sup>	108±4 <sup>abc</sup>
<i>Neonuzhenide/oleuropein glucoside (is 1)</i>	144±53 <sup>ab</sup>	239±121 <sup>ab</sup>	161±39 <sup>ab</sup>	122±29 <sup>ab</sup>	210±76 <sup>ab</sup>	208±61 <sup>ab</sup>	375±205 <sup>b</sup>	42±5 <sup>a</sup>	230±81 <sup>ab</sup>	208±84 <sup>ab</sup>
<i>Neonuzhenide/oleuropein glucoside (is 2)</i>	228±42 <sup>cd</sup>	231±24 <sup>cd</sup>	93±44 <sup>a</sup>	114±21 <sup>ab</sup>	310±70 <sup>de</sup>	357±21 <sup>e</sup>	179±16 <sup>abc</sup>	356±29 <sup>e</sup>	202±23 <sup>bc</sup>	167±16 <sup>abc</sup>
<i>Neonuzhenide/oleuropein glucoside (is 4)</i>	48±10 <sup>a</sup>	99±32 <sup>bcd</sup>	88±25 <sup>abcd</sup>	97±25 <sup>bcd</sup>	69±9 <sup>abc</sup>	53±5 <sup>ab</sup>	128±16 <sup>d</sup>	107±4 <sup>cd</sup>	40±5 <sup>a</sup>	56±8 <sup>ab</sup>
<i>Oleanolic acid</i>	2438±437 <sup>ab</sup>	2790±349 <sup>ab</sup>	3775±1693 <sup>b</sup>	2709±1003 <sup>ab</sup>	1586±674 <sup>a</sup>	2713±684 <sup>ab</sup>	1064±298 <sup>a</sup>	1913±280 <sup>ab</sup>	1015±102 <sup>a</sup>	2542±561 <sup>ab</sup>
<i>Oleoside/secologanoside (isomer 1)</i>	203±17 <sup>a</sup>	402±34 <sup>d</sup>	186±37 <sup>a</sup>	278±15 <sup>abc</sup>	310±28 <sup>bcd</sup>	377±28 <sup>cd</sup>	277±52 <sup>abc</sup>	231±14 <sup>ab</sup>	254±59 <sup>ab</sup>	260±36 <sup>ab</sup>
<i>Oleoside/secologanoside (isomer 2)</i>	851±57 <sup>ab</sup>	1566±100 <sup>cd</sup>	855±97 <sup>ab</sup>	1121±85 <sup>b</sup>	1702±168 <sup>d</sup>	1193±138 <sup>bc</sup>	1027±203 <sup>ab</sup>	623±29 <sup>a</sup>	1211±294 <sup>bc</sup>	1153±66 <sup>bc</sup>
<i>Oleuropein</i>	14793±2356 <sup>a</sup>	34335±2802 <sup>e</sup>	21077±1819 <sup>abc</sup>	17190±2044 <sup>ab</sup>	24208±1113 <sup>bcd</sup>	26303±1532 <sup>cde</sup>	17590±5557 <sup>ab</sup>	30795±2207 <sup>de</sup>	19813±4649 <sup>abc</sup>	18180±1040 <sup>abc</sup>
<i>Oleuropein aglycone (isomer 1)</i>	27±8 <sup>a</sup>	125±36 <sup>a</sup>	109±88 <sup>a</sup>	56±19 <sup>a</sup>	107±27 <sup>a</sup>	101±12 <sup>a</sup>	68±27 <sup>a</sup>	67±14 <sup>a</sup>	16±6 <sup>a</sup>	36±17 <sup>a</sup>

<b>b) Stems</b>	<i>Arbequina</i>	<i>Empeltre</i>	<i>Frantoio</i>	<i>Hojiblanca</i>	<i>Jabali</i>	<i>Koroneiki</i>	<i>Leccino</i>	<i>Mastoidis</i>	<i>Menya</i>	<i>Pical</i>
<i>Oleuropein aglycone (isomer 2)</i>	26±5 <sup>a</sup>	161±41 <sup>abc</sup>	89±77 <sup>ab</sup>	91±9 <sup>ab</sup>	172±54 <sup>bc</sup>	145±34 <sup>ab</sup>	286±108 <sup>c</sup>	153±5 <sup>abc</sup>	26±16 <sup>a</sup>	32±9 <sup>ab</sup>
<i>Oleuroside</i>	351±21 <sup>ab</sup>	884±23 <sup>f</sup>	308±57 <sup>ab</sup>	528±17 <sup>cd</sup>	714±83 <sup>e</sup>	430±11 <sup>bc</sup>	410±78 <sup>bc</sup>	900±48 <sup>f</sup>	266±61 <sup>a</sup>	583±23 <sup>de</sup>
<i>Phenylethyl primeveroside</i>	49±7 <sup>d</sup>	48±4 <sup>cd</sup>	27±11 <sup>ab</sup>	42±3 <sup>bcd</sup>	27±7 <sup>ab</sup>	58±8 <sup>d</sup>	23±3 <sup>a</sup>	54±7 <sup>d</sup>	30±4 <sup>abc</sup>	17±2 <sup>a</sup>
<i>Quercetin-O-glucoside (isomer 1)</i>	37±8 <sup>ab</sup>	27±2 <sup>ab</sup>	45±27 <sup>ab</sup>	22±9 <sup>a</sup>	142±31 <sup>c</sup>	63±6 <sup>b</sup>	41±5 <sup>ab</sup>	22±2 <sup>a</sup>	22±1 <sup>a</sup>	31±8 <sup>ab</sup>
<i>Quercetin-O-glucoside (isomer 2)</i>	35±3 <sup>a</sup>	17±5 <sup>a</sup>	31±24 <sup>a</sup>	26±3 <sup>a</sup>	96±56 <sup>b</sup>	16±5 <sup>a</sup>	8±3 <sup>a</sup>	9±5 <sup>a</sup>	16±3 <sup>a</sup>	16±6 <sup>a</sup>
<i>Quercetin-O-glucoside (isomer 3)</i>	39±6 <sup>a</sup>	18±4 <sup>a</sup>	40±16 <sup>a</sup>	32±3 <sup>a</sup>	102±37 <sup>b</sup>	30±4 <sup>a</sup>	30±9 <sup>a</sup>	10±4 <sup>a</sup>	22±4 <sup>a</sup>	30±7 <sup>a</sup>
<i>Quinic acid</i>	1792±175 <sup>ab</sup>	2710±112 <sup>b</sup>	2300±831 <sup>ab</sup>	2463±471 <sup>ab</sup>	2095±380 <sup>ab</sup>	1490±103 <sup>a</sup>	1761±89 <sup>ab</sup>	1844±206 <sup>ab</sup>	1469±174 <sup>a</sup>	1862±266 <sup>ab</sup>
<i>Rutin</i>	91±34 <sup>ab</sup>	88±9 <sup>ab</sup>	111±68 <sup>ab</sup>	34±7 <sup>a</sup>	157±33 <sup>b</sup>	99±19 <sup>ab</sup>	54±6 <sup>a</sup>	33±6 <sup>a</sup>	47±5 <sup>a</sup>	34±8 <sup>a</sup>
<i>Taxifolin</i>	186±13 <sup>cde</sup>	151±16 <sup>bcd</sup>	199±12 <sup>de</sup>	31±8 <sup>a</sup>	120±26 <sup>bc</sup>	228±42 <sup>ef</sup>	285±45 <sup>f</sup>	145±11 <sup>bcd</sup>	118±19 <sup>bc</sup>	115±17 <sup>b</sup>
<i>Unknown 1</i>	34±5 <sup>a</sup>	85±35 <sup>ab</sup>	41±35 <sup>a</sup>	157±44 <sup>bc</sup>	101±64 <sup>ab</sup>	251±32 <sup>c</sup>	107±19 <sup>ab</sup>	111±22 <sup>ab</sup>	42±15 <sup>a</sup>	60±47 <sup>ab</sup>
<i>Unknown 2</i>	260±3 <sup>a</sup>	194±20 <sup>a</sup>	202±18 <sup>a</sup>	257±13 <sup>a</sup>	261±61 <sup>a</sup>	240±28 <sup>a</sup>	188±32 <sup>a</sup>	253±16 <sup>a</sup>	221±6 <sup>a</sup>	249±16 <sup>a</sup>
<i>Unknown 4</i>	n.d	43±15 <sup>b</sup>	184±14 <sup>c</sup>	n.d	n.d	n.d	176±37 <sup>c</sup>	n.d	14±0 <sup>a</sup>	n.d
<i>Unknown 5</i>	149±31 <sup>ab</sup>	139±18 <sup>ab</sup>	191±119 <sup>b</sup>	104±33 <sup>ab</sup>	112±23 <sup>ab</sup>	120±43 <sup>ab</sup>	106±36 <sup>ab</sup>	62±9 <sup>ab</sup>	56±11 <sup>a</sup>	151±26 <sup>ab</sup>
<i>Verbascoside</i>	319±89 <sup>a</sup>	1196±205 <sup>ab</sup>	1118±547 <sup>ab</sup>	499±146 <sup>a</sup>	883±429 <sup>a</sup>	521±165 <sup>a</sup>	1941±739 <sup>b</sup>	234±58 <sup>a</sup>	661±189 <sup>a</sup>	508±79 <sup>a</sup>

Lower case letters indicate Tukey's post hoc test differences ( $p < 0.05$ ) among different cultivars. Means with a common letter are not significantly different ( $p > 0.05$ ); n.d: not detected

<b>c) Roots</b>	<i>Arbequina</i>	<i>Empeltre</i>	<i>Frantoio</i>	<i>Hojiblanca</i>	<i>Jabali</i>	<i>Koroneiki</i>	<i>Leccino</i>	<i>Mastoidis</i>	<i>Menya</i>	<i>Pical</i>
<i>11-Hydroxyiridodial glucoside pentaacetate</i>	123±50 <sup>ab</sup>	278±31 <sup>cd</sup>	77±23 <sup>ab</sup>	151±13 <sup>abc</sup>	131±56 <sup>abc</sup>	345±19 <sup>d</sup>	188±113 <sup>bc</sup>	16±3 <sup>a</sup>	156±66 <sup>abc</sup>	82±42 <sup>ab</sup>
<i>7-deoxyloganic acid</i>	48±12 <sup>a</sup>	16±11 <sup>a</sup>	17±15 <sup>a</sup>	48±19 <sup>a</sup>	81±43 <sup>a</sup>	986±688 <sup>c</sup>	330±126 <sup>b</sup>	58±29 <sup>a</sup>	20±12 <sup>a</sup>	66±41 <sup>a</sup>
<i>Acetoxipinoresinol</i>	155±57 <sup>b</sup>	62±14 <sup>ab</sup>	149±46 <sup>b</sup>	154±78 <sup>b</sup>	147±49 <sup>b</sup>	57±22 <sup>ab</sup>	17±4 <sup>a</sup>	59±9 <sup>ab</sup>	141±22 <sup>b</sup>	151±12 <sup>ab</sup>
<i>Acetoxypinoresinol glucoside</i>	798±156 <sup>bc</sup>	455±116 <sup>ab</sup>	819±76 <sup>bc</sup>	670±95 <sup>abc</sup>	1001±415 <sup>c</sup>	618±32 <sup>abc</sup>	335±26 <sup>a</sup>	657±10 <sup>abc</sup>	803±130 <sup>bc</sup>	262±87 <sup>a</sup>
<i>Betulinic acid</i>	275±24 <sup>c</sup>	269±40 <sup>bc</sup>	244±27 <sup>bc</sup>	183±13 <sup>abc</sup>	112±13 <sup>a</sup>	174±67 <sup>ab</sup>	179±45 <sup>abc</sup>	179±9 <sup>abc</sup>	276±36 <sup>c</sup>	93±18 <sup>a</sup>
<i>Cycloolivil glucoside (isomer 1)</i>	421±79 <sup>cd</sup>	450±99 <sup>d</sup>	164±15 <sup>a</sup>	164±30 <sup>a</sup>	211±76 <sup>ab</sup>	411±44 <sup>cd</sup>	378±90 <sup>bcd</sup>	370±33 <sup>bcd</sup>	263±60 <sup>abcd</sup>	251±100 <sup>abc</sup>
<i>Cycloolivil glucoside (isomer 2)</i>	190±77 <sup>ab</sup>	426±38 <sup>c</sup>	354±97 <sup>bc</sup>	255±119 <sup>abc</sup>	117±45 <sup>a</sup>	104±7 <sup>a</sup>	142±27 <sup>a</sup>	258±59 <sup>abc</sup>	232±58 <sup>abc</sup>	210±71 <sup>ab</sup>
<i>Elenolic acid glucoside (isomer 1)</i>	286±91 <sup>abc</sup>	767±68 <sup>d</sup>	289±98 <sup>abc</sup>	172±25 <sup>ab</sup>	292±79 <sup>abc</sup>	442±75 <sup>bc</sup>	547±256 <sup>cd</sup>	420±32 <sup>abc</sup>	335±82 <sup>abc</sup>	128±37 <sup>a</sup>
<i>Elenolic acid glucoside (isomer 2)</i>	121±47 <sup>abc</sup>	284±31 <sup>d</sup>	83±22 <sup>ab</sup>	29±8 <sup>a</sup>	76±26 <sup>a</sup>	302±43 <sup>d</sup>	204±98 <sup>bcd</sup>	225±35 <sup>cd</sup>	118±30 <sup>abc</sup>	27±11 <sup>a</sup>
<i>Hydroxy oleuropein</i>	152±36 <sup>a</sup>	450±311 <sup>a</sup>	246±133 <sup>a</sup>	197±90 <sup>a</sup>	184±124 <sup>a</sup>	248±102 <sup>a</sup>	193±28 <sup>a</sup>	429±20 <sup>a</sup>	372±126 <sup>a</sup>	86±8 <sup>a</sup>
<i>Hydroxypinoresinol glucoside</i>	528±48 <sup>bc</sup>	472±32 <sup>abc</sup>	713±27 <sup>de</sup>	545±27 <sup>bc</sup>	347±124 <sup>a</sup>	738±49 <sup>de</sup>	818±52 <sup>e</sup>	603±24 <sup>cd</sup>	573±56 <sup>bcd</sup>	426±66 <sup>ab</sup>
<i>Ligstroside</i>	1502±234	4061±222	1778±268	877±155	1961±1026	3526±739	3111±1616	2542±180	2446±729	914±325
<i>Lucidumoside C</i>	270±89 <sup>ab</sup>	1045±823 <sup>b</sup>	426±259 <sup>ab</sup>	273±146 <sup>ab</sup>	313±277 <sup>ab</sup>	582±307 <sup>ab</sup>	438±92 <sup>ab</sup>	868±88 <sup>ab</sup>	688±255 <sup>ab</sup>	113±12 <sup>a</sup>
<i>Maslinic acid</i>	3082±777 <sup>ab</sup>	3000±774 <sup>ab</sup>	2181±436 <sup>a</sup>	2514±106 <sup>ab</sup>	2535±465 <sup>ab</sup>	2824±692 <sup>ab</sup>	3351±601 <sup>ab</sup>	2780±842 <sup>ab</sup>	3897±391 <sup>b</sup>	2497±170 <sup>ab</sup>
<i>Metoxypinoresinol glucoside</i>	87±6 <sup>bc</sup>	60±12 <sup>ab</sup>	101±15 <sup>c</sup>	97±13 <sup>c</sup>	72±22 <sup>abc</sup>	36±1 <sup>a</sup>	44±10 <sup>a</sup>	83±4 <sup>bc</sup>	45±3 <sup>a</sup>	89±20 <sup>bc</sup>
<i>Neonuzhenide/oleuropein glucoside (isomer 1)</i>	101±47 <sup>abc</sup>	195±52 <sup>abc</sup>	70±19 <sup>ab</sup>	26±9 <sup>a</sup>	101±49 <sup>abc</sup>	339±85 <sup>c</sup>	269±230 <sup>bc</sup>	113±13 <sup>abc</sup>	92±17 <sup>ab</sup>	34±13 <sup>ab</sup>
<i>Neonuzhenide/oleuropein glucoside (isomer 2)</i>	90±35 <sup>ab</sup>	156±12 <sup>bc</sup>	70±30 <sup>ab</sup>	31±9 <sup>a</sup>	138±59 <sup>ab</sup>	394±57 <sup>d</sup>	170±55 <sup>bc</sup>	260±36 <sup>c</sup>	117±19 <sup>ab</sup>	42±9 <sup>a</sup>
<i>Neonuzhenide/oleuropein glucoside (isomer 4)</i>	15±2 <sup>a</sup>	35±1 <sup>cd</sup>	16±2 <sup>ab</sup>	7±1 <sup>a</sup>	13±4 <sup>a</sup>	39±5 <sup>d</sup>	26±5 <sup>bc</sup>	34±5 <sup>cd</sup>	16±3 <sup>ab</sup>	8±3 <sup>a</sup>

<b>c) Roots</b>	<i>Arbequina</i>	<i>Empeltre</i>	<i>Frantoio</i>	<i>Hojiblanca</i>	<i>Jabali</i>	<i>Koroneiki</i>	<i>Leccino</i>	<i>Mastoidis</i>	<i>Menya</i>	<i>Pical</i>
<i>Oleanolic acid</i>	53±11 <sup>a</sup>	43±11 <sup>a</sup>	45±4 <sup>a</sup>	38±4 <sup>a</sup>	30±6 <sup>a</sup>	43±10 <sup>a</sup>	49±15 <sup>a</sup>	38±6 <sup>a</sup>	36±5 <sup>a</sup>	34±4 <sup>a</sup>
<i>Oleoside/secologanoside (isomer 1)</i>	69±15 <sup>ab</sup>	204±15 <sup>e</sup>	61±12 <sup>a</sup>	64±13 <sup>a</sup>	70±13 <sup>abc</sup>	147±26 <sup>de</sup>	130±50 <sup>cd</sup>	125±7 <sup>bcd</sup>	57±9 <sup>a</sup>	38±5 <sup>a</sup>
<i>Oleoside/secologanoside (isomer 2)</i>	267±44 <sup>abc</sup>	323±60 <sup>bc</sup>	244±24 <sup>abc</sup>	366±99 <sup>c</sup>	388±98 <sup>c</sup>	164±37 <sup>ab</sup>	300±24 <sup>abc</sup>	165±7 <sup>ab</sup>	139±29 <sup>a</sup>	227±70 <sup>abc</sup>
<i>Oleuropein</i>	17093±6267 <sup>ab</sup>	37381±5024 <sup>d</sup>	13510±1354 <sup>ab</sup>	6736±898 <sup>a</sup>	11165±4890 <sup>a</sup>	33302±2467 <sup>cd</sup>	24029±8228 <sup>bc</sup>	33049±1922 <sup>cd</sup>	13790±4379 <sup>ab</sup>	6545±2577 <sup>a</sup>
<i>Quinic acid</i>	252±14 <sup>a</sup>	295±50 <sup>a</sup>	356±239 <sup>a</sup>	383±65 <sup>a</sup>	377±73 <sup>a</sup>	245±85 <sup>a</sup>	288±36 <sup>a</sup>	239±5 <sup>a</sup>	370±125 <sup>a</sup>	311±87 <sup>a</sup>
<i>Unknown 1</i>	133±63 <sup>ab</sup>	266±77 <sup>bcd</sup>	124±68 <sup>ab</sup>	81±23 <sup>a</sup>	203±89 <sup>abc</sup>	423±84 <sup>d</sup>	241±68 <sup>abc</sup>	341±11 <sup>cd</sup>	94±31 <sup>ab</sup>	66±36 <sup>a</sup>
<i>Unknown 2</i>	141±25 <sup>ab</sup>	162±17 <sup>b</sup>	135±7 <sup>ab</sup>	123±20 <sup>ab</sup>	103±26 <sup>a</sup>	103±16 <sup>a</sup>	117±9 <sup>ab</sup>	142±14 <sup>ab</sup>	144±3 <sup>ab</sup>	116±29 <sup>ab</sup>
<i>Unknown 3</i>	57±38 <sup>ab</sup>	185±21 <sup>c</sup>	33±14 <sup>a</sup>	18±2 <sup>a</sup>	38±8 <sup>ab</sup>	131±31 <sup>bc</sup>	108±55 <sup>abc</sup>	185±63 <sup>c</sup>	40±10 <sup>ab</sup>	16±8 <sup>a</sup>
<i>Verbascoside</i>	6055±1827 <sup>a</sup>	2778±715 <sup>a</sup>	5655±643 <sup>a</sup>	9359±5461 <sup>a</sup>	8883±4473 <sup>a</sup>	8887±2296 <sup>a</sup>	9913±1546 <sup>a</sup>	4799±1477 <sup>a</sup>	4990±783 <sup>a</sup>	8695±3120 <sup>a</sup>
<i>Isoverbascoside</i>	693±89 <sup>ab</sup>	366±79 <sup>a</sup>	1185±72 <sup>ab</sup>	1237±716 <sup>ab</sup>	1150±306 <sup>ab</sup>	711±19 <sup>ab</sup>	924±68 <sup>ab</sup>	760±52 <sup>ab</sup>	724±157 <sup>ab</sup>	1442±681 <sup>b</sup>

Lower case letters indicate Tukey's post hoc test differences ( $p < 0.05$ ) among different cultivars. Means with a common letter are not significantly different ( $p > 0.05$ )

# Chapter

# 7

## Application of LC-ion mobility spectrometry-MS-based metabolomics to investigate the basal chemical profile of olive cultivars differing in *Verticillium dahliae* resistance

Irene Serrano-García<sup>1</sup>, Ioannis C. Martakos<sup>2,3</sup>, Lucía Olmo-García<sup>1✉</sup>, Lorenzo León<sup>4</sup>, Raúl de la Rosa<sup>4,5</sup>, Ana M. Gómez-Caravaca<sup>1</sup>, Angjelina Belaj<sup>4</sup>, Alicia Serrano<sup>6</sup>, Marilena Dasenaki<sup>3</sup>, Nikolaos S. Thomaidis<sup>2</sup>, Alegría Carrasco-Pancorbo<sup>1</sup>

<sup>1</sup>Department of Analytical Chemistry, Faculty of Sciences, University of Granada, Ave. Fuentenueva s/n, 18071 Granada, Spain

<sup>2</sup>Analytical Chemistry Laboratory, Chemistry Department, National and Kapodistrian University of Athens, Panepistimiopolis Zographou, 15771 Athens, Greece

<sup>3</sup>Food Chemistry Laboratory, Department of Chemistry, National and Kapodistrian University of Athens, Panepistimiopolis Zographou, 15771 Athens, Greece

<sup>4</sup>IFAPA Centro Alameda del Obispo, Av. Menéndez Pidal s/n, 14004 Córdoba, Spain

<sup>5</sup>Instituto de Agricultura Sostenible, Consejo Superior de Investigaciones Científicas, Av. Menéndez Pidal s/n, 14004 Córdoba, Spain

<sup>6</sup>The University Institute of Research into Olives and Olive Oils (INUO). University of Jaén, Campus Las Lagunillas s/n, 23071 Jaén, Spain

✉ luciaolmo@ugr.es

*Journal of Agricultural and Food Chemistry* (under review)



**Abstract:** The limited effectiveness of current strategies to control Verticillium wilt of olive (VWO) prompts the need for innovative approaches. This study explores the basal metabolome of 43 olive cultivars with varying resistance levels to *Verticillium dahliae*, offering alternative insights for olive crossbreeding programmes. The use of an innovative UHPLC-ESI-TimsTOF MS/MS platform enabled the identification of more than 70 compounds across different olive organs (root, stem, and leaf) and the creation of a preliminary <sup>TIMS</sup>CCS<sub>N<sub>2</sub></sub> experimental database for reliable metabolite annotation. Moreover, it allowed the documentation of numerous isomeric species in the studied olive organs by resolving hidden isobaric compounds. Multivariate statistical analyses revealed significant metabolome variability between highly resistant and susceptible cultivars, which was further investigated through supervised PLS-DA. Key markers indicative of VWO susceptibility were identified and characteristic compositional patterns were established. Stem tissue exhibited the highest discriminative capability, while root and leaf tissues also showed significant predictive potential.

**Keywords:** *Olea europaea* L., LC-MS profiling, TIMS, olive roots, olive stems, olive leaves, pathogen resistance, Verticillium wilt of olive.

## 1. INTRODUCTION

*Olea europaea* L. has coexisted with mankind since prehistoric times, undergoing a lengthy process of intentional or accidental domestication [1]. The fruit is the most valued part of the tree and, due to its profitability, its cultivation has been steadily increasing worldwide. Indeed, olive-growing area is currently 19% higher compared to the beginning of the 21st century [2]. Concurrently, the modernisation of olive management has witnessed the emergence of high-density growing systems and the widespread adoption of drip irrigation systems worldwide, with particular prominence in Andalusia, Spain [3,4]. However, a downside of these significant changes has been the rapid spread of some pests and diseases, such as Verticillium wilt of olive (VWO), across olive-growing regions, resulting in substantial economic losses for producers [5,6]. This severe pathology is caused by the soil-borne fungus *Verticillium dahliae* Kleb. and was first diagnosed in 1946 in Italy and, later, in the entire Mediterranean basin [7]. Numerous factors contribute to its uncontrolled expansion, but particularly noteworthy is the fungus's exceptional resistance, facilitated by microsclerotia, which are triggered to germinate by the root exudates of the plant [8]. *V. dahliae* penetrates the olive tree via roots and disseminates rapidly through other organs (trunk, barks, leaves, etc.) to colonise the xylem vessels causing the host plant's water and nutrients collapse [8]. The severity of plant symptoms will vary depending on several factors, including the type of infecting isolates, the density of inoculum, the susceptibility of the cultivar, and environmental conditions. In severe cases, this can lead to the complete death of the tree [9,10]. Since there is not a clear way to eradicate VWO-pathology, the use of olive cultivars possessing inherent resistance to *V. dahliae* as a component of integrated control strategies has

been widely advocated to mitigate disease incidence [9]. Many studies have already categorised in terms of resistance and/or susceptibility a substantial number of olive cultivars by using multiple disease parameters related to physical symptomatology and/or fungus infection rate [11–14]. However, the critical factors defining VWO resistance as a selection criterion in olive breeding programs remain uncertain and further research is needed.

In plant biology, metabolomics has been pivotal in elucidating the physiological and biochemical responses of hosts to biotic and abiotic stresses [15]. Metabolomics is categorised into targeted and non-targeted approaches, which differ mainly in the methodologies and pursued objectives. Regarding VWO, only targeted approaches have been employed so far, covering a limited section of metabolome. Thus, several secondary metabolites (mainly phenolic compounds) have been evaluated in various infected olive organs and tissues (roots, stems, cortex, xylem, etc.) to explore their role in the plant's defence mechanisms against *V. dahliae* [16–19]. Indeed, some of these metabolites such as rutin, oleuropein, luteolin-7-glucoside or hydroxytyrosol have been previously described to exhibit *in-vitro* anti-fungal activity against this vascular pathogen [17,20]. More extensively, Cardoni and co-authors determined 31 secondary metabolites belonging to simple phenols and glycosides, secoiridoids and derivatives, lignans and triterpenic acids to evaluate major changes in metabolic profiles of infected-olive root extracts [21]. In that work, a strong relationship between the quantitative basal metabolic profile and olive cultivar susceptibility was pointed out. Building on these findings and providing additional evidence, Serrano-García and co-authors, in a recent study, depicted the distribution of 56 basal metabolites in three olive organs, emphasising key quantitative differences observed in relation to VWO-resistance levels [22]. These authors also evidenced the capability of the quantified metabolites to discriminate olive cultivars according to the fungus resistance by applying supervised and unsupervised statistical analyses.

Although non-targeted metabolomics has not been applied in VWO-pathology to date, this holistic approach has provided valuable insights trying to elucidate the resistance mechanisms of olive tree against *Xylella fastidiosa* [23], cotton against *Aspergillus tubingensis* [24] or tobacco against *Phytophthora parasitica* var. *nicotianae* [25]. The primary objective of non-targeted metabolomics is to screen the metabolome of samples exhibiting specific traits, such as resistance, as well as to identify discriminant biomarkers without prior knowledge of their identity. The most time-consuming step in this process is metabolite/marker identification, requiring thorough data interpretation. Conventional LC-High Resolution MS (LC-HRMS) platforms widely used in metabolomics provide many ion descriptors (e.g., retention time, accurate mass, molecular formula, isotopic distribution, and MS/MS fragmentation). These descriptors facilitate metabolite identification by comparison with comprehensive databases and published literature. Over the past decade, the integration of ion mobility spectrometry (IMS) with HRMS has introduced an additional molecular descriptor known as the collision cross section (CCS) value. The CCS is a unique physicochemical parameter related to the size, shape and charge of the molecules, which

is measured with a specific buffer gas, pressure, and temperature [26]. The mobility dimension enhances metabolite identification with higher confidence and improves sensitivity by reducing the signal-to-noise ratio. Additionally, it increases the selectivity of the method by boosting peak capacity [27]. Moreover, for isomers that cannot be distinguished chromatographically and evade differentiation by MS, ion mobility offers an additional separation dimension, enabling the elucidation of hidden isomers. Therefore, IMS emerges as a powerful technique for enhancing the performance characteristics of non-targeted LC-MS methods. However, there is a notable lack of CCS-experimental databases in plant metabolomics, particularly for substances without available pure standards, such as those derived from olive matrices. Consequently, the CCS descriptor remains incompletely integrated into the workflow for metabolite characterisation, and further research is needed to achieve widespread acceptance.

Being aware of the existence of a significant information gap regarding VWO disease and the capabilities of the analytical platform used, this study pursued three main objectives: (i) to evaluate the potential of the innovative UHPLC-ESI-TimsTOF MS platform to maximise metabolome information from olive-derived matrices, leading to the creation of a preliminary list of compounds based on collision cross-section values ( $^{TIMS}CCS_{N_2}$ ); (ii) characterise the presence or absence of these secondary metabolites in various olive plant organs; and (iii) apply an untargeted approach to comprehensively investigate and delineate basal metabolic differences in roots, stems, and leaves of 43 olive cultivars as a function of their resistance to *Verticillium dahliae* Kleb. infection.

## 2. MATERIALS AND METHODS

### 2.1. Plant material and sample pre-treatment

Healthy one-year-old plants from 43 different olive cultivars obtained by vegetative propagation of semi-hardwood stem cuttings were provided from the World Olive Germplasm Bank (WOGBC) of Centro IFAPA 'Alameda del Obispo' in Cordoba, Spain [28]. Table 1 includes the cultivars selected in the present study classified according to the VWO-resistance category [9,12]. Plant organs (roots, stems and leaves) were sampled from three different plants of the cultivars under study, resulting thus in a comprehensive collection of 129 samples per each plant organ (387 samples in total considering all the tissues). As plant pre-treatment, olive organs were carefully detached from the tree, followed thorough wet cleaning. Afterward, the detached tissues were air-dried at room temperature in a dark environment until a constant weight was achieved. The dried material was then finely powdered, homogenised to uniform particle size using a 0.5 mm metal sieve, and stored at -23 °C until further use.

**Table 1.** Olive cultivars included in the study, their classification according to VWO-resistance and the code used for their identification

Category	Olive Cultivars and Code Used
High resistant (HR)	'I117-120' (G1), 'Frantoio' (G2), 'I111-2' (G3), 'I117-117' (G4), 'Manzanillera de Huércal-Overa' (G5), 'Empeltre' (G6)
Resistant (R)	'Uslu' (G7), 'Maarri' (G8), 'Koroneiki' (G9), 'Leccino' (G10), 'Mavreya' (G11), 'Dokkar' (G12)
Medium susceptible (MS)	'Fs17' (G13), 'Klon 14-1812' (G14), 'Arbequina' (G15), 'UCI 2-35' (G16), 'Mawi' (G17), 'UCI 10-30' (G18), 'Fishomi' (G19), 'Changlot Real' (G20), 'Piñonera' (G21), 'UCI 2-68' (G22), 'Lianolia Kerkyras' (G23), 'Picual' (G24), 'Barri' (G25), 'Picudo' (G26), 'Myrtolia' (G27), 'Cornicabra' (G28), 'Barnea' (G29), 'Verdial de Vélez Málaga-51' (G30), 'Sikitita' (G31), 'Manzanilla de Sevilla' (G32), 'Morrut' (G33)
Susceptible (S)	'Chemlal del Kabylie' (G34), 'Abadi Abou Gabra' (G35), 'Hojiblanca' (G36), 'Majhol-152' (G37), 'Abou Salt Mohazam' (G38), 'Menya' (G39), 'Temprano' (G40), 'Llumeta' (G41), 'Jabali' (G42), 'Mastoidis' (G43)

## 2.2. Chemicals and reagents

Double deionised water, with a resistivity of 18.2 MΩ·cm, was obtained using a Milli-Q system (Millipore, Bedford, USA). High-quality ethanol (EtOH) with a minimum purity of 99% and LC-MS grade methanol (MeOH) were supplied by Prolabo (Paris, France). ESI-L Low Concentration Tuning Mix was provided by Agilent Technologies (Santa Clara, CA, USA). The pure standards of quinic acid, hydroxytyrosol, rutin, oleuropein, maslinic acid, catechin, luteolin, apigenin, tyrosol, oleanolic acid and verbascoside were acquired from Sigma-Aldrich (St. Louis, MO, USA), as well as the ammonium acetate salt. Mobile phases were filtered through a Nylaflo™ 0.45 µm nylon membrane filter (Pall Corporation (Michigan, MI, USA)) while Clarinet™ 0.22 µm nylon syringe filters (Bonna-Agela Technologies (Wilmington, DE, USA)) were used for extracts and pure standard mixtures. The standard solution mix used for qualitative purposes was prepared by mixing the exact amount of all pure standards mentioned above in EtOH/H<sub>2</sub>O (80:20, v/v) to obtain a concentration of around 15 mg/L for each compound.

## 2.3. Extract preparation

The sample preparation followed the solid-liquid extraction protocol previously outlined by Serrano-García [22]. Briefly, leaf extracts were prepared by mixing 100 mg of dried and homogenised powder with 10 mL of EtOH/H<sub>2</sub>O (60:40, v/v) in a 15 mL falcon tube. After 1.5 min of shaking, the falcon was introduced into an ultrasonic bath working within the range of 50–60 kHz for 30 min and centrifugated for 10 min at 9000 rpm. Once the first supernatant was removed in a dark flask, the remaining solid underwent re-extraction using 10 mL of EtOH/H<sub>2</sub>O (80:20, v/v) in the subsequent step, followed by 10 mL of pure EtOH in the last extraction cycle. All supernatants were combined in the same dark flask (totalling 30 mL in leaf extracts). Before injection, an additional 10-fold dilution was performed using EtOH/H<sub>2</sub>O (80:20, v/v). Stem and root extracts were prepared following the same protocol as described above, with the extractant agent volume

reduced to 5 mL at each step, resulting in a final volume of 15 mL. A 5-fold dilution was carried out for both root and stem extracts. All extracts were stored at -23 °C until analysis.

A quality control (QC) sample was prepared for each plant organ (root, stem, and leaf) by combining aliquots from the extracts of the cultivars included in this study. These samples were utilised as instrumental controls.

#### 2.4. Analytical LC-IMS-MS/MS platform conditions

The entire sample set was analysed using an ultrahigh performance liquid chromatography (UHPLC) equipped with an electrospray ionisation source (ESI) and coupled to trapped ion mobility spectrometry-time of flight system (TimsTOF Pro) powered by the latest parallel accumulation serial fragmentation (PASEF®) technology from Bruker Daltonics (Bremen, Germany). Analytes were eluted using an Acclaim™ RSLC 120 C18 column (2.1 × 100 mm, 2.2 µm) from Thermo Fischer Scientific Inc. (Waltham, MA, USA), equipped with an Acquity UPLC BEH C18 VanGuard Pre-Column (2.1 × 5 mm, 1.7 µm), and maintained at a temperature of 30 °C. The injection volume was set at 2 µL and the autosampler was kept at 4 °C throughout the sequence. Mobile phases were composed by H<sub>2</sub>O/MeOH (90:10, v/v) (phase A) and pure MeOH (phase B), both buffered with 5 mM ammonium acetate. The chromatographic elution conditions, including time, flow rate, and mobile phase composition, were programmed as follows: 0 min, 99.0 % A and 0.2 mL/min; 1.0 min, 99.0 % A and 0.2 mL/min; 3.0 min, 61.0 % A and 0.2 mL/min, 14 min, 0.1 % A and 0.4 mL/min, 16 min, 0.1 % A and 0.48 mL/min, 16.1 min, 99.0 % A and 0.48 mL/min, 19 min, 99.0 % A and 0.48 mL/min, 19.1 min, 99.0 % A and 0.2 mL/min; and 20 min, 99.0 % A and 0.2 mL/min.

Ion mobility spectrometer operated with nitrogen (N<sub>2</sub>) as drift gas and 100.0 ms of ramp time, monitoring features from 0.40 to 1.37 V·s/cm<sup>2</sup>. The ESI operated in negative polarity and *Full Scan* mode (*m/z* 20–1300), with specific setting including +2500 V of capillary, -500 V of end-plate offset, 10 L/min and 220°C of dry gas, and 2.0 Bar of nebuliser pressure. Two different MS acquisition modes were employed depending on the objective pursued. Broadband collision-induced dissociation (bbCID) based on data-independent acquisition (DIA) method was employed to analyse the entire sample set, providing enhanced sensitivity. Additionally, PASEF, which relies on data-dependent acquisition, was exclusively utilised in certain QC samples to generate the auto MS/MS fragmentation pattern. In this latter mode, the same precursor ion was selected and fragmented several times to generate multiple MS<sup>2</sup> spectra. The software used for system control included Compass Hystar and Otof Control, supplied by Bruker Corporation. Data Analysis 5.3 software was applied to examine the acquired chromatograms.

#### 2.5. System calibration, system stability assurance, and data processing

Before starting any sequence, both TIMS and MS systems were subjected to external calibration using sodium formate and commercial ESI-L Low Concentration mix (Agilent, USA) solutions. In addition, a freshly prepared mixture (3:1, v/v) of these solutions was constantly infused to serve as internal calibration for data processing. For successful calibration, at least three reference *m/z* and

ion mobility values from the calibration solution had to correspond with those measured in the system. The QC sample was analysed every 10 samples to evaluate the stability of the instrument response. Additionally, pure solvent (MeOH) injections were performed at the same intervals to clean the column and ensure it remained free of contamination.

Data processing was conducted using the MetaboScape 2023 software, which utilised the T-Rex 4D (LC-TIMS-QTOF MS) algorithm to automatically recalibrate the acquired MS data. This involved conducting molecular feature selection, filtering, and scaling. Key parameters were configured during processing, such as setting the minimum extracted features by the number of occurrences to #3 for each group (in this case, for each cultivar) to ensure consistent feature presence across all cultivar replicates. The intensity threshold for peak detection was established at 1000 counts and the minimum 4D peak size was set at 100 points, while recursive features were defined at 75 points. An EIC correlation of 0.8 related to ion deconvolution was applied. The primary ion was  $[M-H]^-$ , with  $[M+Cl]^-$  as the seed ion and  $[M-H-H_2O]^-$  as the common ion. During data processing, the Within-Batch Correction tool was utilised to address potential drifts that may have occurred during the sequences. Extracted features from solvent analyses were automatically excluded if the analysis/solvent ratio exceeded 3.0. Following this, the extracted features were characterised using a number of tools that are integrated into MetaboScape. These tools include: (i) SmartFormula, which derives the molecular formula of each identified compound based on its accurate mass and isotopic pattern, taking into account any detected adducts; (ii) Compound Crawler, which searches molecular structures for specified molecular formulas in local (AnalyteDB) and online public databases (ChEBI, ChemSpider and PubChem); and (iii) MetFrag, which performs *in silico* fragmentation of potential structures and compares them with acquired MS/MS spectra. The software also supports annotation by comparing with previously established analyte lists and MS/MS spectral libraries (such as Bruker Sumner MetaboBASE Plant Library or public MS/MS databases). Typical bioactive compounds primarily consist of carbon, hydrogen, and oxygen. Therefore, our focus was on annotating compounds containing these elements, aiming for errors below 5 ppm. Additionally, the software provides a CCS prediction tool, crucial for ensuring high-reliability analyte characterisation.

## 2.6. Statistical analysis

SIMCA v14.1 software was used to perform both unsupervised principal components (PCA) and supervised partial least squares-discriminant analysis (PLS-DA). The data matrix included 129 samples (observations) and contained all the detected features (variables) expressed as peak intensity for each olive organ type. Standard data normalisation and unit variance (UV) scaling were implemented as a pre-processing methods. PCA was conducted to investigate data quality, biological diversity, and natural clustering of samples based on VWO-resistance. Hotelling's T<sup>2</sup> (95%) and DModX (DCrit 0.05) plots were examined to detect any potential outliers within the multidimensional space of PCA. Following a thorough examination of the LC-MS data, a supervised PLS-DA statistical analysis was employed to further explore the characteristic

metabolic patterns associated with the most VWO-resistant/susceptible olive cultivars. The quality of PLS-DA models was evaluated with a cross-validation test through the  $R^2X$ ,  $R^2Y$  and  $Q^2$  parameters. These parameters indicate the fraction of explained variance in the X and Y matrices and the predictive capability of the model, respectively. Additionally, permutations plot with 100 iterations were carried out to assess the class discrimination performance by comparing the goodness of fit ( $R^2$  and  $Q^2$ ) of the original model with randomly generated models where the order of Y-observations was permuted while keeping X-matrix intact.

### 3. RESULTS AND DISCUSSION

#### 3.1. Screening of olive organs profiles to build a comprehensive $TIMS_{CCS_{N_2}}$ -database

The limited availability of experimental CCS-libraries remains an unresolved obstacle to integrating ion mobility into metabolomics studies. Therefore, the initial step of this investigation was to conduct a preliminary screening of the LC-IMS-MS metabolic profiles of olive-derived matrices, aiming to build a comprehensive  $TIMS_{CCS_{N_2}}$ -database. Over 70 metabolites were annotated in the olive tree organs, including organic acids, iridoids, coumarins, simple phenols, lignans, secoiridoids, flavonoids, pentacyclic triterpenes, and their derivatives. The identified constituents are listed in Table 1 of Supporting Information (Table S1) including the proposed compound name, chemical family, calculated molecular formula, retention time (Rt), experimental  $m/z$ , error of the mass prediction (ppm), mSigma value,  $TIMS_{CCS_{N_2}}$  value and the main MS/MS fragments observed. All data presented in Table S1 are expressed as deprotonated form  $[M-H]^-$ , as this was the most commonly detected ion in negative polarity. In some cases, other ions such as  $[M-Cl]^-$  and  $[M-H-H_2O]^-$  were also monitored, although they were not included in the table information to contain the size of the table. The proposed compounds were cross-checked with relevant comprehensive studies focused on the in-depth characterisation of olive-derived matrices to ensure their identity or confirmed using Bruker spectral libraries [21,22,29–31]. The ion mobility descriptor was used to support metabolite identification whenever a standard was available, or if the compounds were described in the plant metabolomics  $TIMS_{CCS_{N_2}}$  library generated by Schroeder and collaborators in a previous work [32], or in other works applying TIMS mobility [33,34]. Additionally, it was used to propose a candidate if the predicted CCS value was consistent with the putative identification.

Therefore, the integration of IMS has proven to be crucial in the discrimination of numerous isomeric metabolites within the matrices under study. Notably, several of these metabolites were annotated for the first time in this study. This breakthrough may be attributed to the fact that, until now, LC-MS has primarily provided isomer differentiation based solely on retention time and accurate mass. In specific cases, hidden isomers were distinguishable within a single chromatographic peak solely through the IMS dimension. Furthermore, TIMS has shown its capability to effectively separate widely overlapping peaks that cannot be entirely resolved based

only on retention time and accurate mass. This capability is especially crucial for quantitative applications and represents a significant enhancement for targeted studies. The detailed workflow utilised in both scenarios is described in the following section, along with an examination of the distribution of the identified metabolites throughout the olive tree.

### 3.1.1. Exhaustive qualitative characterisation of the identified compounds within the metabolome of olive root, stem and leaf samples.

In accordance to previous studies, the qualitative metabolic profile is closely linked to the olive organ assessed [22,29–31]. **Table S1** lists the metabolites that were consistently detected in all tested cultivars of each matrix. The table, as specified in the previous section, includes relevant information for each of the substances considered. As expected, most of the compounds identified are of phenolic nature, such as simple phenols, secoiridoids, flavonoids, etc. In the case of **organic acids**, only two metabolites of this chemical class were identified: quinic acid ( $C_7H_{12}O_6$ ) with a CCS of  $134.3 \text{ \AA}^2$ , and citric acid ( $C_6H_8O_7$ ) with  $126.5 \text{ \AA}^2$ . These compounds were consistently present in all organs under investigation. Three instances of **iridoids** (compounds characterised by a six-membered ring containing an oxygen bound to a cyclopentane ring) were identified in the ethanolic extracts. Loganic acid ( $375.1296 m/z$ ), with a CCS of  $184.7 \text{ \AA}^2$ , was found in the three organs examined. It is characterised by the calculated molecular formula  $C_{16}H_{24}O_{10}$  and shows a fragmentation pattern with MS signals of certain intensity at  $213.0764$ ,  $169.0876$ ,  $151.0752$ ,  $125.0606$ ,  $113.0244$  and  $107.0499 m/z$ . The metabolites identified as 11-hydroxyiridodial glucoside pentaacetate ( $555.2082 m/z$ ;  $222.3 \text{ \AA}^2$ ) and 7-deoxyloganic acid ( $359.1347 m/z$ ;  $182.4 \text{ \AA}^2$ ) were exclusively detected in roots and stems. The latter finding is not entirely in line with the results reported by Michael and co-authors, who observed the presence of 7-deoxyloganic acid exclusively in root extracts of 'Koroneiki' and 'Chetoui' cultivars [31]. Serrano-Garcia and co-workers also found 7-deoxyloganic acid only in roots in a recent paper working with 10 cultivars [22]. These differences can be easily explained, taking into account the cultivars considered in each study and the analytical methodologies employed. Two metabolites belonging to the **coumarins group** were also found in the olive-derived tissues. Aesculin ( $C_{15}H_{16}O_9$ ;  $174.6 \text{ \AA}^2$ ), also known as esculetin hexoside, was found exclusively in olive roots and stems. The fragmentation pattern of this compound revealed the detachment of the sugar moiety, releasing its aglycone at  $m/z 177.0192$ . In contrast, aesculetin ( $C_9H_6O_4$ ;  $127.5 \text{ \AA}^2$ ), a dihydroxycoumarin, was detected in roots, stems and leaves, and exhibited MS fragmentation with signals at  $m/z 149.0244$ ,  $133.0300$ ,  $105.0345$  and  $89.0401$ . Both metabolites had been previously documented in various matrices derived from olive trees [29,31].

In general, **simple phenols and derivatives** were distributed throughout the plant, with most of them being detected in the three organs under study, although some exceptions were observed. For example, hydroxytyrosol ( $153.0557 m/z$ ;  $128.8 \text{ \AA}^2$ ) was detected in leaves and stems but it was not found in roots in the dilutions of extracts analysed. Contrary to our results, Michel and colleagues reported the presence of hydroxytyrosol in the roots of 'Koroneiki' and 'Chetoui'

cultivars, albeit at low concentrations [31]. Serrano-García and co-authors only quantified this simple phenol in the leaves of ten olive cultivars [22]. Ammar *et al.* observed the presence of hydroxytyrosol in the wood of the olive cultivar 'Chemlali', but did not detect it in extracts of "olive leaves + stems" [29]. In the same olive cultivar, Toumi and collaborators describe the presence of hydroxytyrosol in roots [35]. The substance identified as isoverbascoside ( $C_{29}H_{36}O_{15}$ ; rt 6.17 min and  $223.4 \text{ \AA}^2$ ) was found only in root tissue, whereas its isomer verbascoside (rt 5.73 min and  $223.2 \text{ \AA}^2$ ) was found in all organs. There were other 4 metabolites detected in the three organs: two isomers of hydroxytyrosol glycoside ( $C_{14}H_{20}O_8$ ), tyrosol glycoside ( $C_{14}H_{20}O_7$ ;  $161.4 \text{ \AA}^2$ ) and phenylethyl primeveroside ( $C_{19}H_{28}O_{10}$ ;  $202.2 \text{ \AA}^2$ ). The two isomers of hydroxytyrosol glucoside were identified by observation of a dual signal peak in the mobilogram ( $163.1 \text{ \AA}^2$  and  $171.8 \text{ \AA}^2$ ) accompanied by a fragmentation pattern with  $m/z$  signals at 153.055, 135.045 and 123.045; the peak at  $163.1 \text{ \AA}^2$  proved to be the predominant one. According to the literature, one of these isomers could coincide with the hydroxytyrosol 4-*O*-glucoside previously described in olive leaves [36].

**Lignans and derivatives** were found exclusively in olive roots and stems. However, although many reports claim the absence of this family of metabolites in olive leaves, other authors have reported the presence of trace amounts of lignans in that particular organ [30,37]. In the present study, three potential isomers of cycloolivil glucoside ( $C_{26}H_{34}O_{12}$ ;  $208.9 \text{ \AA}^2$ ,  $214.5 \text{ \AA}^2$  and  $231.4 \text{ \AA}^2$ ), two isomers of hydroxypinoresinol glucoside ( $C_{26}H_{32}O_{12}$ ;  $229.5 \text{ \AA}^2$  and  $215.9 \text{ \AA}^2$ ), and two isomers of acetoxypinoresinol glucoside ( $C_{28}H_{34}O_{13}$ ;  $210.7 \text{ \AA}^2$  and  $227.9 \text{ \AA}^2$ ) have been described. In all cases, being glycosylated compounds, the HRMS/MS spectra consistently showed a loss of 162  $m/z$ , confirming the association with a glucose unit attached to the lignan aglycone. Several of these isomeric structures, although appearing under a single chromatographic peak, could be elucidated based on the molecular descriptors of the ions and the intensity of the peaks in the ion mobility dimension, as illustrated in Figure 1. For instance, the highest signal of acetoxypinoresinol glucoside with a CCS of  $210.7 \text{ \AA}^2$  was denoted as (+)-1-acetoxypinoresinol-4' $\beta$ -D-glucoside in agreement with the predominant structure described in the literature [31]. In contrast, the signal of  $227.9 \text{ \AA}^2$  would be consistent with 8-acetoxypinoresinol-4'-glucoside, based on the predicted CCS value.

The presence of (+)-1-hydroxypinoresinol 4'- $\beta$ -D-glucoside and (+)-1-hydroxypinoresinol 1'- $\beta$ -D-glucoside has been documented for these matrices [29,31]. However, although we have detected 2 isomers, we have not been able to attribute these identities to the observed peaks, due to lack of consensus on the abundant species; further studies are essential to clarify this. Olivil ( $C_{20}H_{24}O_7$ ), with a CCS of  $197.8 \text{ \AA}^2$ , was identified from the primary fragments observed by HRMS/MS, namely the  $m/z$  360.1227, 345.1360, 327.1252, 195.0670 and 179.0713. In the case of cycloolivil ( $C_{20}H_{24}O_7$ ;  $205.6 \text{ \AA}^2$ ) a fragmentation pattern with two clear signals at 360.1228 and 345.1358  $m/z$  was obtained. The lignan eluting later in the chromatographic profile was 1-acetoxypinoresinol, with a molecular formula of  $C_{22}H_{24}O_8$ . Drakopoulou and co-workers, in an

interesting study, highlighted the presence of two isomers of acetoxypinoresinol at 203.5 Å<sup>2</sup> (1-acetoxypinoresinol) and 285.5 Å<sup>2</sup> (8-acetoxypinoresinol) in extra virgin olive oil [33]. However, in our case, only the signal linked to 1-acetoxypinoresinol was detected in the root and stem extracts, with a CCS value in line with that described by the aforementioned authors. This provides a solid basis to identify with certainty this specific conformation.

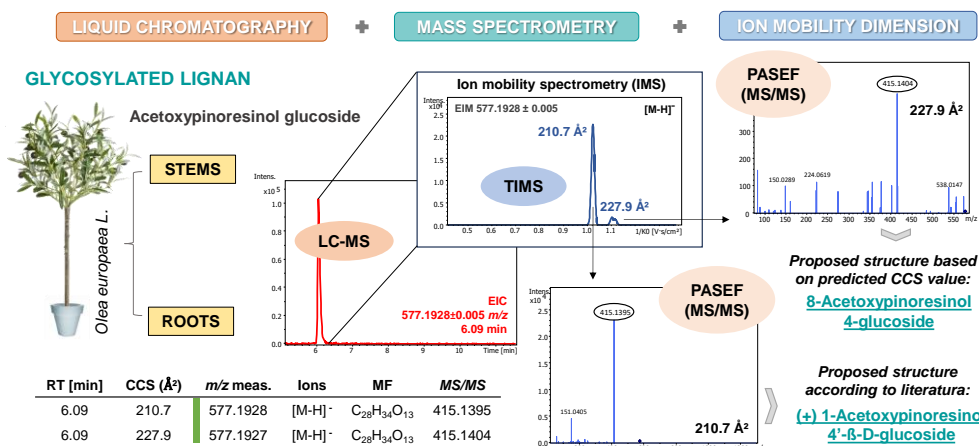


**Figure 1.** Example of the extracted ion chromatogram (EIC), mobilogram (EIM) and HRMS/MS spectra of acetoxypinoresinol glucoside to prove the potential of TIMS coupling to LC-MS/MS in the detection of hidden isomeric species without chromatographic separation

The group with the highest number of metabolites consisted of **secoiridoids and derivatives**, which are undoubtedly one of the most representative families of compounds in olive matrices. In Table S1, 27 compounds belonging to this chemical class have been described. Practically all of them were detected in olive root, stem and leaf. Oleuropein (C<sub>25</sub>H<sub>32</sub>O<sub>13</sub>; 217.5 Å<sup>2</sup>) and some of its derivatives were among the most relevant substances of this group, including demethyl oleuropein (C<sub>24</sub>H<sub>30</sub>O<sub>13</sub>; 213.5 Å<sup>2</sup>), two potential isomers of hydroxy oleuropein (C<sub>25</sub>H<sub>32</sub>O<sub>14</sub>; 218.9 Å<sup>2</sup> and 227.6 Å<sup>2</sup>), methoxyoleuropein (C<sub>26</sub>H<sub>34</sub>O<sub>14</sub>; 223.2 Å<sup>2</sup>), oleuroside (C<sub>25</sub>H<sub>32</sub>O<sub>13</sub>; 217.1 Å<sup>2</sup>) and three isomers of oleuropein aglycone (C<sub>19</sub>H<sub>22</sub>O<sub>8</sub>; 186.0 Å<sup>2</sup>, 185.2 Å<sup>2</sup> and 184.8 Å<sup>2</sup>). Several signals detected at 701.229 m/z, with molecular formula of C<sub>31</sub>H<sub>42</sub>O<sub>18</sub>, would be consistent with isomers of the glycosidic form of oleuropein or neonuzhenide (245.5 Å<sup>2</sup>, 241.8 Å<sup>2</sup> and 248.9 Å<sup>2</sup>). The first two isomers were not detected in leaves, and the latter, together with oleuroside, was absent in root tissue. Another notable subgroup of secoiridoids distributed in the three matrices considered were the compounds related to elenolic acid. Their identifications were achieved by HRMS/MS analysis, revealing two isomers of aldehydic form of decarboxymethyl elenolic acid glucoside (C<sub>16</sub>H<sub>26</sub>O<sub>10</sub>; 188.8 Å<sup>2</sup> and 188.6 Å<sup>2</sup>), five isomers of elenolic acid glucoside (C<sub>17</sub>H<sub>24</sub>O<sub>11</sub>; 192.5 Å<sup>2</sup>, 189.9 Å<sup>2</sup>, 192.1 Å<sup>2</sup>, 190.1 Å<sup>2</sup> and 190.4 Å<sup>2</sup>), elenolic acid dihexose derivative (C<sub>25</sub>H<sub>38</sub>O<sub>18</sub>; 231.5 Å<sup>2</sup>), and elenolic acid dihexose (C<sub>23</sub>H<sub>34</sub>O<sub>15</sub>; 234.9 Å<sup>2</sup>). The signals detected with m/z 389.109 at 1.29 and 1.32 min, respectively, with molecular formula of C<sub>16</sub>H<sub>22</sub>O<sub>11</sub>, were tentatively identified as oleoside/

secologanoside (184.6 Å<sup>2</sup> and 189.5 Å<sup>2</sup>) displaying a fragmentation with *m/z* signals of 345.116, 209.044, 183.066, 121.066 and 113.025. Finally, demethyl ligstroside (C<sub>24</sub>H<sub>30</sub>O<sub>12</sub>; 208.8 Å<sup>2</sup>), nuzhenide (C<sub>31</sub>H<sub>42</sub>O<sub>17</sub>; 241.1 Å<sup>2</sup>), lucidumoside C (C<sub>27</sub>H<sub>36</sub>O<sub>14</sub>; 229.1 Å<sup>2</sup>) and ligstroside (C<sub>25</sub>H<sub>32</sub>O<sub>12</sub>; 214.7 Å<sup>2</sup>) were also consistently identified in all the olive matrices investigated.

**Flavonoids** proved to be another important group of phenolic compounds present mainly in olive stems and leaves. Dihydrokaempferol-*O*-glucoside (C<sub>21</sub>H<sub>22</sub>O<sub>11</sub>; 186.3 Å<sup>2</sup>), identified through the main MS/MS fragments at 287.0550, 259.0633, 243.0664, 151.0034 and 125.0245 *m/z*, and two isomers of dihydroquercetin-*O*-glucoside (C<sub>21</sub>H<sub>22</sub>O<sub>12</sub>; 191.8 Å<sup>2</sup> and 192.5 Å<sup>2</sup>) were found exclusively in stems organ. Their flavanonol aglycones, taxifolin (C<sub>15</sub>H<sub>12</sub>O<sub>7</sub>; 164.7 Å<sup>2</sup>) and dihydrokaempferol (C<sub>15</sub>H<sub>12</sub>O<sub>6</sub>; 163.4 Å<sup>2</sup>), were also detected exclusively in the stem extracts. Both compounds were confidently identified as they showed a typical fragmentation pattern with MS signals at 285.0409, 177.0199 and 125.0263 *m/z* (for taxifolin) and 259.0598, 243.0661, 177.0561, 151.0039 and 125.0244 *m/z* (for dihydrokaempferol) [29–31]. Among the flavonoids that were systematically found in stem and leaf extracts, it is possible to mention the following: naringenin-*O*-glucoside (C<sub>21</sub>H<sub>22</sub>O<sub>10</sub>; 183.1 Å<sup>2</sup>), rutin (C<sub>27</sub>H<sub>30</sub>O<sub>16</sub>; 232.4 Å<sup>2</sup>), three isomers of luteolin-*O*-glucoside (C<sub>21</sub>H<sub>20</sub>O<sub>11</sub>; 210.2 Å<sup>2</sup>, 208.4 Å<sup>2</sup>, and 210.2 Å<sup>2</sup>), two isomers of quercetin-*O*-glucoside (C<sub>21</sub>H<sub>20</sub>O<sub>12</sub>; 202.1 Å<sup>2</sup> and 210.9 Å<sup>2</sup>) and apigenin-7-*O*-glucoside (C<sub>21</sub>H<sub>20</sub>O<sub>10</sub>; 208.1 Å<sup>2</sup>). In all cases, the HRMS/MS spectra of these glycosylated compounds revealed a cleavage of the sugar (-162 *m/z*), releasing the aglycone form. It is worth noting that the following 4 compounds only appeared in the olive leaf samples: two isomers of apigenin-*O*-rutinoside (C<sub>27</sub>H<sub>30</sub>O<sub>14</sub>; 232.7 Å<sup>2</sup> and 224.5 Å<sup>2</sup>), diosmin (C<sub>28</sub>H<sub>32</sub>O<sub>15</sub>; 231.8 Å<sup>2</sup>) and chrysoeriol-7-*O*-glucoside (C<sub>22</sub>H<sub>22</sub>O<sub>11</sub>; 215.9 Å<sup>2</sup>). The two isomers of apigenin-*O*-rutinoside could not be fully distinguished and annotated by LC-MS. However, relying on the TIMS dimension and following the strategy illustrated in Figure 2, both peaks were fully differentiated. Briefly, Figure 2A shows the extracted ion chromatogram (EIC) of *m/z* 577.1563 with a clear shoulder to the left of the main peak (min 6.55 and 6.65). Due to the absence of complete chromatographic separation for this glycosylated flavonoid, an isomeric profile scan was performed in the mobility dimension (Figure 2B). As expected, two distinct peaks emerged at 577.1563 *m/z* in EIM, indicating the possible presence of an isomer, as hinted above. Subsequently, specific mobility values for each segment of the co-eluted peak were evidenced by locking the elution time (*m/z* 577.1563; min 6.4–6.6 and 6.6–7.0) in EIM. HRMS/MS spectra generated by PASEF revealed fragmentation at 269.0458 *m/z*, providing useful extra information for the identification of the metabolites. Finally, by meticulous re-extraction of the features by imposing mobility constraints on the EIC, the initial overlap of the apigenin-*O*-rutinoside isomers was unravelled (Figure 2C). The predominant peak (224.5 Å<sup>2</sup>) was assigned as apigenin-7-*O*-rutinoside according to described in literature [38–40]. To conclude the overview of the described substances belonging to the flavonoid family, 3 metabolites were detected in all organs of all varieties: the flavanone naringenin (C<sub>15</sub>H<sub>12</sub>O<sub>5</sub>; 163.0 Å<sup>2</sup>), and two flavones, luteolin (C<sub>15</sub>H<sub>10</sub>O<sub>6</sub>; 160.6 Å<sup>2</sup>) and apigenin (C<sub>15</sub>H<sub>10</sub>O<sub>5</sub>; 157.6 Å<sup>2</sup>).

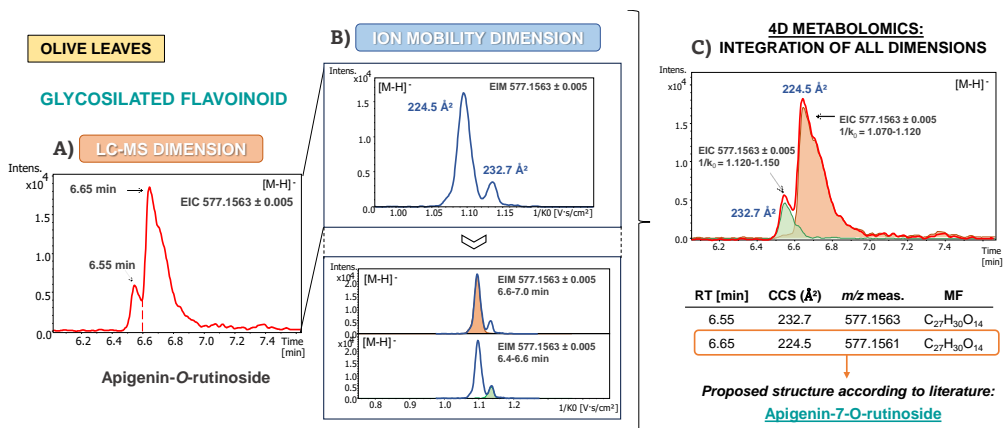


**Figure 2.** Three-step-strategy used for the complete resolution of the overlapping peaks of apigenin-O-rutinoside in olive leaf extracts by incorporating the ion mobility dimension into LC-HRMS/MS methodology

Regarding **pentacyclic triterpenes**, maslinic acid (C<sub>30</sub>H<sub>48</sub>O<sub>4</sub>; rt 13.13 min and 223.4 Å<sup>2</sup>), betulinic acid (C<sub>30</sub>H<sub>48</sub>O<sub>3</sub>; rt 14.00 min and 220.1 Å<sup>2</sup>) and oleanolic acid (C<sub>30</sub>H<sub>48</sub>O<sub>3</sub>; rt 14.14 min and 220.7 Å<sup>2</sup>) were also registered in all analysed parts of olive tree.

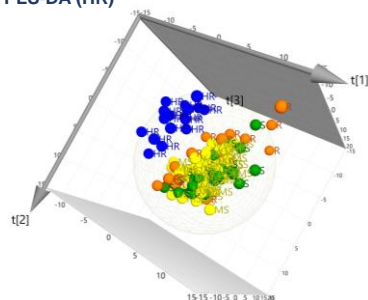
### 3.2. Non-targeted metabolomics for the identification of potential markers related to VWO-resistance level on the basal metabolic profiles of olive root, stem and leaf tissues

To study the possible association between VWO resistance level and basal metabolic profiles of olive organs, all LC-TIMS-HRMS/MS data, extracted as described in Section 2.5, were thoroughly explored by applying multivariate statistics. Initially, unsupervised PCA was employed to assess data quality, biodiversity and natural clustering of samples by matrix; however, this analysis did not reveal a clear natural clustering between groups. Despite this, Hotelling's T<sub>2</sub> (95%) and DModX (DCrit 0.05) plots were carefully evaluated to detect potential outliers across the multidimensional PCA space. Subsequent tests determined that the distant positioning of the suspected outliers was attributed to the inherent heterogeneity of biological specimens. In every instance, these samples remained in proximity to their biological replicates and their exclusion did not enhance the model.

Although the natural groupings observed with the PCA models were not distinctly clear among the resistance categories, the results indicate metabolic differences between most of the evaluated cultivars. Therefore, the LC-IMS-MS data were secondly subjected to a supervised PLS-DA to determine the markers that could presumably serve to describe the characteristic metabolic patterns. By focusing on the extremes of resistance/susceptibility to VWO, two-class PLS-DA models discriminating the highest (HR) and lowest (S) resistance level *versus* the other cultivars were constructed for root, stem and leaf. All the PLS-DA-score plots generated in three dimensions (3D) are represented in Figure 3 using the first three principal components (3PC's).

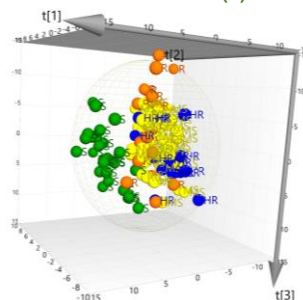
## ROOT TISSUE TYPE

PLS-DA (HR)



$R^2X[1] = 0.0917$     $R^2X[2] = 0.1090$   
 $R^2X[3] = 0.0817$

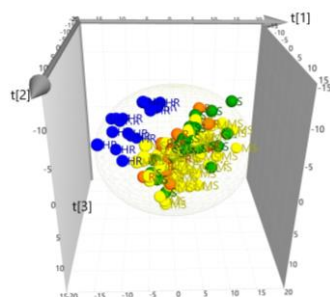
PLS-DA (S)



$R^2X[1] = 0.0769$     $R^2X[2] = 0.0376$   
 $R^2X[3] = 0.0824$

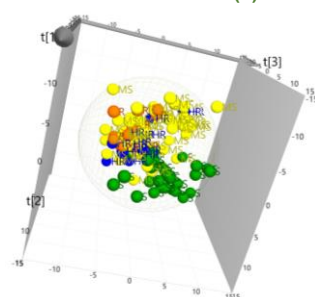
## STEM TISSUE TYPE

PLS-DA (HR)



$R^2X[1] = 0.1510$     $R^2X[2] = 0.0627$   
 $R^2X[3] = 0.0607$

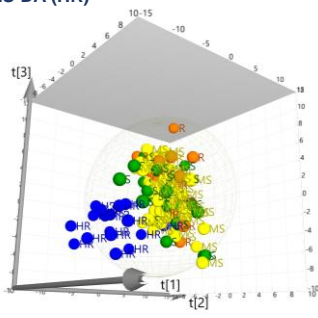
PLS-DA (S)



$R^2X[1] = 0.1090$     $R^2X[2] = 0.1000$   
 $R^2X[3] = 0.0783$

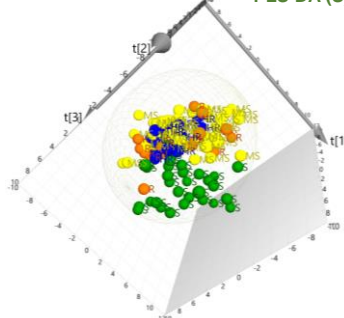
## LEAF TISSUE TYPE

PLS-DA (HR)



$R^2X[1] = 0.0862$     $R^2X[2] = 0.1250$   
 $R^2X[3] = 0.0822$

PLS-DA (S)



$R^2X[1] = 0.0766$     $R^2X[2] = 0.1260$   
 $R^2X[3] = 0.0762$

**Figure 3.** Two-class PLS-DA models and permutation tests of olive root, stem and leaf tissues for the discrimination of highly resistant (HR) and susceptible (S) cultivars to *V. dahliae*. Dots in PLS-DA plots represent different cultivars: High resistant (HR: blue), Resistant (R: orange), Medium Susceptible (MS: yellow), Susceptible (S: green)

Model quality descriptors ( $R^2X$ ,  $R^2Y$  and  $Q^2$ ) are detailed in [Figure S1](#) along with the permutation tests. Adequate linear regression parameters and predictive capacity were obtained in almost every model with values associated of  $R^2Y \geq 0.7$  and  $Q^2 \geq 0.4$  [41]. Besides, the differences of  $R^2Y$  and  $Q^2$  values ranged between 0.2-0.3, which ensures that the models are not being overfitted. The PLS-DA model differentiating leaves of susceptible cultivars deviates somewhat these reference values, although the permutation test results underline the robustness of the model in all cases, as shown by the lower positioning of  $Q^2$  (blue) and  $R^2$  (green) points on the left compared to those on the right. Moreover, the regression line of the  $Q^2$  points intersected the vertical axis at zero or below, reiterating the results of the quality tests above mentioned. When analysing each olive organ individually, stems led to the best cross-validation values in both models. HR cultivars vs. the rest provided the best fitting model considering only 3PCs as optimal ( $R^2Y=0.803$ ;  $Q^2=0.677$ ) while for S cultivars vs. the rest, 5PCs were necessary to reach similar values ( $R^2Y=0.861$ ;  $Q^2=0.630$ ). Roots and leaves, although showing a slightly lower discriminatory efficiency, still exhibited acceptable performance.

Once the PLS-DA-based models were validated, the most influential features were selected taking into account the variable importance in the projection (VIP). Features with the highest relevance in these models (VIP above 1.50) have been highlighted as possible class markers and have been included in [Table 2](#), together with their associated retention time, calculated molecular formula, mass error (ppm), mSigma,  $TIMS_{CCS_{N_2}}$  value, and HRMS/MS fragmentation. In addition, the regression coefficient was also included in the table to indicate the relative abundance of each compound in these categories. Positive regression coefficients marked as '+' indicate a peak of higher intensity, while a negative correlation identified with a '-' indicates the opposite. Relevant compounds described above in olive matrices include the putative name in the table, as well as the reference to the relevant literature used for their characterisation. Other substances previously described in other plant species are mentioned in the discussion when the compound could match the observed one. Some additional markers were annotated in the table through searches in HRMS/MS library and utilising the MetFrag tool. The identification of other important features in the models, as is typical in untargeted studies, proved to be more challenging. This underscores the need for further investigations to propose reliable candidates and facilitate annotation as accurately as possible. Those markers without identity are numbered in order of appearance in [Table 2](#) to facilitate their recognition in the discussion. Compounds that may potentially be isomeric with others in the table are assigned with the same number for clarity.

Before going into detail on the contents of [Table 2](#), it is important to note that the distinctive compositional patterns of cultivars belonging to a particular category will always depend on a set of compounds and their relative concentrations, their possible metabolic pathways, etc. have to be considered, which increases the complexity of the matter.

**Table 2.** Metabolites from olive root, stem and leaf organs from VVO-highly resistant (HR) and susceptible (S) olive cultivars that exhibited the highest relevance in PLS-DA models (VIP  $\geq$  1.50)

Putative Compound Identity	Chemical Class <sup>Δ</sup>	RT (min)	<i>m/z</i> <sub>exp</sub>	Molecular Formula	Error (ppm)	mSigma	CCS (Å <sup>2</sup> )	Main fragments via MS/MS	R.C.	VIP	Ref.
<b>Olive roots of HR-cultivars</b>											
Unknown 1	-	12.75	277.1661	C <sub>13</sub> H <sub>26</sub> O <sub>6</sub>	1.62	48.4	180.3	233.1531	-	2.03	-
Sinapyl alcohol(8- 5)coniferyl aldehyde derivate	Lignans	6.95	337.1080	C <sub>20</sub> H <sub>18</sub> O <sub>5</sub>	-0.02	8.4	189.7	322.0871; 307.0617; 291.0652	-	1.95	[40]
Unknown 2 (potential isomer)	-	1.27	267.0722	C <sub>9</sub> H <sub>16</sub> O <sub>9</sub>	0.91	14.2	200.8	113.0222; 75.0088	-	1.93	-
Vanilloyl glucoside / Vanillic acid hexoside	Phenolic acids	1.28	329.0876	C <sub>14</sub> H <sub>18</sub> O <sub>9</sub>	-0.50	9.1	183.3	167.0357; 152.0107; 123.0450; 108.0218	-	1.86	[38,42]
Unknown 3	-	4.86	313.0929	C <sub>14</sub> H <sub>18</sub> O <sub>8</sub>	0.15	17.4	177.6	151.0406; 150.0333	-	1.82	-
Guaiaconic acid	Lignans	6.51	339.1238	C <sub>20</sub> H <sub>20</sub> O <sub>5</sub>	0.13	41.4	193.8	324.1001; 310.0779; 309.0770; 281.0840	-	1.75	CRW
Methyl gallate glucoside	Phenolic acids	1.35	345.0829	C <sub>14</sub> H <sub>18</sub> O <sub>10</sub>	0.41	43.6	172.7	-	-	1.70	[43]
Unknown 4	-	1.33	557.2084	C <sub>22</sub> H <sub>38</sub> O <sub>16</sub>	-0.46	13.1	223.3	389.1088; 375.1288; 213.0769	-	1.67	-
Unknown 2 (potential isomer)	-	1.27	267.0721	C <sub>9</sub> H <sub>16</sub> O <sub>9</sub>	-0.08	15.7	151.2	113.0230; 75.0080	-	1.67	-
<i>D</i> -Mannitol	Sugars	1.40	181.0719	C <sub>6</sub> H <sub>14</sub> O <sub>6</sub>	0.67	8.9	131.1	101.0257; 85.0307; 71.0145	-	1.55	[29]
Unknown 5	-	1.39	523.1878	C <sub>18</sub> H <sub>36</sub> O <sub>17</sub>	-0.24	11.0	207.2	341.1091	-	1.53	-
Lactone (ester with hydroxytyrosol)	Simple phenols	6.47	321.1342	C <sub>17</sub> H <sub>22</sub> O <sub>6</sub>	-0.24	19.1	168.2	185.0820; 111.0823; 59.0142	+	1.68	[44]
Unknown 6	-	7.37	465.2132	C <sub>24</sub> H <sub>34</sub> O <sub>9</sub>	0.39	28.3	208.9	-	+	1.63	-
<u>Elenolic acid dihexose derivate</u>	Secoiridoids	4.87	625.1986	C <sub>25</sub> H <sub>38</sub> O <sub>18</sub>	0.05	6.9	231.5	223.0601; 179.0564; 119.0353	+	1.61	[21]
Hydroxytyrosol glucoside derivative	Simple phenols	6.81	481.2078	C <sub>24</sub> H <sub>34</sub> O <sub>10</sub>	-0.35	23.5	209.5	315.1078; 135.0441; 101.0231	+	1.56	[31]
Unknown 7	-	1.30	237.0618	C <sub>8</sub> H <sub>14</sub> O <sub>8</sub>	0.66	16.3	144.8	87.0090	+	1.55	-
Unknown 8	-	1.31	279.0512	C <sub>13</sub> H <sub>12</sub> O <sub>7</sub>	0.55	24.4	151.3	207.0705; 189.0584; 115.0180	+	1.54	-
Unknown 9	-	6.97	569.2237	C <sub>27</sub> H <sub>38</sub> O <sub>13</sub>	0.13	11.0	214.6	537.1977; 403.1259; 223.0604; 121.0292	+	1.52	-
<b>Olive roots of S-cultivars</b>											
<u>Cyclooolivil glucoside (is. 3)</u>	Lignans	5.16	537.1975	C <sub>26</sub> H <sub>34</sub> O <sub>12</sub>	-0.27	21.0	214.5	375.1449; 195.0665; 179.0700	-	2.33	[21]
Unknown 10 (potential isomer)	-	1.30	207.0664	C <sub>11</sub> H <sub>12</sub> O <sub>4</sub>	-0.12	7.8	146.6	-	-	1.63	-
Unknown 10 (potential isomer)	-	1.30	207.0661	C <sub>11</sub> H <sub>12</sub> O <sub>4</sub>	-0.81	13.0	178.1	-	-	1.63	-
<i>D</i> -Sedoheptulose	Sugars	1.27	209.0667	C <sub>7</sub> H <sub>14</sub> O <sub>7</sub>	0.47	10.1	139.0	85.0294; 84.0211; 78.9592; 59.1249	-	1.93	[39]

Putative Compound Identity	Chemical Class <sup>Δ</sup>	RT (min)	m/z <sub>exp</sub>	Molecular Formula	Error (ppm)	mSigma	CCS (Å <sup>2</sup> )	Main fragments via MS/MS	R.C.	VIP	Ref.
<b>Olive roots of S-cultivars</b>											
Unknown 11	-	6.70	199.1340	C <sub>11</sub> H <sub>20</sub> O <sub>3</sub>	0.09	11.3	148.1	-	+	1.64	-
Vanilloyl glucoside / Vanillic acid hexoside	Phenolic acids	1.28	329.0876	C <sub>14</sub> H <sub>18</sub> O <sub>9</sub>	-0.50	9.1	183.3	167.0357; 152.0107; 123.0450; 108.0218	+	1.51	[38,42]
Maslinic acid monohydroxylated derivative	Pentacyclic triterpenes	11.22	487.3426	C <sub>30</sub> H <sub>48</sub> O <sub>5</sub>	-0.35	11.3	225.4	-	+	1.57	[30]
<u>Phenylethyl primeveroside</u>	Simple phenols	5.78	415.1609	C <sub>19</sub> H <sub>28</sub> O <sub>10</sub>	-0.12	4.6	202.2	149.0444	+	1.54	[30]
Unknown 2 (potential isomer)	-	1.27	267.0722	C <sub>9</sub> H <sub>16</sub> O <sub>9</sub>	0.91	14.2	200.8	113.0222; 75.0088	+	1.50	-
<b>Olive stems of HR-cultivars</b>											
Unknown 12	-	7.38	283.1187	C <sub>14</sub> H <sub>20</sub> O <sub>6</sub>	-0.01	13.9	166.3	199.0959; 181.0492; 139.0378; 123.0447; 99.0450; 83.0167	+	3.36	-
Elenolic acid-methyl ester	Secoiridoids	5.59	255.0875	C <sub>12</sub> H <sub>16</sub> O <sub>6</sub>	0.28	13.3	156.4	153.0572; 101.0242; 83.0139	+	3.28	[30]
Unknown 13	-	9.87	277.1804	C <sub>17</sub> H <sub>26</sub> O <sub>3</sub>	-0.72	26.5	171.6	233.1531; 205.1627; 59.0144	+	2.94	-
Hydroxydecarboxymethyl elenolic acid	Secoiridoids	1.40	199.0609	C <sub>9</sub> H <sub>12</sub> O <sub>5</sub>	-0.70	20.7	138.5	155.0710	+	2.23	[30]
Unknown 14	-	1.47	363.1659	C <sub>16</sub> H <sub>28</sub> O <sub>9</sub>	-0.46	31.5	177.2	181.0717	+	1.90	-
Unknown 15	-	1.33	353.0878	C <sub>16</sub> H <sub>18</sub> O <sub>9</sub>	0.09	19.3	185.8	191.0536; 111.0798	+	1.60	-
<u>Dihydroquercetin-O-glucoside (is. 1)</u>	Flavonoids	4.67	465.1036	C <sub>21</sub> H <sub>22</sub> O <sub>12</sub>	-0.54	12.9	191.8	303.0505; 285.0399; 177.0191; 125.0261	-	1.58	[45]
<u>Dihydrokaempferol</u>	Flavonoids	6.30	287.0560	C <sub>15</sub> H <sub>12</sub> O <sub>6</sub>	-0.30	2.9	163.4	259.0598; 243.0661; 177.0561; 151.0039; 125.0244	-	1.51	[30]
<b>Olive stems of S-cultivars</b>											
Sinapyl alcohol(8- 5)coniferyl aldehyde derivat	Lignans	6.95	337.1080	C <sub>20</sub> H <sub>18</sub> O <sub>5</sub>	-0.02	8.4	189.7	322.0871; 307.0617; 291.0652	+	2.67	[40]
Unknown 16	-	1.21	333.0623	C <sub>16</sub> H <sub>14</sub> O <sub>8</sub>	2.58	28.7	165.1	241.0129; 217.0518; 78.9594	+	1.58	-
Unknown 17 (potential isomer)	-	4.86	333.1555	C <sub>15</sub> H <sub>26</sub> O <sub>8</sub>	-0.78	13.1	175.9	-	+	1.51	-
<u>Hydroxypinoresinol glucoside (is. 1 and 2)</u>	Lignans	6.33	535.1822 535.1820	C <sub>26</sub> H <sub>32</sub> O <sub>12</sub>	0.25 -0.16	8.9 2.8	229.5 215.9	373.1290 373.1289; 355.1189; 295.0998	-	1.82 1.81	[21]
Unknown 18	-	7.39	315.1813	C <sub>16</sub> H <sub>28</sub> O <sub>6</sub>	-0.03	2.9	176.8	297.1695; 187.1334; 145.05076; 101.0605; 83.0506	-	1.66	-
<b>Olive leaves of HR-cultivars</b>											
Unknown19	-	1.39	395.1558	C <sub>16</sub> H <sub>28</sub> O <sub>11</sub>	-0.26	10.6	188.9	213.0771; 151.0765	+	2.19	-

Putative Compound Identity	Chemical Class <sup>Δ</sup>	RT (min)	m/z <sub>exp</sub>	Molecular Formula	Error (ppm)	mSigma	CCS (Å <sup>2</sup> )	Main fragments via MS/MS	R.C.	VIP	Ref.
<b>Olive leaves of HR-cultivars</b>											
<u>Loganic acid</u>	Iridoids	1.30	375.1296	C <sub>16</sub> H <sub>24</sub> O <sub>10</sub>	0.07	22.7	184.7	213.0764; 169.0876; 151.0752; 125.0606; 113.0244; 107.0499	+	2.13	[46]
Unknown 17 (potential isomer)	-	5.73	333.1553	C <sub>15</sub> H <sub>26</sub> O <sub>8</sub>	-0.45	20.4	175.1	-	+	1.65	-
Unknown 20 (potential isomer)	-	1.33	349.1502	C <sub>15</sub> H <sub>26</sub> O <sub>9</sub>	-0.69	38.7	217.7	-	+	1.60	-
Trihydroxyoctadecadienoic acid	Fatty acids	7.76	327.2178	C <sub>18</sub> H <sub>32</sub> O <sub>5</sub>	0.13	18.7	182.3	291.1971; 229.1439; 211.1338; 171.1006	+	1.54	[30]
Unknown 15	-	1.33	353.0876	C <sub>16</sub> H <sub>18</sub> O <sub>9</sub>	-0.45	20.6	185.9	191.0536; 111.0798	+	1.50	-
Dihydroxyhexadecanoic acid	Fatty acids	8.69	287.2228	C <sub>16</sub> H <sub>32</sub> O <sub>4</sub>	-0.06	17.0	170.3	-	-	1.50	[30]
<b>Olive leaves of S-cultivars</b>											
1-Sinapoyl-2-feruloylgentiobiose	Phenolic acids	6.36	361.1041 [M-H-H] <sup>2-</sup>	C <sub>33</sub> H <sub>40</sub> O <sub>18</sub>	1.94	4.9	263.1	-	+	2.22	[47]
Unknown 21	-	7.98	481.1361 [M-H-H] <sup>2-</sup> ;	C <sub>44</sub> H <sub>52</sub> O <sub>24</sub>	1.78	50.0	348.4	-	+	1.80	-
<u>Naringenin</u>	Flavonoids	7.77	271.0613	C <sub>15</sub> H <sub>12</sub> O <sub>5</sub>	0.35	1.6	163.0	151.0028; 119.0500	+	1.78	[48]
Dihydroxyhexadecanoic acid	Fatty acids	8.69	287.2228	C <sub>16</sub> H <sub>32</sub> O <sub>4</sub>	-0.06	17.0	170.3	-	+	1.69	[30]
<u>Luteolin-O-glucoside (is. 2)</u>	Flavonoids	6.85	447.0931	C <sub>21</sub> H <sub>20</sub> O <sub>11</sub>	-0.45	8.3	208.4	285.0405; 133.0297	+	1.67	[46]
Unknown 11	-	6.70	199.1340	C <sub>11</sub> H <sub>20</sub> O <sub>3</sub>	0.09	11.3	148.1	-	+	1.60	-
Unknown 20 (potential isomer)	-	1.30	349.1502	C <sub>15</sub> H <sub>26</sub> O <sub>9</sub>	-0.57	18.7	178.7	-	+	1.55	-
Coumaroyl hexoside	Phenolic acids	4.95	325.0928	C <sub>15</sub> H <sub>18</sub> O <sub>8</sub>	-0.24	14.0	180.7	145.0292; 119.0485; 117.0340	+	1.54	CRW
<u>Apigenin 7-O-glucoside</u>	Flavonoids	6.73	431.0984	C <sub>21</sub> H <sub>20</sub> O <sub>10</sub>	-0.03	10.5	208.1	269.0459	+	1.53	[48]
<u>Aldehydic form of decarboxymethyl elenolic acid glucoside (is. 1)</u>	Secoiridoids	1.27	377.1452	C <sub>16</sub> H <sub>26</sub> O <sub>10</sub>	-0.15	8.6	188.8	197.0821; 153.0921	+	1.53	[40]
<u>Apigenin</u>	Flavonoids	8.80	269.0456	C <sub>15</sub> H <sub>10</sub> O <sub>5</sub>	0.04	6.5	157.6	225.0554; 201.0547; 149.0238	+	1.51	[48]
<u>Hydroxytyrosol glucoside (is. 1)</u>	Simple phenols	4.33	315.1084	C <sub>14</sub> H <sub>20</sub> O <sub>8</sub>	-0.31	6.4	163.1	153.0559; 135.0451; 123.0459	+	1.50	[40]
Trihydroxyoctadecanoic acid	Fatty acids	8.41	331.2488	C <sub>18</sub> H <sub>36</sub> O <sub>5</sub>	-0.37	17.0	180.3	157.1272	-	1.65	[30]
Octadecanedioic acid	Fatty acids	9.86	313.2383	C <sub>18</sub> H <sub>34</sub> O <sub>4</sub>	-0.32	12.2	180.4	295.2291; 277.2165	-	1.62	[49]
<u>Maslinic acid</u>	Pentacyclic triterpenes	13.13	471.3479	C <sub>30</sub> H <sub>48</sub> O <sub>4</sub>	-0.30	12.7	223.4	-	-	1.57	[30]
Trihydroxyoctadecadienoic acid	Fatty acids	7.76	327.2178	C <sub>18</sub> H <sub>32</sub> O <sub>5</sub>	0.13	18.7	182.3	291.1971; 229.1439; 211.1338; 171.1006	-	1.56	[30]

<sup>Δ</sup>Including glycosylated forms and derivatives within these chemical classes; R.C: regression coefficient, ((sign "+"): high intensity peak, (sign "-"): low intensity peak); CRW: CompoundCrawler; Underlined compounds indicate their previous identification in the initial screening (section 3.1.).

In the model developed to discriminate the **root extracts** of the **HR-cultivars** from the rest, 18 compounds were found to have significance (VIP above 1.50), with 11 of them having negative correlation coefficients (i.e. exhibiting relatively low concentrations in the HR-cultivars). Among the negatively correlated metabolites, the compound eluting at 6.95 min with a predominant MS signal with  $m/z$  of 337.1080 was tentatively identified as a sinapyl alcohol(8-5)coniferyl aldehyde derivate ( $-H_2O$ ,  $-CH_2O$ ), taking the previous results of Contreras *et al.* into account [40]. The following compounds were also negatively correlated in the models for olive root extracts with HR cultivars: vanilloyl glucoside/vanillic acid hexoside, methyl gallate glucoside and *D*-mannitol, which were identified on the basis of previously published reports. Also, guaiaconic acid (3,4-dimethyl-2,5-bis(4-hydroxy-3-methoxyphenyl)furan) which was identified through the use of HRMS/MS spectral libraries. Its molecular structure and the result of MetFrag assignments to the fragments are shown in [Figure S2](#).

Possible tentative identities could not be suggested for unknown 1 at 277.1661  $m/z$  ( $C_{13}H_{26}O_6$ ). The metabolites referred to as unknown 2 ( $C_9H_{16}O_9$ ), were classified as potential isomers due to their different  $TIM^S CCS_{N_2}$  value (200.8Å and 151.2Å, respectively). Considering that they eluted at the beginning of the chromatogram (1.27 min), these metabolites could be some kind of sugar derivatives, such as 3-deoxy-*D*-glycero-*D*-galacto-2-nonulosonic acid, found in roots of transgenic tobacco plants or hexosylglycerate, reported in soybean root nodules [50,51]. To the best of our knowledge, these compounds have not been previously identified in any olive matrix and further attempts should be made to corroborate these hypotheses. The unknown 3 at 313.0929  $m/z$  ( $C_{14}H_{18}O_8$ ) could be vanillin hexoside/vanilloside or *p*-hydroxyphenylacetic acid-*O*-hexoside, taking into account its fragmentation pattern. This hypothesis would be supported by the fact that both aglycones, vanillin and *p*-hydroxyphenylacetic acid, have been found in olive extracts according to the literature [29,30,38,52], which could reinforce the presence of their glycosylated forms in the investigated organs. In fact, both glycosylated metabolites mentioned above have been previously described in other plant species, but so far not in olive matrices [53,54]. Unknown 4, with MS signals at 557.2084  $m/z$  ( $C_{22}H_{38}O_{16}$ ) showed fragments comparable to loganic acid/loganin, suggesting that it could be a derivative. Unknown 5 at 523.1878  $m/z$  ( $C_{18}H_{36}O_{17}$ ), which was also found to be a relevant compound in this category, could not be annotated. Among the positively correlated compounds, significant metabolites identified included a lactone (hydroxytyrosol ester), a dihexose derivative of elenolic acid and a glucoside derivative of hydroxytyrosol. In addition, a compound characterised by the predicted molecular formula  $C_8H_{14}O_8$  (unknown 7) could be tentatively identified as a sugar derivative, as 3-deoxy-*D*-manno-octulosonate, based on its retention time and predicted CCS value. This identification should be conclusively confirmed. The molecular formula of three other metabolites of remarkable significance were established, with  $m/z$  values of 465.2132 (unknown 6;  $C_{24}H_{34}O_9$ ), 279.0512 (unknown 8;  $C_{13}H_{12}O_7$ ) and 569.2237 (unknown 9;  $C_{27}H_{38}O_{13}$ ). However, these substances could not be assigned specific names at this stage.

Regarding **susceptible cultivars (olive roots of S cultivars)**, and paying attention first to the annotated compounds, a negative correlation was found for the isomer 3 of the cycloolivil glycoside ( $C_{26}H_{34}O_{12}$ ;  $214.5 \text{ \AA}^2$ ). This finding is consistent with that previously observed by Serrano-García and co-authors, who also found a correlation between the root content of isomer 2 of the cycloolivil glycoside and susceptibility to *V. dahliae* [22]. Despite the different isomer designation, we are certainly referring to the same compound, as the isomer 3 within the current work involves chromatographic separation of isomer 1, while isomer 2 co-elutes with the initial peak. This may explain why the same isomers were not detected by the aforementioned authors using only LC-MS (without the mobility dimension). Another significant compound was *D*-sedoheptulose. Two possible isomeric metabolites named as unknown 10 ( $C_{11}H_{12}O_4$ ;  $146.6 \text{ \AA}^2$  and  $178.1 \text{ \AA}^2$ ) also showed considerable VIP values (negative correlation). In contrast, vanilloyl glucoside/vanillic acid hexoside, a maslinic acid monohydroxylated derivative, phenylethyl primeveroside and unknowns 2 ( $200.8 \text{ \AA}^2$ ) and 11 showed positive correlation with root extracts of susceptible olive cultivars. Unknown 11 ( $C_{11}H_{20}O_3$ ;  $148.1 \text{ \AA}^2$ ) could be a fatty acid derivative such as 9-hydroxy-10-undecenoic acid, considering its ionisation in MS, the limited *in-source* fragmentation and the predicted CCS value of this molecule. An interesting finding was that vanilloyl glucoside/vanillic acid hexoside and an isomer of unknown 2 ( $200.8 \text{ \AA}^2$ ) were significant at both extreme levels of resistance, underlining their paramount importance in roots for predicting, to some extent, resistance/susceptibility to VWO. According to these results, a higher presence/concentration of certain secoiridoid derivatives in olive roots together with a low content of lignan derivatives could be characteristic of highly resistant cultivars. This general statement was partially suggested by Cardoni and co-authors in a previous work [21].

Eight compounds were identified as the most influential in the model built to discriminate between **HR-cultivars** and the rest based on **stem extracts**. Thus, HR-cultivars correlated positively with elenolic acid-methyl ester, hydroxydecarboxymethyl elenolic acid and four unidentified compounds at  $283.1187 \text{ m/z}$  (unknown 12;  $C_{14}H_{20}O_6$ ),  $277.1804 \text{ m/z}$  (unknown 13;  $C_{17}H_{26}O_3$ ),  $363.1659 \text{ m/z}$  (unknown 14;  $C_{16}H_{28}O_9$ ) and  $353.0878 \text{ m/z}$  (unknown 15;  $C_{16}H_{18}O_9$ ). In contrast, an isomer of dihydroquercetin-*O*-glucoside (is.1) and dihydrokaempferol correlated negatively in this category.

Relatively high concentrations of sinapyl alcohol(8-5)coniferyl aldehyde derivate, unknown 16 ( $C_{16}H_{14}O_8$ ;  $165.1 \text{ \AA}^2$ ) and unknown 17 ( $C_{15}H_{26}O_8$ ; 4.86 min and  $175.9 \text{ \AA}^2$ ), together with low quantities of hydroxypinoresinol glucoside (is. 1 and 2) and unknown 18 ( $C_{16}H_{28}O_6$ ;  $176.8 \text{ \AA}^2$ ) characterised the stem extracts of the **susceptible cultivars (olive stems of S-cultivars)**. Interestingly, as mentioned above, the lignan derivative sinapyl alcohol(8-5)coniferyl aldehyde was also relevant for its low content in the root extracts of the HR-cultivars, highlighting the close relationship of this lignan derivative to VWO resistance/susceptibility. In summary, the distinctive compositional pattern defined for stems of highly resistant cultivars would include high levels of two elenolic acid derivatives together with low amounts of the flavonoids dihydroquercetin-*O*-glucoside (is.1) and

dihydrokaempferol. In contrast, the composition of the stems of susceptible cultivars would be marked by the concentration levels of the sinapyl alcohol(8-5)conferyl aldehyde derivative and the 2 isomers of hydroxy-pinoinosinol glucoside.

When using **olive leaf extracts**, seven compounds were found to have the highest discriminant power in the models separating **HR-cultivars** from the rest of the cultivars, while 16 possible markers were pointed out to characterise the **S-cultivars**. The compositional pattern of HR-cultivars was characterised by relative high concentrations of loganic acid, trihydroxyoctadecadienoic acid, unknown 19 ( $C_{16}H_{28}O_{11}$ ; 1.39 min and 188.9  $\text{\AA}^2$ ), unknown 17 ( $C_{15}H_{26}O_8$ ; 5.73 min and 175.1  $\text{\AA}^2$ ), unknown 20 ( $C_{15}H_{26}O_9$ ; 1.33 min and 217.7  $\text{\AA}^2$ ), and unknown 15 ( $C_{16}H_{18}O_9$ ; 1.33 min and 185.9  $\text{\AA}^2$ ) together with low amounts of the fatty acid dihydroxyhexadecanoic acid. The unknown 20 with 349.1502  $m/z$  had previously been documented in the metabolic profile of olive pomace, although the authors were also unable to assign an identity to it [55]. The same occurred with unknown 17 which had been previously detected in the profiles of olive leaf but also remained as unidentified [52]. It is worth noting that the unknown 17 detected in the leaves could be an isomer of a marker identified in the stems of the **S-varieties**, since they differ only in the retention time (4.86 min in the stems and 5.73 min in the leaf extracts).

Among the 16 compounds identified as potential markers to define the distinctive compositional characteristics of the **S-cultivars**, 12 were positively correlated and the rest negatively correlated. Within the positive correlated biomarkers, the compound with molecular formula  $C_{33}H_{40}O_{18}$  was identified as a phenolic acid derivate named 1-sinapoyl-2-feruloylgentiobiose bearing in mind the information reported by Alcántara and co-authors for olive leaf tissue as well [47]. Coumaroyl hexoside identified through HRMS/MS library (see [Figure S2](#)), naringenin, dihydroxyhexadecanoic acid, luteolin-*O*-glucoside (is. 2), apigenin 7-*O*-glucoside, aldehydic form of decarboxymethyl elenolic acid glucoside (is. 1), apigenin and hydroxytyrosol glucoside (is. 1) were also relevant and exhibited positive correlations; as well as a potential isomer of unknown 20, unknown 21 and unknown 11. Unknown 21 ( $C_{44}H_{52}O_{24}$ ; 7.98 min and 348.4  $\text{\AA}^2$ ) could correspond to the anthocyanidin glycoside known as peonidin-3-feruloyl sophoroside-5-glucoside; however, its identity could not be confirmed since this compound has not been previously described in extracts from olive tree tissues. The unknown compound 11 ( $C_{11}H_{20}O_3$ ), previously suggested to be a fatty acid, acted as a marker due to its higher contents in the leaves of susceptible cultivars. The same observation was noted in the root organ, highlighting the importance of this compound in the basal metabolic profile of olive cultivars.

In contrast, trihydroxyoctadecanoic acid, octadecanedioic acid, trihydroxyoctadecadienoic acid, and maslinic acid were negatively correlated for the **S-cultivar** extracts. Serrano-Garcia and colleagues reported some similarities in a previous work [22]. They also noted the potential of hydroxytyrosol glucoside, aldehydic form of decarboxymethyl elenolic acid-glucoside and maslinic acid as markers to classify olive leaves according to VWO resistance/susceptibility. However, some discrepancies were observed about the correlation of maslinic acid and the aldehydic form of

decarboxymethyl elenolic acid-glucoside in this aerial part of the olive tree. Another notable role was played by the unknown 20 ( $C_{15}H_{26}O_9$ ), as one of its isomers was a marker for HR-cultivars and another for S-cultivars. Moreover, dihydroxyhexadecanoic and trihydroxyoctadecadienoic acids were identified as markers in both resistance categories, making them compelling compounds for evaluation in the basal metabolic profiles of olive leaves. In view of the results obtained for the leaves, it can be affirmed that the precise determination of flavonoids and fatty acids would be of crucial importance to distinguish olive cultivars according to their resistance to VWO.

In conclusion, this work provides an in-depth qualitative analysis of the metabolome of olive root, stem and leaf samples using a UHPLC-ESI-TimsTOF MS/MS platform. Of particular importance is the innovative  $TIMS_{CCS_{N_2}}$  database, which covers more than 70 metabolites distributed in different organs of the olive plant. This database increases confidence in the identification of metabolites for future studies. Importantly, the integration of the ion mobility dimension has enabled the detection and resolution of numerous isomeric species hidden within these matrices. This advance not only improves our understanding of the complex chemical composition of olive, but also establishes a solid basis for future research in plant metabolomics. To corroborate the identification of CCS achieved in this study, further targeted metabolomics studies are essential, using other pure standards and incorporating this fourth dimension together with LC-HRMS.

Furthermore, this comprehensive study, using a non-targeted approach to roots, stems and leaves of 43 different olive cultivars, may represent a significant achievement for the advancement of olive breeding programmes. The construction of PLS-DA models allowed the identification of key markers positively and negatively correlated with HR-cultivars and S-cultivars. In particular, stem extracts showed the highest power to categorise the resistance response. In roots, a high concentration of certain secoiridoid derivatives together with a low content of lignan derivatives could be characteristic of highly resistant cultivars. Besides, the distinctive compositional pattern defined for the stems of highly resistant cultivars would include high levels of two elenolic acid derivatives together with low amounts of the flavonoids dihydroquercetin-O-glucoside (is.1) and dihydrokaempferol. It can also be stated that the precise determination of flavonoids and fatty acids in leaf extracts would be of crucial importance to distinguish olive cultivars according to their resistance to VWO.

These findings offer valuable insights into the fundamental metabolic complexities linked to resistance against VWO. The integration of non-targeted metabolomics and chemometrics represent a powerful tool to unravel the chemical profiles of olive cultivars showing different levels of resistance/susceptibility to *V. dahliae* infection. Defining characteristic metabolic patterns of certain olive organs in relation to their resistance/susceptibility to VWO not only increases our understanding of the molecular mechanisms underlying basal resistance, but also serves as a foundation for fine-tuning breeding strategies and enhances our knowledge on olive plant resistance.

**Funding:** This research received funding from FEDER/Junta de Andalucía-Consejería de Transformación Económica, Industria, Conocimiento y Universidades (Proyecto P20\_00263), FEDER/Junta de Andalucía-Consejería de Economía y Conocimiento (Proyecto B-AGR-416-UGR18) and FEDER/Junta de Andalucía-IFAPA (grant number AVA23.INV2023.016). Additional support was provided by the grant RYC2021-032996-I funded by MCIN/AEI/10.13039/501100011033 and by “European Union NextGenerationEU/PRTR” (L.O-G), and the grant FPU19/00700 from the Ministerio de Ciencia, Innovación y Universidades (I.S-G).

## References

1. Liphshitz, N.; Gophna, R.; Hartman, M.; Biger, G. The Beginning of Olive (*Olea Europaea*) Cultivation in the Old World: A Reassessment. *J. Archaeol. Sci.* **1991**, *18*, 441–453, doi:10.1016/0305-4403(91)90037-P.
2. FAO Statistics Division of Food and Agriculture Organization of the United Nations (FAOSTAT). Available online: <https://www.fao.org/faostat/en/#data> (accessed on 7 March 2024).
3. Rallo, L.; Barranco, D.; Castro-García, S.; Connor, D.J.; del Campo, M.G.; Rallo, P. Chapter 7. High-Density Olive Plantations. In *Horticultural Reviews*, Janick, J., Ed.; Wiley-Blackwell, 2013, Vol. 41, 303–383, doi:10.1002/9781118707418.ch07.
4. Tous, J. Olive Production Systems and Mechanization. *Acta Hort.* **2011**, *924*, 169–184, doi:10.17660/ActaHortic.2011.924.22.
5. López-Escudero, F.J.; Blanco-López, M.A. Effects of Drip Irrigation on Population of *Verticillium Dahliae* in Olive Orchards. *Phytopathology* **2005**, *153*, 238–239, doi:10.1111/j.1439-0434.2005.00961.x.
6. Rodríguez-Jurado, D.; Bejarano-Alcázar, J. Dispersión de “*Verticillium Dahliae*” En El Agua Utilizada Para El Riego de Olivares En Andalucía. *Boletín Sanid. Veg. Plagas* **2007**, *33*, 547–562.
7. Trapero, C.; López Escudero, F.J.; Roca, L.F.; Blanco López, M.A.; Trapero, A. Agricultura. Nutrición y Sanidad Vegetal. 2011, pp. 106–110.
8. Keykhasaber, M.; Thomma, B.P.H.J.; Hiemstra, J.A. *Verticillium Wilt* Caused by *Verticillium Dahliae* in Woody Plants with Emphasis on Olive and Shade Trees. *Eur. J. Plant Pathol.* **2018**, *150*, 21–37, doi:10.1007/s10658-017-1273-y.
9. López-Escudero, F.J.; Mercado-Blanco, J. *Verticillium Wilt* of Olive: A Case Study to Implement an Integrated Strategy to Control a Soil-Borne Pathogen. *Plant Soil* **2011**, *344*, 1–50, doi:10.1007/s11104-010-0629-2.
10. Jiménez-Díaz, R.M.; Cirulli, M.; Bubici, G.; Jiménez-Gasco, M. del M.; Antoniou, P.P.; Tjamos, E.C. *Verticillium Wilt*, A Major Threat to Olive Production: Current Status and Future Prospects for Its Management. *Am. Phytopathol. Soc. Plant Dis.* **2012**, *96*, 304–329, doi:10.1094/PDIS-06-11-0496.
11. Arias-Calderón, R.; Rodríguez-Jurado, D.; León, L.; Bejarano-Alcázar, J.; De la Rosa, R.; Belaj, A. Pre-Breeding for Resistance to *Verticillium Wilt* in Olive: Fishing in the Wild Relative Gene Pool. *Crop Prot.* **2015**, *75*, 25–33, doi:10.1016/j.cropro.2015.05.006.
12. Serrano, A.; Rodríguez-Jurado, D.; Ramírez-Tejero, J.A.; Luque, F.; López-Escudero, F.J.; Belaj, A.; Román, B.; León, L. Response to *Verticillium Dahliae* Infection in a Genetically Diverse Set of Olive Cultivars. *Sci. Hort.* **2023**, *316*, 112008, doi:10.1016/j.scienta.2023.112008.
13. Martos-Moreno, C.; López-Escudero, F.J.; Blanco-López, M.Á. Resistance of Olive Cultivars to the Defoliating Pathotype of *Verticillium Dahliae*. *HortScience* **2006**, *41*, 1313–1316, doi:10.21273/hortsci.41.5.1313.

14. Trapero, C.; Rallo, L.; López-Escudero, F.J.; Barranco, D.; Díez, C.M. Variability and Selection of Verticillium Wilt Resistant Genotypes in Cultivated Olive and in the Olea Genus. *Plant Pathol.* **2015**, *64*, 890–900, doi:10.1111/ppa.12330.
15. Castro-Moretti, F.R.; Gentzel, I.N.; Mackey, D.; Alonso, A.P. Metabolomics as an Emerging Tool for the Study of Plant–Pathogen Interactions. *Metabolites* **2020**, *10*, 52, doi:10.3390/metabo10020052.
16. Markakis, E.A.; Tjamos, S.E.; Antoniou, P.P.; Roussos, P.A.; Paplomatas, E.J.; Tjamos, E.C. Phenolic Responses of Resistant and Susceptible Olive Cultivars Induced by Defoliating and Nondefoliating Verticillium Dahliae Pathotypes. *Plant Dis.* **2010**, *94*, 1156–1162, doi:10.1094/PDIS-94-9-1156.
17. Báidez, A.G.; Gómez, P.; Del Río, J.A.; Ortuño, A. Dysfunctionality of the Xylem in Olea Europaea L. Plants Associated with the Infection Process by Verticillium Dahliae Kleb. Role of Phenolic Compounds in Plant Defense Mechanism. *J. Agric. Food Chem.* **2007**, *55*, 3373–3377, doi:10.1021/jf063166d.
18. Gharbi, Y.; Barkallah, M.; Bouazizi, E.; Hibar, K.; Gdoura, R.; Triki, M.A. Lignification, Phenols Accumulation, Induction of PR Proteins and Antioxidant-Related Enzymes Are Key Factors in the Resistance of Olea Europaea to Verticillium Wilt of Olive. *Acta Physiol. Plant.* **2017**, *39*, 43, doi:10.1007/s11738-016-2343-z.
19. Bruno, G.L.; Sermani, S.; Triozzi, M.; Tommasi, F. Physiological Response of Two Olive Cultivars to Secondary Metabolites of Verticillium Dahliae Kleb. *Plant Physiol. Biochem.* **2020**, *151*, 292–298, doi:10.1016/j.plaphy.2020.03.029.
20. Drais, M.I.; Pannucci, E.; Caracciolo, R.; Bernini, R.; Romani, A.; Santi, L.; Varvaro, L. Antifungal Activity of Hydroxytyrosol Enriched Extracts from Olive Mill Waste against Verticillium Dahliae, the Cause of Verticillium Wilt of Olive. *Pytopathologia Mediterr.* **2021**, *60*, 139–147, doi:10.36253/phyto-12019.
21. Cardoni, M.; Olmo-García, L.; Serrano-García, I.; Carrasco-Pancorbo, A.; Mercado-Blanco, J. The Roots of Olive Cultivars Differing in Tolerance to Verticillium Dahliae Show Quantitative Differences in Phenolic and Triterpenic Profiles. *J. Plant Interact.* **2023**, *18*, 1–14 doi:10.1080/17429145.2023.2206840.
22. Serrano-García, I.; Olmo-García, L.; Monago-Maraña, O.; Muñoz Cabello de Alba, I.; León, L.; de la Rosa, R.; Serrano, A.; Gómez-Caravaca, A.M.; Carrasco-Pancorbo, A. Characterization of the Metabolic Profile of Olive Tissues ( Roots , Stems and Leaves ): Relationship with Cultivars ' Resistance / Susceptibility to the Soil Fungus Verticillium Dahliae. *Antioxidants* **2023**, *12*, 2120, doi:10.3390/antiox12122120.
23. Jililat, A.; Ragone, R.; Gualano, S.; Santoro, F.; Gallo, V.; Varvaro, L.; Mastroilli, P.; Saponari, M.; Nigro, F.; D'Onghia, A.M. A Non-Targeted Metabolomics Study on Xylella Fastidiosa Infected Olive Plants Grown under Controlled Conditions. *Sci. Rep.* **2021**, *11*, 1070, doi:10.1038/s41598-020-80090-x.
24. Khizar, M.; Shi, J.; Saleem, S.; Liaquat, F.; Ashraf, M.; Latif, S.; Haroon, U.; Hassan, S.W.; Rehman, S. ur; Chaudhary, H.J.; et al. Resistance Associated Metabolite Profiling of Aspergillus Leaf Spot in Cotton through Non-Targeted Metabolomics. *PLoS One* **2020**, *15*, e0228675, doi:10.1371/journal.pone.0228675.
25. Cho, K.; Kim, Y.; Wi, S.J.; Seo, J.B.; Kwon, J.; Chung, J.H.; Park, K.Y.; Nam, M.H. Nontargeted Metabolite Pro Fi Ling in Compatible Pathogen- Inoculated Tobacco ( Nicotiana Tabacum L. Cv. Wisconsin 38) Using UPLC-Q-TOF/MS. *J. Agric. Food Chem.* **2012**, *60*, 11015–11028, doi:10.1021/jf303702j.
26. Hernández-Mesa, M.; Ropartz, D.; García-Campaña, A.M.; Rogniaux, H.; Dervilly-Pinel, G.; Le Bizec, B. Ion Mobility Spectrometry in Food Analysis: Principles, Current Applications and Future Trends. *Molecules* **2019**, *24*, 1–28, doi:10.3390/molecules24152706.
27. Mairinger, T.; Causon, T.J.; Hann, S. The Potential of Ion Mobility–Mass Spectrometry for Non-Targeted Metabolomics. *Curr. Opin. Chem. Biol.* **2018**, *42*, 9–15, doi:10.1016/j.cbpa.2017.10.015.
28. Belaj, A.; Ninot, A.; Gómez-Gálvez, F.J.; El Riachy, M.; Gurbuz-Veral, M.; Torres, M.; Lazaj, A.; Klepo, T.; Paz, S.; Ugarte, J.; et al. Utility of EST-SNP Markers for Improving Management and Use of Olive Genetic Resources: A Case Study at the Worldwide Olive Germplasm Bank of Córdoba. *Plants* **2022**,

- 17, 921, doi:10.3390/plants11070921.
29. Ammar, S.; Contreras, M. del M.; Gargouri, B.; Segura-Carretero, A.; Bouaziz, M. RP-HPLC-DAD-ESI-QTOF-MS Based Metabolic Profiling of the Potential *Olea Europaea* by-Product “Wood” and Its Comparison with Leaf Counterpart. *Phytochem. Anal.* **2017**, *28*, 217–229, doi:10.1002/pca.2664.
  30. Olmo-García, L.; Kessler, N.; Neuweger, H.; Wendt, K.; Olmo-Peinado, J.M.; Fernández-Gutiérrez, A.; Baessmann, C.; Carrasco-Pancorbo, A. Unravelling the Distribution of Secondary Metabolites in *Olea Europaea* L.: Exhaustive Characterization of Eight Olive-Tree Derived Matrices by Complementary Platforms (LC-ESI/APCI-MS and GC-APCI-MS). *Molecules* **2018**, *23*, 2419, doi:10.3390/molecules23102419.
  31. Michel, T.; Khlif, I.; Kanakis, P.; Termentzi, A.; Allouche, N.; Halabalaki, M.; Skaltsounis, A.L. UHPLC-DAD-FLD and UHPLC-HRMS/MS Based Metabolic Profiling and Characterization of Different *Olea Europaea* Organs of Koroneiki and Chetoui Varieties. *Phytochem. Lett.* **2015**, *11*, 424–439, doi:10.1016/j.phytol.2014.12.020.
  32. Schroeder, M.; Meyer, S.W.; Heyman, H.M.; Barsch, A.; Sumner, L.W. Generation of a Collision Cross Section Library for Multi-Dimensional Plant Metabolomics Using UHPLC-Trapped Ion Mobility-MS/MS. *Metabolites* **2020**, *10*, 13, doi:10.3390/metabo10010013.
  33. Drakopoulou, S.K.; Damalas, D.E.; Baessmann, C.; Thomaidis, N.S. Trapped Ion Mobility Incorporated in LC-HRMS Workflows as an Integral Analytical Platform of High Sensitivity: Targeted and Untargeted 4D-Metabolomics in Extra Virgin Olive Oil. *J. Agric. Food Chem.* **2021**, *69*, 15728–15737, doi:10.1021/acs.jafc.1c04789.
  34. Drakopoulou, S.K.; Kritikou, A.S.; Baessmann, C.; Thomaidis, N.S. Untargeted 4D-Metabolomics Using Trapped Ion Mobility Combined with LC-HRMS in Extra Virgin Olive Oil Adulteration Study with Lower-Quality Olive Oils. *Food Chem.* **2024**, *434*, 137410, doi:10.1016/j.foodchem.2023.137410.
  35. Toumi, K.; Świątek, Ł.; Boguszewska, A.; Skalicka-Woźniak, K.; Bouaziz, M. Comprehensive Metabolite Profiling of Chemlali Olive Tree Root Extracts Using LC-ESI-QTOF-MS/MS, Their Cytotoxicity, and Antiviral Assessment. *Molecules* **2023**, *28*, 4829, doi:10.3390/molecules28124829.
  36. Zhang, C.; Zhang, J.; Xin, X.; Zhu, S.; Niu, E.; Wu, Q.; Li, T.; Liu, D. Changes in Phytochemical Profiles and Biological Activity of Olive Leaves Treated by Two Drying Methods. *Front. Nutr.* **2022**, *9*, doi:10.3389/fnut.2022.854680.
  37. Cittan, M.; Çelik, A. Development and Validation of an Analytical Methodology Based on Liquid Chromatography–Electrospray Tandem Mass Spectrometry for the Simultaneous Determination of Phenolic Compounds in Olive Leaf Extract. *J. Chromatogr. Sci.* **2018**, *56*, 336–343, doi:10.1093/chromsci/bmy003.
  38. Abbattista, R.; Ventura, G.; Calvano, C.D.; Cataldi, T.R.I.; Losito, I. Bioactive Compounds in Waste By-Products from Olive Oil Production: Applications and Structural Characterization by Mass Spectrometry Techniques. *Foods* **2021**, *10*, 1236, doi:10.3390/foods10061236.
  39. Romero-Márquez, J.M.; Navarro-Hortal, M.D.; Forbes-Hernández, T.Y.; Varela-López, A.; Puentes, J.G.; Pino-García, R. Del; Sánchez-González, C.; Elio, I.; Battino, M.; García, R.; et al. Exploring the Antioxidant, Neuroprotective, and Anti-Inflammatory Potential of Olive Leaf Extracts from Spain, Portugal, Greece, and Italy. *Antioxidants* **2023**, *12*, 1538, doi:10.3390/antiox12081538.
  40. Contreras, M. del M.; Gomez-Cruz, I.; Romero, I.; Castro, E. Olive Pomace-Derived Biomasses Fractionation through a Chemical Characteristics. *Foods* **2021**, *10*, 111, doi:10.3390/foods10010111.
  41. Godzien, J.; Ciborowski, M.; Angulo, S.; Barbas, C. From Numbers to a Biological Sense: How the Strategy Chosen for Metabolomics Data Treatment May Affect Final Results. A Practical Example Based on Urine Fingerprints Obtained by LC-MS. *Electrophoresis* **2013**, *34*, 2812–2826, doi:10.1002/elps.201300053.
  42. Sánchez-Lucas, R. The Effect of Increasing Temperature on Olive Trees (*Olea Europaea* L. Subsp.

- Europaea) Biology: An Integrated Morphological, Phenological and Biomolecular Study, University of Córdoba, Córdoba, Spain, 2019.
43. Cádiz-Gurrea, M. de la L.; Pinto, D.; Delerue-Matos, C.; Rodrigues, F. Olive Fruit and Leaf Wastes as Bioactive Ingredients for Cosmetics—A Preliminary Study. *Antioxidants* **2021**, *10*, 245, doi:10.3390/antiox10020245.
  44. Kanakis, P.; Termentzi, A.; Michel, T.; Gikas, E.; Halabalaki, M.; Skaltsounis, A.L. From Olive Drupes to Olive Oil An HPLC-Orbitrap-Based Qualitative and Quantitative Exploration of Olive Key Metabolites. *Planta Med.* **2013**, *79*, 1576–1587, doi:10.1055/s-0033-1350823.
  45. Vergine, M.; Pavan, S.; Negro, C.; Nicoli, F.; Greco, D.; Sabella, E.; Aprile, A.; Ricciardi, L.; De Bellis, L.; Luvisi, A. Phenolic Characterization of Olive Genotypes Potentially Resistant to Xylella. *J. Plant Interact.* **2022**, *17*, 462–474, doi:10.1080/17429145.2022.2049381.
  46. Ammar, S.; Contreras, M. del M.; Gargouri, B.; Segura-Carretero, A.; Bouaziz, M. RP-HPLC-DAD-ESI-QTOF-MS Based Metabolic Profiling of the Potential Olea Europaea by-Product “Wood” and Its Comparison with Leaf Counterpart. *Phytochem. Anal.* **2017**, *28*, 217–229, doi:10.1002/pca.2664.
  47. Alcántara, C.; Žugcic, T.; Abdelkebir, R.; García-Pérez, J. V.; Jambak, A.R.; Lorenzo, J.M.; Collado, M.C.; Granato, D.; Barba, F.J. Effects of Ultrasound-Assisted Extraction and Solvent on the Phenolic Profile, Bacterial Growth, and Anti-Inflammatory/Antioxidant Activities of Mediterranean Olive and Fig Leaves Extracts. *Molecules* **2020**, *25*, 1718, doi:10.3390/molecules25071718.
  48. Mir-Cerdà, A.; Granados, M.; Saurina, J.; Sentellas, S. Green Extraction of Antioxidant Compounds from Olive Tree Leaves Based on Natural Deep Eutectic Solvents. *Antioxidants* **2023**, *12*, 995, doi:10.3390/antiox12050995.
  49. Nikou, T.; Witt, M.; Stathopoulos, P.; Barsch, A.; Halabalaki, M. Olive Oil Quality and Authenticity Assessment Aspects Employing FIA-MRMS and LC-Orbitrap MS Metabolomic Approaches. *Front. Public Heal.* **2020**, *8*, 1–20, doi:10.3389/fpubh.2020.558226.
  50. Samarah, L.Z.; Khattar, R.; Tran, T.H.; Stopka, S.A.; Brantner, C.A.; Parlanti, P.; Veličković, D.; Shaw, J.B.; Agtuca, B.J.; Stacey, G.; et al. Single-Cell Metabolic Profiling: Metabolite Formulas from Isotopic Fine Structures in Heterogeneous Plant Cell Populations. *Anal. Chem.* **2020**, *92*, 7289–7298, doi:10.1021/acs.analchem.0c00936.
  51. Mungur, R.; Glass, A.D.M.; Goodenow, D.B.; Lightfoot, D.A. Metabolite Fingerprinting in Transgenic *Nicotiana Tabacum* Altered by the *Escherichia Coli* Glutamate Dehydrogenase Gene. *J. Biomed. Biotechnol.* **2005**, *2*, 198–214, doi:10.1155/JBB.2005.198.
  52. Duque-Soto, C.; Quirantes-Piné, R.; Borrás-Linares, I.; Segura-Carretero, A.; Lozano-Sánchez, J. Characterization and Influence of Static In Vitro Digestion on Bioaccessibility of Bioactive Polyphenols from an Olive Leaf Extract. *Foods* **2022**, *11*, 743, doi:10.3390/foods11050743.
  53. Voynikov, Y.; Balabanova, V.; Gevrenova, R.; Zheleva-Dimitrova, D. Chemophenetic Approach to Selected Senecioneae Species, Combining Morphometric and UHPLC-HRMS Analyses. *Plants* **2023**, *12*, 390, doi:10.3390/plants12020390.
  54. Abu-Reidah, I.M.; Arráez-Román, D.; Warad, I.; Fernández-Gutiérrez, A.; Segura-Carretero, A. UHPLC/MS2-Based Approach for the Comprehensive Metabolite Profiling of Bean (*Vicia Faba* L.) by-Products: A Promising Source of Bioactive Constituents. *Food Res. Int.* **2017**, *93*, 87–96, doi:10.1016/j.foodres.2017.01.014.
  55. Cea Pavez, I., Lozano-Sánchez, J., Borrás-Linares, I., Nuñez, H., Robert, P., & Segura-Carretero, A. Obtaining an Extract Rich in Phenolic Compounds from Olive Pomace by Pressurized Liquid Extraction. *Molecules* **2019**, *24*, 3108, doi:10.3390/molecules24173108.

**Table S1.** <sup>TIMS</sup>CCS<sub>N2</sub> Database of many compounds detected in olive-derived matrices by LC-ESI-TimsTOF MS/MS profiling along with its presence in the olive root, stem and leaf organ.

Proposed compound	Molecular Formula	Rt (min)	For experimental [M-H] <sup>-</sup>					Detected in:		
			<i>m/z</i> <sub>exp</sub>	Error (ppm)	mSigma	<sup>TIMS</sup> CCS <sub>N2</sub> (Å <sup>2</sup> )	Main fragments via MS/MS	Root	Stem	Leaf
<b>Organic acids</b>										
quinic acid*	C <sub>7</sub> H <sub>12</sub> O <sub>6</sub>	1.24	191.0562	0.52	4.4	134.3	127.0416; 93.0344; 85.0294	x	x	x
citric acid	C <sub>6</sub> H <sub>8</sub> O <sub>7</sub>	1.26	191.0197	-0.01	11.9	126.5	111.0092; 87.0087; 85.0291	x	x	x
<b>Iridoids</b>										
loganic acid	C <sub>16</sub> H <sub>24</sub> O <sub>10</sub>	1.30	375.1296	0.07	22.7	184.7	213.0764; 169.0876; 151.0752; 125.0606; 113.0244; 107.0499	x	x	x
7-deoxyloganic acid	C <sub>16</sub> H <sub>24</sub> O <sub>9</sub>	4.82	359.1347	-0.36	6.1	182.4	197.0814; 153.0923; 135.0817	x	x	
11-hydroxyiridodial glucoside pentaacetate	C <sub>26</sub> H <sub>36</sub> O <sub>13</sub>	5.66	555.2082	-0.06	9.9	222.3	225.1134; 183.0659; 167.0717; 151.0406	x	x	
<b>Coumarins</b>										
aesculin	C <sub>15</sub> H <sub>16</sub> O <sub>9</sub>	4.44	339.0721	-0.06	27.0	174.6	177.0192; 133.0299	x	x	
aesculetin	C <sub>9</sub> H <sub>6</sub> O <sub>4</sub>	6.39	177.0194	0.39	10.6	127.5	149.0244; 133.0300; 105.0345; 89.0401	x	x	x
<b>Simple phenols and derivatives</b>										
hydroxytyrosol glucoside (is. 1, main peak)	C <sub>14</sub> H <sub>20</sub> O <sub>8</sub>	4.33	315.1084	-0.31	6.4	163.1	153.0559; 135.0451; 123.0459	x	x	x
hydroxytyrosol glucoside (is.2)			315.1085	0.04	2.8	171.8	153.0556; 135.0450; 123.0453	x	x	x
hydroxytyrosol*	C <sub>8</sub> H <sub>10</sub> O <sub>3</sub>	4.49	153.0557	-0.38	5.6	128.8	123.0455; 109.0293		x	x
tyrosol glucoside	C <sub>14</sub> H <sub>20</sub> O <sub>7</sub>	4.69	299.1136	-0.17	10.0	161.4	137.0622; 119.0425	x	x	x
tyrosol*	C <sub>8</sub> H <sub>10</sub> O <sub>2</sub>	5.00	137.0611	1.86	3.5	127.6	119.0449; 107.0508			
verbascoside*	C <sub>29</sub> H <sub>36</sub> O <sub>15</sub>	5.73	623.1979	-0.25	8.2	223.2	461.1663; 179.0351; 161.0242; 135.0446	x	x	x
phenylethyl primeveroside	C <sub>19</sub> H <sub>28</sub> O <sub>10</sub>	5.78	415.1609	-0.12	4.6	202.2	149.0444	x	x	x
isoverbascoside	C <sub>29</sub> H <sub>36</sub> O <sub>15</sub>	6.17	623.1981	0.08	5.5	223.4	461.1665; 161.0245	x		
<b>Lignans and derivatives</b>										
cyclooolivil glucoside (is.1, main peak)	C <sub>26</sub> H <sub>34</sub> O <sub>12</sub>	5.03	537.1977	-0.09	3.8	231.4	375.1450; 195.0661; 179.0710	x	x	
cyclooolivil glucoside (is.2, main peak)			537.1976	-0.32	2.1	208.9	375.1446; 345.1372; 195.0661; 179.0716	x	x	
cyclooolivil glucoside (is.3)	C <sub>26</sub> H <sub>34</sub> O <sub>12</sub>	5.16	537.1975	-0.27	21.0	214.5	375.1449; 195.0665; 179.0700	x	x	
oolivil	C <sub>20</sub> H <sub>24</sub> O <sub>7</sub>	5.54	375.1449	-0.17	11.0	197.8	360.1227; 345.1360; 327.1252; 195.0670; 179.0713	x	x	
cyclooolivil			375.1448	-0.33	10.2	205.6	360.1228; 345.1358	x	x	

Proposed compound	Molecular Formula	Rt (min)	For experimental [M-H] <sup>-</sup>				Detected in:			
			m/z <sub>exp</sub>	Error (ppm)	mSigma	<sup>TIMS</sup> CCS <sub>N<sub>2</sub></sub> (Å <sup>2</sup> )	Main fragments via MS/MS	Root	Stem	Leaf
<b>Lignans and derivatives</b>										
(+)-1-acetoxypinoresinol 4'-β-D-glucoside (is.1, main peak)	C <sub>28</sub> H <sub>34</sub> O <sub>13</sub>	6.09	577.1928	0.23	8.4	210.7	415.1395	x	x	
8-acetoxypinoresinol 4-glucoside (is.2)			577.1927	0.02	3.8	227.9	415.1404	x	x	
hydroxypinoresinol glucoside (is.1)			535.1820	-0.16	2.8	215.9	373.1289; 355.1189; 295.0998	x	x	
hydroxypinoresinol glucoside (is.2, main peak)	C <sub>26</sub> H <sub>32</sub> O <sub>12</sub>	6.33	535.1822	0.25	8.9	229.5	373.1290	x	x	
1-acetoxypinoresinol	C <sub>22</sub> H <sub>24</sub> O <sub>8</sub>	7.15	415.1398	-0.02	12.0	203.5	325.1066; 280.0728; 181.0508; 151.0399; 136.0163	x	x	
<b>Secoiridoids and derivatives</b>										
aldehydic form of decarboxymethyl elenolic acid glucoside (is.1)	C <sub>16</sub> H <sub>26</sub> O <sub>10</sub>	1.27	377.1452	-0.15	8.6	188.8	197.0821; 153.0921	x	x	x
oleoside / secologanoside	C <sub>16</sub> H <sub>22</sub> O <sub>11</sub>	1.29	389.1090	0.08	8.9	184.6	345.1164; 209.0446; 183.0663; 165.0519; 121.0663; 113.0250	x	x	x
oleoside / secologanoside	C <sub>16</sub> H <sub>22</sub> O <sub>11</sub>	1.32	389.1088	-0.44	11.7	189.5	345.1161; 227.0558; 209.0445; 183.0669; 121.0665; 113.0253	x	x	x
elenolic acid glucoside (is.1)	C <sub>17</sub> H <sub>24</sub> O <sub>11</sub>	2.14	403.1245	-0.36	15.7	192.5	371.0975; 223.0598; 181.0504; 179.0557; 127.0393; 101.0243	x	x	x
elenolic acid glucoside (is.2)	C <sub>17</sub> H <sub>24</sub> O <sub>11</sub>	2.69	403.1246	-0.02	10.4	189.9	371.0978; 223.0607; 179.0561; 127.0419; 101.0238	x	x	x
aldehydic form of decarboxymethyl elenolic acid glucoside (is.2)	C <sub>16</sub> H <sub>26</sub> O <sub>10</sub>	4.23	377.1452	0.02	8.8	188.6	197.0823; 153.0915	x	x	x
elenolic acid glucoside (is.3)	C <sub>17</sub> H <sub>24</sub> O <sub>11</sub>	4.49	403.1245	-0.01	13.4	192.1	371.0975; 223.0601; 181.0493; 165.0555; 121.0296; 101.0241	x	x	x
elenolic acid dihexose derivate	C <sub>25</sub> H <sub>38</sub> O <sub>18</sub>	4.85	625.1986	0.05	6.9	231.5	223.0601; 179.0564; 119.0353	x	x	x
demethyl oleuropein	C <sub>24</sub> H <sub>30</sub> O <sub>13</sub>	4.95	525.1606	0.01	8.9	213.5	481.1694; 389.1085; 209.0442; 195.0663; 121.0670	x	x	x
elenolic acid dihexose	C <sub>23</sub> H <sub>34</sub> O <sub>15</sub>	5.16	565.1775	-0.20	5.9	234.9	403.1239; 371.0981; 223.0603; 113.0224; 101.0232; 89.0232	x	x	x
demethyl ligstroside	C <sub>24</sub> H <sub>30</sub> O <sub>12</sub>	5.23	509.1663	-0.22	27.1	208.8	347.1128; 277.0713; 233.0801; 165.0554; 121.0680	x	x	x
hydroxy oleuropein (is.1, main peak)			555.1719	0.03	15.3	218.9	537.1597; 403.1242; 393.1190; 323.0770; 151.0386	x	x	x
hydroxy oleuropein (is.2)	C <sub>25</sub> H <sub>32</sub> O <sub>14</sub>	5.60	555.1721	-0.03	13.2	227.6	537.1595; 403.1241; 151.0383	x	x	x
neonuzhenide / oleuropein glucoside (is.1)	C <sub>31</sub> H <sub>42</sub> O <sub>18</sub>	5.63	701.2293	-0.72	19.1	245.5	539.1770; 377.1241; 307.0795; 275.0925	x	x	

Proposed compound	Molecular Formula	Rt (min)	For experimental [M-H] <sup>-</sup>				Detected in:			
			m/z <sub>exp</sub>	Error (ppm)	mSigma	TIMS <sup>+</sup> CCS <sub>N2</sub> (Å <sup>2</sup> )	Main fragments via MS/MS	Root	Stem	Leaf
<b>Secoiridoids and derivatives</b>										
elenolic acid glucoside (is.4)	C <sub>17</sub> H <sub>24</sub> O <sub>11</sub>	5.94	403.1246	0.00	8.6	190.1	223.0603; 121.0289; 113.0228; 101.0246	x	x	x
nuzhenide	C <sub>31</sub> H <sub>42</sub> O <sub>17</sub>	6.03	685.2347	-0.34	19.0	241.1	523.1813; 453.1391; 421.1499; 299.1132	x	x	x
neonuzhenide / oleuropein glucoside (is.2)	C <sub>31</sub> H <sub>42</sub> O <sub>18</sub>	6.10	701.2297	-0.22	16.1	241.8	539.1773; 377.1238; 307.0830; 275.0925	x	x	
methoxyoleuropein	C <sub>26</sub> H <sub>34</sub> O <sub>14</sub>	6.52	569.1867	-0.55	28.2	223.2	537.1587; 403.1235; 223.0604; 165.0570; 121.0292	x	x	x
neonuzhenide / oleuropein glucoside (is.3)	C <sub>31</sub> H <sub>42</sub> O <sub>18</sub>	6.54	701.2296	-0.33	19.2	248.9	539.1769; 377.1236; 307.0816; 275.0928		x	x
oleuropein*	C <sub>25</sub> H <sub>32</sub> O <sub>13</sub>	6.66	539.1718	0.19	4.5	217.5	403.1233; 377.1234; 307.0822; 275.0924; 223.0609; 179.0558	x	x	x
elenolic acid glucoside (is.5)	C <sub>17</sub> H <sub>24</sub> O <sub>11</sub>	6.86	403.1246	-0.04	6.9	190.4	371.0967; 223.0604; 181.0483; 127.0409; 101.0249; 89.0193	x	x	x
lucidumoside C	C <sub>27</sub> H <sub>36</sub> O <sub>14</sub>	7.13	583.2032	0.03	14.8	229.1	403.1224; 223.0593; 179.0541; 151.0399	x	x	x
ligstroside	C <sub>25</sub> H <sub>32</sub> O <sub>12</sub>	7.26	523.1824	0.37	9.0	214.7	361.1290; 291.0879; 259.0976; 223.0621; 101.0245	x	x	x
oleuroside	C <sub>25</sub> H <sub>32</sub> O <sub>13</sub>	7.35	539.1766	-0.70	10.9	217.1	403.1230; 377.1244; 345.0990; 307.0824; 275.0926; 223.0610		x	x
oleuropein aglycone (is.1)	C <sub>19</sub> H <sub>22</sub> O <sub>8</sub>	8.03	377.1239	-0.73	3.2	186.0	307.0820; 275.0572; 149.0241; 139.0389; 111.0082; 95.0500	x	x	x
oleuropein aglycone (is.2)	C <sub>19</sub> H <sub>22</sub> O <sub>8</sub>	8.33	377.1243	0.41	2.3	185.2	307.0822; 275.0564; 149.0234; 139.0390; 127.0408; 111.0088	x	x	x
oleuropein aglycone (is.3)	C <sub>19</sub> H <sub>22</sub> O <sub>8</sub>	9.00	377.1242	-0.02	17.9	184.8	275.0564; 149.0237; 139.0399; 127.0407; 121.0315	x	x	x
<b>Flavonoids</b>										
dihydroquercetin-O-glucoside (is.1)	C <sub>21</sub> H <sub>22</sub> O <sub>12</sub>	4.67	465.1036	-0.54	12.9	191.8	303.0505; 285.0399; 177.0191; 125.0261		x	
catechin*	C <sub>15</sub> H <sub>14</sub> O <sub>6</sub>	4.80	289.0721	1.23	3.3	156.8	245.0810; 203.0744; 179.0362			
catechin*	C <sub>15</sub> H <sub>14</sub> O <sub>6</sub>		289.0722	1.51	1.2	169.5	245.0811; 203.0746; 179.0358			
dihydrokaempferol-O-glucoside	C <sub>21</sub> H <sub>22</sub> O <sub>11</sub>	4.91	449.1089	0.37	10.6	186.3	287.0550; 259.0633; 243.0664; 151.0034; 125.0245		x	
dihydroquercetin-O-glucoside (is.2)	C <sub>21</sub> H <sub>22</sub> O <sub>12</sub>	5.40	465.1036	0.42	15.7	192.5	303.0504; 285.0406		x	
taxifolin (dihydroquercetin)	C <sub>15</sub> H <sub>12</sub> O <sub>7</sub>	5.77	303.0510	-0.07	3.8	164.7	285.0409; 177.0199; 125.0263		x	
naringenin-O-glucoside	C <sub>21</sub> H <sub>22</sub> O <sub>10</sub>	6.26	433.1138	-0.02	11.2	183.1	271.0615; 151.0018; 119.0515		x	x
dihydrokaempferol	C <sub>15</sub> H <sub>12</sub> O <sub>6</sub>	6.30	287.0560	-0.30	2.9	163.4	259.0598; 243.0661; 177.0561; 151.0039; 125.0244		x	
rutin*	C <sub>27</sub> H <sub>30</sub> O <sub>16</sub>	6.36	609.1471	1.63	2.9	232.4	301.0349; 300.0252		x	x

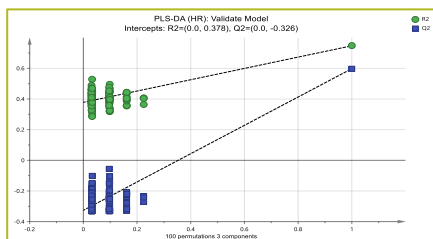
Proposed compound	Molecular Formula	Rt (min)	For experimental [M-H] <sup>-</sup>					Detected in:		
			m/z <sub>exp</sub>	Error (ppm)	mSigma	TIMS <sup>2</sup> CCS <sub>N<sub>2</sub></sub> (Å <sup>2</sup> )	Main fragments via MS/MS	Root	Stem	Leaf
<b>Flavonoids</b>										
luteolin-O-glucoside (is.1)	C <sub>21</sub> H <sub>20</sub> O <sub>11</sub>	6.46	447.0934	-0.06	19.6	210.2	285.0408		x	x
quercetin-O-glucoside (is.1)	C <sub>21</sub> H <sub>20</sub> O <sub>12</sub>	6.50	463.0879	-0.48	17.1	202.1	301.0347; 300.0251		x	x
apigenin-O-rutinoside (is.1)	C <sub>27</sub> H <sub>30</sub> O <sub>14</sub>	6.55	577.1563	0.03	10.4	232.7	269.0458			x
apigenin 7-O-rutinoside (is.2)	C <sub>27</sub> H <sub>30</sub> O <sub>14</sub>	6.65	577.1561	0.25	12.0	224.5	269.0458			x
apigenin-7-O-glucoside	C <sub>21</sub> H <sub>20</sub> O <sub>10</sub>	6.73	431.0984	-0.03	10.5	208.1	269.0459		x	x
diosmin	C <sub>28</sub> H <sub>32</sub> O <sub>15</sub>	6.74	607.1664	-0.75	24.8	231.8	299.0562; 284.0319			x
chrysoeriol-7-O-glucoside	C <sub>22</sub> H <sub>22</sub> O <sub>11</sub>	6.80	461.1089	-0.25	3.7	215.9	446.0858; 299.0561			x
luteolin-O-glucoside (is.2)	C <sub>21</sub> H <sub>20</sub> O <sub>11</sub>	6.85	447.0931	-0.45	8.3	208.4	285.0405; 133.0297		x	x
quercetin-O-glucoside (is.2)	C <sub>21</sub> H <sub>20</sub> O <sub>12</sub>	6.90	463.0879	-0.71	14.7	210.9	301.0345		x	x
luteolin-O-glucoside (is.3)	C <sub>21</sub> H <sub>20</sub> O <sub>11</sub>	7.17	447.0933	-0.02	15.4	210.2	285.0405; 284.0331		x	x
naringenin	C <sub>15</sub> H <sub>12</sub> O <sub>5</sub>	7.77	271.0613	0.35	1.6	163.0	151.0028; 119.0500	x	x	x
luteolin*	C <sub>15</sub> H <sub>10</sub> O <sub>6</sub>	8.71	285.0407	0.89	19.3	160.6	217.0516; 199.0409; 175.0401; 151.0038; 133.0291; 107.0139	x	x	x
apigenin*	C <sub>15</sub> H <sub>10</sub> O <sub>5</sub>	8.80	269.0456	0.04	6.5	157.6	225.0554; 201.0547; 149.0238	x	x	x
<b>Pentacyclic triterpenes</b>										
maslinic acid*	C <sub>30</sub> H <sub>48</sub> O <sub>4</sub>	13.13	471.3479	-0.30	12.7	223.4	-	x	x	x
betulinic acid	C <sub>30</sub> H <sub>48</sub> O <sub>3</sub>	14.00	455.3531	-0.02	2.6	220.1	-	x	x	x
oleanolic acid*	C <sub>30</sub> H <sub>48</sub> O <sub>3</sub>	14.14	455.3530	0.32	5.1	220.7	-	x	x	x

\*Corroborate with a pure standard

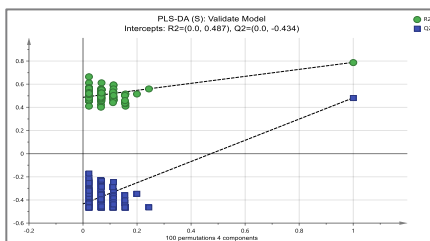
ROOT TISSUE TYPE

	PLS-DA model	A	N	R <sup>2</sup> X (cum)	R <sup>2</sup> Y (cum)	Q <sup>2</sup> (cum)
(1)-	HR vs. Others	3	129	0.283	0.747	0.598
(2)-	S vs. Others	4	129	0.318	0.789	0.482

(1)- Permutations PLS-DA (HR)



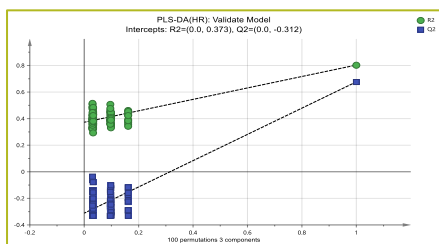
(2)- Permutations PLS-DA (S)



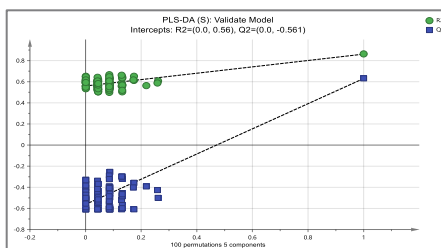
STEM TISSUE TYPE

	PLS-DA model	A	N	R <sup>2</sup> X (cum)	R <sup>2</sup> Y (cum)	Q <sup>2</sup> (cum)
(1)-	HR vs. Others	3	129	0.275	0.803	0.677
(2)-	S vs. Others	5	129	0.391	0.861	0.630

(1)- Permutations PLS-DA (HR)



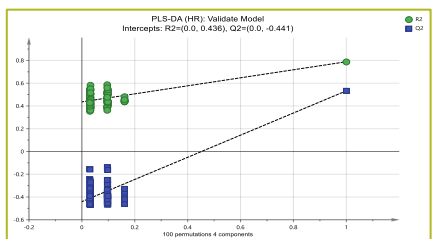
(2)- Permutations PLS-DA (S)



LEAF TISSUE TYPE

	PLS-DA model	A	N	R <sup>2</sup> X (cum)	R <sup>2</sup> Y (cum)	Q <sup>2</sup> (cum)
(1)-	HR vs. Others	4	129	0.339	0.788	0.533
(2)-	S vs. Others	3	129	0.279	0.666	0.318

(1)- Permutations PLS-DA (HR)



(2)- Permutations PLS-DA (S)

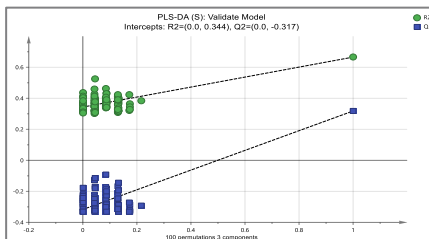
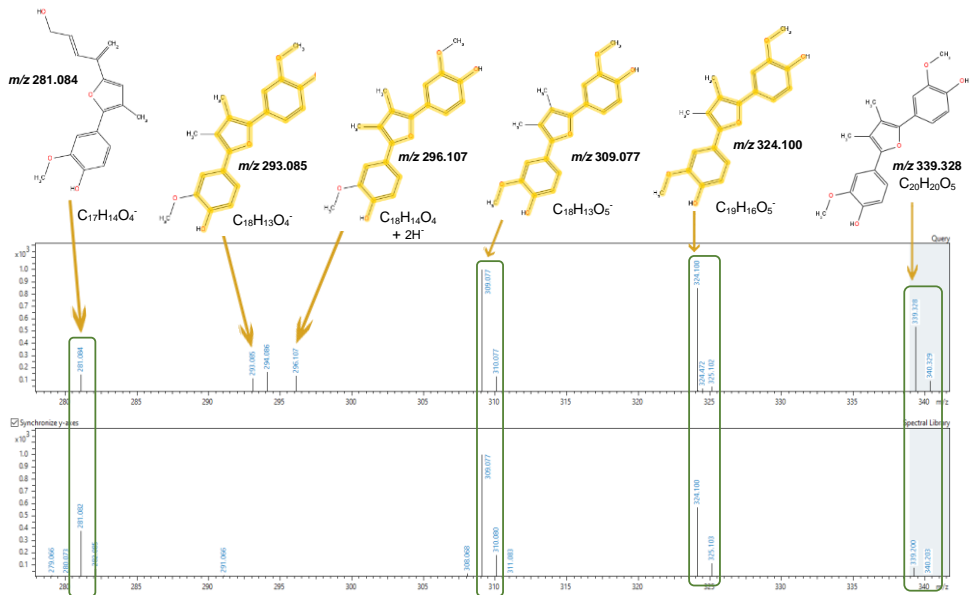


Figure S1. Model quality descriptors (R<sup>2</sup>X, R<sup>2</sup>Y and Q<sup>2</sup>) and permutation tests of PLS-DA models built for each tissue type

## GUAIAICONIC ACID



## COUMAROYL HEXOSIDE

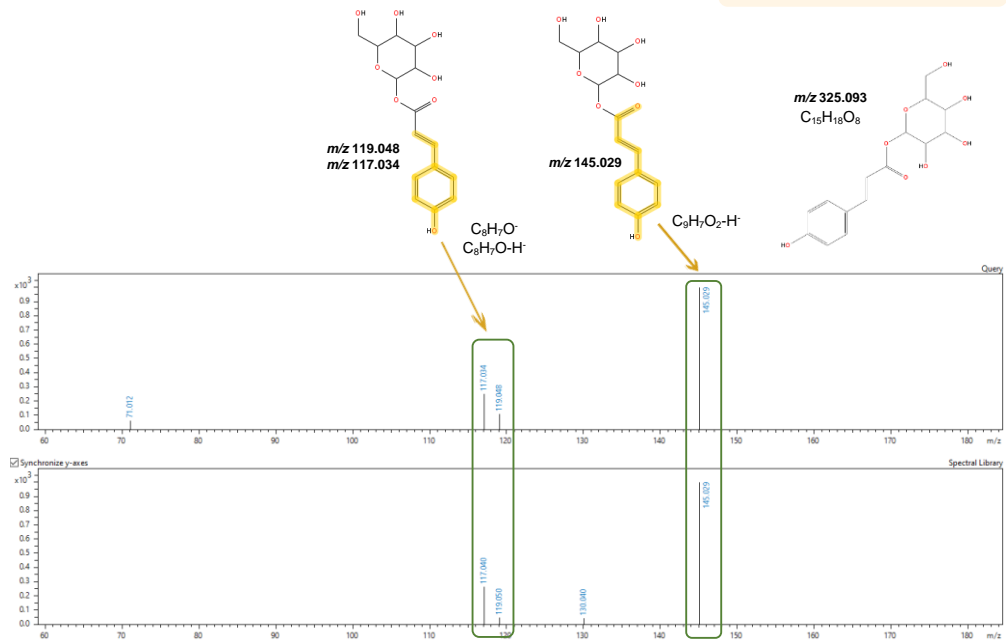


Figure S2. Molecular structure and MetFrag outcomes for guaiacnic and coumaroyl hexoside fragment assignments



**CONCLUSIONS**

**CONCLUSIONES**





## CONCLUSIONS

---

As a part of this Doctoral Thesis, various analytical methodologies have been successfully developed and applied to conduct metabolomic studies on both avocado fruit pulp and different olive tree-derived matrices, including fruits, as well as plant tissues such as leaves, stems, and roots. This section summarizes the most relevant conclusions of the work carried out, following the general structure established in the experimental sections.

### Section I. “Metabolomic approaches applied to the study of avocado fruit”

1. Both the maturation and ripening processes of avocado are closely related to complex metabolic changes that can be significantly modulated by pre- and post-harvest fruit management. Prolonged on-tree maturation has been shown to increase the overall content of phenolic compounds in avocados. Conversely, this content decreases when the fruit is stored in a cold chamber for more than 10 days. Pantothenic acid levels remain relatively stable regardless of the handling method, whereas abscisic acid levels rise in cold-stored fruit, likely due to ethylene accumulation, which stimulates its synthesis (**Chapter 1**).
2. Significant metabolic variations occur during the softening of avocados, with differences depending on the variety (*Hass*, *Bacon*, and *Fuerte*). In general terms, phenolic compound levels increase throughout fruit ripening, particularly in the *Hass* variety, whereas the behavior of amino acids and related compounds varies by cultivar. Other metabolites, such as abscisic acid, uridine, and penstemide, show consistent trends during maturation across the three varieties (**Chapter 2**).
3. *Hass* avocados imported from countries such as Peru or Chile exhibit different metabolic profiles compared to those produced locally in Spain. Statistical classification models were used to define specific compositional patterns for each country. This metabolic differentiation could facilitate the provision of comparative nutritional information on the avocados available in the European market throughout the year (**Chapter 3**).
4. Non-targeted metabolomics using LC-IMS-MS has proven to be an effective tool for investigating the geographical origin of avocados grown in different regions of the Iberian Peninsula. Greater similarities have been observed between the metabolic profiles of fruit from northern regions (Asturias and Galicia) compared with those from more southern regions. Nevertheless, a unique compositional pattern has been identified for each of the eight locations, which has been thoroughly described using two-class OPLS-DA statistical models (**Chapter 4**).

5. Overall, in this Section I, the use of advanced platforms such as LC-MS or LC-IMS-MS has enabled an in-depth exploration of the metabolic profile of avocado pulp, identifying over 100 metabolites from various chemical classes, including phenolic compounds (the most abundant), nucleosides, amino acids, vitamins, sesquiterpenoids, organic acids, etc. Additionally, experimental CCS values have been obtained for these metabolites, providing a solid foundation for future characterization studies (considering this descriptor for compound annotation). These tools have also enabled the precise quantification of a wide range of relevant compounds in the fruit pulp.

## Section II. "Metabolomic approaches applied to the study of olive-related matrices"

6. *Olea europaea* subsp. *cuspidata* represent a valuable genetic resource for olive breeding programs. The drupes of most progeny genotypes tend to be generally richer in certain bioactive compounds than traditional cultivars, particularly in terms of rutin, hydroxytyrosol glucoside, several secoiridoids, and unknown compounds with  $m/z$  values of 421.1494 ( $C_{21}H_{26}O_9$ ) and 363.1440 ( $C_{19}H_{24}O_7$ ) (Chapter 5).
7. The qualitative and quantitative distribution of secondary metabolites across different olive tree organs (roots, stems, and leaves) has been investigated. In general, lignans and their derivatives are not present in olive leaves, whereas flavonoids and related compounds are absent from the roots. In contrast, other chemical families such as organic acids, iridoids, coumarins, simple phenols and their derivatives, secoiridoids and related compounds, and pentacyclic triterpenes are found in all the tissues studied (Chapters 6 and 7).
8. Investigating the basal metabolic profile of olive varieties with varying levels of susceptibility to verticillium wilt using both targeted and non-targeted metabolomic approaches, has revealed that cultivars with similar susceptibility share common metabolic patterns. The use of discriminant statistical models (PLS-DA and OPLS-DA) has enabled the identification of key compounds that could serve as markers of resistance. This information will not only help to understand the potential role of these compounds in plant defense against *V. dahliae* but will also aid in the selection of promising candidates for olive breeding programs (Chapters 6 and 7).
9. Overall, in Section II of this report, the application of powerful LC-MS and LC-IMS-MS methods has proven extremely effective for comprehensive characterization of various olive tissues. These methodologies have facilitated the identification of more than 70 metabolites from diverse chemical classes and the quantification of the most relevant ones. Furthermore, the integration of ion mobility with mass spectrometry has shown great potential for distinguishing coeluting isomers, representing a significant advancement over high-resolution LC-MS.

The findings of this Doctoral Thesis open new avenues for future research in the field of food and plant metabolomics. The successful implementation of advanced LC-MS methodologies provides a robust foundation for exploring new areas that could significantly enrich knowledge and practical applications in these two sectors. Some of the most interesting future directions could include:

- ✚ Analyzing the samples used in this thesis through a complementary analytical platform, such as GC-MS, which would provide additional information and confirm or expand the results already obtained.
- ✚ Investigating the bioavailability of the more than 100 metabolites identified in avocado pulp to understand how they are absorbed, metabolized, and excreted from the body would be key to scientifically supporting the health benefits associated with this tropical fruit.
- ✚ Assessing the potential of lipidomics and stable isotope analysis to differentiate avocados based on their geographical origin would add a valuable dimension to ensuring traceability.
- ✚ Employing structural characterization techniques such as NMR would enable the unambiguous identification of key compounds that act as markers of resistance to *V. dahliae* (in olive trees) or as indicators of maturity, variety, or geographical origin (in avocados).
- ✚ Conducting an in-depth exploration of the metabolic profiles of other wild olive varieties could provide valuable genetic material for improving olive resistance to certain diseases and optimizing the production of high-quality oil.

In short, the application of innovative metabolomic tools and the integration of multi-omics approaches hold great promise for expanding our knowledge and transforming certain practices in agriculture and health, offering new ways to address emerging challenges and leverage potential future opportunities.



En el marco de la presente Tesis Doctoral se han desarrollado y aplicado con éxito diversas metodologías analíticas para la realización de estudios metabolómicos tanto en la pulpa del fruto del aguacate como en distintas matrices derivadas del olivo, que incluyen desde el fruto hasta tejidos vegetales como hojas, tallos y raíces. En esta sección se presentan de manera resumida las conclusiones más relevantes del trabajo realizado, siguiendo la estructura general establecida en las secciones de la parte experimental.

### Sección I. “Aproximaciones metabolómicas aplicadas al estudio del fruto del aguacate”

1. El fenómeno de maduración del aguacate está estrechamente relacionado con cambios metabológicos complejos, que pueden ser modulados de manera significativa por el manejo pre- y postcosecha de los frutos. Se ha demostrado que la maduración prolongada en árbol incrementa el contenido general de compuestos fenólicos en los aguacates. Contrariamente, este contenido disminuye cuando los frutos se almacenan en cámaras frigoríficas durante más de 10 días. El ácido pantoténico no presenta cambios drásticos en función del distinto manejo del aguacate, mientras que los niveles de ácido abscísico aumentan en los frutos almacenados en frío, probablemente debido a la acumulación de etileno, que estimula su síntesis (**Capítulo 1**).
2. Durante el proceso de reblandecimiento del aguacate se producen variaciones significativas a nivel metabólico, con diferencias dependiendo a la variedad (*Hass*, *Bacon* y *Fuerte*). En general, los niveles de compuestos fenólicos aumentan a lo largo de la maduración, especialmente en la variedad *Hass*, mientras que el comportamiento de los aminoácidos y compuestos relacionados varía según el cultivar. Otros metabolitos como el ácido abscísico, la uridina y el penstemide muestran tendencias consistentes durante la maduración en las tres variedades (**Capítulo 2**).
3. Los aguacates de la variedad *Hass* importados de países como Perú o Chile tienen perfiles metabológicos diferentes a los de los producidos localmente en España. Gracias al uso de modelos estadísticos de clasificación, se han definido patrones composicionales específicos para cada país. Esta diferenciación metabólica podría facilitar la obtención de información nutricional comparativa sobre los aguacates disponibles en el mercado europeo a lo largo de todo el año (**Capítulo 3**).
4. La metabolómica no dirigida empleando LC-IMS-MS ha resultado ser una herramienta eficaz para estudiar el origen geográfico de aguacates cultivados en distintas zonas de la Península Ibérica. Se han observado mayores similitudes entre los perfiles metabológicos de los frutos provenientes de las regiones del norte (Asturias y Galicia) en comparación con

aquellos de las regiones más al sur. Sin embargo, se ha podido describir un patrón composicional único para cada una de las ocho localizaciones, que han sido detalladamente descritos mediante el uso de modelos estadísticos OPLS-DA de dos clases (**Capítulo 4**).

5. En términos globales, en esta sección I, el uso de plataformas avanzadas como LC-MS o LC-IMS-MS ha permitido una exploración profunda del perfil metabólico de la pulpa de aguacate, logrando identificar más de 100 metabolitos pertenecientes a diversas clases químicas, tales como compuestos fenólicos (siendo los más abundantes), nucleósidos, aminoácidos, vitaminas, sesquiterpenoides, ácidos orgánicos, etc. Además, se ha obtenido el valor de CCS experimental para dichos metabolitos, proporcionando una base sólida para futuros trabajos de caracterización (anotaciones que consideren este descriptor). Estas herramientas también han permitido llevar a cabo la cuantificación exacta de una amplia variedad de compuestos relevantes en la pulpa del fruto.

## **Sección II. "Aproximaciones metabolómicas aplicadas al estudio de matrices relacionadas con el olivar"**

6. Las drupas de *Olea europaea* subsp. *cuspidata* son una fuente genética valiosa para ser incluidas en programas de mejora del olivo. Los genotipos de la progenie tienden a ser, en general, más ricos en ciertos compuestos bioactivos que los cultivares tradicionales, especialmente en cuando a los contenidos de rutina, hidroxitirosol glicosilado, varios secoiridoides y los compuestos desconocidos con  $m/z$  421.1494 ( $C_{21}H_{26}O_9$ ) y 363.1440 ( $C_{19}H_{24}O_7$ ) (**Capítulo 5**).
7. Se ha investigado la distribución cualitativa y cuantitativa de metabolitos secundarios en distintos órganos del olivo (raíces, tallos y hojas). En términos generales, los lignanos y sus derivados no se encuentran en las hojas de olivo, mientras que los flavonoides y compuestos relacionados están ausentes en las raíces. En cambio, otras familias químicas como los ácidos orgánicos, iridoides, cumarinas, fenoles simples y sus derivados, secoiridoides y compuestos relacionados, y los triterpenos pentacíclicos están presentes en todos los tejidos del árbol que fueron considerados (**Capítulo 6 y 7**).
8. Estudiar el perfil metabólico basal de variedades de olivo con distintos niveles de susceptibilidad a la verticilosis, utilizando tanto enfoques metabolómicos dirigidos como no dirigidos, ha revelado que los cultivares con similar susceptibilidad comparten patrones metabólicos comunes. El empleo de modelos estadísticos discriminantes (PLS-DA y OPLS-DA) ha posibilitado la identificación de compuestos clave que podrían servir como marcadores de resistencia. Esta información no solo contribuirá a comprender el papel potencial de estos compuestos en la defensa de la planta contra *V. dahliae*, sino que también facilitará la selección de candidatos prometedores para los programas de mejora genética del olivo (**Capítulo 6 y 7**).

9. Así pues, en general en la sección II de la presente memoria, el empleo de potentes métodos de LC-MS y LC-IMS-MS ha demostrado ser extremadamente eficaz para realizar caracterizaciones exhaustivas de distintos tejidos del olivo. Estas metodologías han permitido identificar más de 70 metabolitos pertenecientes a distintas clases químicas y cuantificar los más representativos. Además, la integración de la movilidad iónica con la espectrometría de masas ha mostrado un gran potencial para discriminar isómeros coeluyentes, representando un avance significativo respecto a la LC-MS de alta resolución.

Los hallazgos de esta Tesis Doctoral abren nuevas oportunidades para futuras investigaciones en el campo de la metabolómica alimentaria y de plantas. La exitosa implementación de metodologías LC-MS avanzadas proporciona una base robusta para explorar nuevas áreas que podrían enriquecer notablemente el conocimiento y la aplicación práctica en estos dos sectores. Algunas de las direcciones futuras más interesantes podrían incluir:

- ✚ Analizar las muestras usadas en la presente Tesis mediante una plataforma analítica complementaria, como GC-MS, permitiría obtener información adicional y confirmar o ampliar los resultados ya obtenidos.
- ✚ Investigar la biodisponibilidad de los más de 100 metabolitos identificados en la pulpa de aguacate, para comprender cómo son absorbidos, metabolizados y eliminados del cuerpo, sería clave para respaldar científicamente los beneficios para la salud asociados a esta fruta tropical.
- ✚ Evaluar el potencial de la lipidómica y el del análisis de isótopos estables para diferenciar los aguacates según su origen geográfico añadiría una dimensión valiosa en aras de asegurar la trazabilidad de estos productos.
- ✚ Emplear técnicas de caracterización estructural como RMN posibilitaría la identificación de forma inequívoca de compuestos clave que actúan como marcadores de resistencia a *Verticillium dahliae* (en olivo) o como indicadores de madurez, variedad o procedencia geográfica (en aguacate).
- ✚ Explorar en profundidad los perfiles metabólicos de otras variedades silvestres de olivo podría proporcionar material genético valioso para mejorar la resistencia del olivar a ciertas enfermedades y optimizar la producción de aceite de alta calidad.

En definitiva, la aplicación de herramientas metabolómicas innovadoras y la integración de enfoques multi-ómicos prometen ampliar nuestro conocimiento y transformar ciertas prácticas en la agricultura y la salud, ofreciendo nuevas vías para abordar desafíos emergentes y aprovechar posibles oportunidades venideras.